การสังเคราะห์และฤทธิ์ต้านไวรัสเริมของสารกลุ่มกลัยโคกลีเซอโรไลปิด

นายวิชาญ จันทร์วิทยานุชิต

วิทยานิพนธ์นี้เป็นส่วนหนึ่งของการศึกษาตามหลักสูตรปริญญาวิทยาศาสตรดุษฎีบัณฑิต
สาขาวิชาเภสัชเคมีและผลิตภัณฑ์ธรรมชาติ
คณะเภสัชศาสตร์ จุฬาลงกรณ์มหาวิทยาลัย
ปีการศึกษา 2546

ISBN 974-17-3675-4

SYNTHESIS AND ANTI-HERPES SIMPLEX VIRAL ACTIVITY OF GLYCOGLYCEROLIPIDS

Mr. Wicharn Janwitayanuchit

A Dissertation Submitted in Partial Fulfillment of the Requirements
for the Degree of Doctor of Philosophy in Pharmaceutical Chemistry and Natural Products
Faculty of Pharmaceutical Sciences
Chulalongkorn University
Academic Year 2003

ISBN 974-17-3675-4

Thesis Title	Synthesis and anti-herpes simplex viral activity of glycoglycerolipids
By	Mr. Wicharn Janwitayanuchit
Field of Study	Pharmaceutical Chemistry and Natural Products
Thesis Advisor	Khanit Suwanborirux, Ph.D.
Thesis Co-advisor	Assistant Professor Chamnan Patarapanich, Ph.D.

Accepted by the Faculty of Pharmaceutical Sciences, Chulalongkorn University in Partial Fulfillment of the Requirements for the Doctor's Degree

……Dean of Faculty of Pharmaceutical Sciences

(Associate Professor Boonyong Tantisira, Ph.D.)

THESIS COMMITTEE

……Chairman

(Associate Professor Sumphan Wongseripipatana, Ph.D.)

…… Thesis Advisor

(Khanit Suwanborirux, Ph.D.)

…… Thesis Co-advisor

(Assistant Professor Chamnan Patarapanich, Ph.D.)

…… Member

(Associate Professor Sunibhond Pummangura, Ph.D.)

……. Member

(Associate Professor Vimolmas Lipipun, Ph.D.)

…….. Member

(Associate Professor Jiraporn Ungwitayatorn, Ph.D.)

……Member

(Assistant Professor Tirayut Vilaivan, D.Phil.)

นายวิชาญ จันทร์วิทยานุชิต: การสังเคราะห์และฤทธิ์ต้านไวรัสเริมของสารกลุ่มกลัยโคกลีเซอโรไลปิด. (SYNTHESIS AND ANTI-HERPES SIMPLEX VIRAL ACTIVITY OF GLYCOGLYCEROLPIDS) อ. ที่ปรึกษา: ดร. คณิต สุวรรณบริรักษ์, อ.ที่ปรึกษาร่วม: ผศ.ดร. ชำนาญ ภัตรพานิช, 245 หน้า. ISBN 974-17-3675-4

การวิจัยนี้เป็นการศึกษาวิธีการสังเคราะห์ และฤทธิ์ต้านไวรัสเริมของสารกลุ่มกลัยโคกลีเซอโรไลปิด ได้สังเคราะห์อนุกรมของสารโมโนกลัยโคซิล กลีเซอไรด์ 30 ชนิดที่มีน้ำตาลกลูโคสหรือแกแลคโตสเป็นองค์ประกอบและมีกรดไขมันอิ่มตัวและไม่อิ่มตัวที่มีความยาวของจำนวนคาร์บอนต่างๆกัน รวมทั้งโมโนกลีเซอไรด์ 3 ชนิดและไดกลีเซอไรด์ 1 ชนิด และรายงานความสัมพันธ์ระหว่างโครงสร้างทางเคมีและการออกฤทธิ์ต้านไวรัสเริมของสารดังกล่าว

การพิสูจน์เอกลักษณ์ของสารใช้เทคนิคทางสเปกโตรสโคปีและการวิเคราะห์องค์ประกอบธาตุ การทดสอบฤทธิ์ต้านไวรัสเริมใช้วิธีตรวจนับจำนวนพลาคที่ลดลง จากการทดสอบฤทธิ์พบว่า 1,2-ได-โอ-ลิโนเลโนอิล-3-โอ-เบต้า-ดี-กลูโคพัยราโนซิล-เอสเอน-กลีเซอรอล มีฤทธิ์ต้านไวรัสเริมชนิดที่ 1และชนิดที่ 2 ดีที่สุด โดยมีค่าความเข้มข้นในการยับยั้งการเจริญของไวรัสได้ 50 เปอร์เซ็นต์ต่อไวรัสเริมชนิดที่ 1 และชนิดที่ 2 เท่ากับ 16.1 และ 23.9 ไมโครโมลาร์ตามลำดับ จากการศึกษาความสัมพันธ์ระหว่างโครงสร้างทางเคมีและการออกฤทธิ์พบว่า หมู่ฟังก์ชันส่วนที่เป็นกรดไขมันเป็นส่วนที่มีความสำคัญต่อการออกฤทธิ์ โดยที่สารจะมีฤทธิ์ต้านไวรัสดีเมื่อหมู่ฟังก์ชันดังกล่าวมีสมบัติเป็นโอลิฟีนมากขึ้น ส่วนน้ำตาลเป็นองค์ประกอบที่มีความสำคัญต่อการออกฤทธิ์เช่นกัน อย่างไรก็ตามชนิดของน้ำตาลที่เป็นองค์ประกอบ(กลูโคสหรือแกแลคโตส) ไม่มีผลทำให้ฤทธิ์ในการต้านไวรัสเริมแตกต่างกัน และสเตอริโอเคมีที่ตำแหน่ง 2 ของโครงสร้างส่วนที่เป็นกลีเซอรอลไม่มีผลทำให้ฤทธิ์ต้านไวรัสเริมแตกต่างกันอย่างมีนัยสำคัญ

สาขาวิชา เภสัชเคมีและผลิตภัณฑ์ธรรมชาติ ลายมือชื่อนิสิต.....

ปีการศึกษา 2546 ลายมือชื่ออาจารย์ที่ปรึกษา.....

ลายมือชื่ออาจารย์ที่ปรึกษาร่วม.....

33410 : MAJOR PHARMACEUTICAL CHEMISTRY AND NATURAL PRODUCTS

KEY WORD: SYNTHESIS/ ANTI-HERPES SIMPLEX VIRAL ACTIVITY/
GLYCOGLYCEROLIPIDS
WICHARN JANWITAYANUCHIT: SYNTHESIS AND ANTI-HERPES SIMPLEX VIRAL ACTIVITY OF GLYCOGLYCEROLIPIDS: THESIS ADVISOR: KHANIT SUWANBORIRUX, Ph.D.,: THESIS CO-ADVISOR: ASST. PROF. CHAMNAN PATARAPANICH, Ph.D., 245 pp. ISBN 974-17-3675-4

This research was aimed to study the synthesis and anti-herpes simplex viral activity of glycoglycerolipids. A series of monoglycosyl glycerides bearing either glucose or galactose and related derivatives were synthesized. Thirty monoglycosyl glycerides bearing various chain lengths of saturated and unsaturated fatty acids were successfully prepared. Three monoglycerides and one diglyceride were also synthesized. Preliminary structure-activity relationships were reported.

The chemical structures of the synthesized compounds were confirmed by spectroscopic techniques and elemental analysis. The anti-HSV activity was determined *via* the plaque reduction assay. Among the compounds synthesized, 1,2-di-*O*-linolenoyl-3-*O*-β-D-glucopyranosyl-*sn*-glycerol shows the highest inhibitory activity against HSV-1 and HSV-2 with the IC_{50} values of 16.1 and 23.9 μM, respectively. A study of the structure-activity relationships of these synthetic compounds indicates that the fatty acyl moieties are critical for inhibitory action with higher activity displayed as the acyl groups become more olefinic in character. The sugar moiety is also important for anti-HSV action; however, the type of sugar (glucose or galactose) exhibits no different activity. The stereochemistry at C-2 of the glycerol backbone displays no significant effect on anti-HSV activity.

Field of Study Pharmaceutical Chemistry and Natural Products — Student's signature……

Academic Year 2003 — Advisor's signature……...

Co-advisor's signature……..

ACKNOWLEDGEMENTS

I am indebted to my thesis advisor, Dr. Khanit Suwanborirux, for his valuable advice, continual guidance, kindness, and understanding.

I am grateful to my thesis co-advisor, Assistant Professor Chamnan Patarapanich, for helpful discussion and suggestion.

It is great pleasure to acknowledge Associate Professor Vimolmas Lipipun for providing anti-herpes simplex viral activity test and valuable advice.

Financial supports for this work were provided by the Thailand Research Fund, grant No. RDG3/33/2543, the Graduate School of Chulalongkorn University and Huachiew Chalermprakiet University

I thank the Pharmaceutical Research Instrument Center, Faculty of Pharmaceutical Sciences for providing 300 MHz NMR spectrometer, the Scientific and Technological Research Equipment Center, Chulalongkorn University for elemental analysis and transmission electron micrograph, and Assoc. Prof. Naoki Saito, Meiji Pharmaceutical University, for his support in recording mass spectra.

Finally, I would like to thank the members of thesis committee for their valuable suggestions and discussion.

CONTENTS

LIST OF TABLES

LIST OF FIGURES

Figure Page

Figure Page

Figure Page

Figure Page

Figure Page

Figure Page

Figure Page

Figure Page

Figure Page

Figure Page

Figure Page

Figure Page

Figure Page

Figure Page

LIST OF SCHEMES

CHAPTER I
INTRODUCTION

Herpes simplex is a result of an infection caused by herpes simplex virus (HSV), which has an affinity for the skin, mucous membranes and nervous system. The word herpes is derived from the Greek word “herpein”, which means “to creep”. HSV is one of the most difficult viruses to control and has plagued mankind worldwide for thousands of years. There are two distinct types of these viruses: herpes simplex virus 1 (HSV-1) and herpes simplex virus 2 (HSV-2) which can be differentiated by serologic tests (Goldstein et al., 1983). HSV-1 mainly involves the oral cavity, often as the so-called “cold sores”, while HSV-2 attacks the genital area. Either type, however, can occasionally be found in either area or at the other sites. Once HSV enters the body, it penetrates vulnerable cells in the lower layers of human skin tissue and attempts to replicate itself in the cell nuclei. This process can destroy host cells, causing inflammation and fluid-filled blisters or ulcers in this area due to rupture of the blisters, these remain intact for several days in dermal infections, before they crust over and heal. In rare cases, the virus can further spread to the central nervous system causing meningitis or encephalitis (Craig and Nahmias, 1973). The virus travels from the site of primary infection through branches of nerve cells to root ganglia. Here, the virus persists in an inactive (latent) form, in which complete viral replication does not occur but both the host cells and the viruses survive. Infection is not apparent during these periods. In many cases, the virus begins multiplying again and in symptomatic patients, flare-ups often occur. After an initial infection with oral HSV-1, between 20-40% of patients experience recurrent flare-ups. In patients with HSV-2 genital herpes, the recurrent rate is even higher: up to 80% (Mertz, 1997). It is not completely known what triggers this renewed infection, but a number of different factors may be involved, such as sunlight, wind, fever, local physical injury, menstruation, suppression of the immune system, or emotional stress. The body does mount an immune response to HSV, and in healthy people recurring infections tend to become progressively less severe and less frequent. The immune system, however, can not eradicate the virus completely.

HSV-1 and HSV-2 represent two members of a group of at least 8 human herpes viruses, including varicella-zoster virus (VZV), Epstein-Barr virus (EBV), cytomegalovirus (CMV), human herpes virus 6 (HHV-6), human herpes virus 7 (HHV-7), and human herpes virus 8 (HHV-8). HSV particles are complex, some 120 to 200 nm in diameter with an enveloped structure and an icosahedral nucleocapsid. The genomic linear double-stranded DNA consists of approximately 125 kbps and codes for about 100 polypeptides. Whilst the functions of these encoded proteins are poorly understood, a number of them are well characterized including DNA polymerase, thymidine kinase (TK) which provides excellent targets for chemotherapy.

The management of mucocutaneous herpes infection usually involves symptomatic relief, preventing transmission, and eradication of virus by antiviral agents. Most herpes simplex infections can be managed with pain killer pills or local anesthetics for alleviation of pain, fever, and local tenderness, and for severe itching, anti-histamines may be useful.

Of the large number of agents being under development for treatment of herpes simplex virus infection, the nucleoside analogs are apparently effective. However, the ever increasing resistance of HSV to the current nucleoside analogs antiviral agents have been described (Kost et al., 1993; Fife et al., 1994; Pottage and Kessler, 1995), leading to the need for developing novel antiviral prototype molecules. As a part of our screening program to investigate the anti-HSV activity from natural products, we have explored that the galactosyl diglycerides isolated from *Clinacanthus nutans* leaves, exhibited promising anti-HSV activity (Satakhun, 2001). However, these natural glycoglycerolipids were found in a small amount and the isolation and purification process of these compounds is the main obstacle to their anti-HSV study. This prompted us to synthesize and study the structure activity relationships of these compounds on anti-HSV activity. In this research, the effect of fatty acyl moieties, sugar moiety and the stereochemistry at C-2 of glycerol backbone on anti-HSV activity would be investigated. In order to study the effect of fatty acyl moieties on anti-HSV activity, a series of the designed 1,2-di-*O*-acyl-3-*O*-β-D-glucopyranosyl-*rac*-glycerols bearing various chain length of either saturated or

unsaturated fatty acids were synthesized. The chemical structures and synthetic approach of these compounds are shown in Table 1 and Scheme 1, respectively.

Table 1. Chemical structures of 1,2-di-*O*-acyl-3-*O*-β-D-glucopyranosyl-*rac*-glycerols and derivatives.

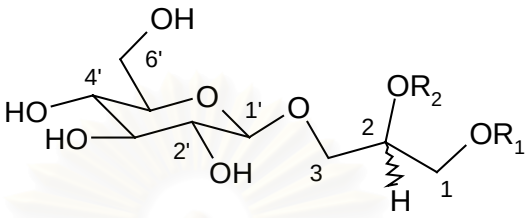

Compounds	R_1	R_2	Compounds	R_1	R_2
6a	caproyl (C10:0)	caproyl	**6k**	lauroyl	oleoyl
6b	lauroyl (C12:0)	lauroyl	**6l**	stearoyl	lauroyl
6c	myristoyl (C14:0)	myristoyl	**6m**	stearoyl	behenoyl
6d	palmitoyl (C16:0)	palmitoyl	**6n**	behenoyl	lauroyl
6e	stearoyl (C18:0)	stearoyl	**6o**	behenoyl	oleoyl
6f	behenoyl (C22:0)	behenoyl	**6p**	α-linolenoyl	linoleoyl
6g	oleoyl (C18:1)	oleoyl	**6q**	benzoyl	lauroyl
6h	linoleoyl (C18:2)	linoleoyl	**8a**	lauroyl	H
6i	α-linolenoyl (C18:3)	α-linolenoyl	**8b**	α-linolenoyl	H
6j	benzoyl	benzoyl			

Scheme 1. Synthesis of 1,2-di-*O*-acyl-3-*O*-β-D-glycopyranosyl-*rac*-glycerols and related derivatives.

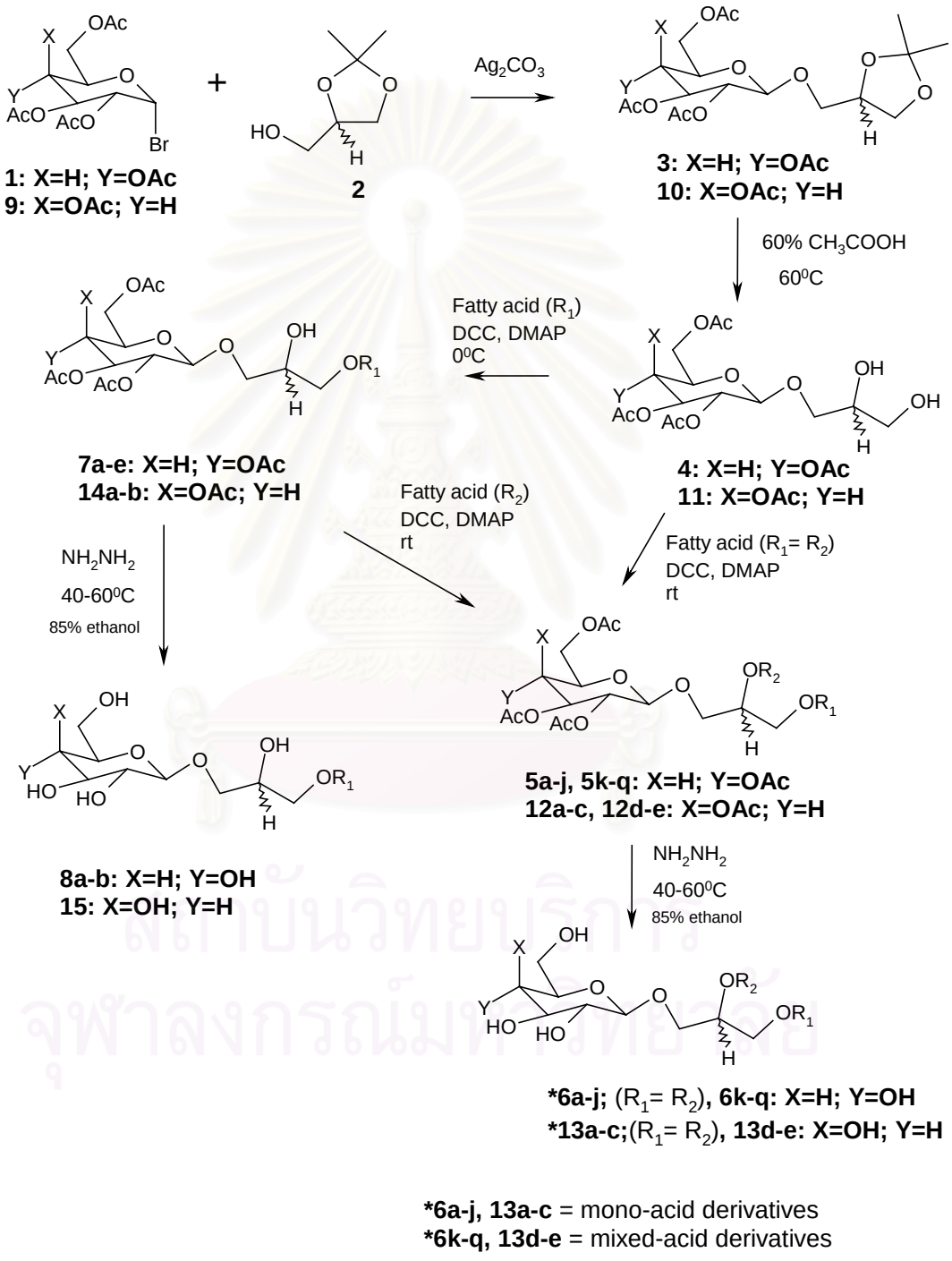

***6a-j, 13a-c** = mono-acid derivatives
***6k-q, 13d-e** = mixed-acid derivatives

To investigate the effect of sugar moiety on anti-HSV activity, the designed 1,2-di-*O*-acyl-3-*O*-β-D-galactopyranosyl-*rac*-glycerols, mono- and diacyl glycerols were synthesized and evaluated for activity. The chemical structures and synthetic approach of these compounds are outlined in Table 2 and Schemes 1-3, respectively.

Table 2. Chemical structures of 1,2-di-*O*-acyl-3-*O*-β-D-galactopyranosyl-*rac*-glycerols and related derivatives.

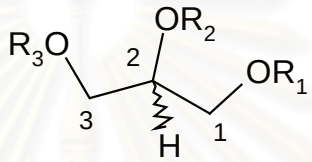

Compounds	**R_1**	**R_2**	**R_3**
13a	lauroyl	lauroyl	galactosyl
13b	linoleoyl	linoleoyl	galactosyl
13c	α-linolenoyl	α-linolenoyl	galactosyl
13d	behenoyl	lauroyl	galactosyl
13e	α-linolenoyl	linoleoyl	galactosyl
15	α-linolenoyl	H	galactosyl
19	lauroyl	lauroyl	H
21a	lauroyl	H	H
21b	stearoyl	H	H
21c	behenoyl	H	H

Scheme 2. Synthesis of 1,2-di-*O*-acyl-glycerol (**19**).

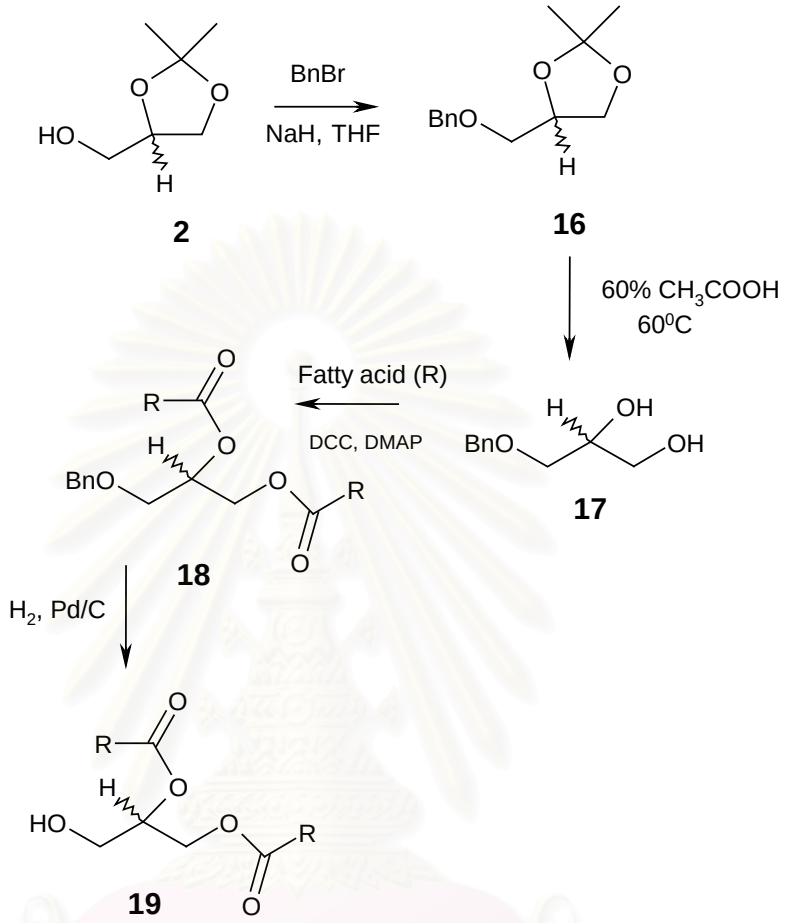

Scheme 3. Synthesis of 1-O-acyl-glycerols (**21a-c**).

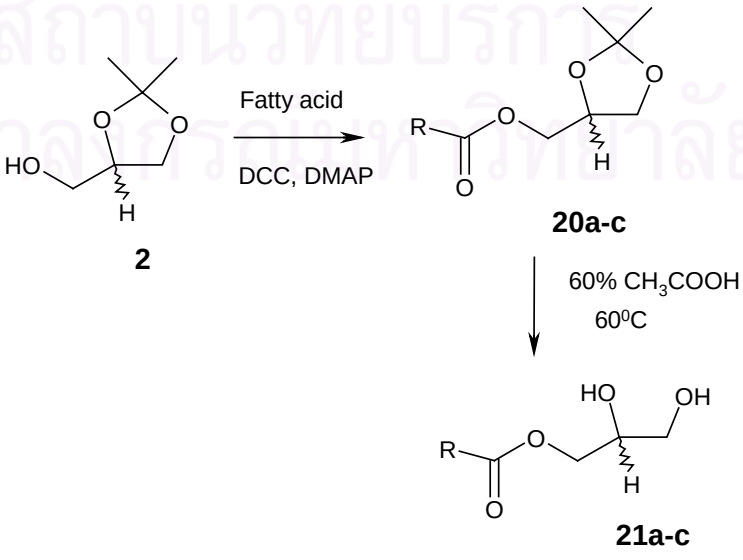

In order to determine the effect of the stereochemistry at C-2 of glycerol backbone, the selected 1,2-di- and 1-*O*-acyl-3-*O*-β-D-glycopyranosyl-*sn*-glycerols were synthesized. The chemical structures and synthetic approach are illustrated in Table 3 and Scheme 4, respectively.

Table 3. Chemical structures of 1,2-di- and 1-*O*-acyl-3-*O*-β-D-glycopyranosyl-*sn*-glycerols.

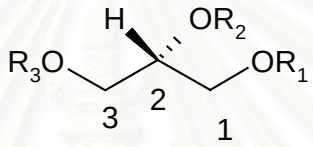

Compounds	**R_1**	**R_2**	**R_3**
32a	lauroyl	lauroyl	glucosyl
32b	α-linolenoyl	α-linolenoyl	glucosyl
32c	α-linolenoyl	lauroyl	glucosyl
34	α-linolenoyl	H	glucosyl
38	α-linolenoyl	H	galactosyl

Scheme 4. Synthesis of 1,2-di-*O*-acyl-3-*O*-β-D-glycopyranosyl-*sn*-glycerols and derivatives.

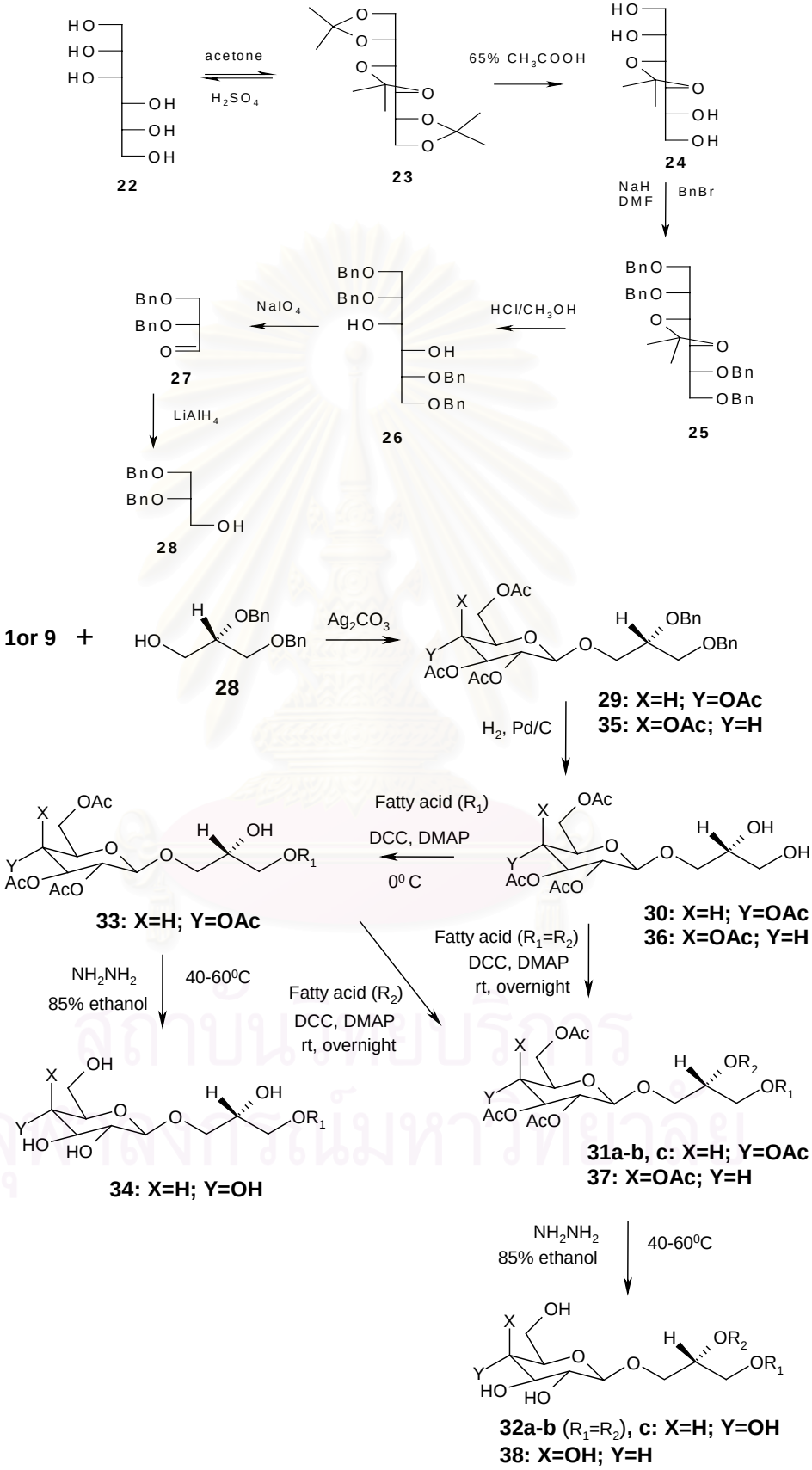

CHAPTER II
HISTORICAL

In considering the future development of antiviral agents, it is first worth reflecting on what has been achieved so far. Chemotherapy of viral infections has lagged significantly behind chemotherapy of bacterial infections. One reason for this is that viral metabolic processes resemble the host process and a virus will frequently utilize host enzymes to meet its metabolic needs. A mean of attack on the invading virus by blocking the metabolic transformation without toxicity to host is much more difficult than that of bacteria. In this chapter, the discovery and development of anti-HSV agents from natural sources and nucleoside analogs are reviewed. And also the biological activities and chemical synthetic approach to the glycoglycerolipids are concerned.

1. Anti-HSV Agents

1.1 Nucleoside Analogs as Anti-HSV Agents

For years, investigators have explored the potential of nucleoside analogs as inhibitors of viral infections, with much of the effort focused on modification of base and sugar moiety. To this time, the number of nucleoside analogs has been investigated for antiviral activity; however, few compounds have been approved for treatment of herpes simplex virus (Alrabiah and Sacks, 1996; Koszalka et al., 1998).

1.1.1 Purine Nucleoside Analogs

A major breakthrough in antiviral drug development occurred with the discovery of acyclovir (**39**). This compound is effective against both herpes simplex and varicella-zoster virus and has established an excellent safety profile in clinical practice. Acyclovir has profound effects on the viral DNA polymerase function through obligatory chain termination and competitive inhibition, acting as its triphosphate form. It is a substrate for viral thymidine kinase, but not for any host kinases, which accounts for overall selectivity, as the drug can only be phosphorylated to its active form in infected cell. Despite its potency and safety, it has several clinical limitations, including poor oral absorption (bioavailability is only 15 to 30%

after oral administration (de Miranda and Blum, 1983). However, this drawback has been overcome by the use of prodrugs. The L-valyl ester of acyclovir, valaciclovir (**40**) was found to have improved 3-5 fold greater bioavailability (Beauchamp et al., 1992; Weller et al., 1993). Ganciclovir (**41**), an analog of acyclovir, differs structurally from acyclovir by addition of a 3′ hydroxymethylene on the acyclic chain, also has activity against HSV-1, HSV-2 and cytomegalovirus. However, due to the extra functionality, it is not necessarily a chain terminator, so its antiviral effect must be somewhat different from that of acyclovir. Penciclovir (**42**), like acyclovir and ganciclovir, is an acyclic guanosine analog having an antiviral spectrum against herpes viruses similar to that of acyclovir (Boyd et al., 1987). This compound may be considered to be structurally related to ganciclovir. The active form, penciclovir triphosphate, inhibits the viral DNA polymerase through competition with deoxyguanosine triphosphate and is incorporated into the viral DNA. As penciclovir has two hydroxyl groups on the acyclic chain, it can be incorporated into the growing DNA chain and does allow limited chain elongation. Although active intravenously, penciclovir is very poorly absorbed orally. Famciclovir (**43**), the diacetyl ester of 6-deoxy penciclovir, is the orally active form of penciclovir. Following oral administration, famciclovir is rapidly absorbed and converted to penciclovir with bioavailability about 77% (Pue and Benet, 1993). Lobucavir (**44**) is another deoxyguanosine analog having antiviral activity against HSV-1, HSV-2 and CMV similar to that of ganciclovir. Lobucavir is phosphorelated to the active triphosphate form by TK which is believed to act as a nonobligate DNA chain terminator (Bisacchi et al., 1991). Adefovir (**45**) or PMEA (9-(2-(phosphonomethoxy)ethyl)adenine), a nucleotide analog, effectively inhibits a wide range of DNA viruses. One major problem often encountered in the use of nucleotide analogs as potential therapeutic viral infection is one of low lipophilicity. Dipivoxil and butenolide ester exhibited higher lipophilicity and water solubility as compared to adefovir, were reported to be more potent than adefovir *in vivo* (Hakimelahi et al., 2001)

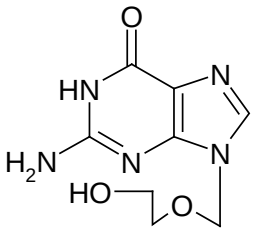

acyclovir (**39**)

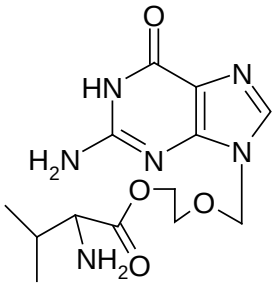

valaciclovir (**40**)

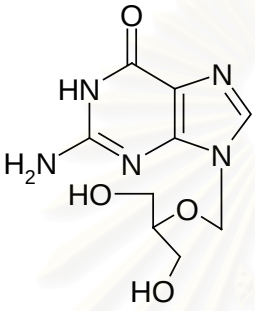

ganciclovir (**41**)

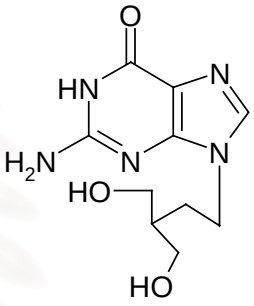

penciclovir (**42**)

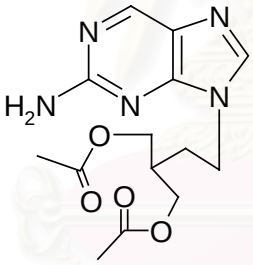

famciclovir (**43**)

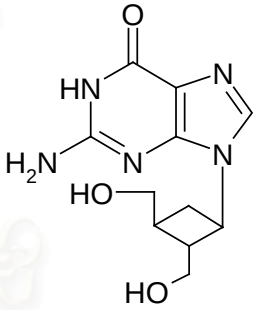

lobucavir (**44**)

adefovir (**45**)

Figure 1. Purine nucleoside analogs as anti-HSV agents.

1.1.2 Pyrimidine Nucleoside Analogs as Anti-HSV Agents

Idoxuridine (**46**) and trifluorothymidine (**47**) are examples of older, non selective thymidine analogs. The clinical usage of these two compounds is limited to topical formulations because of adverse effects. These compounds are phosphorylated by the viral kinases, however, they are also phosphorylated in uninfected cells by host kinases and are substrates for human DNA polymerase, which limit their selectivity. Sorivudine (**48**) is a synthetic arabinosyluracil analog which is taken up by HSV- and VZV-infected cells, and is only phosphorylated by viral TK. Thus, phosphorylation does not occur in uninfected cells and the active sorivudine triphosphate does not act as a chain terminator, but as an inhibitor of virus-encoded DNA polymerase (Machida et al., 1981). Brivudine (**49**), chemically closely related to sorivudine, is characterized by the presence of the (E)-5-(2-bromovinyl) substituent in the 5-position of uracil. Oral bioavailability of brivudine is greater than that of sorivudine, however, it demonstrates an antiviral activity similar to that of sorivudine. Both compounds interfere with the degradation of 5-fluorouracil by blocking the dihydropyrimidine dehydrogenase. Thus, they should not be administered to patients receiving 5-fluorouracil therapy. Cidofovir (**50**) (or HPMPC) belongs to the acyclic nucleotide analogs as a potent broad-spectrum antiviral agent, with activity against a wide variety of DNA viruses, such as HSV-1, HSV-2, TK-negative HSV-1, VZV, CMV, EBV and HPV (DeClerq et al., 1986). Unlike acyclovir or other nucleoside analogs, which require intracellular activation by viral kinase, cidofovir is already a nucleotide which is converted to the active compound, independently of virus infection. Cidofovir inhibits HSV-1 and HSV-2 DNA polymerases at concentrations 50-to 600-fold lower than those needed to inhibit human DNA polymerases (DeClerq et al., 1991)

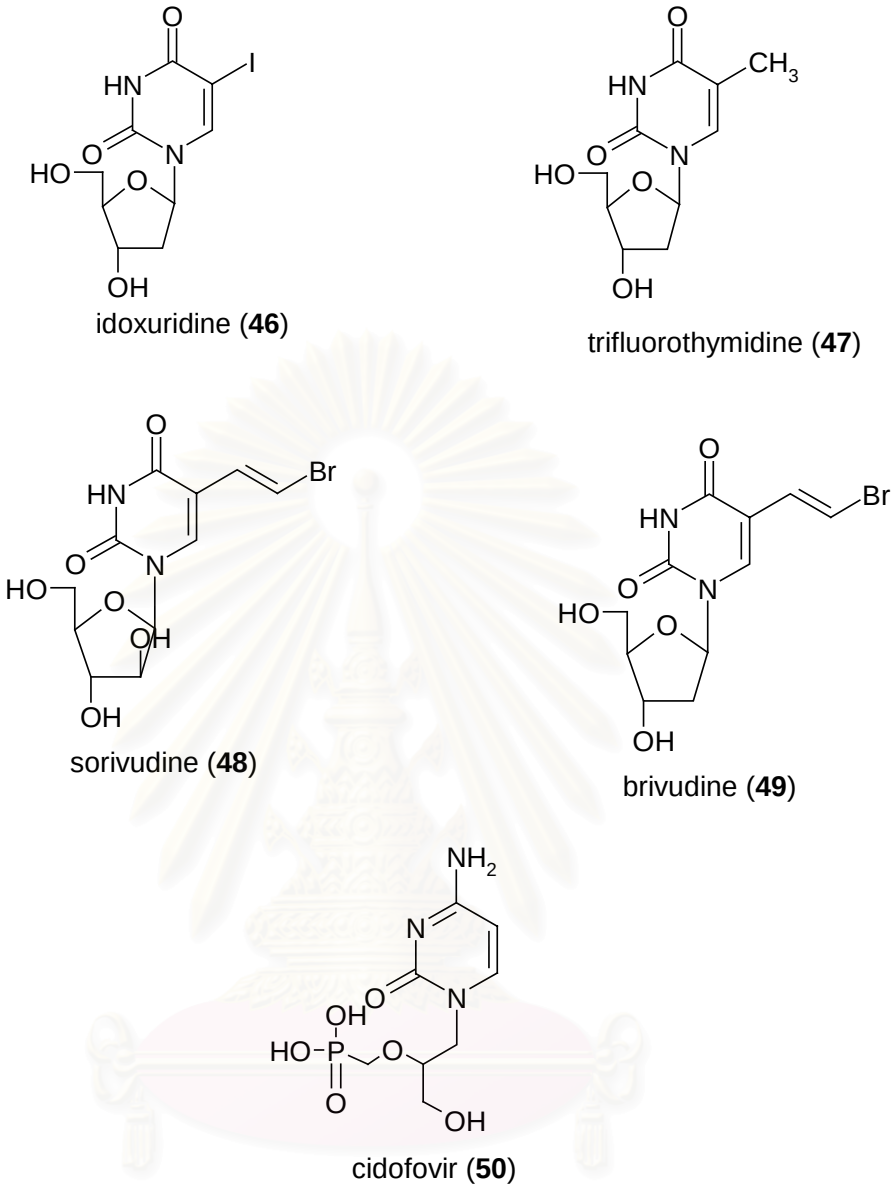

Figure 2. Pyrimidine nucleoside analogs as anti-HSV agents.

1.2 Other Synthetic Non-nucleoside Anti-HSV Agents

1.2.1 Pyrophosphate Analogs

Pyrophosphate analogs might also be thought of as fragmentary nucleotides, with only the oligophosphate moiety mimicked. The earliest pyrophosphate analog found to possess antiviral activity was phosphonoacetic acid (PAA) (**51**).

Phosphonate analogs of pyrophosphate, which contain P-C bonds instead of labile P-O bonds are much more resistant to enzymatic hydrolysis. They act by blocking phosphate binding site with pyrophosphate isosteres preventing nucleic acid synthesis. Such compounds have advantage of not requiring any activation and they often show broad spectrum of activity, though these are compromised by poor selectivity. Foscarnet (phosphonoformic acid) (**52**), the other pyrophosphate antagonist, exhibits broad activity against DNA and RNA viruses (Helgstrand et al., 1978). As it does not require any previous metabolic activation to inhibit the viral replication, it is active against thymidine kinase-deficient HSV and VZV strains. However, this drug is relatively toxic causing acute renal failure, gastro-intestinal symptoms limiting widespread use. Foscarnet is approved for use in treatment of acyclovir-resistant herpes virus infection.

phosphonoacetic acid (**51**) foscarnet (**52**)

Figure 3. Pyrophosphate analogs as anti-HSV agents.

1.2.2 Ribonucleoside Reductase Inhibitors

Herpes simplex viruses are known to induce virus specific ribonucleoside reductase (RR) in infected cells. This enzyme catalyses the reduction of ribonucleosides to 2′-deoxyribonucleosides, essential for the formation of new copies of viral DNA. Thus, RR is considered as a possible target for development of antiviral agents (Nutter et al., 1985). BILD 1263 (**53**) and BILD 1633 SE (**54**) were reported as novel peptidomimetic inhibitors of HSV ribonucleoside reductase in animal models (Duan et al., 1998).

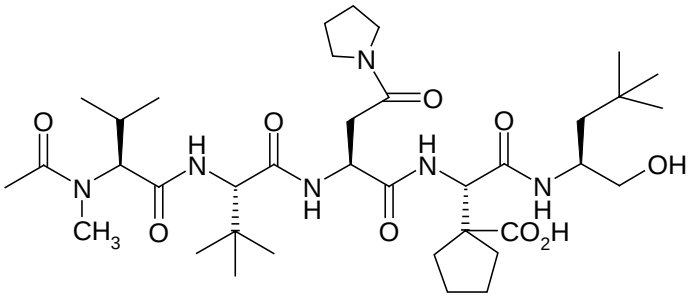

BILD 1263 (**53**)

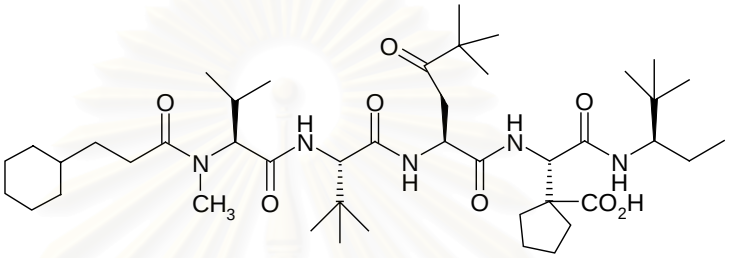

BILD 1633 SE (**54**)

Figure 4. Ribonucleoside reductase inhibitors as anti-HSV agents.

1.2.3 Fatty Alcohol

n-Docosanol, also known as behenyl alcohol, is a 22-carbon fatty alcohol produced by high-pressure, catalytic hydrogenation of a mixture of fatty acids. *In vitro* studies have demonstrated that this compound exhibits broad spectrum antiviral activity against several lipid-enveloped viruses including HSV-1 and HSV-2 (Katz et al., 1991). n-Docosanol is believed to interfere viral entry into host cells, possibly by inhibition of the fusion of viral particles with cell membranes. n-Docosanol is being developed as a 10% topical antiviral cream for treatment of recurrent herpes labialis.

1.3 Natural Products as Anti-HSV Agents

Apart from synthetic nucleoside analogs, natural products are potential sources for anti-HSV agents. Many research approachs are currently aimed at developing novel prototype molecules of antiviral agents. Natural products are increasingly appreciated as leads for drug discovery and development. A number of reports concerning the antiviral constituents of plants have appeared, and several bioactive constituents showing anti-HSV activity have been isolated. These included flavonoids, terpenoids, alkaloids, steroids, and glycolipids.

Flavonoids

Robustaflavone (**55**) a biflavonoid, isolated from *Rhus succedanea* exhibited moderately anti-HSV-1 and HSV-2 activities with EC_{50} values of 8.6 μg/ml and 8.5 μg/ml, respectively (Lin et al., 1999). Isoquercitrin (**56**) isolated from *Waldsteinia fragarioides* Tratt. showed antiviral activity against HSV-1 with EC_{50} value of 40 μg/ml (Abou-Karam et al., 1992). Galangin (**57**) from *Helichrysum aureanitens* Sch. Bip. a medicinal plant of south Africa displayed anti-HSV-1 at concentration 12-47 μg/ml (Meyer et al., 1997). Hayashi et al. (1992) found that ginkgetin (**58**) isolated from *Cephalotaxus drupacea* Sieb.& Zucc. exhibited potent anti-HSV-1 and HSV-2 activities with EC_{50} values of 0.76 and 0.83 μg/ml, respectively. (-)-Epigallocatechin-3-0-gallate (**59**) and samarangenin B (**60**) isolated from the root of *Limonium sinense* (Girard) Ktzc exhibited inhibitory activity in HSV-1 replication with IC_{50} values of 38.6 and 11.4 μM, respectively (Lin et al., 2000).

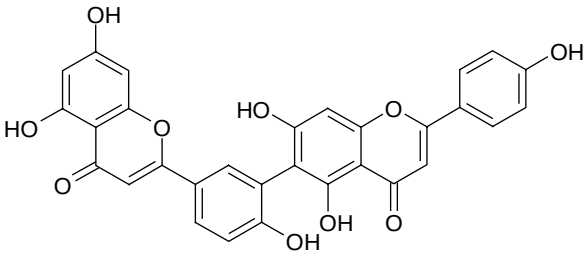

robustaflavone (**55**)

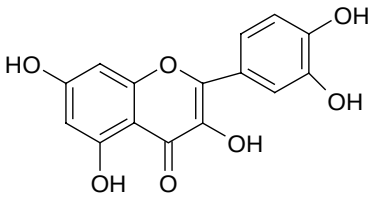

isoquercitrin (**56**)

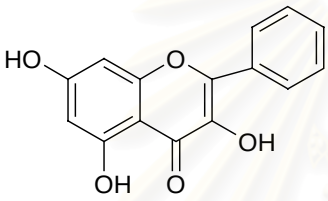

galangin (**57**)

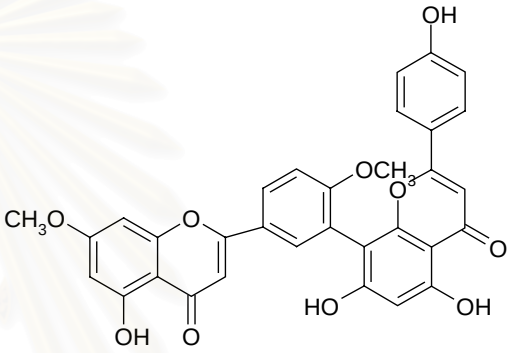

ginkgetin (**58**)

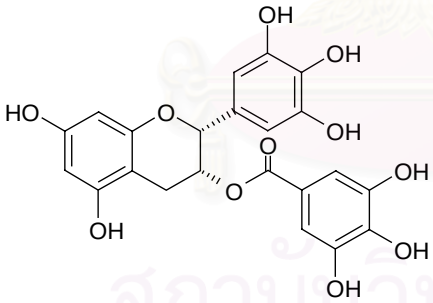

(-)-epigallocatechin 3-O-gallate (**59**)

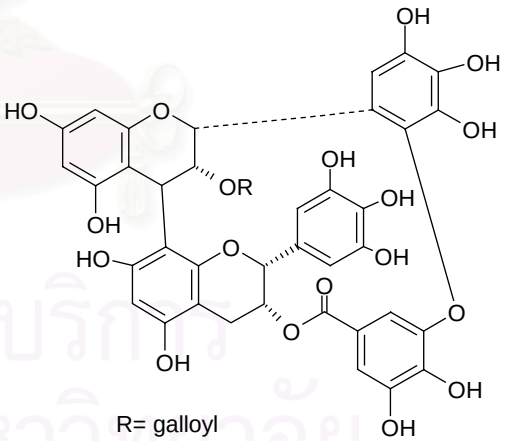

R= galloyl

samarangenin B (**60**)

Figure 5. Flavonoids as anti-HSV agents.

Terpenoids

Sclerocarpic acid (**61**), a sesquiterpene, isolated from the stem bark of *Glyptopetalum sclerocarpum* Laws displayed anti-HSV-1 and HSV-2, with the concentrations required for 50% inhibition of plaque formation (EC_{50}) of 5 and 12.5 μg/ml, respectively (Sotanaphun et al., 1999). Other terpenoids were reported as having anti-HSV activity such as scopadulcic acid B (**62**) (Hayashi et al., 1990), dehydrosoyasaponin I (**63**) (Kinjo et al., 2000) and euphosalicin (**64**) (Mucsi et al., 2001).

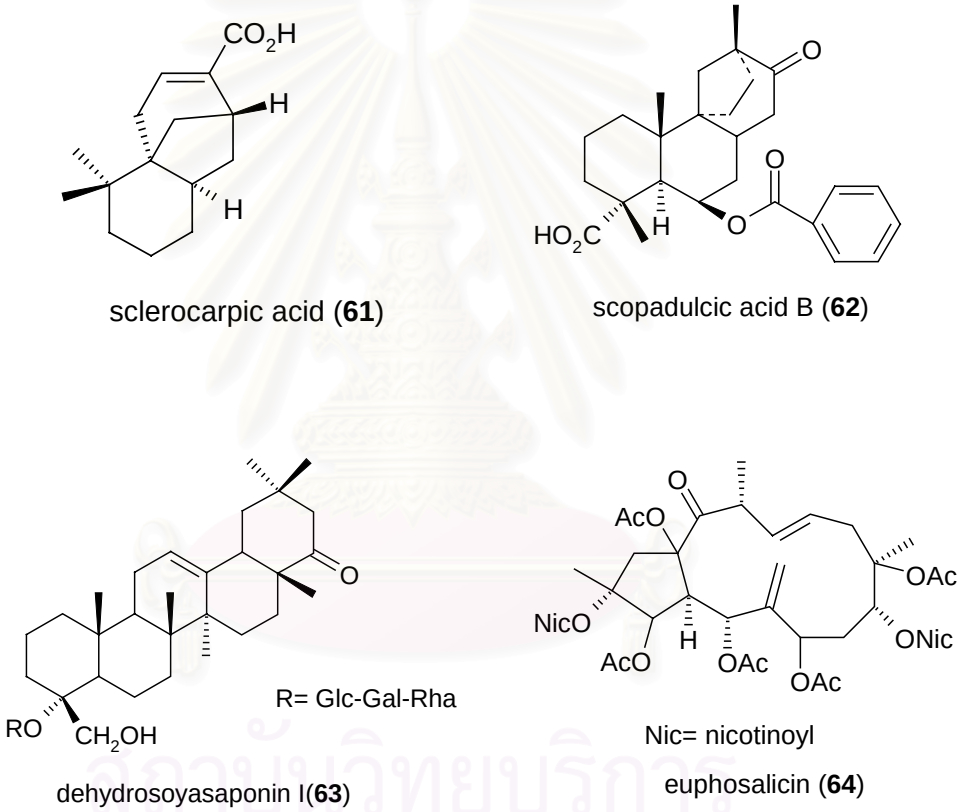

Figure 6. Terpenoids as anti-HSV agents.

Alkaloids

(-)-Norcycleanine (**65**), a bisbenzylisoquinoline isolated from the root of *Stephania cepharantha* displayed anti-HSV-1 and HSV-2 with ED_{50} values of 18.1

and 23.1 μg/ml, respectively. FK-3000 (**66**), a morphinan alkaloid, from the same plant showed potent anti-HSV-1 and HSV-2 with ED_{50} values of 7.8 and 8.7 μg/ml, respectively (Nawawi et al., 1999).

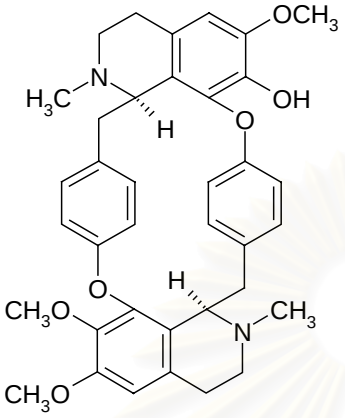

(-)-norcycleanine (**65**)

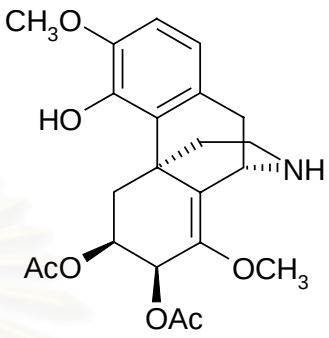

FK-3000 (**66**)

Figure 7. Alkaloids as anti-HSV agents.

Steroid glycosides

Ikeda et al. (2000) reported that steroid glycosides isolated from *Solanum muricatum* showed anti-HSV activity, and β-solamarine (**67**) exhibited the most potent anti-HSV-1 with ED_{50} value of 0.90 μg/ml.

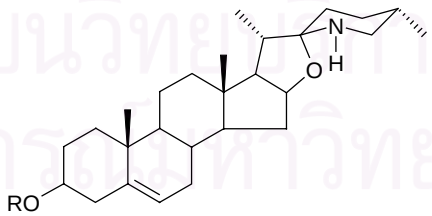

R= -Glc-Rha
Rha

beta-solamarine (**67**)

Figure 8. Steroid glycoside as anti-HSV agent.

Glycolipids

As part of our search for active anti-HSV constituents from *Clinacanthus nutans* (Burm.f.) leaves, a well-known Thai medicinal plant promoted for the treatment of herpes simplex, we found that glycoglycerolipids (**68**) showed 95% inhibition to HSV-1 and HSV-2 at equal concentration of 50 μg/ml. To continue our efforts to study the structure-activity relationships of this new class of anti-HSV agents, we synthesized and evaluated the anti-HSV activity of these compounds as described in this following research.

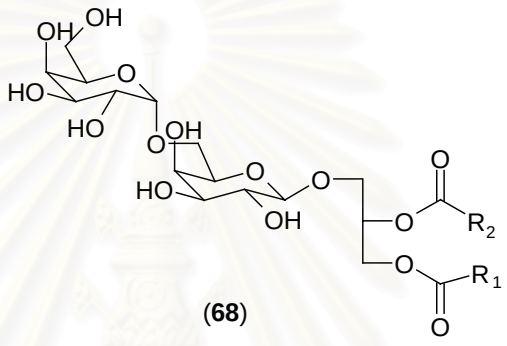

(**68**)

R_1=hexadecanoyl; R_2=hexadecatrienoyl

Figure 9. Glycoglycerolipid as anti-HSV agent.

2. Glycoglycerolipids

Glycolipid designates any compound containing one or more monosaccharide residues bound by a glycosidic linkage to a hydrophobic moiety such as an acylglycerol, a sphingoid, a ceramide or prenols. Glycolipids are a structurally heterogeneous group of membrane components found in all species ranging from bacteria to man, which can be divided, roughly, into two groups, i.e. glycoglycerolipids and glycosphingolipids. Herein, only glycoglycerolipids will be focused on.

The term glycoglycerolipids are used to designate glycolipids containing one or more glycerol residues. They are especially important in higher plants, algae and bacteria where they are located in photosynthetic membranes, they are also found in animals but in lesser amounts. In plants, mono- and digalactosyl diglycerides are

major components of the stacked thylakoid membranes of chloroplasts, while tri- and tetragalactosyl diglycerides or acyl galactosyl diglycerides may be present in much smaller amounts. Sulfoquinovosyl diglyceride, found in all photosynthetic plants, algae, and bacteria, is another glycosyl diglyceride but the sugar in this case is 6-deoxyglucose (quinovose) containing a sulfonic acid group at position 6. In bacteria and algae, a large number of glycoglycerolipids containing a wide variety of sugar combinations including glucose, galactose, mannose, rhamnose, gluconic acid and glucosamine have been reported (Kopitz, 1991).

2.1 Biological activities of glycoglycerolipids

Although various glycoglycerolipids have been isolated and characterized, the biological functions of these compounds have not fully elucidated (Kopitz, 1991). Several glycoglycerolipids were reported to possess various biological activities e.g., antitumor-promoting activity (Baruah et al., 1983; Murakami et al., 1995; Shirahashi et al., 1996; Colombo et al., 1998; Colombo et al., 1999), oxygen scavenging activity (Nakata, 2000), anti-HIV activity (Loya et al., 1998; Ohta et al., 1998), and anti-HSV activity (Satakhun, 2001).

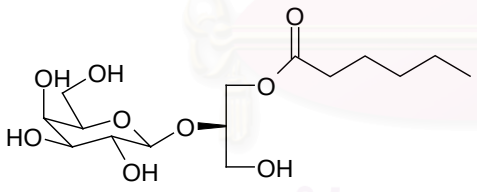

antitumor promotor (**69**)

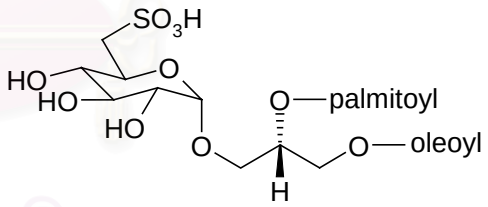

anti-HIV sulfolipid (**71**)

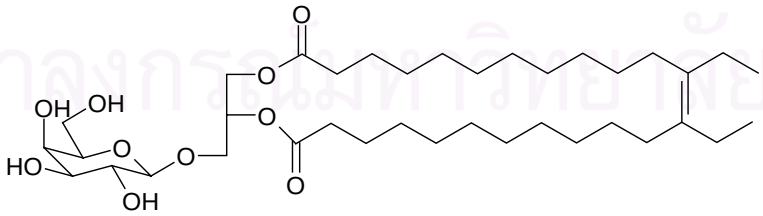

oxygen scavenger (**70**)

Figure 10. Chemical structures and bioactivities of some glycoglycerolipids.

2.2 Chemical synthetic strategies of glycoglycerolipids

Glycoglycerolipids constitute from polyhydroxyl sugars glycosidic linked with glycerol and hydrophobic fatty acids. A versatile method for glycosylation involves a two-step procedure. The first step, activation of the anomeric center provides the glycosyl donor. The second step, the glycosyl transfer to the acceptor provides the glycoside. To achieve this synthesis, the suitable protection of hydroxyl groups not involved in the glycoside bond formation and glycosyl donor must be designed (Gigg, 1980). The commonly used hydroxyl group protection and glycosyl donors are reviewed as following (Greene and Wuts, 1991; Toshima and Tatsuta, 1993).

2.2.1 Hydroxyl group protection

The considerable effort has been directed towards the development of effective hydroxyl protecting groups. In general, hydroxyl functionality is most frequently protected by conversion into esters, ethers, acetals or ketals.

Esters:

Acetates and benzoates are usually used to protect hydroxyl compounds, especially, carbohydrates. Regioselective esterification is possible, primary hydroxyl groups react more rapidly than secondary ones while tertiary hydroxyl groups tend to be unreactive groups. Several factors influence the selective removal of ester groups, including ester types, steric hindrance, strength of deprotecting reagents, etc. For instance, chloroacetyl protection can be removed in the presence of acetyl and benzoyl groups by treatment with thiourea. Hydrazine selectively deprotects *O*-1 acetyl group in 1,2,3-tri-*O*-acetyl-4,6-di-*O*-benzyl-α-D-galactose without reaction at *O*-2 or *O*-3

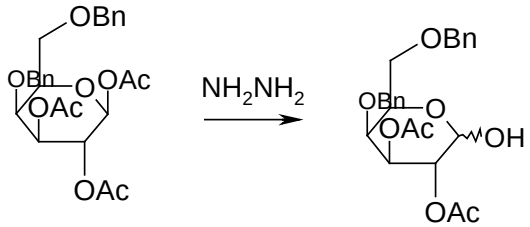

Figure 11. Selective deprotection of *O*-1 acetyl group by hydrazine.

Ethers:

Several simple and substituted alkyl, benzyl, silyl, and trityl ether protecting groups have been developed. They are formed and removal under a wide variety of conditions. Among common protecting groups, the benzyl ether holds a position of considerable importance. It is stable over a broader range of conditions, including both acidic and basic media, than any other common protecting groups. Deprotection of benzyl ethers, is always accomplished by catalytic hydrogenolysis under mild conditions. Trialkyl silyl ether protecting groups are stable under neural and basic conditions but undergo hydrolysis in the presence of aqueous acids. Regioselectivity in silylation can be achieved by using hindered silylating agents such as tri-isopropyl chlorosilane (TIPSCl), t-butyl chlorodimethylsilane (TBDMSCl). An effective method for desilylation has been accomplished by treatment with tetrabutyl ammonium fluoride under various conditions. Trityl ether protecting groups are used as the regioselective protection of primary hydroxyl groups in the presence of secondary and tertiary ones. Trityl ethers are readily deprotected by several acids conditions.

Acetals and ketals:

The acyclic and cyclic acetals or ketals are useful protecting groups. These could be introduced by treating the carbonyl with an alcohol or diol. Cyclic and acyclic acetals and ketals are stable to aqueous and non aqueous bases, hydride reduction, including organometallic reagents. They are also stable to most oxidants, but readily cleaved by acid hydrolysis. Isopropylidene ketals and benzylidene acetals are the common protecting groups often introduced into a molecule under similar reaction condition, however, benzylidene groups prefer to be part of six-membered ring acetals, while isopropylidene groups generally are five-membered ring ketals. Both benzylidene and isopropylidene groups can be removed by aqueous acids. In addition, partial deprotection of benzylidene acetals can be achieved by reductive cleavage with metal hydride (Binkley, 1988).

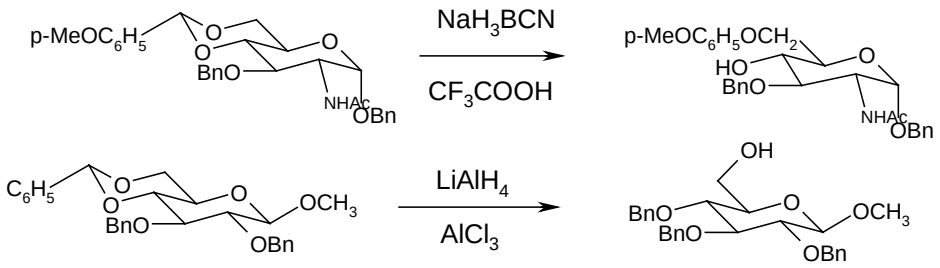

Figure 12. Partial deprotection of benzylidene acetal by metal hydride reduction.

2.2.2 Glycosylation

Glycosylation or glycosidic bond formation, is a crucial synthetic organic methodology to attach sugar to the other molecules, the efficiency of the glycosylation reaction generally involves a high chemical yield, regioselectivity, and stereoselectivity. The type of glycosyl donor and the hydroxyl group next to the anomeric center exert strong influence on the anomeric stereocontrol. Successful glycosylation can be achieved by the requirement of suitable group protecting strategies and glycosyl donors (Kochetkov et al., 1967; Paulsen, 1982; Schmidt, 1986; Schmidt, 1989). The type of glycosyl donor is decisive step in the chemical method for glycosylation. Several glycosyl donors have been developed and some are classified as following (Schmidt, 1989; Toshima and Tatsuta, 1993; Schmidt, 1997).

Glycosyl halides:

The use of glycosyl bromide or chloride as an effective glycosyl donor in glycosylation reaction was first introduced by Koenigs and Knorr in 1901 (Koenigs and Knorr, 1901; Wallace and Schroeder, 1976). Glycosyl halides formation is carried out with typical halogenation reaction and the α-anomers are mainly obtained. The stability and the reactivity of glycosyl halides are highly dependent on the halogen, the sugar residue and the protecting groups. For instance, the thermal stability of glycosyl halides increases from bromide to chloride. However, reactivity increases in reverse order compared with stability. For the glycosylation reaction, at least equimolar amounts of a “promoter” are required. Various silver and mercury salts have been used as promoters. The order of reactivity of some representative promoters is $AgOTf/Ag_2CO_3$ > $AgClO_4$ > $Hg(CN)_2/HgBr_2$ > $Hg(CN)_2$ (Binkley, 1988). Further, Ag_2CO_3, Ag_2O, HgO are used as acid scavengers and water is usually

removed by Drierite or molecular sieves. On the other hand, several Lewis acids such as $SnCl_4$, TrCl-$ZnCl_2$ and phase transfer catalysts such as $Bu_4N^+Br^-$ have been used as promoters (Toshima and Tatsuta, 1993). Solvents of low donicity are commonly used, which favor S_N-2 type reaction. Glycosyl fluoride has been investigated for glycoside synthesis. Although the higher stability towards many reagents and temperature compared with other halides, appropriated fluorophilic promoters limit the use of this glycosyl donor.

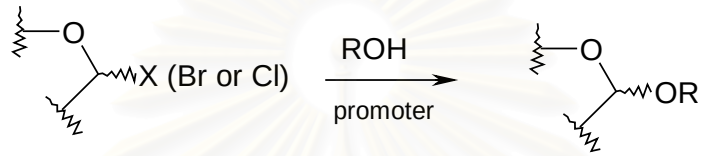

promoters: silver or mercury salts, Lewis acids, phase-transfer catalysts
drying agents: Drierite, molecular sieves

Figure 13. Glycosylation of glycosyl halide.

Thioglycosides:

Thioglycosides have been extensively studied as useful glycosyl donors due to their high stability in many organic operations. Several kinds of alkyl- and arylthio groups were developed with their appropriate promoters (Toshima and Tatsuta, 1993). However, thioglycosides require at least equimolar amounts of the promoters, which can lead to undesired side reactions.

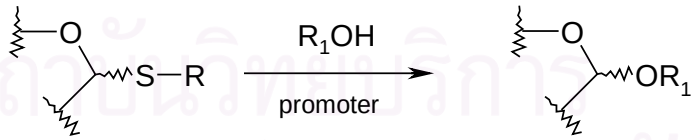

promoters: silver or mercury salts, NIS, NBS,etc.

Figure 14. Glycosylation of thioglycoside.

Trichloroimidates:

Trichloroimidate-mediated glycosylation appears to be one of the most ideal glycosylation method. The thermally and chemically stable trichloroimidate glycosyl donor has been synthesized from the corresponding 1-hydroxyl sugar by treatment of trichloroacetonitrile in the presence of a base such as K_2CO_3, NaH, or 1,8-diazabicyclo(5.4.0)undec-7-ene (DBU). The glycosylation reaction is promoted by only 0.005-0.02 equivalents of an acid catalyst under wide range of temperature. The most frequently employed catalysts are trimethylsilyl trifluoromethane sulfonate (TMSOTf), AgOTf, $Sn(OTf)_2$. Anomeric form of glycosyl trichloroimidate and neighboring group participation are crucial for the anomer stereocontrol. When non-participating protecting group are selected, α-trichloroimidates yield β-glycosides and β-trichloroimidates yield α-glycosides (Schmidt and Micheal, 1984).

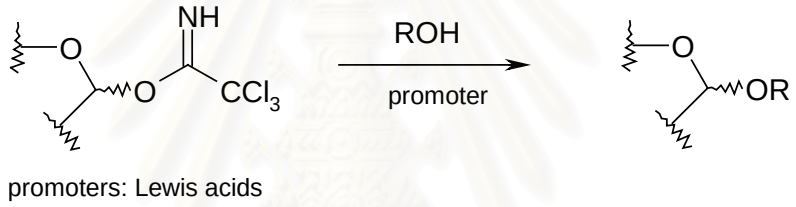

Figure 15. Glycosylation of trichloroimidate.

Glycals:

Glycal is a versatile synthetic intermediate in the synthesis of 2-deoxy glycoside. The reaction of glycal and alcohol in the presence of I_2, NBS, iodinium dicollidine perchlorate (IDCP) gives 2-deoxy-2-halo-glycoside which is subsequently converted into the desired 2-deoxy-glycoside by reductive dehalogenation.

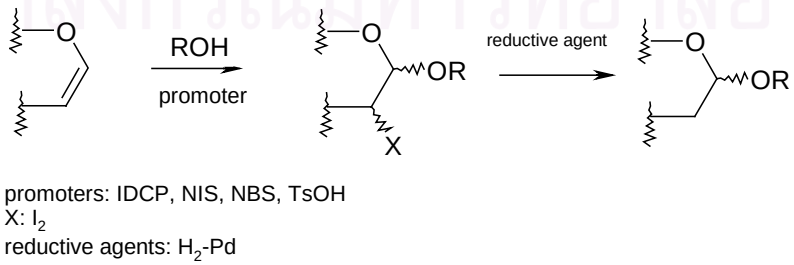

Figure 16. Glycosylation of glycal.

1,2-anhydro sugars:

The formation of 1,2-anhydro (1,2-epoxide) sugars start from the glycal as precursors for the individual sugars; therefore, stereocontrol is required not only at C-1 but also at C-2 in product formation. Generally, the anhydro sugar is smoothly coupled with alcohol in the presence of $ZnCl_2$ to exclusively give the 1,2-trans-glycoside.

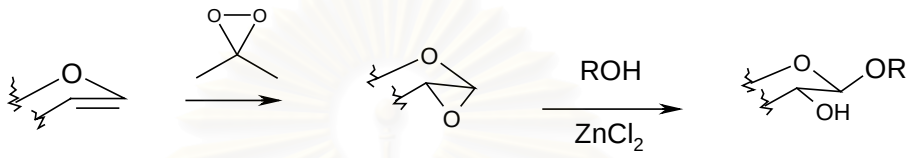

Figure 17. Glycosylation of 1,2-anhydro sugar.

4-pentyl glycosides:

In general, 4-pentyl glycosides are prepared as a mixture of α- and β-anomers by the reaction of 1-hydroxyl sugars and 4-pentyl alcohol in the presence of acid catalyst. Usually, the glycosylation reactions could be promoted by at least equimolar amounts of IDCP, NIS/TfOH or TESOTf

Figure 18. Glycosylation of 4-pentyl glycoside.

CHAPTER III
EXPERIMENTAL

1. Instruments

1. Bruker AVANCE DPX-300 FT-NMR spectrometer
2. Infrared spectrophotometer: Perkin Elmer model 2000
3. Polarimeter: Perkin Elmer 341
4. CHNS/O Analyser: Perkin Elmer PE 2400 Series II
5. HR-FAB mass spectrometer JEOL JMS-700
6. Transmission electron microscope JEOL JEM 200CX

2. Chemicals

Acetic acid	Merck
Acetobromo-α-D-galactose	Fluka
Acetobromo-α-D-glucose	Fluka
Acetone	Merck
Behenic acid	Fluka
Benzoic acid	Merck
Benzyl bromide	Fluka
Calcium hydride	Fluka
Caproic acid	Fluka

Dicyclohexyl carbodiimide (DCC)	Fluka
4-Dimethyl aminopyridine (DMAP)	Fluka
Drierite	Fluka
Hydrazine monohydrate	Sigma
Hydrochloric acid, concentrated	Merck
DL-α,β-Isopropylidene glycerol	Fluka
Iodine	Fluka
Lauric acid	Fluka
Linoleic acid	Fluka
α-Linolenic acid	Sigma
Lithium aluminium hydride	Fluka
D-Mannitol	Fluka
Myristic acid	Fluka
Potassium dichromate	Fluka
Oleic acid	Fluka
10% Palladium on activated charcoal	Merck
Palmitic acid	Fluka
Silver carbonate	Sigma
Sodium carbonate	Merck
Sodium hydride	Fluka
Sodium (meta) periodate	Fluka

Sodium sulfate, anhydrous	Merck
Stearic acid	Fluka
Sulfuric acid concentrated	Merck
Tetrabutyl ammonium bromide	Fluka

All solvents used were either analytical or laboratory grade and were redistilled prior to use. Dichloromethane was predried with calcium hydride, acetone was dried with molecular sieve type 4A, and tetrahydrofuran was refluxed and distilled from sodium. Reactions were monitored by TLC on silica gel plates, spots were visualized by spraying with 2% potassium dichromate in 30% aqueous sulfuric acid followed by heating

3. Biologicals

Cell line and medium

Vero cells, the kidney cell of African green monkey (*Cercopithecus sethiops*) were obtained from the Department of Microbiology, Faculty of Medicine, Mahidol University (Siriraj Hospital). Culture medium was consisted of Modified Eagle medium (MEM) (GIBCO, U.S.A.), 10% fetal calf serum (GIBCO, U.S.A.) and 1% of antibiotics (penicillin, streptomycin and fungizone, GIBCO, U.S.A.)

Cell line culture

The cell line was washed twice with phosphate buffer and trypsin-EDTA was added to lyse the adhesive cells from the flask. Trypsin- EDTA was then removed and the medium was added to the flask. The cells were incubated at 37^{O} C under moisture and 5% CO_2 condition (Abou-Karam and Shier, 1990; Jayawasu et al., 1992).

Herpes simplex viruses

Herpes simplex virus type 1 (HSV-1), KOS strain and herpes simplex virus type 2 (HSV-2), 186 strain were obtained from the Department of Microbiology, Faculty of Medicine, Mahidol University (Siriraj Hospital).

Viral titer was determined by plaque assay. Five-fold serial dilutions of virus, 50 μl each, were added into the wells of Vero cell monolayer containing cultures medium (in triplicate). The viruses were allowed to adsorb for 3 hours at 37^{O} C under moisture and 5% CO_2 condition, then 100 μl of the overlay medium (1% gum tragacanth) was added. The overlay medium was discarded after further incubated for 2 days and the infected cells were stained with 1% crystal violet in 10% formalin for 30 minutes, and then washed with water. Plaque was counted and expressed as plaque forming unit (PFU).

Examination of anti-HSV-1 and HSV-2 activity

Plaque reduction, inactivation assay performed in 96-well tissue culture plates. The samples were dissolved with 1% DMSO in medium (25 μl) and mixed with 30 PFU (25 μl) of viruses, then left for 1 hour at room temperature. The Vero cells suspension (50 μl/well) was added into triplicate wells. The viruses were allowed to adsorb for 3 hours at 37^{O} C under moisture and 5% CO_2 condition, then 75 μl of overlay medium (1% gum tragacanth in medium) was added. The culture was incubated for 2 days and plaques were observed and counted under inverted microscope then the infected cells were stained with 1% crystal violet in 10% formalin for 30 minutes, and washed with water. Antiviral activity was expressed as a score of % inhibition and 50% inhibitory concentration (EC_{50}). Acyclovir was used as a positive control.

Examination of HSV-particles by Transmission Electron Microscope

Transmission electron microscope was used for examining the effect of glycosyl diglycerides on herpes simplex viral particles. HSV was concentrated by ultracentrifugation at 55,000 rpm for 50 minutes, and then, the sample dissolved with 1% DMSO in medium was added with concentrated HSV to constitute 100 μg/ml, then, left for 1 h at room temperature. The mixture was applied on carbon-coated grid and negatively stained with 2% phosphotungstic acid (Thormar et al., 1987). The specimens were examined by using a JEOL JEM 200CX electron microscope.

4. Synthesis of 1,2-di-*O*-acyl-3-*O*-β-D-glycopyranosyl-*rac*-glycerols

4.1 General Procedure for Glycosylation

A mixture of D,L-α,β-isopropylideneglycerol (**2**) (2.0 mmol), Ag_2CO_3 (1.0 mmol), fine Drierite 2.5 g in 40 ml of dry dichloromethane was stirred and protected from light under a nitrogen atmosphere. After being stirred for half an hour, iodine (0.2 mmol) was added and acetobromo-α-D-glucose (**1**) (or acetobromo-α-D-galactose (**9**)) (2.0 mmol) in 10 ml dry dichloromethane was then added dropwise over a peroid of 1 h. The reaction mixture was stirred overnight at room temperature and then filtered. The residue was washed with dry dichloromethane, and the filtrate was evaporated *in vacuo* to give colorless syrupy mixture. The mixture was purified by column chromatography on silica gel, eluted with ethyl acetate: hexane (1:8) to give the 1:1 mixtures of two diastereomers **3** (or **10**).

*1,2-O-isopropylidene-3-O-(β-D-2',3',4',6'-tetra-O-acetyl-glucopyranosyl)-rac-glycerol (**3**)* (470 mg, 50.8%)

^{1}H-NMR (300 MHz, $CDCl_3$, Figure 19) δ: 1.34, 1.42 (each 2 × 3H, *s*, acetonide), 2.01, 2.03, 2.05, 2.11(each 2 × 3H, *s*, acetyl), 3.60-4.33 (2 × 8H, H_2-1, H-

2, H_2-3, H-5' and H_2-6'), 4.61 and 4.63 (each 1H, *d*, *J* = 7.6 Hz, H-1'), 5.01 and 5.03 (each 1H, *dd* (apparent *t*), *J* = 9.8 and 7.5 Hz, H-2'), 5.09 (2 × 1H, *dd* (apparent *t*), *J* = 9.8 and 9.5 Hz, H-4'), 5.22 and 5.23 (each 1H, *dd* (apparent *t*), *J* = 9.4 and 9.4 Hz, H-3').

1,2-O-isopropylidene-3-O-(β-D-2',3',4',6'-tetra-O-acetyl-galactopyranosyl)-rac-glycerol ***(10)*** (458 mg, 49.7 %)

^{1}H-NMR (300 MHz, $CDCl_3$, Figure 20) δ: 1.35, 1.43 (each 2 × 3H, *s*, acetonide), 1.96, 2.01, 2.02, 2.14 (each 2 x 3H, *s*, acetyl), 3.60-4.20 (2 × 8H, H_2-1, H-2, H_2-3, H-5' and H_2-6'), 4.48 and 4.50 (each 1H, *d*, *J* = 7.6 Hz, H-1'), 5.01 (2 × 1H, *br d*, *J* = 10.4 Hz, H-3'), 5.18 (2 × 1H, *br t*, *J* = 8.3 Hz, H-2'), 5.37 (2 × 1H, *br s*, H-4')

4.2 General Procedure for Deacetonization

A solution of **3** (or **10**) 400 mg in 20 ml of 60% acetic acid aqueous solution was stirred at 60 ^{o} C for 1.5 h. The mixture was concentrated and co-evaporated with toluene three times. Then, the residue was purified by column chromatography on silica gel column, eluted with ethyl acetate: hexane (5:1) to give semisolid substance **4** (or **11**)

1-O-(β-D-2',3',4',6'-tetra-O-acetyl-glucopyranosyl)-rac-glycerol ***(4)***
(363 mg, 100 %)

^{1}H-NMR (300 MHz, $CDCl_3$, Figure 21) δ: 2.01, 2.04, 2.06, 2.10 (each 2 × 3H, *s*, acetyl), 3.52-3.95 (2 × 6H, H_2 -1, H-2, H_2-3 and H-5'), 4.22 (2 × 2H, *br s*, H_2-6'), 4.56 (2 × 1H, *d*, *J* = 7.8 Hz, H-1'), 5.02 (2 × 1H, *dd* (apparent *t*), *J* = 9.4 and 7.5 Hz, H-2'), 5.09 (2 × 1H, *dd* (apparent *t*), *J* = 9.4 and 9.5 Hz, H-4'), 5.23 (2 × 1H, *dd* (apparent *t*), *J* = 9.4 and 9.3 Hz, H-3')

^{13}C-NMR (75 MHz, $CDCl_3$, Figure 22) δ: 61.8, 63.2 and 63.3, 68.4, 70.4, 71.2 and 71.3, 72.0, 72.5 and 72.6, 72.8, 101.3 and 101.4, 169.4, 169.5, 170.2, 170.6

^{1}H-^{1}H COSY (Figure 23)

*1-O-(β-D-2',3',4',6'-tetra-O-acetyl-galactopyranosyl)-rac-glycerol (**11**)*
(360 mg, 99 %)

^{1}H-NMR (300 MHz, $CDCl_3$, Figure 24) δ: 1.98, 2.01, 2.02, 2.13 (each 2 × 3H, *s*, acetyl), 3.53-3.96 (2 × 6H, H_2-1, H-2, H_2-3 and H-5'), 4.14 (2 × 2H, *br* s, H_2-6'), 4.48 (2 × 1H, *d*, *J* = 7.8 Hz, H-1'), 5.01 (2 × 1H, *dd*, *J* = 10.4 and 3.3 Hz, H-3'), 5.18 (2 × 1H, *dd*, *J* = 9.9 and 8.4 Hz, H-2'), 5.38 (2 × 1H, *br d*, *J* = 3.0 Hz, H-4')

4.3 General Procedure for Preparation of Mono-acid 1,2-di-*O*-acyl-3-*O*-(β-D-2',3',4',6'-tetra-*O*-acetyl-glycopyranosyl)-*rac*-glycerols

To a solution of **4** (or **11**) (0.3 mmol), fatty acid (0.7 mmol), and DMAP (0.03 mmol) in 8 ml dry dichloromethane, DCC (0.7 mmol) was added and stirred for 24 h at room temperature. The solid was filtered off and the solvent was evaporated *in vacuo*. The residue was purified by column chromatography on silica gel column, eluted with ethyl acetate: hexane (1:3) to give the products **5a-j** (or **12a-c**). All compounds were obtained as the 1:1 mixtures of two diastereomers.

*1,2-di-O-caproyl-3-O-(β-D-2',3',4',6'-tetra-O-acetyl-glucopyranosyl)-rac-glycerol (**5a**)* (198.2 mg, 90.5%)

^{1}H-NMR (300 MHz, $CDCl_3$, Figure 25) δ: 0.83 (2 × 6H, *br t*, *J* = 6.9 Hz), 1.25 (2 × 24H, *br s*), 1.59 (2 × 4H, *br*), 1.90, 1.92, 1.94, 1.98 (each 2 × 3H, *s*, acetyl), 2.26 (2 × 4H, *br t*, *J* = 6.9 Hz), 3.61-3.72 (2 × 2H, H_a-3 and H-5'), 3.89 (2 × 1H, *dd*, *J* = 10.9 and 4.9 Hz, H_b-3), 4.00-4.15 (2 × 2H, H_a-1 and H_a-6'), 4.18-4.30 (2 × 2H, H_b-1 and H_b-6'), 4.48 and 4.50 (each 1H, *d*, *J* = 7.8 Hz, H-1'), 4.95 and 4.96 (each 1H, *dd* (apparent *t*), *J* = 9.5 and 7.9 Hz, H-2'), 5.04 (2 × 1H, *dd* (apparent *t*), *J* = 9.5 Hz, H-4'), 5.10-5.21 (2 × 2H, H-2 and H-3')

^{13}C-NMR (75 MHz, $CDCl_3$, Figure 26) δ: 14.6, 21.1, 23.2, 25.4, 29.5, 29.6, 29.7, 29.9, 32.4, 34.6, 34.7, 62.3, 62.7, 68.0, 68.1, 68.7, 70.1, 70.2, 71.5, 71.6, 72.4, 73.1, 73.2, 101.2, 101.4, 169.4, 169.5, 170.4, 170.8, 173.0, 173.2, 173.5

*1,2-di-O-lauroyl-3-O-(β-D-2',3',4',6'-tetra-O-acetyl-glucopyranosyl)-rac-glycerol (**5b**)* (212.8 mg, 90.2%)

^{1}H-NMR (300 MHz, $CDCl_3$, Figure 27) δ: 0.79 (2 × 6H, *br t*, *J* = 6.9 Hz), 1.18 (2 × 32H, *br s*), 1.51 (2 × 4H, *br*), 1.90, 1.92, 1.94, 2.01 (each 2 × 3H, *s*, acetyl), 2.20 (2 × 4H, *br t*, *J* = 7.0 Hz), 3.53-3.68 (2 × 2H, H_a-3 and H-5'), 3.83 (2 × 1H, *dd*, *J* = 10.9, 4.9 Hz, H_b-3), 3.97-4.10 (2 × 2H, H_a-1 and H_a-6'), 4.11-4.26 (2 × 2H, H_b-1 and H_b-6'), 4.43 and 4.45 (each 1H, *d*, *J* = 7.8 Hz, H-1'), 4.89 and 4.90 (each 1H, *dd* (apparent *t*), *J* = 9.4 and 7.6 Hz, H-2'), 4.99 (2 × 1H, *dd* (apparent *t*), *J* = 9.6 Hz, H-4'), 5.10-5.21 (2 × 2H, H-2 and H-3')

^{13}C-NMR (75 MHz, $CDCl_3$, Figure 28) δ: 14.5, 20.8, 20.9, 22.9, 25.2, 29.4, 29.5, 29.6, 29.8, 29.9, 32.2, 34.3, 34.4, 34.5, 60.6, 62.2, 62.5, 67.9, 68.0, 68.6, 68.7, 70.0, 70.1, 71.3, 71.4, 72.3, 73.0, 101.1, 101.3, 169.5, 169.6, 170.5, 170.9, 173.1, 170.2, 173.5, 173.6

^{1}H-^{1}H COSY (Figure 29)

IR (cm^{-1}): 2921 (ν C-H), 1746 (ν C=O) (Figure 30)

*1,2-di-O-myristoyl-3-O-(β-D-2',3',4',6'-tetra-O-acetyl-glucopyranosyl)-rac-glycerol (**5c**)* (210.3 mg, 83.5%)

^{1}H-NMR (300 MHz, $CDCl_3$, Figure 31) δ: 0.85 (2 × 6H, *br t*, *J* = 6.9 Hz), 1.25 (2 × 40H, *br s*), 1.95, 1.98, 2.00, 2.08 (each 2 × 3H, *s*, acetyl), 2.25 (2 × 4H, *br t*, *J* = 7.0 Hz), 3.60-3.70 (2 × 2H, H_a-3 and H-5'), 3.91 (2 × 1H, *dd*, *J* = 10.9, 4.9 Hz, H_b-3), 4.01-4.15 (2 × 2H, H_a-1 and H_a-6'), 4.18-4.30 (2 × 2H, H_b-1 and H_b-6'), 4.48 and 4.50 (each 1H, *d*, *J* = 7.8 Hz, H-1'), 4.91 and 4.92 (each 1H, *dd* (apparent *t*), *J* = 9.4 and 7.6 Hz, H-2'), 5.01 (2 × 1H, *dd* (apparent *t*), *J* = 9.6 Hz, H-4'), 5.10-5.21 (2 × 2H, *dd* (apparent *t*), *J* = 9.6 and 7.4 Hz, H-3' and H-2)

*1,2-di-O-palmitoyl-3-O-(β-D-2',3',4',6'-tetra-O-acetyl-glucopyranosyl)-rac-glycerol (**5d**)* (209.4 mg, 77.5%)

^{1}H-NMR (300 MHz, $CDCl_3$, Figure 32) δ: 0.85 (2 × 6H, *br t*, *J* = 6.9 Hz), 1.23 (2 × 48H, *br s*), 1.57 (2 × 4H, *br*), 1.95, 1.97, 2.01, 2.08 (each 2 × 3H, *s*, acetyl), 2.28 (2 × 4H, *br t*, *J* = 7.0 Hz), 3.60-3.69 (2 × 2H, H_a-3 and H-5'), 3.90 (2 × 1H, *dd*, *J* = 10.9, 4.9 Hz, H_b-3), 4.01-4.15 (2 × 2H, H_a-1 and H_a-6'), 4.18-4.30 (2 × 2H, H_b-1 and

H_b-6'), 4.49 and 4.50 (each 1H, *d*, *J* = 7.8 Hz, H-1'), 4.91 and 4.92 (each 1H, *dd* (apparent *t*), *J* = 9.4 and 7.6 Hz, H-2'), 5.03 (2 × 1H, *dd* (apparent *t*), *J* = 9.6 Hz, H-4'), 5.10-5.21 (2 × 2H, *dd* (apparent *t*), *J* = 9.6 and 7.4 Hz, H-3' and H-2)

*1,2-di-O-stearoyl-3-O-(β-D-2',3',4',6'-tetra-O-acetyl-glucopyranosyl)-rac-glycerol (**5e**)* (223.5 mg, 78.1%)

^{1}H-NMR (300 MHz, $CDCl_3$, Figure 33) δ: 0.85 (2 × 6H, *br t*, *J* = 6.9 Hz), 1.22 (2 × 56H, *br s*), 1.95, 1.98, 2.01, 2.08 (each 2 × 3H, *s*, acetyl), 2.28 (2 × 4H, *br t*, *J* = 6.9 Hz), 3.60-3.72 (2 × 2H, H_a-3 and H-5'), 3.92 (2 × 1H, *dd*, *J* = 11.0 and 4.9 Hz, H_b-3), 4.03-4.17 (2 × 2H, H_a-1 and H_a-6'), 4.19-4.32 (2 × 2H, H_b-1 and H_b-6'), 4.50 and 4.51 (each 1H, *d*, *J* = 7.7 Hz, H-1'), 4.96 and 4.97 (each 1H, *dd* (apparent *t*), *J* = 9.5 and 7.9 Hz, H-2'), 5.05 (2 × 1H, *dd* (apparent *t*), *J* = 9.5 Hz, H-4'), 5.10-5.23 (2 × 2H, *dd* (apparent *t*), *J* = 9.6 and 7.2 Hz, H-3' and H-2)

*1,2-di-O-behenoyl-3-O-(β-D-2',3',4',6'-tetra-O-acetyl-glucopyranosyl)-rac-glycerol (**5f**)* (176.1 mg, 55.1%)

^{1}H-NMR (300 MHz, $CDCl_3$, Figure 34) δ: 0.85 (2 × 6H, *br t*, *J* = 6.9 Hz), 1.25 (2 × 72H, *br s*), 2.01, 20.2, 2.04, 2.08 (each 2 × 3H, *s*, acetyl), 2.29 (2 × 4H, *br t*, *J* = 6.9 Hz), 3.61-3.72 (2 × 2H, H_a-3 and H-5'), 3.90 (2 × 1H, *dd*, *J* = 10.8 and 4.8 Hz, H_b-3), 4.05-4.18 (2 × 2H, H_a-1 and H_a-6'), 4.19-4.32 (2 × 2H, H_b-1 and H_b-6'), 4.50 and 4.51 (each 1H, *d*, *J* = 7.8 Hz, H-1'), 4.96 and 4.97 (each 1H, *dd* (apparent *t*), *J* = 9.5 and 7.9 Hz, H-2'), 5.05 (2 x 1H, *dd* (apparent *t*), *J* = 9.7 Hz, H-4'), 5.11-5.22 (2 × 2H, *dd* (apparent *t*), *J* = 9.6 and 7.2 Hz, H-3' and H-2)

^{1}H-^{1}H COSY (Figure 35)

*1,2-di-O-oleoyl-3-O-(β-D-2',3',4',6'-tetra-O-acetyl-glucopyranosyl)-rac-glycerol (**5g**)* (207.1 mg, 72.6%)

^{1}H-NMR (300 MHz, $CDCl_3$, Figure 36) δ: 0.83 (2 × 6H, *br t*, *J* = 6.7 Hz), 1.30 (2 × 40H, *br*), 1.55 (2 × 4H, *br*), 1.92-2.05 (2 × 20H), 2.25 (2 × 4H, *br t*, *J* = 7.0 Hz), 3.60-3.72 (2 × 2H, H_a-3 and H-5'), 3.90 (2 × 1H, *dd*, *J* = 10.9 and 4.9 Hz, H_b-3), 4.03-4.18 (2 × 2H, H_a-1 and H_a-6'), 4.19-4.33 (2 × 2H, H_b-1 and H_b-6'), 4.49 and 4.50 (each 1H, *d*, *J* = 7.8 Hz, H-1'), 4.96 and 4.97 (each 1H, *dd* (apparent *t*), *J* = 9.5 and 7.5

Hz, H-2'), 5.05 (2 × 1H, *dd* (apparent *t*), *J* = 9.6 Hz, H-4'), 5.10-5.20 (2 × 2H, *dd* (apparent *t*), *J* = 9.6 and 7.6 Hz, H-3' and H-2), 5.28-5.38 (2 × 4H, *br*)

IR(cm^{-1}): 2931 (ν C-H), 1746 (ν C=O) (Figure 37)

*1,2-di-O-linoleoyl-3-O-(β-D-2',3',4',6'-tetra-O-acetyl-glucopyranosyl)-rac-glycerol (**5h**)* (mixture, 198.3 mg, 69.9%)

^{1}H-NMR (300 MHz, $CDCl_3$, Figure 38) δ: 0.87 (2 × 6H, *br t*, *J* = 6.8 Hz), 1.26 (2 × 36H, *br*), 1.95-2.10 (2 × 20H), 2.28 (2 × 4H, *br t*, *J* = 7.0 Hz), 2.78 (2 × 3H, *br t*, *J* = 5.5 Hz), 3.60-3.74 (2 × 2H, H_a-3 and H-5'), 3.93 (2 × 1H, *dd*, *J* = 10.9 and 4.9 Hz, H_b-3), 4.02-4.17 (2 × 2H, H_a-1 and H_a-6'), 4.18-4.34 (2 × 2H, H_b-1 and H_b-6'), 4.50 and 4.51 (each 1H, *d*, *J* = 7.8 Hz, H-1'), 4.96 and 4.97 (each 1H, *dd* (apparent *t*), *J* = 9.3 and 8.1 Hz, H-2'), 5.06 (2 × 1H, *dd* (apparent *t*), *J* = 9.6 Hz, H-4'), 5.10-5.21 (2 × 2H, *dd* (apparent *t*), *J* = 9.4 and 7.2 Hz, H-3' and H-2), 5.22-5.40 (2 × 6H, *br*)

*1,2-di-O-linolenoyl-3-O-(β-D-2',3',4',6'-tetra-O-acetyl-glucopyranosyl)-rac-glycerol (**5i**)* (158.5 mg, 56.1%)

^{1}H-NMR (300 MHz, $CDCl_3$, Figure 39) δ: 0.92 (2 × 6H, *t*, *J* = 7.5 Hz), 1.29 (2 × 19H, *br s*), 1.56 (2 × 4H, *br*), 1.95-2.08 (2 × 20H), 2.25 (2 × 4H, *br t*, *J* = 7.0 Hz), 2.75 (2 × 8H, *br t*, *J* = 5.5 Hz), 3.58-3.68 (2 × 2H, H_a-3 and H-5'), 3.90 (2 × 1H, *br d*, *J* = 11.7 Hz, H_b-3), 4.01-4.15 (2 × 2H, H_a-1 and H_a-6'), 4.16-4.30 (2 × 2H, H_b-1 and H_b-6'), 4.50 and 4.51 (each 1H, *br*, H-1'), 4.90-4.96 (2 × 1H, *br*, H-2'), 5.05 (2 × 1H, *dd* (apparent *t*), *J* = 9.6 Hz, H-4'), 5.10-5.20 (2 × 2H, *dd* (apparent *t*), *J* = 9.6 and 7.4 Hz, H-3' and H-2), 5.20-5.40 (2 × 12H, *br*)

^{13}C-NMR (75 MHz, $CDCl_3$, Figure 40) δ: 14.6, 21.1, 21.2, 25.2, 26.1, 27.9, 29.3, 29.4, 29.5, 29.6, 29.9, 34.2, 34.4, 62.1, 62.6, 67.9, 68.1, 68.7, 70.0, 70.1, 71.4, 71.5, 72.3, 73.0, 73.1, 101.1,101.3, 127.4, 128.0, 128.4, 128.5, 130.4, 132.1, 169.4, 169.5, 170.3, 170.7, 172.9, 173.0, 173.3

*1,2-di-O-benzoyl-3-O-(β-D-2',3',4',6'-tetra-O-acetyl-glucopyranosyl)-rac-glycerol (**5j**)* (94.5 mg, 50.0 %)

^{1}H-NMR (300 MHz, $CDCl_3$, Figure 41) δ: 1.96, 1.98, 20.2, 2.04 (each 2 × 3H, *s*, acetyl), 3.48 (2 × 1H), 3.68 (2 × 1H), 3.92 (2 × 1H), 4.05-4.25 (2 × 3H), 4.59

(2 × 2H), 4.98 (2 × 1H, *dd* (apparent *t*), *J* = 9.5 and 7.9 Hz, H-2'), 5.05 (2 × 1H, *dd* (apparent *t*), *J* = 9.7 Hz, H-4'), 5.14 (2 × 1H, *dd* (apparent *t*), *J* = 9.6 and 7.3 Hz, H-3'), 5.58 (2 × 1H, *br*, H-2), 7.45-7.60 and 8.00 (2 × 10H, aromatic)

1,2-di-O-lauroyl-3-O-(β-D-2',3',4',6'-tetra-O-acetyl-galactopyranosyl)-rac-glycerol ***(12a)*** (210.2 mg, 89.1 %)

^{1}H-NMR (300 MHz, $CDCl_3$, Figure 42) δ: 0.85 (2 × 6H, *br t*, *J* = 6.5 Hz), 1.29 (2 × 32H, *br s*), 1.98, 2.01, 2.02, 2.14 (each 2 × 3H, *s*, acetyl), 2.28 (2 × 4H, *br t*, *J* = 7.0 Hz), 3.65 (2 × 1H, *dd*, *J* = 10.8 and 5.5 Hz, H_a-3), 3.85-3.96 (2 × 2H, H_b-3 and H-5'), 4.01-4.15 (2 × 3H, H_a-1 and H_2-6'), 4.27 (2 × 1H, *br d*, *J* = 11.0 Hz, H_b-1), 4.44 and 4.46 (each 1H, *d*, *J* = 7.6 Hz, H-1'), 4.96 (2 × 1H, *br d*, *J* = 10.3 Hz, H-3'), 5.12-5.22 (2 × 2H, *br*, H-2 and H-2'), 5.35 (2 × 1H, *br s*, H-4')

^{1}H-^{1}H COSY (Figure 43)

1,2-di-O-linoleoyl-3-O-(β-D-2',3',4',6'-tetra-O-acetyl-galactopyranosyl)-rac-glycerol ***(12b)*** (mixture, 149.1 mg, 52.7 %)

^{1}H-NMR (300 MHz, $CDCl_3$, Figure 44) δ: 0.85 (2 × 6H, *br*), 1.25 (2 × 28H, *br s*), 1.95-2.10(2 × 20H, overlapped), 2.23 (2 × 4H, *br t*, *J* = 7.0 Hz), 2.76 (2 × 3H, *br*), 3.61 (2 × 1H, *br*, H_a-3), 3.82-3.95 (2 × 2H, H_b-3 and H-5'), 4.01-4.15 (2 × 3H, H_a-1 and H_2-6'), 4.27 (2 × 1H, *br d*, *J* = 11.0 Hz, H_b-1), 4.42-4.48 (2 × 1H, *br*, H-1'), 4.96 (2 × 1H, *br d*, *J* = 10.2 Hz, H-3'), 5.10-5.18 (2 × 2H, *br*, H-2 and H-2'), 5.25-5.40 (2 × 7H, overlapped, H-4' and olefinic)

1,2-di-O-linolenoyl-3-O-(β-D-2',3',4',6'-tetra-O-acetyl-galactopyranosyl)-rac-glycerol ***(12c)*** (150.7 mg, 53.3%)

^{1}H-NMR (300 MHz, $CDCl_3$, Figure 45) δ: 0.92 (2 × 6H, *t*, *J* = 7.5 Hz), 1.26 (2 × 20H, *br s*), 1.53 (2 × 4H, *br*), 1.90-2.10 (2 × 20H, overlapped), 2.23 (2 × 4H, *br t*, *J* = 7.0 Hz), 2.76 (2 × 8H, *br*), 3.61 (2 × 1H, *dd*, *J* = 10.8 and 5.5 Hz, H_a-3), 3.80-3.92 (2 × 2H, H_b-3 and H-5'), 4.01-4.15 (2 × 3H, H_a-1 and H_2-6'), 4.24 (2 × 1H, *br d*, *J* = 11.9 Hz, H_b-1), 4.41 and 4.42 (each 1H, *d*, *J* = 7.8 Hz, H-1'), 4.95 (2 × 1H, *br d*, *J* = 10.5 Hz, H-3'), 5.05-5.15 (2 × 2H, *br*, H-2 and H-2'), 5.20-5.40 (2 × 13H, *br*, overlapped, H-4' and olefinic)

^{13}C-NMR (75 MHz, $CDCl_3$, Figure 46) δ: 14.6, 21.1, 21.2, 25.2, 26.1, 27.9, 29.3, 29.4, 29.5, 29.6, 29.9, 34.2, 34.4, 61.5, 61.6, 62.6, 67.3, 67.9, 68.0, 68.9, 69.0, 70.1, 70.2, 71.2, 101.6, 101.9, 127.3, 128.0, 128.4, 128.5, 130.4, 132.1, 169.4, 170.2, 170.3, 170.4, 172.9, 173.0, 173.3

4.4 General Procedure for Preparation of 1-*O*-acyl-3-*O*-(β-D-2',3',4',6'-tetra-*O*-acetyl-glycopyranosyl)-*rac*-glycerols

To a solution of **4** (or **11**) (0.3 mmol), the fatty acid (0.4 mmol) and DMAP (0.03 mmol) in 8 ml dry dichloromethane, DCC (0.4 mmol) was added and stirred for 6 h at 0 ^{o} C. The solid was filtered off and the solvent was evaporated *in vacuo*. The residue was purified by column chromatography on silica gel column, eluted with ethyl acetate: hexane (1:3) to give the glycosyl monoglycerides (**7a-e** or **14a-b**)

*1-O-lauroyl-3-O-(β-D-2',3',4',6'-tetra-O-acetyl-glucopyranosyl)-rac-glycerol(**7a**)*
(112.2 mg, 67.8 %)

^{1}H-NMR (300 MHz, $CDCl_3$, Figure 47) δ: 0.81 (2 × 3H, *br t*, *J* = 6.9 Hz), 1.18 (2 × 20H, *br s*), 1.52 (2 × 2H, *br*), 1.90, 1.92, 1.94, 2.01 (each 2 × 3H, *s*, acetyl), 2.20 (2 × 2H, *br t*, *J* = 7.0 Hz), 3.53-3.72 (2 × 2H, H_a-3 and H-5'), 3.83 (2 × 1H, *dd*, *J* = 10.9, 4.9 Hz, H_b-3), 3.90 (2 × 1H, H-2), 3.97-4.26 (2 × 4H, H_2-1 and H_2-6'), 4.49 and 4.50 (each 1H, *d*, *J* = 7.8 Hz, H-1'), 4.91 (2 × 1H, *dd* (apparent *t*), *J* = 9.4 and 7.6 Hz, H-2'), 5.02 (2 × 1H, *dd* (apparent *t*), *J* = 9.6 Hz, H-4'), 5.15 (2 × 1H, *dd* (apparent *t*), *J* = 9.6 and 7.4 Hz, H-3')

^{13}C-NMR (75 MHz, $CDCl_3$, Figure 48) δ: 14.5, 20.8, 20.9, 22.9, 25.2, 29.4, 29.5, 29.6, 29.8, 29.9, 32.2, 34.3, 34.4, 34.5, 62.3, 65.2, 65.4, 68.7, 69.1, 69.3, 71.6, 71.7, 72.2, 72.3, 72.5, 73.0, 101.6, 101.7, 169.5, 169.6, 170.3, 170.4, 170.8, 173.9, 174.1

*1-O-linolenoyl-3-O-(β-D-2',3',4',6'-tetra-O-acetyl-glucopyranosyl)-rac-glycerol(**7b**)*
(120.1 mg, 63.5%)

^{1}H-NMR (300 MHz, $CDCl_3$, Figure 49) δ: 0.95 (2 × 3H, *t*, *J* = 7.5 Hz), 1.25 (2 × 10H, *br s*), 1.58 (2 × 2H, *br*), 1.95-2.10 (2 × 16H, overlapped), 2.28 (2 × 2H, *br t*, *J* = 7.0 Hz), 2.78 (2 × 4H, *br*), 3.60-3.78 (2 × 2H), 3.85 (2 × 1H, *br d*, *J*=10.6 Hz), 3.95 (2 × 1H, *br*), 4.01-4.35 (2 × 4H), 4.50 (2 × 1H, *br*, H-1'), 4.95 (2 × 1H, *br t*, *J* = 8.4 Hz, H-2'), 5.00 (2 × 1H, *br t*, *J*= 9.5 Hz, H-4'), 5.19 (2 × 1H, *br t*, *J*= 9.5 Hz , H-3'), 5.22-5.45 (2 × 6H, *br*)

^{13}C-NMR (75 MHz, $CDCl_3$, Figure 50) δ: 14.7, 21.1, 21.2, 25.4, 26.0, 26.1, 27.7, 29.6, 29.7, 30.0, 34.5, 62.3, 65.2, 65.4, 68.8, 69.2, 69.3, 71.7, 72.3, 72.4, 72.5, 73.0, 101.6, 101.7, 127.4, 128.0, 128.5, 128.6, 130.5, 132.2, 169.5, 169.6, 170.3, 170.7, 173.9, 174.0

*1-O-stearoyl-3-O-(β-D-2',3',4',6'-tetra-O-acetyl-glucopyranosyl)-rac-glycerol(**7c**)* (130.0 mg, 68.1%)

^{1}H-NMR (300 MHz, $CDCl_3$, Figure 51) δ: 0.85 (2 × 3H, *br t*, *J* = 6.9 Hz), 1.25 (2 × 26H, *br s*), 1.51 (2 × 2H, *br*), 1.90, 1.92, 1.94, 2.01 (each 2 × 3H, *s*, acetyl), 2.20 (2 × 2H, *br t*, *J* = 7.0 Hz), 3.63-3.72 (2 × 2H, H_a-3 and H-5'), 3.83 (2 × 1H, *dd*, *J* = 10.9, 4.9 Hz, H_b-3), 3.90 (2 × 1H, H-2), 4.02-4.26 (2 × 4H, H_2-1 and H_2-6'), 4.49 and 4.50 (each 1H, *d*, *J* = 7.8 Hz, H-1'), 4.93 (2 × 1H, *dd* (apparent *t*), *J* = 9.4 and 7.6 Hz, H-2'), 5.02 (2 × 1H, *dd* (apparent *t*), *J* = 9.6 Hz, H-4'), 5.15 (2 × 1H, *dd* (apparent *t*), *J* = 9.6 and 7.4 Hz, H-3')

*1-O-behenoyl-3-O-(β-D-2',3',4',6'-tetra-O-acetyl-glucopyranosyl)-rac-glycerol(**7d**)* (118.5 mg, 57.1%)

^{1}H-NMR (300 MHz, $CDCl_3$, Figure 52) δ: 0.87 (2 × 3H, *br t*, *J* = 6.9 Hz), 1.21 (2 × 31H, *br s*), 1.90, 1.92, 1.94, 2.01 (each 2 × 3H, *s*, acetyl), 2.30 (2 × 2H, *br t*, *J* = 7.0 Hz), 3.63-3.72 (2 × 2H, H_a-3 and H-5'), 3.83 (2 × 1H, *dd*, *J* = 10.9, 4.9 Hz, H_b-3), 3.95 (2 × 1H, H-2), 4.03-4.26 (2 × 4H, H_2-1 and H_2-6'), 4.49 and 4.50 (each 1H, *d*, *J* = 7.8 Hz, H-1'), 4.92 (2 × 1H, *dd* (apparent *t*), *J* = 9.4 and 7.6 Hz, H-2'), 5.02 (2 × 1H, *dd* (apparent *t*), *J* = 9.6 Hz, H-4'), 5.185 (2 × 1H, *dd* (apparent *t*), *J* = 9.6 and 7.4 Hz, H-3')

IR (cm^{-1}): 2916 (ν C-H), 1752 (ν C=O) (Figure 53)

*1-O-benzoyl-3-O-(β-D-2',3',4',6'-tetra-O-acetyl-glucopyranosyl)-rac-glycerol(**7e**)* (71.3 mg, 50.1%)

^{1}H-NMR (300 MHz, $CDCl_3$, Figure 54) δ: 1.92, 1.94, 1.98, 2.10 (each 2 × 3H, *s*, acetyl), 3.65-3.75 (2 × 1H), 3.80-4.00 (2 × 2H), 4.05-4.20 (2 × 3H), 4.35 (2 × 2H), 4.54 and 4.55 (each 1H, *d*, *J* = 7.8 Hz, H-1'), 4.98 (2 × 1H, *dd* (apparent *t*), *J* = 9.1 Hz, H-2'), 5.02 (2 × 1H, *dd* (apparent *t*), *J* = 9.6 Hz, H-4'), 5.18 (2 × 1H, *dd* (apparent *t*), *J* = 9.5 Hz, H-3'), 7.25-7.60 and 8.01 (2 × 5H, aromatic)

*1-O-linolenoyl-3-O-(β-D-2',3',4',6'-tetra-O-acetyl-galactopyranosyl)-rac-glycerol (**14a**)* (117.5 mg, 62.2%)

^{1}H-NMR (300 MHz, $CDCl_3$, Figure 55) δ: 0.95 (2 × 3H, *t*, *J* = 6.8 Hz), 1.25 (2 × 10H, *br s*), 1.60 (2 × 2H, *br*), 1.94-2.10 (2 × 16H, overlapped), 2.28 (2 × 2H, *br t*, *J* = 7.0 Hz), 2.78 (2 × 4H, *br*), 3.65 (2 × 1H, *dd*, *J* = 10.5 and 5.9 Hz, H_a-3), 3.75 (2 × 1H), 3.85-3.95 (2 × 3H), 4.00-4.18 (2 × 3H), 4.48 and 4.49 (each 1H, *d*, *J* = 7.8 Hz, H-1'), 4.99 (2 × 1H, *dd*, *J* = 10.5 and 3.3 Hz, H-3'), 5.16 (2 × 1H, *br t*, *J*= 10.1 Hz, H-2'), 5.23-5.45 (2 × 7H, *br*, olefinic and H-4')

^{13}C-NMR (75 MHz, $CDCl_3$, Figure 56) δ: 14.7, 21.1, 21.2, 25.4, 26.0, 26.1, 27.7, 29.6, 29.7, 30.0, 34.5, 61.8, 65.3, 65.4, 67.4, 69.2, 69.3, 71.2, 71.3, 72.2, 72.5, 102.2, 102.3, 127.4, 128.0, 128.5, 128.6, 130.5, 132.2, 170.2, 170.3, 170.6, 173.9, 174.0

*1-O-behenoyl-3-O-(β-D-2',3',4',6'-tetra-O-acetyl-galactopyranosyl)-rac-glycerol (**14b**)* (115.2 mg, 55.5%)

^{1}H-NMR (300 MHz, $CDCl_3$, Figure 57) δ: 0.85 (2 × 3H, *br t*), 1.25 (2 × 32H, *br s*), 1.94-2.12 (2 × 12H, acetyl), 2.23 (2 × 2H, *br t*, *J* = 7.0 Hz), 3.65 (2 × 1H, *br*), 3.76 (2 × 1H, *br*), 3.85-4.01 (2 × 3H), 4.05-4.20 (2 × 3H), 4.46 (2 × 1H, *br*, H-1'), 4.99 (2 × 1H, *br d*, *J* = 10.5 Hz, H-3'), 5.17 (2 × 1H, *br t*, *J*= 10.1 Hz, H-2'), 5.36 (2 × 1H, *br s*, H-4')

IR: (Figure 58)

4.5 General Procedure for Preparation of Mixed-acid 1,2-*di*-*O*-acyl-3-*O*-(β-D-2',3',4',6'-tetra-*O*-acetyl-glycopyranosyl)-*rac*-glycerols

To a solution of **4** (or **11**) (0.3 mmol), the first fatty acid (0.4 mmol) and DMAP (0.03 mmol) in 8 ml dry dichloromethane, DCC (0.4 mmol) was added and stirred for 6 h at 0 ^{o} C. The solid was filtered off and the solvent was evaporated *in vacuo*. The residue was purified by column chromatography on silica gel column, eluted with ethyl acetate: hexane (1:3) to give the glycosyl monoglycerides (**7a-e** or **14a-b**) which were subsequently reacted with equimolar of the second fatty acid, DCC and a little amount of DMAP at room temperature overnight. The solid was filtered off and the solvent was evaporated *in vacuo*. The residue was purified by column chromatography on silica gel column, eluted with ethyl acetate: hexane (1:3) to give the 1:1 mixtures of two diastereomers **5k-q** (or **12d-e**).

*1-O-lauroyl-2-O-oleoyl-3-O-(β-D-2',3',4',6'-tetra-O-acetyl-glucopyranosyl)-rac-glycerol (**5k**)* (187.5 mg, 72.0%)

^{1}H-NMR (300 MHz, $CDCl_3$, Figure 59) δ: 0.85 (2 × 6H, *br t*, *J* = 6.7 Hz), 1.25 (2 × 36H, *br*), 1.54 (2 × 4H, *br*), 1.95-2.05 (2 × 14H, overlapped), 2.25 (2 × 4H, *br t*, *J* = 7.0 Hz), 3.60-3.70 (2 × 2H, H_a-3 and H-5'), 3.90 (2 × 1H, *dd*, *J* = 10.9 and 4.9 Hz, H_b-3), 4.01-4.14 (2 × 2H, H_a-1 and H_a-6'), 4.15-4.30 (2 × 2H, H_b-1 and H_b-6'), 4.49 and 4.50 (each 1H, *d*, *J* = 7.8 Hz, H-1'), 4.95 and 4.96 (each 1H, *dd* (apparent *t*), *J* = 9.5 and 7.5 Hz, H-2'), 5.06 (2 × 1H, *dd* (apparent *t*), *J* = 9.6 Hz, H-4'), 5.10-5.20 (2 × 2H, *dd* (apparent *t*), *J* = 9.4 and 7.2 Hz, H-3' and H-2), 5.28-5.32 (2 × 2H, *br*)

^{13}C-NMR (75 MHz, $CDCl_3$, Figure 60): δ 14.5, 21.1, 23.0, 25.1, 25.2, 27.5, 27.6, 29.4, 29.5, 29.6, 29.7, 29.8, 62.2, 62.6, 67.9, 68.1, 68.7, 70.1, 71.4, 71.5, 72.3, 73.0, 101.2, 101.4, 130.1, 130.4, 169.6, 169.7, 170.6, 171.0, 173.2, 173.3, 173.4

*1-O-stearoyl-2-O-lauroyl-3-O-(β-D-2',3',4',6'-tetra-O-acetyl-glucopyranosyl)-rac-glycerol (**5l**)* (mixture, 221.5 mg, 84.9%)

^{1}H-NMR (300 MHz, $CDCl_3$, Figure 61) δ: 0.85 (2 × 6H, *br t*, *J* = 6.7 Hz), 1.27 (2 × 47H, *br s*), 1.98, 2.01, 2.03, 2.06 (each 2 × 3H, *s*, acetyl), 2.29 (2 × 4H, *br t*, *J* = 7.0 Hz), 3.60-3.72 (2 × 2H, H_a-3 and H-5'), 3.92 (2 × 1H, *dd*, *J* = 10.9 and 4.9 Hz,

H_b-3), 4.01-4.18 (2 × 2H, H_a-1 and H_a-6'), 4.19-4.33 (2 × 2H, H_b-1 and H_b-6'), 4.49 and 4.50 (each 1H, *d*, *J* = 7.8 Hz, H-1'), 4.96 and 4.97 (each 1H, *dd* (apparent *t*), *J* = 9.5 and 7.5 Hz, H-2'), 5.05 (2 × 1H, *dd* (apparent *t*), *J* = 9.6 Hz, H-4'), 5.11-5.23 (2 × 2H, overlapped, H-2 and H-3')

*1-O-stearoyl-2-O-behenoyl-3-O-(β-D-2',3',4',6'-tetra-O-acetyl-glucopyranosyl)-rac-glycerol (**5m**)* (196.3 mg, 64.8%)

^{1}H-NMR (300 MHz, $CDCl_3$, Figure 62) δ: 0.87 (2 × 6H, *br t*, *J* = 6.7 Hz), 1.38 (2 × 64H, *br s*), 2.01, 2.03, 2.05, 2.08 (each 2 × 3H, *s*, acetyl), 2.30 (2 × 4H, *br t*, *J* = 7.0 Hz), 3.61-3.75 (2 × 2H, H_a-3 and H-5'), 3.92 (2 × 1H, *dd*, *J* = 10.9 and 4.9 Hz, H_b-3), 4.02-4.19 (2 × 2H, H_a-1 and H_a-6'), 4.20-4.33 (2 × 2H, H_b-1 and H_b-6'), 4.50 and 4.51 (each 1H, *d*, *J* = 7.8 Hz, H-1'), 4.96 and 4.97 (each 1H, *dd* (apparent *t*), *J* = 9.5 and 7.5 Hz, H-2'), 5.07 (2 × 1H, *dd* (apparent *t*), *J* = 9.6 Hz, H-4'), 5.11-5.23 (2 × 2H, overlapped, H-2 and H-3')

*1-O-behenoyl-2-O-lauroyl-3-O-(β-D-2',3',4',6'-tetra-O-acetyl-glucopyranosyl)-rac-glycerol (**5n**)* (194.2 mg, 69.9%)

^{1}H-NMR (300 MHz, $CDCl_3$, Figure 63) δ: 0.88 (2x6H, *br t*, *J* = 6.7 Hz), 1.25 (2x52H, *br s*), 1.54 (2x4H, *br*), 1.98, 2.01, 2.03, 2.07 (each 2x3H, *s*, acetyl), 2.28 (2x4H, *br t*, *J* = 7.0 Hz), 3.60-3.72 (2x2H, H_a-3 and H-5'), 3.92 (2x1H, *dd*, *J* = 10.9 and 4.9 Hz, H_b-3), 4.01-4.17 (2x2H, H_a-1 and H_a-6'), 4.18-4.32 (2x2H, H_b-1 and H_b-6'), 4.50 and 4.51 (each 1H, *d*, *J* = 7.8 Hz, H-1'), 4.96 and 4.97 (each 1H, *dd* (apparent *t*), *J* = 9.5 and 7.5 Hz, H-2'), 5.05 (2x1H, *dd* (apparent *t*), *J* = 9.6 Hz, H-4'), 5.11-5.23 (2x2H, overlapped, H-2 and H-3')

*1-O-behenoyl-2-O-oleoyl-3-O-(β-D-2',3',4',6'-tetra-O-acetyl-glucopyranosyl)-rac-glycerol (**5o**)*(205.8 mg, 68.1%)

^{1}H-NMR (300 MHz, $CDCl_3$, Figure 64) δ: 0.87 (2 × 6H, *br t*, *J* = 6.7 Hz), 1.25 (2 × 56H, *br s*), 2.02 (2 × 4H, overlapped), 2.01, 2.03, 2.05, 2.10 (each 2 × 3H, *s*, acetyl), 2.25 (2 × 4H, *br t*, *J* = 7.0 Hz), 3.60-3.73 (2 × 2H, H_a-3 and H-5'), 3.92 (2 × 1H, *dd*, *J* = 10.9 and 4.9 Hz, H_b-3), 4.04-4.17 (2 × 2H, H_a-1 and H_a-6'), 4.19-4.33 (2x2H, H_b-1 and H_b-6'), 4.50 and 4.51 (each 1H, *d*, *J* = 7.8 Hz, H-1'), 4.96 and 4.97 (each 1H, *dd* (apparent *t*), *J* = 9.5 and 7.5 Hz, H-2'), 5.05 (2 × 1H, *dd* (apparent *t*), *J* =

9.6 Hz, H-4'), 5.11-5.23 (2x2H, *dd* (apparent *t*), *J* = 9.8 and 7.3 Hz, H-3' and H-2), 5.27-5.35 (2 × 2H, *br*)

*1-O-linolenoyl-2-O-linoleoyl-3-O-(β-D-2',3',4',6'-tetra-O-acetyl-glucopyranosyl)-rac-glycerol (**5p**)* (169.5 mg, 59.9%)
(spectral data not reported)

*1-O-benzoyl-2-O-lauroyl-3-O-(β-D-2',3',4',6'-tetra-O-acetyl-glucopyranosyl)-rac-glycerol (**5q**)* (110.5 mg, 52.0%)
(spectral data not reported)

*1-O-behenoyl-2-O-lauroyl-3-O-(β-D-2',3',4',6'-tetra-O-acetyl-galactopyranosyl)-rac-glycerol (**12d**)* (190.0 mg, 68.4 %)

^{1}H-NMR (300 MHz, $CDCl_3$, Figure 65) δ: 0.85 (2 × 6H, *br t*, *J* = 6.7 Hz), 1.29 (2 × 52H, *br s*), 1.98, 2.01, 2.02, 2.14 (each 2 × 3H, *s*, acetyl), 2.28 (2 × 4H, *br t*, *J* = 7.0 Hz), 3.64 (2 × 1H, *dd*, *J* = 10.8 and 5.5 Hz, H_a-3), 3.82-3.96 (2 × 2H, H_b-3 and H-5'), 4.01-4.17 (2 × 3H, H_a-1 and H_2-6'), 4.26 (2 × 1H, *br d*, *J* =11.0 Hz, H_b-1), 4.44 and 4.46 (each 1H, *d*, *J* = 7.6 Hz, H-1'), 4.95 (2 × 1H, *br d*, *J*=10.4 Hz, H-3'), 5.12-5.21 (2 × 2H, H-2 and H-2'), 5.35 (2 × 1H, *br s*, H-4')

*1-O-linolenoyl-2-O-linoleoyl-3-O-(β-D-2',3',4',6'-tetra-O-acetyl-galactopyranosyl)-rac-glycerol (**12e**)* (mixture, 151.5 mg, 53.5 %)

^{1}H-NMR (300 MHz, $CDCl_3$, Figure 66) δ: 0.85 (2 × 3H, *br t*, *J* = 6.7 Hz), 0.95 (2 × 3H, *t*, *J* = 7.6 Hz), 1.29 (2 × 35H, *br s*), 1.98-2.20 (2 × 20H, overlapped), 2.30 (2 × 4H, *br t*, *J* = 6.9 Hz), 2.78 (2 × 6H, *br*), 3.64 (2 × 1H, *br*, H_a-3), 3.82-3.95 (2 × 2H, H_b-3 and H-5'), 4.01-4.15 (2 × 3H, H_a-1 and H_2-6'), 4.27 (2 × 1H, *br d*, *J* = 11.0 Hz, H_b-1), 4.44 and 4.46 (each 1H, *d*, *J* = 7.6 Hz, H-1'), 4.96 (2 × 1H, *br d*, *J* = 10.4 Hz, H-3'), 5.12-5.22 (2 × 2H, H-2 and H-2'), 5.25-5.50 (2 × 13H, overlapped, H-4' and olefinic)

4.6 General Procedure for Selective Removal of Acetyl Protecting Groups from 1,2-di-*O*-acyl-3-*O*-(β-D-2',3',4',6'-tetra-*O*-acetyl-glycopyranosyl) glycerols

To a solution of **5a-q** (or **12a-e**) (0.1 mmol) in 85% EtOH, $NH_2NH_2.H_2O$ (1.2 mmol) was added. The mixture was stirred for 4-6 h at 40-60 ^{o} C, and then, the mixture was poured into ice-cold water and extracted 3 times with 50 ml of chloroform. The combined chloroform layers were dried with anhydrous Na_2SO_4 and evaporated to give syrupy mixture. The mixture was purified by column chromatography on silica gel column, eluted with $CHCl_3$:CH_3OH (8:1) to give the 1:1 mixtures of two diastereomers **6a-q** (or **13a-e**).

*1,2-di-O-caproyl-3-O-β-D-glucopyranosyl-rac-glycerol (**6a**)*

(31.9 mg, 56.7%)

^{1}H-NMR (300 MHz, $CDCl_3$, Figure 67) δ: 0.85 (2 × 6H, *br t*, *J* = 6.7 Hz), 1.24 (2 × 24H, *br s*), 1.57 (2 × 4H, *br*), 2.29 (2 × 4H, *br t*, *J* = 7.0 Hz), 3.24-3.38 (2 × 2H, H-2' and H-5'), 3.41-3.59 (2 × 2H, H-3' and H-4'), 3.62 and 3.65 (each 1H, *dd*, *J* = 10.7 and 6.4 Hz, H_a-3), 3.80 (2 × 2H, *br s*, H_2-6'), 3.87 (each 1H, *br d*, *J* = 10.7 Hz, H_b-3), 4.08 and 4.13 (each 1H, *dd*, *J* = 12.0 and 6.7 Hz, H_a-1), 4.28 (2 × 1H, *d*, *J* = 7.8 Hz, H-1'), 4.35 (2 × 1H, *br d*, *J* = 12.1 Hz, H_b-1), 5.24 (2 × 1H, *br*, H-2)

^{13}C-NMR (75 MHz, $CDCl_3$, Figure 68) δ: 14.6 (*q*), 23.2 (*t*), 25.4 (*t*), 29.6 (*t*), 29.8 (*t*), 30.0 (*t*), 32.4 (*t*), 34.6 (*t*), 34.8 (*t*), 61.9 (*t*, C-6'), 63.2 and 63.3 (*t*, C-1), 68.6 (*t*, C-3), 69.8 (*d*, C-3'), 70.5 (*d*, C-2), 73.7 and 73.8 (*d*, C-2'), 76.2 and 76.3 (*d*, C-5'), 76.7 (*d*, C-4'), 103.7 and 103.8 (*d*, C-1'), 173.6 and 173.7 (*s*, carbonyl), 173.9 and 174.0 (*s*, carbonyl)

Elemental analysis for $C_{29}H_{54}O_{10}$ calcd. C: 61.881 H: 9.677
found C: 61.859 H: 9.695

*1,2-di-O-lauroyl-3-O-β-D-glucopyranosyl-rac-glycerol (**6b**)*

(31.6 mg, 51.1%)

^{1}H-NMR (300 MHz, $CDCl_3$, Figure 69) δ: 0.83 (2 × 6H, *br t*, *J* = 6.7 Hz), 1.22 (2 × 32H, *br s*), 1.55 (2 × 4H, *br*), 2.28 (2 × 4H, *br t*, *J* = 7.0 Hz), 3.25-3.38 (2 ×

2H, H-2' and H-5'), 3.42-3.59 (2 × 2H, H-3' and H-4'), 3.62 and 3.65 (each 1H, *dd*, *J* = 10.7 and 6.4 Hz, H_a-3), 3.79 (2 × 2H, *br s*, H_2-6'), 3.85 (2 × 1H, *br d*, *J* = 10.5 Hz, H_b-3), 4.08 and 4.12 (each 1H, *dd*, *J* = 12.0 and 6.7 Hz, H_a-1), 4.25 (2 × 1H, *d*, *J* = 7.7 Hz, H-1'), 4.38 (2 × 1H, *br d*, *J* = 10.4 Hz, H_b-1), 5.22 (2 × 1H, *br*, H-2)

^{13}C-NMR (75 MHz, $CDCl_3$, Figure 70) δ: 14.5 (*q*), 23.0 (*t*), 25.2 (*t*), 25.3 (*t*), 29.5 (*t*), 29.6(*t*), 29.7 (*t*), 29.9 (*t*), 30.0 (*t*), 32.3 (*t*), 34.5 (*t*), 34.6 (*t*), 61.7 (*t*, C-6'), 63.2 and 63.3 (*t*, C-1), 68.4 (*t*, C-3), 69.6 (*d*, C-3'), 70.4 (*d*, C-2), 73.6 and 73.7 (*d*, C-2'), 76.2 (*d*, C-5'), 76.6 (*d*, C-4'), 103.7 and 103.8 (*d*, C-1'), 173.7 and 173.8 (*s*, carbonyl), 174.1 and 174.2 (*s*, carbonyl)

^{1}H-^{1}H COSY: (Figure 71)

IR (cm^{-1}): 3294 (ν O-H), 2917 (ν C-H), 1746 (ν C=O) (Figure 72)

Positive-ion FABMS $[M + K]^+$ *m/z* : 657.3 (Figure 73)

Negative-ion FABMS $[M - H]^-$ *m/z*: 617.3 (Figure 74)

Positive-ion FABMS (m-Nitrobenzyl alcohol) (Figure 75)

Negative-ion FABMS (diethanolamine) (Figure 76)

Elemental analysis for $C_{33}H_{62}O_{10}$ calcd. C: 64.036 H: 10.104

found C: 63.984 H: 10.122

*1,2-di-O-myristoyl-3-O-β-D-glucopyranosyl-rac-glycerol (**6c**)*

(35.5 mg, 52.9%)

^{1}H-NMR (300 MHz, $CDCl_3$, Figure 77) δ: 0.85 (2 × 6H, *br t*, *J* = 6.7 Hz), 1.22 (2 × 40H, *br s*), 1.55 (2 × 4H, *br*), 2.26 (2 × 4H, *br t*, *J* = 7.0 Hz), 3.25-3.38 (2 × 2H, H-2' and H-5'), 3.42-3.59 (2 × 2H, H-3' and H-4'), 3.62 and 3.65 (each 1H, *dd*, *J* = 10.7 and 6.4 Hz, H_a-3), 3.79 (2 × 2H, *br s*, H_2-6'), 3.85 (2 × 1H, *br d*, *J* = 10.5 Hz, H_b-3), 4.08 and 4.12 (each 1H, *dd*, *J* = 12.0 and 6.7 Hz, H_a-1), 4.25 (2 × 1H, *d*, *J* = 7.7 Hz, H-1'), 4.38 (2 × 1H, *br d*, *J* = 10.4 Hz, H_b-1), 5.22 (2 × 1H, *br*, H-2)

^{13}C-NMR (75 MHz, $CDCl_3$, Figure 78) δ: 14.5 (*q*), 23.0 (*t*), 25.2 (*t*), 25.3 (*t*), 27.6 (*t*), 29.5 (*t*), 29.6(*t*), 29.7 (*t*), 29.9 (*t*), 30.0 (*t*), 30.1 (*t*), 30.4 (*t*), 32.3 (*t*), 34.5 (*t*), 34.6 (*t*), 61.8 (*t*, C-6'), 63.2 and 63.3 (*t*, C-1), 68.5 (*t*, C-3), 69.8 (*d*, C-3'), 70.4 (*d*, C-2), 73.6 and 73.7 (*d*, C-2'), 76.2 (*d*, C-5'), 76.6 (*d*, C-4'), 103.7 and 103.8 (*d*, C-1'), 173.8 and 173.9 (*s*, carbonyl), 174.1 and 174.2 (*s*, carbonyl).

Elemental analysis for $C_{37}H_{70}O_{10}$ calcd. C: 65.827 H: 10.459

found C: 65.854 H: 10.498

*1,2-di-O-palmitoyl-3-O-β-D-glucopyranosyl-rac-glycerol (**6d**)*

(34.6 mg, 47.5%)

^{1}H-NMR (300 MHz, $CDCl_3$, Figure 79) δ: 0.86 (2 × 6H, *br t*, *J* = 6.7 Hz), 1.22 (2 × 48H, *br s*), 1.55 (2 × 4H, *br*), 2.26 (2 × 4H, *br t*, *J* = 7.0 Hz), 3.25-3.38 (2 × 2H, H-2' and H-5'), 3.42-3.59 (2 × 2H, H-3' and H-4'), 3.65 and 3.70 (each 1H, *dd*, *J* = 10.7 and 6.4 Hz, H_a-3), 3.79 (2 × 2H, *br s*, H_2-6'), 3.85 (2 × 1H, *br d*, *J* = 10.5 Hz, H_b-3), 4.08 and 4.12 (each 1H, *dd*, *J* = 12.0 and 6.7 Hz, H_a-1), 4.27 (2 × 1H, *d*, *J* = 7.7 Hz, H-1'), 4.36 (2 × 1H, *br d*, *J* = 10.4 Hz, H_b-1), 5.22 (2 × 1H, *br*, H-2)

^{13}C-NMR (75 MHz, $CDCl_3$, Figure 80) δ: 14.5 (*q*), 23.0 (*t*), 25.2 (*t*), 25.3 (*t*), 29.5 (*t*), 29.6(*t*), 29.7 (*t*), 29.9 (*t*), 30.0 (*t*), 32.3 (*t*), 34.5 (*t*), 34.6 (*t*), 61.7 (*t*, C-6'), 63.1 and 63.2 (*t*, C-1), 68.4 (*t*, C-3), 69.7 (*d*, C-3'), 70.5 (*d*, C-2), 73.6 and 73.7 (*d*, C-2'), 76.2 (*d*, C-5'), 76.6 (*d*, C-4'), 103.7 and 103.8 (*d*, C-1'), 173.7 and 173.8 (*s*, carbonyl), 174.1 and 174.2 (*s*, carbonyl).

Elemental analysis for $C_{41}H_{78}O_{10}$ calcd. C: 67.346 H: 10.760

found C: 67.401 H: 10.809

*1,2-di-O-stearoyl-3-O-β-D-glucopyranosyl-rac-glycerol (**6e**)*

(27.8 mg, 35.4%)

^{1}H-NMR (300 MHz, $CDCl_3$, Figure 81) δ: 0.84 (2 × 6H, *br t*, *J* = 6.5 Hz), 1.23 (2 × 56H, *br s*), 1.57 (2 × 4H, *br*), 2.29 (2 × 4H, *br t*, *J* = 6.9 Hz), 3.30-3.38 (2 × 2H, H-2' and H-5'), 3.45-3.58 (2 × 2H, H-3' and H-4'), 3.62 and 3.65 (each 1H, *dd*, *J* = 10.7 and 6.4 Hz, H_a-3), 3.79 (2 × 2H, *br s*, H_2-6'), 3.85 (2 × 1H, *br d*, *J* = 10.5 Hz, H_b-3), 4.06 and 4.12 (each 1H, *dd*, *J* = 12.0 and 6.7 Hz, H_a-1), 4.28 (2 × 1H, *d*, *J* = 7.8 Hz, H-1'), 4.35 (2 × 1H, *br d*, *J* = 11.0 Hz, H_b-1), 5.24 (2 × 1H, *br*, H-2)

^{13}C-NMR (75 MHz, $CDCl_3$, Figure 82) δ: 14.5 (*q*), 23.0 (*t*), 25.3 (*t*), 29.5 (*t*), 29.6 (*t*), 29.8 (*t*), 29.9 (*t*), 30.1 (*t*), 32.3 (*t*), 34.6 (*t*), 34.7 (*t*), 61.9 (*t*, C-6'), 63.1 and 63.2 (*t*, C-1), 68.5 (*t*, C-3), 69.8 (*d*, C-3'), 70.4 and 70.5 (*d*, C-2), 73.7 and 73.8 (*d*, C-2'), 76.2 (*d*, C-5'), 76.6 (*d*, C-4'), 103.7 and 103.9 (*d*, C-1'), 173.8 and 173.9 (*s*, carbonyl), 174.1 and 174.2 (*s*, carbonyl)

IR (cm^{-1}): 3295 (ν O-H), 2917 (ν C-H), 1736 (ν C=O) (Figure 83)

Positive-ion FABMS $[M + Na]^+$ *m/z* : 809.6 (Figure 84)

Negative-ion FABMS $[M - H]^-$ *m/z*: 785.3 (Figure 85)

Elemental analysis for $C_{45}H_{86}O_{10}$ calcd. C: 68.648 H: 11.018

found C: 68.727 H: 11.268

*1,2-di-O-behenoyl-3-O-β-D-glucopyranosyl-rac-glycerol (**6f**)*

(25.2 mg, 28.1%)

^{1}H-NMR (300 MHz, $CDCl_3$, Figure 86) δ: 0.76 (2 × 6H, *br t*, *J* = 6.5 Hz), 1.16 (2 × 72H, *br s*), 1.49 (2 × 4H, *br*), 2.20 (2 × 4H, *br t*, *J* = 6.9 Hz), 3.20-3.30 (2 × 2H, H-2' and H-5'), 3.32-3.53 (2 × 2H, H-3' and H-4'), 3.62-3.90 (2 × 4H, H_2-3 and H_2-6'), 4.07 and 4.14 (each 1H, *dd*, *J* = 12.0 and 6.7 Hz, H_a-1), 4.23 (2 × 1H, *d*, *J* = 7.8 Hz, H-1'), 4.30 (2 × 1H, *br d*, *J* = 11.0 Hz, H_b-1), 5.20 (2 × 1H, *br*, H-2)

^{13}C-NMR (75 MHz, $CDCl_3$, Figure 87) δ: 14.5 (*q*), 23.0 (*t*), 25.3 (*t*), 29.5 (*t*), 29.6 (*t*), 29.8 (*t*), 29.9 (*t*), 30.1 (*t*), 32.3 (*t*), 34.6 (*t*), 34.7 (*t*), 62.4 (*t*, C-6'), 62.8 and 63.0 (*t*, C-1), 68.2 (*t*, C-3), 70.4 and 70.5 (*d*, C-3'), 70.7 (*d*, C-2), 73.7 and 73.8 (*d*, C-2'), 76.4 (*d*, C-5'), 76.8 (*d*, C-4'), 103.8 and 103.9 (*d*, C-1'), 173.8-174.2 (*s*, carbonyl)

Positive-ion FABMS $[M + Na]^+$ *m/z* : 921.9 (Figure 88)

Negative-ion FABMS $[M - H]^-$ *m/z*: 897.7 (Figure 89)

Elemental analysis for $C_{53}H_{102}O_{10}$ calcd. C: 70.765 H: 11.438

found C: 70.885 H: 11.569

*1,2-di-O-oleoyl-3-O-β-D-glucopyranosyl-rac-glycerol (**6g**)*

(28.0 mg, 35.9%)

^{1}H-NMR (300 MHz, $CDCl_3$, Figure 90) δ: 0.85 (2 × 6H, *br t*, *J* = 6.7 Hz), 1.25 (2 × 40H, *br*), 1.57 (2 × 4H, *br*), 1.99 (2 × 8H, *br*), 2.25 (2 × 4H, *br t*, *J* = 7.0 Hz), 3.22-3.37 (2 × 2H, H-2' and H-5'), 3.35-3.58 (2 × 2H, H-3' and H-4'), 3.62 and 3.65 (each 1H, *dd*, *J* = 10.7 and 6.4 Hz, H_a-3), 3.79 (2 × 2H, *br s*, H_2-6'), 3.86 (2 × 1H, *br d*, *J* = 10.6 Hz, H_b-3), 4.07 and 4.14 (each 1H, *dd*, *J* = 12.0 and 6.7 Hz, H_a-1), 4.29 (2 × 1H, *d*, *J* = 7.5 Hz, H-1'), 4.34 (2 × 1H, *br d*, *J* = 11.8 Hz, H_b-1), 5.22 (2 × 1H, *br*, H-2), 5.27-5.36 (2 × 4H, *br*)

^{13}C-NMR (75 MHz, $CDCl_3$, Figure 91) δ: 14.5 (*q*), 23.0 (*t*), 25.2 (*t*), 25.3 (*t*), 27.6 (*t*), 27.7 (*t*), 29.5 (*t*), 29.6 (*t*), 29.7 (*t*), 29.8 (*t*), 29.9 (*t*), 30.1 (*t*), 30.3 (*t*), 30.4 (*t*), 32.3 (*t*), 34.5 (*t*), 34.6 (*t*), 61.8 (*t*, C-6'), 63.2 and 63.3 (*t*, C-1), 68.4 (*t*, C-3), 69.8 (*d*, C-3'), 70.4 and 70.5 (*d*, C-2), 73.6 and 73.7 (*d*, C-2'), 76.2 and 76.3 (*d*, C-5'), 76.6

and 76.7 (*d*, C-4'), 103.7 and 103.9 (*d*, C-1'), 130.1 (*d*), 130.4 (*d*), 173.8 and 173.9 (*s*, carbonyl), 174.2 and 174.3 (*s*, carbonyl)

^{1}H-^{1}H COSY: (Figure 92)

HMQC: (Figure 93)

Positive-ion FABMS $[M + Na]^+$ *m/z* : 805.6 (Figure 94)

Negative-ion FABMS $[M - H]^-$ *m/z* : 781.3 (Figure 95)

Elemental analysis for $C_{45}H_{82}O_{10}$ calcd. C: 69.002 H: 10.560

found C: 69.120 H: 10.665

*1,2-di-O-linoleoyl-3-O-β-D-glucopyranosyl-rac-glycerol (**6h**)*

(25.7 mg, 33.0%)

^{1}H-NMR (300 MHz, $CDCl_3$, Figure 96) δ: 0.85 (2 × 6H, *br t*, *J* = 6.6 Hz), 1.24 (2 × 33H, *br*), 1.54 (2 × 4H, *br*), 1.99 (2 × 6H, *br*), 2.24 (2 × 4H, *br t*, *J* = 7.0 Hz), 2.78 (2 × 2H, *br t*, *J* = 5.5 Hz), 3.22-3.37 (2 × 2H, H-2' and H-5'), 3.41-3.59 (2 × 2H, H-3' and H-4'), 3.62 and 3.65 (each 1H, *dd*, *J* = 10.7 and 6.4 Hz, H_a-3), 3.79 (2 × 2H, *br s*, H_2-6'), 3.86 (2 × 1H, *br d*, *J* = 10.6 Hz, H_b-3), 4.09 and 4.14 (each 1H, *dd*, *J* = 12.0 and 6.7 Hz, H_a-1), 4.27 (2 × 1H, *d*, *J* = 7.6 Hz, H-1'), 4.35 (2 × 1H, *br d*, *J* = 10.4 Hz, H_b-1), 5.23 (2 × 1H, H-2), 5.24-5.40 (2 × 6H, *br*)

^{13}C-NMR (75 MHz, $CDCl_3$, Figure 97) δ: 14.4 (*q*), 22.9 (*t*), 23.0 (*t*), 25.1 (*t*), 25.2 (*t*), 25.3 (*t*), 26.0 (*t*), 27.5 (*t*), 29.4 (*t*), 29.5 (*t*), 29.6 (*t*), 29.7 (*t*), 29.9 (*t*), 30.0 (*t*), 30.1 (*t*), 31.9 (*t*), 32.3 (*t*), 34.5 (*t*), 34.6 (*t*), 62.1 (*t*, C-6'), 63.0 and 63.1 (*t*, C-1), 68.6 (*t*, C-3), 69.7 (*d*, C-3'), 70.4 and 70.5 (*d*, C-2), 73.7 and 73.8 (*d*, C-2'), 76.1 (*d*, C-5'), 76.6 (*d*, C-4'), 103.7 and 103.8 (*d*, C-1'), 128.3 (*d*), 128.5 (*d*), 130.4 (*d*), 130.5 (*d*), 173.8 and 173.9 (*s*, carbonyl), 174.1 (*s*, carbonyl)

Positive-ion FABMS $[M + Na]^+$ *m/z* : 801.6 (Figure 98)

Negative-ion FABMS $[M - H]^-$ *m/z* : 777.4 (Figure 99)

Elemental analysis for $C_{45}H_{78}O_{10}$ calcd. C: 69.359 H: 10.097

found C: 69.596 H: 10.390

*1,2-di-O-linolenoyl-3-O-β-D-glucopyranosyl-rac-glycerol (**6i**)*

(23.5 mg, 30.4%)

^{1}H-NMR (300 MHz, $CDCl_3$, Figure 100) δ: 0.93 (2 × 6H, *t*, *J* = 7.5 Hz), 1.24 (2 × 21H, *br*), 1.54 (2 × 4H, *br*), 2.00 (2 × 8H, *br*), 2.25 (2 × 4H, *br t*, *J* = 6.9 Hz),

2.76 (2 × 8H, *br t*, *J* = 5.3 Hz), 3.21-3.40 (2 × 2H, H-2' and H-5'), 3.41-3.60 (2 × 2H, H-3' and H-4'), 3.62 and 3.65 (each 1H, *dd*, *J* = 10.7 and 6.4 Hz, H_a-3), 3.80 (2 × 2H, *br s*, H_2-6'), 3.85 (2 × 1H, *br d*, *J* = 10.6 Hz, H_b-3), 4.07 and 4.13 (each 1H, *dd*, *J* = 12.0 and 6.7 Hz, H_a-1), 4.27 (2 × 1H, *d*, *J* = 7.5 Hz, H-1'), 4.35 (2 × 1H, *br d*, *J* =10.5 Hz, H_b-1), 5.21-5.42 (2 × 13H, *br*, overlapped, H-2 and olefinic)

^{13}C-NMR (75 MHz, $CDCl_3$, Figure 101) δ: 14.8 (*q*), 21.1 (*t*), 25.4 (*t*), 26.0 (*t*), 26.1 (*t*), 26.2 (*t*), 27.5 (*t*), 27.6 (*t*), 27.7 (*t*), 29.6 (*t*), 29.7 (*t*), 29.8 (*t*), 29.9 (*t*), 30.2 (*t*), 34.6 (*t*), 34.7 (*t*), 61.8 (*t*, C-6'), 63.2 and 63.3 (*t*, C-1), 68.5 (*t*, C-3), 69.7 (*d*, C-3'), 70.5 and 70.6 (*d*, C-2), 73.7 (*d*, C-2'), 76.3 (*d*, C-5'), 76.6 (*d*, C-4'), 103.7 and 103.8 (*d*, C-1'), 127.4 (*d*), 128.0 (*d*), 128.5 (*d*), 128.6 (*d*), 130.4 (*d*), 132.2 (*d*), 173.5 and 173.6 (*s*, carbonyl), 173.9 and 174.0 (*s*, carbonyl)

Positive-ion FABMS $[M + Na]^+$ *m/z* : 797.5 (Figure 102)

Negative-ion FABMS $[M - H]^-$ *m/z* : 773.2 (Figure 103)

Elemental analysis for $C_{45}H_{74}O_{10}$ calcd. C: 69.720 H: 9.629

found C: 69.829 H: 9.989

*1,2-di-O-benzoyl-3-O-β-D-glucopyranosyl-rac-glycerol (**6j**)*

(14.8 mg, 32.0%)

^{1}H-NMR (300 MHz, $CDCl_3$, Figure 104) 3.22 (2 × 1H, *br*, H-5'), 3.35 (2 × 1H, *br*, H-2'), 3.40-3.56 (2 × 2H, *br*, H-3' and H-4'), 3.70 (2 × 2H, *br s*, H_2-6'), 3.85 (2 × 1H, *br dd*, *J* = 10.6 and 5.6 Hz, H_a-3), 4.05 (2 × 1H, *br d*, *J* = 10.0 and 5.6 Hz, H_b-3), 4.32 (2 × 1H, *d*, *J* = 7.5 Hz, H-1'), 4.52 (2 × 1H, *br dd*, *J* = 11.0 and 5.2 Hz, H_a-1), 4.64 (2 × 1H, *br d*, *J* =10.5 Hz, H_b-1), 5.55 (2 × 1H, *br s*, H-2), 7.30-7.45 (2 × 10H, aromatic)

^{13}C-NMR (75 MHz, $CDCl_3$, Figure 105) δ: 14.8 (*q*), 21.1 (*t*), 25.4 (*t*), 26.0 (*t*), 26.1 (*t*), 26.2 (*t*), 27.5 (*t*), 27.6 (*t*), 27.7 (*t*), 29.6 (*t*), 29.7 (*t*), 29.8 (*t*), 29.9 (*t*), 30.2 (*t*), 34.6 (*t*), 34.7 (*t*), 61.4 (*t*, C-6'), 64.2, 68.4 and 68.5, 69.6, 71.5 and 71.6, 73.5 and 73.6, 76.2 and 76.3, 103.7 and 103.8 (*d*, C-1'), 128.7 (*d*), 130.0 (*d*), 130.2 (*d*), 133.5 and 133.6 (*d*), 166.5 and 166.6 (*s*, carbonyl), 166.9 (*s*, carbonyl)

^{1}H-^{1}H COSY: (Figure 106)

Elemental analysis for $C_{23}H_{26}O_{10}$ calcd. C: 59.721 H: 5.670

found C: 60.201 H: 5.799

*1-O-lauroyl-2-O-oleoyl-3-O-β-D-glucopyranosyl-rac-glycerol (**6k**)*

(30.7 mg, 43.9%)

^{1}H-NMR (300 MHz, $CDCl_3$, Figure 107) δ: 0.85 (2 × 6H, *br t*, *J* = 6.5 Hz), 1.23 (2 × 40H, *br s*), 1.57 (2 × 4H, *br*), 1.98 (2 × 4H, *br*), 2.29 (2 × 4H, *br t*, *J* =6.9 Hz), 3.27-3.35 (2 × 2H, H-2' and H-5'), 3.43-3.56 (2 × 2H, H-3' and H-4'), 3.64 and 3.67 (each 1H, *dd*, *J* = 10.7 and 6.4 Hz, H_a-3), 3.80 (2 × 2H, *br s*, H_2-6'), 3.87 (2 × 1H, *br d*, *J* = 10.6 Hz, H_b-3), 4.07 and 4.14 (each 1H, *dd*, *J* = 12.0 and 6.7 Hz, H_a-1), 4.28 (2 × 1H, *d*, *J* = 7.8 Hz, H-1'), 4.35 (2 × 1H, *br d*, *J* = 10.5 Hz, H_b-1), 5.23 (2 × 1H, *br*, H-2), 5.28-5.32 (2 × 2H, *br*)

^{13}C-NMR (75 MHz, $CDCl_3$, Figure 108) δ: 14.5 (*q*), 23.1 (*t*), 25.3 (*t*), 27.5 (*t*), 27.6 (*t*), 29.2 (*t*), 29.6 (*t*), 29.7 (*t*), 29.8 (*t*), 29.9 (*t*), 30.0 (*t*), 30.1 (*t*), 32.3 (*t*), 34.5 (*t*), 34.7 (*t*), 61.8 (*t*, C-6'), 63.1 and 63.2 (*t*, C-1), 68.6 (*t*, C-3), 69.8 (*d*, C-3'), 70.5 (*d*, C-2), 73.8 (*d*, C-2'), 76.2 (*d*, C-5'), 76.6 (*d*, C-4'), 103.7 and 103.9 (*d*, C-1'), 130.1 (*d*), 130.4 (*d*), 173.8 and 173.9 (*s*, carbonyl), 174.1 and 174.2 (*s*, carbonyl)

IR (cm^{-1}): 3309 (ν O-H), 2923 (ν C-H), 1737 (ν C=O) (Figure 109)

Positive-ion FABMS $[M + Na]^+$ *m/z* : 723.6 (Figure 110)

Negative-ion FABMS $[M - H]^-$ *m/z* : 699.2 (Figure 111)

Elemental analysis for $C_{39}H_{72}O_{10}$ calcd. C: 66.808 H: 10.359

found C: 66.879 H: 10.398

*1-O-stearoyl-2-O-lauroyl-3-O-β-D-glucopyranosyl-rac-glycerol (**6l**)*

(28.2 mg, 40.2%)

^{1}H-NMR (300 MHz, $CDCl_3$, Figure 112) δ: 0.85 (2 × 6H, *br t*, *J* = 6.8 Hz), 1.23 (2 × 44H, *br s*), 1.57 (2 × 4H, *br*), 2.29 (2 × 4H, *br t*, *J* = 6.9 Hz), 3.27-3.35 (2 × 2H, H-2' and H-5'), 3.39-3.58 (2 × 2H, H-3' and H-4'), 3.62 and 3.65 (each 1H, *dd*, *J* = 10.7 and 6.4 Hz, H_a-3), 3.79 (2 × 2H, *br* s, H_2-6'), 3.89 (2 × 1H, *br d*, *J* = 10.6 Hz, H_b-3), 4.09 and 4.15 (each 1H, *dd*, *J* = 12.0 and 6.6 Hz, H_a-1), 4.28 (2 × 1H, *d*, *J* = 7.8 Hz, H-1'), 4.35 (2 × 1H, *br d*, *J* = 11.0 Hz, H_b-1), 5.24 (2 × 1H, *br*, H-2)

^{13}C-NMR (75 MHz, $CDCl_3$, Figure 113) δ: 14.6 (*q*), 23.2 (*t*), 25.4 (*t*), 25.5 (*t*), 29.6 (*t*), 29.7 (*t*), 29.8 (*t*), 30.0 (*t*), 30.1 (*t*), 30.2 (*t*), 32.4 (*t*), 34.7 (*t*), 34.8 (*t*), 62.0 (*t*, C-6'), 63.1 and 63.2 (*t*, C-1), 68.6 (*t*, C-3), 70.0 (*d*, C-3'), 70.5 and 70.6 (*d*, C-2),

73.7 (*d*, C-2'), 76.2 and 76.3 (*d*, C-5'), 76.5 (*d*, C-4'), 103.7 and 103.8 (*d*, C-1'), 173.6 and 173.7 (*s*, carbonyl), 173.9 (*s*, carbonyl)

^{1}H-^{1}H COSY: (Figure 114)

IR (cm^{-1}): 3295 (ν O-H), 2919 (ν C-H), 1733 (ν C=O) (Figure 115)

Positive-ion FABMS $[M + Na]^{+}$ *m/z* : 725.5 (Figure 116)

Negative-ion FABMS $[M - H]^{-}$ *m/z* : 701.4 (Figure 117)

Elemental analysis for $C_{39}H_{74}O_{10}$ calcd. C: 66.617 H: 10.616

found C: 66.520 H: 10.566

*1-O-stearoyl-2-O-behenoyl-3-O-β-D-glucopyranosyl-rac-glycerol (**6m**)*

(26.1 mg, 31.0%)

^{1}H-NMR (300 MHz, $CDCl_3$, Figure 118) δ: 0.84 (2 × 6H, *br t*, *J* = 6.8 Hz), 1.23 (2 × 64H, *br s*), 1.57 (2 × 4H, *br*), 2.29 (2 × 4H, *br t*, *J* = 7.0 Hz), 3.28-3.37 (2 × 2H, H-2' and H-5'), 3.45-3.59 (2 × 2H, H-3' and H-4'), 3.62 and 3.65 (each 1H, *dd*, *J* = 10.7 and 6.4 Hz, H_a-3), 3.79 (2 × 2H, *br s*, H_2-6'), 3.87 (2 × 1H, *br d*, *J* = 10.6 Hz, H_b-3), 4.07 and 4.13 (each 1H, *dd*, *J* = 12.0 and 6.7 Hz, H_a-1), 4.29 (2 × 1H, *d*, *J* = 7.8 Hz, H-1'), 4.35 (2 × 1H, *br d*, *J* = 11.0 Hz, H_b-1), 5.27 (2 × 1H, *br*, H-2)

^{13}C-NMR (75 MHz, $CDCl_3$, Figure 119) δ: 14.6 (*q*), 23.2 (*t*), 25.4 (*t*), 29.6 (*t*), 29.7 (*t*), 29.8 (*t*), 29.9 (*t*), 30.2 (*t*), 32.4 (*t*), 34.6 (*t*), 34.8 (*t*), 39.9 (*t*), 40.3 (*t*), 40.5 (*t*), 40.8 (*t*), 62.7 (*t*, C-6'), 62.9 and 63.0 (*t*, C-1), 68.4 and 68.5 (*t*, C-3), 70.5 and 70.5 (*d*, C-3'), 70.9 (*d*, C-2), 73.9 and 74.0 (*d*, C-2'), 76.3 and 76.4 (*d*, C-5'), 76.9 (*d*, C-4'), 103.8 and 103.9 (*d*, C-1'), 173.5 and 173.6 (*s*, carbonyl), 173.7 (*s*)

IR (cm^{-1}): 3295 (ν O-H), 2917 (ν C-H), 1740 (ν C=O) (Figure 120)

Positive-ion FABMS $[M + Na]^{+}$ *m/z* : 865 (Figure 121)

Negative-ion FABMS $[M - H]^{-}$ *m/z* : 841 (Figure 122)

Elemental analysis for $C_{49}H_{94}O_{10}$ calcd. C: 69.777 H: 11.242

found C: 69.809 H: 11.012

*1-O-behenoyl-2-O-lauroyl-3-O-β-D-glucopyranosyl-rac-glycerol (**6n**)*

(28.6 mg, 37.7%)

^{1}H-NMR (300 MHz, $CDCl_3$, Figure 123) δ: 0.85 (2 × 6H, *br t*, *J* = 6.9 Hz), 1.23 (2 × 52H, *br s*), 1.57 (2 × 4H, *br*), 2.29 (2 × 4H, *br t*, *J* = 7.0 Hz), 3.28-3.39 (2 ×

2H, H-2' and H-5'), 3.45-3.60 (2 × 2H, H-3' and H-4'), 3.62 and 3.65 (each 1H, *dd*, *J* = 10.7 and 6.4 Hz, H_a-3), 3.79 (2 × 2H, *br s*, H_2-6'), 3.88 (2 × 1H, *br d*, *J* = 10.6 Hz, H_b-3), 4.08 and 4.15 (each 1H, *dd*, *J* = 12.0 and 6.7 Hz, H_a-1), 4.28 (2 × 1H, *d*, *J* = 7.8 Hz, H-1'), 4.35 (2 × 1H, *br d*, *J* = 12.1 Hz, H_b-1), 5.23 (2 × 1H, *br*, H-2)

^{13}C-NMR (75 MHz, $CDCl_3$, Figure 124) δ: 14.5 (*q*), 23.1 (*t*), 25.3 (*t*), 29.5 (*t*), 29.6 (*t*), 29.7 (*t*), 30.0 (*t*), 30.1 (*t*), 32.3 (*t*), 34.5 (*t*), 34.7 (*t*), 61.6 (*t*, C-6'), 63.2 and 63.3 (*t*, C-1), 68.5 (*t*, C-3), 69.6 (*d*, C-3'), 70.4 and 70.5 (*d*, C-2), 73.5 and 73.6 (*d*, C-2'), 76.2 (*d*, C-5'), 76.6 (*d*, C-4'), 103.7 and 103.8 (*d*, C-1'), 173.8 and 173.9 (*s*, carbonyl), 174.2 and 174.3 (*s*, carbonyl)

^{1}H-^{1}H COSY: (Figure 125)

IR (cm^{-1}): 3295 (ν O-H), 2917 (ν C-H), 1736 (ν C=O) (Figure 126)

Positive-ion FABMS $[M + Na]^+$ *m/z* : 781.6 (Figure 127)

Negative-ion FABMS $[M - H]^-$ *m/z* : 757.5 (Figure 128)

Elemental analysis for $C_{43}H_{82}O_{10}$ calcd. C: 68.021 H: 10.894

found C: 68.290 H: 11.094

*1-O-behenoyl-2-O-oleoyl-3-O-β-D-glucopyranosyl-rac-glycerol (**6o**)*

(26.8 mg, 31.9%)

^{1}H-NMR (300 MHz, $CDCl_3$, Figure 129) δ: 0.85 (2 × 6H, *br t*, *J* = 6.8 Hz), 1.23 (2 × 61H, *br s*), 1.57 (2 × 4H, *br*), 1.98 (2 × 2H, *br*), 2.29 (2 × 4H, *br t*, *J* = 6.9 Hz), 3.28-3.39 (2 × 2H, H-2' and H-5'), 3.44-3.61 (2 × 2H, H-3' and H-4'), 3.62 and 3.65 (each 1H, *dd*, *J* = 10.7 and 6.4 Hz, H_a-3), 3.80 (2 × 2H, *br s*, H_2-6'), 3.89 (2 × 1H, *br d*, *J* = 10.6 Hz, H_b-3), 4.07 and 4.14 (each 1H, *dd*, *J* = 12.0 and 6.6 Hz, H_a-1), 4.28 (2 × 1H, *d*, *J* = 7.8 Hz, H-1'), 4.34 (2 × 1H, *br d*, *J* = 12.0 Hz, H_b-1), 5.23 (2 × 1H, *br*, H-2), 5.31 (2 × 2H, *br*)

^{13}C-NMR (75 MHz, $CDCl_3$, Figure 130) δ: 14.5 (*q*), 23.1 (*t*), 25.3 (*t*), 27.5 (*t*), 27.6 (*t*), 29.6 (*t*), 29.7 (*t*), 29.8 (*t*), 29.8 (*t*), 29.9 (*t*), 30.1 (*t*), 30.6 (*t*), 31.6 (*t*), 32.3 (*t*), 34.5 (*t*), 34.7 (*t*), 38.5 (*t*), 62.5 (*t*, C-6'), 62.9 and 63.1 (*t*, C-1), 68.4 (*t*, C-3), 70.5 (*d*, C-3'), 70.7 (*d*, C-2), 73.7 and 73.8 (*d*, C-2'), 76.4 (*d*, C-5'), 76.8 (*d*, C-4'), 103.7 and 103.9 (*d*, C-1'), 129.9 (*d*), 130.2 (*d*), 173.4 (*s*, carbonyl), 173.6 (*s*, carbonyl)

^{1}H-^{1}H COSY: (Figure 131)

Positive-ion FABMS $[M + Na]^+$ *m/z* : 863.7 (Figure 132)

Negative-ion FABMS $[M - H]^-$ *m/z* : 839.3 (Figure 133)

Elemental analysis for $C_{49}H_{92}O_{10}$ calcd. C: 69.944 H: 11.029
found C: 69.817 H: 10.898

*1-O-linolenoyl-2-O-linoleoyl-3-O-β-D-glucopyranosyl-rac-glycerol (**6p**)*
(24.0 mg, 30.9%)

^{1}H-NMR (300 MHz, $CDCl_3$, Figure 134) δ: 0.85 (2 × 3H, *br t*, *J* = 6.9 Hz), 0.93 (2 × 3H, *t*, *J* = 7.5 Hz), 1.24 (2 × 35H, *br*), 1.54 (2 × 4H, *br*), 2.08 (2 × 8H, *br*), 2.25 (2 × 10H, *br t*, *J* = 7.0 Hz), 2.76 (2 × 5H, *br t*, *J* = 5.5 Hz), 3.21-3.40 (2 × 2H, H-2' and H-5'), 3.41-3.60 (2 × 2H, H-3' and H-4'), 3.62 and 3.65 (each 1H, *dd*, *J* = 10.7 and 6.4 Hz, H_a-3), 3.80 (2 × 2H, *br* s, H_2-6'), 3.87 (2 × 1H, *br d*, *J* = 10.6 Hz, H_b-3), 4.07 and 4.13 (each 1H, *dd*, *J* = 12.0 and 6.6 Hz, H_a-1), 4.27 (2 × 1H, *d*, *J* = 7.5 Hz, H-1'), 4.35 (2 × 1H, *br d*, *J* = 12.0 Hz, H_b-1), 5.21-5.42 (2 × 10H, *br*, overlapped, H-2 and olefinic)

^{13}C-NMR (75 MHz, $CDCl_3$, Figure 135) δ: 14.8 (*q*), 21.1 (*t*), 25.4 (*t*), 26.0 (*t*), 26.1 (*t*), 26.2 (*t*), 27.5 (*t*), 27.6 (*t*), 27.7 (*t*), 29.6 (*t*), 29.7 (*t*), 29.8 (*t*), 29.9 (*t*), 30.2 (*t*), 34.6 (*t*), 34.7 (*t*), 62.2 (*t*, C-6'), 63.1 and 63.2 (*t*, C-1), 68.6 (*t*, C-3), 70.0 (*d*, C-3'), 70.5 and 70.6 (*d*, C-2), 73.8 and 73.9 (*d*, C-2'), 76.1 and 76.2 (*d*, C-5'), 76.7 (*d*, C-4'), 103.7 and 103.8 (*d*, C-1'), 127.4 (*d*), 128.0 (*d*), 128.1 (*d*), 128.4 (*d*), 128.5 (*d*), 128.6 (*d*), 130.1 (*d*), 130.2 (*d*), 130.4 (*d*), 130.5 (*d*), 132.2 (*d*), 173.5 and 173.6 (*s*, carbonyl), 173.9 (*s*, carbonyl)

Elemental analysis for $C_{45}H_{76}O_{10}$ calcd. C: 70.446 H: 9.992
found C: 70.801 H: 10.285

*1-O-benzoyl-2-O-lauroyl-3-O-β-D-glucopyranosyl-rac-glycerol (**6q**)*
(18.4 mg, 34.0%)

^{1}H-NMR (300 MHz, $CDCl_3$, Figure 136) δ: 0.85 (2 × 3H, *br t*, *J* = 6.9 Hz), 1.23 (2 × 18H, *br s*), 1.54 (2 × 2H, *br*), 2.20 (2 × 2H, *br t*, *J* = 7.0 Hz), 3.20-3.42 (2 × 2H, H-2' and H-5'), 3.43-3.62 (2 × 2H, H-3' and H-4'), 3.80 (2 × 2H, *br* s, H_2-6'), 3.90-4.15(2 × 2H, *br*), 4.30 (2 × 1H, *br*, H-1'), 4.32-4.75 (2 × 2H, *br*, H_2-1), 5.35 (2 × 1H, *br*, H-2), 7.30-7.50 and 7.85 (2 × 5H, aromatic)

^{13}C-NMR (75 MHz, $CDCl_3$, Figure 137) δ:14.6 (*q*), 23.0 (*t*), 25.2 (*t*), 25.3 (*t*), 29.5 (*t*), 29.6(*t*), 29.7 (*t*), 29.9 (*t*), 30.0 (*t*), 32.3 (*t*), 34.5 (*t*), 34.6 (*t*), 62.1 (*t*, C-6'),

63.7 (*t*, C-1), 68.5 and 68.6 (*t*, C-3), 70.1 (*d*, C-3'), 70.4 (*d*, C-2), 73.9 (*d*, C-2'), 76.1 and 76.2 (*d*, C-5'), 76.6 (*d*, C-4'), 103.7 and 103.9 (*d*, C-1'), 128.8, 130.1, 133.7, 166.5 and 166.8 (*s*, carbonyl), 173.8 (*s*, carbonyl)

Elemental analysis for $C_{28}H_{44}O_{10}$ calcd. C: 62.188 H: 8.208

found C: 62.286 H: 8.395

*1,2-di-O-lauroyl-3-O-β-D-galactopyranosyl-rac-glycerol (**13a**)*

(30.8 mg, 49.8%)

^{1}H-NMR (300MHz, $CDCl_3$-D_2O, Figure 138) δ: 0.85 (2 × 6H, *br t*, *J* = 6.7 Hz), 1.24 (2 × 32H, *br s*), 1.52 (2 × 4H, *br*), 2.24 (2 × 4H, *br t*, *J* = 7.0 Hz), 3.45-3.62 (2 × 3H, H-2', 3' and 5'), 3.63-3.74 (2 × 1H, *br*, H_a-3), 3.80 (2 × 2H, *br s*, H_2-6'), 3.86-3.92 (2 × 1H, *br*, H_b-3), 3.96 (2 × 1H, *br s*, H-4'), 4.08-4.18 (2 × 1H, H_a-1), 4.22 (2 × 1H, *d*, *J* = 7.8 Hz, H-1'), 4.39 (2 × 1H, *br d*, *J* = 11.4 Hz, H_b-1), 5.23 (2 × 1H, *br*, H-2)

^{13}C-NMR (75 MHz, $CDCl_3$, Figure 139) δ: 14.7 (*q*), 23.2 (*t*), 25.5 (*t*), 29.4 (*t*), 29.7 (*t*), 29.9 (*t*), 30.0 (*t*), 30.2 (*t*), 32.4 (*t*), 34.7 (*t*), 34.8 (*t*), 61.8 (*t*, C-6'), 63.4 (*t*, C-1), 68.5 (*t*, C-3), 69.2 (*d*, C-4'), 70.6 (*d*, C-2), 71.5 (*d*, C-2'), 73.6 (*d*, C-3'), 74.9 and 75.0 (*d*, C-5'), 104.2 and 104.3 (*d*, C-1'), 173.7 and 173.8 (*s*, carbonyl), 174.1 and 174.3 (*s*, carbonyl)

^{1}H-^{1}H COSY: (Figure 140)

HMQC: (Figure 141)

IR (cm^{-1}): 3264 (ν O-H), 2920 (ν C-H), 1736 (ν C=O) (Figure 142)

Positive-ion FABMS $[M + Na]^+$ *m/z* : 641.4 (Figure 143)

Negative-ion FABMS $[M - H]^-$ *m/z* : 617.2 (Figure 144)

Elemental analysis for $C_{33}H_{62}O_{10}$ calcd. C: 64.036 H: 10.104

found C: 64.138 H: 10.305

*1,2-di-O-linoleoyl-3-O-β-D-galactopyranosyl-rac-glycerol (**13b**)*

(mixture, 24.0 mg, 31.3%)

^{1}H-NMR ($CDCl_3$, Figure 145) δ: 0.85 (2 × 6H, *br*), 1.30 (2 × 35H, *br*), 1.58 (2 × 4H, *br*), 2.02 (2 × 8H, *br*), 2.28 (2 × 4H, *br t*, *J* = 7.0 Hz), 2.76 (2 × 3H, *br t*, *J* = 5.5 Hz), 3.45-3.60 (2 × 3H, H-2', 3' and 5'), 3.63 and 3.70 (each 1H, *dd*, *J* = 10.9 and 5.4 Hz, H_a-3), 3.80 (2 × 2H, *br s*, H_2-6'), 3.84-3.93 (2 × 1H, *br*, H_b-3), 3.98 (2 × 1H,

br s, H-4'), 4.08-4.18 (2 × 1H, *br*, H_a-1), 4.24 (2 × 1H, *d*, *J* = 7.5 Hz, H-1'), 4.37 (2 × 1H, *br d*, *J* = 9.0 Hz, H_b-1), 5.21-5.40 (2 × 8H, *br*, H-2 and olefinic)

^{13}C-NMR (75 MHz, $CDCl_3$, Figure 146) δ: 14.7 (*q*), 22.2 (*t*), 23.0 (*t*), 25.3 (*t*), 27.3 (*t*), 27.5 (*t*), 29.4 (*t*), 29.6 (*t*), 29.8 (*t*), 29.9 (*t*), 30.1(*t*), 30.2 (*t*), 31.2 (*t*), 34.5 (*t*), 34.6 (*t*), 35.0 (*t*), 62.4 and 62.5 (*t*, C-6'), 63.1 and 63.2 (*t*, C-1), 68.5 and 68.6 (*t*, C-3), 69.5 (*d*, C-4'), 70.6 (*d*, C-2), 71.5 and 71.6 (*d*, C-2'), 73.6 (*d*, C-3'), 74.8 and 74.9 (*d*, C-5'), 104.2 and 104.4 (*d*, C-1'), 128.3 (*d*), 128.5 (*d*), 130.4 (*d*), 130.6 (*d*), 173.9 and 174.0 (*s*, carbonyl), 174.2 (*s*, carbonyl)

Positive-ion FABMS $[M + Na]^+$ *m/z* : 801.6 (Figure 147)

Negative-ion FABMS $[M - H]^-$ *m/z* : 777.2 (Figure 148)

Elemental analysis for $C_{45}H_{78}O_{10}$ calcd. C: 69.359 H: 10.097

found C: 68.995 H: 10.386

*1,2-di-O-linolenoyl-3-O-β-D-galactopyranosyl-rac-glycerol (**13c**)*

(mixture, 24.0 mg, 31.0%)

^{1}H-NMR (300 MHz, $CDCl_3$, Figure 149) δ: 0.95 (2 × 6H, *br t*, *J* = 6.7 Hz), 1.26 (2 × 30H, *br s*), 1.50 (2 × 4H, *br*), 2.02 (2 × 11H, *br*), 2.30 (2 × 4H, *br t*, *J* = 7.0 Hz), 2.76 (2 × 7H, *br t*, *J* = 5.5 Hz), 3.45-3.60 (2 × 3H, H-2', 3' and 5'), 3.62-3.73 (2 × 1H, H_a-3), 3.80 (2 × 2H, *br s*, H_2-6'), 3.84 and 3.89 (each 1H, *dd*, *J* = 10.9 and 4.9 Hz, H_b-3), 3.96 (2 × 1H, *br s*, H-4'), 4.08 and 4.12 (each 1H, *dd*, *J* = 12.0 and 3.3 Hz, H_a-1), 4.22 (2 × 1H, *d*, *J* = 7.1 Hz, H-1'), 4.35 (2 × 1H, *br d*, *J* = 10.4 Hz, H_b-1), 5.20-5.40 (2 × 13H, *br*, H-2 and olefinic)

^{13}C-NMR (75 MHz, $CDCl_3$, Figure 150) δ: 14.7 (*q*), 22.2 (*t*), 23.0 (*t*), 25.3 (*t*), 27.3 (*t*), 27.5 (*t*), 29.4 (*t*), 29.6 (*t*), 29.8 (*t*), 29.9 (*t*), 30.1(*t*), 30.2 (*t*), 31.2 (*t*), 34.5 (*t*), 34.6 (*t*), 35.0 (*t*), 62.1 and 62.2 (*t*, C-6'), 63.2 and 63.3 (*t*, C-1), 68.5 (*t*, C-3), 69.4 (*d*, C-4'), 70.6 (*d*, C-2), 71.5 and 71.6 (*d*, C-2'), 73.6 (*d*, C-3'), 74.8 and 74.9 (*d*, C-5'), 104.1 and 104.3 (*d*, C-1'), 127.4(*d*), 128.0 (*d*), 128.5 and 128.6 (*d*), 130.5 (*d*), 132.0 (*d*), 173.7 and 173.8 (*s*, carbonyl), 174.0 and 174.1 (*s*, carbonyl)

IR (cm^{-1}): 3295 (ν O-H), 2926 (ν C-H), 1739 (ν C=O) (Figure 151)

Elemental analysis for $C_{45}H_{74}O_{10}$ calcd. C: 69.720 H: 9.629

found C: 69.918 H: 9.807

*1-O-behenoyl-2-O-lauroyl-3-O-β-D-galactopyranosyl-rac-glycerol (**13d**)*

(30.2 mg, 39.8%)

^{1}H-NMR (300 MHz, $CDCl_3$, Figure 152) δ: 0.85 (2 × 6H, *br t*, *J* = 6.9 Hz), 1.23 (2 × 52H, *br s*), 1.57 (2 × 4H, *br*), 2.29 (2 × 4H, *br t*, *J* = 7.0 Hz), 3.45-3.63 (2 × 3H, H-2', 3' and 5'), 3.68-3.75 (2 × 1H, *br*, H_a-3), 3.80 (2 × 2H, *br s*, H_2-6'), 3.86-3.94 (2 × 1H, *br*, H_b-3), 3.97 (2 × 1H, *br s*, H-4'), 4.09 and 4.14 (each 1H, *dd*, 12.0 and 4.6 Hz, H_a-1), 4.22 (2 × 1H, *d*, *J* = 7.8 Hz, H-1'), 4.35 (2 × 1H, *br d*, *J* = 12.1 Hz, H_b-1), 5.25 (2 × 1H, *br*, H-2)

^{13}C-NMR (75 MHz, $CDCl_3$, Figure 153) δ: 14.5 (*q*), 23.0 (*t*), 25.3 (*t*), 29.5 (*t*), 29.6 (*t*), 29.7 (*t*), 29.9 (*t*), 30.0 (*t*), 30.1 (*t*), 32.3 (*t*), 34.6 (*t*), 34.7 (*t*), 61.9 and 62.0 (*t*, C-6'), 63.2 and 63.3 (*t*, C-1), 68.5 (*t*, C-3), 69.2 (*d*, C-4'), 70.5 and 70.6 (*d*, C-2), 71.4 and 71.5 (*d*, C-2'), 73.6 (*d*, C-3'), 74.8 and 74.9 (*d*, C-5'), 104.2 and 104.4 (*d*, C-1'), 173.9 and 174.0 (*s*, carbonyl), 174.2 and 174.3 (*s*, carbonyl)

IR (cm^{-1}): 3253 (ν O-H), 2918 (ν C-H), 1736 (ν C=O) (Figure 154)

Elemental analysis for $C_{43}H_{82}O_{10}$ calcd. C: 68.021 H: 10.894

found C: 68.208 H: 10.998

*1-O-linolenoyl-2-O-linoleoyl-3-O-β-D-galactopyranosyl-rac-glycerol (**13e**)*

(23.2 mg, 29.9 %)

^{1}H-NMR (300 MHz, $CDCl_3$, Figure 155) δ: 0.85 (2 × 3H, *br*), 0.95 (2 × 3H, *t*, *J* = 7.5 Hz), 1.28 (2 × 29H, *br s*), 1.60 (2 × 4H, *br*), 2.02 (2 × 8H, *br*), 2.31 (2 × 4H, *br t*, *J* = 7.0 Hz), 2.78 (2 × 5H, *br t*, *J* = 5.5 Hz), 3.45-3.62 (2 × 3H, H-2', 3' and 5'), 3.65-3.72 (2 × 1H, *m*, H_a-3), 3.80 (2 × 2H, *br*, H_2-6'), 3.85-3.92 (2 × 1H, *m*, H_b-3), 3.98 (2 × 1H, *br s*, H-4'), 4.08 and 4.13 (each 1H, *dd*, *J* = 12.0 and 4.4 Hz, H_a-1), 4.22 (2 × 1H, *br d*, *J* = 7.5 Hz, H-1'), 4.38 (2 × 1H, *br d*, *J* = 10.4 Hz, H_b-1), 5.22-5.40 (2 × 10H, *br*, H-2 and olefinic)

^{13}C-NMR (75MHz, $CDCl_3$, Figure 156) δ: 14.6 (*q*), 14.7 (*q*), 21.1(*t*), 23.1 (*t*), 25.4 (*t*), 26.0 (*t*), 26.2 (*t*), 27.7 (*t*), 29.6 (*t*), 29.7 (*t*), 29.8 (*t*), 30.1(*t*), 32.0 (*t*), 34.6 (*t*), 34.8 (*t*), 62.3 (*t*, C-6'), 63.2 and 63.3 (*t*, C-1), 68.5 and 68.6 (*t*, C-3), 69.4 (*d*, C-4'), 70.6 (*d*, C-2), 71.6 (*d*, C-2'), 73.7 (*d*, C-3'), 74.8 and 74.9 (*d*, C-5'), 104.1 and 104.3

(*d*, C-1'), 127.4 (*d*), 128.0 (*d*), 128.2 (*d*), 128.4 (*d*), 128.5 (*d*), 130.1 (*d*), 130.3 (*d*), 130.4 (*d*), 130.5 (*d*), 132.2 (*d*), 173.7 and 173.8 (*s*, carbonyl), 174.0 and 174.1 (*s*, carbonyl)

Elemental analysis for $C_{45}H_{76}O_{10}$	calcd.	C: 70.446	H: 9.992
	found	C: 70.725	H: 10.188

4.7 Preparation of 1-*O*-acyl-3-*O*-β-D-glycopyranosyl-*rac*-glycerols (8a-b, 15)

*1-O-lauroyl-3-O-β-D-glucopyranosyl-rac-glycerol(**8a**)*

(26.6 mg, 61%)

8a was prepared from **7a** according to the general procedure for selective removal of acetyl protecting groups in ***Sec 4.6***

^{1}H-NMR (300 MHz, $CDCl_3$, Figure 157) δ: 0.85 (2 × 3H, *br t*, *J* = 6.9 Hz), 1.25 (2 × 17H, *br s*), 2.30 (2 × 2H, *br t*, *J* = 7.0 Hz), 3.25-3.42 (2 × 2H, H-2' and H-5'), 3.43-3.55 (2 × 2H, H-3' and H-4'), 3.65-3.90 (2 × 4H, H_2-3, H_2-6'), 3.91-4.10 (2 × 3H, H_2-1, H-2) 4.35 (2 × 1H, H-1')

^{13}C-NMR (75 MHz, $CDCl_3$, Figure 158) δ: 14.5 (*q*), 23.1 (*t*), 25.3 (*t*), 29.5 (*t*), 29.6 (*t*), 29.7 (*t*), 30.0 (*t*), 30.1 (*t*), 32.3 (*t*), 34.5 (*t*), 34.7 (*t*), 61.4 and 61.5 (*t*, C-6'), 65.4 and 65.5 (*t*, C-1), 68.9 and 69.2 (*t*, C-2), 69.6 (*d*, C-3'), 71.7 (*d*, C-3), 72.2 (*d*, C-2'), 73.8 (*d*, C-5'), 76.2 and 76.5 (*d*, C-4'), 103.2 and 103.6 (*d*, C-1'), 174.3 and 174.4 (*s*, carbonyl)

Elemental analysis for $C_{21}H_{40}O_9$	calcd.	C: 57.763	H: 9.241
	found	C: 57.853	H: 9.407

*1-O-linolenoyl-3-O-β-D-glucopyranosyl-rac-glycerol (**8b**)*

(24.8 mg, 48.3%)

8b was prepared from **7b** according to the general procedure for selective removal of acetyl protecting groups in ***Sec 4.6***

^{1}H-NMR (300 MHz, $CDCl_3$, Figure 159) δ: 0.95 (2 × 3H, *br t*, *J* = 6.9 Hz), 1.25 (2 × 10H, *br s*), 1.60 (2 × 2H, *br*), 2.00 (2 × 4H, *br*), 2.30 (2 × 2H, *br t*, *J* = 7.0 Hz), 2.76 (2 × 4H, *br t*, *J* = 5.5 Hz), 3.25-3.37 (2 × 2H, H-2' and H-5'), 3.38-3.50 (2 ×

2H, H-3' and H-4'), 3.60-3.90 (2 × 4H, H_2-3, H_2-6'), 4.00-4.10 (2 × 3H, H_2-1, H-2), 4.35 (2 × 1H, *d*, *J* = 7.6 Hz, H-1'), 5.20-5.40 (2 × 6H, *br*)

^{13}C-NMR (75 MHz, $CDCl_3$, Figure 160) δ: 14.8 (*q*), 21.1 (*t*), 25.4 (*t*), 26.0 (*t*), 26.1 (*t*), 26.2 (*t*), 27.5 (*t*), 27.6 (*t*), 27.7 (*t*), 29.6 (*t*), 29.7 (*t*), 29.8 (*t*), 29.9 (*t*), 30.2 (*t*), 34.6 (*t*), 34.7 (*t*), 61.1 and 61.2 (*t*, C-6'), 65.4 and 65.5 (*t*, C-1), 68.7 and 69.0 (*t*, C-2), 69.6 and 69.7 (*d*, C-3'), 7.1.5 and 71.9 (*d*, C-3), 73.6 (*d*, C-2'), 76.5 and 76.6 (*d*, C-5', C-4'), 103.1 and 103.5 (*d*, C-1'), 127.4 (*d*), 128.0 (*d*), 128.5 (*d*), 128.6 (*d*), 130.4 (*d*), 132.2 (*d*), 174.5 and 174.6 (*s*, carbonyl)

Elemental analysis for $C_{27}H_{46}O_9$ calcd. C: 62.997 H: 9.014

found C: 63.086 H: 9.110

*1-O-linolenoyl-3-O-β-D-galactopyranosyl-rac-glycerol (**15**)*

(22.4 mg, 43.6%)

15 was prepared from **14a** according to the general procedure for selective removal of acetyl protecting groups in ***Sec 4.6***

^{1}H-NMR (300 MHz, $CDCl_3$, Figure 161) δ: 0.95 (2 × 3H, *t*, *J* = 7.5 Hz), 1.25 (2 × 10H, *br s*), 1.56 (2 × 2H, *br*), 2.00 (2 × 4H, *br*), 2.31 (2 × 2H, *br t*, *J* = 7.2 Hz), 2.78 (2 × 4H, *br*), 3.50-4.35 (2 × 12, not assigned), 5.20-5.45 (2 × 6H, *br*)

^{13}C-NMR (75MHz, $CDCl_3$, Figure 162) δ: 14.6, 14.7, 21.1, 23.1, 25.4, 26.0, 26.2, 27.7, 29.6, 29.7, 29.8, 30.1, 32.0, 34.6, 34.8, 61.5, 65.4 and 65.5, 68.9, 69.2, 71.6 and 71.9, 73.7 and 73.8, 74.9, 103.8, 104.3, 127.4, 128.0,128.2, 128.5, 128.6, 130.5, 132.2, 174.3, 174.4

IR (cm^{-1}): 3327 (ν O-H), 2930 (ν C-H), 1734 (ν C=O) (Figure 163)

Elemental analysis for $C_{27}H_{46}O_9$ calcd. C: 62.997 H: 9.014

found C: 63.189 H: 9.195

5. Synthesis of 1,2-di-*O*-acyl-*rac*-glycerols

1,2-O-isopropylidene-3-O-benzyl-rac-glycerol **(*16*)** (150.2 mg, 67.6%)

To a suspension of NaH (1.5 mmol) in dry THF was added a solution of **2** (1 mmol) in THF. Then, a solution of BnBr (2 mmol) in THF was added dropwise, the solution was stirred overnight. One ml of ethanol was added, the solvent was evaporated and the residue was purified by column chromatography to give liquid **16**

^{1}H-NMR (300 MHz, $CDCl_3$, Figure 164) δ: 1.30, 1.40 (each 2 × 3H), 3.45 (2 × 1H, *dd*, *J* = 5.5 and 9.5 Hz, H_a-3), 3.55 (2 × 1H, 5.7 and 9.7 Hz, H_b-3), 3.73 (2 × 1H, *dd*, *J* = 6.4 and 8.1 Hz, H_a-1), 4.03 (2 × 1H, *dd*, *J* = 6.5 and 8.1 Hz, H_b-1), 4.28 (2 × 1H, *q*, 5.9 Hz, H-2), 4.51 (2 × 2H), 7.30 (2 × 5H, aromatic)

1-O-benzyl-rac-glycerol **(*17*)** (86.1 mg, 95.6%)

A solution of **16** (90 mg) in 15 ml of 60% acetic acid aqueous solution was stirred at 60 ^{o} C for 1.5 h. The mixture was concentrated and co-evaporated with toluene three times. The residue was then purified by column chromatography on silica gel column eluted with hexane : EtOAc (1:1) to give liquid **17**

^{1}H-NMR (300 MHz, $CDCl_3$, Figure 165) δ: 3.40-3.71(2 × 4H), 3.85 (2 × 1H, *br s*), 4.51 (2 × 2H), 7.30 (2 × 5H, aromatic)

^{13}C-NMR (75MHz, $CDCl_3$, Figure 166) δ: 64.5, 71.1, 72.2, 74.0, 128.1, 128.2, 128.8, 138.0

1,2-di-O-lauroyl-3-O-benzyl-rac-glycerol **(*18*)** (120.5 mg, 73.8%)

To a solution of **17** (0.3 mmol), lauric acid (0.7 mmol), and DMAP (0.03 mmol) in 8 ml dry dichloromethane, DCC (0.7 mmol) was added and stirred for 24 h at room temperature. The solid was filtered off and the solvent was evaporated *in vacuo*. The residue was purified by column chromatography on silica gel column eluted with hexane : EtOAc (5:1) to give white solid **18**

^{1}H-NMR (300 MHz, $CDCl_3$, Figure 167) δ: 0.85 (2 × 6H, *t*, *J* = 6.9 Hz), 1.26 (2 × 40H, *br s*), 1.56 (2 × 4H, *br*), 2.25 (2 × 4H), 3.56 (2 × 2H), 4.15 (2 × 1H, *dd*, *J* = 6.4 and 11.8 Hz), 4.35 (2 × 1H, *dd*, *J* = 3.7 and 11.8 Hz), 4.53 (2 × 2H), 5.22 (2 × 1H), 7.30 (2 × 5H, *br*)

^{13}C-NMR (75MHz, $CDCl_3$, Figure 168) δ: 14.6, 22.5, 25.2, 29.8, 29.9, 30.0, 30.2, 32.2, 34.8, 34.9, 35.0, 63.1, 68.7, 70.4, 73.7, 128.1, 128.8, 138.1, 173.3, 173.6

1,2-di-O-lauroyl-rac-glycerol ***(19)*** (55.8 mg, 61.5%)

A mixture of **18** (109 mg) and 30 mg of 10% Pd/C in 10 ml of ethyl acetate containing 0.25 ml each of ethanol and acetic acid was vigorous shaken under H_2 gas using Parr apparatus for 5 h. The catalyst was filtered off, the filtrate was evaporated

and purified by column chromatography, eluted with hexane : EtOAc (1:1) to give white solid **19**

^{1}H-NMR (300 MHz, $CDCl_3$, Figure 169) δ: 0.85 (2 × 6H, *t*, *J* = 6.8 Hz), 1.26 (2 × 37H, *br s*), 1.55 (2 × 4H, *br*), 2.25 (2 × 4H), 3.64 (2 × 2H, *br*, H-3), 4.15 (2 × 1H, *dd*, *J* = 5.9 and 11.9 Hz, H_a-1), 4.28 (2 × 1H, *dd*, *J* = 4.2 and 11.9 Hz, H_b-1), 5.02 (2 × 1H, *q*, 4.9 Hz, H-2)

^{13}C-NMR (75MHz, $CDCl_3$, Figure 170) δ: 14.6, 23.0, 25.4, 29.8, 29.9, 30.0, 30.2, 32.2, 32.4, 34.4, 34.5, 34.6, 34.8, 34.9, 61.8, 62.6, 72.5, 173.6, 173.9

DEPT 135: (Figure 171)

Elemental analysis: calcd. C: 70.993 H: 11.483

found C: 70.918 H: 11.505

6. Synthesis of 1-*O*-acyl-*rac*-glycerols

6.1 General Procedure for Acylation

To a solution of **2** (0.3 mmol), fatty acid (0.7 mmol), and DMAP (0.03 mmol) in 8 ml dry dichloromethane, DCC (0.7 mmol) was added and stirred for 24 h at room temperature. The solid was filtered off and the solvent was evaporated *in vacuo*. The residue was purified by column chromatography on silica gel column eluted with hexane:EtOAc (10:1) to give **20a-c**

*1-O-lauroyl-2,3-isopropylidene-rac-glycerol (**20a**)* (80.5 mg, 85.5%)

^{1}H-NMR (300 MHz, $CDCl_3$, Figure 172) δ: 0.85 (2 × 3H, *br t*, 6.8 Hz), 1.25 (2 × 26H *br s*), 1.30 and 1.40 (each 2 × 3H, *s*), 1.52 (2 × 2H, *br*), 2.30 (2 × 2H, *t*, 7.5 Hz), 3.71 (2 × 1H, *dd*, *J* = 6.2 and 8.4 Hz, H_a-3), 4.08 (2 × 1H, *dd*, *J* = 6.5 and 8.0 Hz, H_b-3), 4.09 (2 × 1H, *dd*, *J* = 4.5 and 11.2 Hz, H_a-1), 4.14 (2 × 1H, *dd*, *J* = 4.6 and 11.5 Hz, H_b-1), 4.28 (2 × 1H, *q*, 5 Hz, H-2)

^{13}C-NMR (75MHz, $CDCl_3$, Figure 173) δ: 14.4, 23.0, 25.2, 25.6, 25.7, 27.0, 29.4, 29.5, 29.6, 29.7, 29.8, 29.9, 32.2, 34.4, 64.8, 66.7, 74.0, 110.1, 173.9

1-O-strearoyl-2,3-isopropylidene-rac-glycerol ***(20b)*** (94.5 mg, 79.1%)

^{1}H-NMR (300 MHz, $CDCl_3$, Figure 174) δ: 0.85 (2 × 3H, *t*, 6.8 Hz), 1.25 (2 × 33H *br s*), 1.30 and 1.40 (each 2 × 3H, *s*), 1.52 (2 × 2H, *br*), 2.30 (2 × 2H, *t*, 7.5 Hz), 3.71 (2 × 1H, *dd*, *J* = 6.2 and 8.4 Hz, H_a-3), 4.08 (2 × 1H, *dd*, *J* = 6.5 and 8.0 Hz, H_b-3), 4.09 (2 × 1H, *dd*, *J* = 4.5 and 11.2 Hz, H_a-1), 4.14 (2 × 1H, *dd*, *J* = 4.6 and 11.5 Hz, H_b-1), 4.28 (2 × 1H, *q*, 5 Hz, H-2)

^{13}C-NMR (75MHz, $CDCl_3$, Figure 175) δ: 14.5, 23.0, 25.2, 25.6, 25.7, 27.0, 29.4, 29.5, 29.6, 29.7, 29.8, 29.9, 32.2, 34.4, 34.5, 34.6, 64.9, 66.7, 74.0, 110.1, 173.9

1-O-behenoyl-2,3-isopropylidene-rac-glycerol ***(20c)*** (98.8 mg, 72.6%)

^{1}H-NMR (300 MHz, $CDCl_3$, Figure 176) δ: 0.85 (2 × 3H, *t*, 6.8 Hz), 1.25 (2 × 47H *br s*), 1.30 and 1.40 (each 2 × 3H, *s*), 2.30 (2 × 2H, *t*, 7.5 Hz), 3.71 (2 × 1H, *dd*, *J* = 6.2 and 8.4 Hz, H_a-3), 4.08 (2 × 1H, *dd*, *J* = 6.5 and 8.0 Hz, H_b-3), 4.09 (2 × 1H, *dd*, *J* = 4.5 and 11.2 Hz, H_a-1), 4.14 (2 × 1H, *dd*, *J* = 4.6 and 11.5 Hz, H_b-1), 4.28 (2 × 1H, *q*, 5 Hz, H-2)

IR (cm^{-1}): 2918 (ν C-H), 1732 (ν C=O) (Figure 177)

6.2 General Procedure for Deacetonization

0.2 mmol of **20a-c** were deacetonized according to the general procedure for deacetonization in ***Sec 4.2***

1-O-lauroyl-rac-glycerol ***(21a)*** (50.3 mg, 91.8%)

^{1}H-NMR (300 MHz, $CDCl_3$, Figure 178) δ: 0.85 (2 × 3H), 1.25 (2 × 20H), 2.05 (2 × 1H, OH), 2.32 (2 × 2H), 2.50 (2 × 1H, OH), 3.55 (2 × 1H, *dd*, 5.6 and 11.2 Hz, H_a-3), 3.65 (2 × 1H, *dd*, 4.0 and 10.5 Hz, H_b-3), 3.90 (2 × 1H, *q*, 4.7 Hz, H-2), 4.12 (2 × 1H, *dd*, 6.0 and 11.6 Hz, H_a-1), 4.14 (2 × 1H, *dd*, 6.0 and 11.6 Hz, H_b-1)

^{13}C-NMR (75MHz, $CDCl_3$, Figure 179) δ: 14.4, 23.0, 25.3, 29.6-29.9, 32.2, 34.5, 63.7, 65.5, 70.6,174.7

IR (cm^{-1}): 3245 (ν O-H), 2917 (ν C-H), 1731 (ν C=O) (Figure 180)

Elemental analysis: calcd. C: 65.642 H: 11.026

found C: 65.583 H: 11.108

*1-O-stearoyl-rac-glycerol **(21b)*** (65.8 mg, 91.9%)

^{1}H-NMR (300 MHz, $CDCl_3$, Figure 181) δ: 0.85 (2 × 3H), 1.25 (2 × 26H), 1.60 (2 × 2H), 2.32 (2 × 2H), 3.55 (2 × 1H, *br*, H_a-3), 3.65 (2 × 1H, *br*, H_b-3), 3.90 (2 × 1H, *br s*, H-2), 4.08-4.22 (2 × 2H, *br*, H_2-1)

^{13}C-NMR (75MHz, $CDCl_3$, Figure 182) δ: 14.4, 23.0, 25.3, 29.6-29.9, 30.0, 32.3, 32.4, 34.5, 63.7, 65.5, 70.6, 174.7

Elemental analysis: calcd. C: 70.331 H: 11.814

found C: 70.399 H: 11.901

*1-O-behenoyl-rac-glycerol **(21c)*** (75.5 mg, 90.7%)

^{1}H-NMR (300 MHz, $CDCl_3$, Figure 183) δ: 0.85 (2 × 3H), 1.25 (2 × 34H), 1.60 (2 × 2H), 2.32 (2 × 2H), 3.55 (2 × 1H, *br*, H_a-3), 3.65 (2 × 1H, *br*, H_b-3), 3.90 (2 × 1H, *br s*, H-2), 4.08-4.22 (2 × 2H, *br*, H_2-1)

^{13}C-NMR (75MHz, $CDCl_3$, Figure 184) δ: 14.5, 23.0, 25.3, 29.6-29.9, 30.1, 32.3, 34.5, 63.7, 65.5, 70.7, 174.7

IR (cm^{-1}): 3295 (ν O-H), 2917 (ν C-H), 1734 (ν C=O) (Figure 185)

Elemental analysis: calcd. C: 72.399 H: 12.161

found C: 72.534 H: 12.289

7. Synthesis of 1,2-di-*O*-acyl-3-*O*-β-D-glycopyranosyl-*sn*-glycerols

*1,2:3,4:5,6-tri-O-isopropylidene-D-mannitol **(23)*** (14.6 g, 60.4%)

To a stirred solution of acetic acid (5 ml) and concentrated H_2SO_4 (10 ml) in 400 ml dry acetone was added 14.5 g (80 mmol) of dry D-mannitol (**22**). After 2 h at room temperature, the reaction mixture was then poured into a cooled, vigorously stirred suspension of 80 g Na_2CO_3 in 150 ml water until the pH was neutral. The precipitated salts were filtered on a Buchner funnel and washed with dry acetone. The filtrate and washings were then combined and evaporated under high vacuum, to give semisolid residue which was crystallized in C_2H_5OH : H_2O (1:1)

^{1}H-NMR (300 MHz, $CDCl_3$, Figure 186) δ: 1.30, 1.34, 1.38 (each 6H), 3.85-4.30 (8H, *m*)

3,4-O-isopropylidene-D-mannitol ***(24)*** (6.3 g, 70.9%)

12 g of **23** (40 mmol) was added to a stirred solution of 200 ml 65% aqueous acetic acid at 40^{o}C. After 1 h, the solution was evaporated and the residual acetic acid was removed by repeated co-distillation of toluene. Dry acetone was added and the mixture was thoroughly stirred with excess anhydrous Na_2CO_3 and then filtered. The residue was purified by column chromatography eluted with EtOAc : CH_3OH (50:1)

^{1}H-NMR (300 MHz, $CDCl_3$, Figure 187) δ: 1.35 (6H, *s*, acetonide), 3.60-3.95 (8H, *m*)

^{13}C-NMR (75 MHz, $CDCl_3$, Figure 188) δ: 27.4, 64.3, 73.5, 80.0, 110.0

1,2:5,6-tetra-O-benzyl-3,4-O-isopropylidene-D-mannitol ***(25)*** (8.2 g, 70.4%)

To a stirred solution of **24** 4.5 g (20 mmol) in dry dimethylformamide was added in portions of NaH (0.2 mol). The suspension was stirred for 0.5 h at room temperature and then cooled to 0^{o}C in ice bath. Then 120 mmol of benzyl bromide were added and the stirring continued at room temperature overnight. Methanol was added to destroy the excess NaH, the solution was diluted with water and the product was extracted with ether, then washed with water, dried with anhydrous Na_2CO_3 and evaporated to a syrup. The product was purified by column chromatography eluted with hexane : EtOAc (30:1)

^{1}H-NMR (300 MHz, $CDCl_3$, Figure 189) δ: 1.35 (6H, *s*, acetonide), 3.58-3.85 (6H, C$\underline{H}_2$OCH_2Ph, C$\underline{H}$OCH_2Ph), 4.18 (2H, *br s*), 4.46 (4H, *s*, CH_2OC$\underline{H}_2$Ph), 4.57 (2H, *d*, 11.7 Hz, CHOC$\underline{H}_2$Ph), 4.72 (2H, *d*, 11.7 Hz, CHOC$\underline{H}_2$Ph), 7.35 (20H)

^{13}C-NMR (75 MHz, $CDCl_3$, Figure 190) δ: 28.0, 71.0, 73.2, 73.7, 78.9, 79.7, 127.8, 127.9, 128.2, 128.5, 138.9, 139.0

1,2:5,6-tetra-O-benzyl-D-mannitol ***(26)*** (3.6 mg, 66.2%)

To a solution of 1M aqueous HCl /methanol (1:9 v/v) was added 6 g (10 mmol) of **25**, the mixture was stirred under reflux condition. After 3 h $NaHCO_3$ was

added to neutralize the excess acid, then extracted with ether, dried, and evaporated to give a syrup. The product was purified by column chromatography eluted with hexane : EtOAc (5:1)

^{1}H-NMR (300 MHz, $CDCl_3$, Figure 191) δ: 3.10-3.20 (2H, OH), 3.65-3.88 (6H, C<u>H</u>$_2$OCH$_2$Ph, C<u>H</u>OCH$_2$Ph), 4.00-4.10 (2H, *br*), 4.55 (4H, CH$_2$OC<u>H</u>$_2$Ph), 4.60 (2H, *d* 11.7 Hz, CHOC<u>H</u>$_2$Ph), 4.75 (2H, *d*, 11.7 Hz, CHOC<u>H</u>$_2$Ph), 7.35 (20H, aromatic)

^{13}C-NMR (75 MHz, $CDCl_3$, Figure 192) δ: 70.5, 70.7, 73.5, 74.0, 79.7, 128.0, 128.1, 128.3, 128.7, 138.4, 138.6

*1,2-di-O-benzyl-sn-glycerol **(28)*** (910 mg, 60.3%)

A solution of 3 g **26** in 25 ml ether/ethanol (4:1 v/v) and 20 ml water containing 3 g of $NaIO_4$ and 80 mg tetrabutyl ammonium bromide was vigorously stirred for 4 h. Then, 0.5 ml ethylene glycol was added to destroy the excess $NaIO_4$. The ether phase was collected and the aqueous phase was re-extracted with ether 3 times. The combined ether solution was washed with water and dried, then evaporated to syrupy aldehyde (**27**). This syrup was dissolved in 15 ml dry THF and added dropwise over 30 min to 30 ml dry THF containing 0.6 g of $LiAlH_4$. After 1 h the mixture was cooled to 0^{o}C in ice bath and excess ethyl acetate was added, followed by a little amount of water. The product was extracted with ether and purified by column chromatography eluted with 0.5% CH_3OH in $CHCl_3$.

^{1}H-NMR (300 MHz, $CDCl_3$, Figure 193)δ: 3.55-3.80 (5H, C<u>H</u>$_2$OH, C<u>H</u>$_2$OCH$_2$Ph, C<u>H</u>OCH$_2$Ph), 4.58 (2H, *s*, CH$_2$OC<u>H</u>$_2$Ph), 4.61(1H, *d*, 11.7 Hz), 4.70 (1H, *d*, 11.7 Hz, CHOC<u>H</u>(<u>H</u>)Ph), 7.35 (10H, aromatic)

^{13}C-NMR (75 MHz, $CDCl_3$, Figure 194)δ: 63.2, 70.7, 72.6, 74.0, 78.7, 128.0, 128.5, 128.8, 138.3, 138.6

*1,2-di-O-benzyl-3-O-(β-D-2',3',4',6'-tetra-O-acetyl-glucopyranosyl)-sn-glycerol **(29)*** (618.2mg, 51.6 %)

29 was prepared from **28** according to the general procedure for glycosylation as described in ***Sec.4.1***. The product was purified by column chromatography eluted with hexane : EtOAc (4:1).

^{1}H-NMR (300 MHz, $CDCl_3$, Figure 195) δ: 1.90, 1.96, 1.97, 2.01 (each 3H, *s*, acetyl), 3.50-3.78 (5H, H_2-1, H_2-3, H-5'), 3.86-3.97 (1H, *m*, H-2), 4.09 (1H, *br d*, *J* = 12.1 Hz, H_a-6'), 4.28 (1H, *dd*, *J* = 12.2 and 4.3 Hz, H_b-6'), 4.51 (1H, overlapped, H-1'), 4.51 and 4.63 (each 2H, *s*, O$C\underline{H}_2$Ph), 4.97 (1H, *dd* (apparent *t*), *J* = 8.7 Hz, H-2'), 5.03 (1H, *dd* (apparent *t*), *J* = 9.6 Hz, H-4'), 5.16 (1H, *dd* (apparent *t*), *J* = 9.2 Hz, H-3'), 7.30 (10H, *br*, aromatic H)

^{13}C-NMR (75 MHz, $CDCl_3$, Figure 196) δ: 62.4, 68.9, 69.7, 70.2, 71.8, 72.3, 72.5, 73.3, 73.9, 77.3, 101.4, 127.9, 128.6, 128.7, 138.5, 138.7, 169.4, 169.6, 170.4, 170.8

^{1}H-^{1}H COSY: (Figure 197)

*1-O-(β-D-2',3',4',6'-tetra-O-acetyl-glucopyranosyl)-sn-glycerol (**30**)*

(224 mg, 80.4 %)

A mixture of 400 mg of **29** and 90 mg of 10% Pd/C in 10 ml of ethyl acetate containing 0.25 ml each of ethanol and acetic acid was vigorous shaken under H_2 gas using Parr apparatus for 5 h. The catalyst was filtered off, the filtrate was evaporated and purified by column chromatography, eluted with ethyl acetate: hexane 3:1 to give semisolid substance **30.**

^{1}H-NMR (300 MHz, $CDCl_3$, Figure 198) δ: 2.01, 2.04, 2.06, 2.10 (each 3H, *s*, acetyl), 3.52-3.95 (6H, H_2-1, H-2, H_2-3, H-5'), 4.22 (2H, *br s*, H_2-6'), 4.56 (1H, *d*, *J* = 7.8 Hz, H-1'), 5.02 (1H, *dd* (apparent *t*), *J* = 9.4 and 7.5 Hz, H-2'), 5.09 (1H, *dd* (apparent *t*), *J* = 9.4 Hz, H-4'), 5.23 (1H, *dd* (apparent *t*), *J* = 9.4 Hz, H-3')

*1,2-di-O-lauroyl-3-O-(β-D-2',3',4',6'-tetra-O-acetyl-glucopyranosyl)-sn-glycerol (**31a**)* (210.2 mg, 89.1%)

31a was prepared from **30** according to the general procedure for preparation of mono-acid 1,2-di-*O*-acyl-3-*O*-(β-D-2',3',4',6'-tetra-*O*-acetyl-glycopyranosyl)-*rac*-glycerols as described in ***Sec 4.3***.

^{1}H-NMR (300 MHz, $CDCl_3$, Figure 199) δ: 0.83 (6H, *br t*, *J* = 6.9 Hz), 1.22 (32H, *br s*), 1.54 (4H, *br*), 1.94, 1.96, 1.98, 2.02 (each 3H, *s*, acetyl), 2.23 (4H, *br t*, *J* = 7.9 Hz), 3.57-3.70 (2H, H_a-3 and H-5'), 3.89 (1H, *dd*, *J* = 10.4 and 4.9 Hz, H_b-3), 4.05 (1H, *dd*, (apparent *t*), *J* = 6.2 Hz, H_a-1) 4.09 (1H, *br s*, H_a-6'), 4.15 (1H, *br d*, 4.6 Hz, H_b-1) 4.24 (1H, *dd*, *J* = 12.1 and 3.3 Hz, H_b-6'), 4.48 (1H, *d*, *J* = 7.8 Hz, H-1'),

4.93 (1H, *dd* (apparent *t*), *J* = 9.4 and 8.1 Hz, H-2'), 5.01 (1H, *dd* (apparent *t*), *J* = 9.6 Hz, H-4'), 5.10-5.20 (2x2H, overlapped, H-2 and H-3')

^{13}C-NMR (75 MHz, $CDCl_3$, Figure 200) δ: 14.6, 21.1, 23.2, 25.4, 26.1, 29.6, 29.7, 29.8 29.9, 30.1, 32.4, 34.4, 34.5, 34.6, 62.3, 62.6, 68.1, 68.8, 70.1, 71.5, 72.3, 73.1, 101.4, 169.4, 169.5, 170.3, 170.7, 172.9, 173.4

^{1}H-^{1}H COSY: (Figure 201)

*1,2-di-O-linolenoyl-3-O-(β-D-2',3',4',6'-tetra-O-acetyl-glucopyranosyl)-sn-glycerol (**31b**)* (160.2 mg, 56.7 %)

31b was prepared from **30** according to the general procedure for preparation of mono-acid 1,2-di-*O*-acyl-3-*O*-(β-D-2',3',4',6'-tetra-*O*-acetyl-glycopyranosyl)-*rac*-glycerols as described in ***Sec 4.3.***

^{1}H-NMR (300 MHz, $CDCl_3$, Figure 202) δ: 0.92 (6H, *t*, *J* = 7.5 Hz), 1.25 (16H, *br s*), 1.53 (4H, *br*), 1.98-2.08 (20H, overlapped), 2.25 (4H, *br t*, *J* = 7.0 Hz), 2.76 (8H, *br t*, *J* = 6.3 Hz), 3.58-3.68 (2H, H_a-3 and H-5'), 3.90 (1H, *dd*, *J* = 10.9 and 4.9 Hz, H_b-3), 4.05 (1H, *dd* (apparent *t*), *J* = 6.3 Hz, H_a-1) 4.11 (1H, *br* s, H_a-6'), 4.20 (1H, *br d*, *J* = 4.6 Hz, H_b-1) 4.27 (1H, *dd*, *J* = 12.0 and 3.6 Hz, H_b-6'), 4.48 (1H, *d*, *J* = *7.8* Hz, H-1'), 4.93 (1H, *dd* (apparent *t*), *J* = 9.3 and 8.0 Hz, H-2'), 5.03 (1H, *dd* (apparent *t*), *J* = 9.7 Hz, H-4'), 5.14 (1H, overlapped, H-2), 5.16 (1H, *dd* (apparent *t*), *J* = 9.3 Hz, H-3'), 5.20-5.41 (12H, *br*)

^{13}C-NMR (75 MHz, $CDCl_3$, Figure 203) δ: 14.8, 21.1, 25.4, 25.5, 26.0, 26.1, 26.2, 27.7, 29.6, 29.7, 30.1, 30.2, 34.6, 34.7, 62.3, 62.6, 68.2, 68.8, 70.1, 71.5, 72.3, 73.1, 101.4, 127.4, 128.0, 128.5, 128.6, 130.5, 132.2, 169.4, 169.5, 170.4, 170.8, 172.9, 173.4

*1-O-linolenoyl-2-O-lauroyl-3-O-(β-D-2',3',4',6'-tetra-O-acetyl-glucopyranosyl)-sn-glycerol (**31c**)* (165.9 mg, 64.0%)

31c was prepared from **30** according to the general procedure for preparation of mixed-acid 1,2-di-*O*-acyl-3-*O*-(β-D-2',3',4',6'-tetra-*O*-acetyl-glycopyranosyl)-*rac*-glycerols as described in ***Sec. 4.5*** .

^{1}H-NMR (300 MHz, $CDCl_3$, Figure 204) δ: 0.85 (3H, *br t*), 0.92 (3H, *t*, *J* = 7.5 Hz), 1.15-1.37 (29H, *br*), 1.53 (4H, *br*), 1.92-2.08 (16H, overlapped), 2.25 (4H, *br t*, *J* = 7.0 Hz), 2.76 (4H, *br t*, *J* = 6.3 Hz), 3.58-3.68 (2H, H_a-3 and H-5'), 3.89 (1H,

dd, *J* = 10.9 and 4.9 Hz, H_b-3), 4.05 (1H, *dd* (apparent *t)*, *J* = 6.3 Hz, H_a-1) 4.09 (1H, *br* s, H_a-6'), 4.19 (1H, *br d*, *J* = 4.6 Hz, H_b-1) 4.25 (1H, *dd*, *J* = 12.0 and 3.6 Hz, H_b-6'), 4.46 (1H, *d*, *J = 7.8* Hz, H-1'), 4.91 (1H, *dd* (apparent *t*), *J* = 9.3 and 8.0 Hz, H-2'), 5.01 (1H, *dd* (apparent *t*), *J* = 9.7 Hz, H-4'), 5.10-5.18 (2H, H-2, H-3'), 5.20-5.40 (6H, *br*)

^{13}C-NMR (75 MHz, $CDCl_3$, Figure 205) δ: 14.8, 21.1, 25.4, 26.0, 26.2, 27.5, 27.6, 27.7, 29.6, 29.7, 29.8, 29.9, 30.1, 30.2, 32.0, 34.6, 34.7, 62.3, 62.6, 68.1, 68.7, 70.1, 71.5, 72.3, 73.1, 101.4, 127.4, 128.0, 128.4, 128.5, 130.4, 132.2, 169.5, 170.3, 170.7, 172.9 173.4

*1,2-di-O-lauroyl-3-O-β-D-glucopyranosyl-sn-glycerol (**32a**)* (29.8 mg, 48.2 %)

32a was prepared from **31a** according to the general procedure for selective removal of acetyl protecting groups as described in ***Sec*. *4.6***.

$[\alpha]_D^{25}$ – 12.4° ($CHCl_3$, *c* 1.0)

^{1}H-NMR (300 MHz, $CDCl_3$, Figure 206) δ: 0.81 (6H, *br*), 1.22 (32H, *br s*), 1.55 (4H, *br*), 2.26 (4H, *br*), 3.25-3.38 (2H, H-2' and H-5'), 3.42-3.59 (2H, H-3' and H-4'), 3.62-3.70 (1H, *br*, H_a-3), 3.78 (2H, *br* s, H_2-6'), 3.85-3.87 (1H, *br*, H_b-3), 4.10-4.19 (1H, *m*, H_a-1), 4.25 (1H, *d*, *J* = 7.7 Hz, H-1'), 4.38 (1H, *br d*, *J* = 10.4 Hz, H_b-1), 5.22 (1H, *br*, H-2)

^{13}C-NMR (75 MHz, $CDCl_3$, Figure 207) δ: 14.5 (*q*), 23.0 (*t*), 25.2 (*t*), 25.3 (*t*), 29.5 (*t*), 29.6(*t*), 29.7 (*t*), 29.9 (*t*), 30.0 (*t*), 32.3 (*t*), 34.5 (*t*), 34.6 (*t*), 61.9 (*t*, C-6'), 63.2 (*t*, C-1), 68.5 (*t*, C-3), 69.8 (*d*, C-3'), 70.5 (*d*, C-2), 73.8 (*d*, C-2'), 76.2 (*d*, C-5'), 76.6 (*d*, C-4'), 103.9 (*d*, C-1'), 173.8 (*s*), 174.2 (*s*)

Elemental analysis for $C_{33}H_{62}O_{10}$ calcd. C: 64.036 H: 10.104
found C: 64.115 H: 10.189

*1,2-di-O-linolenoyl-3-O-β-D-glucopyranosyl-sn-glycerol (**32b**)* (21.5 mg, 27.7 %)

32b was prepared from **31b** according to the general procedure for selective removal of acetyl protecting groups as described in ***Sec*. *4.6***.

$[\alpha]_D^{25}$ – 9.5° ($CHCl_3$, *c* 1.0)

^{1}H-NMR (300 MHz, $CDCl_3$, Figure 208) δ: 0.93 (6H, *t*, *J* = 7.6 Hz), 1.25 (22H, *br*), 1.55 (4H, *br*), 1.95-2.12 (8H, *br*), 2.25 (4H, *br t*, *J* = 7.0 Hz), 2.75 (8H, *br t*, *J* = 5.5 Hz), 3.23-3.42 (2H, H-2' and H-5'), 3.44-3.60 (2H, H-3' and H-4'), 3.66 (1H,

dd, *J* = 10.8 and 6.6 Hz, H_a-3), 3.78 (2H, *br* s, H_2-6'), 3.85 (1H, *dd*, *J* = 11.0 and 5.2 Hz, H_b-3), 4.15 (1H, *dd*, *J* = 11.9 and 6.6 Hz, H_a-1), 4.28 (1H, *d*, *J* = 7.7 Hz, H-1'), 4.38 (1H, *br d*, *J* = 10.4 Hz, H_b-1), 5.18-5.45 (12H, *br*, H-2 and olefinic)

^{13}C-NMR (75 MHz, $CDCl_3$, Figure 209) δ: 14.8 (*q*), 21.1 (*t*), 25.4 (*t*), 26.0 (*t*), 26.2 (*t*), 27.5 (*t*), 27.6 (*t*), 27.7 (*t*), 29.6 (*t*), 29.7 (*t*), 29.8 (*t*), 29.9 (*t*), 30.1 (*t*), 30.2 (*t*), 32.0 (*t*), 34.6 (*t*), 34.7 (*t*), 61.9 (*t*, C-6'), 63.3 (*t*, C-1), 68.5 (*t*, C-3), 69.8 (*d*, C-3'), 70.6 (*d*, C-2), 73.8 (*d*, C-2'), 76.2 (*d*, C-5'), 76.6 (*d*, C-4'), 103.8 (*d*, C-1'), 127.4 (*d*), 128.1 (*d*), 128.5 (*d*), 128.6 (*d*), 130.4 (*d*), 132.2 (*d*), 173.5 (*s*), 174.0 (s)

Elemental analysis for $C_{45}H_{74}O_{10}$ calcd. C: 69.720 H: 9.629

found C: 69.809 H: 9.778

*1-O-linolenoyl-2-O-lauroyl-3-O-β-D-glucopyranosyl-sn-glycerol (**32c**)*

(mixture, 24.0 mg, 34.5%)

32c was prepared from **31c** according to the general procedure for selective removal of acetyl protecting groups as described in ***Sec.4.6***.

$[\alpha]_D^{25}$ – 11.6° ($CHCl_3$, *c* 1.0)

^{1}H-NMR (300 MHz, $CDCl_3$, Figure 210) δ: 0.85 (3H, *br*), 0.93 (3H, *t*, *J* = 7.6 Hz), 1.25 (29H, *br*), 1.58 (4H, *br*), 2.02 (4H, *br*), 2.27 (4H, *br t*, *J* = 7.0 Hz), 2.75 (3H, *br t*), 3.23-3.42 (2H, H-2' and H-5'), 3.44-3.60 (2H, H-3' and H-4'), 3.66 (1H, *dd*, *J* = 10.8 and 6.6 Hz, H_a-3), 3.79 (2H, *br* s, H_2-6'), 3.87 (1H, *dd*, *J* = 11.0 and 5.2 Hz, H_b-3), 4.15 (1H, *dd*, *J* = 11.9 and 6.6 Hz, H_a-1), 4.28 (1H, *d*, *J* = 7.7 Hz, H-1'), 4.38 (1H, *br d*, *J* = 10.4 Hz, H_b-1), 5.22 (1H, overlapped, H-2), 5.23-5.45 (6H, *br*)

^{13}C-NMR (75 MHz, $CDCl_3$, Figure 211) δ: 14.8 (*q*), 21.1 (*t*), 25.4 (*t*), 26.0 (*t*), 26.2 (*t*), 27.5 (*t*), 27.6 (*t*), 27.7 (*t*), 29.6 (*t*), 29.7 (*t*), 29.8 (*t*), 29.9 (*t*), 30.1 (*t*), 30.2 (*t*), 32.0 (*t*), 34.6 (*t*), 34.7 (*t*), 61.8 (*t*, C-6'), 63.4 (*t*, C-1), 68.5 (*t*, C-3), 69.7 (*d*, C-3'), 70.6 (*d*, C-2), 73.8 (*d*, C-2'), 76.2 (*d*, C-5'), 76.6 (*d*, C-4'), 103.8 (*d*, C-1'), 127.4 (*d*), 128.0 (*d*), 128.5 (*d*), 128.6 (*d*), 130.5 (*d*), 132.2 (*d*), 173.5 (*s*), 173.6 (s), 173.9 (s), 174.0 (s)

IR (cm^{-1}): 3295 (ν O-H), 2925 (ν C-H), 1737 (ν C=O) (Figure 212)

Elemental analysis for $C_{39}H_{68}O_{10}$ calcd. C: 67.195 H: 9.840

found C: 67.316 H: 9.990

1-O-linolenoyl-3-O-(β-D-2',3',4',6'-tetra-O-acetyl-glucopyranosyl)-sn-glycerol ***(33)*** (165.1 mg, 58.4%)

33 was prepared from **30** according to the general procedure for preparation of 1-*O*-acyl-3-*O*-(β-D-2',3',4',6'-tetra-*O*-acetyl-glycopyranosyl)-*rac*-glycerols as described in ***Sec***. ***4.4***.

^{1}H-NMR (300 MHz, $CDCl_3$, Figure 213) δ: 0.93 (2x3H, *t*, *J* = 7.6 Hz), 1.27 (10H, *br*), 1.60 (2x2H), 1.98-2.08 (16H, overlapped), 2.30 (2H, *br t*, *J* = 7.0 Hz), 2.78 (2x4H, *br t*, *J* = 5.5 Hz), 3.60-3.76 (3H, H_2-3 and H-5'), 3.95 (1H, *m*, H-2), 4.06 (2H, H_2-6'), 4.10-4.22 (2H, H_2-1), 4.51 (1H, *d*, *J* = 7.7 Hz, H-1'), 4.95 (1H, H-2'), 5.01 (1H, H-4'), 5.16 (1H, H-3'), 5.20-5.40 (6H)

^{13}C-NMR (75 MHz, $CDCl_3$, Figure 214) δ: 14.8 (*q*), 21.1 (*t*), 25.4 (*t*), 26.0 (*t*), 26.2 (*t*), 27.5 (*t*), 27.6 (*t*), 27.7 (*t*), 29.6 (*t*), 29.7 (*t*), 29.8 (*t*), 29.9 (*t*), 30.1 (*t*), 30.2 (*t*), 32.0 (*t*), 34.6 (*t*), 34.7 (*t*), 62.3 (*t*, C-6'), 65.4 (*t*, C-1), 68.7 (*d*, C-2), 69.2 (*d*, C-3'), 71.6 (*t*, C-3), 72.3 (*d*, C-2'), 72.5 (*d*, C-4'), 73.0 (*d*, C-5'), 101.7 (*d*, C-1'), 127.4 (*d*), 128.0 (*d*), 128.5 (*d*), 128.6 (*d*), 130.5 (*d*), 132.2 (*d*), 169.5,169.6, 170.3 (*s*), 170.7, 174.0 (s)

1-O-linolenoyl-3-O-β-D-glucopyranosyl-sn-glycerol ***(34)*** (24.5 mg, 31.6%)

34 was prepared from **33** according to the general procedure for selective removal of acetyl protecting groups as described in ***Sec.4.6***.

$[\alpha]_D^{25}$ – 9.4° ($CHCl_3$, *c* 1.0)

^{1}H-NMR (300 MHz, $CDCl_3$-D_2O, Figure 215) δ: 0.94 (3H, *t*, *J* = 7.6 Hz), 1.29 (10H, *br*), 1.59 (2H), 1.95-2.10 (4H, *m*), 2.30 (2H, *br t*, *J* = 7.0 Hz), 2.78 (4H, *br*), 3.25-3.39 (2H, H-2' and H-5'), 3.40-3.52 (2H, H-3' and H-4'), 3.65-3.90 (4H, H_2-6', H_2-3) 3.95-4.15 (3H, H_2-1, H-2), 4.32 (1H, *d*, *J* = 7.7 Hz, H-1'), 5.20-5.40 (6H)

^{13}C-NMR (75 MHz, $CDCl_3$, Figure 216) δ: 14.8 (*q*), 21.1 (*t*), 25.4 (*t*), 26.0 (*t*), 26.2 (*t*), 27.5 (*t*), 27.6 (*t*), 27.7 (*t*), 29.6 (*t*), 29.7 (*t*), 29.8 (*t*), 29.9 (*t*), 30.1 (*t*), 30.2 (*t*), 32.0 (*t*), 34.6 (*t*), 34.7 (*t*), 61.2 (*t*, C-6'), 65.5 (*t*, C-1), 68.7 (*d*, C-2), 69.6 (*d*, C-3'), 71.6 (*t*, C-3), 73.6 (*d*, C-2'), 76.3 (*d*, C-4' and C-5'), 103.1 (*d*, C-1'), 127.4 (*d*), 128.0 (*d*), 128.5 (*d*), 128.6 (*d*), 130.5 (*d*), 132.2 (*d*), 174.6 (s)

DEPT 135 (Figure 217)

^{1}H-^{1}H COSY: (Figure 218)

HMQC: (Figure 219)

Elemental analysis for $C_{45}H_{74}O_{10}$ calcd. C: 62.997 H: 9.014
found C: 62.889 H: 9.156

1,2-di-O-benzyl-3-O-(β-D-2',3',4',6'-tetra-O-acetyl-galactopyranosyl)-sn-glycerol ***(35)*** (605.5 mg, 50.5%)

35 was prepared from **28** according to the general procedure for glycosylation as described in ***Sec.4.1***. The product was purified by column chromatography eluted with hexane : EtOAc (4:1)

^{1}H-NMR (300 MHz, $CDCl_3$, Figure 220) δ: 1.96, 1.98, 2.01, 2.10 (each 3H, acetonide), 3.51-3.60 (2H), 3.64-3.78 (2H), 3.84 (1H) 3.95 (1H), 4.12 (2H), 4.45(1H, *d*, *J* = 7.7 Hz, H-1'), 4.51 (2H), 4.62 (2H), 4.97 (1H, *dd*, *J* = 3.3 and 10.5 Hz, H-3'), 5.17 (1H, *dd*, *J* = 8.0 and 10.4 Hz, H-2'), 5.35 (1H, d, 3.0 Hz, H-4')

^{13}C-NMR (75 MHz, $CDCl_3$, Figure 221) δ: 61.7, 67.5, 69.3, 69.6, 70.2, 71.1, 71.3, 72.5, 73.9, 77.3, 101.9, 127.9, 128.0, 128.6, 128.7, 138.5, 138.7, 169.6, 170.3, 170.4, 170.5

*1-O-(β-D-2',3',4',6'-tetra-O-acetyl-galactopyranosyl)-sn-glycerol (****36****)*
(206 mg, 73.9%)

36 was prepared from **35** according to the procedure for preparation of **30**

^{1}H-NMR (300 MHz, $CDCl_3$, Figure 222) δ: 1.98, 2.01, 2.02, 2.13 (each 3H, *s*, acetyl), 3.53-3.96 (6H, H_2-1, H-2, H_2-3 and H-5'), 4.14 (2H, *br* s, H_2-6'), 4.48 (1H, *d*, *J* = 7.8 Hz, H-1'), 5.01 (1H, *dd*, *J* = 10.4 and 3.3 Hz, H-3'), 5.18 (1H, *dd*, *J* = 9.9 and 8.4 Hz, H-2'), 5.38 (1H, *br d*, *J* = 3.0 Hz, H-4')

1,2-di-O-linolenoyl-3-O-(β-D-2',3',4',6'-tetra-O-acetyl-galactopyranosyl)-sn-glycerol ***(37)*** (159.0 mg, 56.3%)

37 was prepared from **36** according to the general procedure for preparation of mono-acid 1,2-*O*-diacyl-3-*O*-(β-D-2',3',4',6'-tetra-*O*-acetyl-glycopyranosyl)-*rac*-glycerols as described in ***Sec 4.3***.

^{1}H-NMR (300 MHz, $CDCl_3$, Figure 223) δ: 0.92(6H, *br t*, 6.5 Hz), 1.25 (18H, *br*), 1.55 (4H, *br*), 1.92-2.10 (20H, overlapped), 2.25 (4H, *br t*, 6.3 Hz), 2.75 (8H, *br s*), 3.58-3.64 (1H, *br*, H_a-3), 3.80-3.95 (2H, H_b-3 and H-5'), 4.01-4.15 (3H, H_a-1 and H_2-6'), 4.25 (1H, *br d*, *J* = 11.7 Hz, H_b-1), 4.42 (1H, *br d*, *J* = 7.4 Hz, H-1'),

4.95 (1H, *br d*, *J* = 10.4 Hz, H-3'), 5.10-5.20 (2H, H-2 and H-2'), 5.21-5.40 (13H, *br*, H-4' and olefinic)

^{13}C-NMR (75 MHz, $CDCl_3$, Figure 224) δ: 61.6, 62.7, 67.4 , 68.0, 69.0, 70.1, 71.1, 71.2, 101.9, 127.4 (*d*), 128.0 (*d*), 128.4 (*d*), 128.5 (*d*), 130.4 (*d*), 132.2 (*d*), 169.6 (*s*), 170.2 (*s*), 170.3 (*s*), 170.5 (s), 172.9 (*s*), 173.4 (*s*)

*1,2-di-O-linolenoyl-3-O-β-D-galactopyranosyl-sn-glycerol (**38**)*

(mixture, 20.2 mg, 26.0%)

38 was prepared from **37** according to the general procedure for selective removal of acetyl protecting groups as described in ***Sec*.*4.6***.

$[\alpha]_D^{25}$ – 10.5° ($CHCl_3$, *c* 1.0)

^{1}H-NMR (300 MHz, $CDCl_3$, Figure 225) δ: 0.95 (6H), 1.30 (26H), 1.58 (4H), 2.01 (8H), 2.32 (4H), 2.78 (6H), 3.50 (1H, *t*, *J* = 5.5 Hz, H-5'), 3.58 (1H, *br d*, *J* = 9.7 Hz, H-3'), 3.65 (1H, *br d*, *J* = 9.8 Hz, H-2'), 3.70 (1H, *dd J* =6.5 and 11.1 Hz, H_a-3), 3.80 (1H, *dd*, J = 4.3 and 12.0 Hz, H_a-6'), 3.89 (1H, *dd*, *J* = 3.8 and 10.9 Hz, H_b-3), 3.94 (1H, *br d*, *J* = 12.3 Hz, H_b-6'), 3.99 (1H, *br s*, H-4'), 4.18 (1H, *dd*, *J* = 6.6 and 12.0 Hz, H_a-1), 4.25 (1H, *d*, *J* = 7.3 Hz, H-1'), 4.38 (1H, *dd*, *J* = 3.5 and 12.0 Hz, H_b-1), 5.20-5.40 (13H, overlapped, H-2 and olefinic H)

^{13}C-NMR (75 MHz, $CDCl_3$, Figure 226) δ: 14.7 (*q*), 22.2 (*t*), 23.0 (*t*), 25.3 (*t*), 27.3 (*t*), 27.5 (*t*), 29.4 (*t*), 29.6 (*t*), 29.8 (*t*), 29.9 (*t*), 30.1(*t*), 30.2 (*t*), 31.2 (*t*), 34.5 (*t*), 34.6 (*t*), 35.0 (*t*), 63.1 (*t*, C-6'), 63.2 (*t*, C-1), 68.7 (*t*, C-3), 69.9 (*d*, C-4'), 70.6 (*d*, C-2), 71.9 (*d*, C-2'), 73.9 (*d*, C-3'), 75.0 (*d*, C-5'), 104.3 (*d*, C-1'), 127.4 (*d*), 128.0 (*d*), 128.5 (*d*), 130.5 (*d*), 132.0 (*d*), 173.7 (*s*, carbonyl), 173.9 (*s*, carbonyl)

Elemental analysis for $C_{45}H_{74}O_{10}$ calcd. C: 69.720 H: 9.629

Found C: 69.459 H: 9.898

CHAPTER IV
RESULTS AND DISCUSSION

β-galactosyl diglycerides isolated from *C. nutans* leaves, as mentioned, showed promising anti-HSV activity. In order to investigate the structure-activity relationships against HSV of this class of compounds, the target compounds were designed, synthesized, and evaluated for activity. In this research, the effect of fatty acyl moieties, sugar, and the effect of stereochemistry at C-2 position on anti-HSV activity were investigated.

1. Effect of Fatty Acyl Moieties at C-1 and C-2 on Anti-HSV Activity

Our first attempt is to study only the effect of the fatty acyls in the glycoglycerolipids, therefore, glucose was selected as the sugar part. A series of 1,2-di-*O*-acyl-3-*O*-β-D-glucopyranosyl-*rac*-glycerols bearing various chain length of either saturated or unsaturated fatty acids were synthesized as the racemic mixture which could be divided into 2 groups, i.e. mono-acid 1,2-di-*O*-acyl-3-*O*-(β-D-2′,3′,4′,6′-tetra-*O*-acetyl-glucopyranosyl)-*rac*-glycerols and mixed-acid 1,2-di-*O*-acyl-3-*O*-(β-D-2′,3′,4′,6′-tetra-*O*-acetyl-glucopyranosyl)-*rac*-glycerols. The mono-acid 1,2-di-*O*-acyl-3-*O*-(β-D-2′,3′,4′,6′-tetra-*O*-acetyl-glucopyranosyl-*rac*-glycerols refer to the compounds bearing the same fatty acyl moieties at C-1 and C-2 wheares the mixed-acid1,2-di-*O*-acyl-3-*O*-(β-D-2′,3′,4′,6′-tetra-*O*-acetyl-glucopyranosyl)-*rac*-glycerols refer to the compounds bearing the different fatty acyl moieties at C-1 and C-2 position. The general structures of compounds to be synthesized are shown in Figure 227 and the synthetic procedures are outlined in Scheme 1.

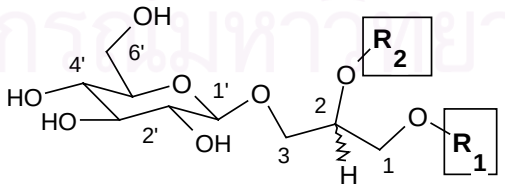

R_1, R_2 = various acyls(fatty acyls, aromatic acyl)

Figure 227. The general chemical structures of 1,2-di-*O*-acyl-3-*O*-β-D-glucopyranosyl-*rac*-glycerols to be synthesized.

The initial step, glycosylation, was carried on *via* the classical Koenigs-Knorr procedure. In this reaction, acetobromo-α-D-glucose (**1**) using as the glycosyl donor was allowed to react with the glycosyl acceptor, D,L-α,β-isopropylidene glycerol (**2**) in the presence of an equivalent amount of silver carbonate in dry dichloromethane providing the 1:1 mixtures of two diastereomeric 1,2-*O*-isopropylidene-3-*O*-(β-D-2′,3′,4′,6′-tetra-*O*-acetyl-glucopyranosyl)-*rac*-glycerol (**3**) which was confirmed by the 1:1 ratio of the anomeric protons signals at δ 4.61 and 4.63 (two overlapped doublets) in the ^{1}H-NMR spectrum (Table 4 and Figure 19).

Table 4. Chemical structure and ^{1}H-NMR assignment of 1,2-*O*-isopropylidene-3-*O*-(β-D-2′,3′,4′,6′-tetra-*O*-acetyl-glucopyranosyl)-*rac*-glycerol (**3**).

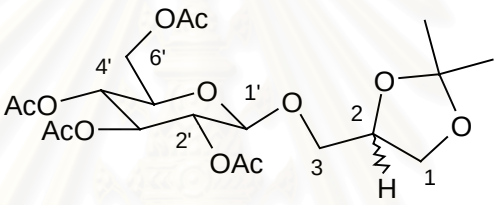

(**3**)

Position	**δ ^{1}H (ppm), (mult., *J* in Hz)**
acetonide	1.34, 1.42 (*s*, each 2 × 3H)
acetyl	2.01, 2.03, 2.05, 2.11 (*s*, each 2 × 3H)
1, 2, 3, 5′, 6′	3.60-4.33 (not assigned, 2 × 8H)
1′	4.61 and 4.63 (*d*, 7.6, each 1H)
2′	5.01 and 5.03 (*dd*, 9.8, 7.5, each 1H)
3′	5.22 and 5.23 (*dd*, 9.4, 9.4, each 1H)
4′	5.09 (*dd*, 9.5, 9.8, 2 × 1H)

The coupling constants of the anomeric protons were 7.6 Hz indicating that the diastereomeric products obtained as β-glucosidic linkage. The β-selective glycosidic bond formation was attained by the use of acetobromo-α-D-glucose with a neighboring-group-active acetyl substituent at 2-OH in the presence of an insoluble silver carbonate. The acetobromo-α-D-glucose adsorbed onto the silver carbonate

underwent a concerted reaction with the alcohol (**2**) by assuming a S_N2 mechanism. On the other hand, this β-glycosylation reaction could be explained by assuming a S_N1 mechanism *via* an acyloxonium ion intermediate as illustrated in Figure 228.

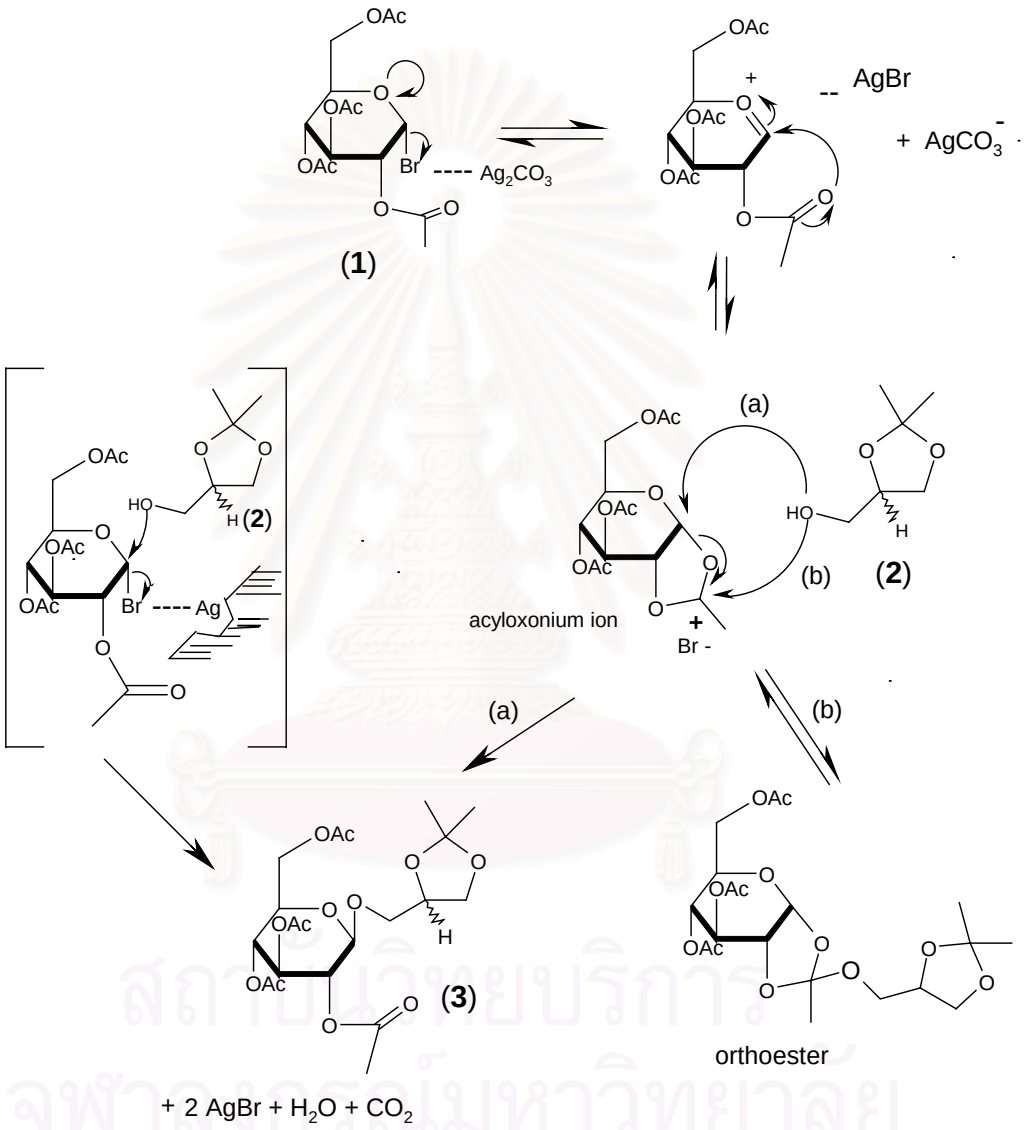

Figure 228. The proposed mechanism of glycosylation reaction.

However, this S_N1 reaction rendered the formation of orthoester by-products lowering the β-glycoside formation. Moreover, the water formed in this reaction also reacted with acetobromo-α-D-glucose and reduced the yields,

nevertheless, this water could be removed with Drierite or molecular sieves. Then the peracetylated glucoside (**3**) was deacetonized by 60% acetic acid in aqueous solution at 60° C to provide 1-*O*-(β-D-2′,3′,4′,6′-tetra-*O*-acetyl-glucopyranosyl)-*rac*-glycerol (**4**) in quantitative yield. The anomeric proton of **4** in the ^{1}H-NMR spectrum (Figure 21 and 229) showed only a doublet signal (J = 7.8 Hz) at δ 4.56 ppm, however, anomeric carbons (Figure 22) showing 1:1 ratio carbon signals separated about 0.1 ppm confirmed the 1:1 mixture of **4**.

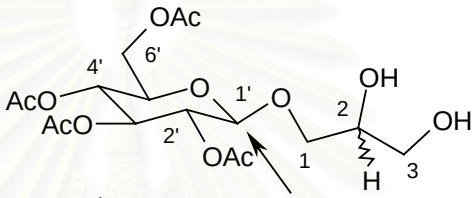

δ ^{1}H 4.56 (*d*, *J* = 7.8 Hz, 2x1H)

δ ^{13}C 101.3 and 101.4 ppm

Figure 229. Chemical structure of 1-*O*-(β-D-2′,3′,4′,6′-tetra-*O*-acetyl-glucopyranosyl)-*rac*-glycerol (**4**).

Then, **4** was subjected to perform acylation reaction under mild esterification providing peracetylated glucosyl diglycerides. The mono-acid 1,2-di-*O*-acyl-3-*O*-(β-D-2′,3′,4′,6′-tetra-*O*-acetyl-glucopyranosyl)-*rac*-glycerols (**5a-j**) were prepared by one step diacylation of **4** with a little excess of the desired fatty acids in the presence of dicyclohexyl carbodiimide (DCC) and dimethylamino pyridine (DMAP) at room temperature. The proposed mechanism of reaction is depicted in Figure 230.

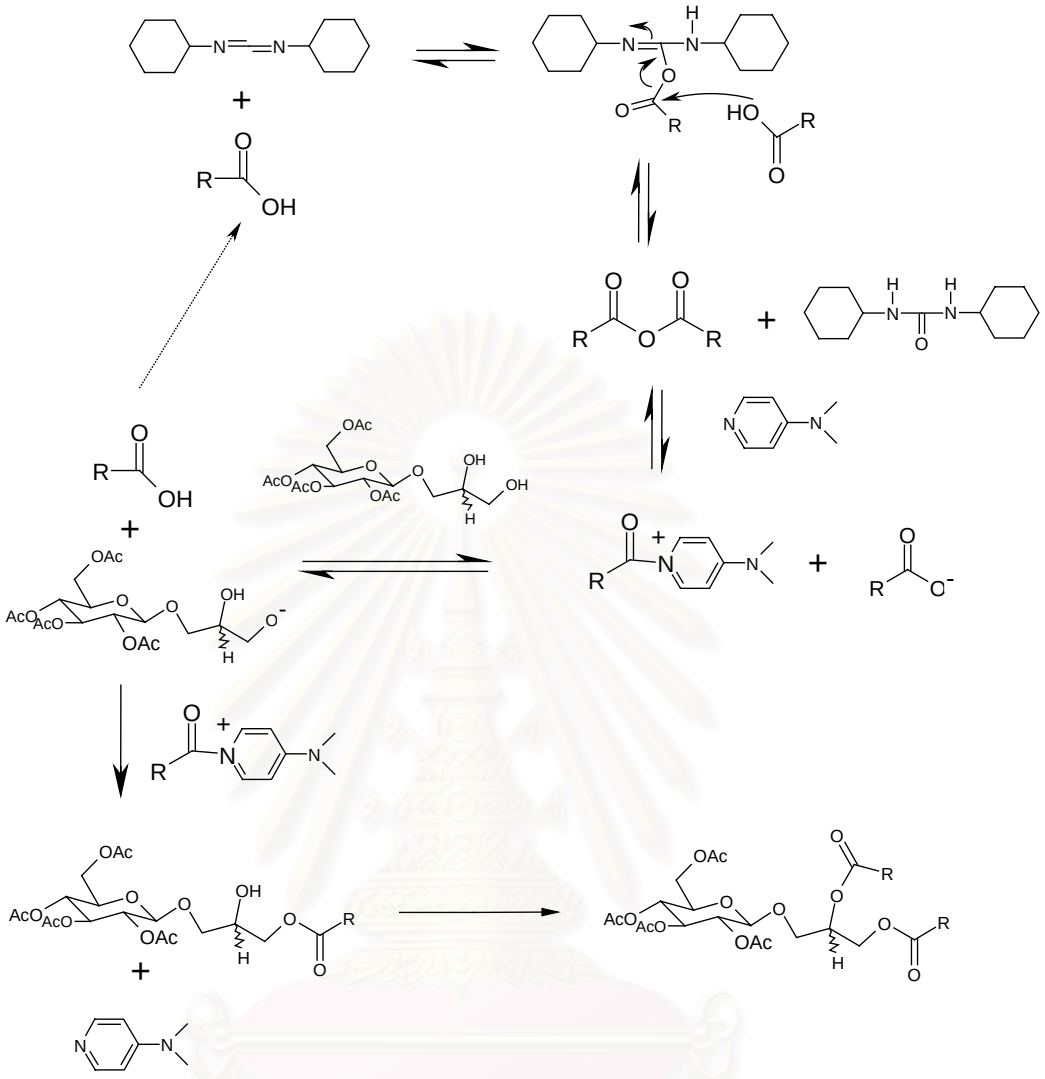

Figure 230. The proposed mechanism of esterification reaction.

The chemical structures and some physical properties of **5a-j** are illustrated in Table 5.

Table 5. The chemical structures and some physical properties of compounds **5a-j.**

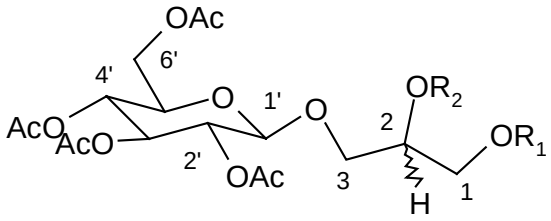

Compounds	**R_1**	**R_2**	**description**	**Yield (%)**
5a	caproyl	caproyl	amorphous solid	90.5
5b	lauroyl	lauroyl	amorphous solid	90.2
5c	myristoyl	myristoyl	amorphous solid	83.5
5d	palmitoyl	palmitoyl	amorphous solid	77.5
5e	stearoyl	stearoyl	amorphous solid	78.1
5f	behenoyl	behenoyl	amorphous solid	55.1
5g	oleoyl	oleoyl	syrupy mass	72.6
5h	linoleoyl	linoleoyl	syrupy mass	69.9
5i	α-linolenoyl	α-linolenoyl	syrupy mass	56.1
5j	benzoyl	benzoyl	amorphous solid	50.0

The percentage yields of these compounds were in the range of 50-90% and the chemical structures of these compounds were analyzed by NMR spectroscopy. The mono-acid peracetylated glucosyl diglycerides containing saturated fatty acyl moieties (**5a-f**) showed the similar pattern of proton signals at δ 0.80-0.90 (2 × 6H, *br t*, *J* = 6.9Hz, terminal methyl), 1.18-1.25 (*br*, bulk methylene), 1.50-1.56 (2 × 4H, *br*, β-CH_2-), 1.90-2.08 (2 × 12H, 4*s*, acetyl), 2.20-2.29 (2 × 4H, α-CH_2-), 3.50-3.72 (2 × 2H, H_a-3, H-5′,), 3.80-3.94 (2 × 1H, H_b-3), 3.95-4.10 (2 × 2H, H_a-1, H_a-6′), 4.11-4.30 (2 × 2H, H_b-1, H_a-6′), 4.42-4.52 (2 × 1H, two overlapped doublets, *J* = 7.7-7.9 Hz, H-1′), 4.88-4.97 (2 × 1H, *dd*, 9.4, 7.6 Hz, H-2′), 4.98-5.05 (2 × 1H, apparent *t*, 9.6 Hz, H-4′), 5.10-5.14 (2 × 2H, overlapped, H-3′and H-2)

(Figures 25, 27, 31-34). The general structures and proton assignments of these compounds are summarized in Figure 231.

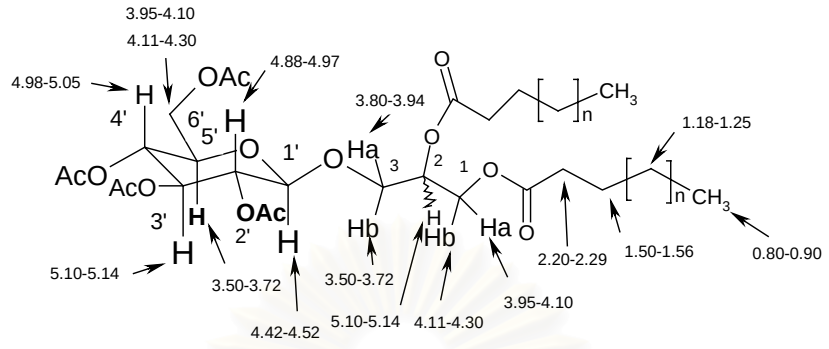

5a-f

Figure 231. The general structures and proton assignment of compounds **5a-f**.

The connectivities of these protons were confirmed by the correlations in the 2D ^{1}H-^{1}H COSY spectra (Figures 29, 35). The ^{1}H-NMR spectra of mono-acid peracetylated glucosyl diglycerides containing unsaturated fatty acyl moieties (**5g-i**) (Figures 36, 38-39) showed the similar pattern of proton signals as observed in those of **5a-f** with additional signals at δ 5.20-5.40 (olefinic protons), 1.98-2.08 (allylic methylene protons), 2.76-2.78 (methylene protons lying between two double bonds of linoleic or linolenic acid alkyl chains). Furthermore, the outstanding sharp triplet at δ 0.93-0.95 (J = 7.5 Hz) were observed in ^{1}H-NMR spectra of compounds bearing α-linolenoyl moiety. The chemical structure of **5j** bearing aromatic acyl moiety was confirmed by ^{1}H-NMR spectrum of which showing 12 acetyl protons at δ 1.96, 1.98, 2.02, 2.04 (each 3H, 4*s*,), δ 3.48-5.58 (2 × 12H, sugar and glycerol protons), 7.45-8.00 (2 × 10H, aromatic protons) (Figure 41)

The synthesis of the defined mixed-acid 1,2-di-*O*-acyl-3-*O*-(β-D-2′,3′,4′,6′-tetra-*O*-acetyl-glucopyranosyl-*rac*-glycerols could be furnished by stepwise acylation of **4** with the desired fatty acyls at 0^o C to provide 1-*O*-acyl-3-*O*-(β-D-2′,3′,4′,6′-tetra-*O*-acetyl-glucopyranosyl)-*rac*-glycerols (**7a-e**). Table 6 illustrates the chemical structures and some properties of these compounds.

Table 6. The chemical structures and some properties of compounds **7a-e.**

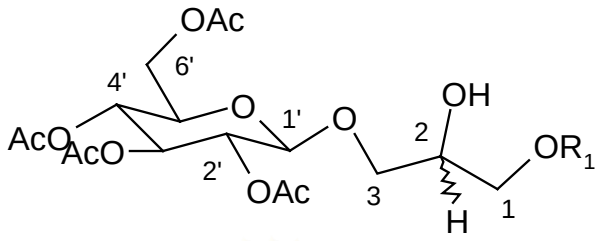

Compounds	**R_1**	**Description**	**Yield (%)**
7a	lauroyl	amorphous solid	67.8
7b	α-linolenoyl	syrupy mass	63.5
7c	stearoyl	amorphous solid	68.1
7d	behenoyl	amorphous solid	57.1
7e	benzoyl	amorphous solid	50.1

The proton signals patterns of these compounds in the ^{1}H-NMR spectra (Figures 47, 49, 51-52, 54) were similar to those of 1,2-di-*O*-acyl-3-*O*-(β-D-2′,3′,4′,6′-tetra-*O*-acetyl-glucopyranosyl)-*rac*-glycerols. However, the proton signals of H-2 of these glucosyl monoglycerides were observed at δ 3.90-3.95 ppm instead of at 5.10-5.14 ppm as observed in the ^{1}H-NMR spectra of the peracetylated glucosyl diglycerides indicating that the fatty acyl moiety were attached to C-1 hydroxyl of the glycerol backbone. Subsequent acylation of **7a-e** with the second fatty acids at room temperature provided the defined mixed-acid 1,2-di-*O*-acyl-3-*O*-(β-D-2′,3′,4′,6′-tetra-*O*-acetyl-glucopyranosyl)-*rac*-glycerols (**5k-q**). The chemical structures and some properties are shown in Table 7, and the chemical structures of these compounds were confirmed by NMR spectra (Figures 59-64).

Table 7. The chemical structures and some properties of compounds **5k-q.**

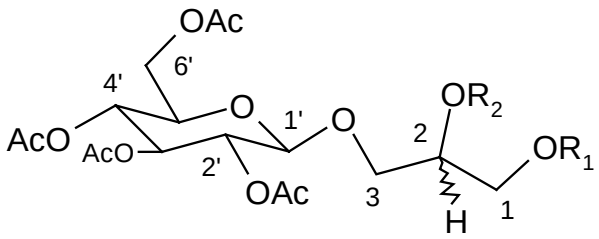

Compounds	**R_1**	**R_2**	**Description**	**Yield (%)**
5k	lauroyl	oleoyl	semisolid	72.0
5l	stearoyl	lauroyl	amorphous solid	84.9
5m	stearoyl	behenoyl	amorphous solid	64.8
5n	behenoyl	lauroyl	amorphous solid	69.9
5o	behenoyl	oleoyl	semisolid	68.1
5p	α-linolenoyl	linoleoyl	syrupy mass	59.9
5q	benzoyl	lauroyl	amorphous solid	52.0

The most difficult step in this synthetic procedure was the selective removal of the acetate moieties of peracetylated glucosyl diglycerides without affecting the fatty acyl groups on the glycerol backbone. Successful deacetylation was carried out by hydrazinolysis of those compounds (**5a-q**) using hydrazine hydrate (3 moles per acetate group) in 85% ethanol aqueous solution to give the corresponding 1,2-di-*O*-acyl-3-*O*-β-D-glucopyranosyl-*rac*-glycerols (**6a-q**). The preferential removal of acetyl groups in the presence of long chain acyl groups was considered to be due rather to the insoluble ability in water of the hydrophobic fatty acid chains, than to the polar sugar moiety. The glucosyl diglycerides form micelles with a hydrophilic center and expose the more polar sugar acetates to the polar solvent. The hydrophilic coat might protect the fatty acid esters from attack by hydrazine (Wehrli and Pomeranz, 1969). All of these synthetic glucosyl diglycerides could not be purified by crystallization, and then, column chromatographic technique was used for purification. The chemical structures of these final compounds were

elucidated by extensive analysis of the spectroscopic data, mainly NMR spectra. All of the ^{1}H-NMR spectra of the glucosyl diglycerides bearing saturated fatty acyls at C-1 and C-2 displayed the similar proton signals at δ 0.80-0.95 (2 × 6H, *br t*, *J* = 6.7 Hz), 1.15-1.28 (*br s*), 1.50-1.60 (2 × 4H, *br*), 1.98-2.28 (2 × 4H, *br t*, *J* = 7.0 Hz), 3.20-3.40 (2 × 2H, H-2' and H-5'), 3.41-3.60 (2 × 2H, H-3' and H-4'), 3.62-3.65 (each 1H, *dd*, *J* = 10.7 and 6.4 Hz, H_a-3), 3.79-3.80 (2 × 2H, *br s*, H_2-6'), 3.85-3.89 (2 × 1H, *br d*, *J* = 10.5 Hz, H_b-3), 4.06- 4.15 (each 1H, *dd*, *J* = 12.0 and 6.7 Hz, H_a-1), 4.25-4.29 (2 × 1H, *d*, *J* = 7.7 Hz, H-1'), 4.34-4.35 (2 × 1H, *br d*, *J* = 10.4 Hz, H_b-1), 5.24-5.27 (2 × 1H, *br*, H-2).(Figure 67, 69, 77, 79, 81, 86, 112, 118, 123). The general structures and proton assignments of these compounds are summarized in Figure 232.

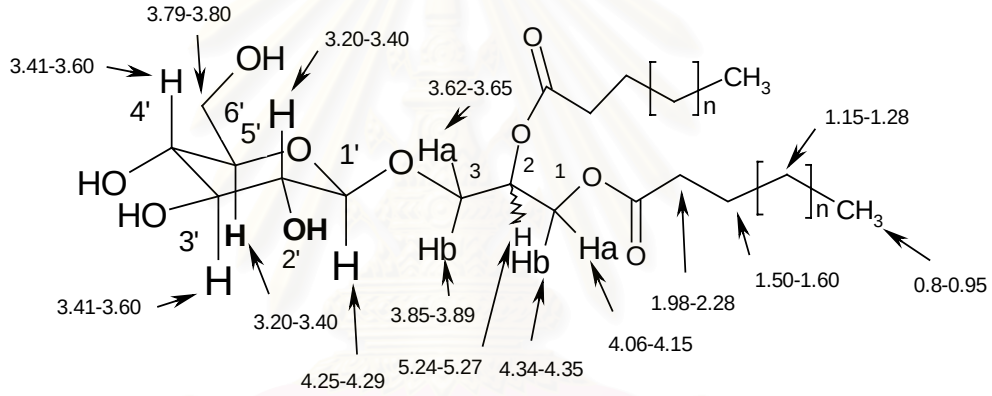

6a-f, 6l, 6m, 6n

Figure 232. The general structures and proton assignments of compounds bearing saturated fatty acyls **6a-f, 6l, 6m, 6n.**

For the compounds containing unsaturated fatty acyl moieties, additional olefinic and related methylene proton signals were observed as above-mentioned (Figures 90, 96, 100, 107, 129, 134). The chemical structures and some physical properties are summarized in Table 8.

Table 8. The chemical structures and some physical properties of compounds **6a-q.**

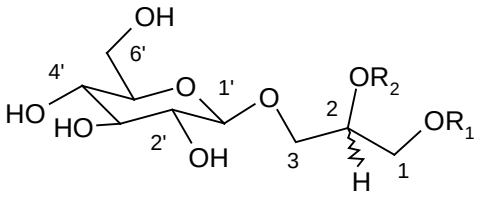

Compounds	R_1	R_2	Description	Yield (%)	Elemental Analysis C	H
6a	caproyl	caproyl	amorphous solid	56.7	Calcd. 61.881 Found 61.859	9.677 9.695
6b	lauroyl	lauroyl	amorphous solid	51.1	Calcd. 64.036 Found 63.984	10.104 10.122
6c	myristoyl	myristoyl	amorphous solid	52.9	Calcd. 65.827 Found 65.854	10.459 10.498
6d	palmitoyl	palmitoyl	amorphous solid	47.5	Calcd. 67.346 Found 67.401	10.760 10.809
6e	stearoyl	stearoyl	amorphous solid	35.4	Calcd. 68.648 Found 68.727	11.018 11.268
6f	behenoyl	behenoyl	amorphous solid	28.1	Calcd. 70.765 Found 70.885	11.438 11.569
6g	oleoyl	oleoyl	semisolid	35.9	Calcd. 69.002 Found 69.120	10.560 10.665
6h	linoleoyl	linoleoyl	syrupy mass	33.0	Calcd. 69.359 Found 69.596	10.097 10.390
6i	α-linolenoyl	α-linolenoyl	syrupy mass	30.4	Calcd. 69.720 Found 69.829	9.629 9.989
6j	benzoyl	benzoyl	amorphous solid	32.0	Calcd. 59.721 Found 60.201	5.670 5.799
6k	lauroyl	oleoyl	semisolid	43.9	Calcd. 66.808 Found 66.879	10.359 10.398
6l	stearoyl	lauroyl	amorphous solid	40.2	Calcd. 66.617 Found 66.520	10.616 10.566

Table 8. The chemical structures and some physical properties of compounds **6a-q** (continued).

Compounds	R_1	R_2	Description	Yield (%)	Elemental analysis C	H
6m	stearoyl	behenoyl	amorphous solid	31.0	Calcd. 69.777	11.242
					Found 69.809	11.012
6n	behenoyl	lauroyl	amorphous solid	37.7	Calcd. 68.021	10.894
					Found 68.290	11.094
6o	behenoyl	oleoyl	semisolid	31.9	Calcd. 69.994	11.029
					Found 69.817	10.898
6p	α-linolenoyl	linoleoyl	syrupy mass	30.9	Calcd. 70.446	9.992
					Found 70.801	10.285
6q	benzoyl	lauroyl	amorphous solid	34.0	Calcd. 62.188	8.208
					Found 62.286	8.395

The correlations in 2D ^{1}H-^{1}H COSY spectral data (Figures 71, 92, 106, 114, 125, 131) confirmed the connectivities of these protons. The connectivities of these protons to the oxygenated carbons were obtained from the HMQC spectra. Table 9 summarizes the assignments for ^{1}H, ^{13}C-NMR, ^{1}H-^{1}H COSY and HMQC of **6g**. Interestingly, the anomeric protons of most peracetylated glucosyl diglycerides were observed as 1:1 ratio of two overlapped doublets (J = 7.5-7.8 Hz), indicating the 1:1 mixtures of the diastereomers while those of the corresponding deacetylated final products as a doublet. However, the ^{13}C-NMR spectra of these final products showing 1:1 ratio of anomeric carbon signals separated about 0.1-0.2 ppm confirmed the 1:1 mixtures of the final diastereomeric glucosyl diglycerides. In addition, some compounds were not so pure which could be observed by NMR spectral data, for instance, the ^{1}H-NMR spectrum of 1,2-*O*-dilinolenoyl-3-*O*-β-D-glucopyranosyl-*rac*-glycerol (**6h**) (Figure 96) showed only two methylene protons at δ 2.78, actually they should be four methylene protons, and olefinic protons were observed only six protons instead of eight protons.

Table 9. Peak assignments for ^{1}H-NMR, ^{13}C-NMR, ^{1}H-^{1}H COSY and HMQC of 1,2-di-*O*-oleoyl-3-*O*-β-D-glucopyranosyl-*rac*-glycerol (**6g**).

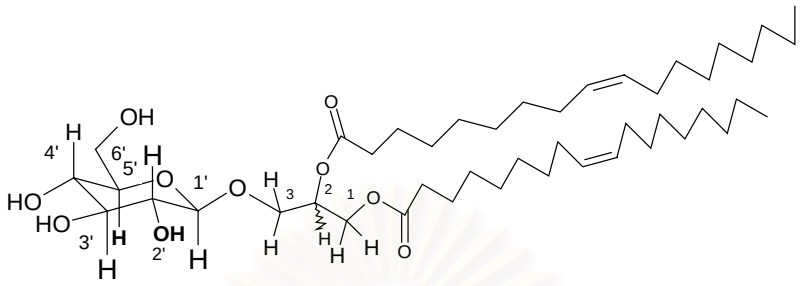

Position	**δ ^{13}C (ppm)**	**δ ^{1}H (ppm)**	**^{1}H-^{1}H COSY**	**HMQC ^{1}H to ^{13}C**
1a	63.2 and 63.3	4.07, 4.14 (*dd*, 12.0, 6.7)	H_b-1, H-2	C-1
1b		4.34 (*br d*, 11.8)	H_a-1, H-2	C-1
2	70.4 and 70.5	5.22 (*br*)	H_a-1, H_a-3	C-2
			H_b-1, H_b-3	
3a	68.4	3.62, 3.65 (*dd*, 10.7, 6.4)	H_b-3, H-2	C-3
3b		3.86 (*br d*, 10.6)	H_a-3, H-2	C-3
1′	103.7 and 103.9	4.29 (*d*, *J*=7.5 Hz)	H-2′	C-1′
2′	73.6 and 73.7	3.33 (*m*)	H-1′, H-3′	C-2′
3′	69.7	3.54 (*m*)	H-2′, H-4′	C-3′
4′	76.6 and 76.7	3.50 (*m*)	H-3′, H-5′	C-4′
5′	76.2 and 76.3	3.26 (*m*)	H-4′, H-6′	C-5′
6′	61.8	3.79 (*br s*)	H-5′	C-6′

The mass analysis of these glucosyl diglycerides was performed by both positive and negative-ion FABMS. In the positive–ion FABMS, a good quality spectra showing quasi-molecular ion $(M + Na)^{+}$ were obtained only upon adding alkaline salt to the matrix, however, free fatty carboxyl ions fragmentations were not observed. In the negative-ion FABMS of these compounds with diethanolamine as the matrix gave the spectra showing quasi-molecular ion $(M - H)^{-}$ and fatty

carboxylate ions fragmentation. The proposed positive-ion and negative-ion FABMS fragmentation patterns are shown in Figure 233 and Figure 234, respectively.

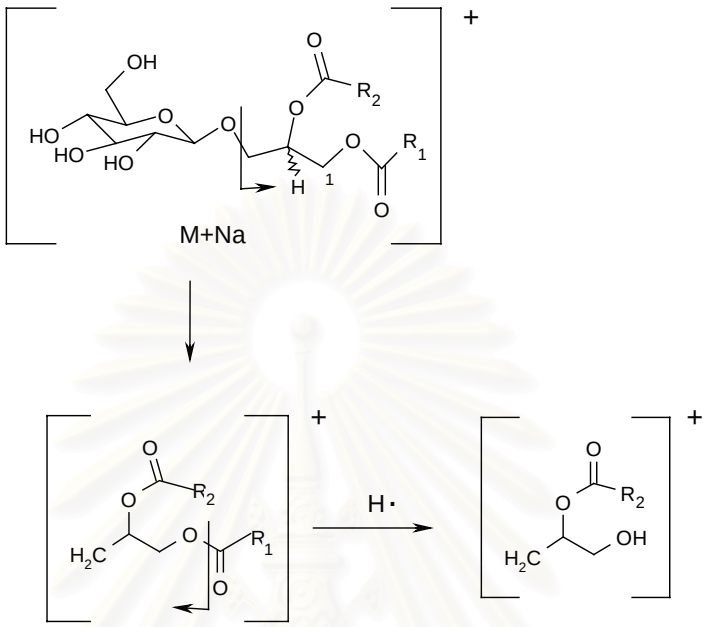

Figure 233. The proposed positive-ion FABMS fragmentation pattern.

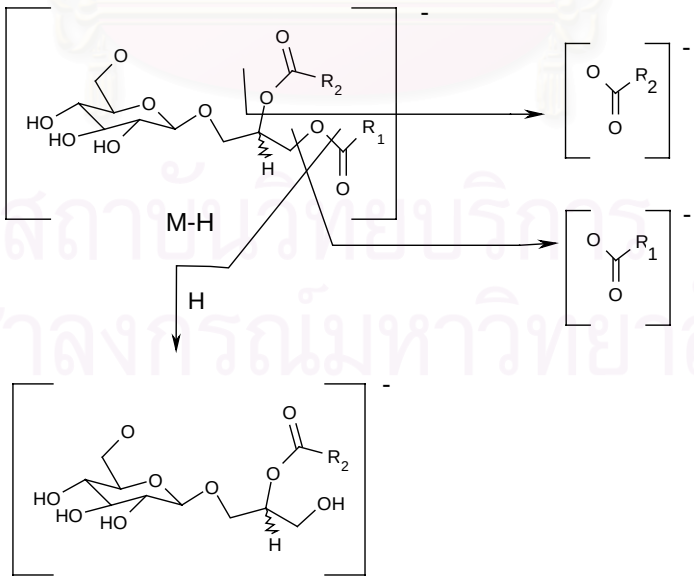

Figure 234. The proposed negative-ion FABMS fragmentation pattern.

The anti-HSV activity of these synthetic glucosyl diglycerides was determined as shown in Table 10.

Table 10. Anti-HSV activity of glucosyl diglycerides and related derivatives.

Compounds	**Concentration (μg/ml)**	**Plaque reduction assay (% inhibition)**	
		HSV-1	**HSV-2**
3	50	n.a.	n.a.
4	50	n.a.	n.a.
5a	50	n.a.	n.a.
5b	50	n.a.	n.a.
5c	50	n.a.	n.a.
5d	50	n.a.	n.a.
5e	50	n.a.	n.a.
5f	50	n.a.	n.a.
5g	50	n.a.	n.a.
5h	50	n.a.	n.a.
5i	50	n.a.	n.a.
5j	50	n.a.	n.a.
5j	50	n.a.	n.a.
5k	50	n.a.	n.a.
5l	50	n.a.	n.a.
5m	50	n.a.	n.a.
5n	50	n.a.	n.a.
5o	50	n.a.	n.a.
5p	50	n.a.	n.a.
5q	50	n.a.	n.a.
6a	50	n.a.	n.a.
6b	50	80	50
6c	50	20	n.a.

Table 10. Anti-HSV activity of glucosyl diglycerides and derivatives (continued).

compounds	Concentration (μg/ml)	Plaque reduction assay (% inhibition)	
		HSV-1	HSV-2
6d	50	n.a.	n.a.
6e	50	n.a.	n.a.
6f	50	n.a.	n.a.
6g	50	n.a.	25
6h	50	50	50
6i	50	94	97
6j	50	n.a.	n.a.
6k	50	13	17
6l	50	n.a.	n.a.
6m	50	n.a.	n.a.
6n	50	n.a.	20
6o	50	n.a.	10
6p	50	90	70
6q	50	n.a.	n.a.

n.a.= not active

The data showed that the peracetylated glucosyl diglycerides (**5a-q**) did not possess anti-HSV activity at concentration 50 μg/ml. The glucosyl diglycerides bearing the same saturated fatty acyl moiety (**6a-f**) and different fatty acyls (**6l-n**) at C-1 and C-1 position displayed little or no inhibitory activity, except **6b** containing dilauroyl (C12:0) moiety. On the other hand, glucosyl diglycerides bearing the same unsaturated fatty acyls (**6g-i**) and different fatty acyls (**6k, 6o-p**) exhibited higher inhibitory activity than those bearing saturated fatty acyls. The glucosyl diglycerides bearing aromatic acyls (**6j, 6q**) showed no activity. By comparing anti-HSV activity of four compounds containing 18 carbon atoms fatty acyls (**6g-i, 6p**), the data showed that inhibitory activity of these compounds followed the order **6i** > **6p** > **6h** > **6g**. These observations suggested that glucosyl diglycerides possessing more olefinic character displayed higher anti-HSV activity, however, the peracetylated form of

these compounds displayed no activity, indicating a requirement for free hydroxyl groups in these compounds for anti-HSV action.

In addition, glucoside derivative lacking fatty acyl moiety (**4**) exhibited no activity.

These results indicated that fatty acyl moiety at C-1 and C-2 positions were important for activity and 1,2-di-*O*-lauroyl-3-*O*-β-D-glucopyranosyl-*rac*-glycerol (**6b**) and 1,2-di-*O*-linolenoyl-3-*O*-β-D-glucopyranosyl-*rac*-glycerol (**6i**) were the promising anti-HSV compounds for further investigations.

Then, 1-*O*-lauroyl-3-*O*-β-D-glucopyranosyl-*rac*-glycerol (**8a**) and 1-*O*-linolenoyl-3-*O*-β-D-glucopyranosyl-*rac*-glycerol (**8b**) bearing only one fatty acyl at C-1 position were synthesized and evaluated for anti-HSV activity. Glucosyl monoglycerides **8a** and **8b** were prepared by hydrazinolysis of **7a** and **7b**, respectively. The chemical structures and some properties of these compounds are shown in Table 11.

Table 11. The chemical structures of glucosyl monoglycerides **8a-b.**

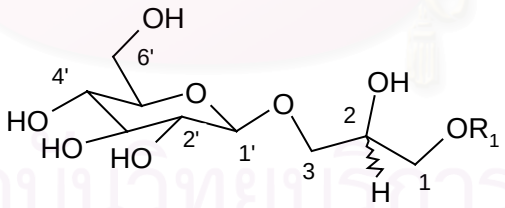

Compounds	**R_1**	**Description**	**Yield (%)**	**Elemental analysis**	**C**	**H**
8a	lauroyl	amorphous solid	61.0	Calcd.	57.763	9.241
				Found	57.853	9.407
8b	α-linolenoyl	syrupy mass	48.3	Calcd.	62.997	9.014
				Found	63.086	9.110

The chemical structures of these two compounds were confirmed by ^{1}H-NMR and ^{13}C-NMR spectra. The ^{1}H-NMR spectrum of **8a** (Figure **157**) showed broad signals at δ 0.85 (2 × 3H), 1.18-1.36 (*br*), 1.58 (2 × 2H, *br*), 2.30 (2 × 2H, *br t*), 3.26-4.50 (sugar and glycerol protons, not assigned) and the ^{13}C-NMR spectrum (Figure 158) showed carbon signals at δ 14.5-35.0 (alkyl), 61.4-76.6 (oxygenated sugar carbons), 103.3 and 103.7 (anomeric carbons), 174.3 and 174.4 (carbonyl). The ^{1}H-NMR spectrum of compound **8b** (Figure 159) in $CDCl_3$ with one drop of deuterium oxide showed relatively clear signals compared to that of **8a**. The ^{13}C-NMR spectrum of **8b** (Figure 160) showed five chemical types of carbon signals resembled that of its glucosyl diglycerides, i.e. 14.5-35.0 (alkyl), 61.1-76.5 (oxygenated carbons), 103.1 and 103.5 (acetal), 127.4-132.2 (olefinic), 174.5 and 174.6 (carbonyl). The anti-HSV activity of these two compounds is shown in Table 12.

Table 12. The anti-HSV activity of glucosyl monoglycerides **8a-b.**

Compounds	**Concentration (μg/ml)**	**Plaque reduction assay (% inhibition)**	
		HSV-1	**HSV-2**
8a	50	n.a.	33.3
	100	95	95
8b	25	n.a.	18.5
	50	24.5	40.4
	100	97.5	98.0

n.a.= not active

At concentration 50 μg/ml, glucosyl monoglyceride **8a** showed no activity against HSV-1, but displayed 33.3% inhibition to HSV-2 while **8b** exhibited 24.5% and 40.4% inhibition to HSV-1 and HSV-2, respectively. The activity of **8a** decreased dramatically compared to that of its glucosyl diglyceride **6b**. The similar result was also observed in compound **8b** and its glucosyl diglyceride **6i**. However, **8a** and **8b** exhibited almost completely inhibition to HSV-1 and HSV-2 at concentration 100 μg/ml.

In conclusion, studies on the effect of fatty acyl moiety on the anti-HSV activity indicated that the appropriate acyl moieties of these glycoglycerolipids were essential for anti-HSV activity and glycoglycerolipids bearing 1,2-di-*O*-acyl moieties possessed higher anti-HSV activity than that bearing only 1-*O*-acyl moiety, and these results suggested that lauroyl (C12:0) and α-linolenoyl (C18:3) moiety were the promising acyl moieties for anti-HSV action.

2. Effect of Sugar Moiety on Anti-HSV Activity

To study the effect of the sugar moiety on anti-HSV activity, the desired galactosyl diglycerides bearing the selected fatty acyl moieties expected to have good activity based on the above-mentioned evidence were synthesized and evaluated. The galactosyl diglycerides bearing the same fatty acyls and different fatty acyls were synthesized following the procedure for the synthesis of 1,2-di-*O*-acyl-3-*O*-β-D-glucopyranosyl-*rac*-glycerols as described above. Acetobromo-α-D-galactose (**9**) replaced the acetobromo-α-D-glucose in glycosylation reaction resulting in diastereomeric 1,2-*O*-isopropylidene-3-*O*-(β-D-2′,3′,4′,6′-tetra-*O*-acetyl-galactopyranosyl)-*rac*-glycerol (**10**) which was confirmed by signals of 1:1 ratio of anomeric protons at δ 4.49 and 4.51 (two overlapped doublet) in ^{1}H-NMR spectrum (Figure 20). The proton assignment is summarized in Table 13. Then **10** was treated with 60% acetic acid aqueous solution to give 1-*O*-(β-D-2′,3′,4′,6′-tetra-*O*-acetyl-galactopyranosyl)-*rac*-glycerol (**11**) which was subsequently acylated with the defined fatty acids providing the peracetylated galactosyl diglycerides (**12a-e**). The chemical structures and some properties of these compounds are shown in Table 14.

Table 13. The proton assignment of compound **10.**

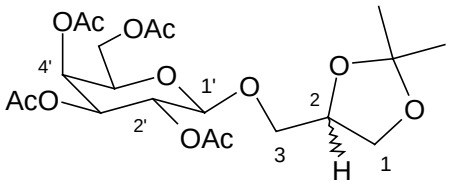

Position	**δ ^{1}H (ppm), (mult., *J* in Hz)**
acetonide	1.35, 1.43 (*s*, each 2x3H)
acetyl	1.98, 2.01, 2.02, 2.13, (*s*, each 2x3H)
1, 2, 3, 5′, 6′	3.60-4.20 (not assigned, 2x8H)
1′	4.49 and 4.51 (*d*, 7.6, each 1H)
2′	5.18 (*br t*, 8.3, 2x1H)
3′	5.01 (*br d*, 10.4, 2x1H)
4′	5.38 (*br s*, 2x1H)

Table 14. The chemical structures and some properties of compounds **12a-e.**

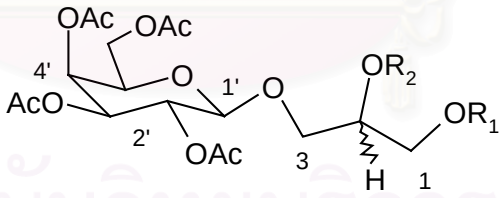

Compounds	**R1**	**R2**	**Description**	**Yield (%)**
12a	lauroyl	lauroyl	amorphous solid	89.1
12b	linoleoyl	linoleoyl	syrupy mass	52.7
12c	α-linolenoyl	α-linolenoyl	syrupy mass	53.3
12d	behenoyl	lauroyl	amorphous solid	68.4
12e	α-linolenoyl	linoleoyl	syrupy mass	53.5

The chemical structures of these peracetylated compounds (**12a-e**) were elucidated by NMR spectral data. The ^{1}H-NMR spectra of these compounds showed similar proton signals at δ 0.85-0.95 (2 × 6H, terminal CH_3), 1.27-1.38 (2 × 32H-52H, bulk $–CH_2$-), 1.51-1.54 (2 × 4H, β-CH_2), 1.95-2.14 (2 × 12H, acetyl), 2.23-2.30 (2 × 4H, α-CH_2), 3.60-3.70 (2 × 1H, H_a-3), 3.80-3.95 (2 × 2H, H_b-3, H-5'), 4.01-4.17 (2 × 3H, H_a-1, H_2-6'), 4.24-4.27 (2 × 1H, H_b-1), 4.41- 4.46 (2 × 1H, H-1'), 4.95-4.96 (2 × 1H, H-3'), 5.05-5.20 (2 × 2H, H-2, H-2'), 5.35 (2 × 1H, H-4') (Figure 42, 44, 45, 65, 66). The general structures and proton assignments of these compounds are summarized in Figure 235.

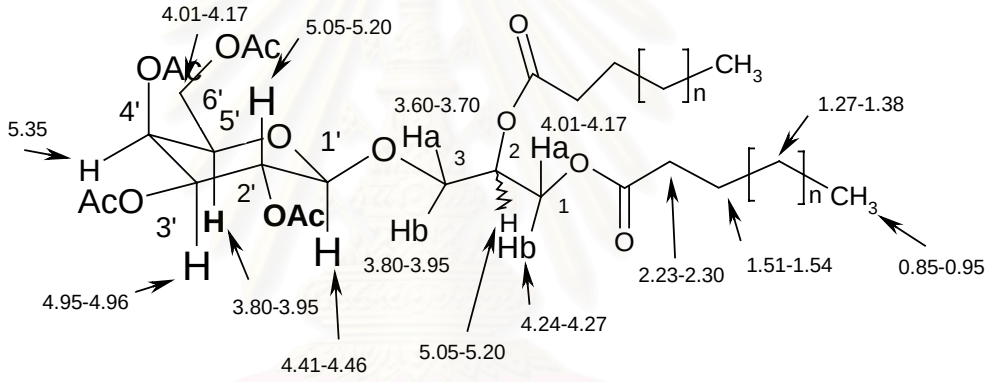

Figure 235. The general structures and proton assignments of compound **12a-e**.

The additional proton signals at δ 2.78 and 5.20-5.40 (olefinic) were observed in compounds bearing linoleoyl or α-linolenoyl moiety. The connectivities of these protons were confirmed by correlations in 2D ^{1}H-^{1}H COSY spectra (Figure 43). Finally, **12a-e** were allowed to react with hydrazine to give the corresponding galactosyl diglycerides (**13a-e**). The chemical structures and some properties are shown in Table 15.

Table 15. The chemical structures and some properties of compounds **13a-e**

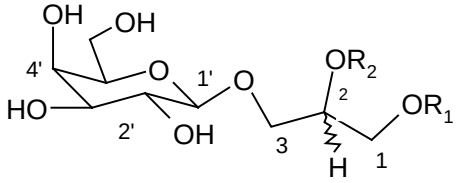

Compounds	R_1	R_2	Description	Yield (%)	Elemental analysis	C	H
13a	lauroyl	lauroyl	amorphous solid	49.8	Calcd.	64.036	10.104
					Found	64.138	10.305
13b	linoleoyl	linoleoyl	syrupy mass	31.3	Calcd.	69.359	10.097
					Found	68.995	10.386
13c	α-linolenoyl	α-linolenoyl	syrupy mass	31.0	Calcd.	69.720	9.629
					Found	69.918	9.807
13d	behenoyl	lauroyl	amorphous solid	39.8	Calcd.	68.021	10.894
					Found	68.208	10.998
13e	α-linolenoyl	linoleoyl	syrupy mass	29.9	Calcd.	70.446	9.992
					Found	70.725	10.188

The structure elucidations of these compounds (**13a-e**) were extensively analyzed by NMR spectral data. The ^{1}H-NMR of galactosyl diglycerides bearing saturated fatty acyl showed the similar proton signals at δ 0.85-0.95 (2 × 6H), 1.24-1.30 (2 × 32-52H), 1.56-1.60 (2 × 4H), 2.24-2.29 (2 × 4H), 3.40-3.62 (2 × 3H, H-2', H-3', H-5'), 3.63-3.71 (2 × 1H, H_a-3), 3.80-3.81 (2 × 2H, H_2-6'), 3.84-3.91 (2 × 1H, H_b-3), 3.96-3.98 (2 × 1H, H-4'), 4.08-4.15 (2 × 1H, H_a-1), 4.21-4.22 (2 × 1H, H-1'), 4.35-4.39 (2 × 1H, H_b-1), 5.21-5.28 (2 × 1H, H-2) (Figures 138, 145, 149, 152, 155). The general structures and proton assignments of these compounds are summarized in Figure 236.

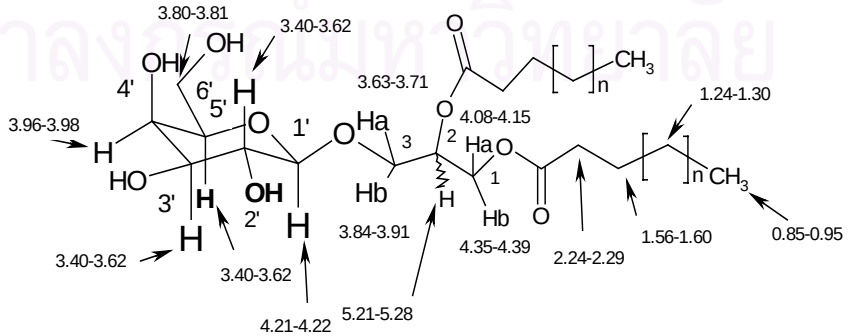

Figure 236. The general structures and proton assignments of **13a-e**.

The spectra also showed additional proton signals δ 2.78 and 5.20-5.40 (olefinic) of compounds bearing linoleoyl or α-linolenoyl moiety (**13b-c, 13e)** as observed in peracetylated compounds. The correlations in the 2D ^{1}H-^{1}H COSY spectra (Figure 140) confirmed the connectivities of these protons. In addition, the proton integration of compound **13c** at δ 2.78 (6H) should be 8H, accompany with broad triplet at δ 0.85, indicating some contaminants. The anti-HSV activity of these galactosyl diglycerides are illustrated in Table 16.

Table 16. The anti-HSV activity of galactosyl diglycerides and derivatives.

Compounds	**Concentration (μg/ml)**	**Plaque reduction assay (% inhibition)**	
		HSV-1	**HSV-2**
10	50	n.a.	n.a.
11	50	n.a.	n.a.
12a	50	n.a.	n.a.
12b	50	n.a.	n.a.
12c	50	n.a.	n.a.
12d	50	n.a.	n.a.
12e	50	n.a.	n.a.
13a	50	80	50
13b	50	55	50
13c	50	95	95
13d	50	n.a.	25
13e	50	95	90

n.a.= not active

The peracetylated galactosyl diglycerides (**12a-e**) did not show any anti-HSV activity, while the selected galactosyl diglycerides showed inhibitory action against both HSV-1 and HSV-2 as expected. Compound **13a** showed activity against HSV-1 and HSV-2 comparable to that of its glucosyl diglyceride analog (**6b**). The

similar results were observed in the other galactosyl diglycerides and their glucosyl diglyceride analogs as shown in Table 17.

Table 17. Comparison of anti-HSV activity of galactosyl diglycerides and their glucosyl diglycerides analogs.

compounds	**sugar**	**R_1**	**R_2**	**Plaque reduction assay [a] (% inhibition)**	
				HSV-1	**HSV-2**
13a	galactose	lauroyl	lauroyl	80	50
6b	glucose	lauroyl	lauroyl	80	50
13b	galactose	linoleoyl	linoleoyl	55	50
6h	glucose	linoleoyl	linoleoyl	50	50
13c	galactose	α-linolenoyl	α-linolenoyl	95	95
6i	glucose	α-linolenoyl	α-linolenoyl	94	97
13d	galactose	behenoyl	lauroyl	n.a.	25
6n	glucose	behenoyl	lauroyl	n.a.	20
13e	galactose	α-linolenoyl	linoleoyl	95	90
6p	glucose	α-linolenoyl	linoleoyl	93	95

[a] concentration tested = 50 μg/ml; n.a.= not active

These observations revealed that the anti-HSV activity of the galactosyl diglycerides possessed activity profile like that of glucosyl diglycerides.

Then, the anti-HSV activity of galactosyl monoglycerides was studied, the selected 1-*O*-linolenoyl-3-*O*-β-D-galactopyranosyl-*rac*-glycerols(**15**) was synthesized by hydrazinolysis of **14a**. The chemical structure of **15** was confirmed by NMR specta (Figures 161-162 and 237).

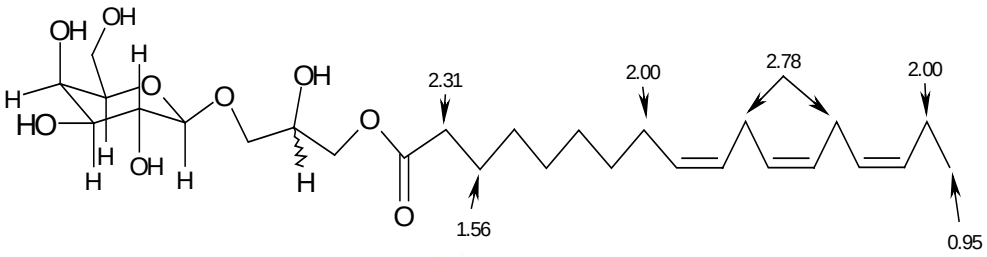

Figure 237. The chemical structure of 1-*O*-linolenoyl-3-*O*-β-D-galactopyranosyl-*rac*-glycerols (**15**).

The activity of **15** was subjected to comparison with its glucosyl monoglyceride analog (**8b**) as shown in Table 18 .

Table 18. Comparison of anti-HSV activity of galactosyl monoglyceride (**15**) and its glucosyl monoglycerides analog (**8b**).

compounds	**sugar**	**R_1**	**Concentration (μg/ml)**	**Plaque reduction assay (% inhibition)**	
				HSV-1	**HSV-2**
15	galactose	α-linolenoyl	50	22.5	48.3
			100	91	93
8b	glucose	α-linolenoyl	25	n.a.	18.5
			50	24.5	40.4
			100	97.5	98.0

n.a.= not active

The data showed that galactosyl monoglyceride possessed anti-HSV activity not significantly different from that of its glucosyl monoglyceride analog.

Extended studies were carried on synthesis and anti-HSV determination of compounds with no sugar moiety. The desired 1,2-dilauroyl glycerol (**19**) was selected as model compound, and the synthetic procedure is outlined in Scheme 2 Benzylation of **2** in the presence of sodium hydride in dry THF resulted in isopropylidene glycerol benzyl ether (**16**) (Figures 164 and 238).

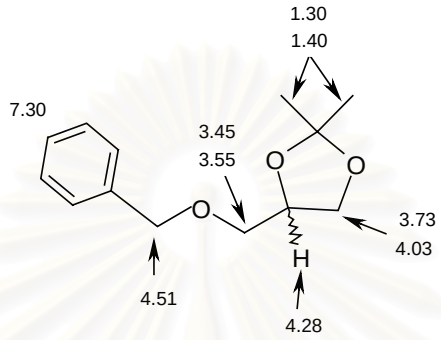

Figure 238. The chemical structure and proton assignment of **16**.

Then, **16** was deacetonized with 60% acetic acid to give glycerol benzyl ether (**17**) (Figures 165-166) which was acylation with lauric acid in the presence of DCC and DMAP providing 1,2-dilauroyl-3-benzyl glycerol (**18**) (Figures 167-168 and 239).

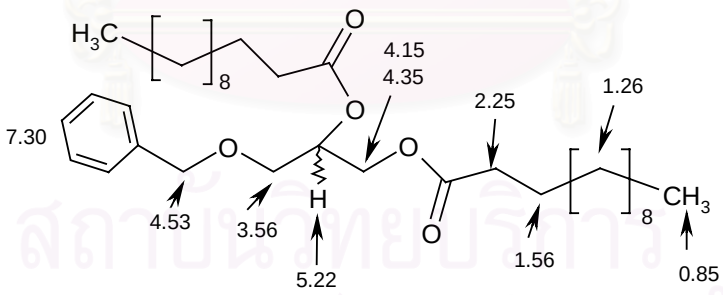

Figure 239. The chemical structure and proton assignment of **18**.

Catalytic hydrogenolysis of **18** afforded 1,2-dilauroyl glycerol (**19**) (Figures 169-171 and 240) combined with a little amount of by product, 1,3-dilauroyl glycerol which could be detected in NMR spectra. The side reaction resulted from acyl migration occurring during preparation.

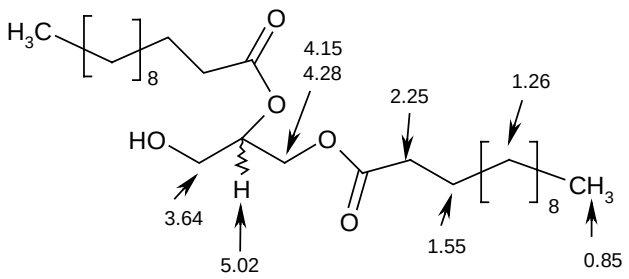

Figure 240. The chemical structure and proton assignment of **19**.

Further investigation on effect of sugar moiety either went on synthesis and evaluation of 1-monoacyl glycerols. The synthesis of these 1-monoacyl glycerols were accomplished in two-step reactions as shown in Scheme 3. The first step, acylation of **2** with the desired fatty acid to give 1-*O*-acyl-2,3-isopropylidene glycerol (**20a-c**) (Table 19 and Figures 172-177) which were subsequently reacted with 60% acetic acid to afford 1-*O*-monoacyl glycerols (**21a-c**) (Table 20 and Figures 178-185). The ^{1}H-NMR spectra of these compounds showed the similar proton signals at δ 0.85 (2 × 3H), 1.15-1.40 (*br*), 1.60 (2 × 2H, *br*), 2.32 (2 × 2H, *t*, *J* = 7.0 Hz), 3.55 (2 × 1H, *dd*, *J* = 5.6 and 11.2 Hz, H_a-3), 3.65 (2 × 1H, *dd*, *J* = 4.0 and 10.5 Hz, H_b-3), 3.90 (2 × 1H, *m*, H-2), 4.12 (2 × 1H, *dd*, *J* = 6.0 and 11.6 Hz, H_a-1), 4.14 (2 × 1H, *dd*, *J* = 6.0 and 11.6 Hz, H_b-1). However, each compound could be distinguished by observation on the number of methylene protons at δ 1.15-1.40 ppm.

Table 19. The chemical structures and some properties of **20a-c**.

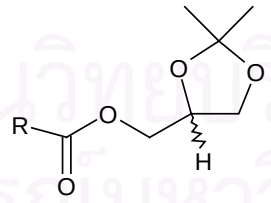

compounds	R	Description	Yield (%)
20a	lauroyl	liquid	85.5
20b	stearoyl	liquid	79.1
20c	behenoyl	liquid	72.6

Table 20. The chemical structures and some properties of **21a-c**.

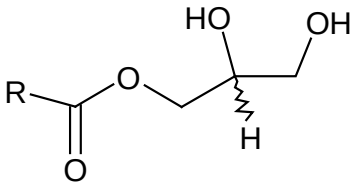

Compounds	**R**	**Description**	**Yield (%)**	**Elemental analysis**	**C**	**H**
21a	lauroyl	amorphous solid	91.8	Calcd.	65.642	11.026
				Found	65.583	11.108
21b	stearoyl	amorphous solid	91.9	Calcd.	70.331	11.814
				Found	70.399	11.901
21c	behenoyl	amorphous solid	90.7	Calcd.	72.399	12.161
				Found	72.534	12.289

The anti-HSV activity of these compounds was summarized in Table 21.

Table 21. The anti-HSV activity of glyceride derivatives

Compounds	**Concentration (μg/ml)**	**Plaque reduction assay (% inhibition)**	
		HSV-1	**HSV-2**
18	50	n.a.	n.a.
19	50	<10	n.a.
20a	50	n.a.	n.a.
20b	50	n.a.	n.a.
20c	50	n.a.	n.a.
21a	50	<10	n.a.
21b	50	n.a.	n.a.
21c	50	n.a.	n.a.

n.a.= not active

The data from Table 21 indicated that compounds lacking sugar moiety did not have any anti-HSV action.

In summary, studies on the effect of sugar moiety on anti-HSV activity indicated that sugar moiety was essential for anti-herpes simplex viral activity. Compounds containing no sugar moiety did not show any inhibitory activity, yet glucosyl or galactosyl glycerides displayed no significantly different inhibitory action.

3. Effect of the Stereochemistry at C-2 of Glycerol Backbone of Glycoglycerolipids on Anti-HSV Activity.

In order to study the effect of the stereochemistry at C-2 of glycerol backbone on anti-HSV activity, 1,2-di-*O*-acyl-3-*O*-β-D-glycopyranosyl-*sn*-glycerols were synthesized and evaluated. The compounds containing glucose or galactose bearing lauroyl and linolenoyl moiety expected to have good activity were selected as model compounds. Five compounds were synthesized, three compounds were glucosyl diglycerides, one compound was galactosyl diglyceride and the other one was glucosyl monoglyceride. In this synthesis strategy, 1,2-di-*O*-benzyl-*sn*-glycerol (**28**) was used as a glycosyl acceptor. Compound **28** could be prepared from D-mannitol according to the method of Mannock et al (1987) as shown in Scheme 4. D-mannitol (**22**) was treated with dry acetone and concentrated sulfuric acid to give 1,2:3,4:5,6-tri-*O*-isopropylidene-D-mannitol (**23**) (Figure 186). Then, **23** was converted to 3,4-*O*-isopropylidene-D-mannitol (**24**) (Figures 187-188) by a controlled acid hydrolysis using 65% acetic acid aqueous solution. Benzylation of **24** to form 1,2:5,6-tetra-*O*-benzyl-3,4-isopropylidene-D-mannitol (**25**) (Figures 189-190) was carried out under mild conditions at room temperature in the presence of benzyl bromide and sodium hydride. Hydrolysis of **25** with 1M hydrochloric acid in methanol yielded 1,2:5,6-tetra-*O*-benzyl-D-mannitol (**26**) (Figures 191-192). Oxidative cleavage of **26** with sodium periodate using tetrabutyl ammonium bromide as a phase transfer catalyst provided aldehyde (**27**) which was subsequently reduced using lithium aluminium hydride to give **28** (Figures 193-194).

The synthesis procedure of the diastereomeric pure isomer of glucosyl diglycerides are depicted in Scheme 4. Compound **28** was subjected to glycosylation with acetobromo-α-D-glucose (**1**) using Koenigs-Knorr condition afforded 1,2-di-*O*-benzyl-3-*O*-(β-D-2′,3′,4′,6′-tetra-*O*-acetyl-glucopyranosyl)-*sn*-glycerol (**29**) (Figures 195-197 and 241).

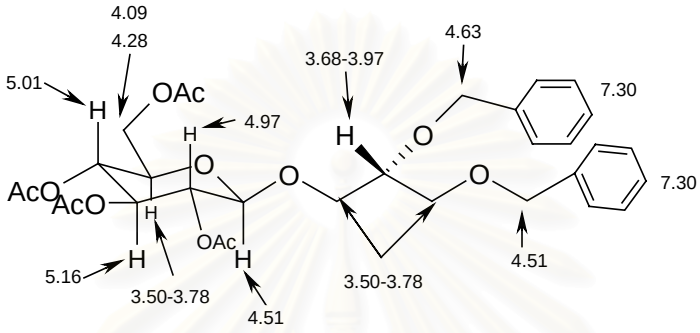

Figure 241. The chemical structure and proton assignment of **29**.

Then, **29** was debenzylated by catalytic hydrogenolysis to give 1-*O*-(β-D-2′,3′,4′,6′-tetra-*O*-acetyl-glucopyranosyl)-*sn*-glycerol (**30**) (Figures 198 and 242).

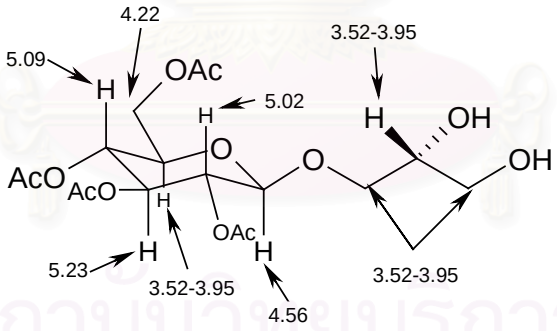

Figure 242. The chemical structure and proton assignment of **30**.

Acylation of **30** with the desired fatty acids gave peracetylated glycosyl diglycerides (**31a-c**) (Table 22 and Figures 199-205) which were deacetylated by hydrazinolysis to give the corresponding diastereomeric pure glucosyl diglycerides (**32a-c**) (Table 23).

Table 22. The chemical structures and some properties of **31a-c**.

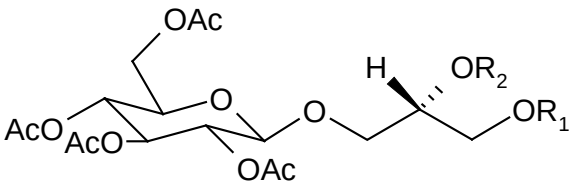

Compounds	R_1	R_2	Description	Yield (%)
31a	lauroyl	lauroyl	amorphous solid	89.1
31b	linolenoyl	linolenoyl	syrupy mass	56.7
31c	linolenoyl	lauroyl	syrupy mass	64.0

Table 23. The chemical structures and some properties of **32a-c**.

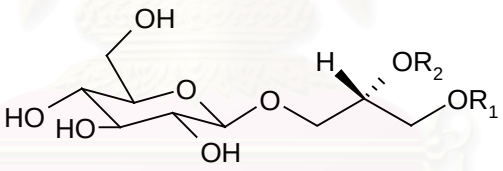

Compounds	R_1	R_2	Description	Yield (%)	Elemental analysis	C	H
32a	lauroyl	lauroyl	amorphous solid	48.2	Calcd.	64.036	10.104
					Found	64.115	10.189
32b	α-linolenoyl	α-linolenoyl	syrupy mass	27.7	Calcd.	69.720	9.629
					Found	69.809	9.778
32c	α-linolenoyl	lauroyl	syrupy mass	34.5	Calcd.	67.195	9.840
					Found	67.316	9.990

The ^{1}H-NMR and ^{13}C-NMR spectra of **32a-c** (Figures 206-212, 243) showed the signals which were characteristically attributable to glucosyl diglycerides

as early mentioned. Nevertheless, the proton and carbon signals of **32a-c** clearly indicated that each one contained only one diastereomeric pure isomer.

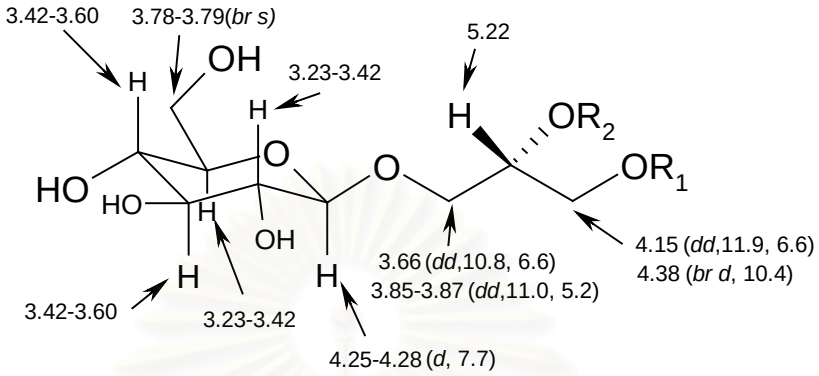

Figure 243. The general structures and proton assignments of **32a-c**.

The synthesis of 1-*O*-linolenoyl-3-*O*-β-D-glucopyranosyl-*sn*-glycerol (**34**) followed the synthesis procedure mentioned above. Controlled acylation of **30** with linolenic acid at 0 ^{0}C provided 1-*O*-linolenoyl-3-*O*-(β-D-2′,3′,4′,6′-tetra-*O*-acetyl-glucopyranosyl)-*sn*-glycerol (**33**) (Figures 213-214). Then, **33** was treated with hydrazine monohydrate to form **34**. The chemical structure of **34** was elucidated by analysis of NMR spectral data (Figures 215-217, 244). The ^{1}H-NMR and ^{13}C-NMR spectra of **34** resembled those of **8b**, however, the spectra of **34** showed clear splitting patterns in proton signals and singlet sharp carbon signals in the ^{13}C-NMR spectrum indicating only one diastereomeric isomer.

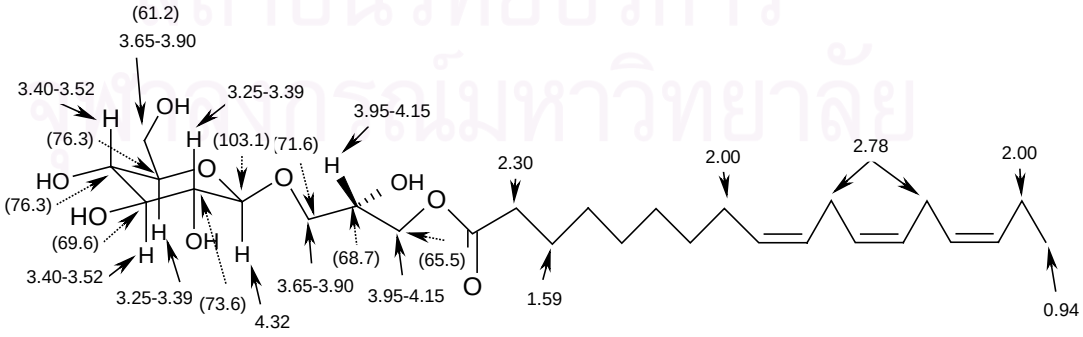

Figure 244. The chemical structure and proton assignment of **34**.

The connectivities of these protons and the connectivities of these protons to the oxygenated carbons were obtained from the correlations in 2D ^{1}H-^{1}H COSY (Figure 218) and HMQC spectra (Figure 219), respectively.

The synthesis of 1,2-di-*O*-linolenoyl-3-*O*-β-D-galactopyranosyl-*sn*-glycerol (**38**) was achieved following the above synthesis procedure (Scheme 4). **28** was glycosylated with acetobromo-α-D-galactose under Koenigs-Knorr condition to give1,2-di-*O*-benzyl-3-*O*-(β-D-2′,3′,4′,6′-tetra-*O*-acetyl-galactopyranosyl)-*sn*-glycerol (**35**) (Figures 220-221).

Then, **35** was debenzylated by catalytic hydrogenolysis to give 1-*O*-(β-D-2′,3′,4′,6′-tetra-*O*-acetyl-galactpyranosyl)-*sn*-glycerol (**36**) (Figure 222).

Acylation of **36** with α-linolenic acid afforded peracetylated galactosyl diglyceride (**37**) which was deacetylated by hydrazinolysis to give the corresponding diastereomeric pure galactosyl diglyceride (**38**). The chemical structure and purity of **38** could be deduced by analysis of NMR spectral data. The ^{1}H-NMR spectrum of **38** (Figure 225) showed characteristic signals of galactosyl diglycerides with some contaminant signals, at δ 0.85 (contaminant), 0.95 (6H, *t*, *J* = 7.5 Hz), 1.30 (26H, should be 16H), 1.58 (4H, *br*), 2.01 (8H, *m*), 2.27 (4H, *t*, *J* = 7.5Hz), 2.78 (6H, should be 8H), 3.50 (1H, *t*, *J* = 5.5 Hz, H-5′), 3.58 (1H, *br d*, *J* = 9.7 Hz, H-3′), 3.65 (1H, *br d*, *J* = 9.8 Hz, H-2′), 3.70 (1H, *dd*, *J* = 6.5, 11.1 Hz, H_a-3), 3.80 (1H, *dd*, *J* = 4.3, 12.0 Hz, H_a-6′), 3.89 (1H, *dd*, *J* = 3.8, 10.9 Hz, H_b-3), 3.94 (1H, *br d*, *J* = 12.3 Hz, H_b-6′) 3.99 (1H, *br s*, H-4′) 4.18 (1H, *dd*, *J* = 6.6, 12.0 Hz, H_a-1), 4.25 (1H, *d*, *J* = 7.3 Hz, H-1′), 4.38 (1H, *dd*, *J* = 3.5, 12.0 Hz, H_b-1), 5.20 (1H, overlapped), 5.20-5.40 (12H, olefnic). The ^{13}C-NMR spectra (Figure 226) also showed the characteristic signals of galactosyl diglycerides i.e. 14.5-34.0 (alkyl region), 63.0-75.0 (oxygenated carbons region), 104.3 (acetal region), 127.4-132.2 (olefinic region) and 173.7, 173.9 (carbonyl region) as observed in compound **13c**. Figure 245 shows proton and carbon assignments of **38**

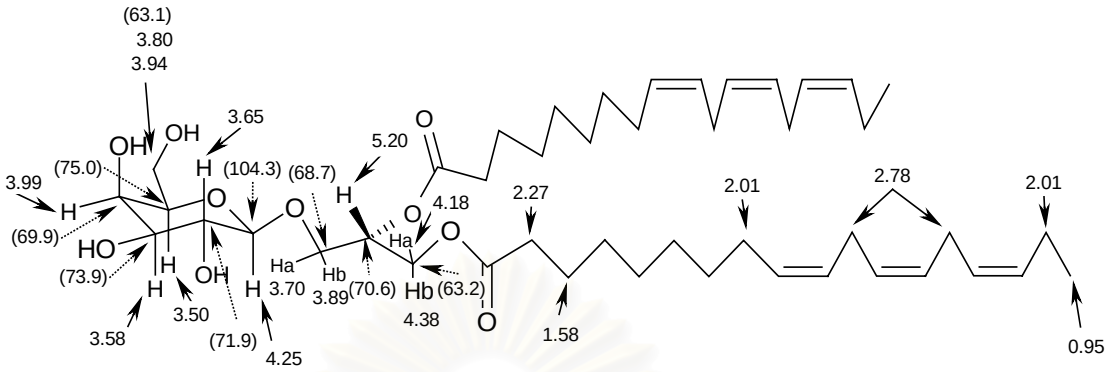

Figure 245. The chemical structure, proton and carbon assignments of **38**.

The anti-HSV activities of these diastereomeric pure isomers were determined as shown in Table 24.

Table 24. The anti-HSV activity of diastereomeric pure isomer **32a-c, 34, 38**

compounds	**Concentration (μg/ml)**	**Plaque reduction assay (% inhibition)**	
		HSV-1	**HSV-2**
32a	50	80	50
32b	50	100	100
32c	50	18	15
	100	21	39
34	50	24	40
38	50	93	90

The anti-HSV activity data showed that both mono-acid 1,2-di-*O*-acyl-glucopyranosyl-*sn*-glycerols bearing lauroyl and linolenoyl moiety (**32a-b**) exhibited high inhibitory action as expected. Surprisingly, mixed-acid glucosyl diglyceride bearing linolenoyl and lauroyl moiety at C-1 and C-2, respectively (**32c**) displayed

relatively low activity. In comparison, the anti-HSV activity of the diastereomeric mixtures (**6b**) and its diastereomeric pure isomer (**32a**) was not significantly different. The similar result was observed in the case of the diastereomeric mixtures **6i** and its diastereomeric pure isomer (**32b**). On the other hand, diastereomeric pure galactosyl diglyceride (**38**) displayed anti-HSV activity no significant difference from that of its diastereomeric mixtures (**13c**) (Table 25).

Table 25. Comparison of anti-HSV activity of diastereomeric mixtures and their diastereomeric pure isomers.

compound	**sugar**	**R_1**	**R_2**	**Conc. (μg/ml)**	**C-2 configuration**	**Plaque reduction assay (% inhibition)**	
						HSV-1	**HSV-2**
6b	glucose	lauroyl	lauroyl	50	R,S	80	50
32a	glucose	lauroyl	lauroyl	50	S	80	50
6i	glucose	α-linolenoyl	α-linolenoyl	50	R,S	94	97
32b	glucose	α-linolenoyl	α-linolenoyl	50	S	100	100
13c	galactose	α-linolenoyl	α-linolenoyl	50	R,S	95	95
38	galactose	α-linolenoyl	α-linolenoyl	50	S	93	90

In conclusion, studies on the effect of the stereochemistry at C-2 of the glycerol backbone on anti-HSV activity revealed that the stereochemistry at C-2 of the glycerol backbone of these compounds did not seem to influence the anti-HSV activity. Moreover, the 50% inhibitory concentration (IC_{50}) and toxicity of promising compounds **32a** and **32b** were also determined as shown in Table 26.

Table 26. The 50% inhibitory concentration (IC_{50}) and toxicity of **32a** and **32b**.

Compounds	IC_{50} (μg/ml)		Toxicity (μg/ml)
	HSV-1	HSV-2	
32a	23.0 (37.2 μM)	40.0 (64.7 μM)	>100
32b	12.5 (16.1 μM)	18.5 (23.9 μM)	>100
acyclovir	0.06 (0.26 μM)	0.5 (2.2 μM)	-

The data showed that **32b** displayed the potency about two times higher than that of **32a** and did not show toxicity at concentrations up to 100 μg/ml.

4. Effect of Glycoglycerolipids on Herpes Simplex Viral Particles

The preliminary structure activity relationships study of glycoglycerolipids on anti-HSV activity revealed that glycosyl diglycerides bearing linolenoyl or lauroyl moieties (**6b, 6i**) possessed promising anti-HSV activity. Although the mechanism of action was still unknown, we postulated that these compounds targeted the viral lipid envelope, causing leakage or disruption of viral envelope. To study the effect of these compounds on viral particles, the transmission electron microscope experiment was established to observe the morphology of viral particles. Staining of HSV-1 without sample showed transparent round-shaped particles (Figure 246).

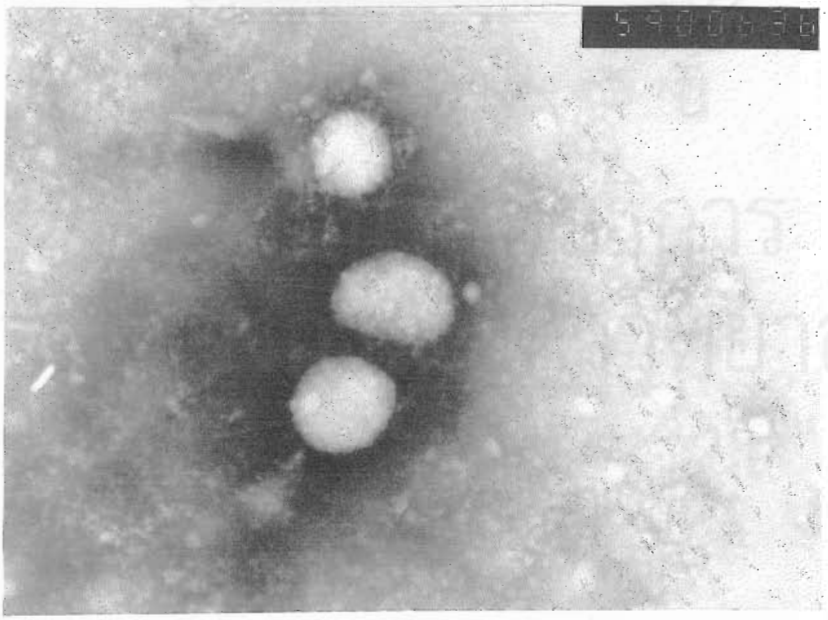

Figure 246. Transmission electron micrograph of staining of HSV-1 without sample (bar, 100 nm.) (magnification × 102,000).

In contrast to the staining of HSV-1 with **6b** or **6i** showed distorted particles with staining inside (Figures 247-248). These results suggested that the inhibitory activity due to the disruption of viral envelope was one of the possible antiviral mechanisms of these compounds.

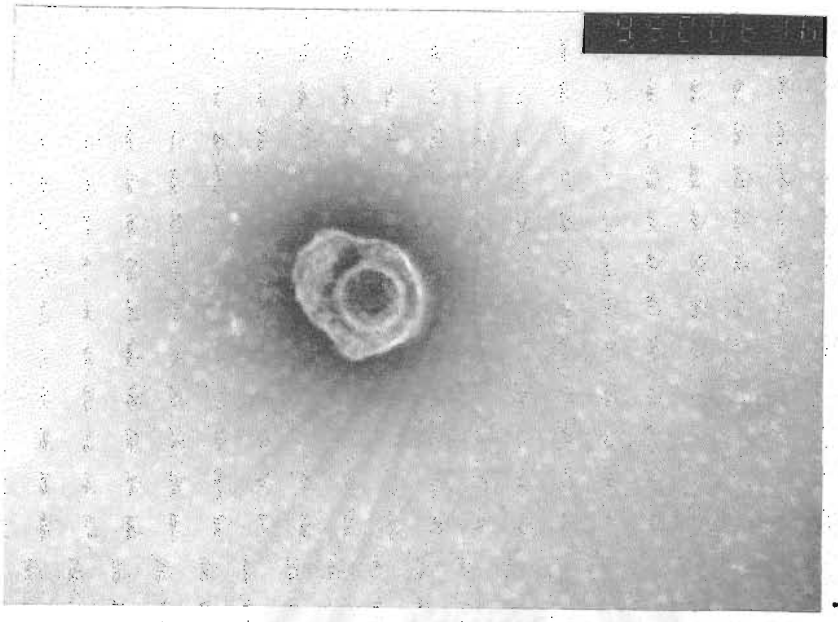

Figure 247. Transmission electron micrograph of staining of HSV-1 with **6b** (bar, 100 nm.) (magnification × 102,000).

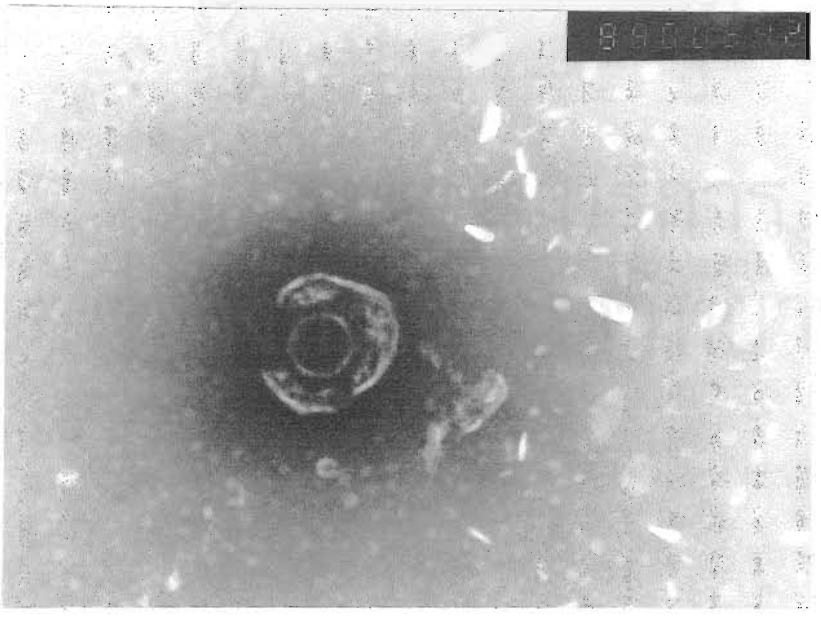

Figure 248. Transmission electron micrograph of staining of HSV-1 with **6i** (bar, 100 nm.) (magnification × 102,000).

CHAPTER V
CONCLUSION

This present investigation aimed to study the synthesis and anti-HSV activity of glycoglycerolipids, the new class of compounds possessing anti-HSV activity. Herein, preliminary structure-activity relationships of these compounds on anti-HSV activity were explored. A variety of compounds were synthesized which could be classified and summarized as following.

1. 1,2-di-*O*-acyl-3-*O*-β-D-glycopyranosyl-*rac*-glycerols and 1-*O*-acyl-3-*O*-β-D-glycopyranosyl-*rac*-glycerols. Diastereomeric mixtures of these compounds were prepared by glycosylation of D,L-α,β-isopropylidene glycerol and acetobromosugar under Koenigs-Knorr condition. The 1,2-*O*-isopropylidene-3-*O*-(β-D-2′,3′,4′,6′-tetra-*O*-acetyl-glycopyranosyl)-*rac*-glycerols obtained were deacetonized by 60% CH_3COOH to give 1-*O*-(β-D-2′,3′,4′,6′-tetra-*O*-acetyl-glycopyranosyl)-*rac*-glycerols which were subsequently acylated with the desired fatty acids to form 1,2-*O*-diacyl- or 1-*O*-acyl-3-*O*-(β-D-2′,3′,4′,6′-tetra-*O*-acetyl-glycopyranosyl)-*rac*-glycerols. Finally, 1,2-di-or 1-*O*-acyl-3-*O*-(β-D-2′,3′,4′,6′-tetra-*O*-acetyl-glycopyranosyl)-*rac*-glycerols were selectively deacetylated by hydrazinolysis to yield the corresponding 1,2-di-*O*-acyl-3-*O*-β-D-glycopyranosyl-*rac*-glycerols or 1-*O*-acyl-3-*O*-β-D-glycopyranosyl-*rac*-glycerols.

2. 1,2-di-*O*-acyl-3-*O*-β-D-glycopyranosyl-*sn*-glycerols and 1-*O*-acyl-3-*O*-β-D-glycopyranosyl-*sn*-glycerols. These diastereomeric pure compounds were prepared by glycosylation of acetobromosugar and 1,2-*O*-dibenzyl-*sn*-glycerol under Koenigs-Knorr condition to give 1,2-di-*O*-benzyl-3-*O*-(β-D-2′,3′,4′,6′-tetra-*O*-acetyl-glycopyranosyl)-*sn*-glycerols, which were then removed benzyl protecting groups by catalytic hydrogenolysis. The 1-*O*-(β-D-2′,3′,4′,6′-tetra-*O*-acetyl-glycopyranosyl)-*sn*-glycerols obtained were acylated with the desired fatty acids to form 1,2-di- or 1-*O*-acyl-3-*O*-(β-D-2′,3′,4′,6′-tetra-*O*-acetyl-glycopyranosyl)-*sn*-glycerols. Finally, the products obtained were reacted with hydrazine to yield the corresponding 1,2-di-*O*-acyl-3-*O*-β-D-glycopyranosyl-*sn*-glycerols or 1-*O*-acyl-3-*O*-β-D-glycopyranosyl-*sn*-glycerols.

3. 1,2-di-*O*-acyl- or 1-*O*-acyl-*rac*-glycerols. 1,2-di-*O*-acyl-*rac*-glycerol was prepared by benzylation of D,L-α,β-isopropylidene glycerol to give 1,2-*O*-isopropylidene-3-*O*-benyl-*rac*-glycerol, which was then removed isopropylidene protecting group by 60% CH_3COOH. The 1-*O*-benzyl-*rac*-glycerol obtain was acylated with the desired fatty acid and finally, was debenzylated to give the 1,2-di-*O*-acyl glycerol. 1-*O*-acyl glycerols were prepared by acylation of D,L-α,β-isopropylidene with the desired fatty acids, then, the 1-*O*-acyl-2,3-*O*-isopropylidene-*rac*-glycerols were removed isopropylidene protecting groups to give the 1-*O*-acyl-glycerols.

The chemical structures of all compounds were elucidated by spectroscopic techniques, mainly NMR spectra, mass spectra and elemental analysis.

Study on the anti-HSV activity of these compounds revealed that, of all the synthetic compounds, 1,2-di-*O*-acyl-3-*O*-β-D-glycopyranosyl-glycerols exhibited the most active anti-HSV activity. Preliminary structure-activity relationships study indicated that the fatty acyl moieties were critical for inhibitory action with higher activity displayed as the acyl groups became more olefinic in character. The sugar moiety was also important for anti-HSV action; however, the type of sugar (glucose or galactose) exhibited no different activity. The stereochemistry at C-2 of the glycerol backbone displayed no significant effect on anti-HSV activity. Among the compounds synthesized, **32b** showed the highest inhibitory activity against HSV-1 and HSV-2 with the IC_{50} values of 12.5 and 18.5 μg/ml, respectively. The transmission electron micrographs of staining HSV-1 with these compounds showing distortion of viral parpticles suggested that the disruption of viral envelopes by these compounds was one of the possible antiviral mechanisms.

REFERENCES

Abou-Karam, M., and Shier, W.T. Isolation and characterization of an antiviral flavonoid from *Waldsteinia fragraioides*. J. Nat. Prod. 55 (10) (1992): 1525-1527.

Abou-Karam, M., and Shier, W.T. A simplified plaque reduction assay for antiviral agents from plants, demonstration of sequence of antiviral activity in higher plants. J. Nat. Prod. 5 (1990): 340-344.

Alrabiah, F.A., and Sacks, S.L. New anti-herpes virus agents: their targets and therapeutic potential. Drugs 52(1) (July 1996): 17-32.

Baruah, P., Baruah, N.C., Shama, R.P., Baruah, J.N., Kulanthaivel, P., and Herz, W. A monoacyl galactosylglycerol from *Sonchus arvensis*. Phytochemistry 22 (1983): 1741-1744.

Beauchamp, L.M., Orr, G.F., de Miranda et al. Amino acid ester prodrugs of acyclovir. Antivir. Chem. Chemother. 3 (1992): 157-164.

Binkley, R.W. Modern carbohydrate chemistry. New York: Marcel Dekker, 1988.

Bisacchi, G.S., Braitman, A., Cianci, C.W., et al. Synthesis and antiviral activity of enantiomeric forms of cyclobutyl nucleoside analogues. J. Med. Chem. 34 (1991): 1415-1421.

Boyd, M.R., Bacon, T.H., Sutton, D., et al. Anti-herpes virus activity of 9-(4-hydroxy-3-hydroxymethylbut-1-yl) guanine (BRL 39123) in cell culture. Antimicrob. Agents Chemother. 31 (1987): 1238-1242.

Colombo, D., Scala, A., Taino, I.M., Toma, L., Ronchetti, F., Tokuda, H., Nishino, H., Nagatsu, A., Sakakibara, J. Inhibitory effects of fatty acid monoesters of 2-O-beta-D-glycosylglycerol on Epstein-Barr virus activation. Cancer Lett. 16: 123(1) (1998): 83-86.

Colombo, D., Compostella, F., Ronchetti, F., Scala, A., Toma, L., Tokuda, H., Nishino, H. Chemoenzymatic synthesis and antitumor promoting activity of 6'-and 3-esters of 2-O-beta-D-glucosylglycerol. Bioorg. Med. Chem. 7(9) (1999): 1867-1871.

Craig, C.P., and Nahmias, A.D. Different patterns of neurologic involvement with herpes simplex virus types 1 and 2: isolation of herpes simplex virus type 2 from the buffy coat of two adults with meningitis. J. Infect. Dis. 127 (1973):

365-372.

DeClerq, E., Holy, A. Efficacy of (S)-2-(3-hydroxy-2-phosphonyl methoxy propyl) cytosine in various models of herpes simplex virus infection in mice. Antimicrob. Agents Chemother. 35 (1991): 701-706.

DeClerq, E., Holy, A., Rosenberg, I., et al. A novel selective broad spectrum anti-DNA virus agent. Nature 323 (1986): 464-467.

de Miranda, P., and Blum, M.R. Pharmacokinetics of acyclovir after intravenous and oral administration. J. Antimicrob. Chemother. 12 (suppl.B) (1983): 29-37.

Douce, R., and Joyard, J. Plant galactolipids. In P.K. Stumpf, and E.E. Conn (eds.), The biochemistry of plants vol. 4, pp. 321-362. New York: Academic Press, 1980.

Duan, J., Liuzzi, M., Paris, W., Lambert, M., Lawetz, C., Moss, N., Jaramillo, J., Gauthier, J., Deziel, R., Cordingley, M.G. Antiviral activity of a selective ribonucleotide reductase inhibitor agent: Acyclovir-resistant herpes virus type I *in vivo*. Antimicrob. Agents Chemother. 42 (7) (July 1998): 1629-1635.

Fife, K.H., Crumpacker, C.S., Mertz, G.J., et al. Recurrence and resistance patterns of herpes simplex following cessation of >6 years of chronic acyclovir suppression. J. Infect. Dis. 169 (1994): 1338-1341.

Gigg, R. Synthesis of glycolipids. Chem. Phys. Lipids 26 (1980): 287-404.

Golstein, L.C., Corey, L., McDougall, J.K., et al. Monoclonal antibodies to herpes simplex viruses: use in antigenic typing and rapid diagnosis. J. Infect. Dis. 147 (1983): 829-837.

Greene, T., and Wuts, P. G. M. Protective groups in organic synthesis. 2 nd ed. New York: John Wiley & Sons, 1991.

Hakimelahi, G.H., Ly, T.W., Moosavi-Movahedi, A.A., Jain, M.L., Zakerinia, M., Davari, H., Mei, H.C., Sambaiah, T., Moshfegh, A.A., and Hakimelahi, S. Design, synthesis, and biological evaluation of novel nucleoside and nucleotide analogues as agents against DNA viruses and/or retroviruses. J. Med. Chem. 44 (2001): 3710-3720.

Hayashi, K., Hayashi, T., Morita, N. Mechanism of action of the antiherpes virus biflavone ginkgetin. Antimicrob. Agents Chemother. 39(9) (1992): 1890-1893.

Hayashi, T., Hayashi, K., Uchida, K., Niwatama, S., Morita, N. Antiviral agents of

plants origins II; antiviral activity of scopadulcic acid B derivatives. Chem. Pharm. Bull. 38(1) (1990): 239-242.

Helgstrand, E., Eriksson, B., Johansson, N.G., Lannero, B., Larsson, A., Misiorny, A., Noren, J.O., Sjoberg, B., Stenberg, K., Stenning, G., Stridh, S., Oberg, B. Trisodium phosphonoformate, a new antiviral compound. Science 201 (1978): 819-821.

Ikeda, T., Ando, J., Miyazono, A., Zhu, X.H., Tsumagari, H., Nohara, T., Yokomizo, K., and Uyeda, M. Anti-herpes virus activity of solanum steroidal glycosides. Biol. Pharm. Bull. 23(3) (2000): 363-364.

Jayawasu, C., Dechatiwongse, T., Balschandra, K. The virucidal activity of *Clinacanthus nutans* Lindau extract against herpes simplex virus type 2: An *in vitro* study. Bull. Dept. of Med. Sci. 34 (1992): 153-158.

Katz, D.H., Marcelletti, J.F., Khalil, M.H., et al. Antiviral activity of 1-docosanol, an inhibitor of lipid-enveloped viruses including herpes simplex. Proc. Natl. Acad. Sci. USA 88 (1991): 10825-9.

Kinjo, J., Yokomizo, K., Hirakawa, T., Shii, Y., Nohara, T., Uyeda, M. Anti-herpes virus activity of fabaceous triterpenoidal saponins. Biol. Pharm. Bull. 23 (7) (2000): 887-889.

Kochetkov, N.K., Khorlin, A.J., and Bochkov, A.F. A new method of glycosylation. Tetrahedron 23 (1967): 693-707.

Koenigs, W., and Knorr, E. Uber einige derivate des traubenzuckers und der galactose. Ber. Dtsch. Chem. Ges. 34 (1901): 957-960.

Kopitz, J. Glycolipids: Structure and function. In H. J. Gabius, and S. Gabius (eds.), Glycosciences, pp. 163-189. Weinheim: Chapman & Hall, 1997.

Kost, R.G., Hill, E.L., Tigges, M., and Straus, S.E. Recurrent acyclovir-resistant genital herpes in an immunocompetent patient. N. Engl. J.Med. 329 (1993): 1777-1782.

Koszalka, G.W., Daluge, S.M., and Boyd, F.L. Chapter 16 Advances in nucleoside and nucleotide antiviral therapies. Annual Reports in Medicinal Chemistry 33 (1998): 163-171.

Lin, Y.M., Flavin, M.T., Schure, R., Sidwell, R., Barnard, D., Huffman, J.H., Kern, E.R. Antiviral activities of biflavonoids. Planta Med. 65 (1999): 120-125.

Lin, L.M., Kuo, Y.C., Chou, C.J. Anti-herpes simplex virus type-1 flavonoids and a

new flavanone from the root of *Limonium sinense*. Planta Med. 66 (2000): 333-336.

Loya, S., Reshef, V., Mizrachi, E., Silberstein, C. and Rachamin, Y. The inhibition of the reverse transcriptase of HIV-1 by the natural sulfoglycolipids from cyanobacteria: contribution of different moieties to their high potency. J. Nat. Prod. 61 (1998): 891-895.

Machida, H., Sakata, S., Kuninaka, A., et al. Antiherpes viral and anti-cellular effects of 2-β-D-arabinofuranosyl-E-5-(2-halogenovinyl) uracils. Antimicrob. Agents Chemother. 20 (1981): 47-52.

Mannock, D.M., Lewis, R.N.A.H., McElhaney. R.N. An improved procedure for the preparation of 1,2-di-O-acyl-3-O-(β-D-glucopyranosyl)-*sn*-glycerols. Chem. Phys. Lipids 43 (1987):113-127.

Mertz, G. J. Herpes simplex virus infections. In G. J. Galasso, R. J. Whitley, and T.C. Merigan (eds.), Antiviral agents and viral diseases. 4 th ed., pp. 305-341. Philadelphia: Lippincott-Raven Publishers, 1997.

Meyer, J.J.M., Afolayan, A.J., Taylor, M.B., Erasmus, D. Antiviral activity of galangin isolated from the aerial parts of *Helichrysum aureonitens*. J. Ethnopharmacol. 56 (1996): 165-169.

Mucsi, I., Molnar, J., Hohmann, J., Redei, D. Cytotoxicities and anti-herpes simplex virus activities of diterpenes isolated from *Euphorbia* species. Planta Med. 67 (2001): 672-674.

Murakami, A., Nakamura, Y., Koshimizu, K. and Ohigashi, H. Glyceroglycolipids from *Citrus hystrix*, a traditional herb in Thailand, potently inhibit the tumor-promoting activity of 12-O-tetradecanoylphorbol 13-acetate in mouse skin. Journal of Agricultural and Food Chemistry 43 (1995): 2779-2783.

Nakata, K. High resistance to oxygen radicals and heat is caused by a galactolipid in *Microbacterium* sp. M874. J. Biochem. 127 (2000):731-737.

Nawawi, A., Ma, C., Nakamura, N., Hattori, M., Kurokawa, M. Anti-herpes simplex virus activity of alkaloids isolated from *Stephania cepharantha*. Biol. Pharm. Bull. 22(3) (1999): 268-274.

Nutter, L.M., Grill, S.D., Cheng, Y.C. Can ribonucleoside reductase be considered as an effective target for developing antiherpes simplex virus type II (HSV-2) compounds ? Biopharm. Pharmacol. 34(6) (1985):777-780.

Ohta, K., Mizushina, Y., Hirata, N., Takemura, M., Sugawara, F., Matsukage, A., Yoshida, S., and Sakaguchi, K. Sulfoquinovosyldiacylglycerol, KM043, a new potent inhibitor of eukaryotic DNA polymerases and HIV-reverse transcriptase type1 from a marine red alga, *Gigartina tenella*. Chem. Pharm. Bull. 46 (4) (1998): 684-686.

Paulsen, H. Advances in selective chemical syntheses of complex oligosaccharides. Angew. Chem. Int. Ed. Engl. 21 (1982): 155-173.

Pottage, J.C., and Kessler, H.A. Herpes simplex virus resistance to acyclovir: clinical relevance. Infectious Agents and Diseases 4 (1995): 115-124.

Pue, M.A., and Benet, L.Z. Pharmacokinetics of famciclovir in man. Antiviral Chem. Chemother. 4 (suppl. 1) (1993): 47-55.

Shirahashi, H., Morimoto, T., Nagatsu, A., Murakami, N., Tatta, K., Sakakibara, J., Tokuda, H., Nishino, H. Antitumor-promoting activities of various synthetic 1-O-acyl-3-O-(6'-O-acyl-β-galactopyranosyl)-*sn*-glycerols related to natural product from fresh water cyanobacterium *Anabaena flos-aquae* f. flos-aquae. Chem. Pharm. Bull. 44 (1996): 1404-1406.

Satakhun, S. Chemical constituents of *Clinacanthus nutans* leaves. Master thesis, Department of Pharmacognosy, The Faculty of Pharmaceutical sciences, Gruduate School, Chulalongkorn University, 2001.

Schmidt, R.R. New methods for the synthesis of glycosides and oligosaccharides-Are there alternatives to the Koenigs-Knorr method?. Angew. Chem. Int. Ed. Engl. 25 (1986): 212-235.

Schmidt, R.R. Recent developments in the synthesis of glycoconjugates. Pure & Appl. Chem. 61(7) (1989): 1257-1270

Schmidt, R.R. Strategies for the chemical synthesis of glycoconjugates. In H. J. Gabius, and S. Gabius (eds.), Glycosciences, pp. 31-53. Weinheim: Chapman & Hall, 1997.

Schmidt, R.R., and Micheal, J. Direct O-glycosylation trichloroacetimidate formation. Nucleophilicity of the anomeric oxygen atom. Tetrahedron Lett. 25 (1984): 821-824.

Sotanaphun, U., Lipipun, V., Suttisri, R., and Bavovada, R., A new antiviral and antimicrobial sesquiterpene from *Glyptopetalum sclerocarpum*. Planta Med. 65 (1999): 257-258.

Thormar, H., Isaacs, C.E., Brown, H.R., Barshatzky, M.R., and Pessolano, T. Inactivation of enveloped viruses and killing of cells by fatty acids and monoglycerides. Antimicrob. Agents Chemother. 31(1) (1987): 27-31.

Toshima, K., and Tatsuta, K. Recent progress in O-glycosylation methods and its application to natural products synthesis. Chem. Rev. 93 (1993): 1503-1531.

Wallace, J.E., and Schroeder, L.R. Koenigs-Knorr reactions. Part 1. Effects of a 2-O-acetyl substituent, the promoter, and the alcohol concentration on the stereoselectivity of reactions of 1,2-cis-glucopyranosyl bromide. J. Chem. Soc. Perkin I (1976): 1938-1941.

Wehrli, H.P., and Pomeranz, Y. Synthesis of galactosyl glycerides and related lipids. Chem. Phys. Lipids 3 (1969): 357-370.

Weller, S., Blum, M.R., Doucette, M., et al. Pharmacokinetics of the acyclovir prodrug valaciclovir after escalating single and multiple-dose administration to normal volunteers. Clin. Pharmacol. Ther. 54 (1993): 595-605.

Wulff, G., and Rohle, G. Results and problems of O-glycoside synthesis. Angew. Chem. Int. Ed. Engl. 13(3) (1974): 157-216.

Wutzler, P. Antiviral therapy of herpes simplex and varicella-zoster virus infections. Intervirology 40 (1997): 343-356.

APPENDICES

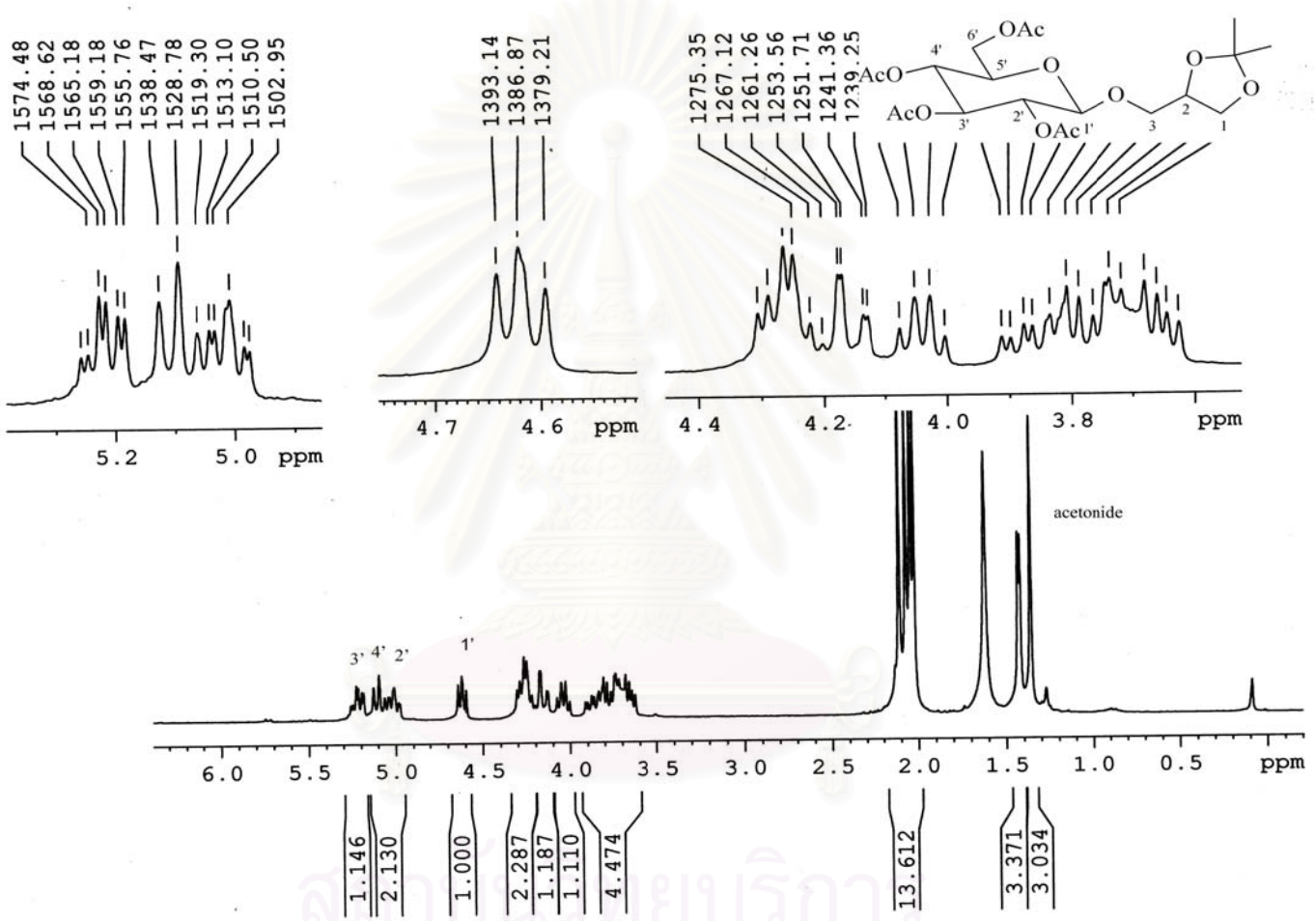

Figure 19. The 300 MHz ^{1}H-NMR spectrum of 1,2-*O*-isopropylidene-3-*O*-(β-D-2′,3′,4′,6′-tetra-*O*-acetyl-glucoopyranosyl)-*rac*-glycerol (**3**) in $CDCl_3$.

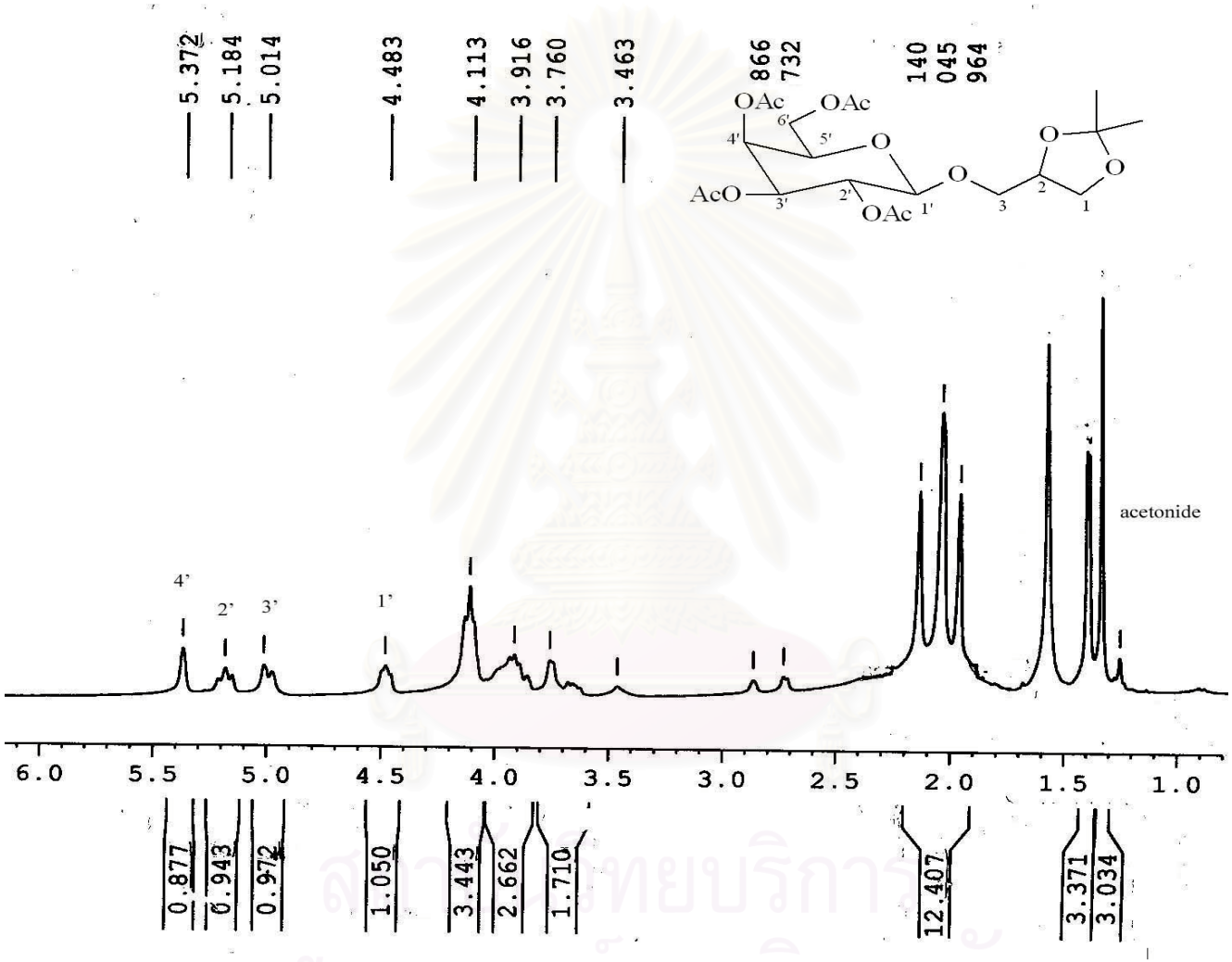

Figure 20. The 300 MHz ^{1}H-NMR spectrum of 1,2-*O*-isopropylidene-3-*O*-(β-D-2′,3′,4′,6′-tetra-*O*-acetyl-galactopyranosyl)-*rac*-glycerol (**10**) in

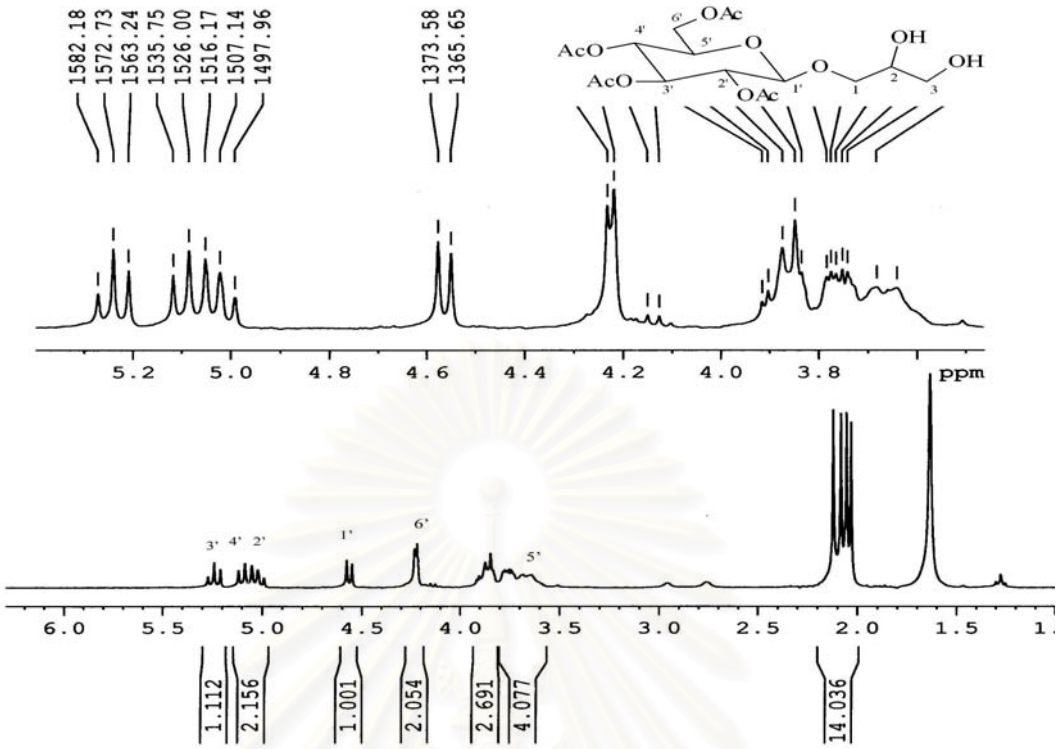

Figure 21. The 300 MHz ^{1}H-NMR spectrum of 1-*O*-(β-D-2′,3′,4′,6′-tetra-*O*-acetyl-glucopyranosyl)-*rac*-glycerol (**4**) in $CDCl_3$.

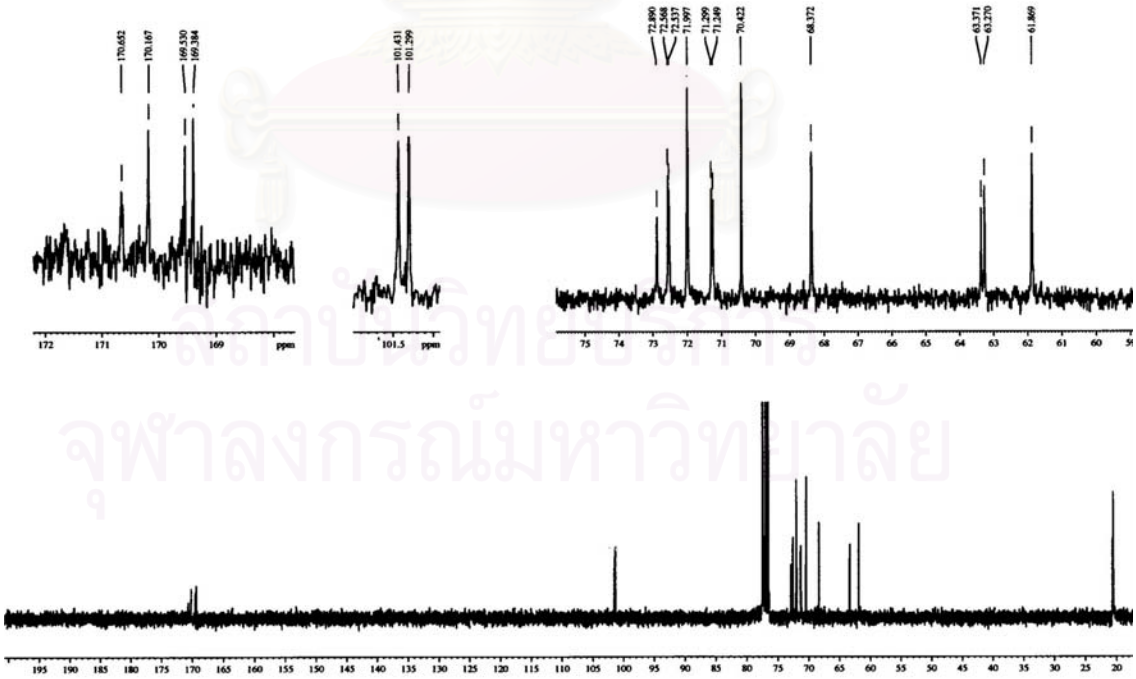

Figure 22. The 75 MHz ^{13}C-NMR spectrum of 1-*O*-(β-D-2′,3′,4′,6′-tetra-*O*-acetyl-glucopyranosyl)-*rac*-glycerol (**4**) in $CDCl_3$.

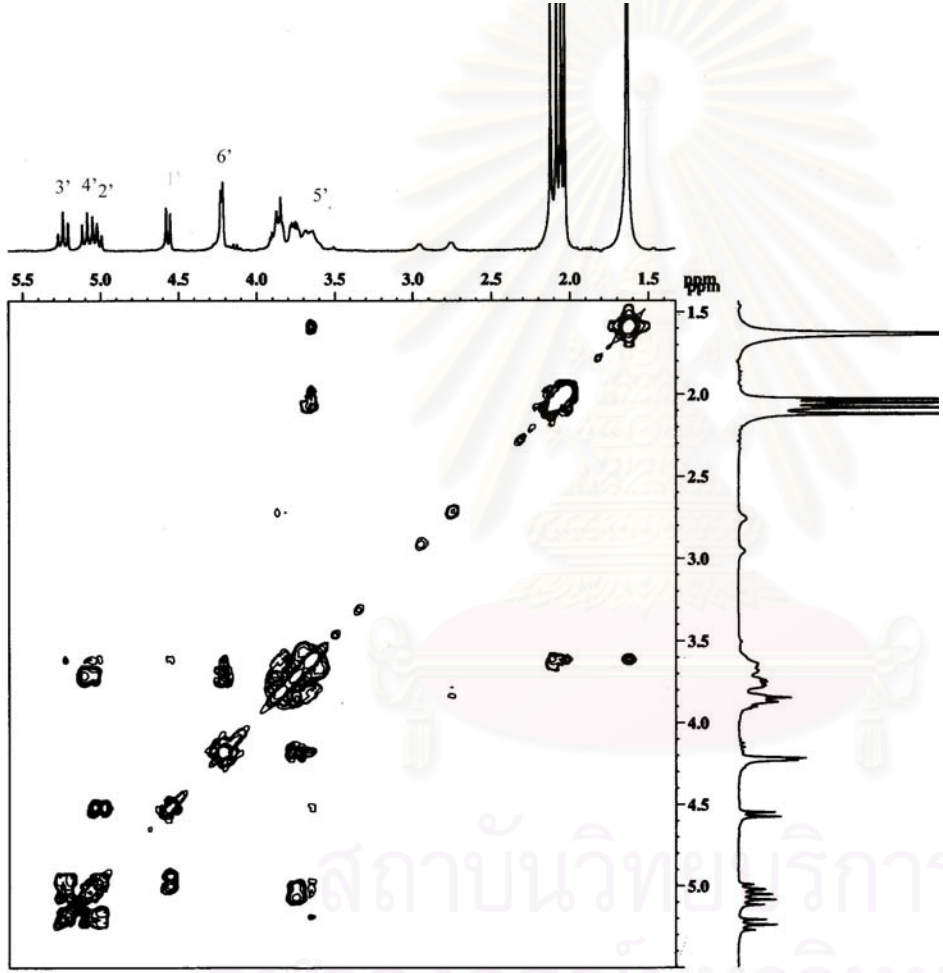

Figure 23. The ^{1}H-^{1}H COSY spectrum of 1-*O*-(β-D-2′,3′,4′,6′-tetra-*O*-acetyl-glucopyranosyl)-*rac*-glycerol (**4**) in $CDCl_3$.

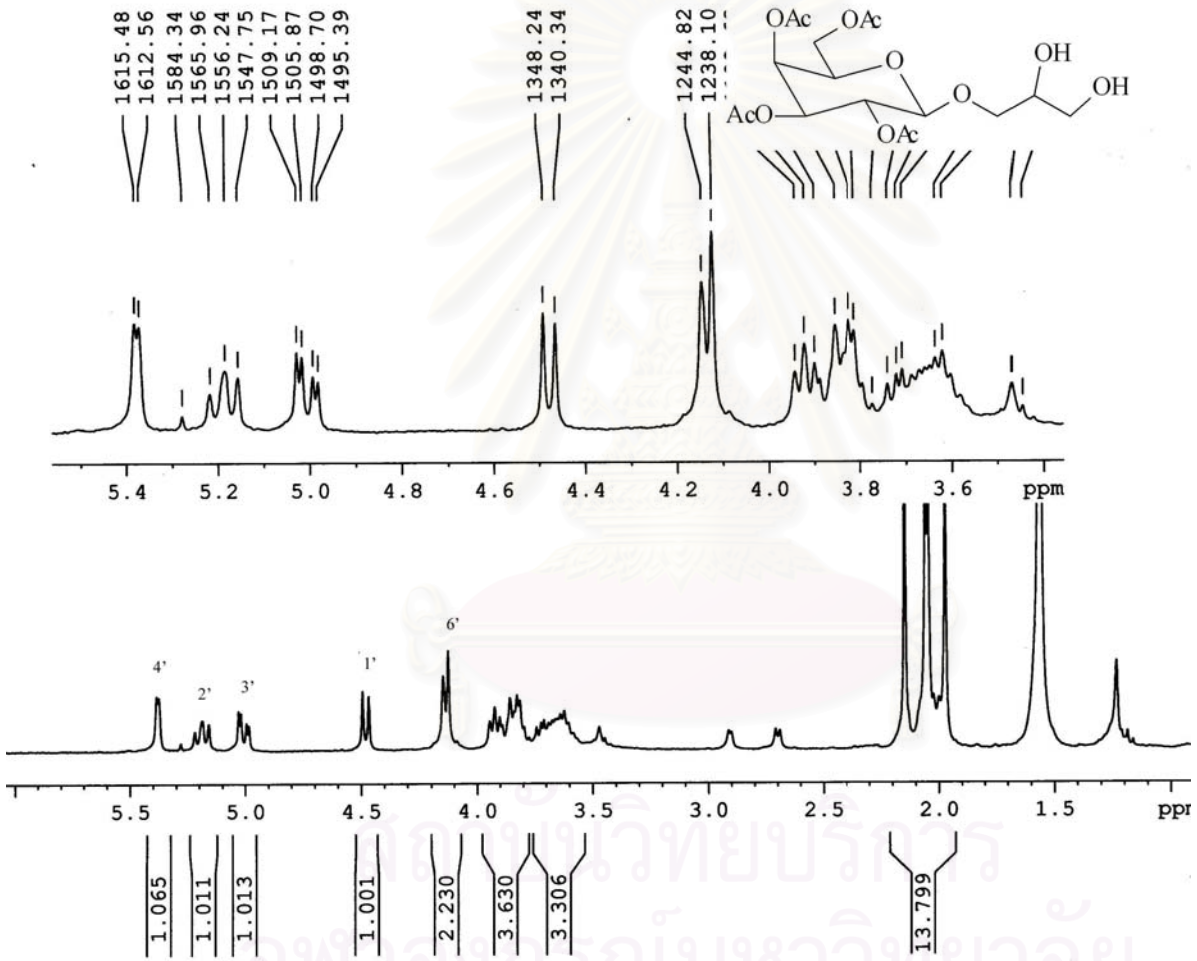

Figure 24. The 300 MHz ^{1}H-NMR spectrum of 1-*O*-(β-D-2′,3′,4′,6′-tetra-*O*-acetyl-galactopyranosyl)-*rac*-glycerol (**11**) in $CDCl_3$.

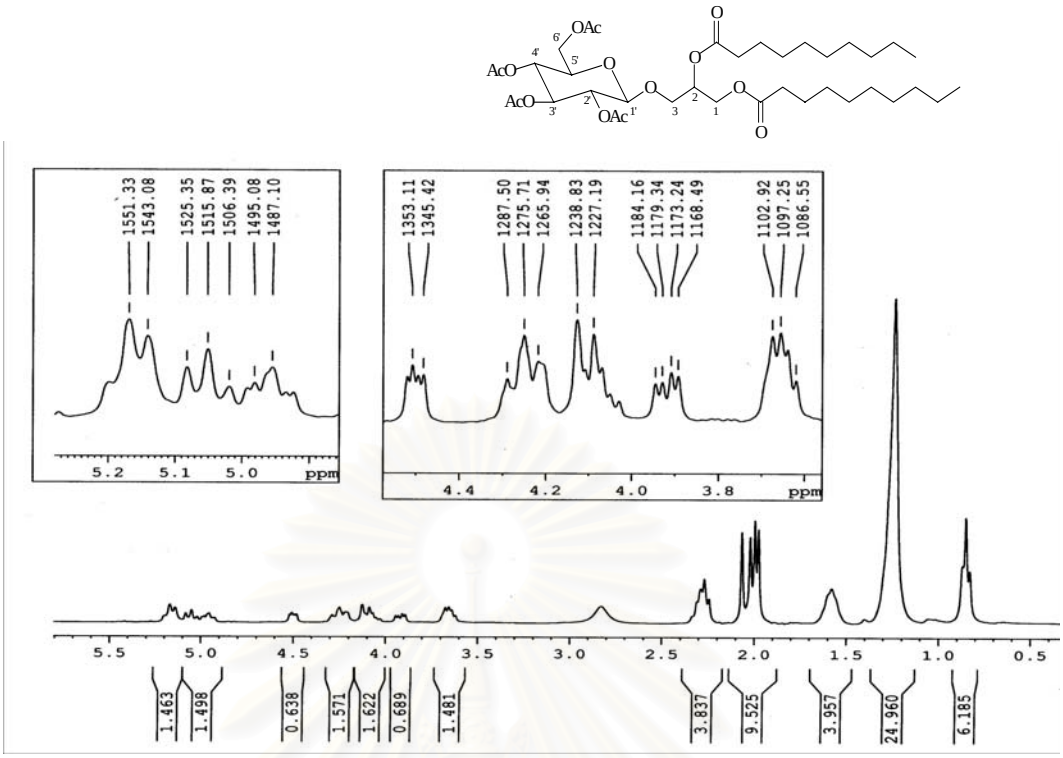

Figure 25. The 300 MHz ^{1}H-NMR spectrum of 1,2-di-*O*-carproyl-3-*O*-(β-D-2′,3′,4′,6′-tetra-*O*-acetyl-glucopyranosyl)-*rac*-glycerol (**5a**) in $CDCl_3$.

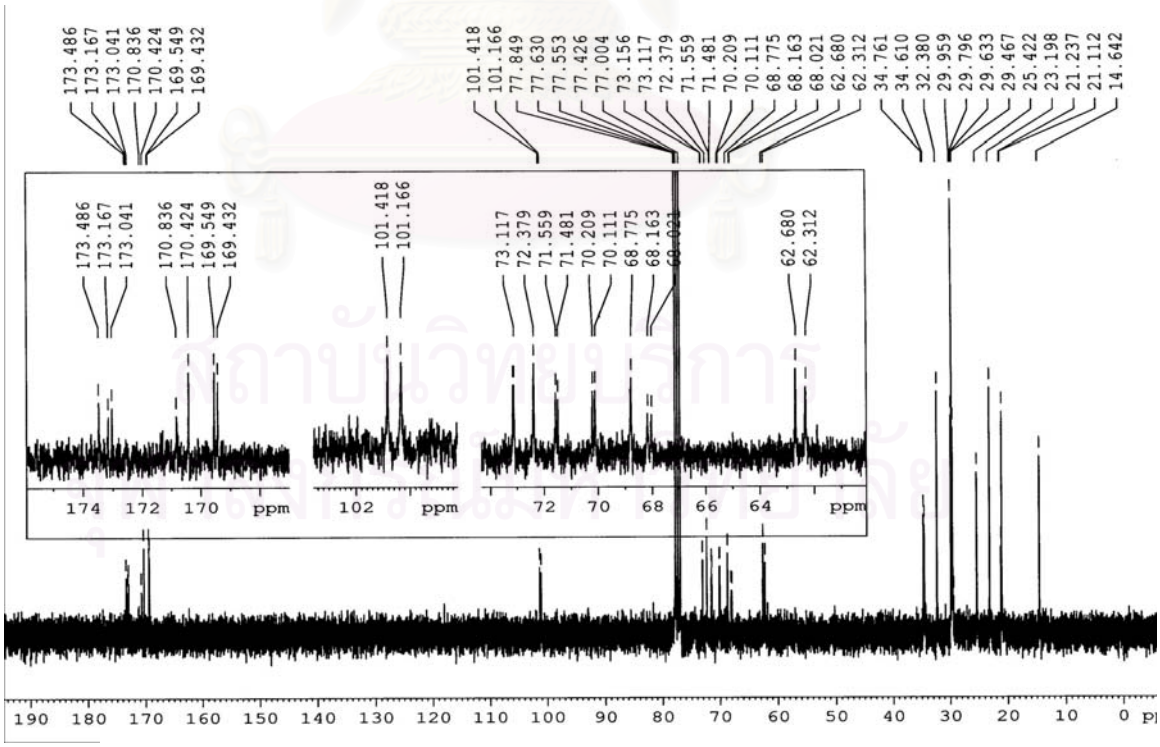

Figure 26. The 75 MHz ^{13}C-NMR spectrum of 1,2-di-*O*-carproyl-3-*O*-(β-D-2′,3′,4′,6′-tetra-*O*-acetyl-glucopyranosyl)-*rac*-glycerol (**5a**) in $CDCl_3$.

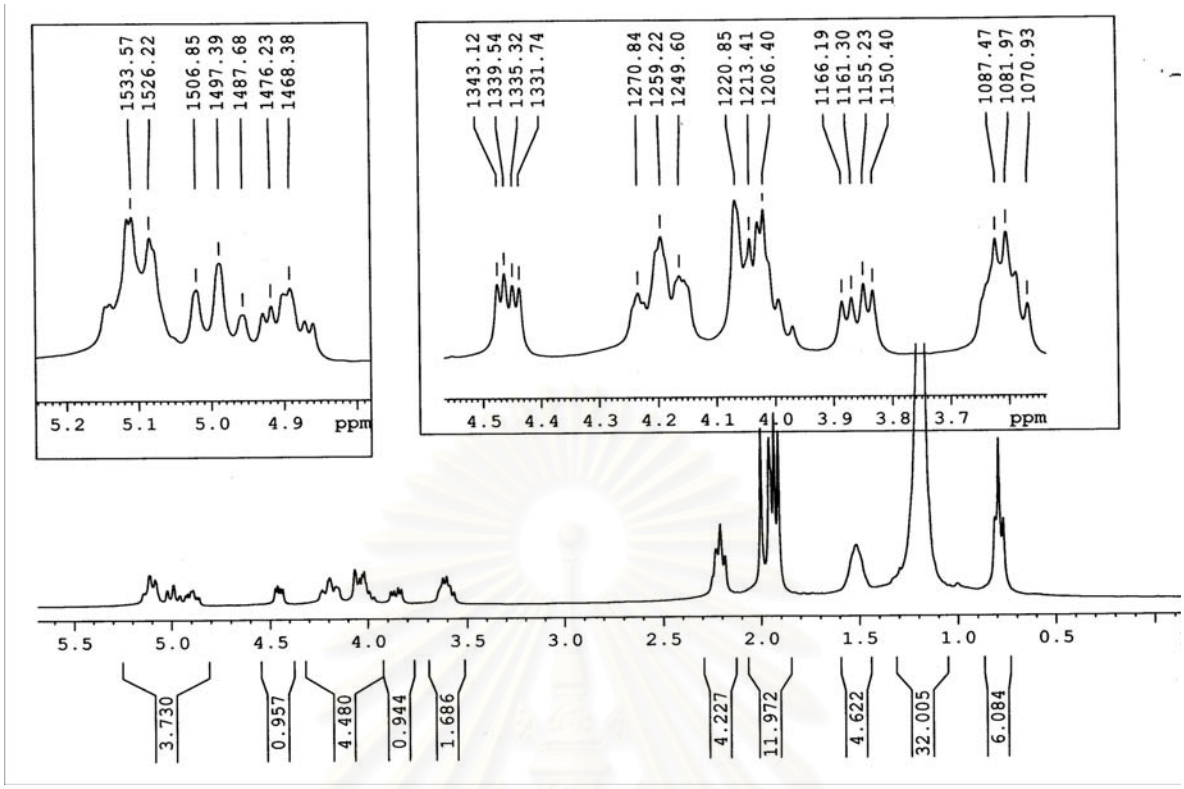

Figure 27. The 300 MHz ^{1}H-NMR spectrum of 1,2-di-*O*-lauroyl-3-*O*-(β-D-2′,3′,4′,6′-tetra-*O*-acetyl-glucopyranosyl)-*rac*-glycerol (**5b**) in $CDCl_3$.

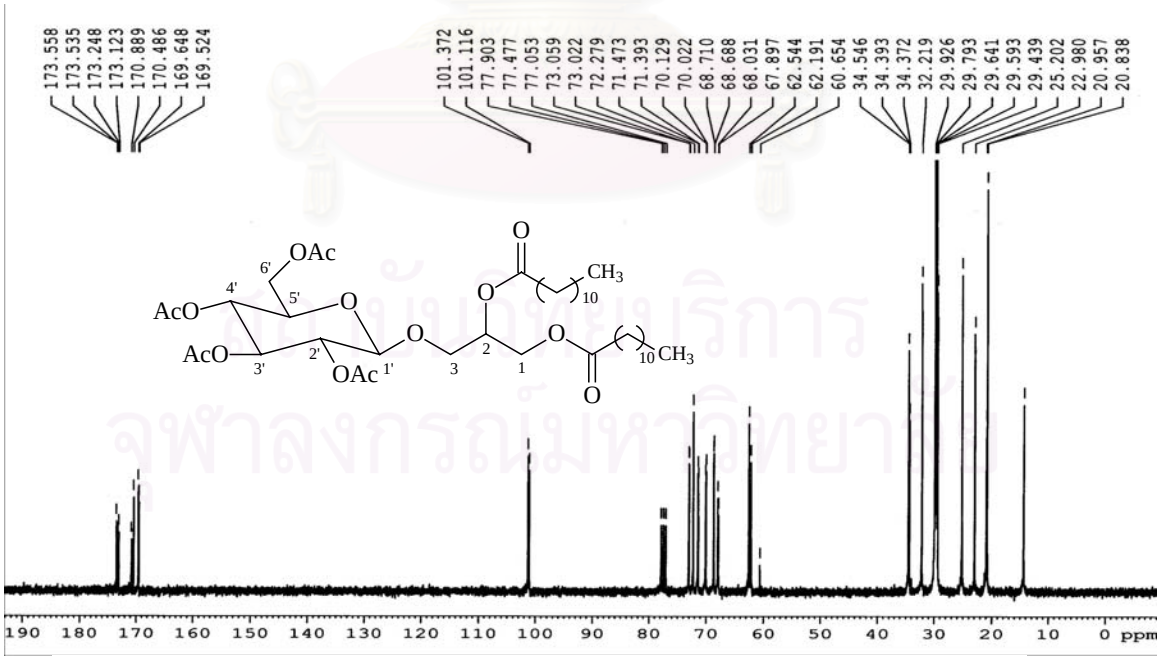

Figure 28. The 75 MHz ^{13}C-NMR spectrum of 1,2-di-*O*-carproyl-3-*O*-(β-D-2′,3′,4′,6′-tetra-*O*-acetyl-glucopyranosyl)-*rac*-glycerol (**5b**).

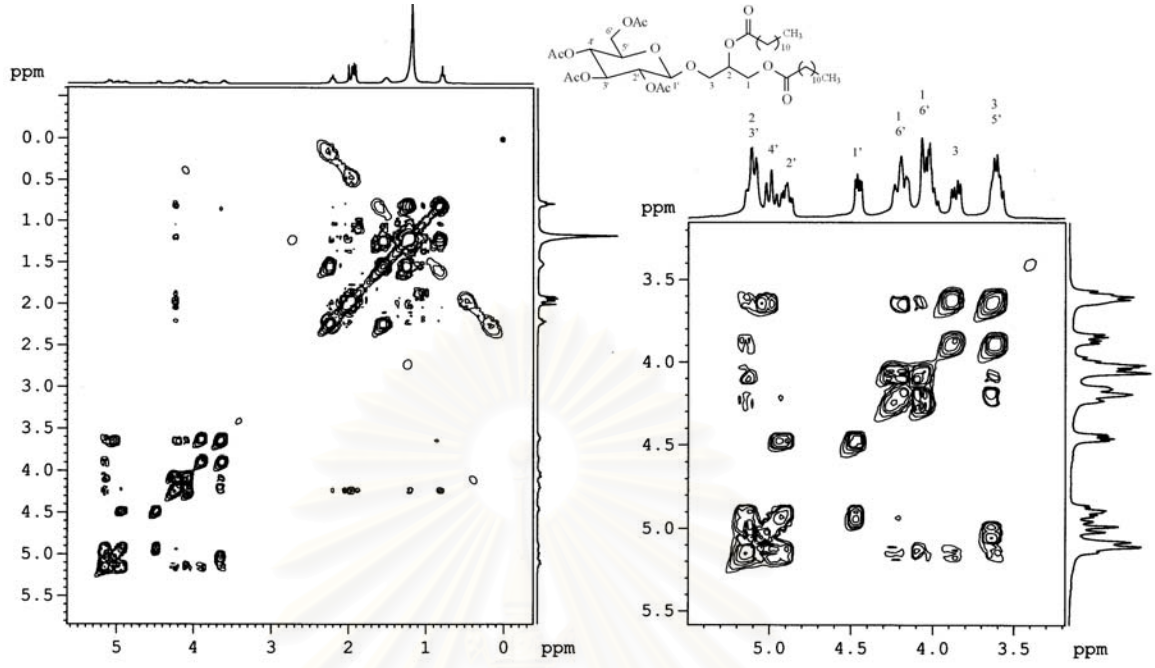

Figure 29. The ^{1}H-^{1}H COSY spectrum of 1,2-di-*O*-carproyl-3-*O*-(β-D-2′,3′,4′,6′-tetra-*O*-acetyl-glucopyranosyl)-*rac*-glycerol (**5b**) in $CDCl_3$.

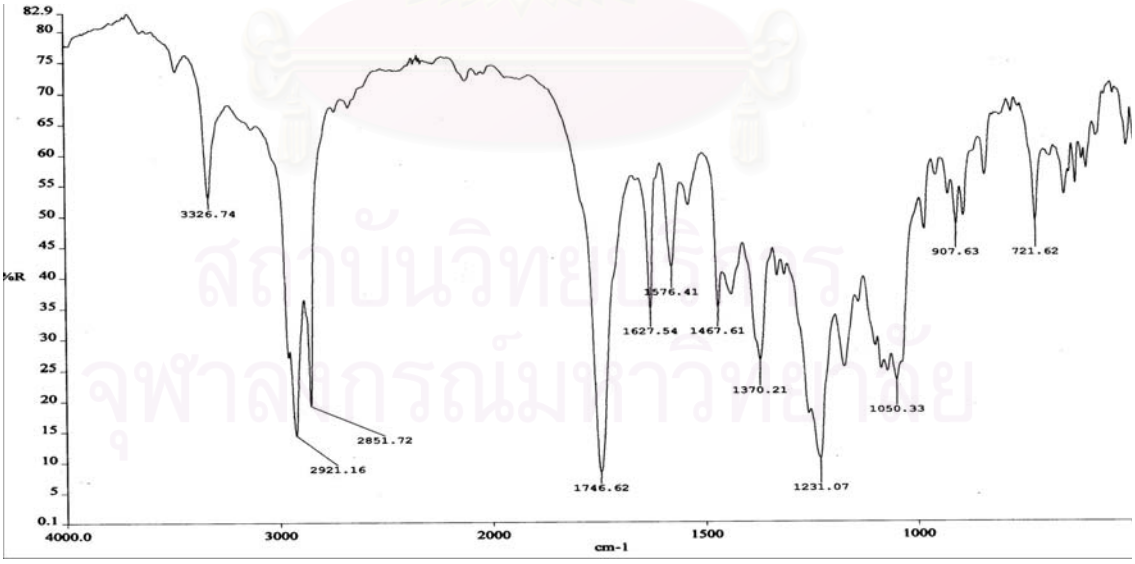

Figure 30. The infrared spectrum of 1,2-di-*O*-carproyl-3-*O*-(β-D-2′,3′,4′,6′-tetra-*O*-acetyl-glucopyranosyl)-*rac*-glycerol (**5b**).

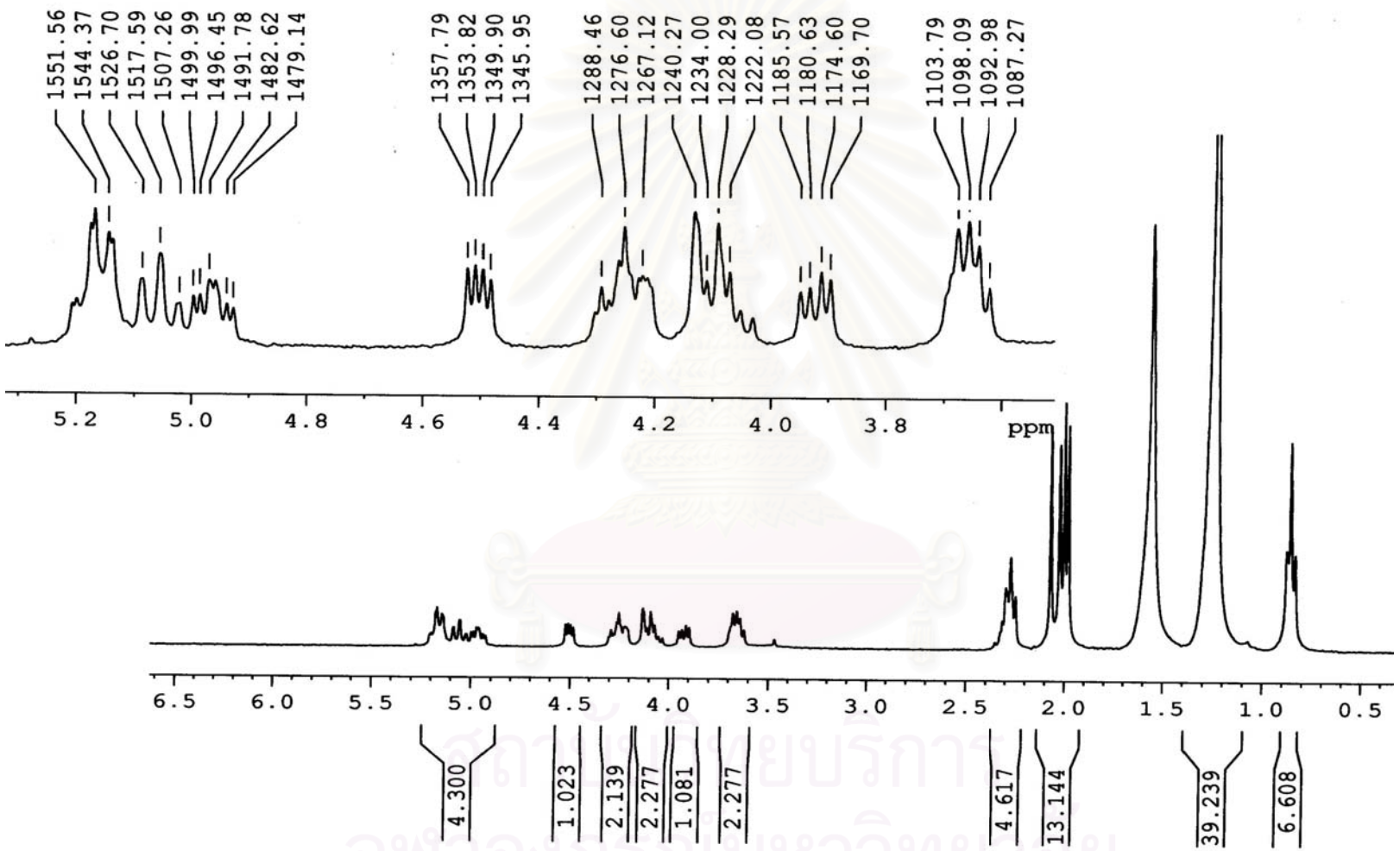

Figure 31. The 300 MHz ^{1}H-NMR spectrum of 1,2-di-*O*-myristoyl-3-*O*-(β-D-2′,3′,4′,6′-tetra-*O*-acetyl-glucopyranosyl)-*rac*-glycerol (**5c**) in $CDCl_3$.

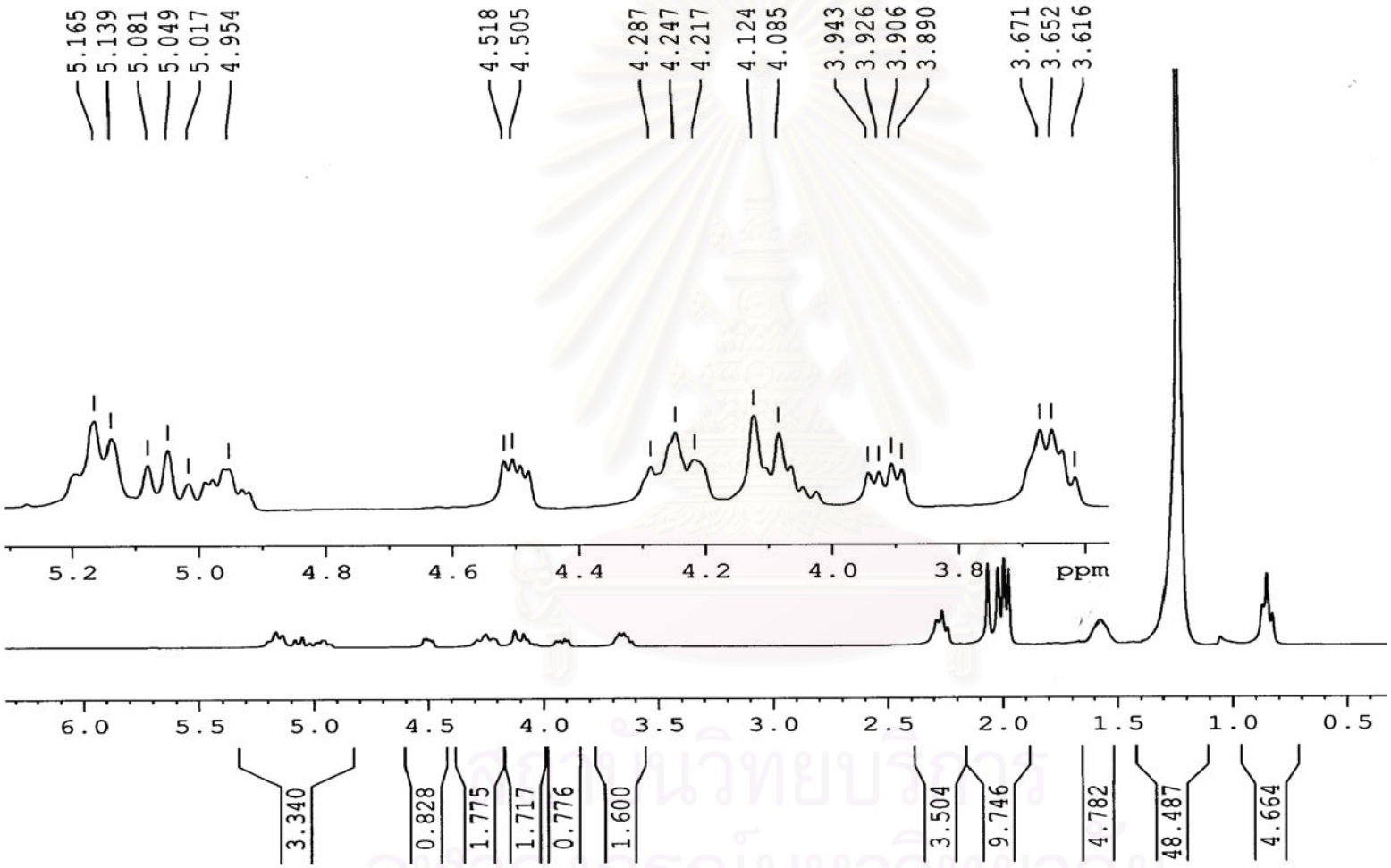

Figure 32. The 300 MHz ^{1}H-NMR spectrum of 1,2-di-*O*-palmitoyl-3-*O*-(β-D-2′,3′,4′,6′-tetra-*O*-acetyl-glucopyranosyl)-*rac*-glycerol (**5d**) in $CDCl_3$.

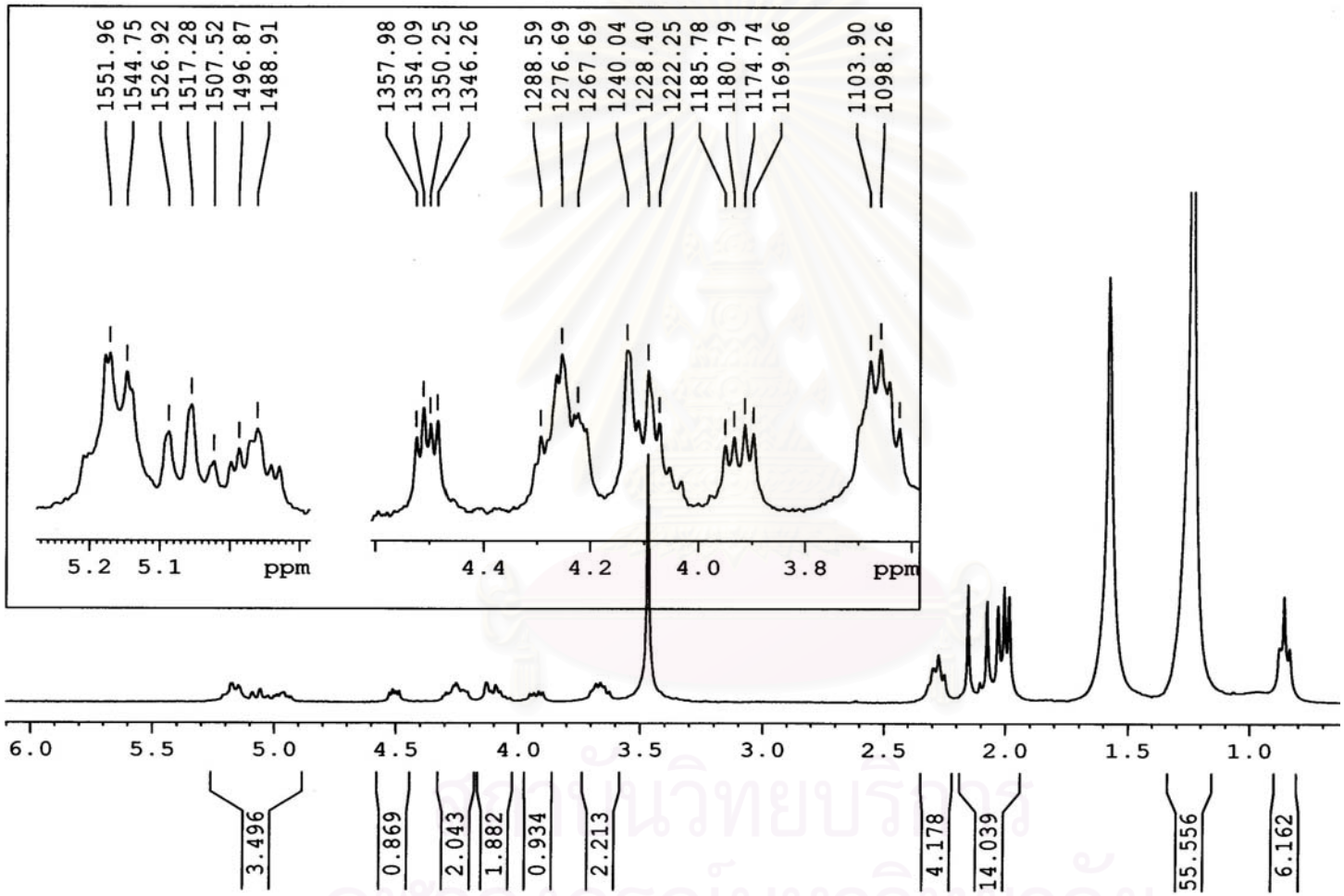

Figure 33. The 300 MHz ^{1}H-NMR spectrum of 1,2-di-*O*-stearoyl-3-*O*-(β-D-2′,3′,4′,6′-tetra-*O*-acetyl-glucopyranosyl)-*rac*-glycerol (**5e**) in $CDCl_3$.

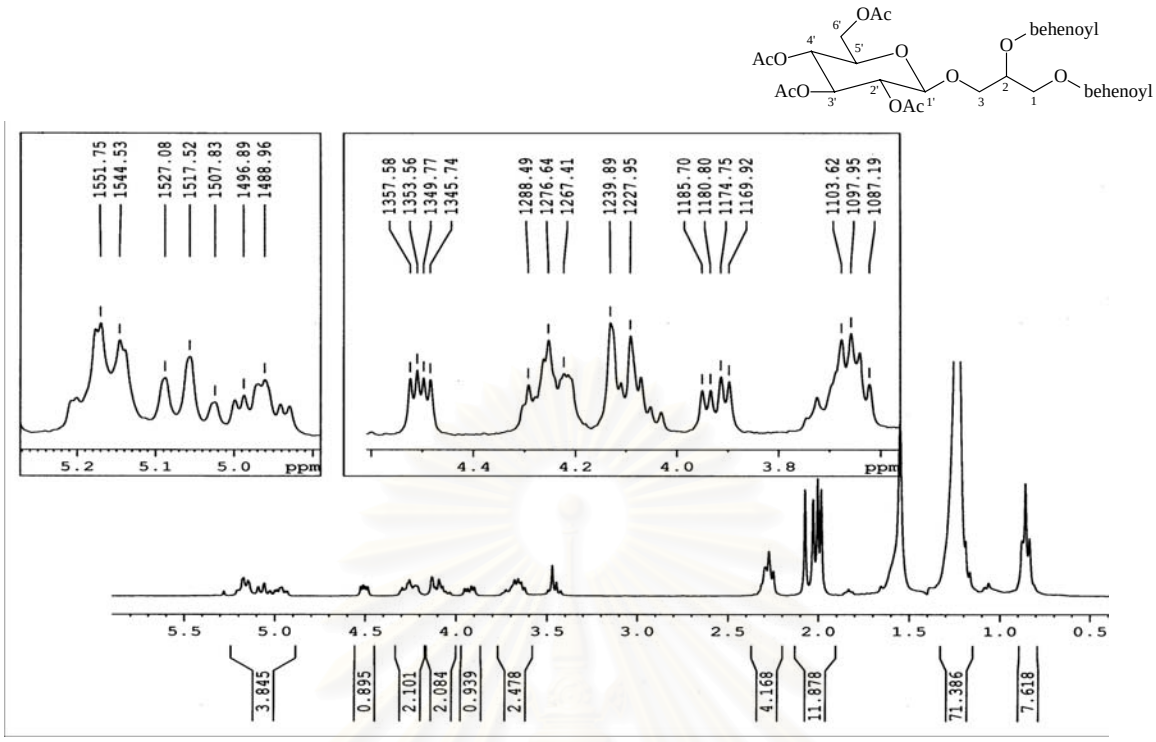

Figure 34. The 300 MHz ^{1}H-NMR spectrum of 1,2-di-*O*-behenoyl-3-*O*-(β-D-2′,3′,4′,6′-tetra-*O*-acetyl-glucopyranosyl)-*rac*-glycerol (**5f**) in $CDCl_3$.

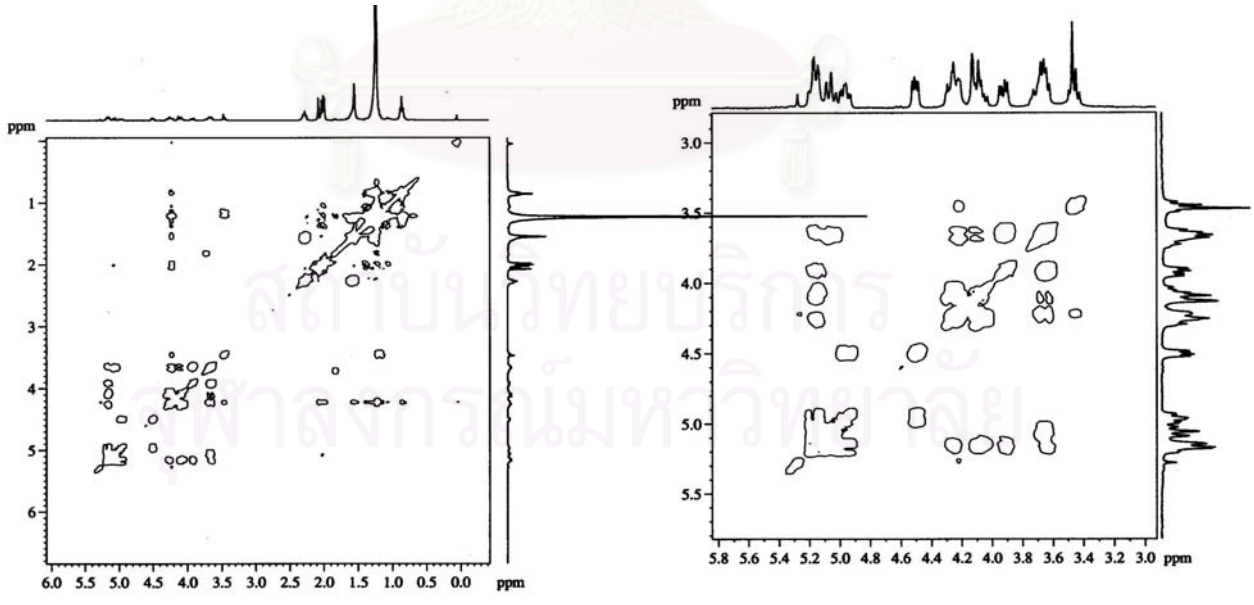

Figure 35. The ^{1}H-^{1}H COSY spectrum of 1,2-di-*O*-behenoyl-3-*O*-(β-D-2′,3′,4′,6′-tetra-*O*-acetyl-glucopyranosyl)-*rac*-glycerol (**5f**) in $CDCl_3$.

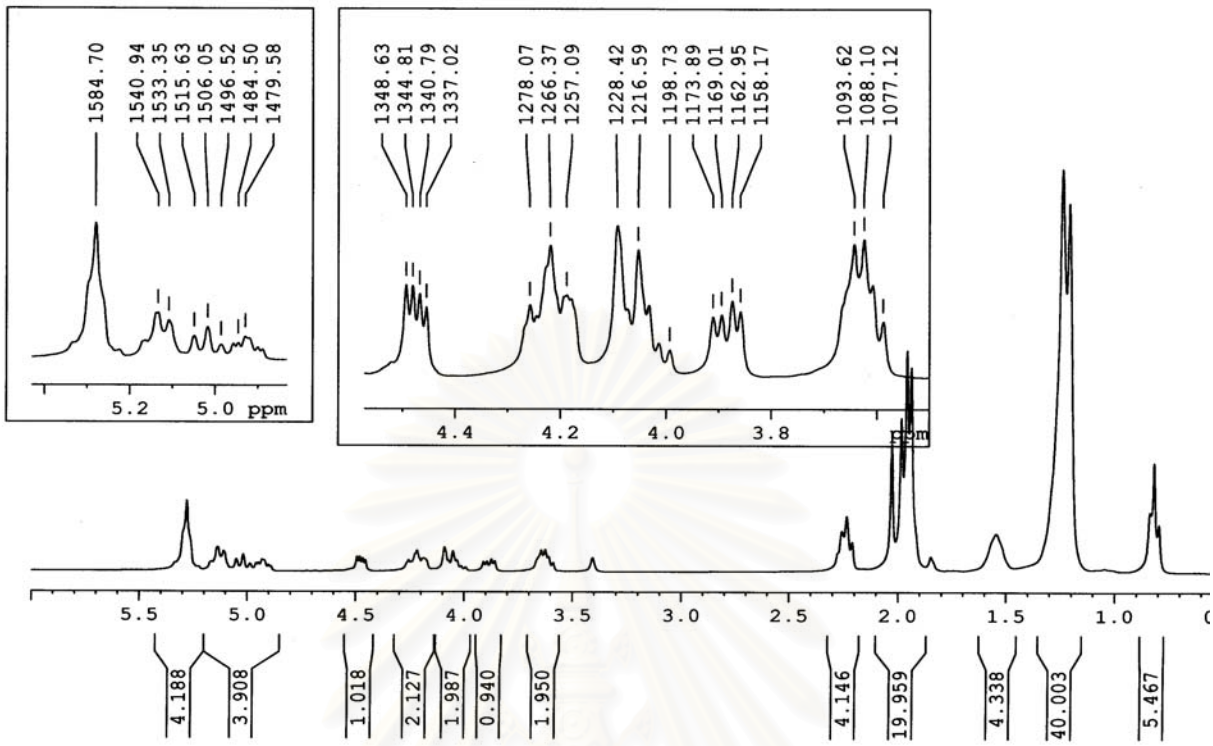

Figure 36. The 300 MHz ^{1}H-NMR spectrum of 1,2-di-*O*-oleoyl-3-*O*-(β-D-2′,3′,4′,6′-tetra-*O*-acetyl-glucopyranosyl)-*rac*-glycerol (**5g**).

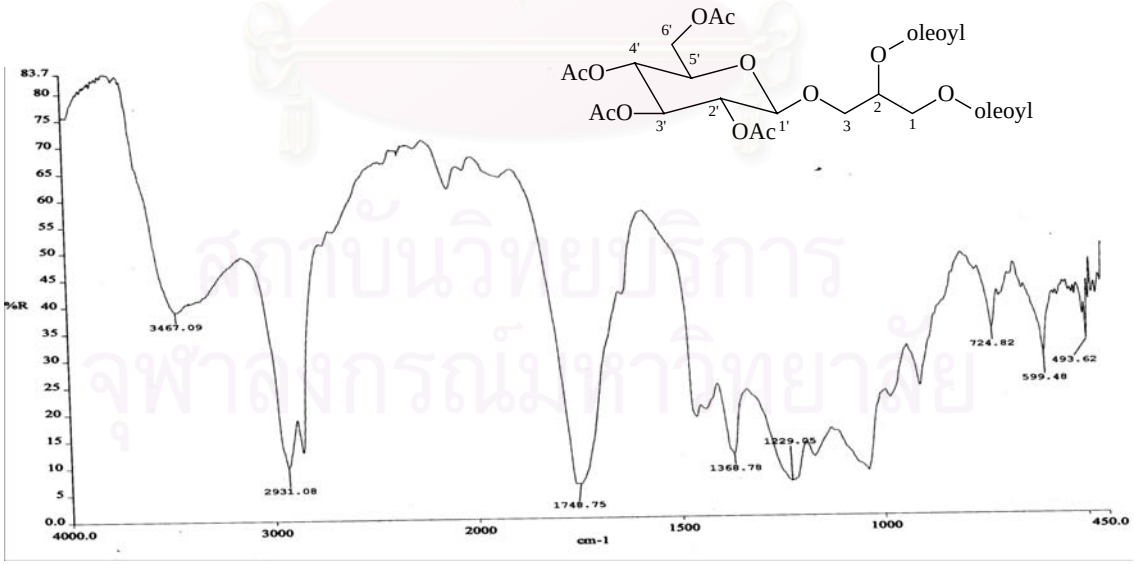

Figure 37. The infrared spectrum of 1,2-di-*O*-oleoyl-3-*O*-(β-D-2′,3′,4′,6′-tetra-*O*-acetyl-glucopyranosyl)-*rac*-glycerol (**5g**).

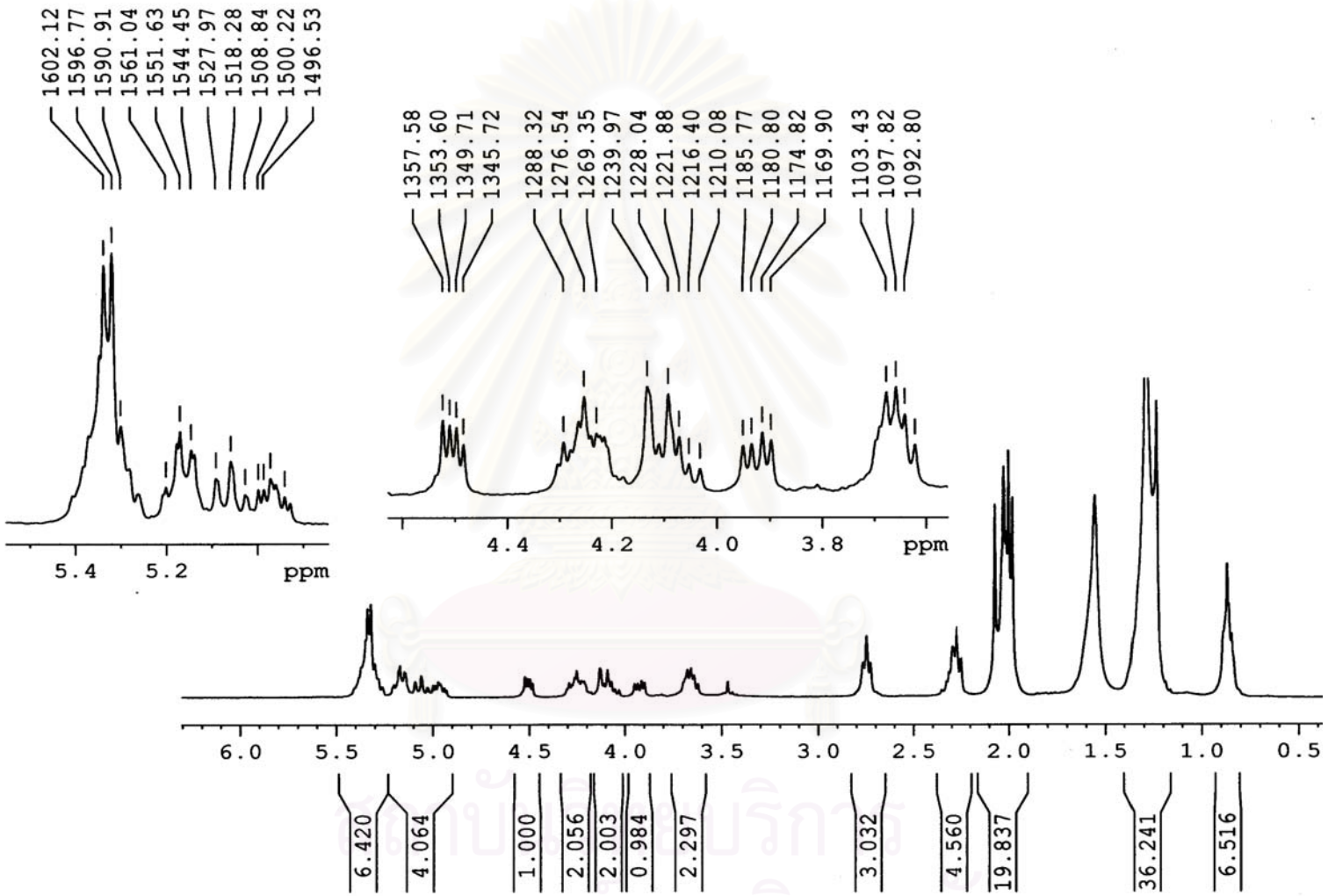

Figure 38. The 300 MHz ^{1}H-NMR spectrum of 1,2-di-*O*-linoleoyl-3-*O*-(β-D-2′,3′,4′,6′-tetra-*O*-acetyl-glucopyranosyl)-*rac*-glycerol (**5h**) in $CDCl_3$.

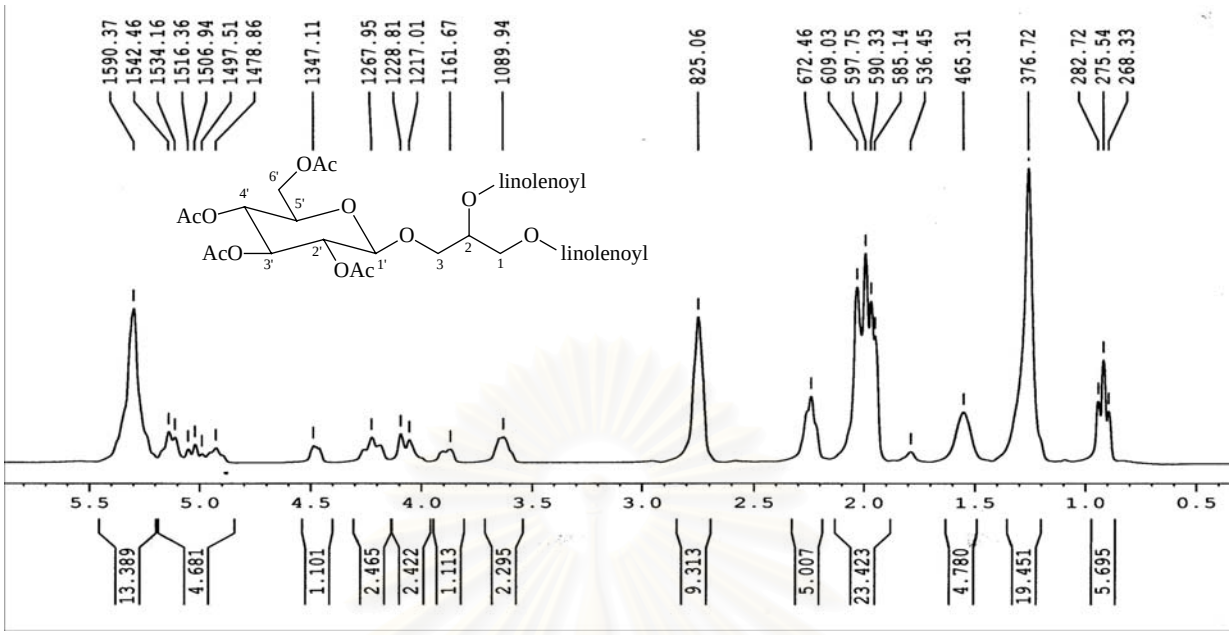

Figure 39. The 300 MHz ^{1}H-NMR spectrum of 1,2-di-*O*-linolenoyl-3-*O*-(β-D-2′,3′,4′,6′-tetra-*O*-acetyl-glucopyranosyl)-*rac*-glycerol (**5i**) in $CDCl_3$.

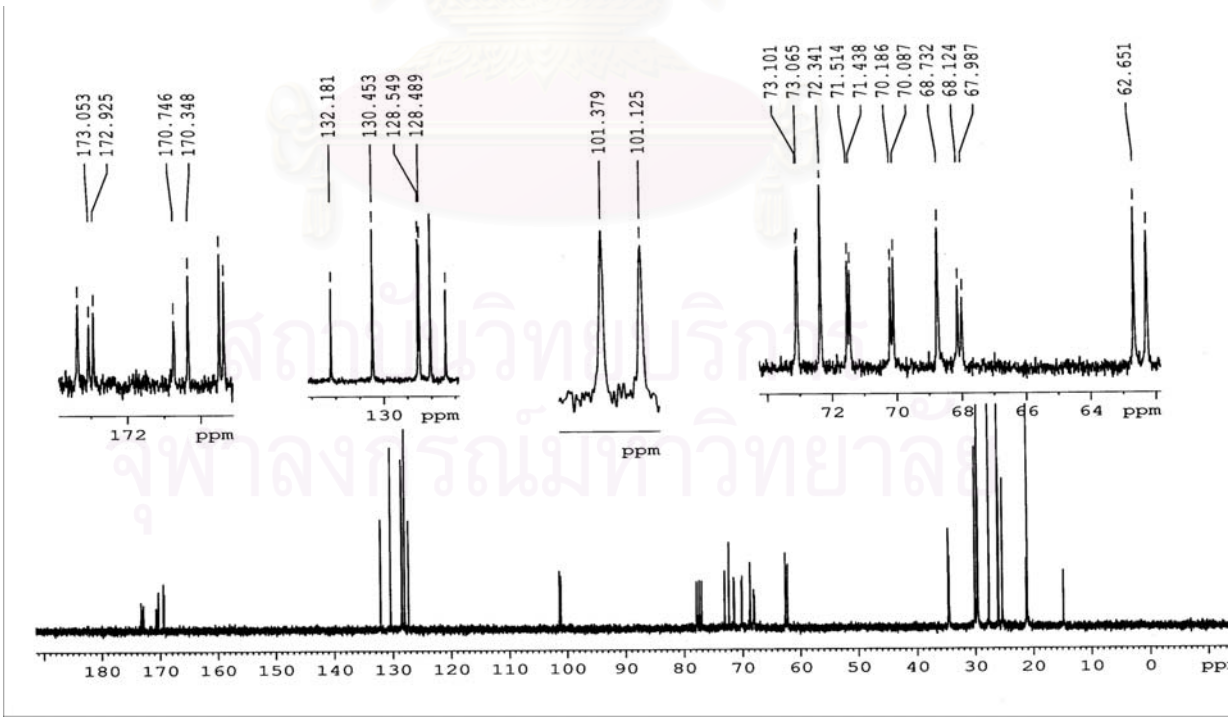

Figure 40. The 75 MHz ^{13}C-NMR spectrum of 1,2-di-*O*-linolenoyl-3-*O*-(β-D-2′,3′,4′,6′-tetra-*O*-acetyl-glucopyranosyl)-*rac*-glycerol (**5i**) in $CDCl_3$.

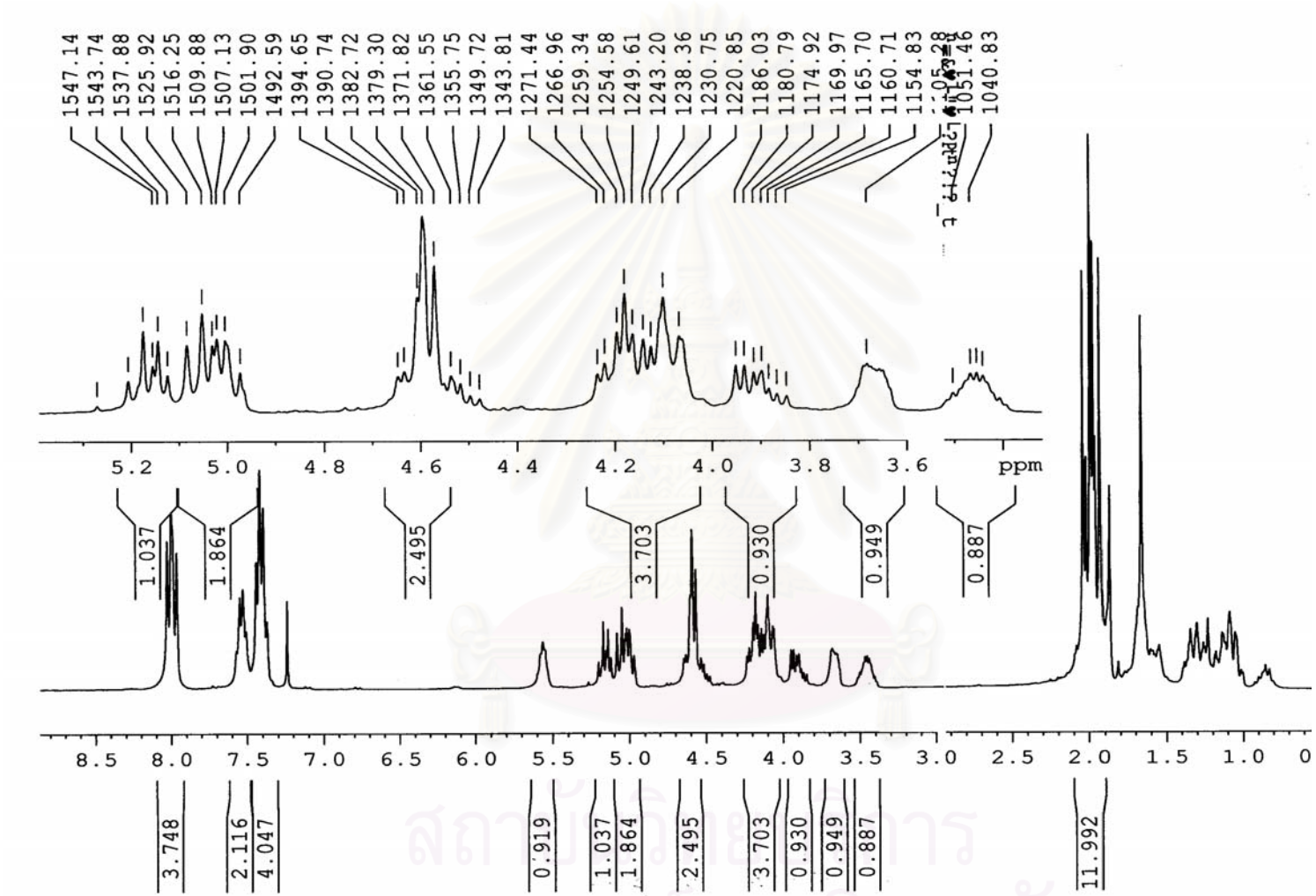

Figure 41. The 300 MHz ^{1}H-NMR spectrum of 1,2-di-*O*-benzoyl-3-*O*-(β-D-2′,3′,4′,6′-tetra-*O*-acetyl-glucopyranosyl)-*rac*-glycerol (**5i**) in $CDCl_3$.

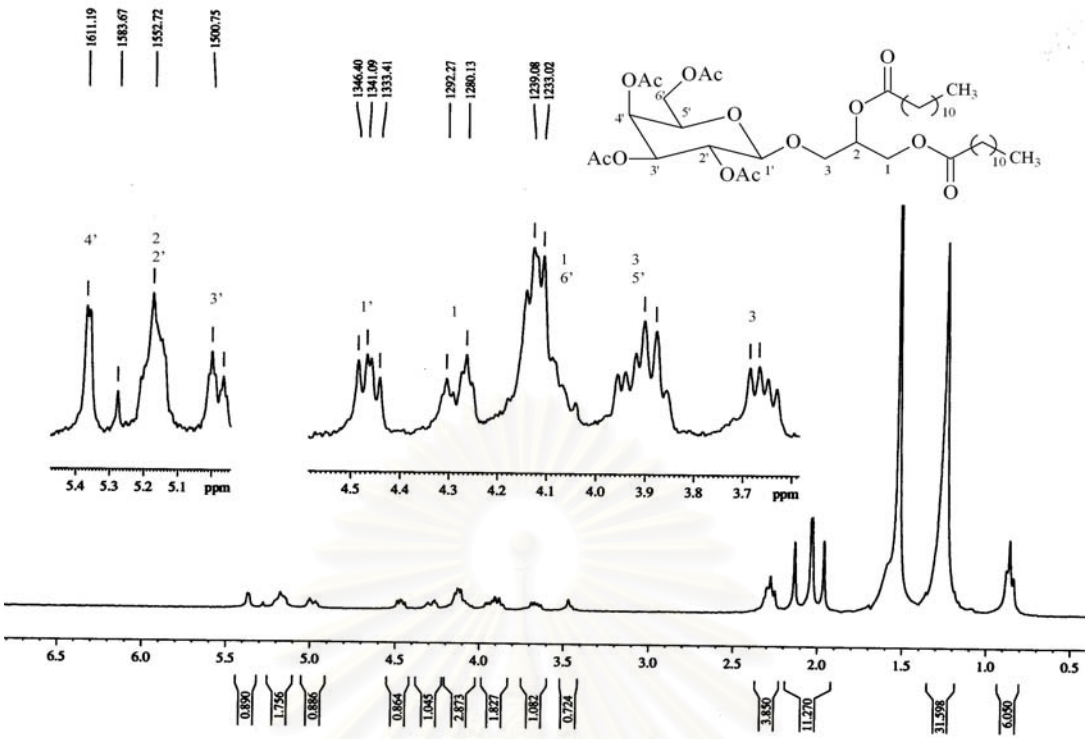

Figure 42. The 300 MHz ^{1}H-NMR spectrum of 1,2-di-*O*-lauroyl-3-*O*-(β-D-2′,3′,4′,6′-tetra-*O*-acetyl-galactopyranosyl)-*rac*-glycerol (**12a**) in $CDCl_3$.

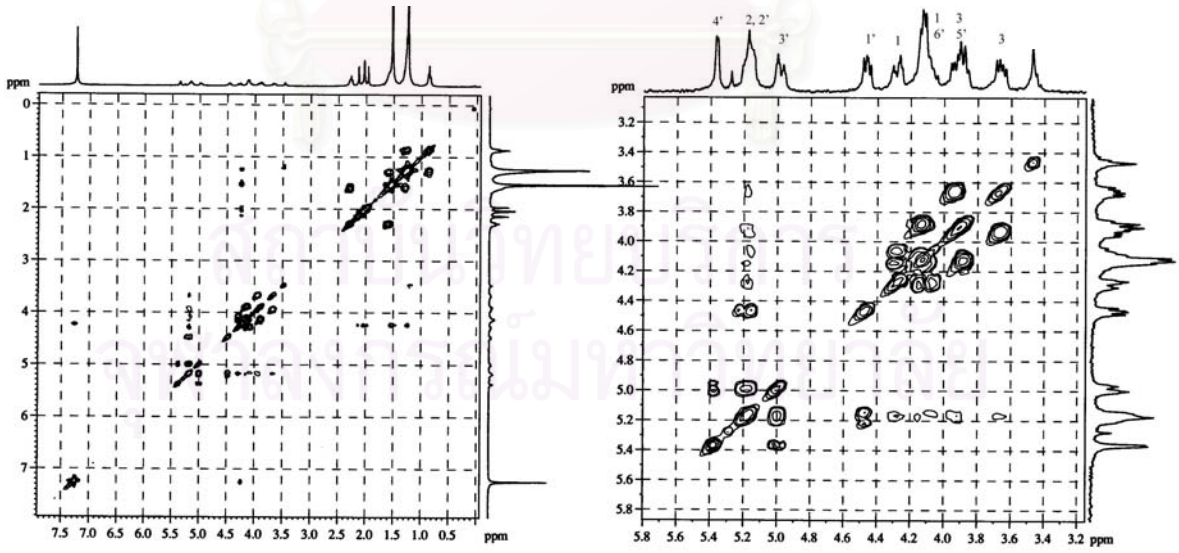

Figure 43. The ^{1}H-^{1}H COSY spectrum of 1,2-di-*O*-lauroyl-3-*O*-(β-D-2′,3′,4′,6′-tetra-*O*-acetyl-galactopyranosyl)-*rac*-glycerol (**12a**) in $CDCl_3$.

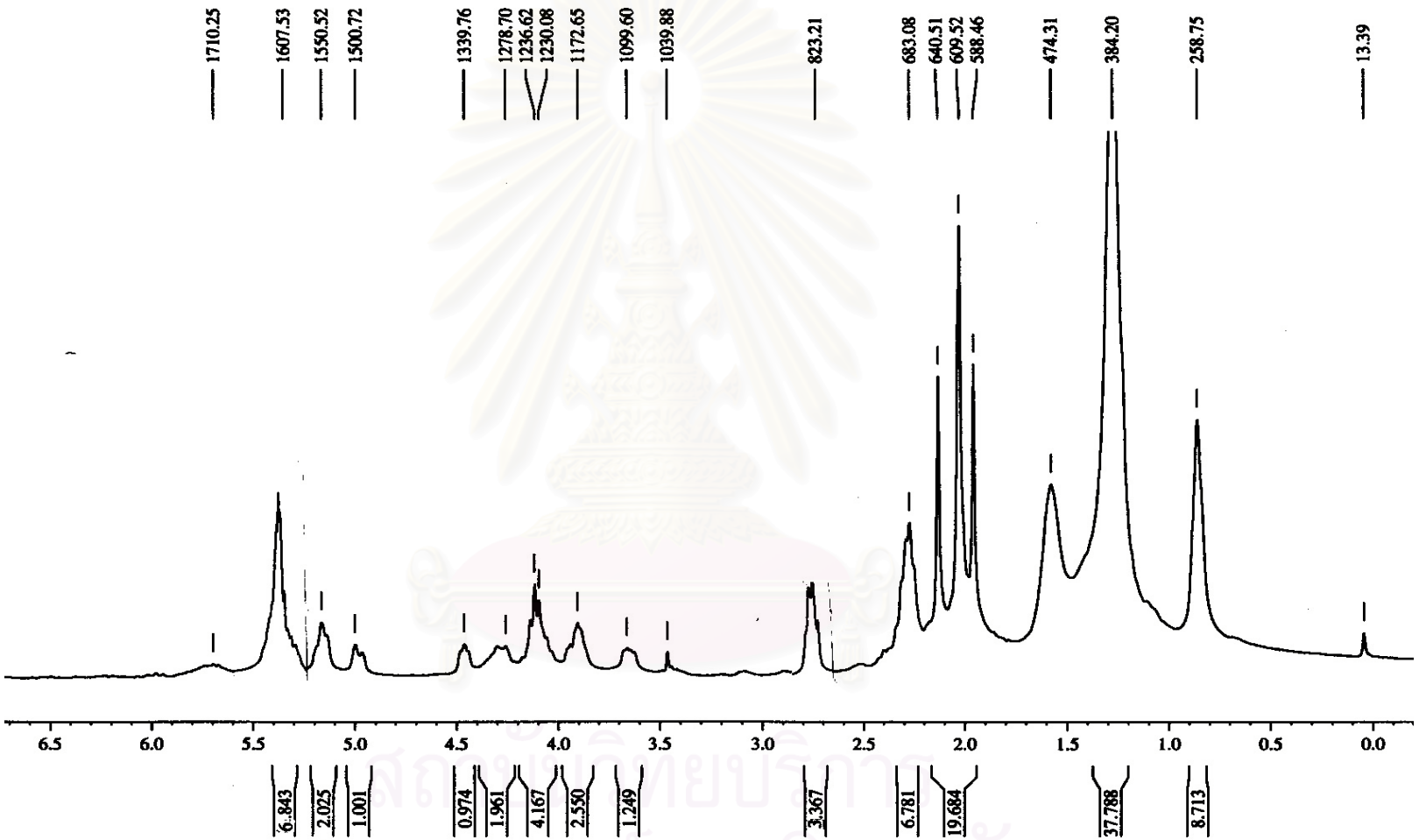

Figure 44. The 300 MHz ^{1}H-NMR spectrum of 1,2-di-*O*-linoleoyl-3-*O*-(β-D-2′,3′,4′,6′-tetra-*O*-acetyl-galactopyranosyl)-*rac*-glycerol (**12b**) in $CDCl_3$.

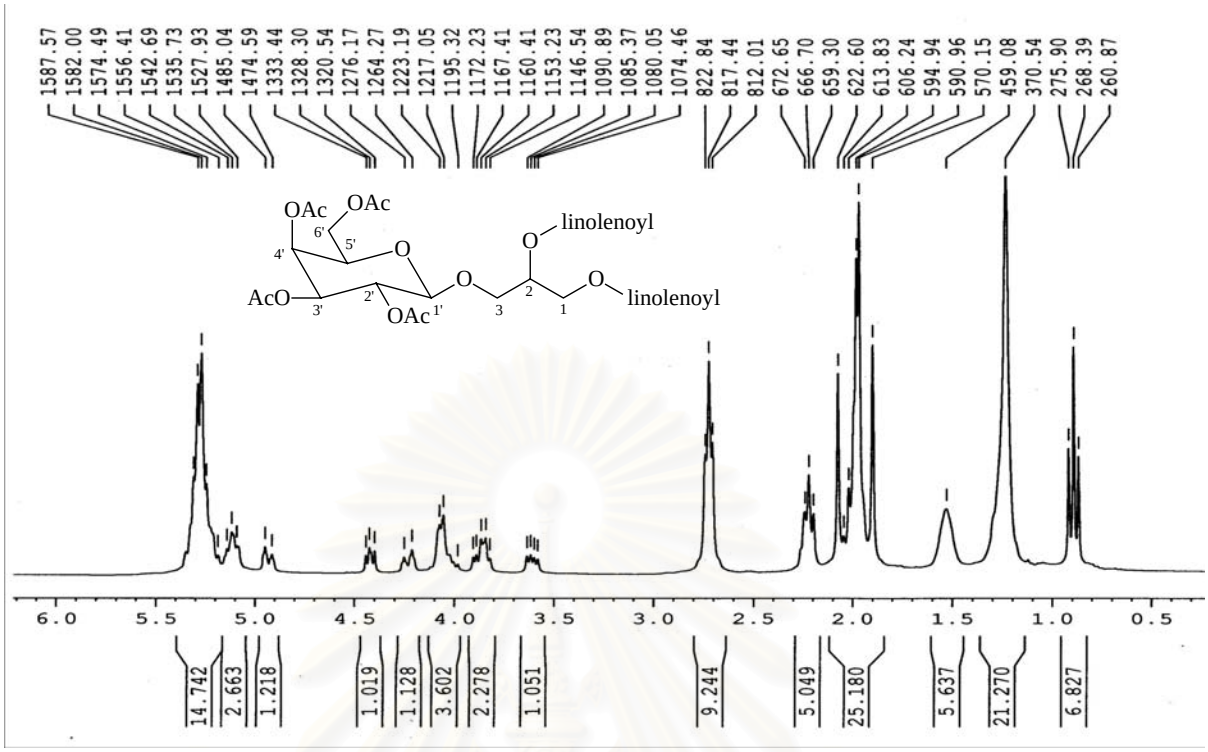

Figure 45. The 300 MHz ^{1}H-NMR spectrum of 1,2-di-*O*-linolenoyl-3-*O*-(β-D-2′,3′,4′,6′-tetra-*O*-acetyl-galactopyranosyl)-*rac*-glycerol (**12c**) in $CDCl_3$.

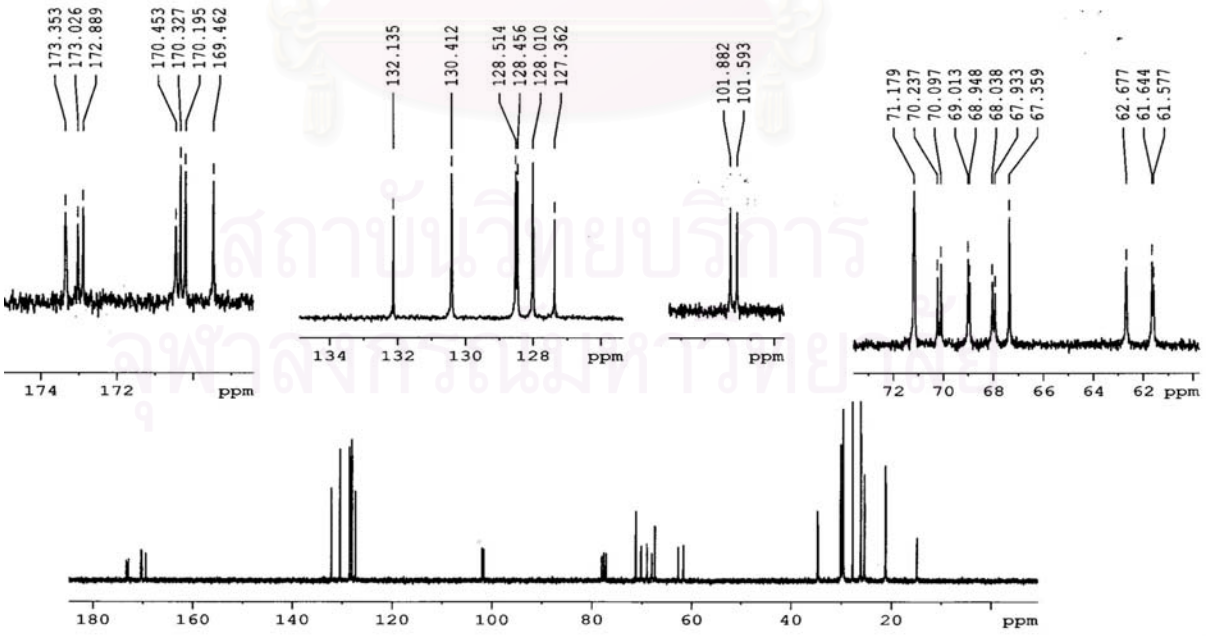

Figure 46. The 75 MHz ^{13}C-NMR spectrum of 1,2-di-*O*-linolenoyl-3-*O*-(β-D-2′,3′,4′,6′-tetra-*O*-acetyl-galactopyranosyl)-*rac*-glycerol (**12c**) in $CDCl_3$.

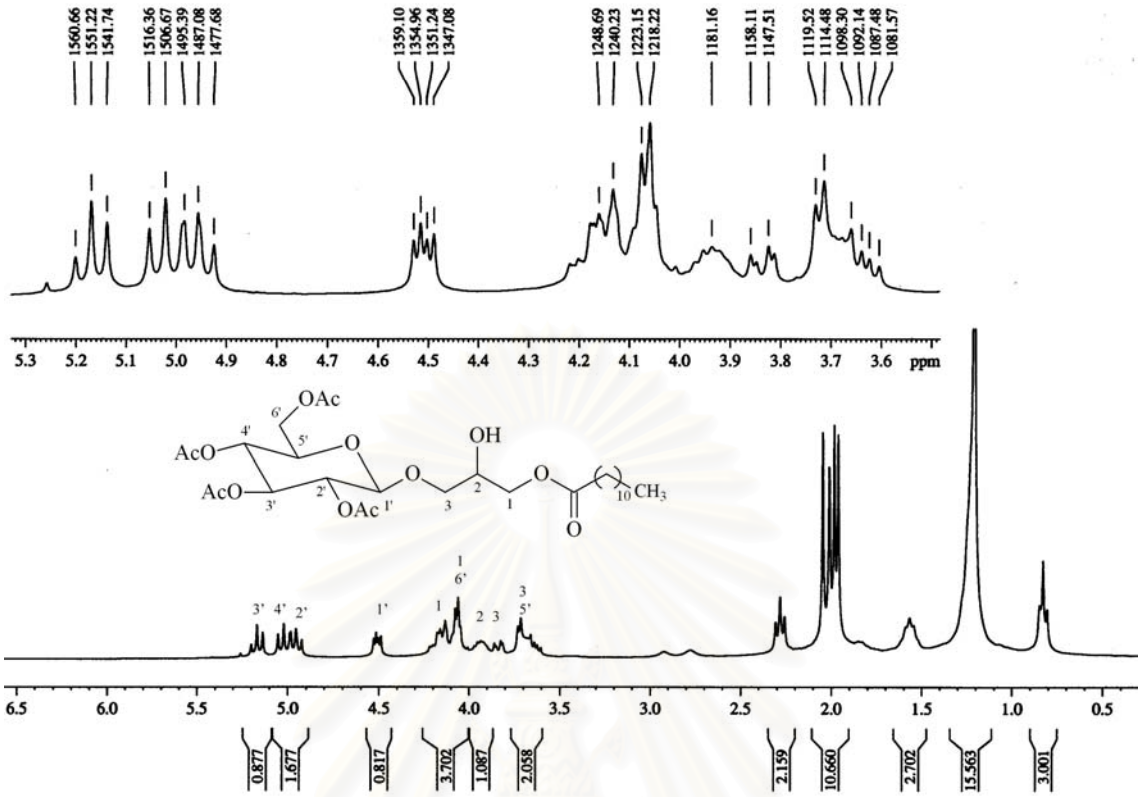

Figure 47. The 300 MHz ^{1}H-NMR spectrum of 1-*O*-lauroyl-3-*O*-(β-D-2′,3′,4′,6′-tetra-*O*-acetyl-glucopyranosyl)-*rac*-glycerol (**7a**) in $CDCl_3$.

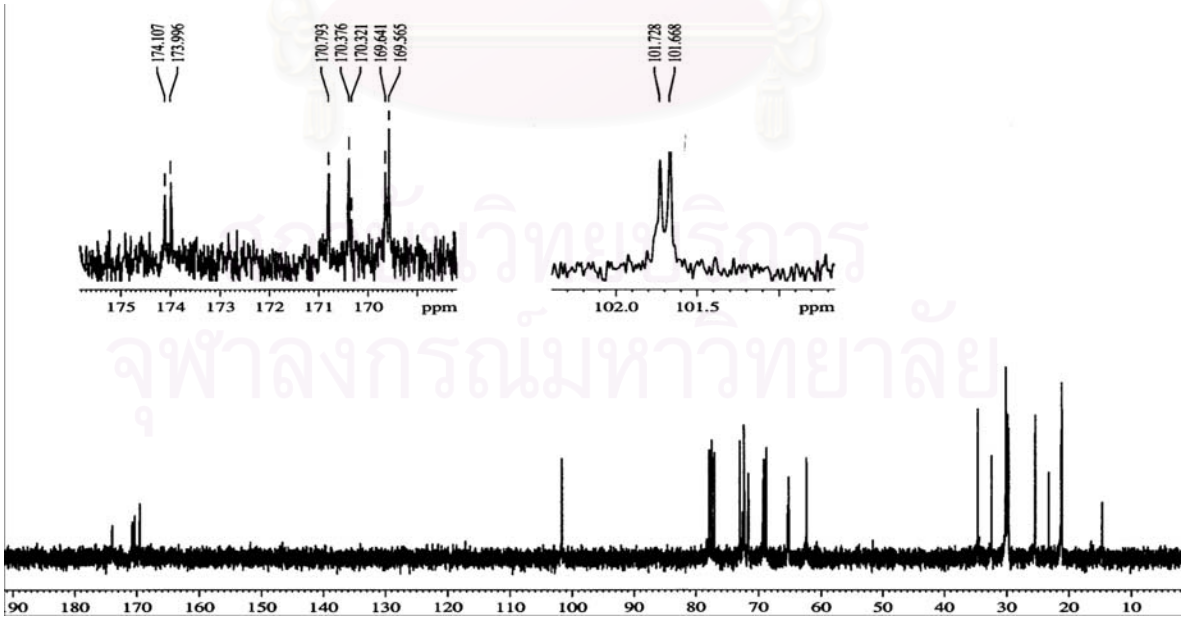

Figure 48. The 75 MHz ^{13}C-NMR spectrum of 1-*O*-lauroyl-3-*O*-(β-D-2′,3′,4′,6′-tetra-*O*-acetyl-glucopyranosyl)-*rac*-glycerol (**7a**) in $CDCl_3$.

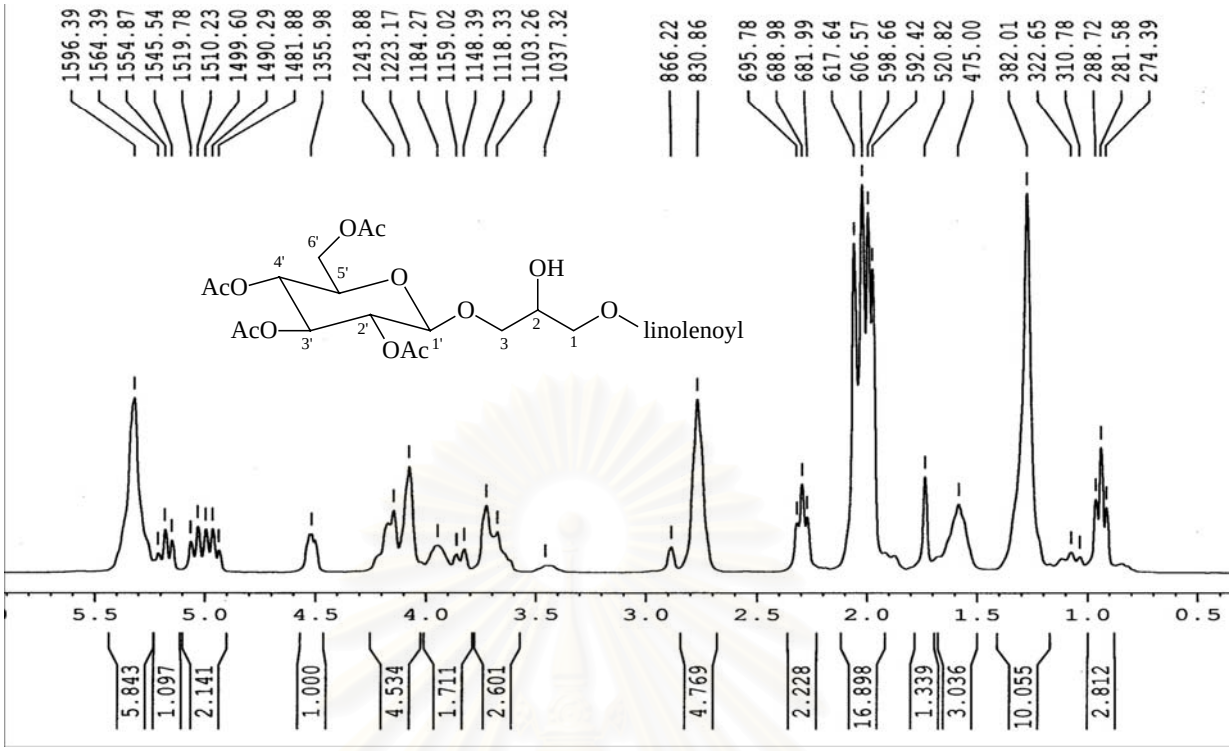

Figure 49. The 300 MHz ^{1}H-NMR spectrum of 1-*O*-linolenoyl-3-*O*-(β-D-2′,3′,4′,6′-tetra-*O*-acetyl-glucopyranosyl)-*rac*-glycerol (**7b**) in $CDCl_3$.

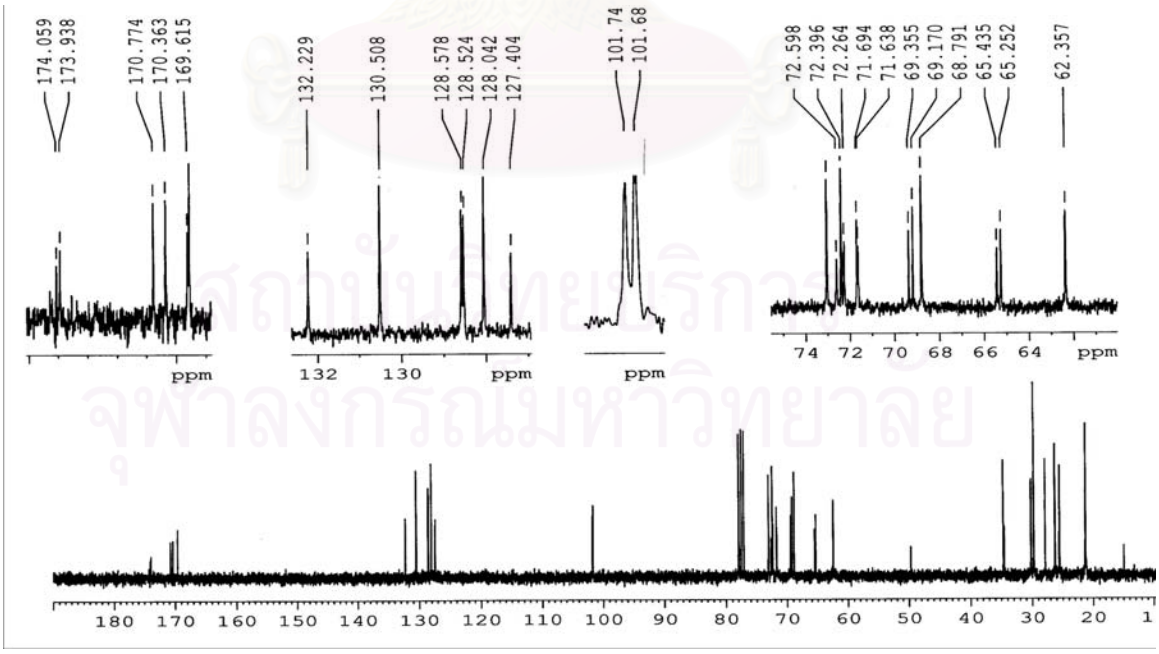

Figure 50. The 75 MHz ^{13}C-NMR spectrum of 1-*O*-linolenoyl-3-*O*-(β-D-2′,3′,4′,6′-tetra-*O*-acetyl-glucopyranosyl)-*rac*-glycerol (**7b**) in $CDCl_3$.

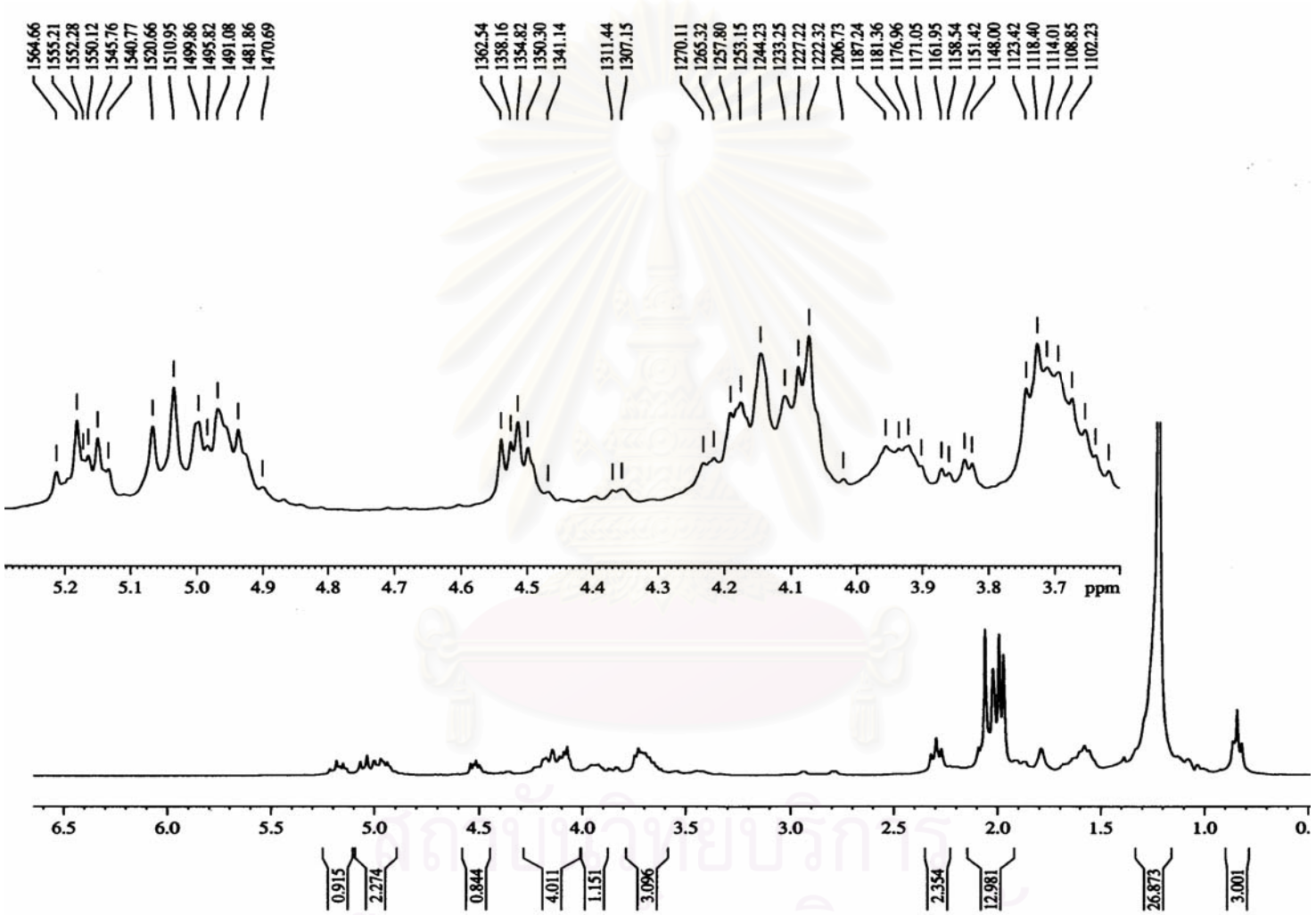

Figure 51. The 300 MHz ^{1}H-NMR spectrum of 1-*O*-stearoyl-3-*O*-(β-D-2′,3′,4′,6′-tetra-*O*-acetyl-glucopyranosyl)-*rac*-glycerol (**7c**) in $CDCl_3$.

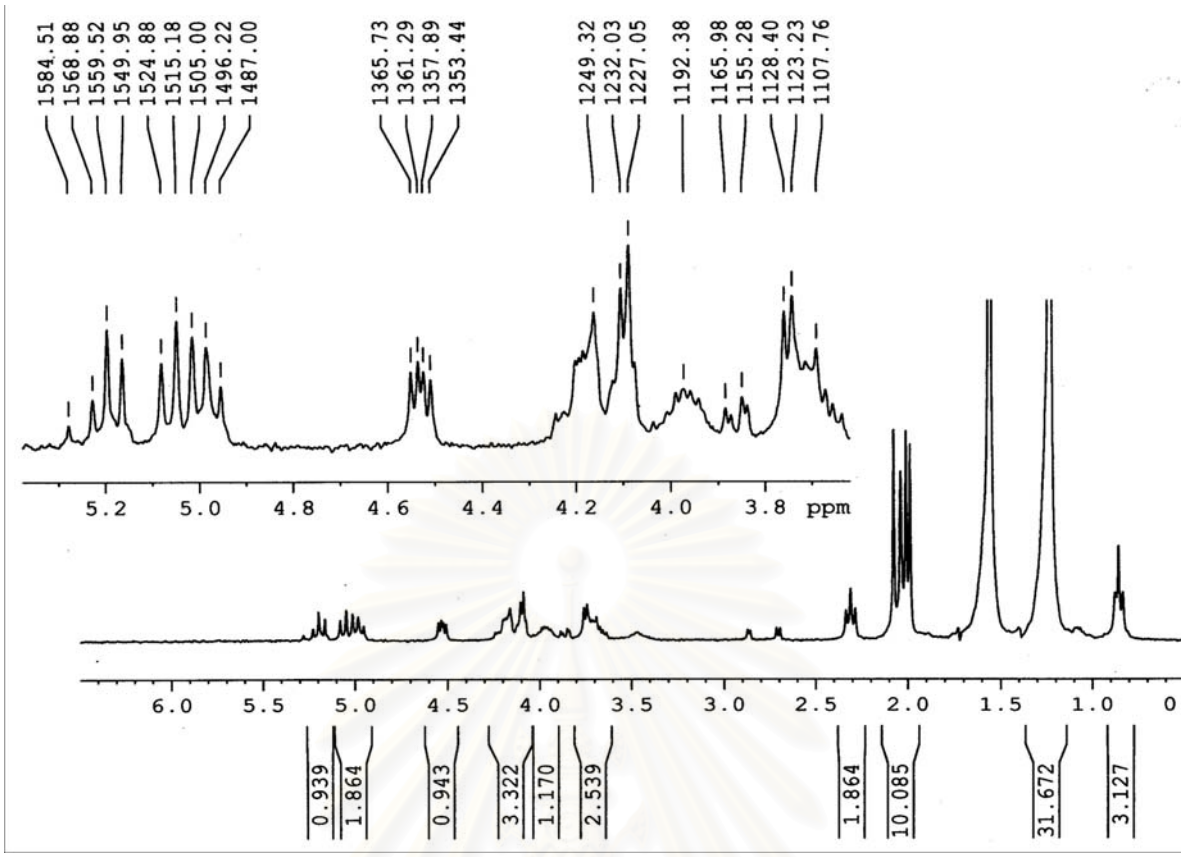

Figure 52. The 300 MHz ^{1}H-NMR spectrum of 1-*O*-behenoyl-3-*O*-(β-D-2′,3′,4′,6′-tetra-*O*-acetyl-glucopyranosyl)-*rac*-glycerol (**7d**) in $CDCl_3$.

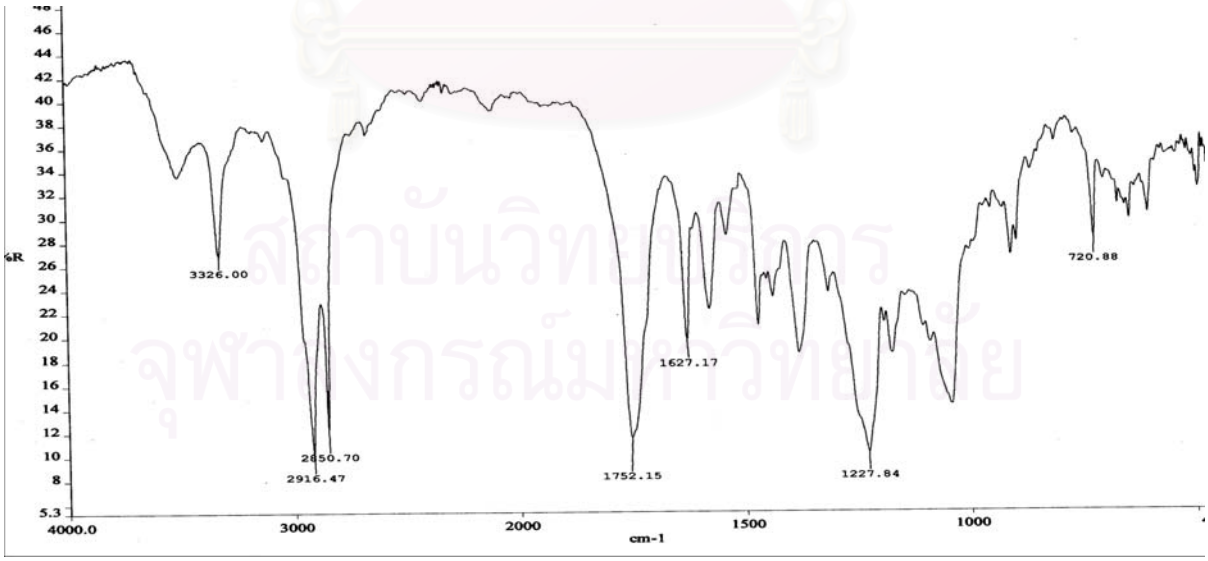

Figure 53. The infrared spectrum of 1-*O*-behenoyl-3-*O*-(β-D-2′,3′,4′,6′-tetra-*O*-acetyl-glucopyranosyl)-*rac*-glycerol (**7d**).

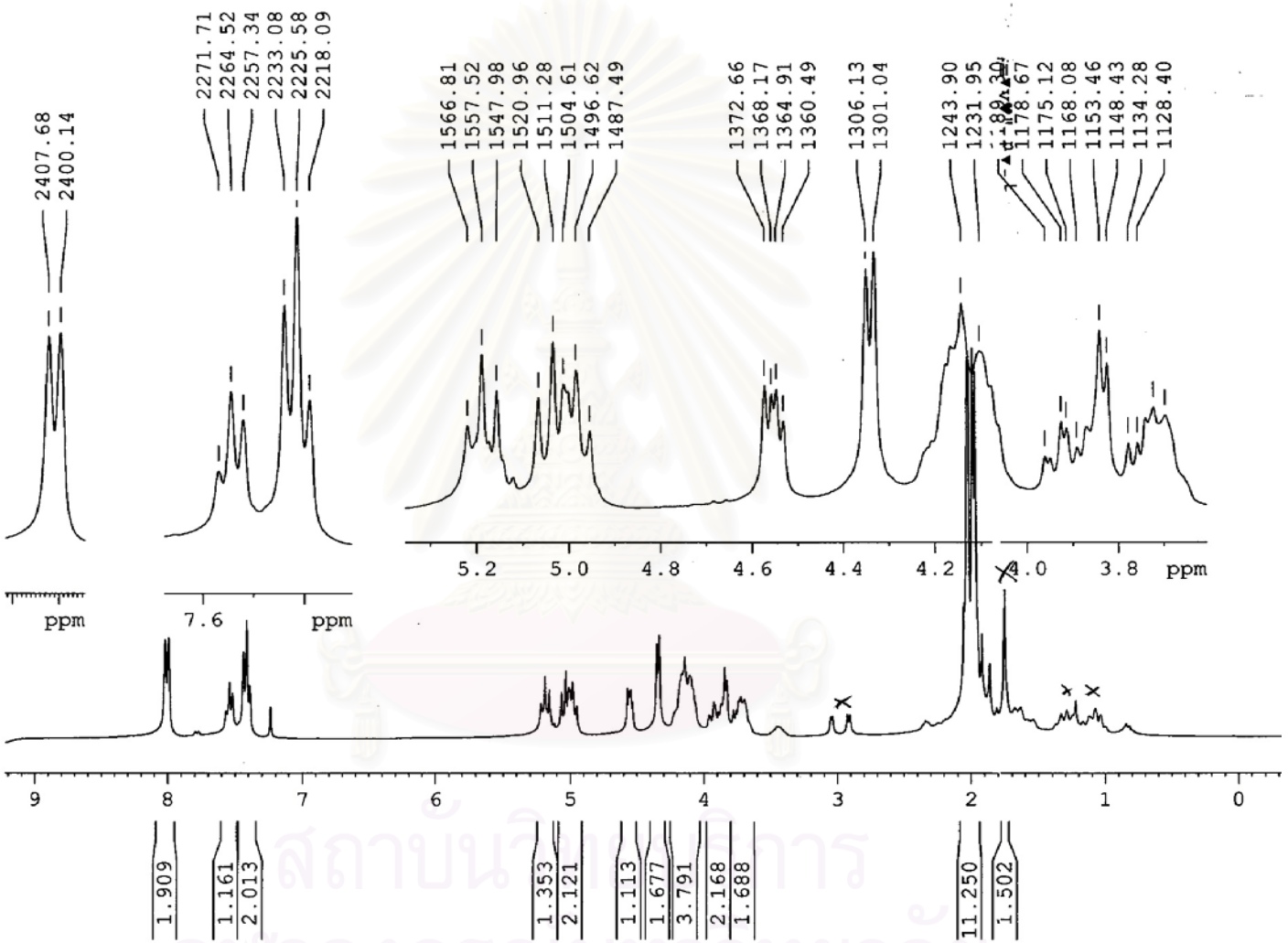

Figure 54. The 300 MHz ^{1}H-NMR spectrum of 1-*O*-benzoyl-3-*O*-(β-D-2′,3′,4′,6′-tetra-*O*-acetyl-glucopyranosyl)-*rac*-glycerol (**7e**) in $CDCl_3$.

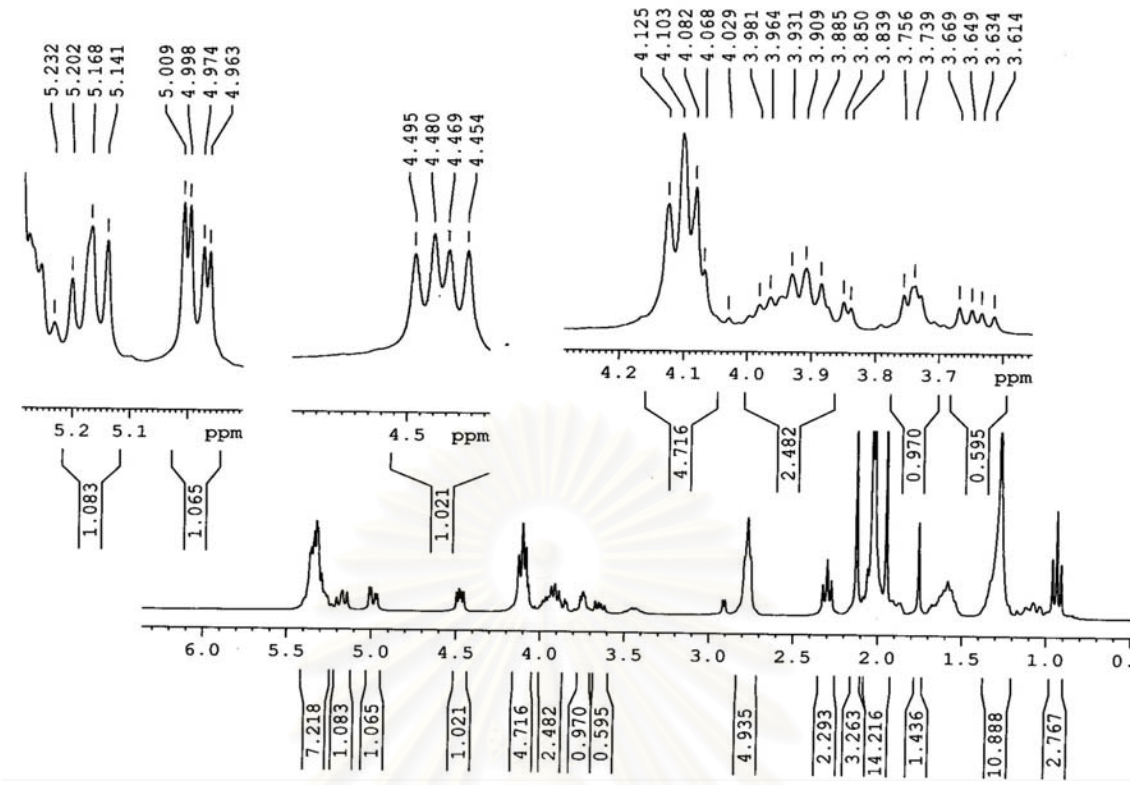

Figure 55. The 300 MHz ^{1}H-NMR spectrum of 1-*O*-linolenoyl-3-*O*-(β-D-2′,3′,4′,6′-tetra-*O*-acetyl-galactopyranosyl)-*rac*-glycerol (**14a**) in $CDCl_3$.

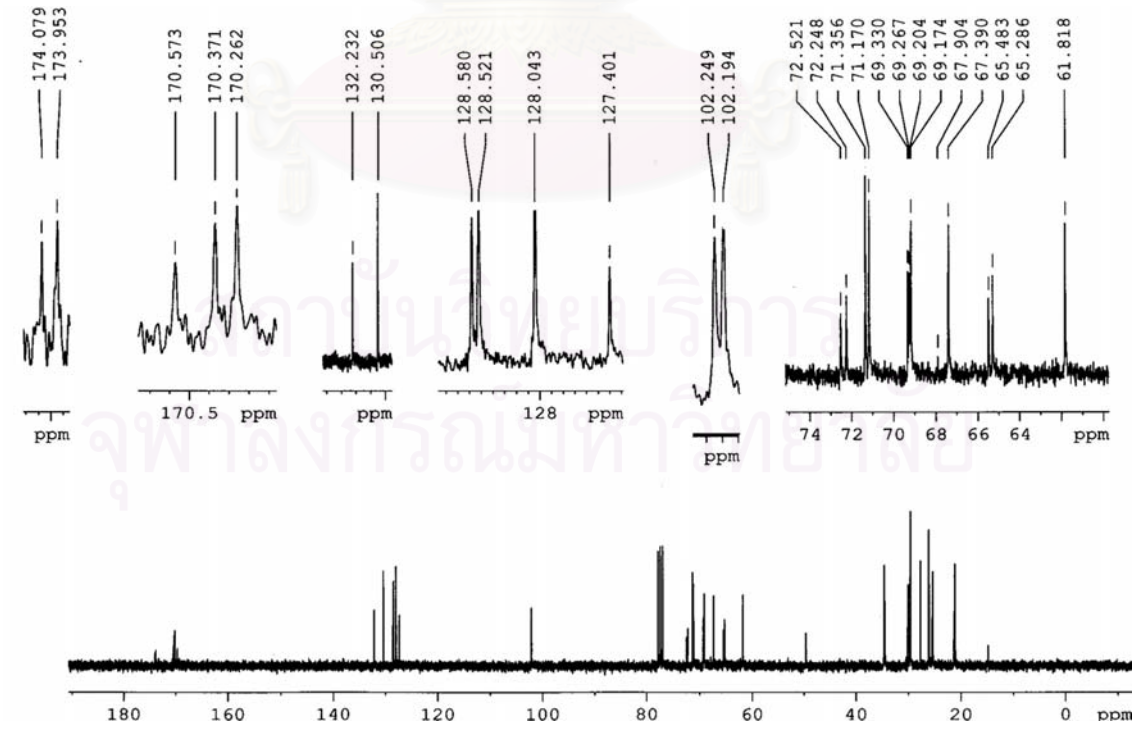

Figure 56. The 75 MHz ^{13}C-NMR spectrum of 1-*O*-linolenoyl-3-*O*-(β-D-2′,3′,4′,6′-tetra-*O*-acetyl-galactopyranosyl)-*rac*-glycerol (**14a**) in $CDCl_3$.

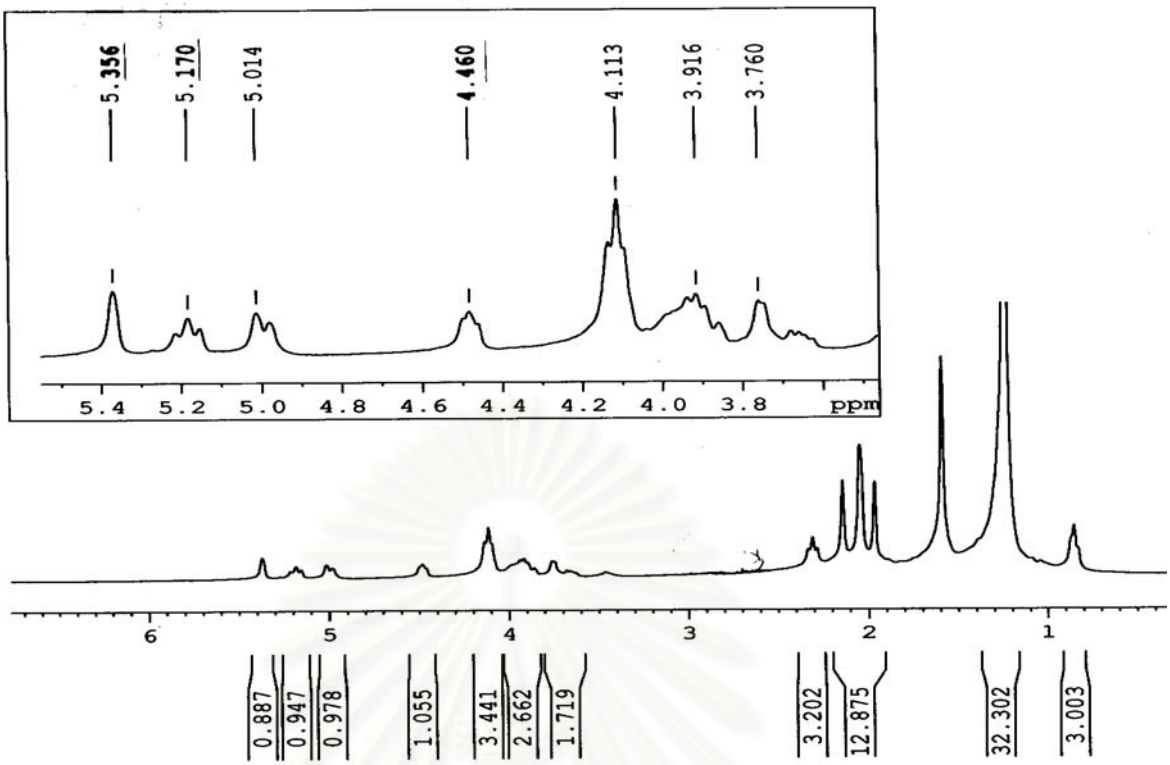

Figure 57. The 300 MHz ^{1}H-NMR spectrum of 1-*O*-behenoyl-3-*O*-(β-D-2′,3′,4′,6′-tetra-*O*-acetyl-galactopyranosyl)-*rac*-glycerol (**14b**) in $CDCl_3$.

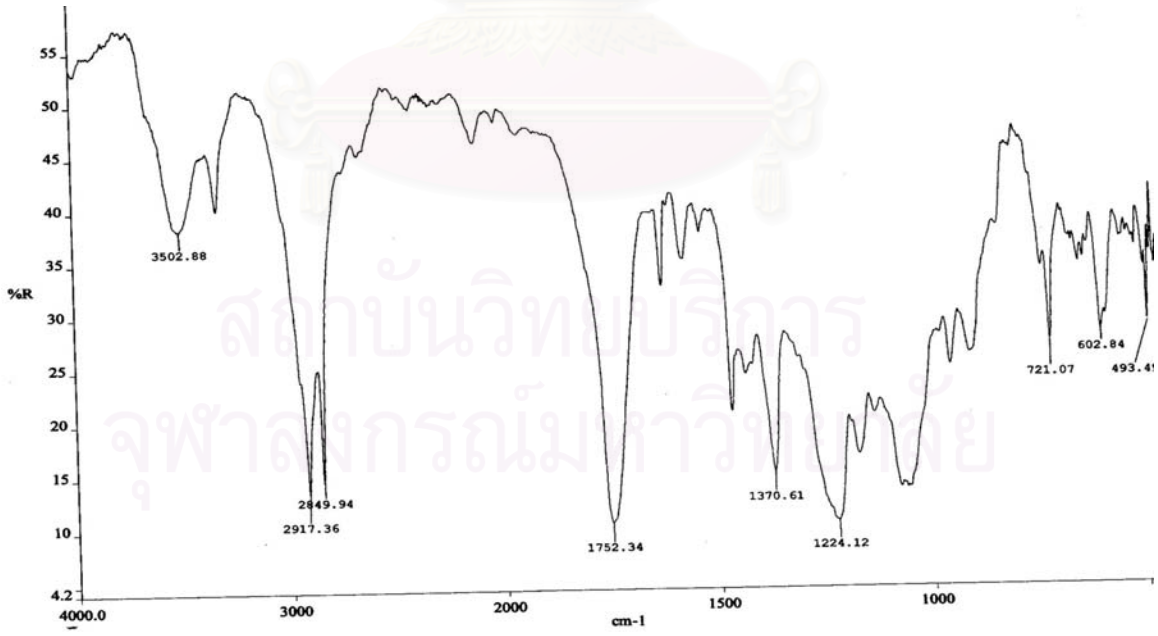

Figure 58. The infrared spectrum of 1-*O*-behenoyl-3-*O*-(β-D-2′,3′,4′,6′-tetra-*O*-acetyl-galactopyranosyl)-*rac*-glycerol (**14b**).

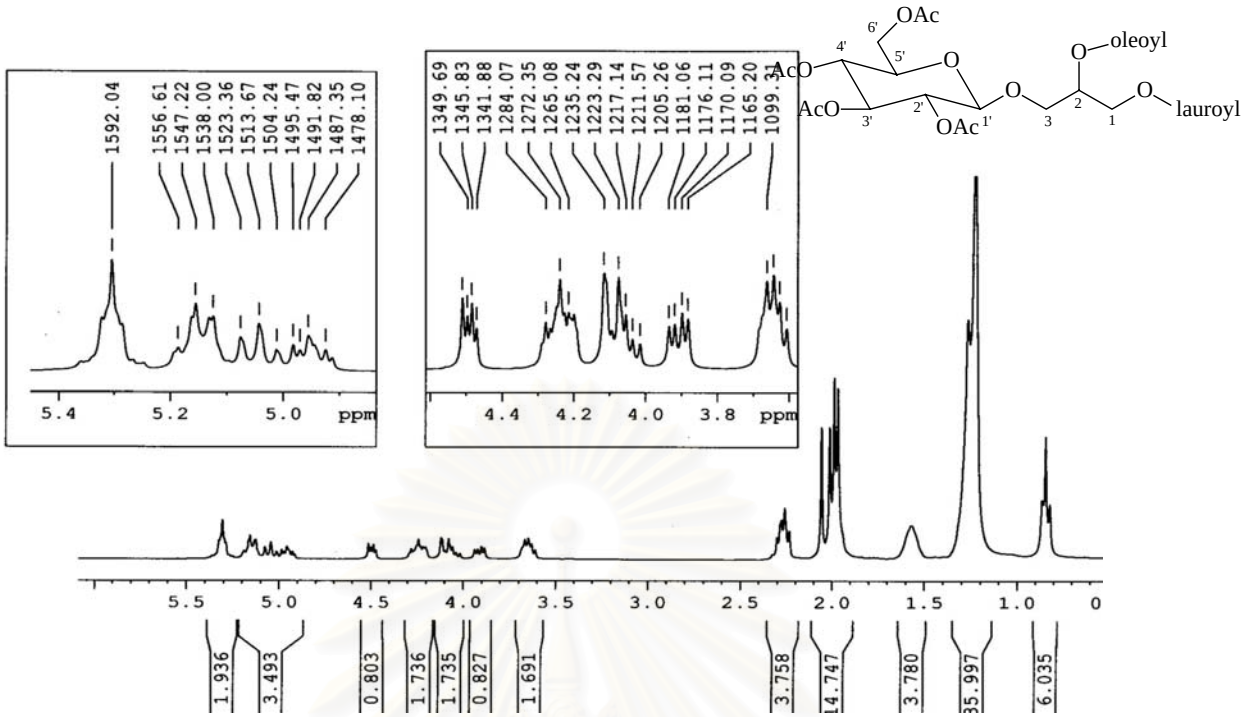

Figure 59. The 300 MHz ^{1}H-NMR spectrum of 1-*O*-lauroyl-2-*O*-oleoyl-3-*O*-(β-D-2′,3′,4′,6′-tetra-*O*-acetyl-glucopyranosyl)-*rac*-glycerol (**5k**) in $CDCl_3$.

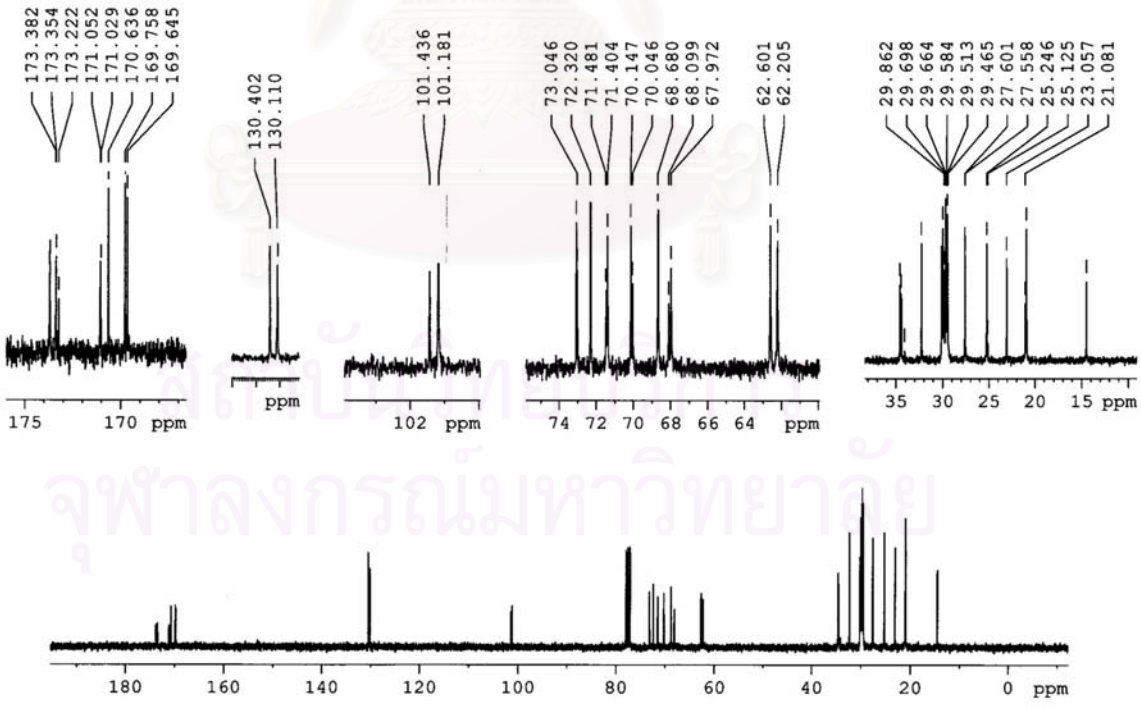

Figure 60. The 75 MHz ^{13}C-NMR spectrum of 1-*O*-lauroyl-2-*O*-oleoyl-3-*O*-(β-D-2′,3′,4′,6′-tetra-*O*-acetyl-glucopyranosyl)-*rac*-glycerol (**5k**) in $CDCl_3$.

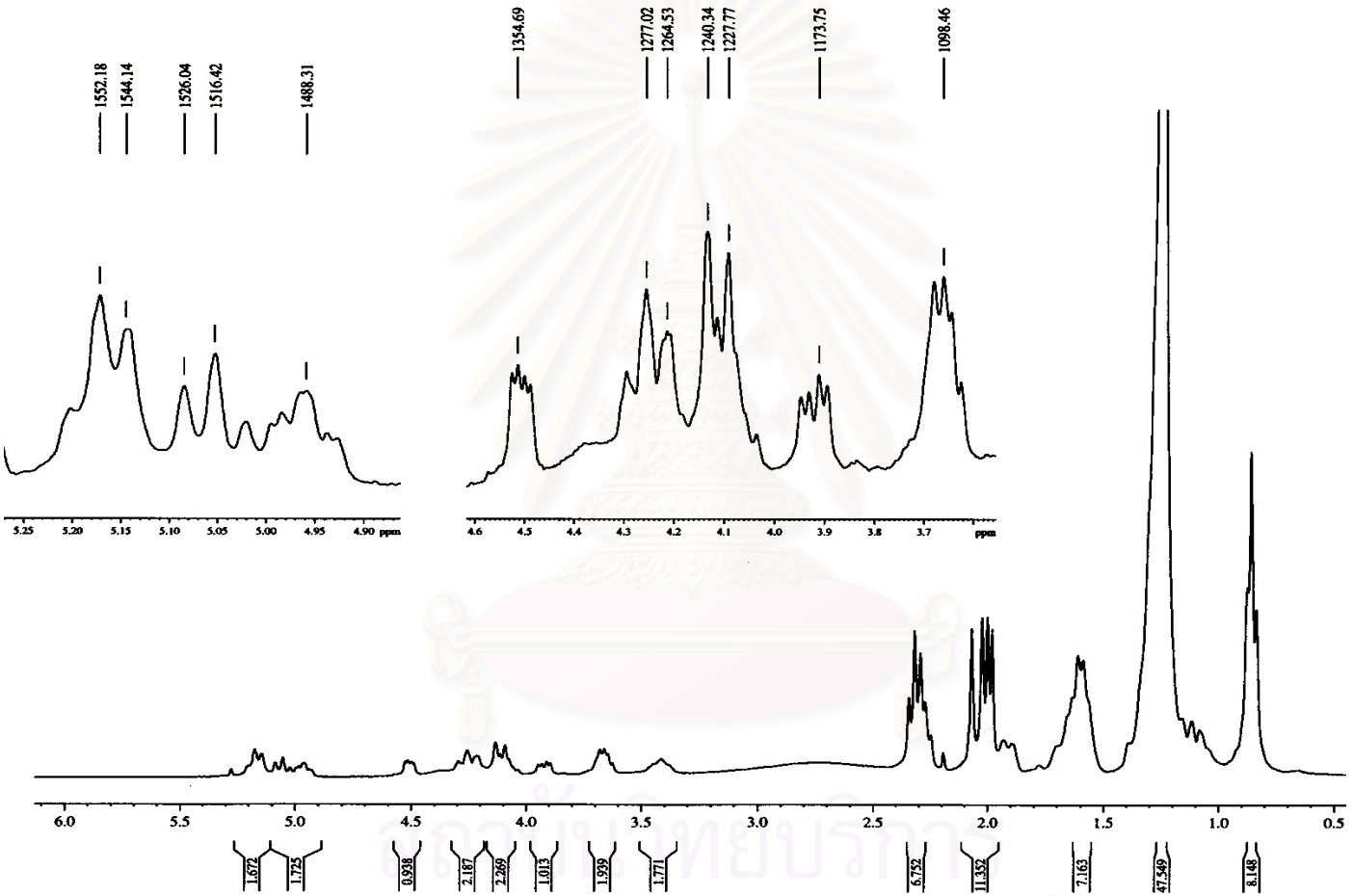

Figure 61. The 300 MHz ^{1}H-NMR spectrum of 1-*O*-stearoyl-2-*O*-lauroyl-3-*O*-(β-D-2′,3′,4′,6′-tetra-*O*-acetyl-glucopyranosyl)-*rac*-glycerol (**5l**) in $CDCl_3$.

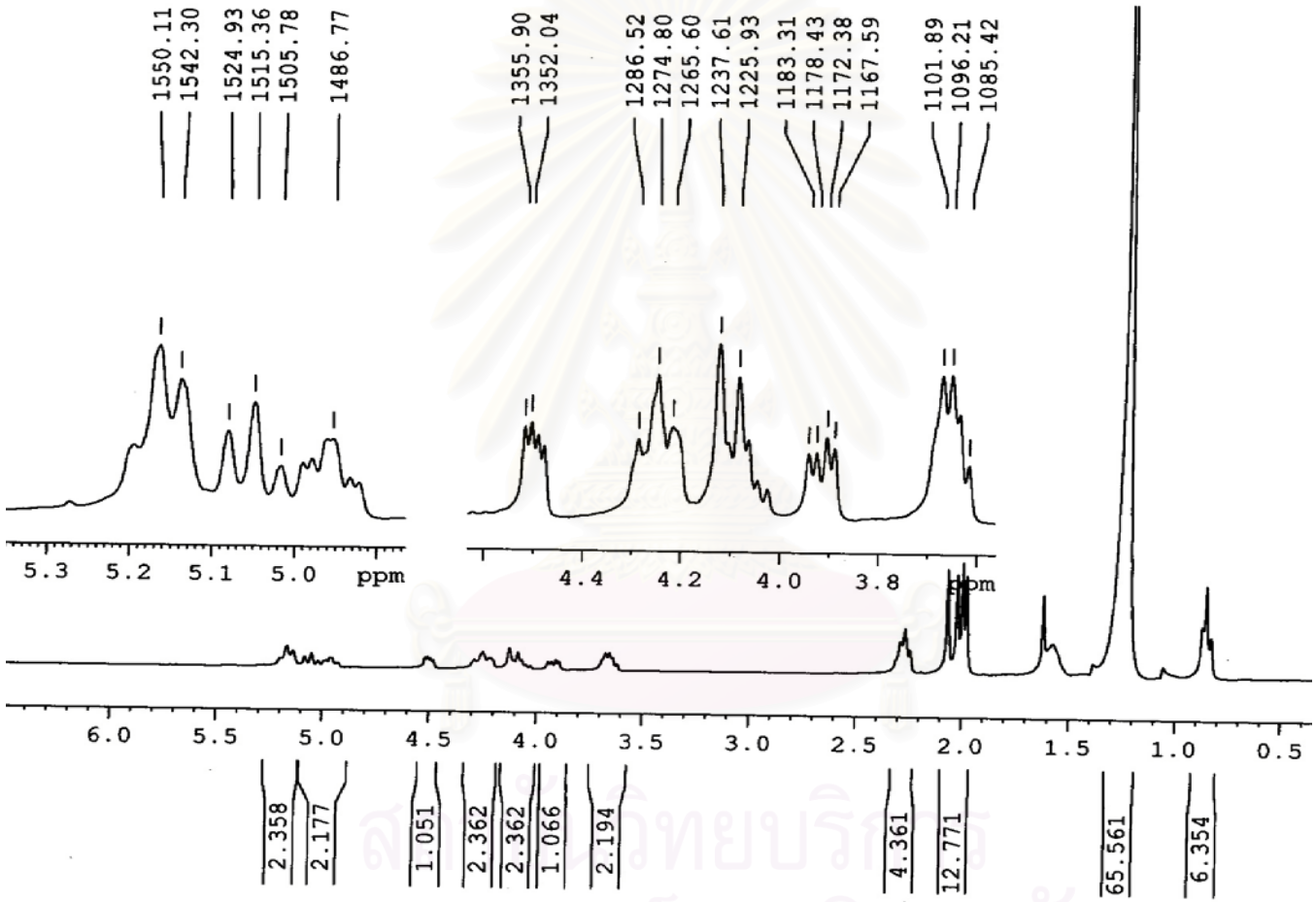

Figure 62. The 300 MHz ^{1}H-NMR spectrum of 1-*O*-stearoyl-2-*O*-behenoyl-3-*O*-(β-D-2′,3′,4′,6′-tetra-*O*-acetyl-glucopyranosyl)-*rac*-glycerol (**5m**) in $CDCl_3$.

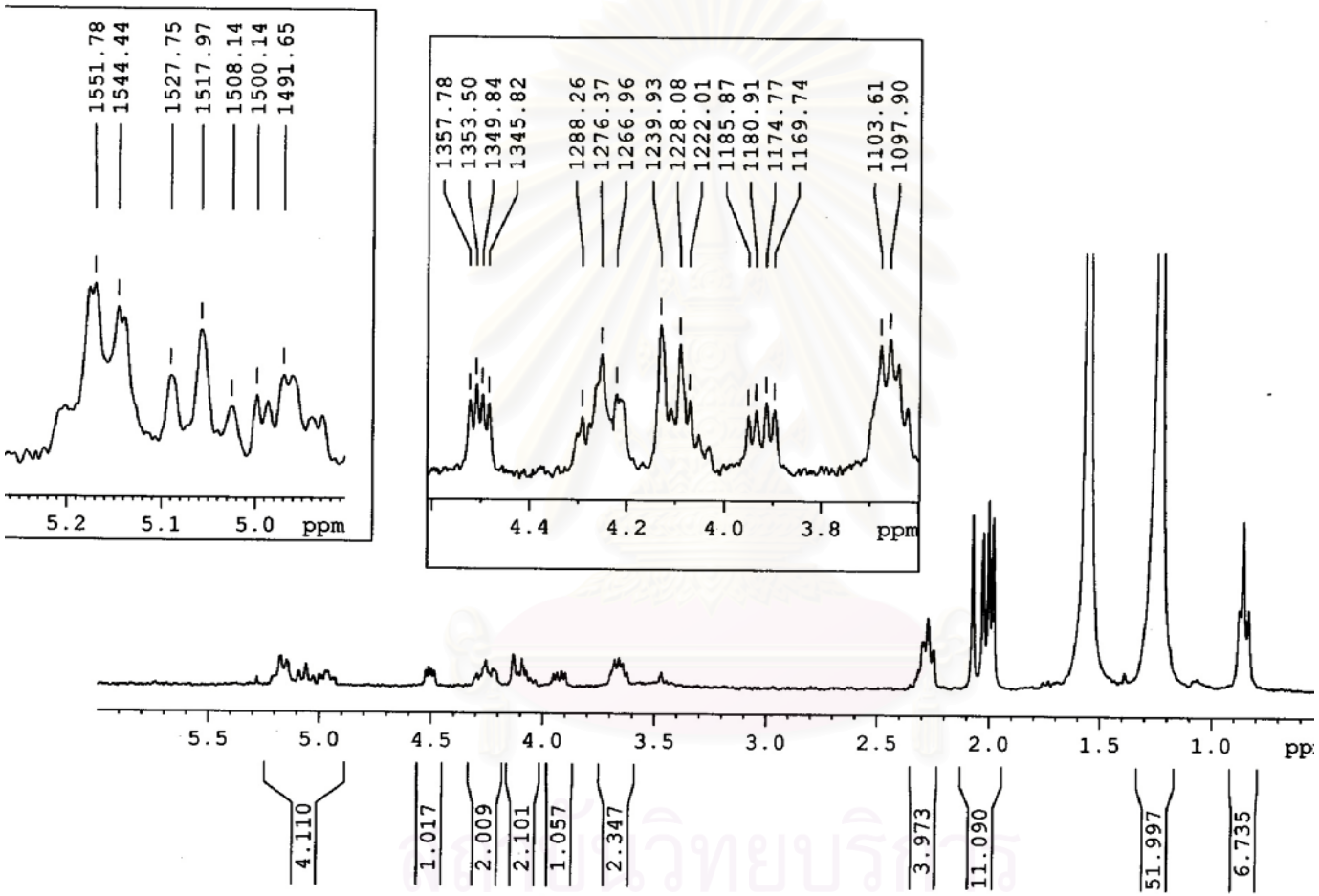

Figure 63. The 300 MHz ^{1}H-NMR spectrum of 1-*O*-behenoyl -2-*O*-lauroyl-3-*O*-(β-D-2′,3′,4′,6′-tetra-*O*-acetyl-glucopyranosyl)-*rac*-glycerol (**5n**) in $CDCl_3$.

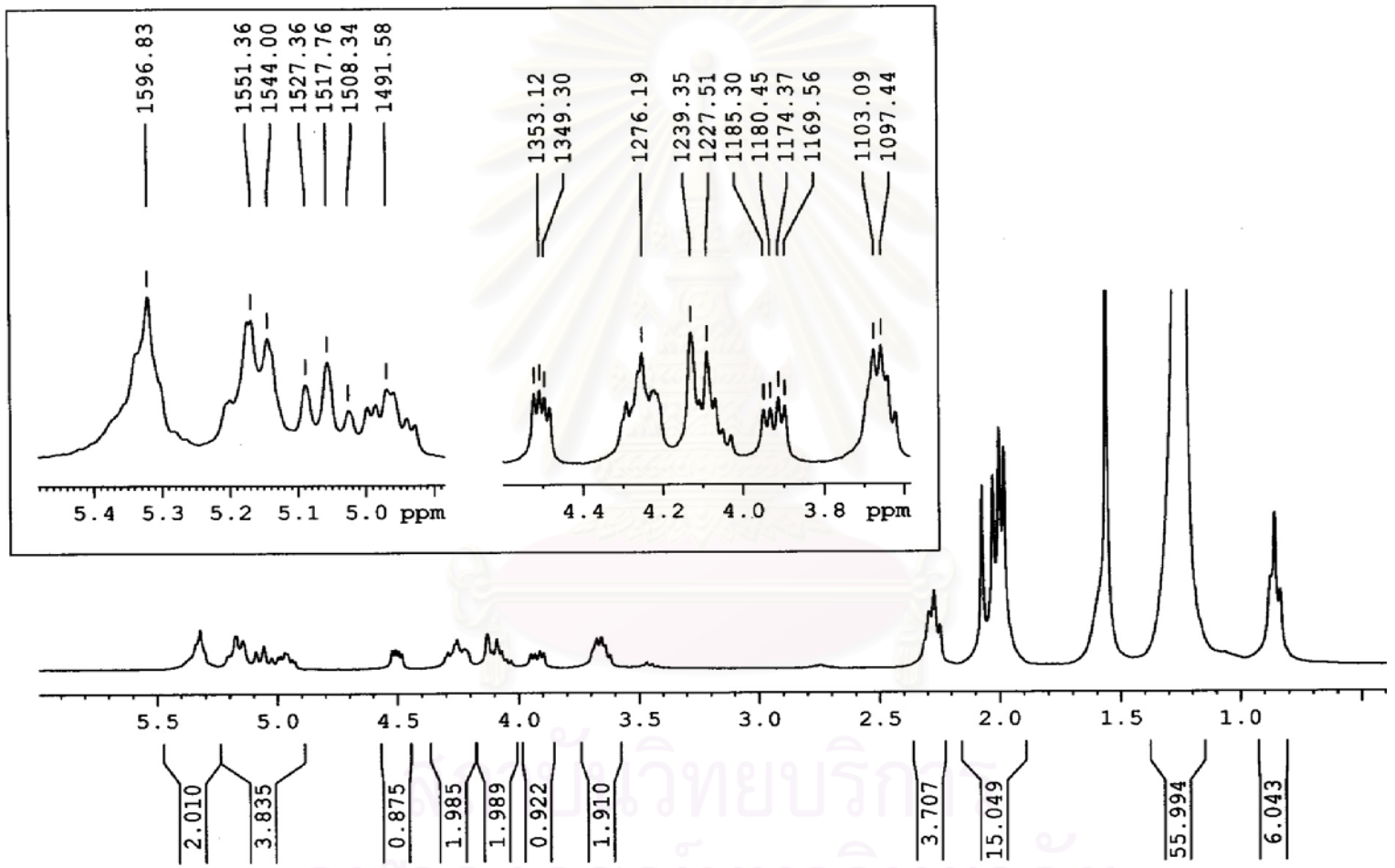

Figure 64. The 300 MHz ^{1}H-NMR spectrum of 1-*O*-behenoyl-2-*O*-oleoyl-3-*O*-(β-D-2′,3′,4′,6′-tetra-*O*-acetyl-glucopyranosyl)-*rac*-glycerol (**5o**) in $CDCl_3$.

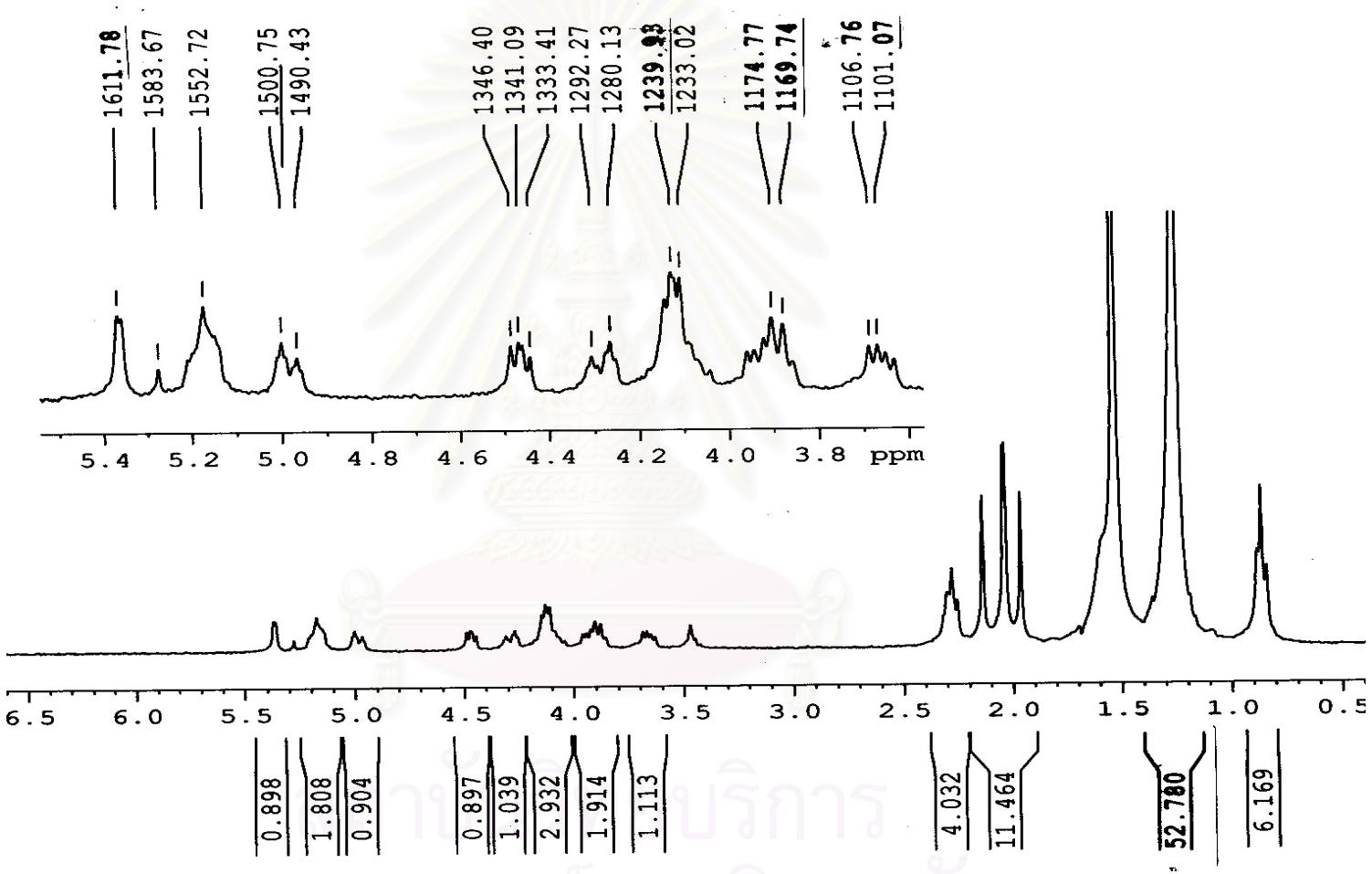

Figure 65. The 300 MHz ^{1}H-NMR spectrum of 1-*O*-behenoyl-2-*O*-lauroyl-3-*O*-(β-D-2′,3′,4′,6′-tetra-*O*-acetyl-galactopyranosyl)-*rac*-glycerol (**12d**) in $CDCl_3$.

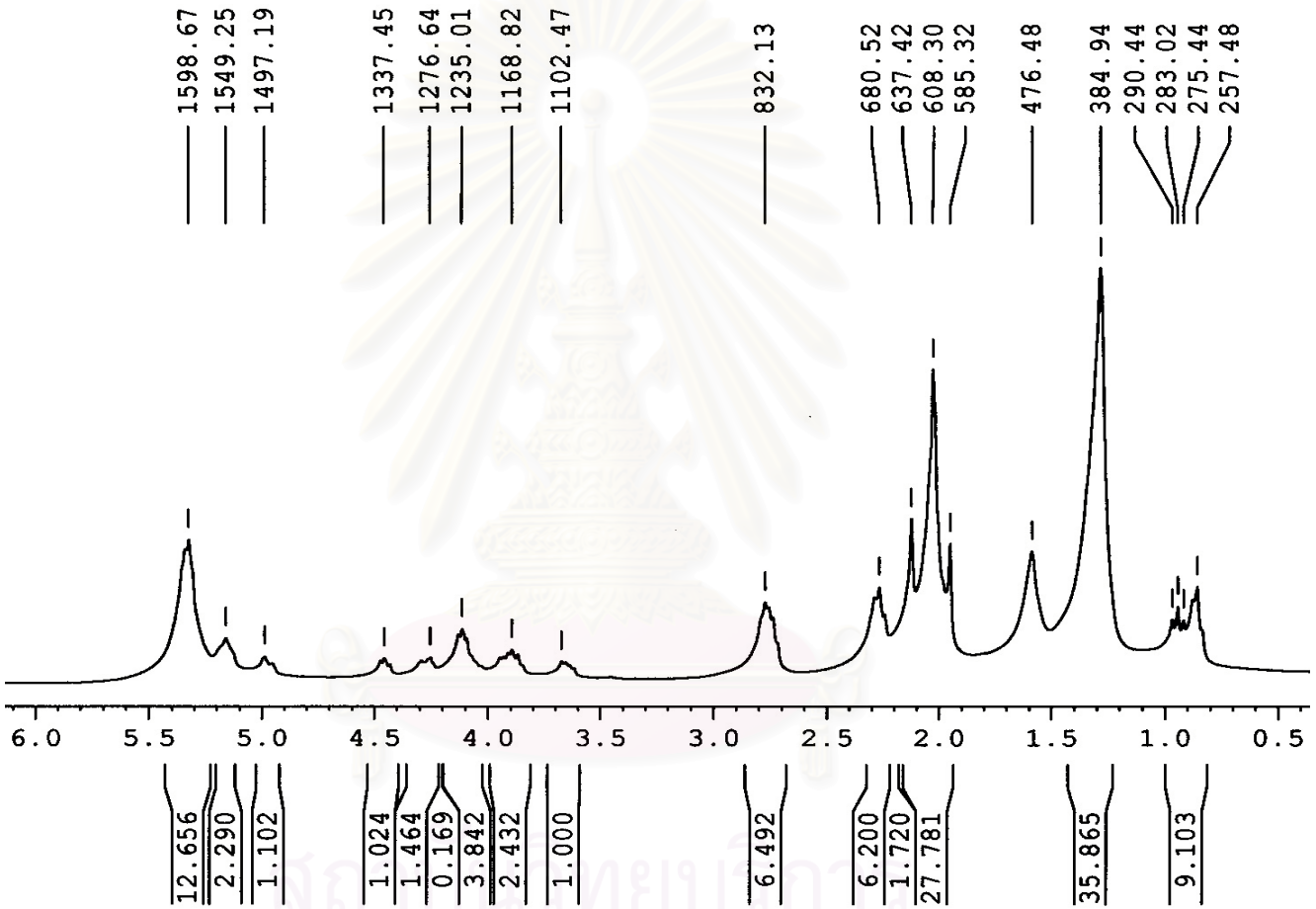

Figure 66. The 300 MHz ^{1}H-NMR spectrum of 1-*O*-linolenoyl-2-*O*-linoleoyl-3-*O*-(β- D-2′,3′,4′,6′-tetra-*O*-acetyl-galactopyranosyl)-*rac*-glycerol (**12e**) in $CDCl_3$.

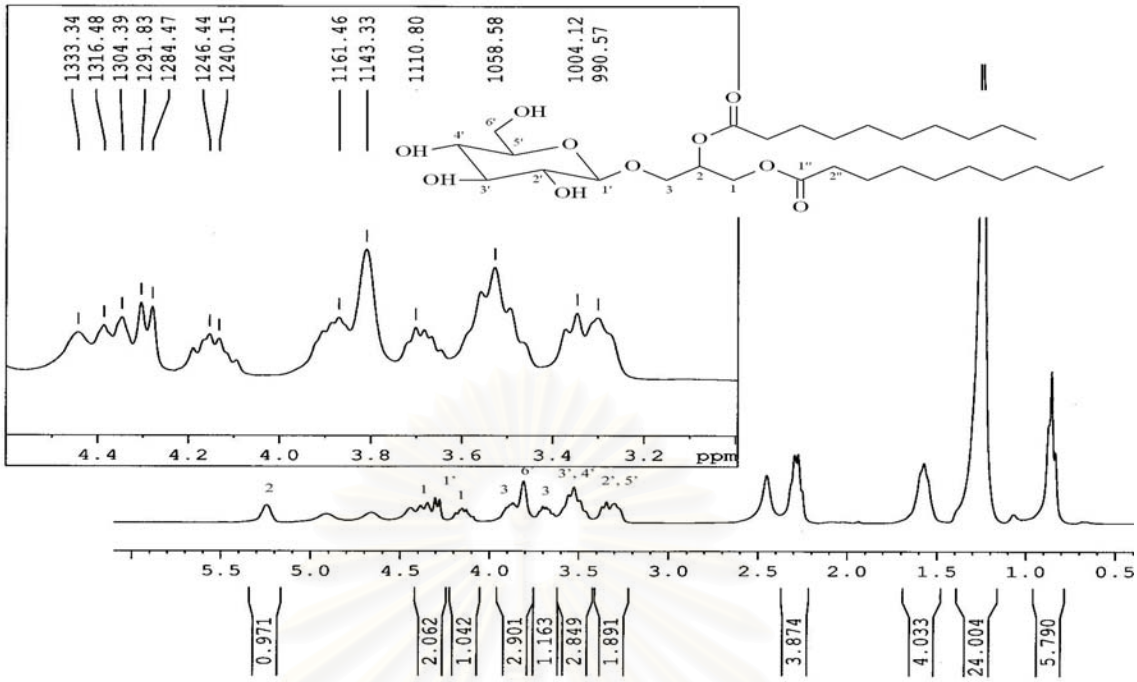

Figure 67. The 300 MHz ^{1}H-NMR spectrum of 1,2-di-*O*-caproyl-3-*O*-β-D-glucopyranosyl-*rac*-glycerol (**6a**) in $CDCl_3$.

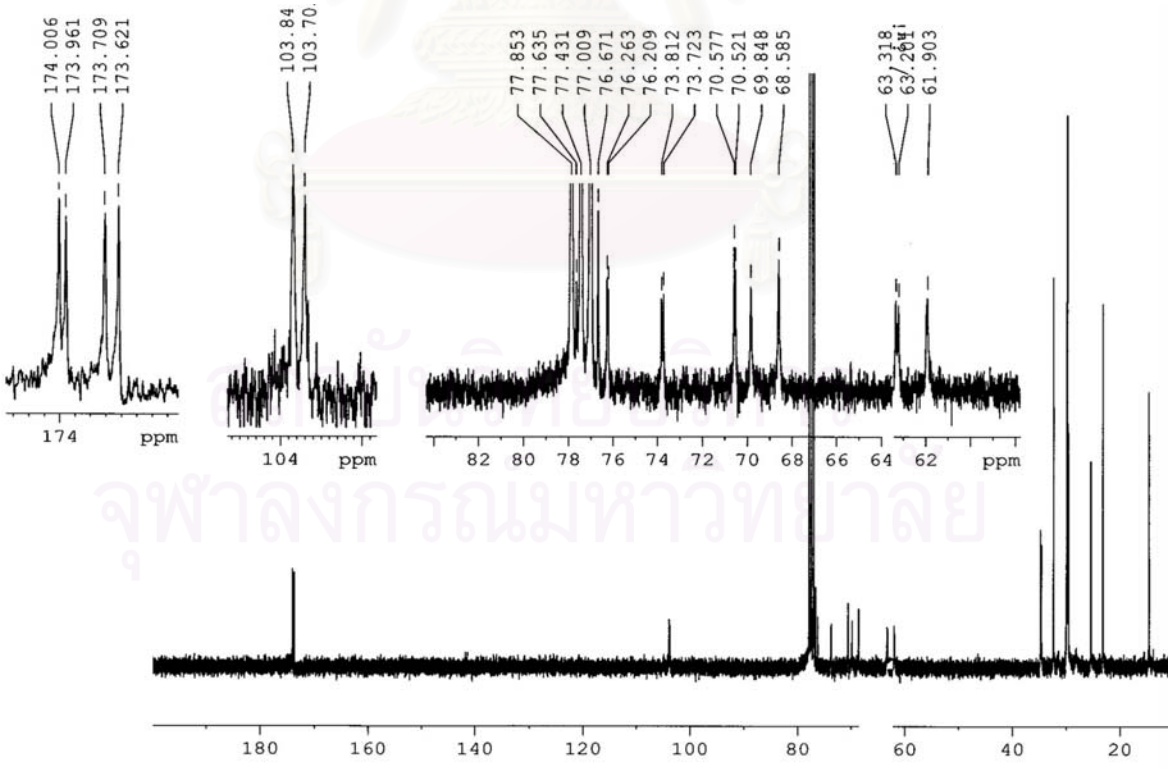

Figure 68. The 75 MHz ^{13}C-NMR spectrum of 1,2-di-*O*-caproyl-3-*O*-β-D-glucopyranosyl-*rac*-glycerol (**6a**) in $CDCl_3$.

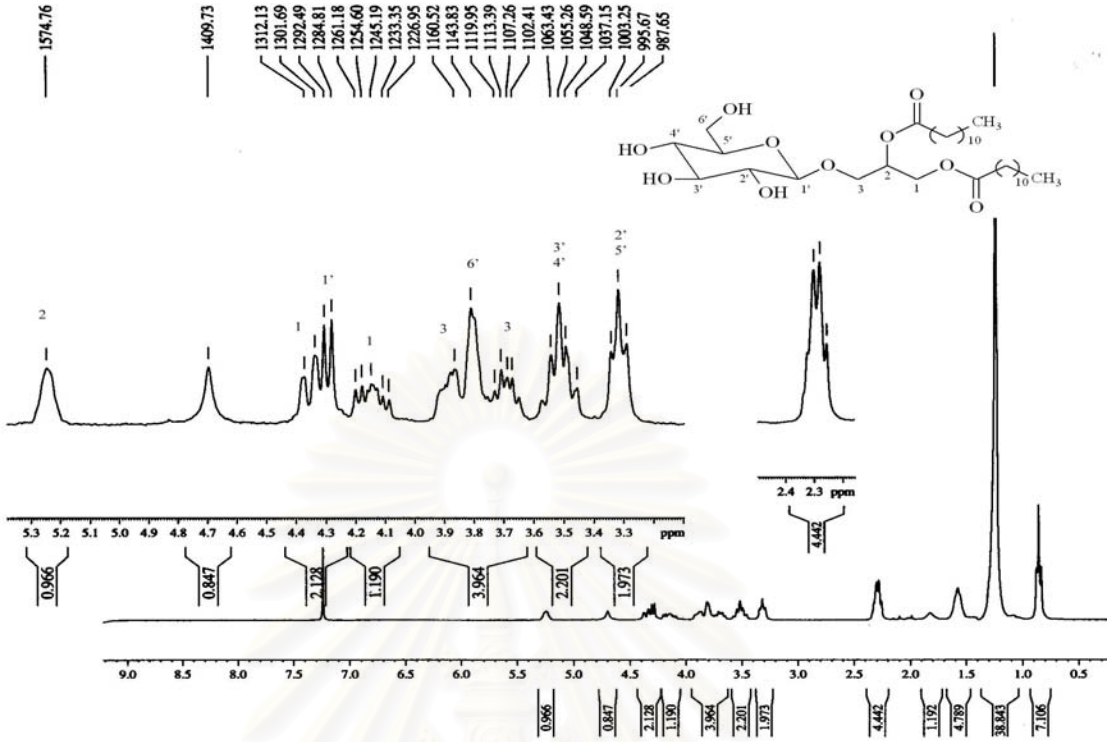

Figure 69. The 300 MHz ^{1}H-NMR spectrum of 1,2-di-*O*-lauroyl-3-*O*-β-D-glucopyranosyl-*rac*-glycerol (**6b**) in $CDCl_3$.

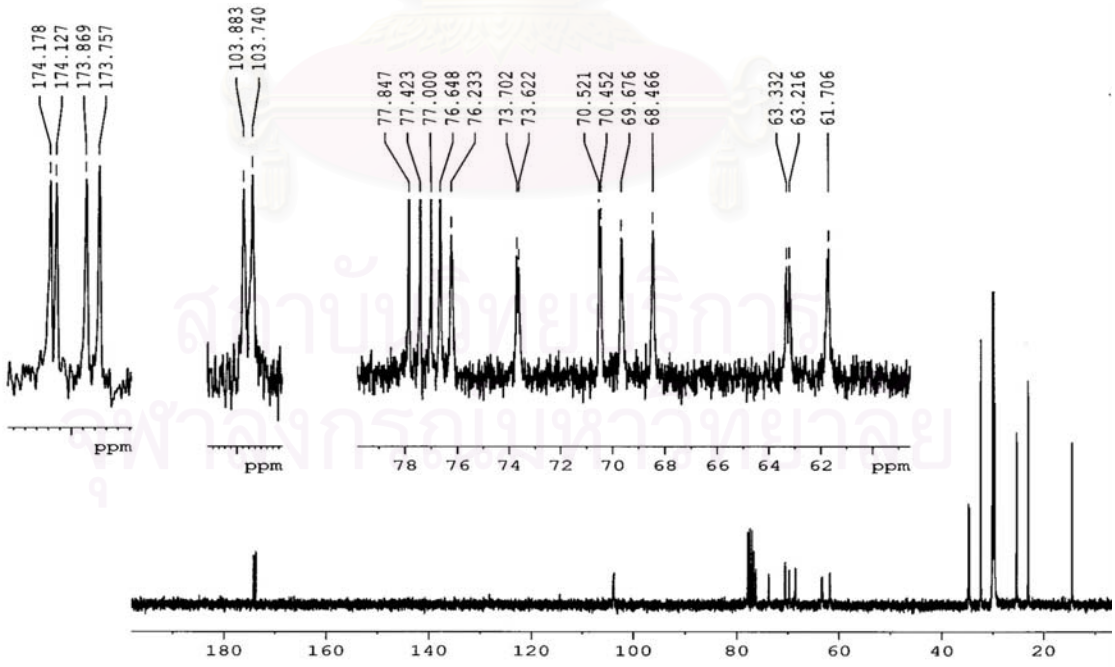

Figure 70. The 75 MHz ^{13}C-NMR spectrum of 1,2-di-*O*-lauroyl-3-*O*-β-D-glucopyranosyl-*rac*-glycerol (**6b**) in $CDCl_3$.

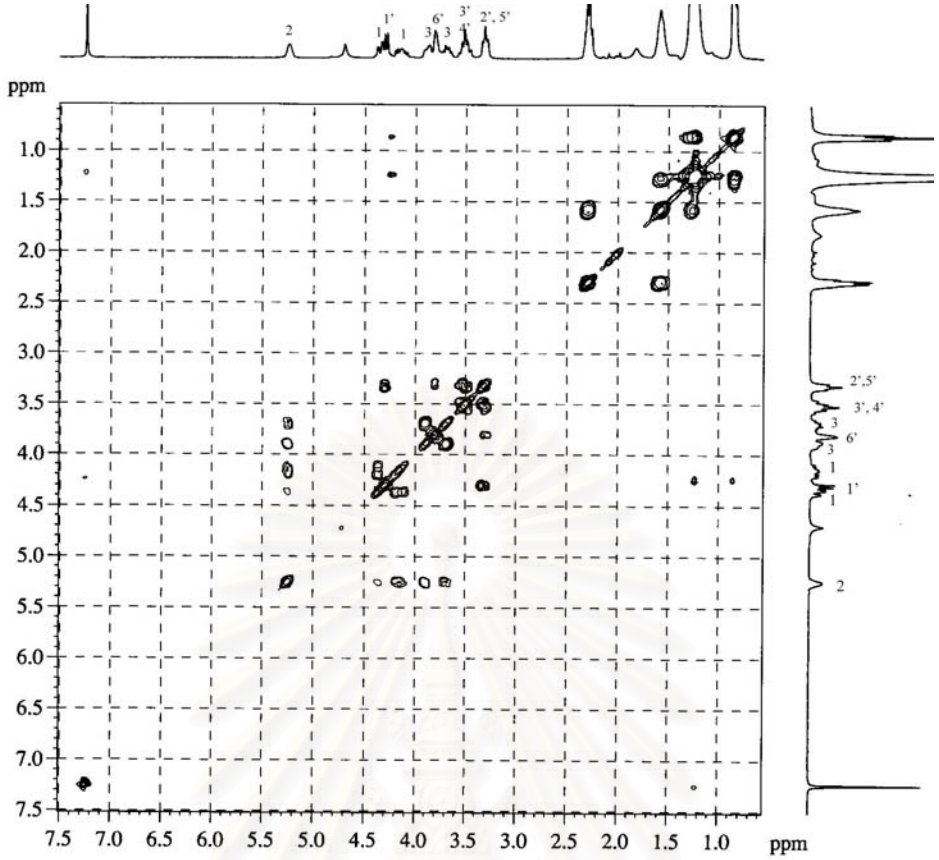

Figure 71. The ^{1}H-^{1}H COSY spectrum of 1,2-di-*O*-lauroyl-3-*O*-β-D-glucopyranosyl-*rac*-glycerol (**6b**) in $CDCl_3$.

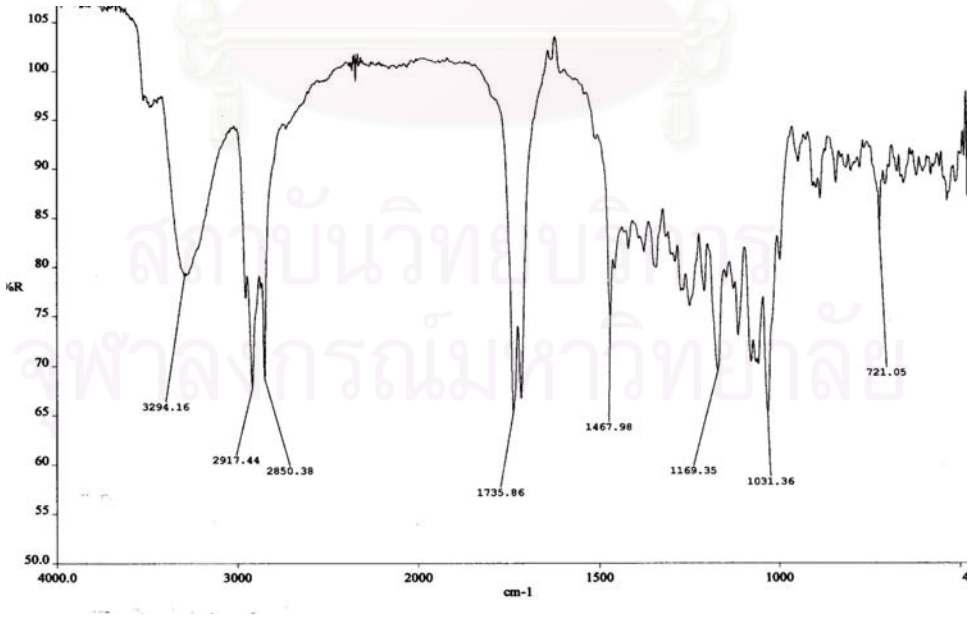

Figure 72. The infrared spectrum of 1,2-di-*O*-lauroyl-3-*O*-β-D-glucopyranosyl-*rac*-glycerol (**6b**).

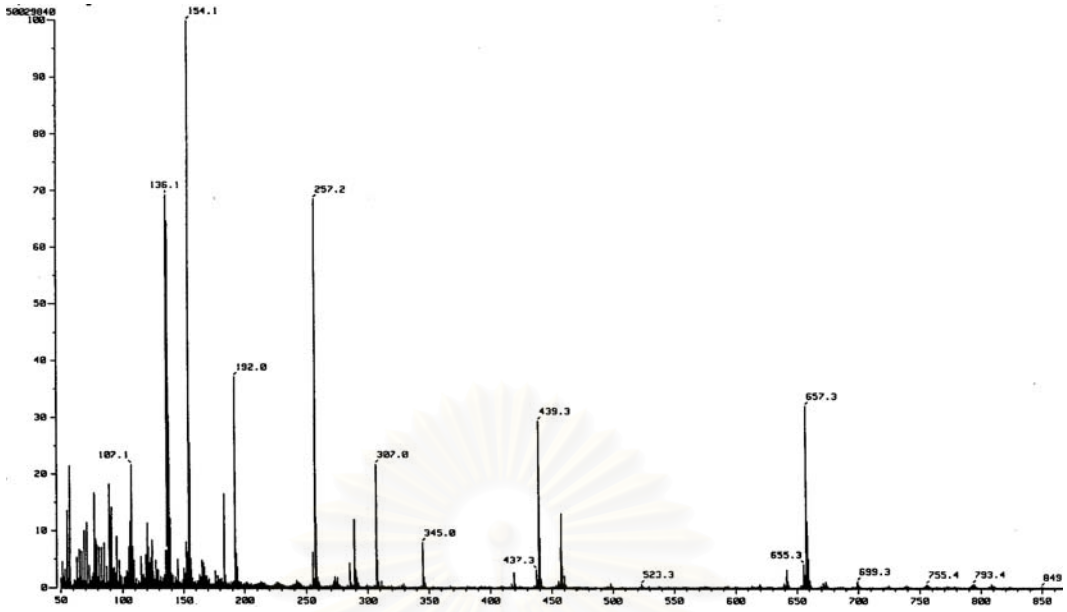

Figure 73. The positive ion FABMS of 1,2-di-*O*-lauroyl-3-*O*-β-D-glucopyranosyl-*rac*-glycerol (**6b**) in the presence of m-Nitrobenzyl alcohol.

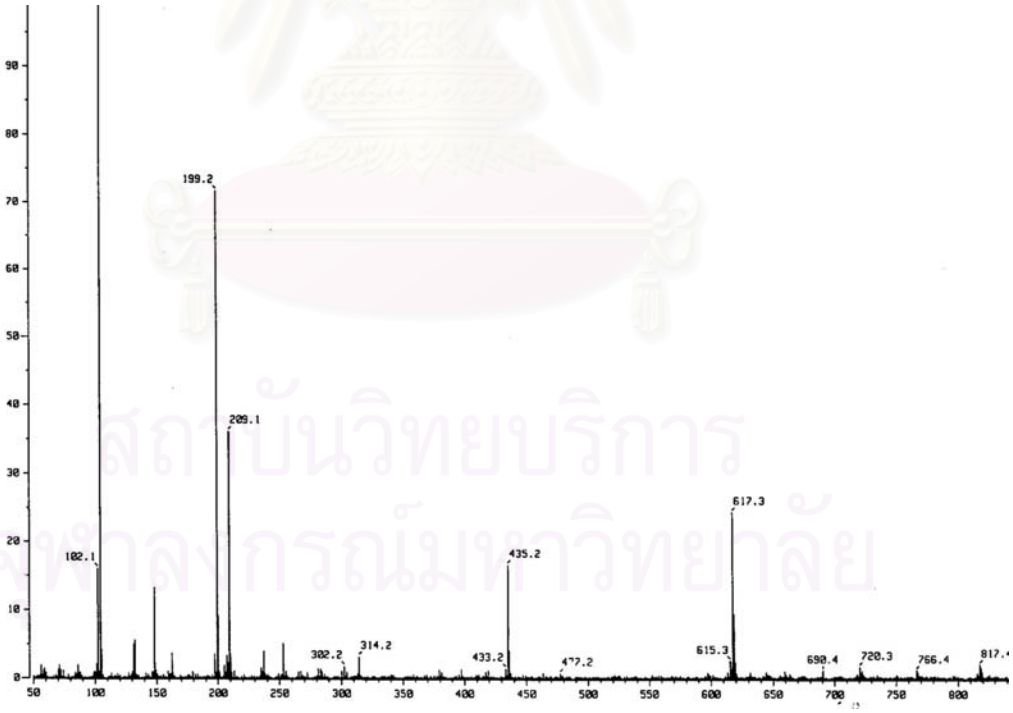

Figure 74. The negative ion FABMS of 1,2-di-*O*-caproyl-3-*O*-β-D-glucopyranosyl-*rac*-glycerol (**6b**) in the presence of diethanolamine.

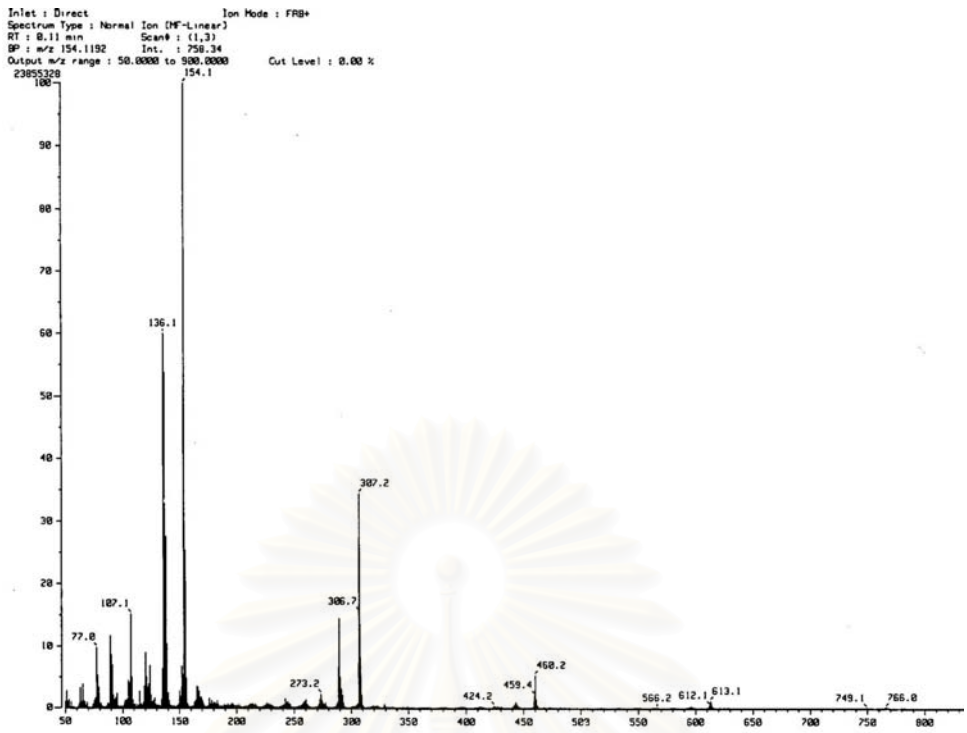

Figure 75. The positive ion FABMS of m-Nitrobenzyl alcohol

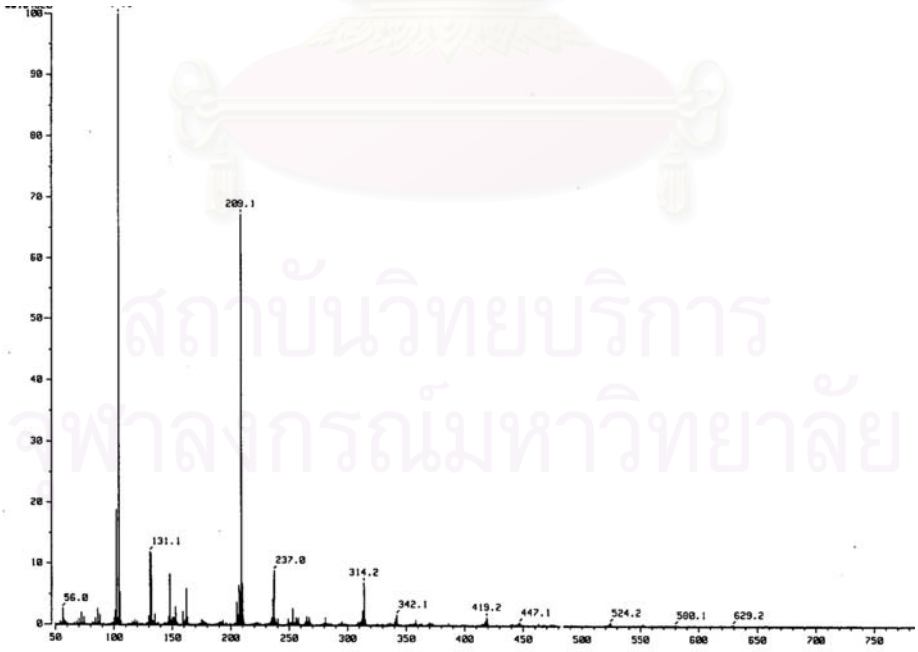

Figure 76. The negative ion FABMS of diethanolamine

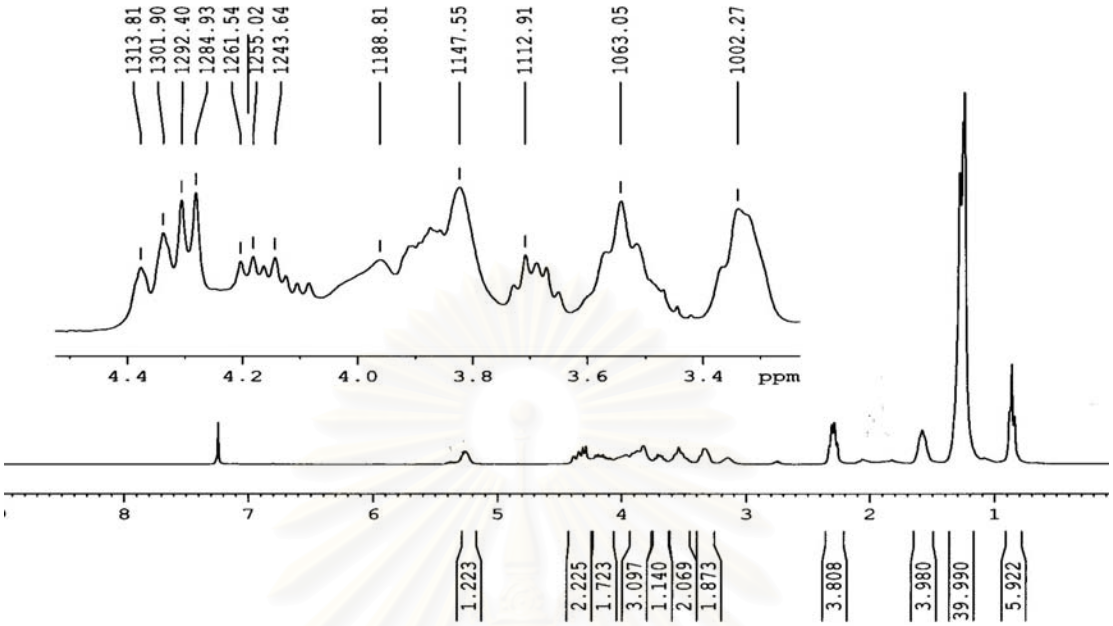

Figure 77. The 300 MHz ^{1}H-NMR spectrum of 1,2-di-*O*-myristoyl-3-*O*-β-D-glucopyranosyl-*rac*-glycerol (**6c**) in $CDCl_3$.

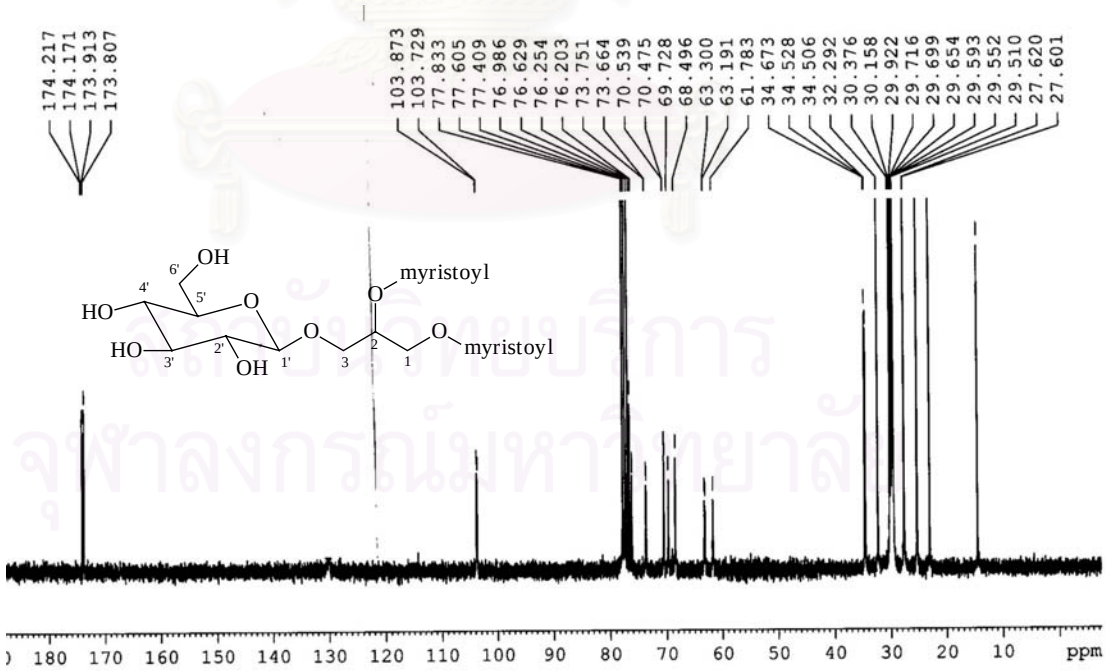

Figure 78. The 75 MHz ^{13}C-NMR spectrum of 1,2-di-*O*-myristoyl-3-*O*-β-D-glucopyranosyl-*rac*-glycerol (**6c**) in $CDCl_3$.

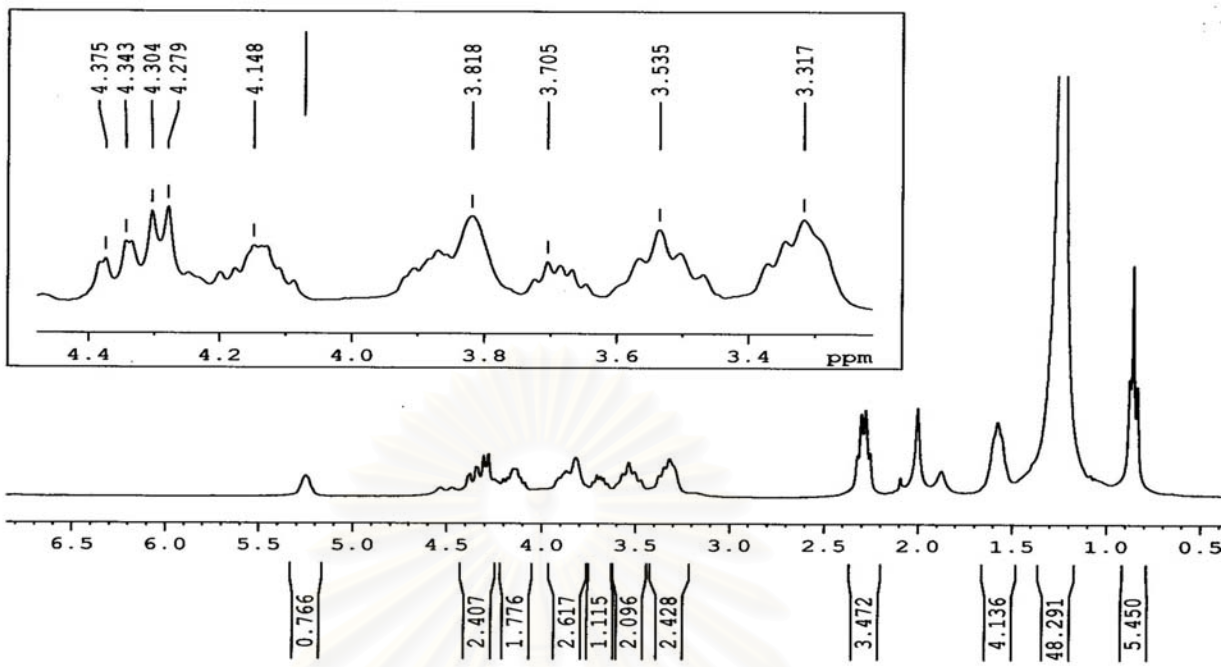

Figure 79. The 300 MHz ^{1}H-NMR spectrum of 1,2-di-*O*-palmitoyll-3-*O*-β-D-glucopyranosyl-*rac*-glycerol (**6d**)) in $CDCl_3$.

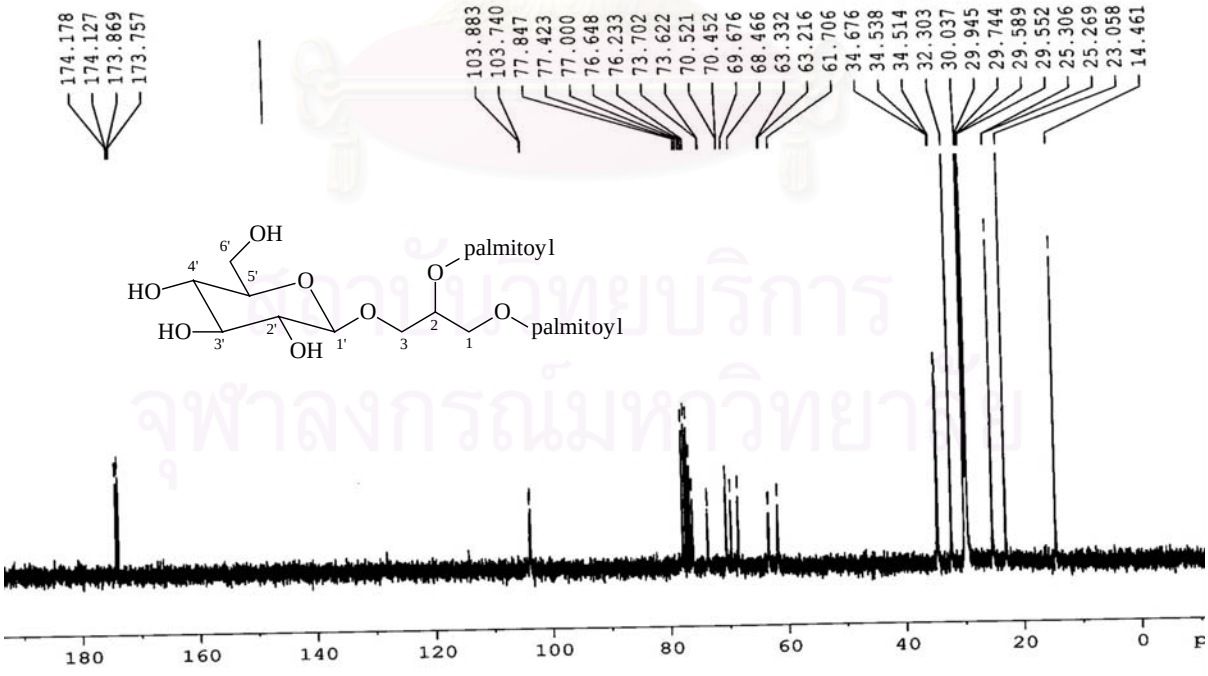

Figure 80. The 75 MHz ^{13}C-NMR spectrum of 1,2-di-*O*-palmitoyl-3-*O*-β-D-glucopyranosyl-*rac*-glycerol (**6d**)) in $CDCl_3$.

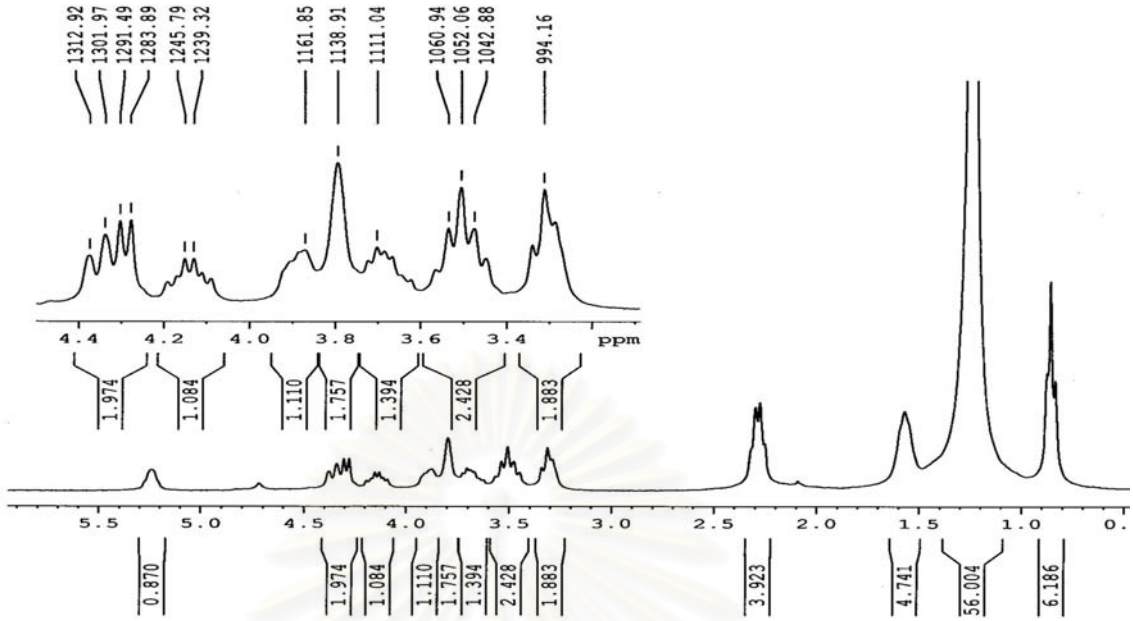

Figure 81. The 300 MHz ^{1}H-NMR spectrum of 1,2-di-*O*-stearoyl-3-*O*-β-D-glucopyranosyl-*rac*-glycerol (**6e**)) in $CDCl_3$.

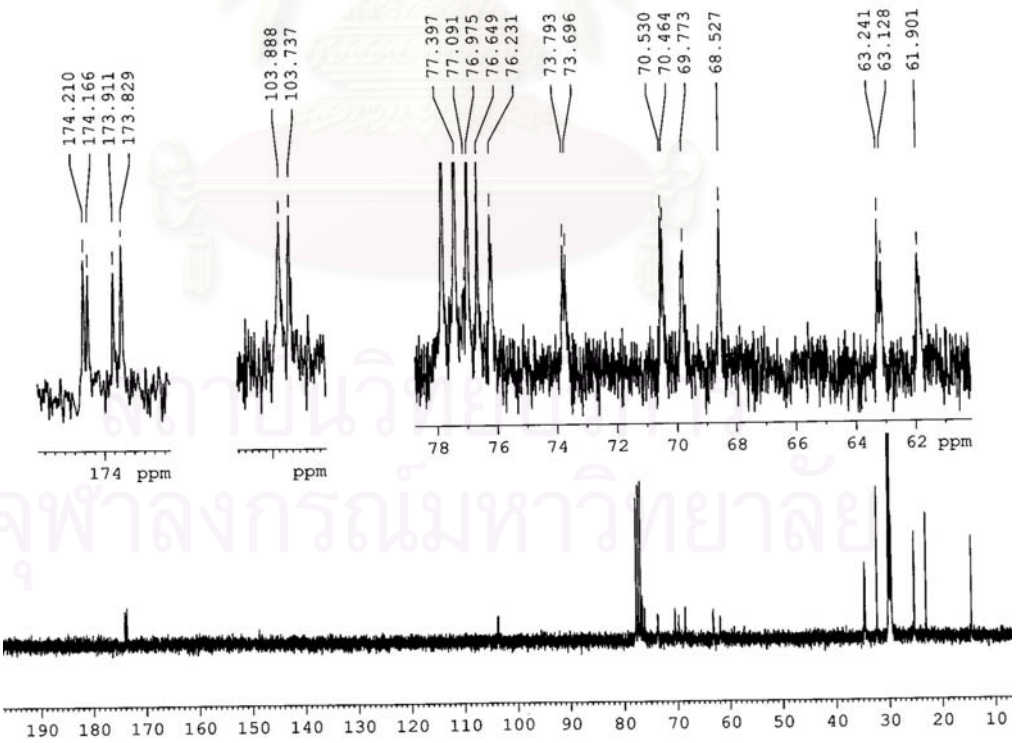

Figure 82. The 75 MHz ^{13}C-NMR spectrum of 1,2-di-*O*-stearoyl-3-*O*-β-D-glucopyranosyl-*rac*-glycerol (**6e**)) in $CDCl_3$.

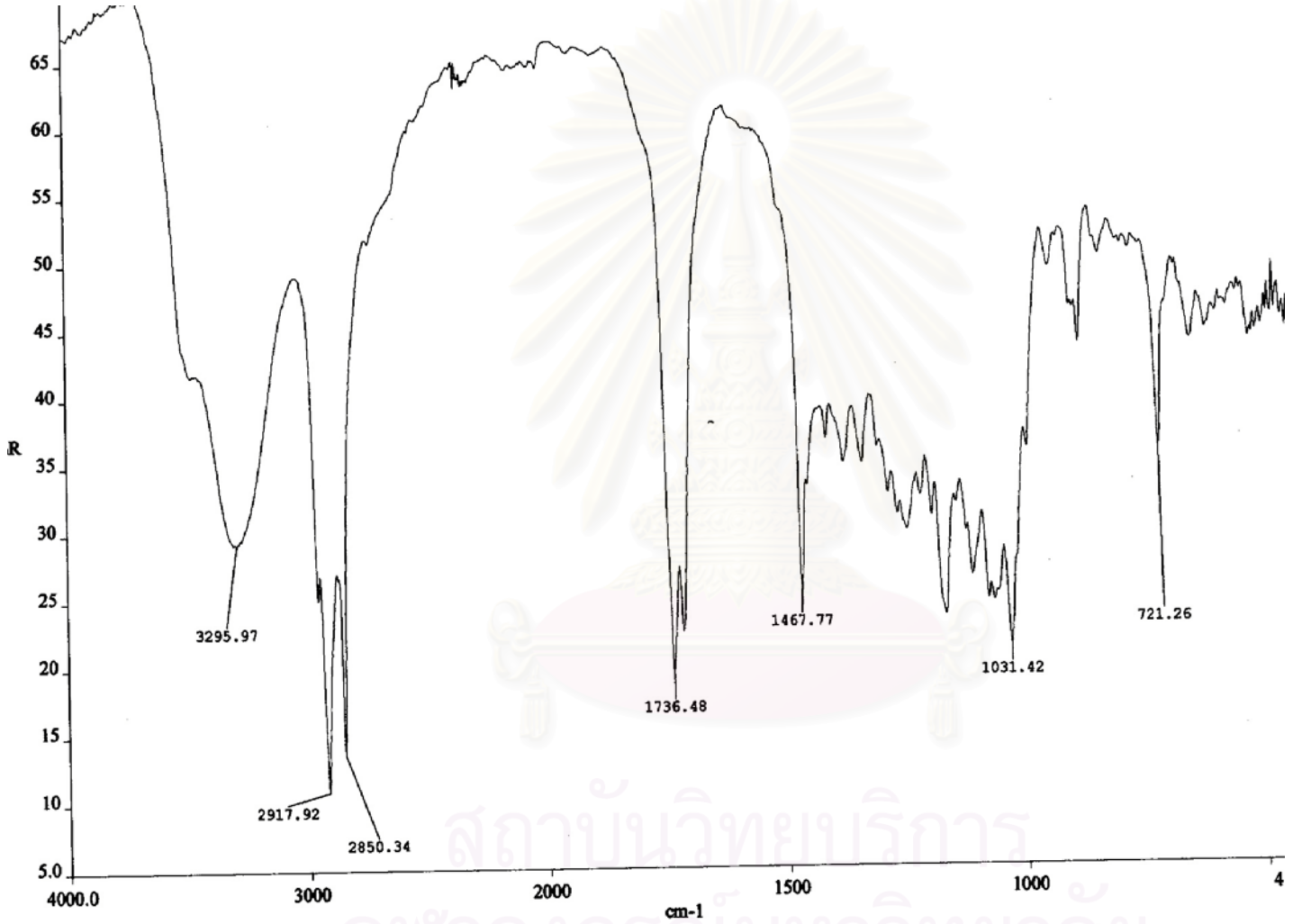

Figure 83. The infrared spectrum of 1,2-di-*O*-stearoyl-3-*O*-β-D-glucopyranosyl-*rac*-glycerol (**6e**).

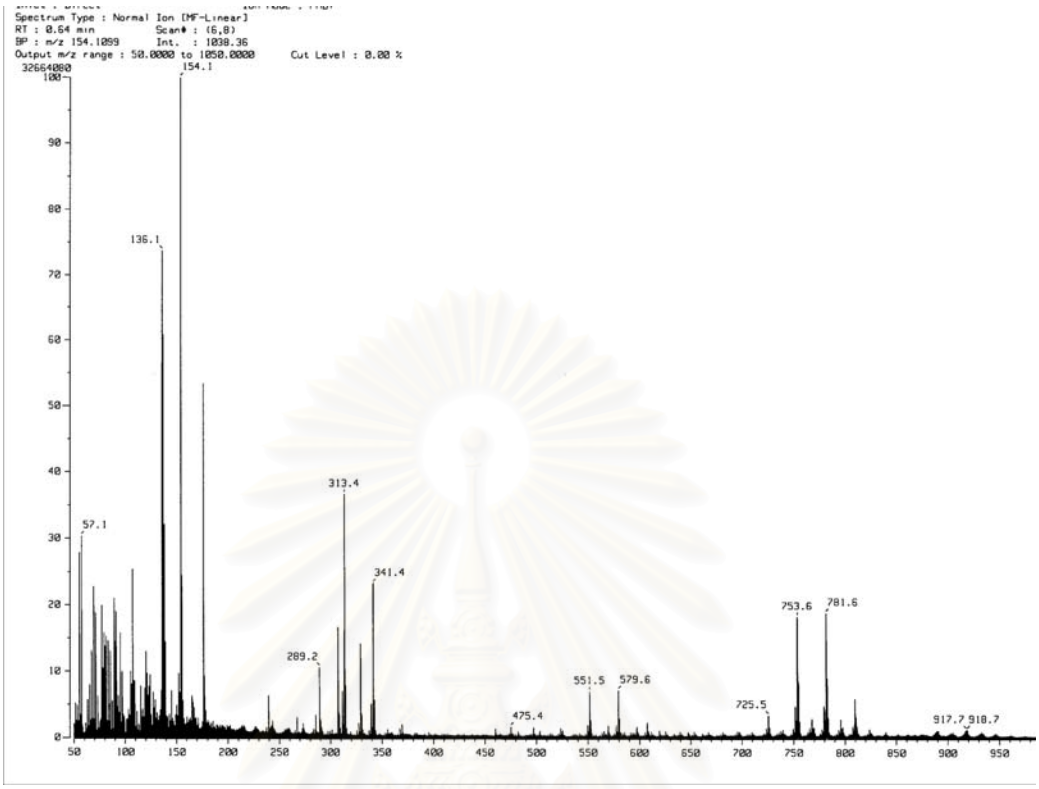

Figure 84. The positive ion FABMS of 1,2-di-*O*-stearoyl-3-*O*-β-D-glucopyranosyl-*rac*-glycerol (**6e**).

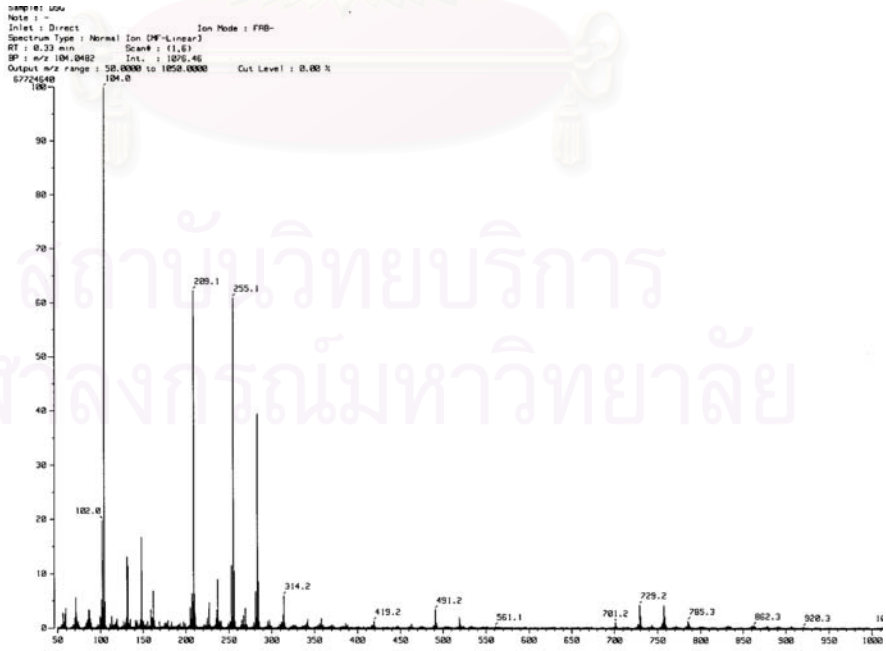

Figure 85. The negative ion FABMS of 1,2-di-*O*-stearoyl-3-*O*-β-D-glucopyranosyl-*rac*-glycerol (**6e**).

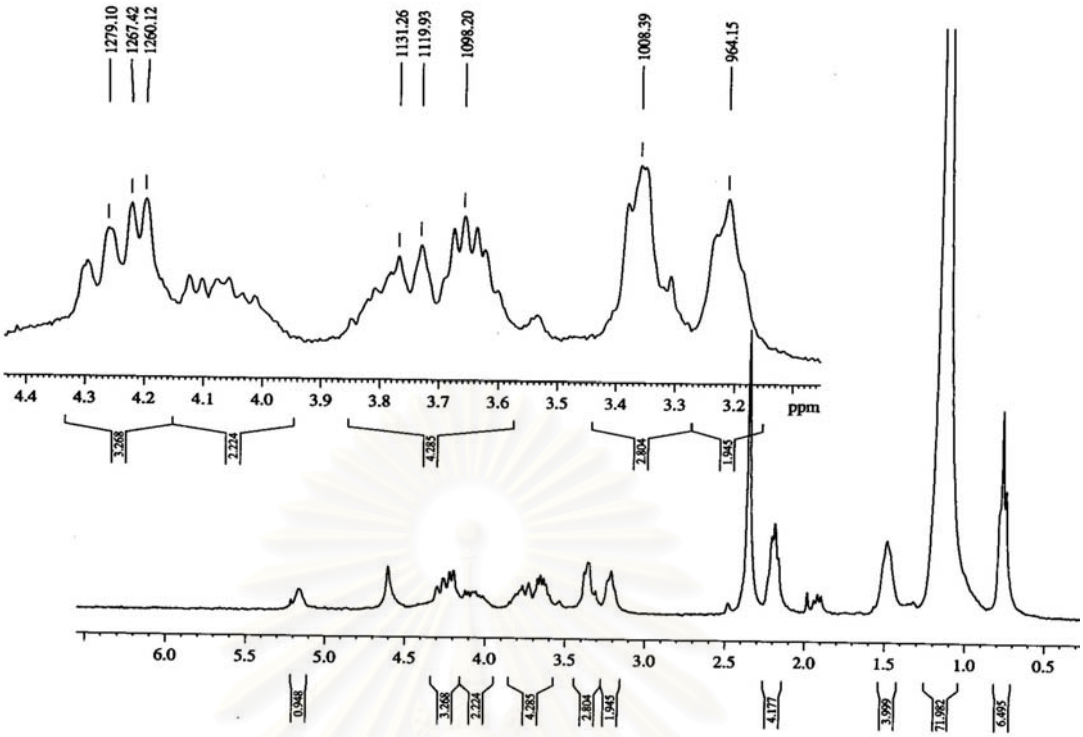

Figure 86. The 300 MHz ^{1}H-NMR spectrum of 1,2-di-*O*-behenoyl-3-*O*-β-D-glucopyranosyl-*rac*-glycerol (**6f**)) in $CDCl_3$.

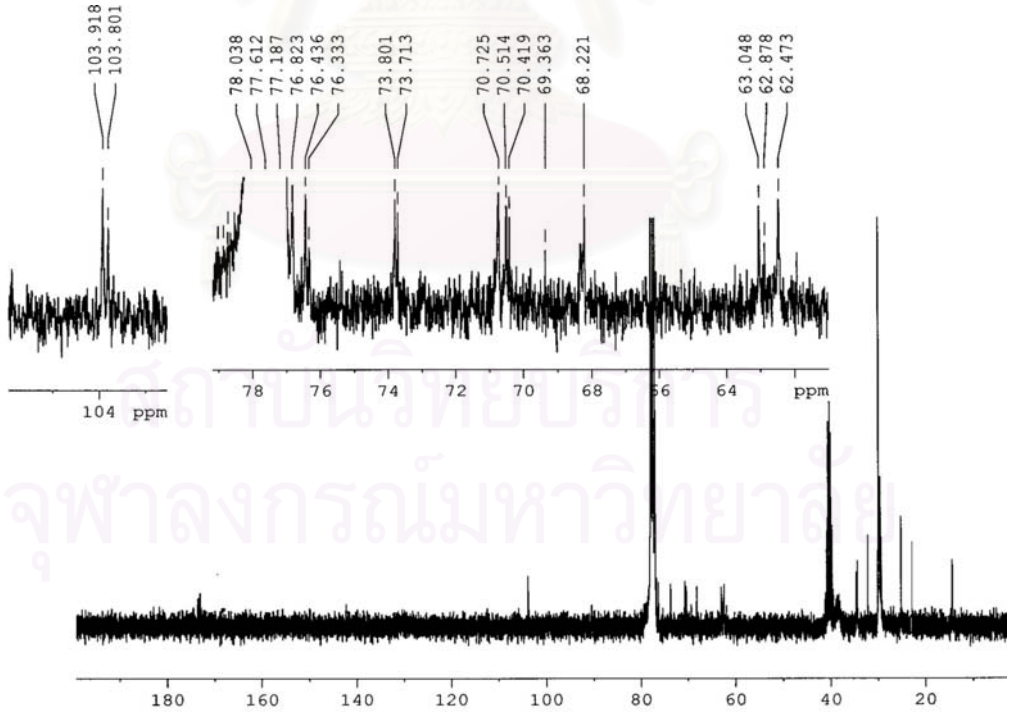

Figure 87. The 75 MHz ^{13}C-NMR spectrum of 1,2-di-*O*-behenoyl-3-*O*-β-D-glucopyranosyl-*rac*-glycerol (**6f**)) in $CDCl_3$.

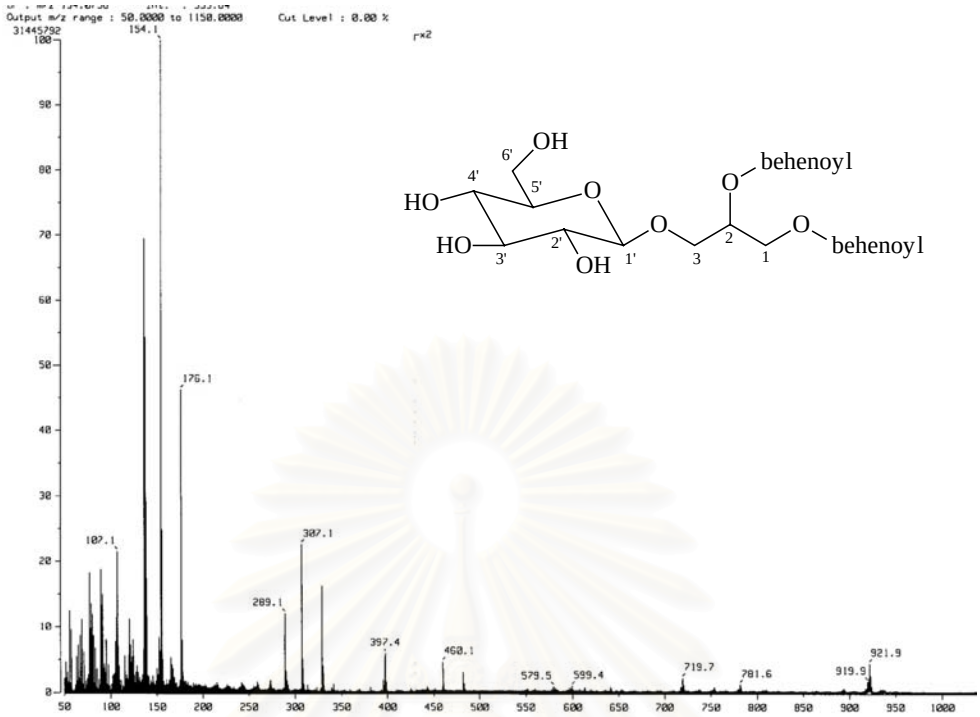

Figure 88. The positive ion FABMS of 1,2-di-*O*-behenoyl-3-*O*-β-D-glucopyranosyl-*rac*-glycerol (**6f**).

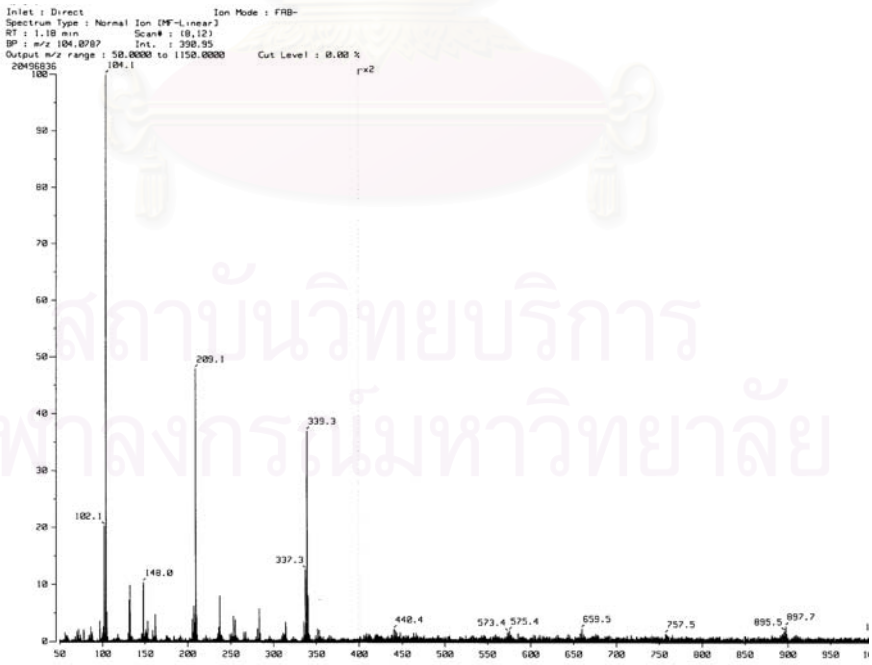

Figure 89. The negative ion FABMS of 1,2-di-*O*-behenoyl-3-*O*-β-D-glucopyranosyl-*rac*-glycerol (**6f**).

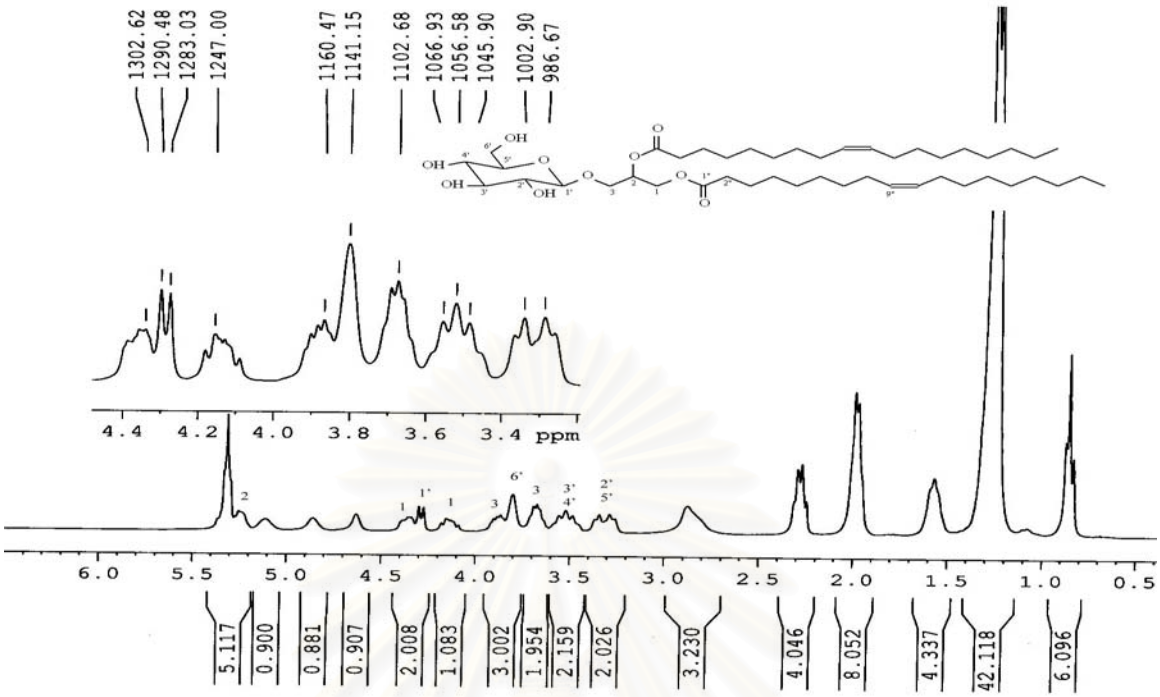

Figure 90. The 300 MHz ^{1}H-NMR spectrum of 1,2-di-*O*-oleoyl-3-*O*-β-D-glucopyranosyl-*rac*-glycerol (**6g**)) in $CDCl_3$.

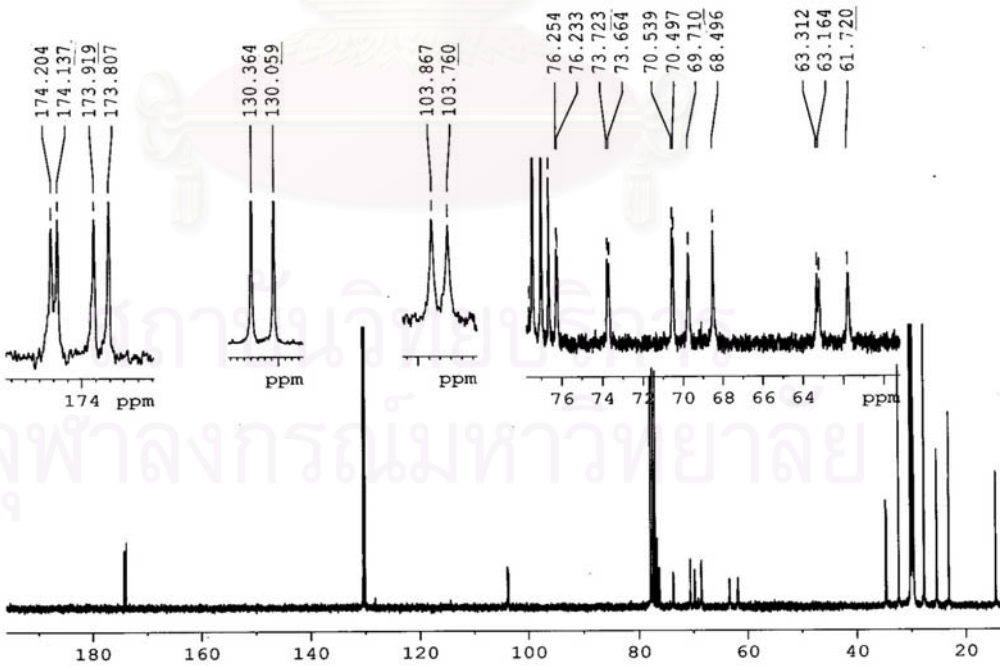

Figure 91. The 75 MHz ^{13}C-NMR spectrum of 1,2-di-*O*-oleoyl-3-*O*-β-D-glucopyranosyl-*rac*-glycerol (**6g**) in $CDCl_3$.

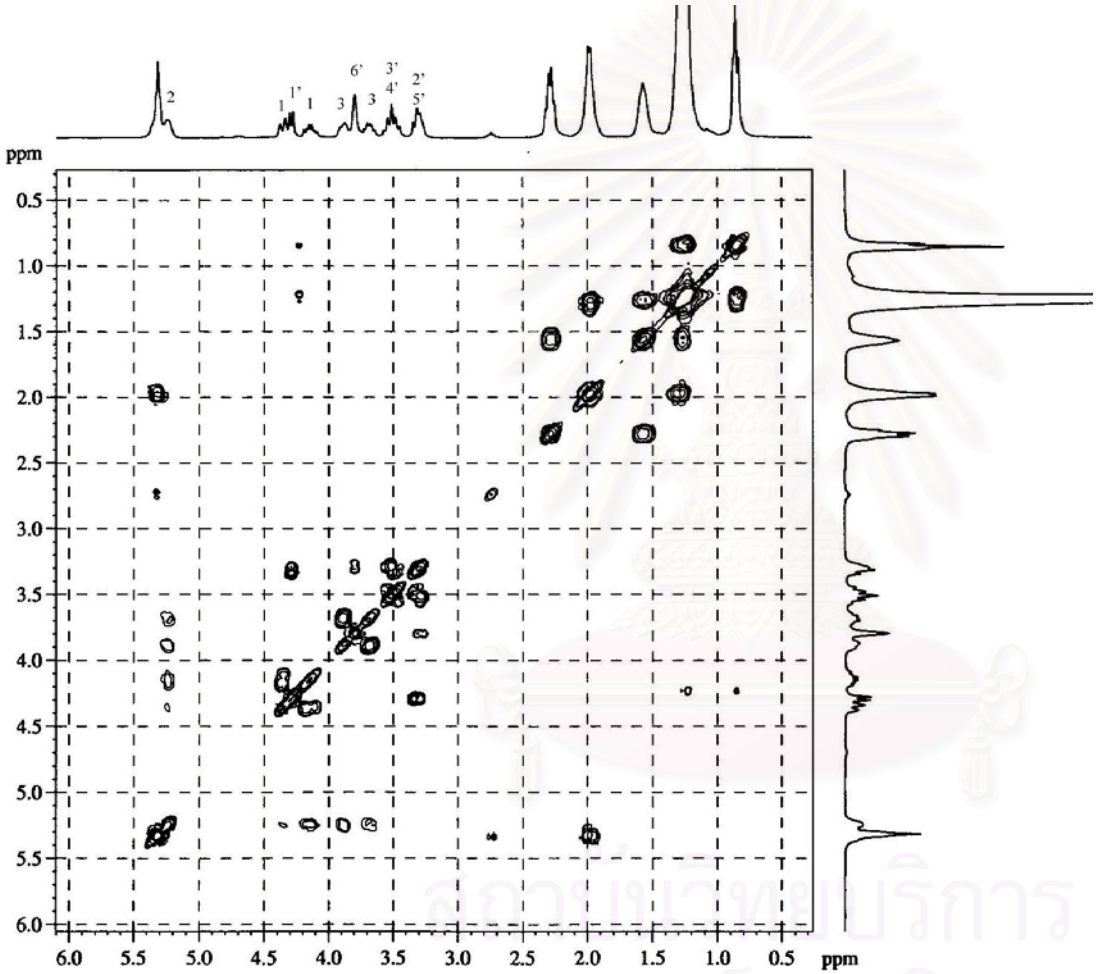

Figure 92. The ^{1}H-^{1}H COSY spectrum of 1,2-di-*O*-oleoyl-3-*O*-β-D-glucopyranosyl-*rac*-glycerol (**6g**) in $CDCl_3$.

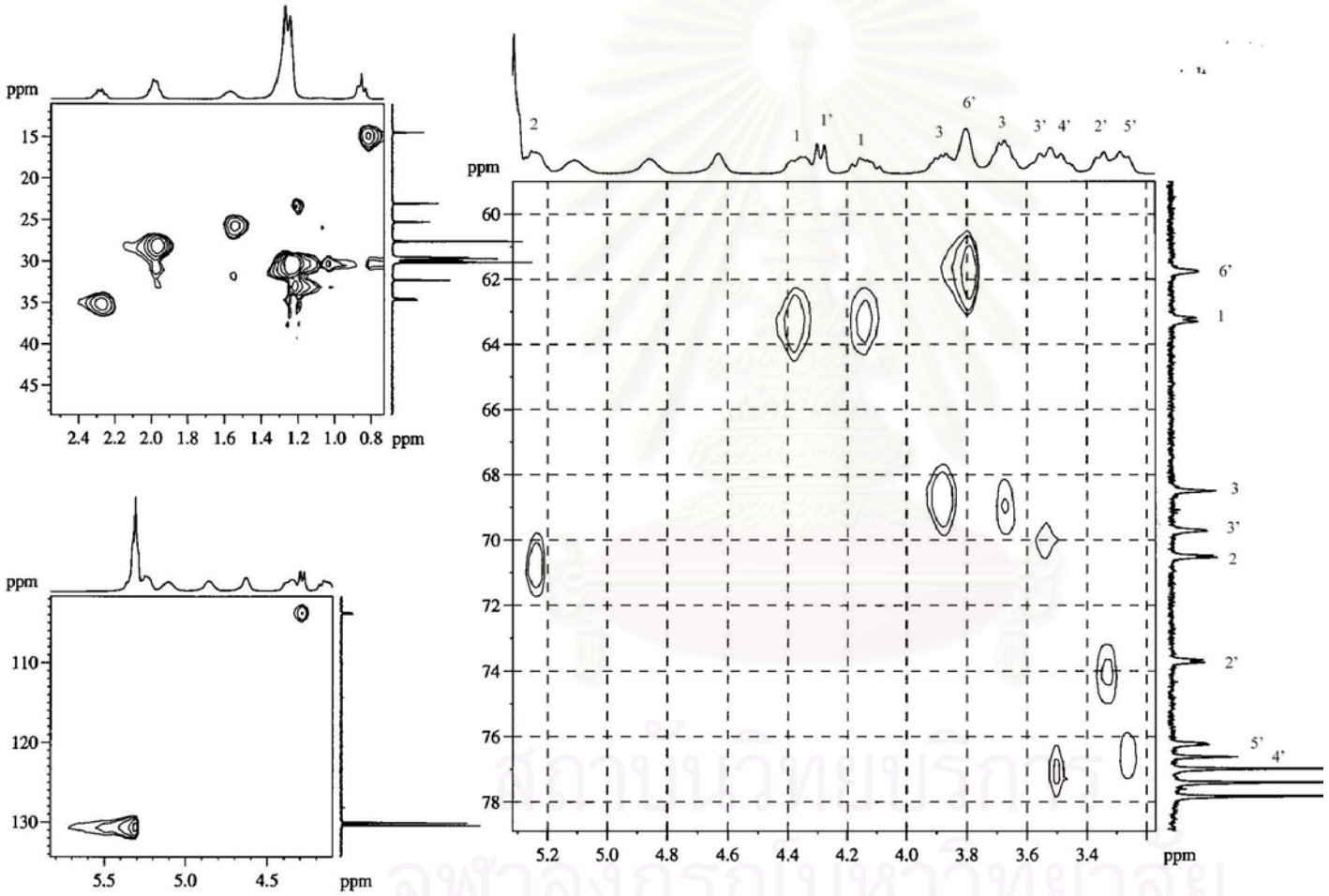

Figure 93. The HMQC spectrum of 1,2-di-*O*-oleoyl-3-*O*-β-D-glucopyranosyl-*rac*-glycerol (**6g**) in $CDCl_3$.

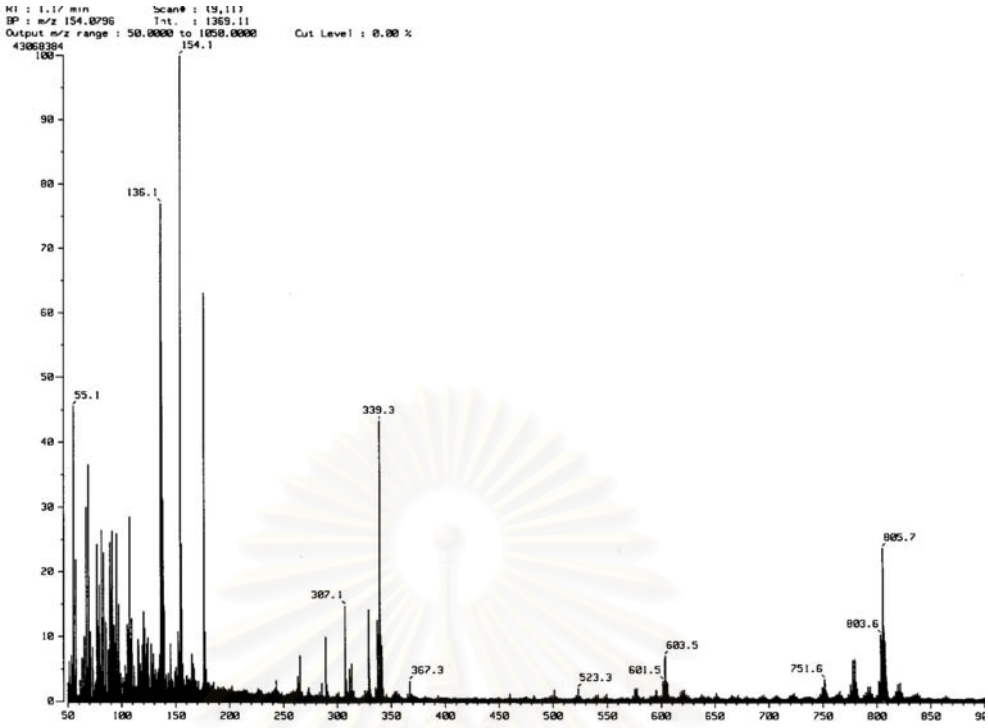

Figure 94. The positive ion FABMS of 1,2-di-*O*-oleoyl-3-*O*-β-D-glucopyranosyl-*rac*-glycerol (**6g**).

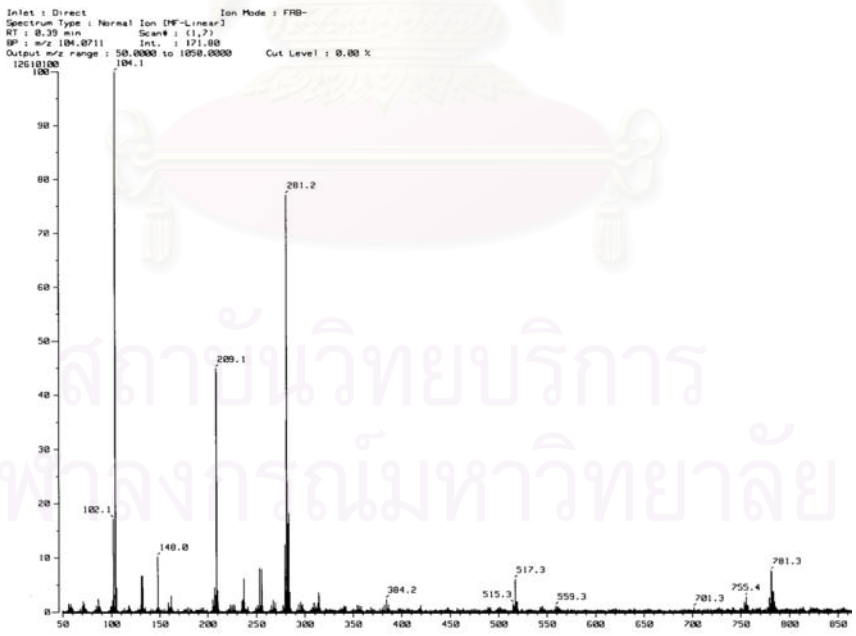

Figure 95. The negative ion FABMS of 1,2-di-*O*-oleoyl-3-*O*-β-D-glucopyranosyl-*rac*-glycerol (**6g**).

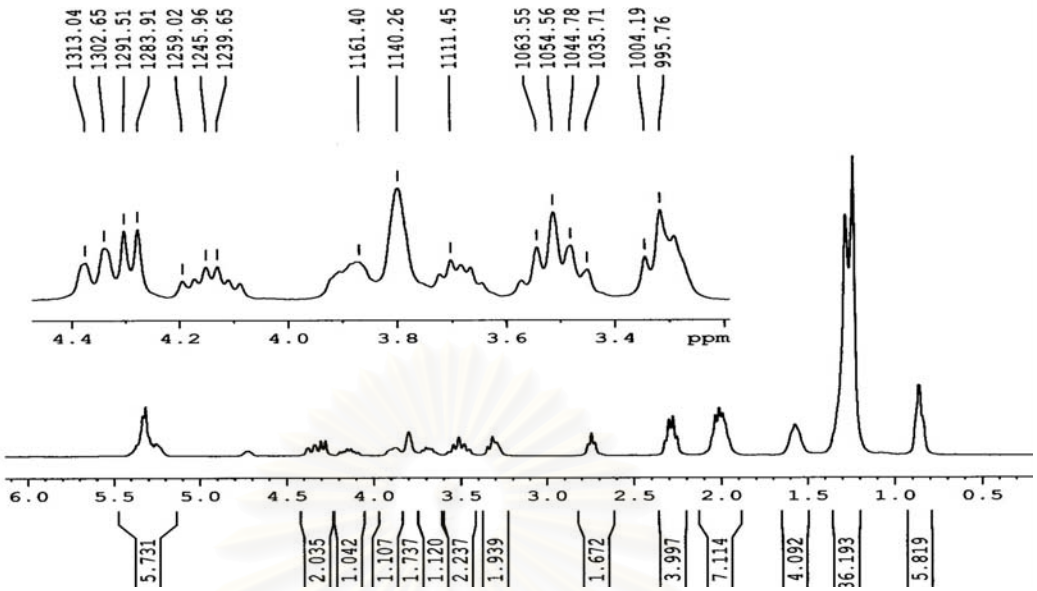

Figure 96. The 300 MHz ^{1}H-NMR spectrum of 1,2-di-*O*-linoleoyl-3-*O*-β-D-glucopyranosyl-*rac*-glycerol (**6h**) in $CDCl_3$.

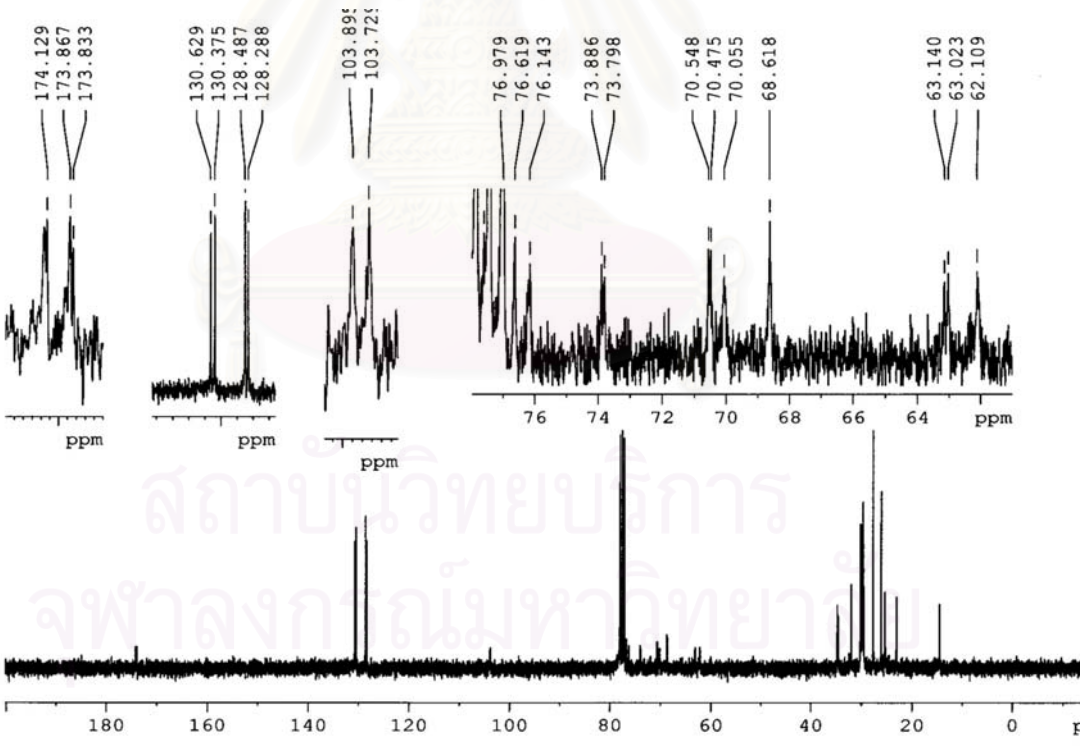

Figure 97. The 75 MHz ^{13}C-NMR spectrum of 1,2-di-*O*-linoleoyl-3-*O*-β-D-glucopyranosyl-*rac*-glycerol (**6h**) in $CDCl_3$.

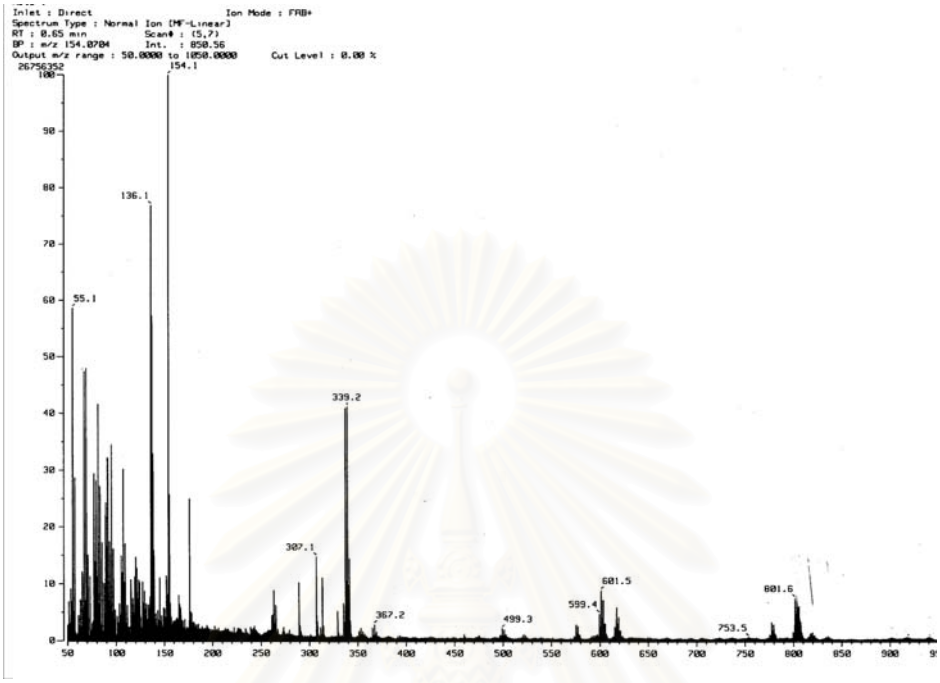

Figure 98. The positive ion FABMS of 1,2-di-*O*-linoleoyl-3-*O*-β-D-glucopyranosyl-*rac*-glycerol (**6h**).

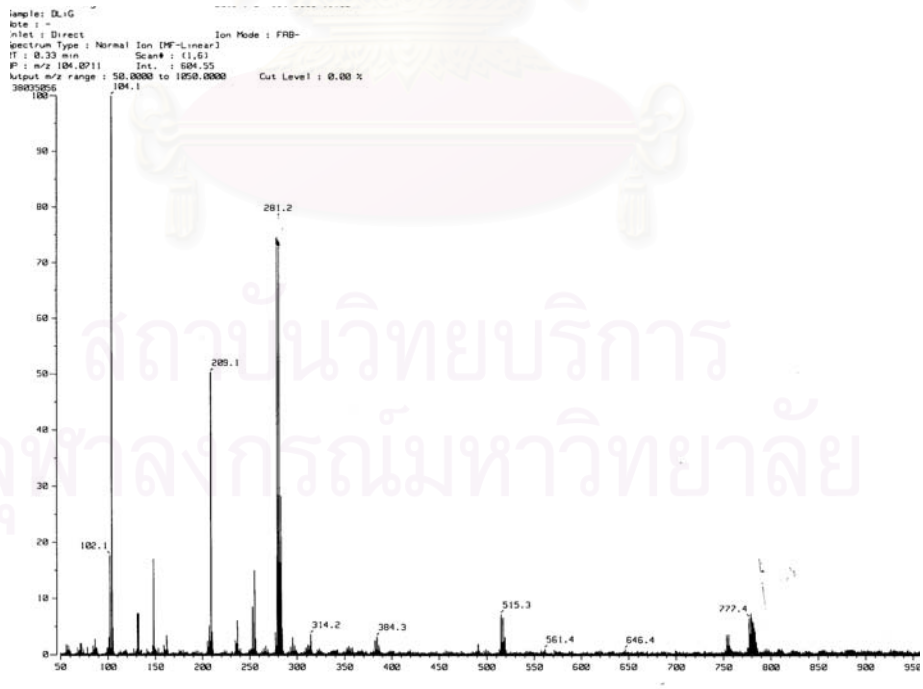

Figure 99. The negative ion FABMS of 1,2-di-*O*-linoleoyl-3-*O*-β-D-glucopyranosyl-*rac*-glycerol (**6h**).

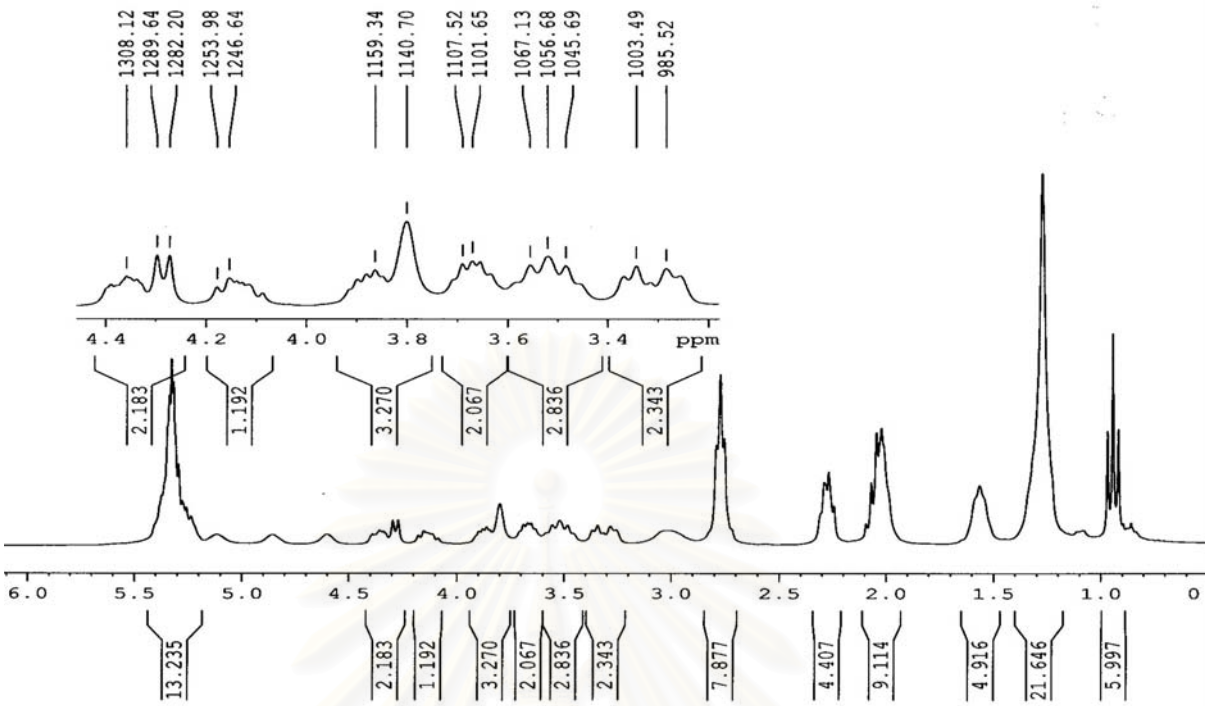

Figure 100. The 300 MHz ^{1}H-NMR spectrum of 1,2-di-*O*-linolenoyl-3-*O*-β-D-glucopyranosyl-*rac*-glycerol (**6i**) in $CDCl_3$.

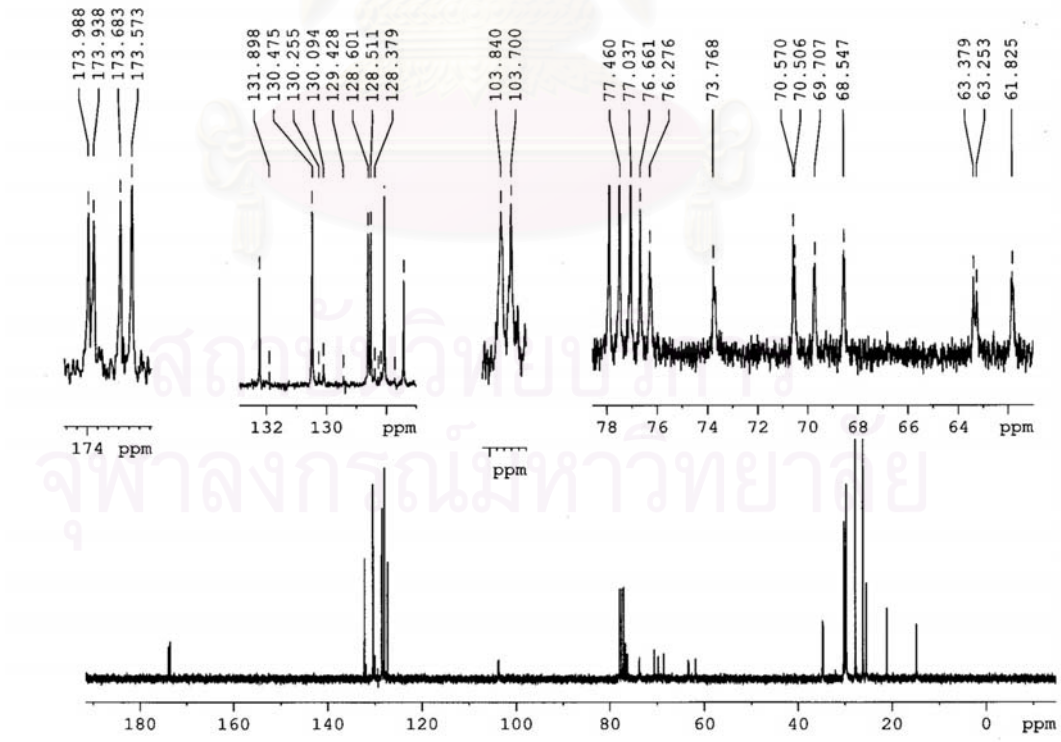

Figure 101. The 75 MHz ^{13}C-NMR spectrum of 1,2-di-*O*-linolenoyl-3-*O*-β-D-glucopyranosyl-*rac*-glycerol (**6i**) in $CDCl_3$.

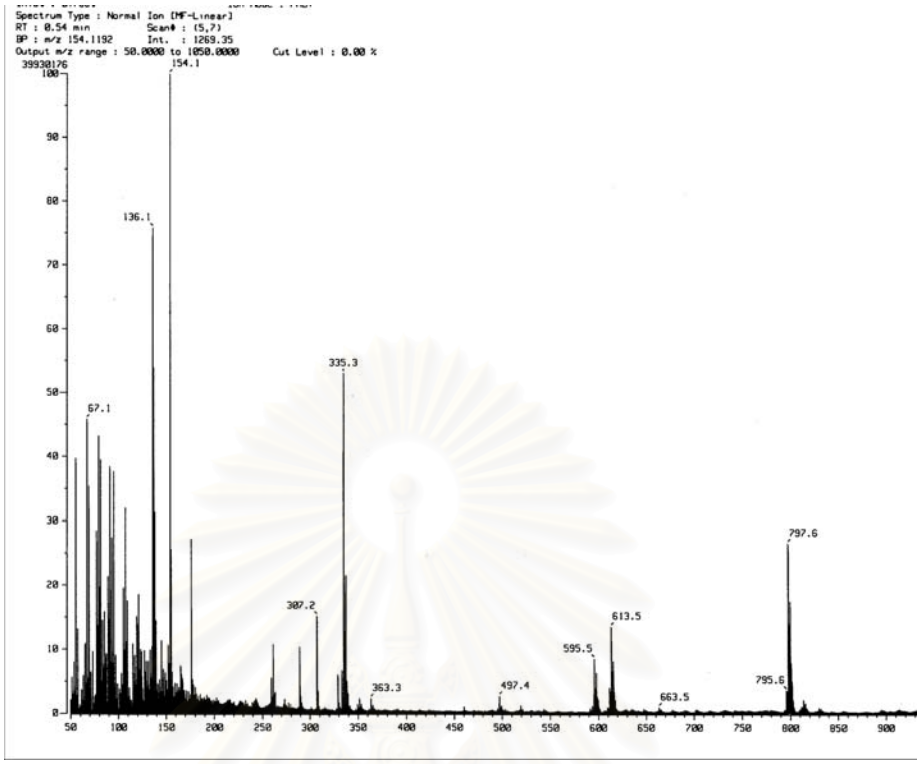

Figure 102. The positive ion FABMS of 1,2-di-*O*-linolenoyl-3-*O*-β-D-glucopyranosyl-*rac*-glycerol (**6i**).

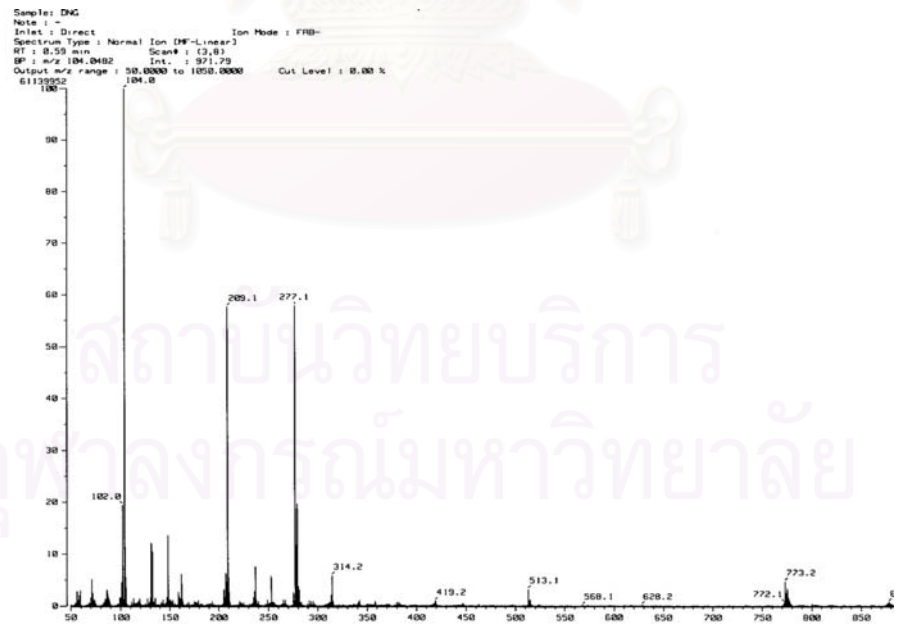

Figure 103. The negative ion FABMS of 1,2-di-*O*-linolenoyl-3-*O*-β-D-glucopyranosyl-*rac*-glycerol (**6i**).

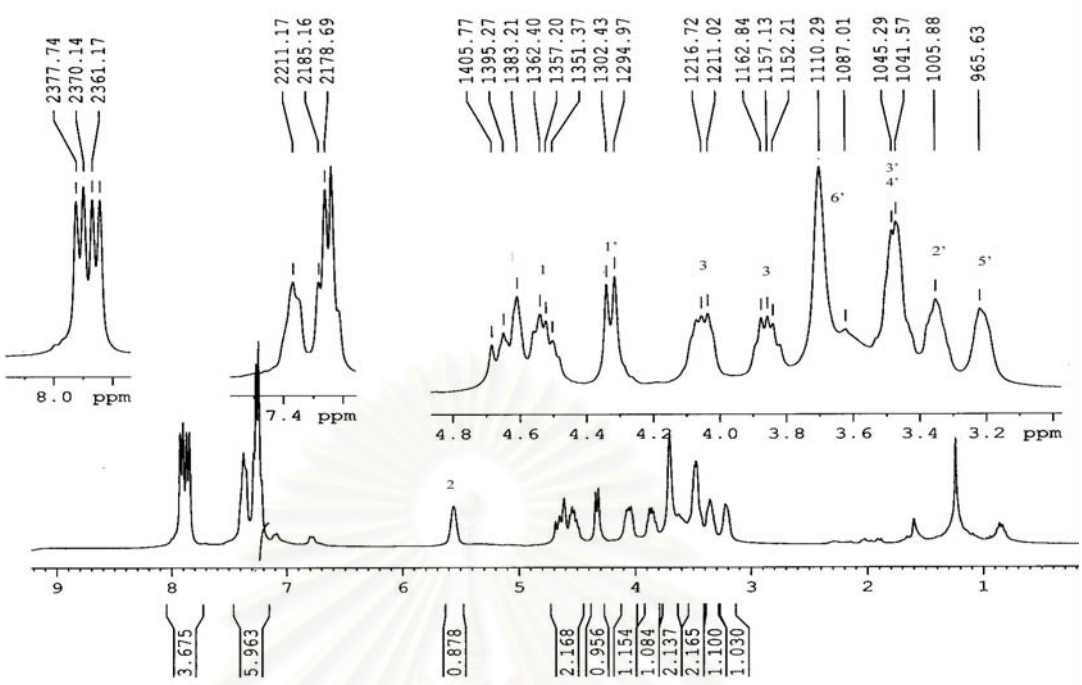

Figure 104. The 300 MHz ^{1}H-NMR spectrum of 1,2-di-*O*-benzoyl-3-*O*-β-D-glucopyranosyl-*rac*-glycerol (**6j**) in $CDCl_3$.

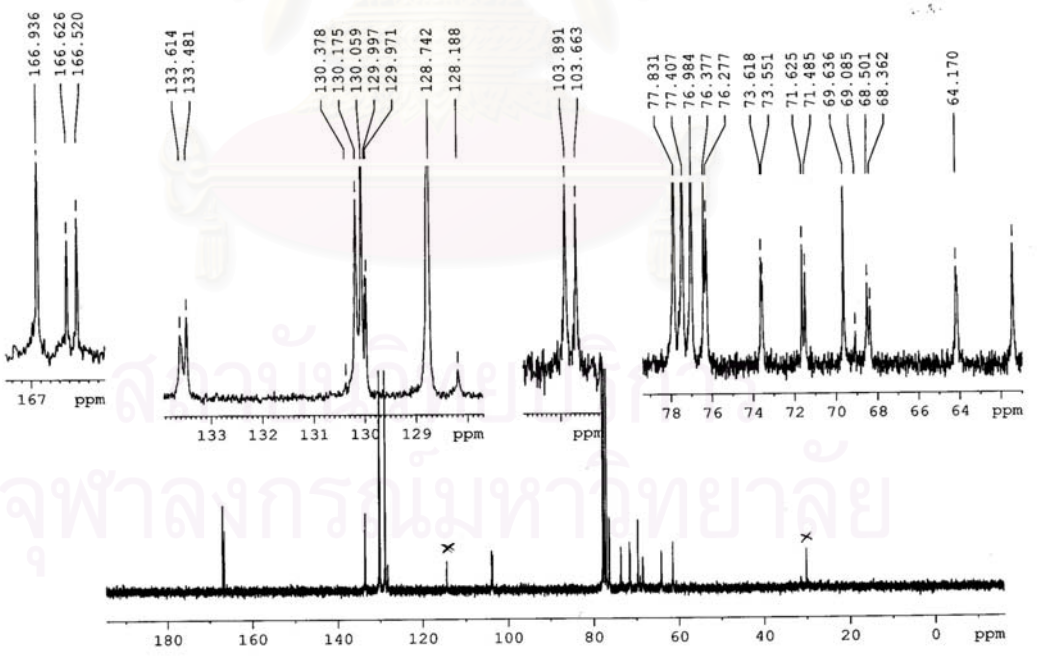

Figure 105. The 75 MHz ^{13}C-NMR spectrum of 1,2-di-*O*-benzoyl-3-*O*-β-D-glucopyranosyl-*rac*-glycerol (**6j**) in $CDCl_3$.

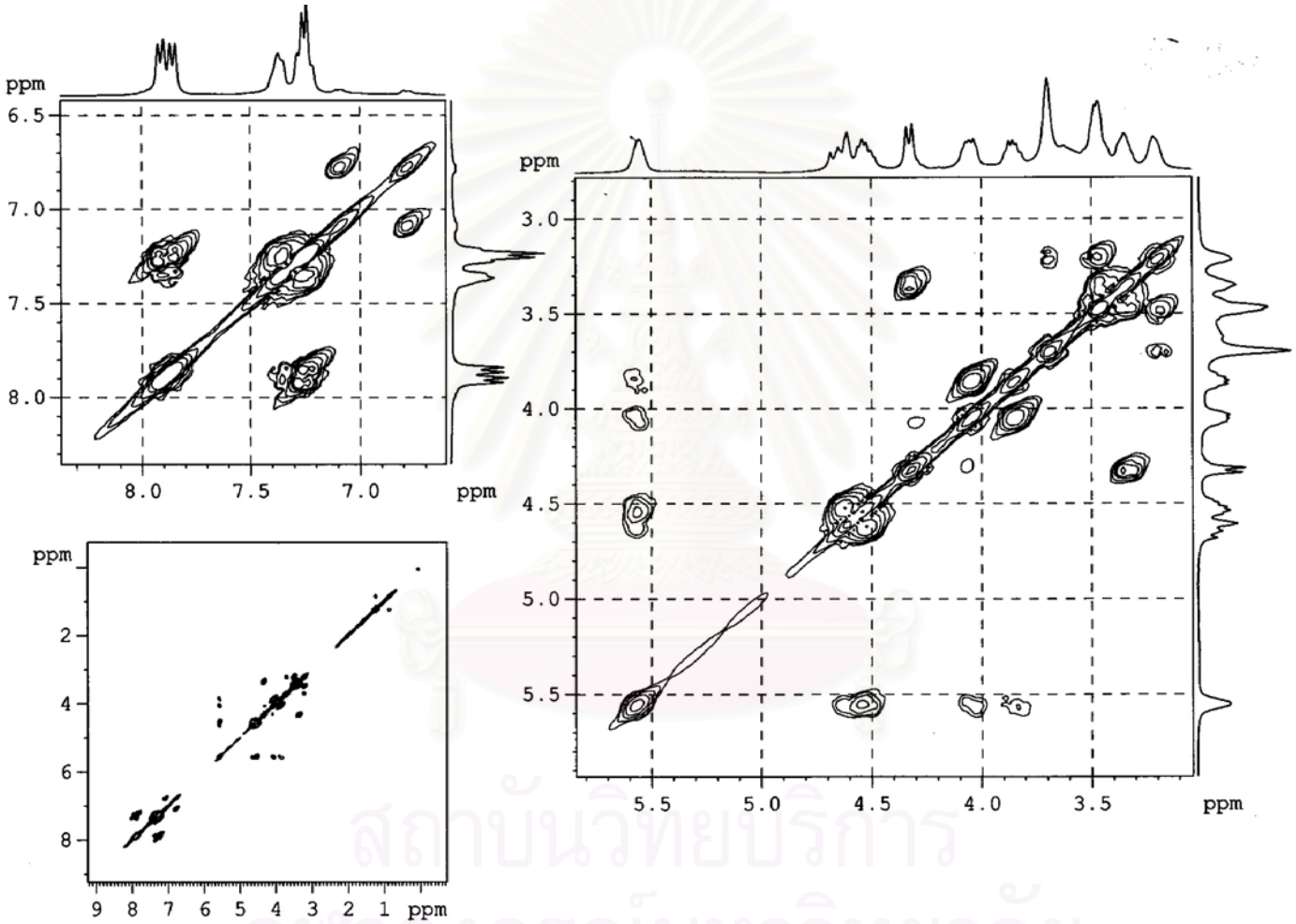

Figure 106. The ^{1}H-^{1}H COSY spectrum of 1,2-di-*O*-benzoyl-3-*O*-β-D-glucopyranosyl-*rac*-glycerol (**6j**) in $CDCl_3$.

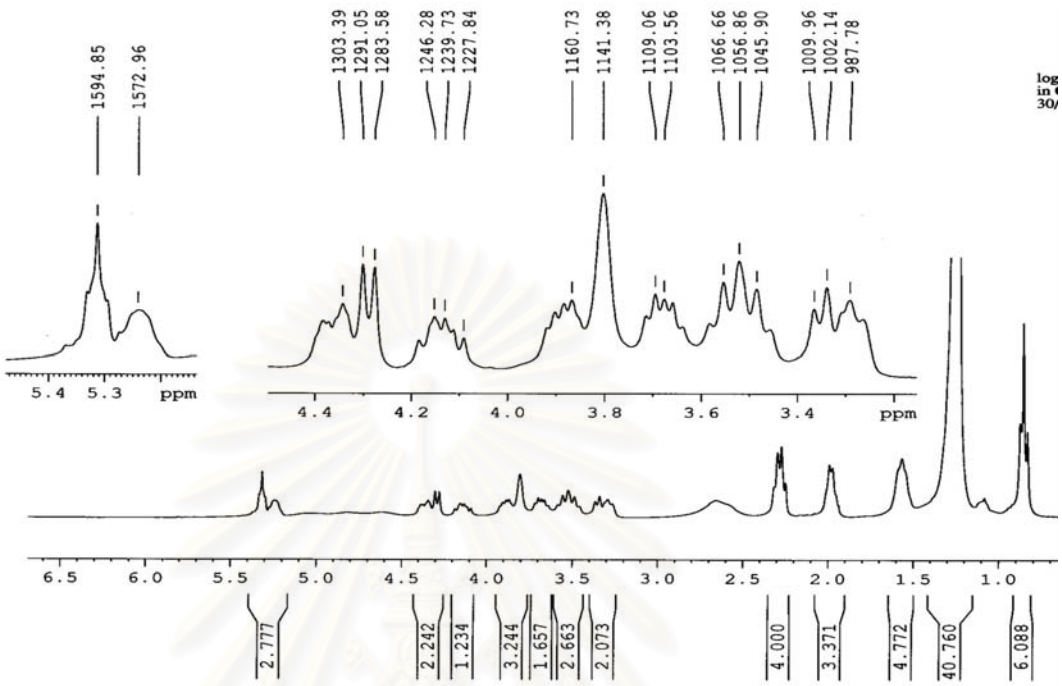

Figure 107. The 300 MHz ^{1}H-NMR spectrum of 1-*O*-lauroyl-2-*O*-oleoyl-3-*O*-β-D-glucopyranosyl-*rac*-glycerol (**6k**) in $CDCl_3$.

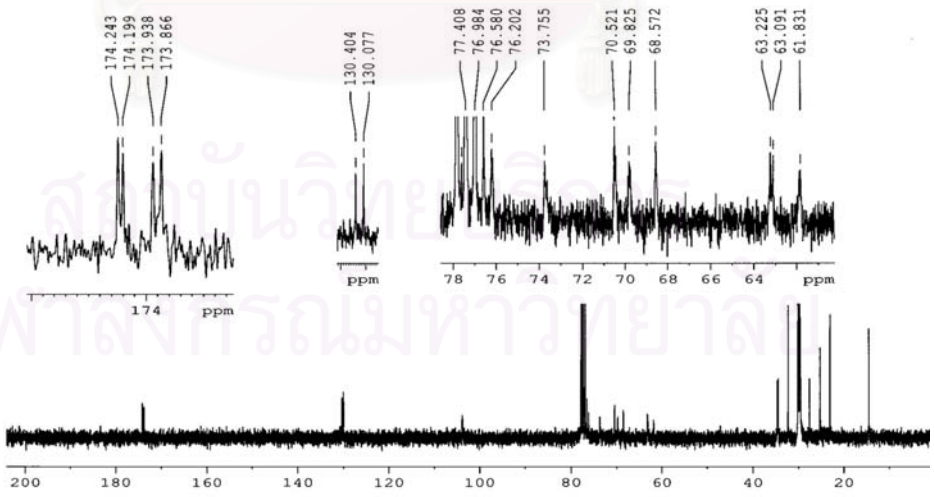

Figure 108. The 75 MHz ^{13}C-NMR spectrum of 1-*O*-lauroyl-2-*O*-oleoyl-3-*O*-β-D-glucopyranosyl-*rac*-glycerol (**6k**) in $CDCl_3$.

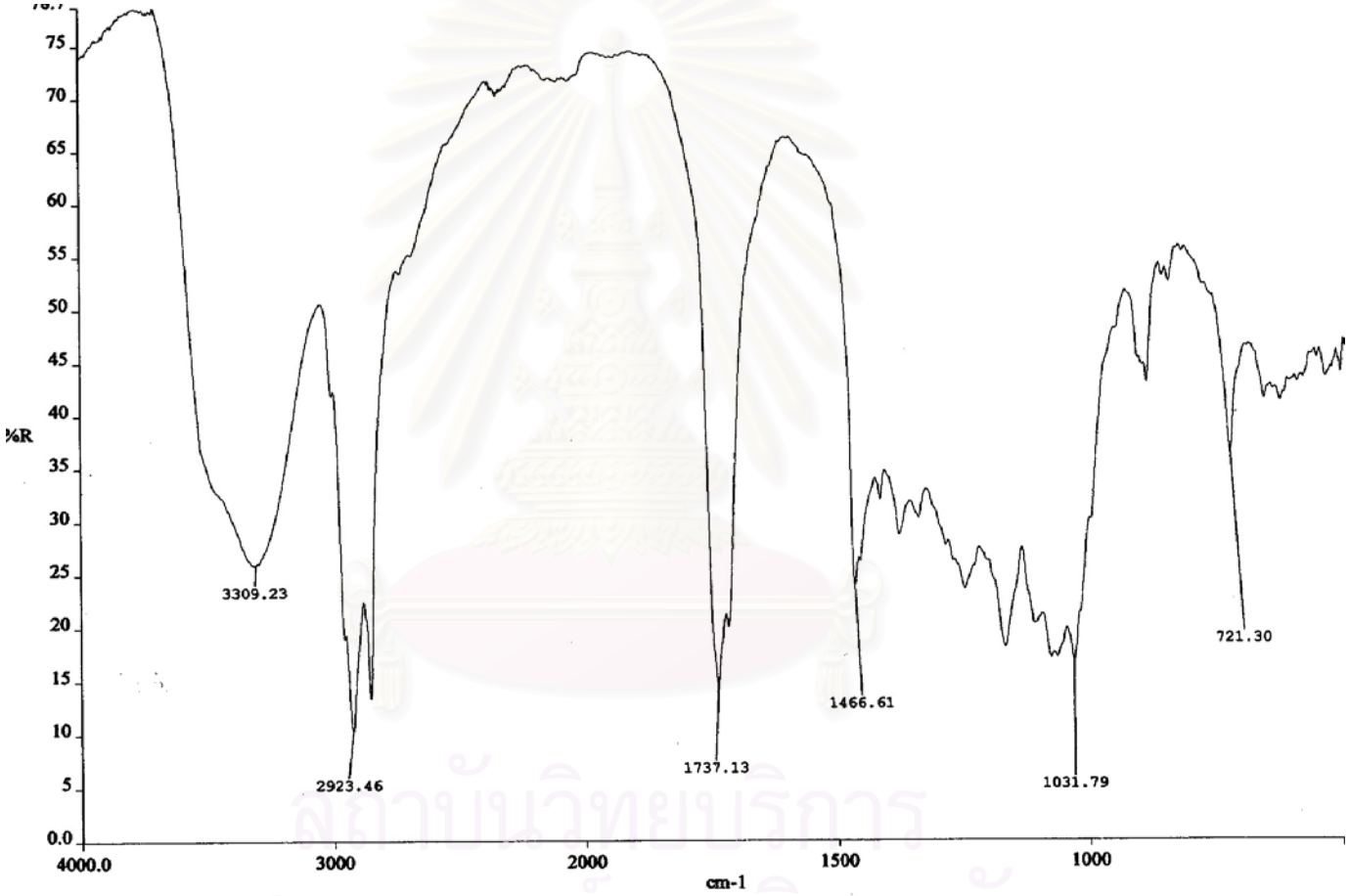

Figure 109. The infrared spectrum of 1-*O*-lauroyl-2-*O*-oleoyl-3-*O*-β-D-glucopyranosyl-*rac*-glycerol (**6k**).

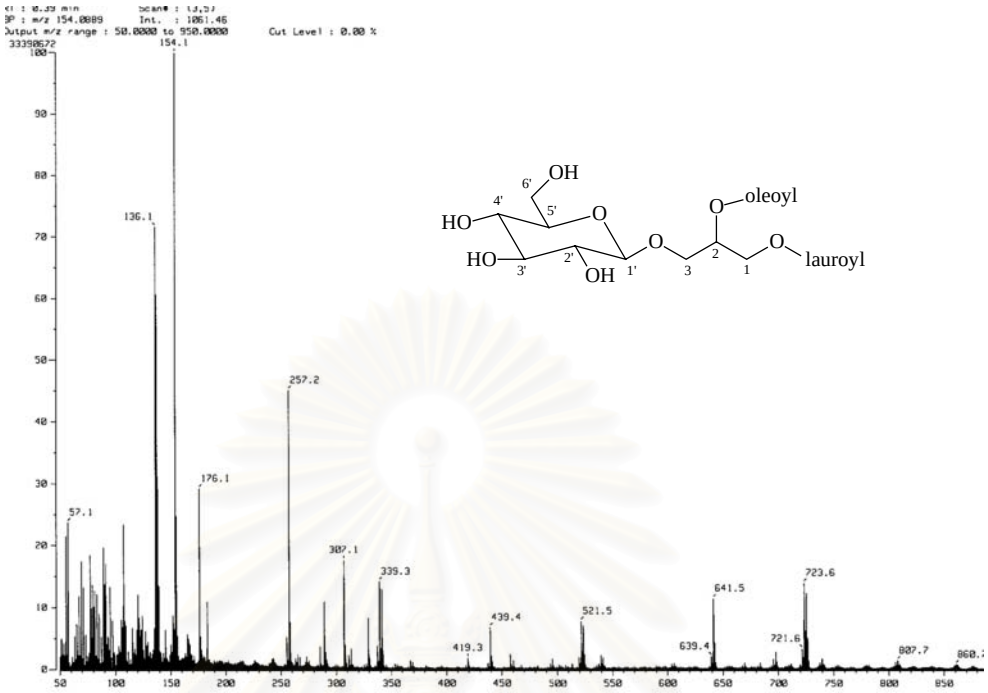

Figure 110. The positive ion FABMS of 1-*O*-lauroyl-2-*O*-oleoyl-3-*O*-β-D-glucopyranosyl-*rac*-glycerol (**6k**).

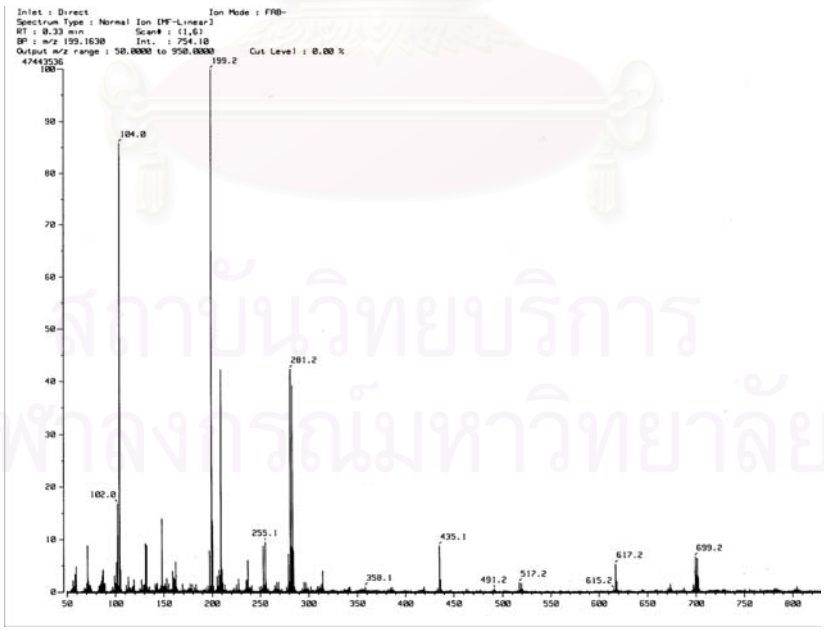

Figure 111. The negative ion FABMS of 1-*O*-lauroyl-2-*O*-oleoyl-3-*O*-β-D-glucopyranosyl-*rac*-glycerol (**6k**).

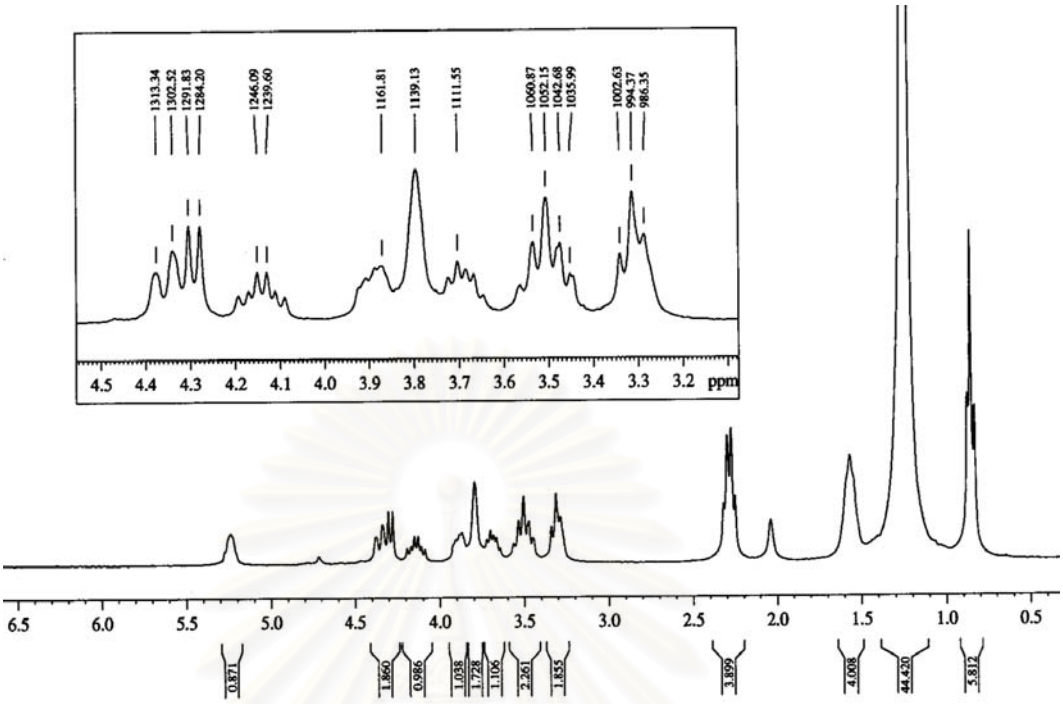

Figure 112. The 300 MHz ^{1}H-NMR spectrum of 1-*O*-stearoyl-2-*O*-lauroyl-3-*O*-β-D-glucopyranosyl-*rac*-glycerol (**6l**) in $CDCl_3$.

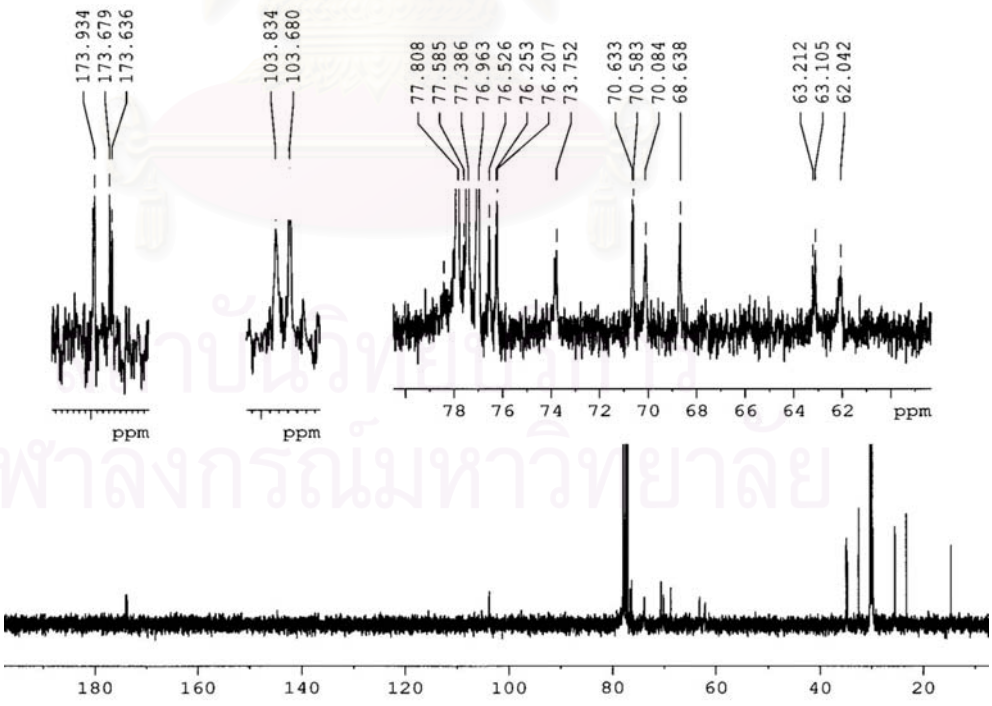

Figure 113. The 75 MHz ^{13}C-NMR spectrum of 1-*O*-stearoyl-2-*O*-lauroyl-3-*O*-β-D-glucopyranosyl-*rac*-glycerol (**6l**) in $CDCl_3$.

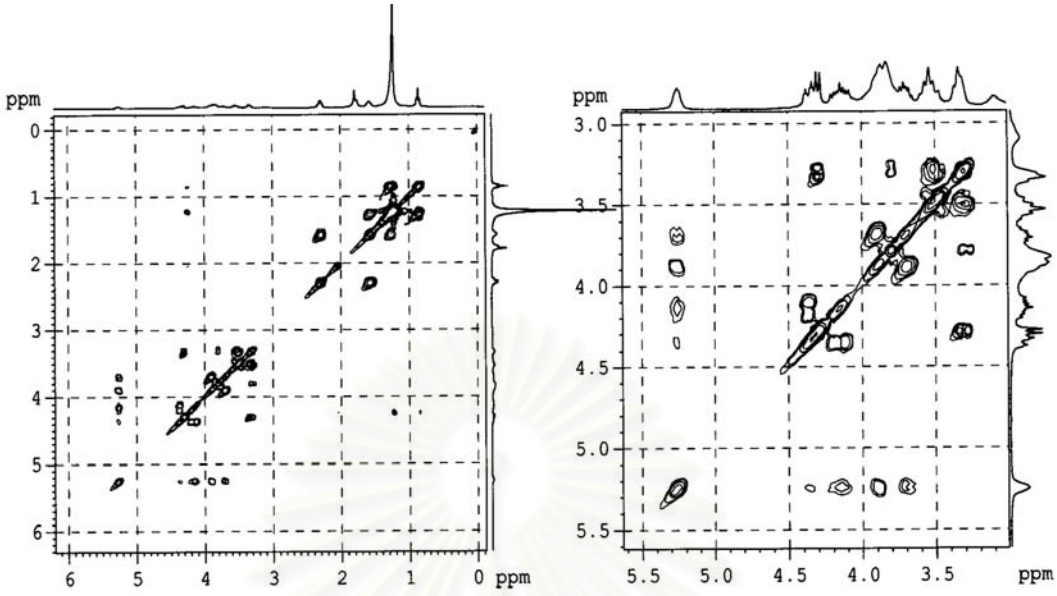

Figure 114. The ^{1}H-^{1}H COSY spectrum of 1-*O*-stearoyl-2-*O*-lauroyl-3-*O*-β-D-glucopyranosyl-*rac*-glycerol (**6l**) in $CDCl_3$.

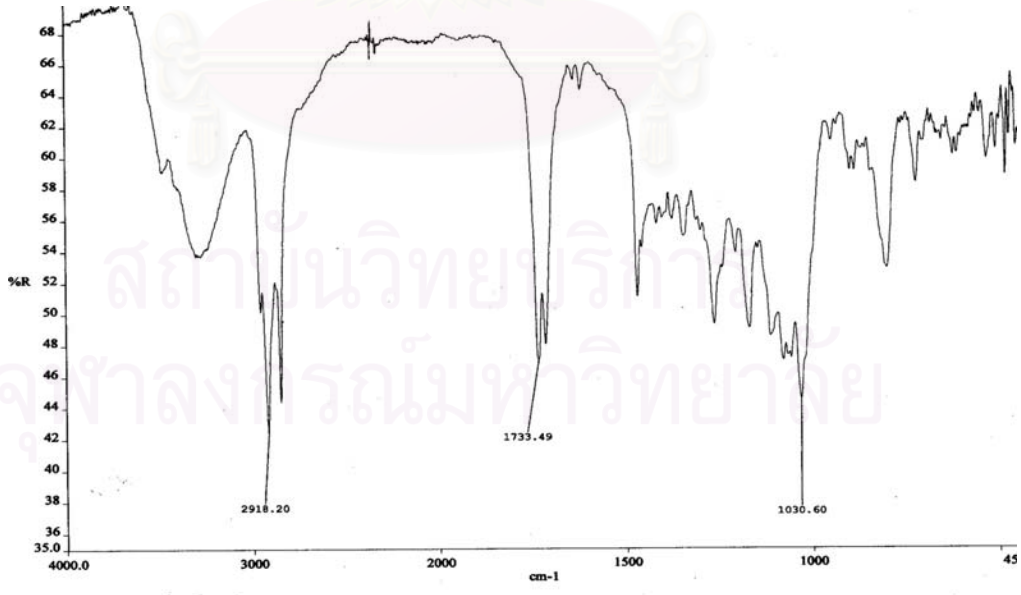

Figure 115. The infrared spectrum of 1-*O*-stearoyl-2-*O*-lauroyl-3-*O*-β-D-glucopyranosyl-*rac*-glycerol (**6l**).

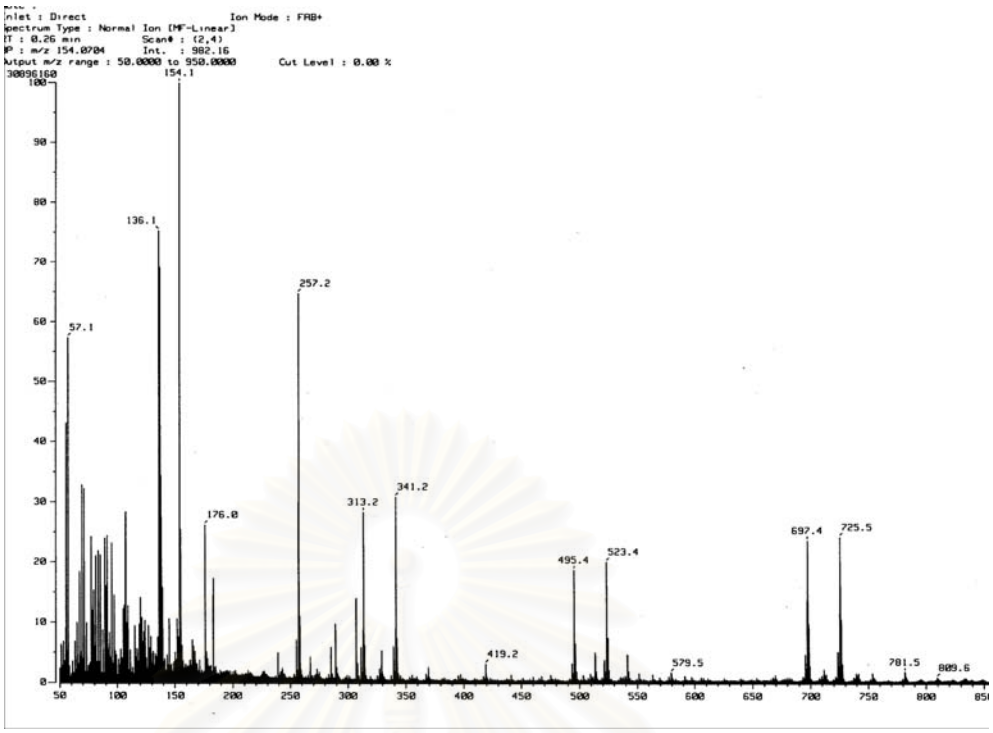

Figure 116. The positive ion FABMS of 1-*O*-stearoyl-2-*O*-lauroyl-3-*O*-β-D-glucopyranosyl-*rac*-glycerol (**6l**).

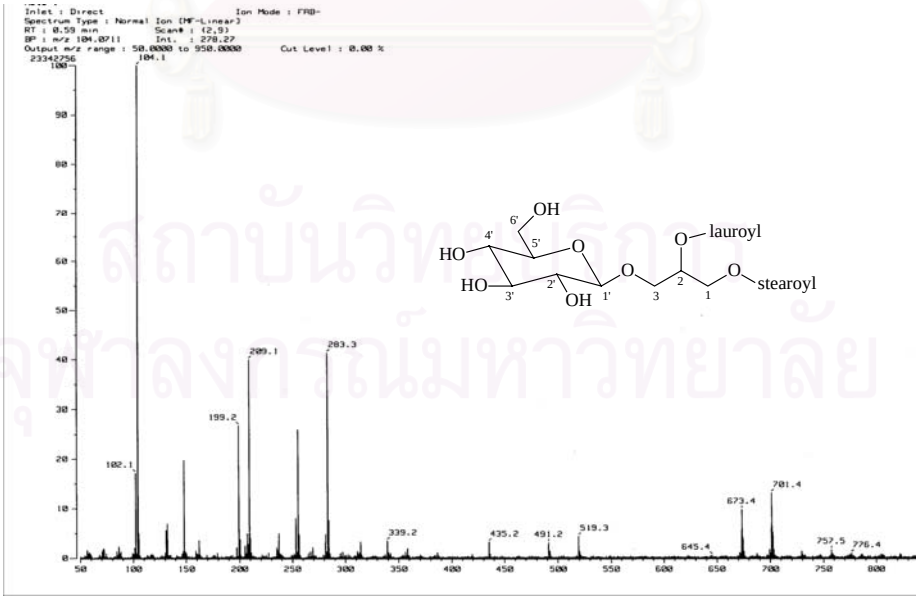

Figure 117. The negative ion FABMS of 1-*O*-stearoyl-2-*O*-lauroyl-3-*O*-β-D-glucopyranosyl-*rac*-glycerol (**6l**).

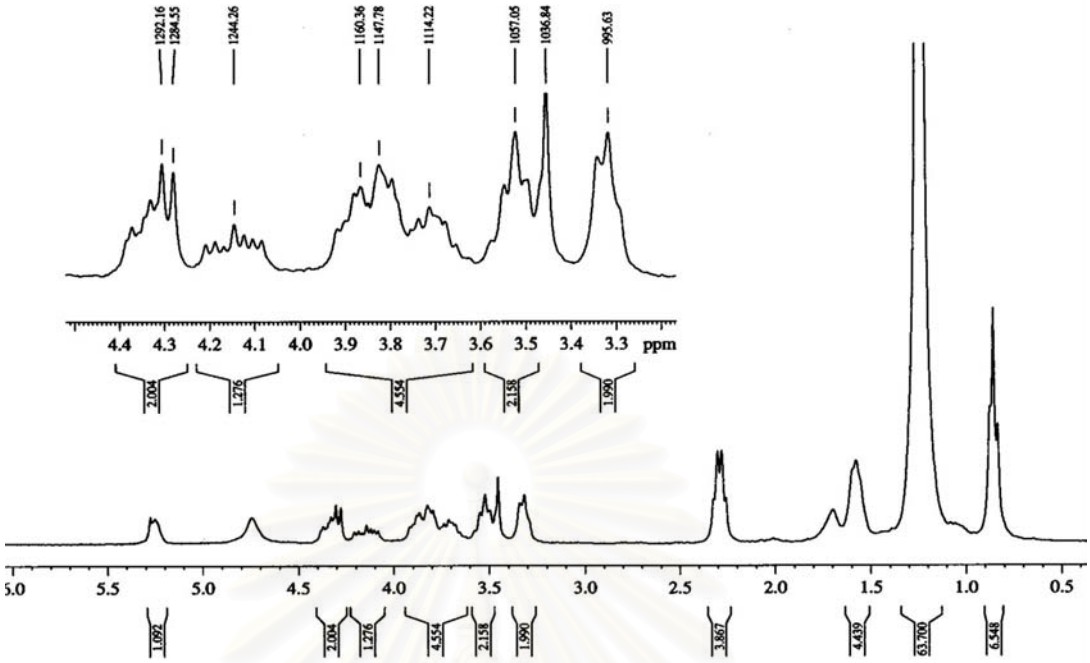

Figure 118. The 300 MHz ^{1}H-NMR spectrum of 1-*O*-stearoyl-2-*O*-behenoyl-3-*O*-β-D-glucopyranosyl-*rac*-glycerol (**6m**) in $CDCl_3$.

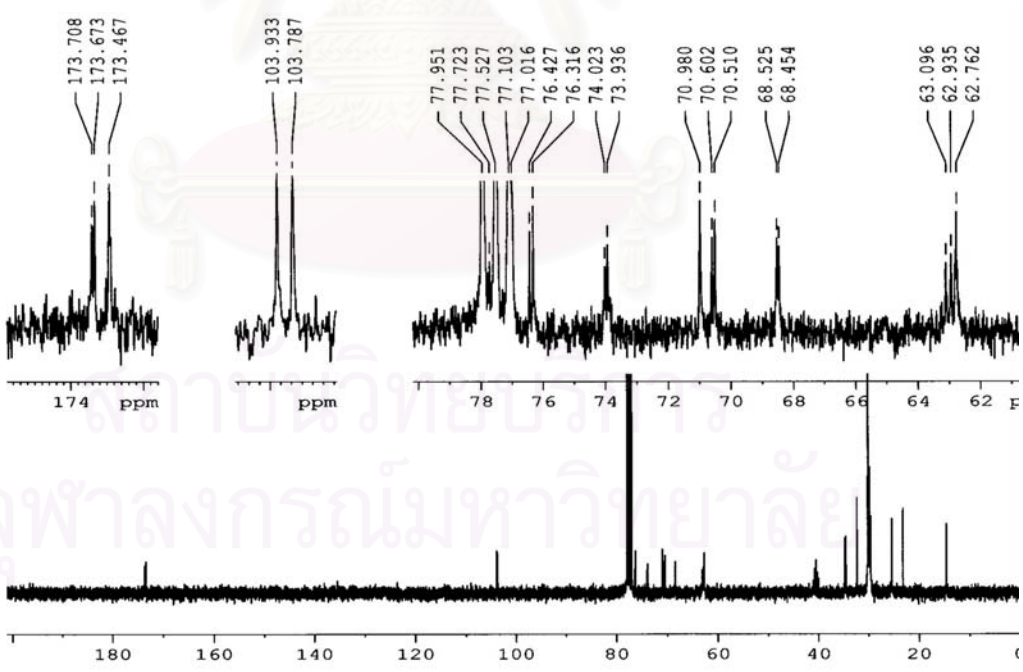

Figure 119. The 75 MHz ^{13}C-NMR spectrum of 1-*O*-stearoyl-2-*O*-behenoyl-3-*O*-β-D-glucopyranosyl-*rac*-glycerol (**6m**) in $CDCl_3$.

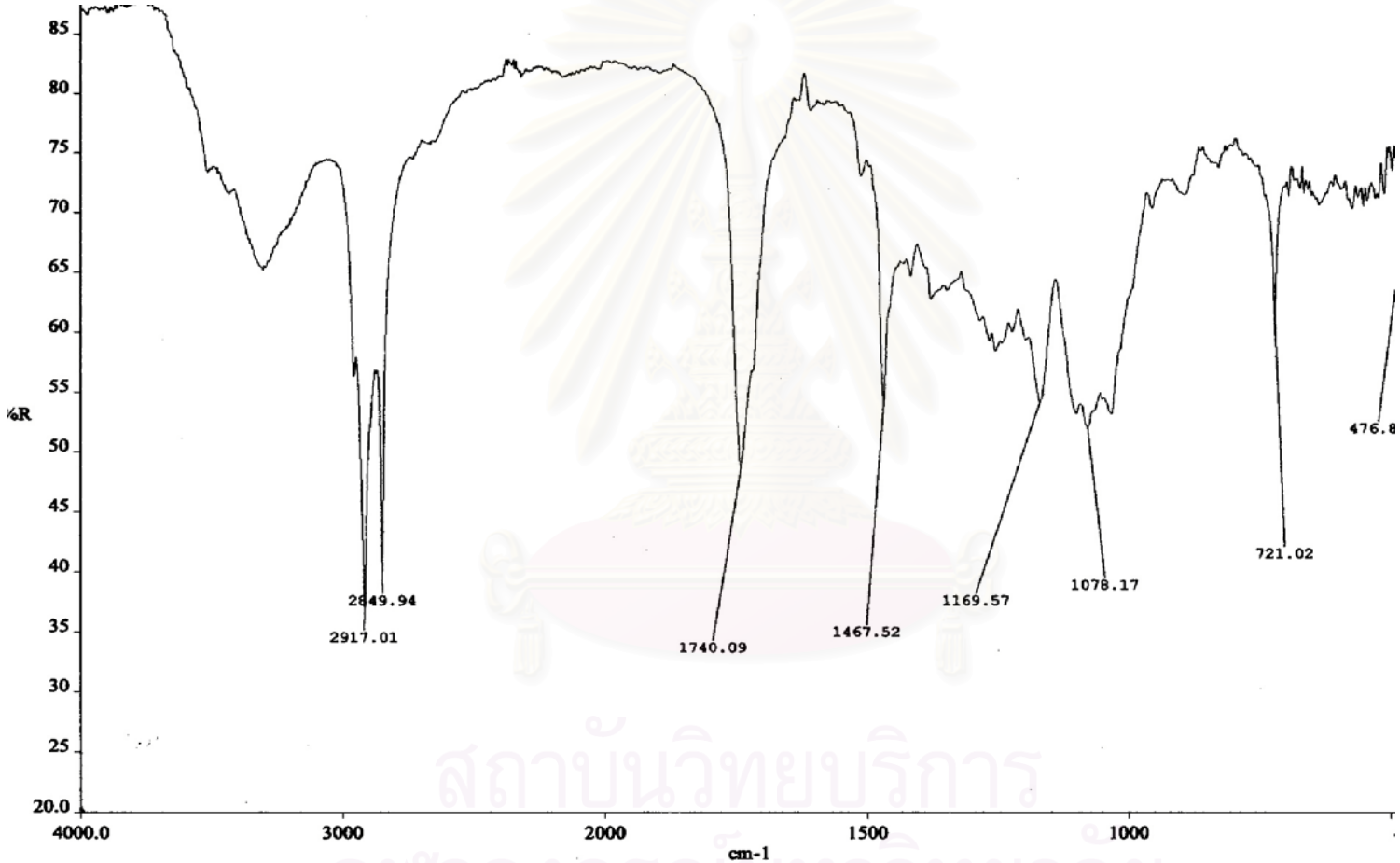

Figure 120. The infrared spectrum of 1-*O*-stearoyl-2-*O*-behenoyl-3-*O*-β-D-glucopyranosyl-*rac*-glycerol (**6m**).

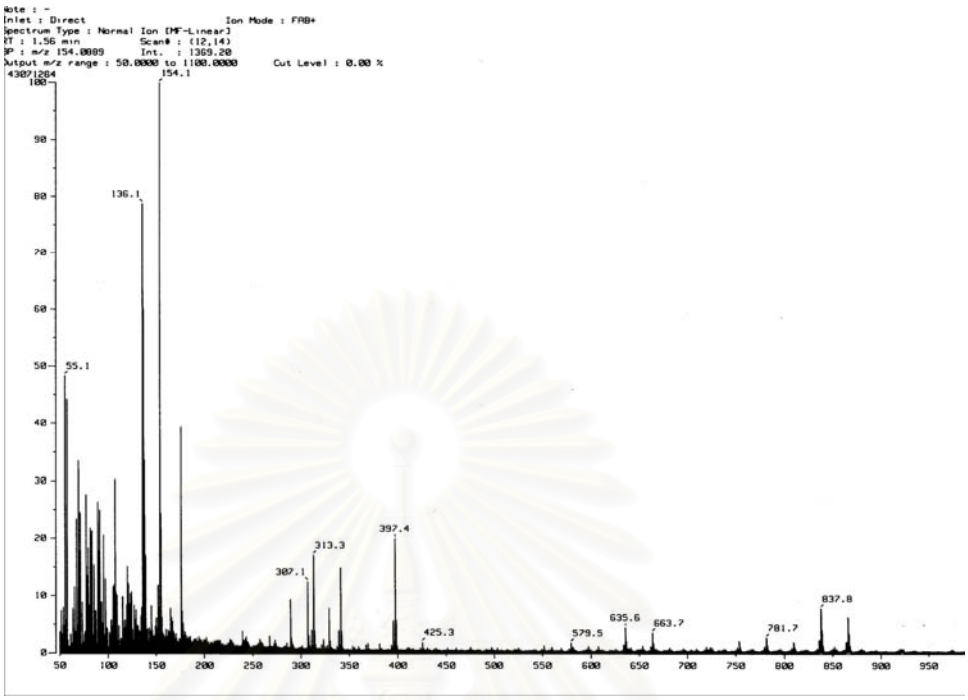

Figure 122. The negative ion FABMS of 1-*O*-stearoyl-2-*O*-behenoyl-3-*O*-β-D-glucopyranosyl-*rac*-glycerol (**6m**).

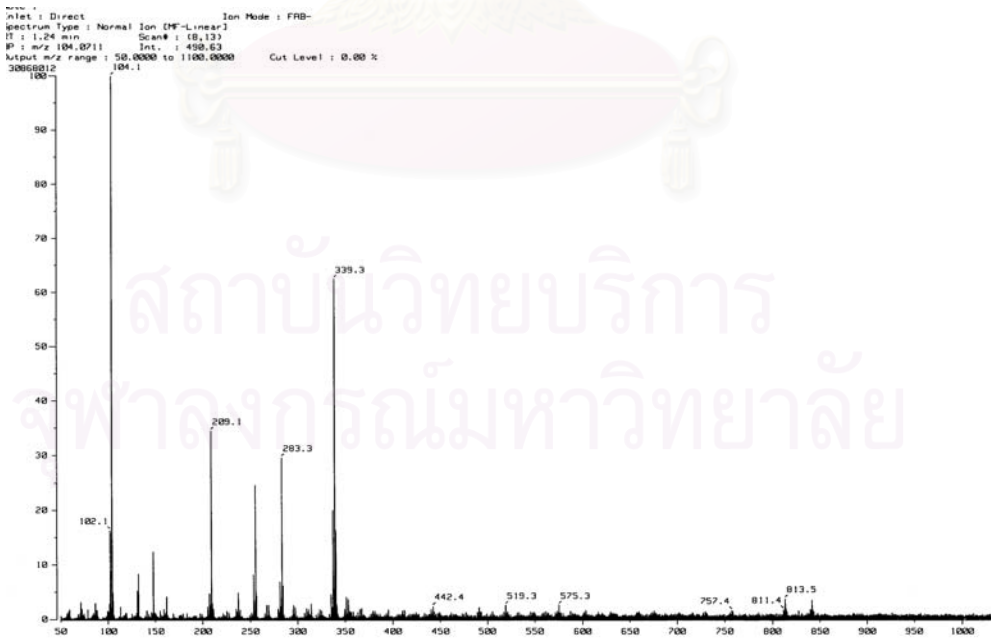

Figure 121. The positive ion FABMS of 1-*O*-stearoyl-2-*O*-behenoyl-3-*O*-β-D-glucopyranosyl-*rac*-glycerol (**6m**).

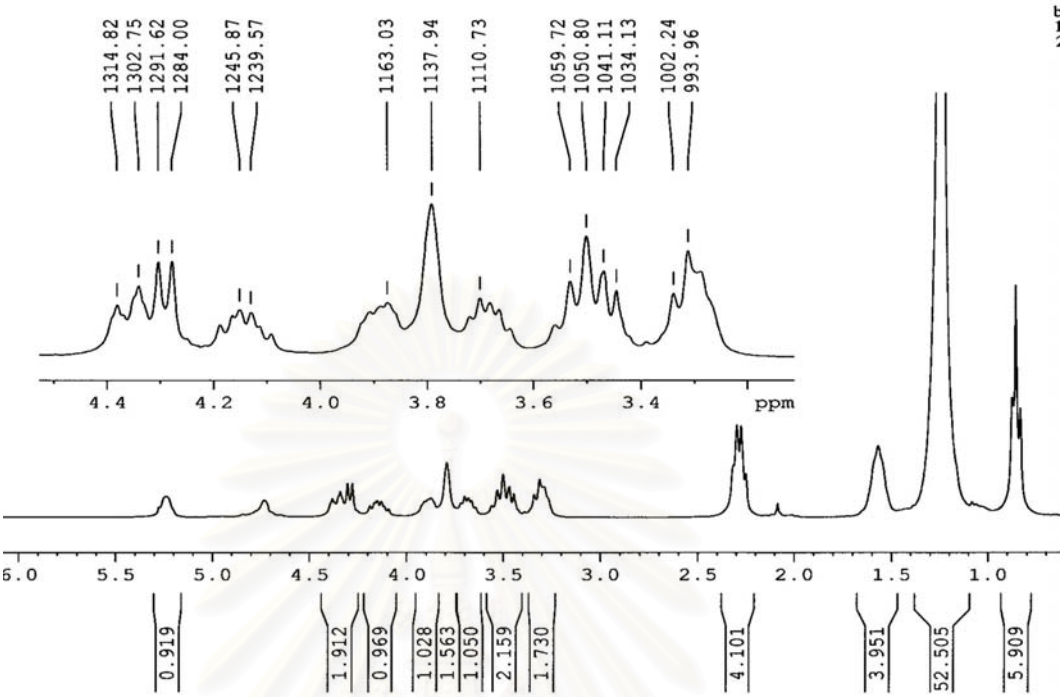

Figure 123. The 300 MHz ^{1}H-NMR spectrum of 1-*O*-behenoyl-2-*O*-lauroyl-3-*O*-β-D-glucopyranosyl-*rac*-glycerol (**6n**) in $CDCl_3$.

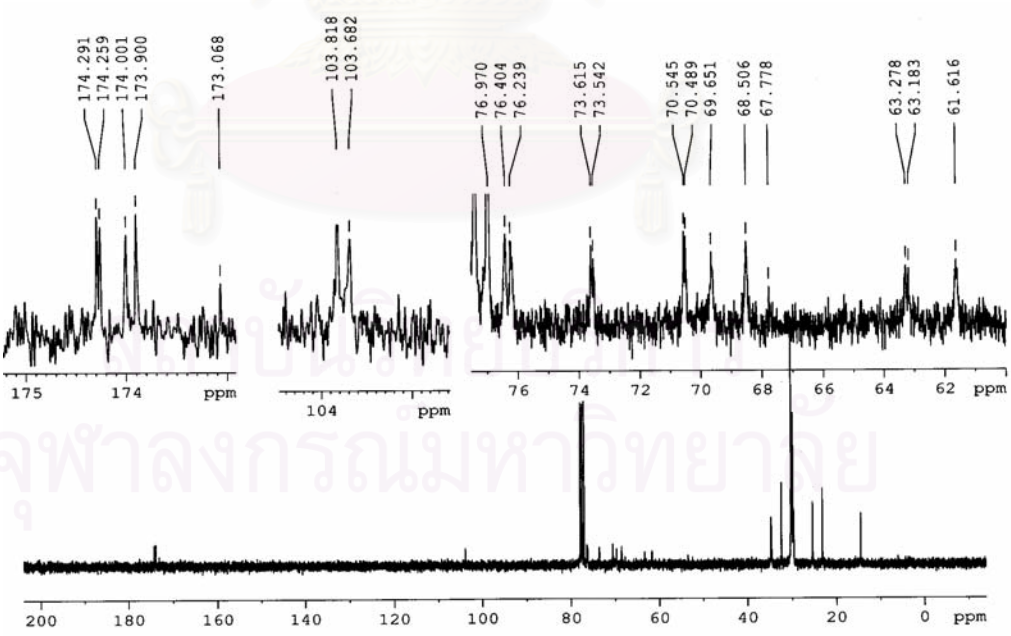

Figure 124. The 75 MHz ^{13}C-NMR spectrum of 1-*O*-behenoyl-2-*O*-lauroyl-3-*O*-β-D-glucopyranosyl-*rac*-glycerol (**6n**) in $CDCl_3$.

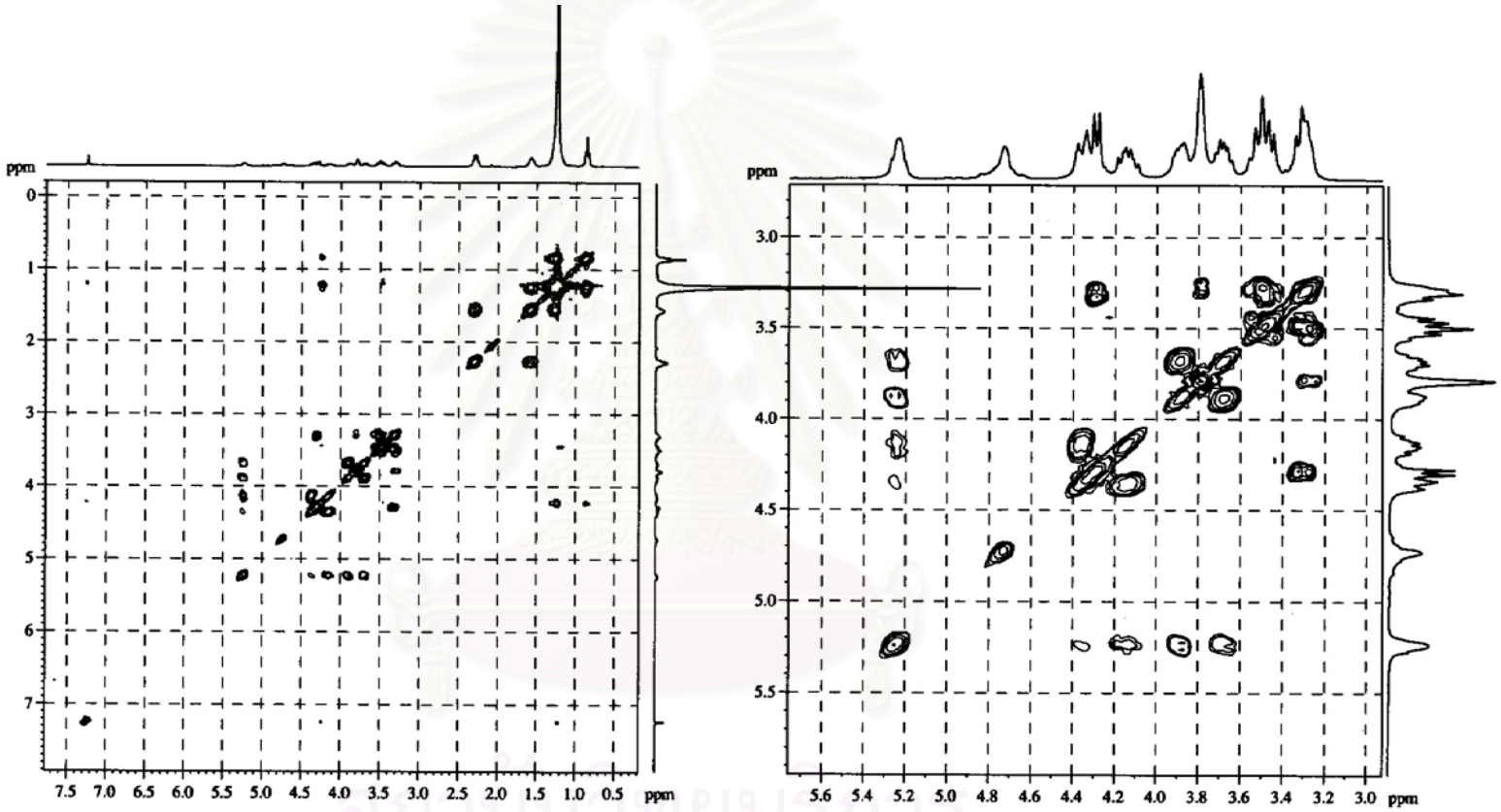

Figure 125. The ^{1}H-^{1}H COSY spectrum of 1-*O*-behenoyl-2-*O*-lauroyl-3-*O*-β-D-glucopyranosyl-*rac*-glycerol (**6n**) in $CDCl_3$.

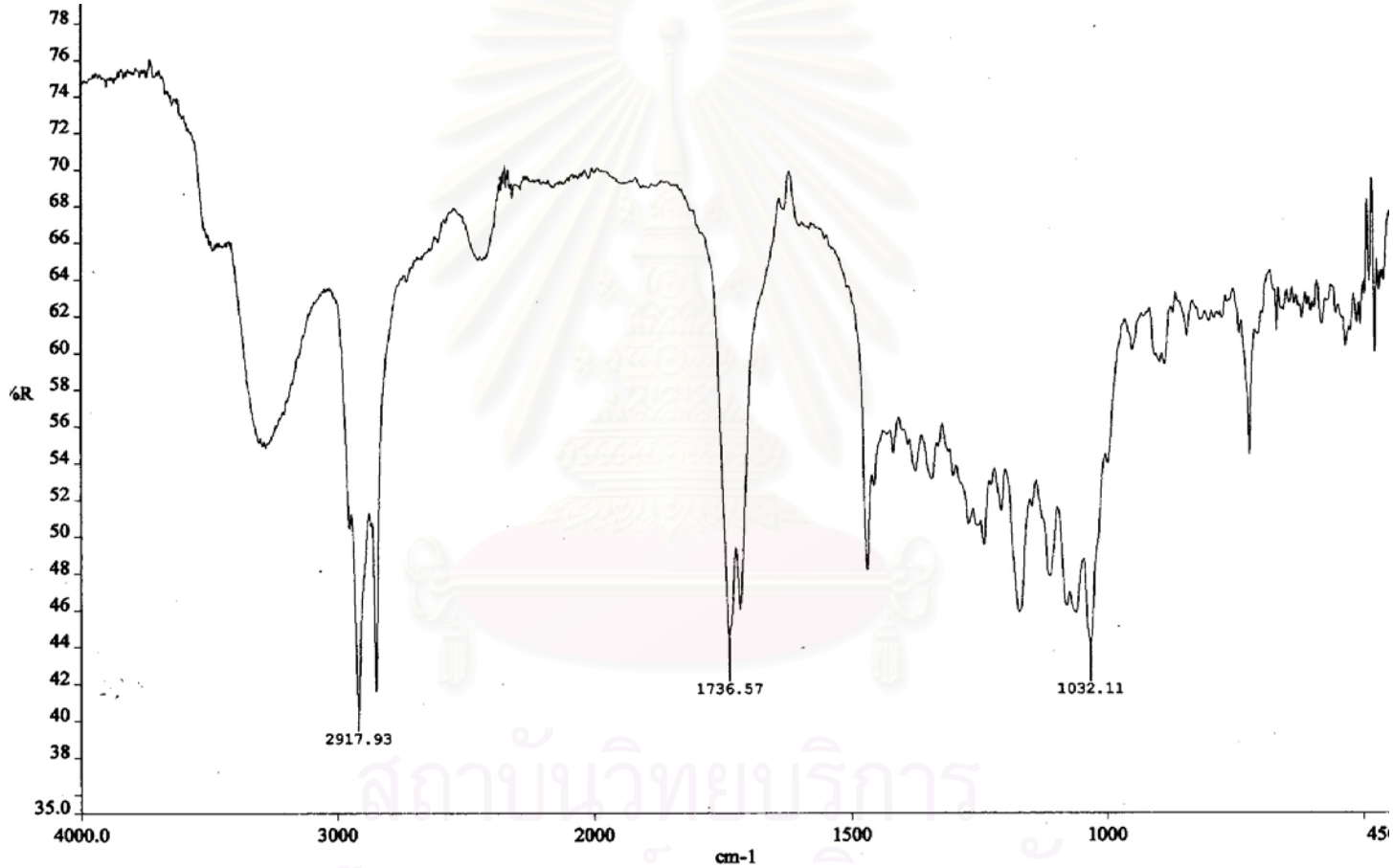

Figure 126. The infrared spectrum of 1-*O*-behenoyl-2-*O*-lauroyl-3-*O*-β-D-glucopyranosyl-*rac*-glycerol (**6n**).

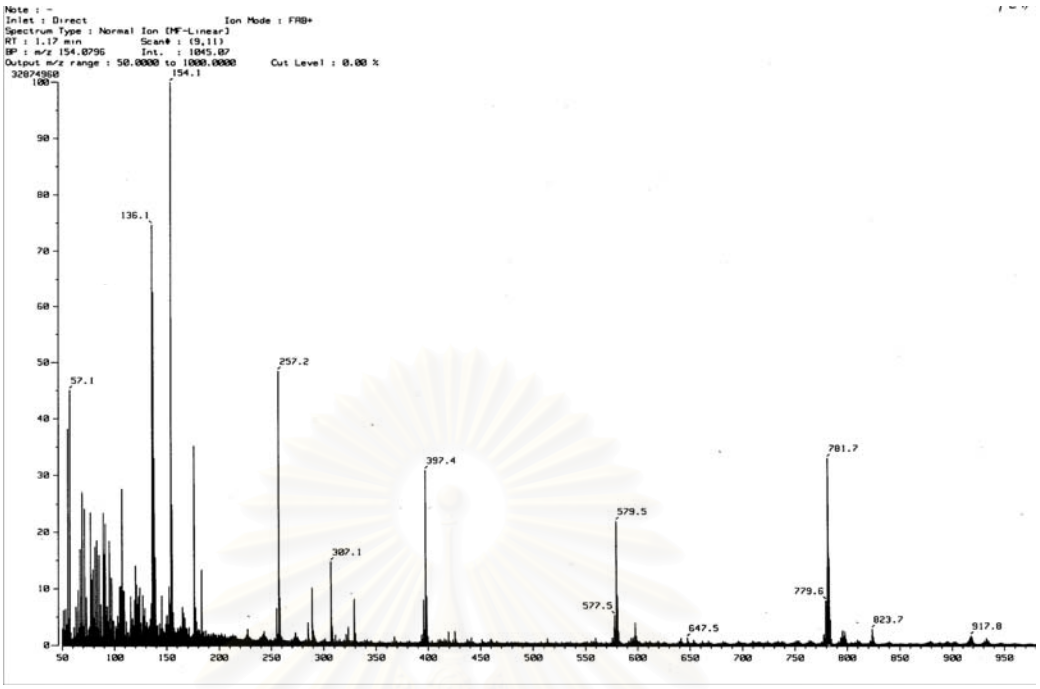

Figure 127. The positive ion FABMS of 1-*O*-behenoyl-2-*O*-lauroyl-3-*O*-β-D-glucopyranosyl-*rac*-glycerol (**6n**).

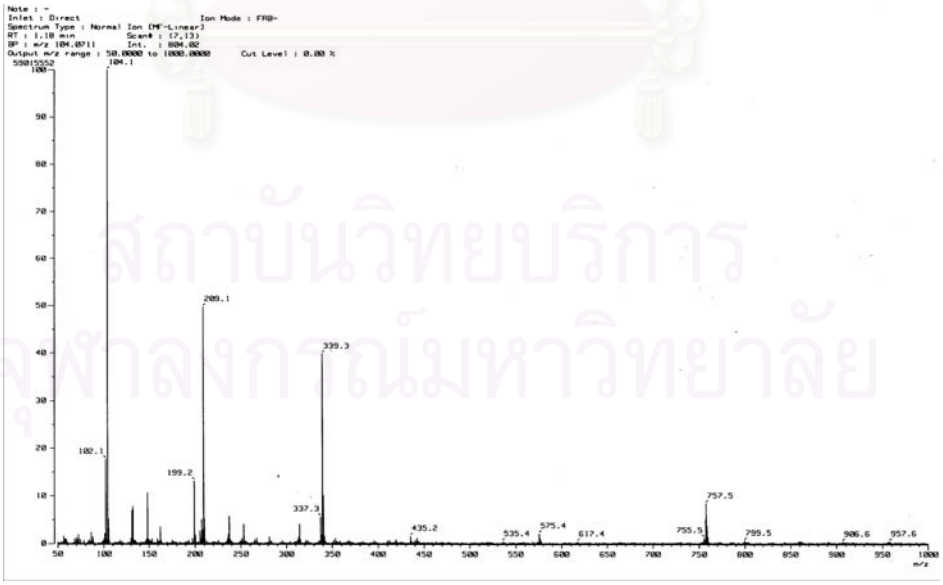

Figure 128. The negative ion FABMS of 1-*O*-behenoyl-2-*O*-lauroyl-3-*O*-β-D-glucopyranosyl-*rac*-glycerol (**6n**).

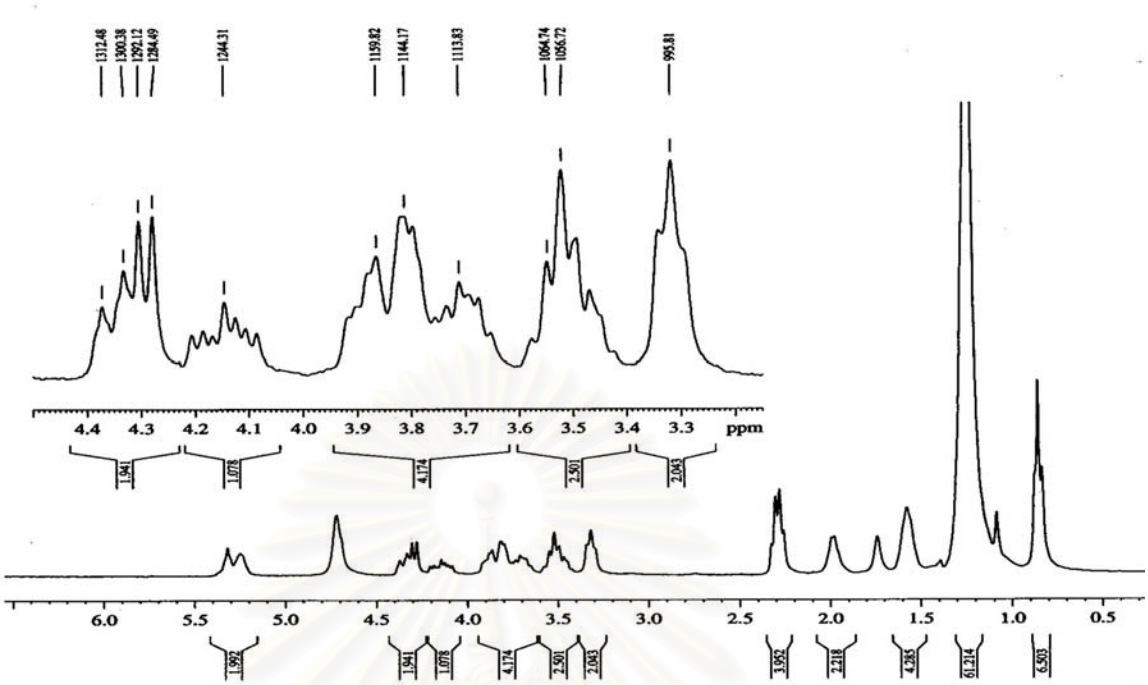

Figure 129. The 300 MHz ^{1}H-NMR spectrum of 1-*O*-behenoyl-2-*O*-oleoyl-3-*O*-β-D-glucopyranosyl-*rac*-glycerol (**6o**) in $CDCl_3$.

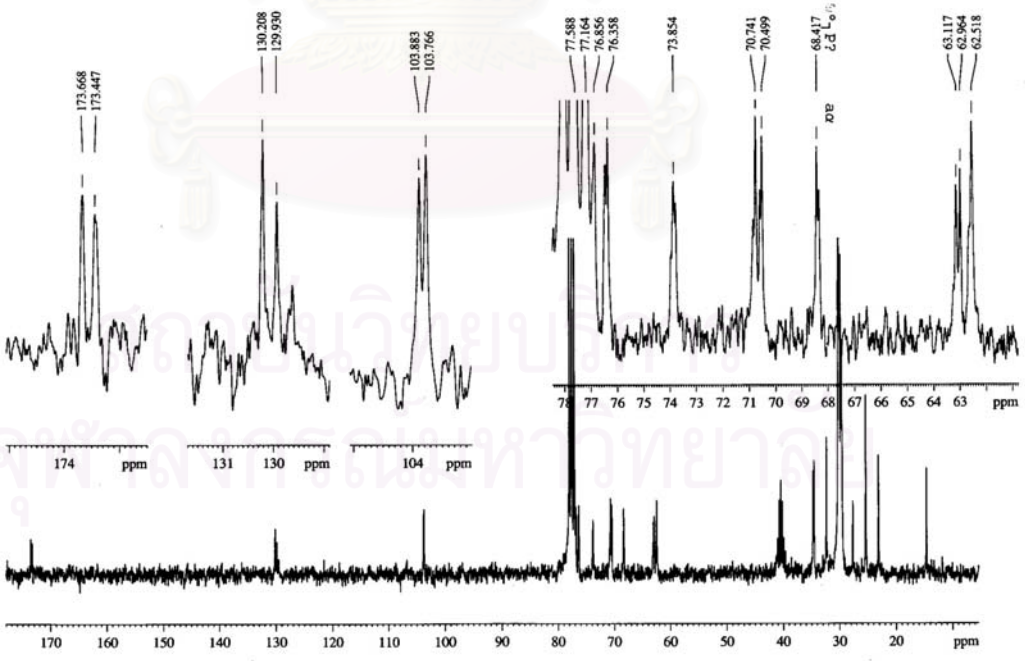

Figure 130. The 75 MHz ^{13}C-NMR spectrum of 1-*O*-behenoyl-2-*O*-oleoyl-3-*O*-β-D-glucopyranosyl-*rac*-glycerol (**6o**) in $CDCl_3$.

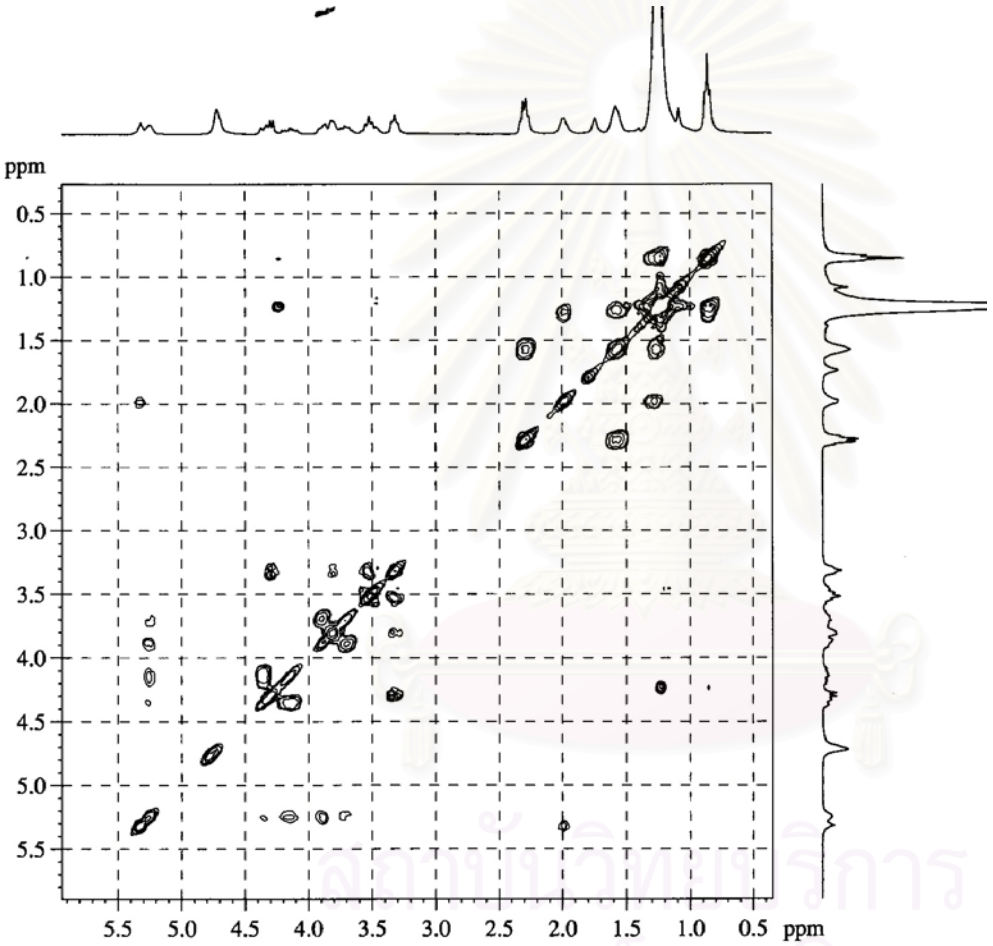

Figure 131. The ^{1}H-^{1}H COSY spectrum of 1-*O*-behenoyl-2-*O*-oleoyl-3-*O*-β-D-glucopyranosyl-*rac*-glycerol (**6o**) in $CDCl_3$.

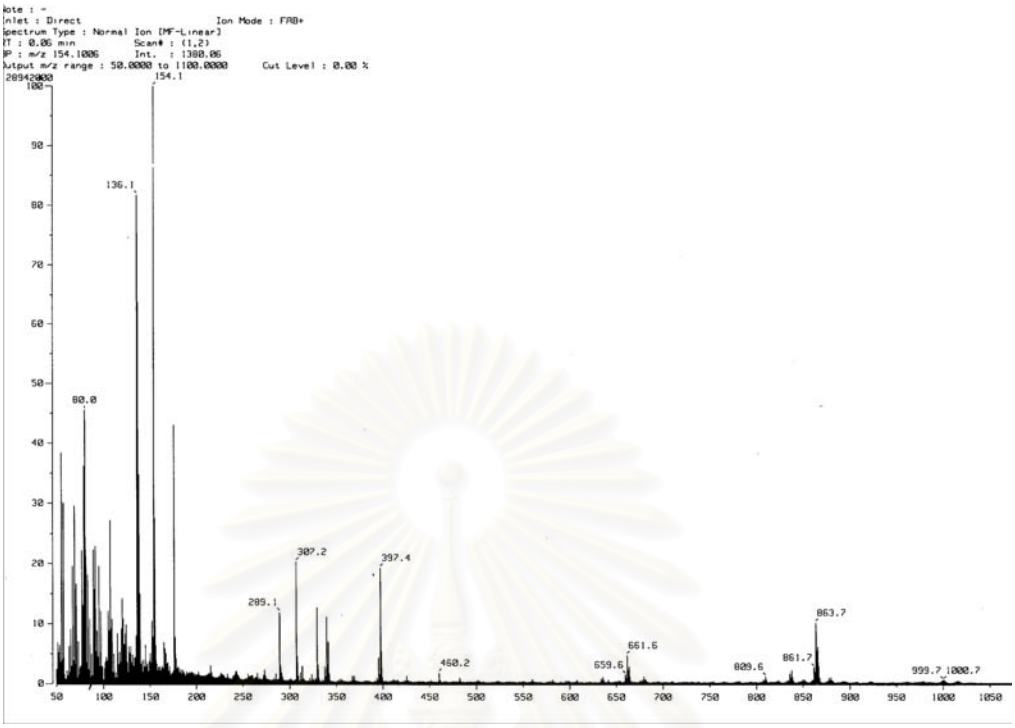

Figure 132. The positive ion FABMS of 1-*O*-behenoyl-2-*O*-oleoyl-3-*O*-β-D-glucopyranosyl-*rac*-glycerol (**6o**).

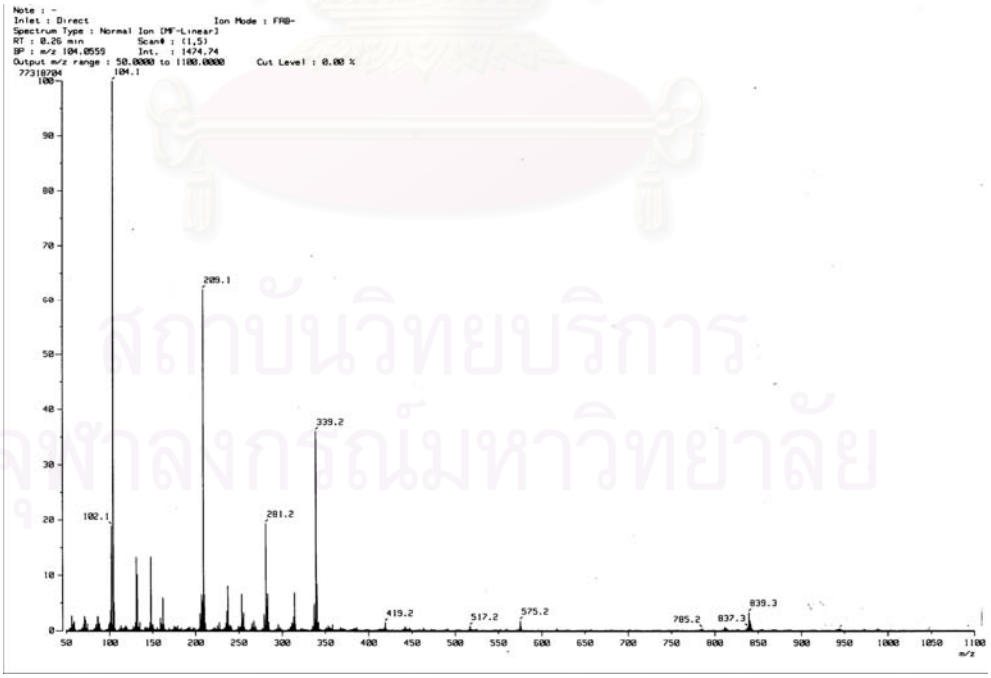

Figure 133. The negative ion FABMS of 1-*O*-behenoyl-2-*O*-oleoyl-3-*O*-β-D-glucopyranosyl-*rac*-glycerol (**6o**).

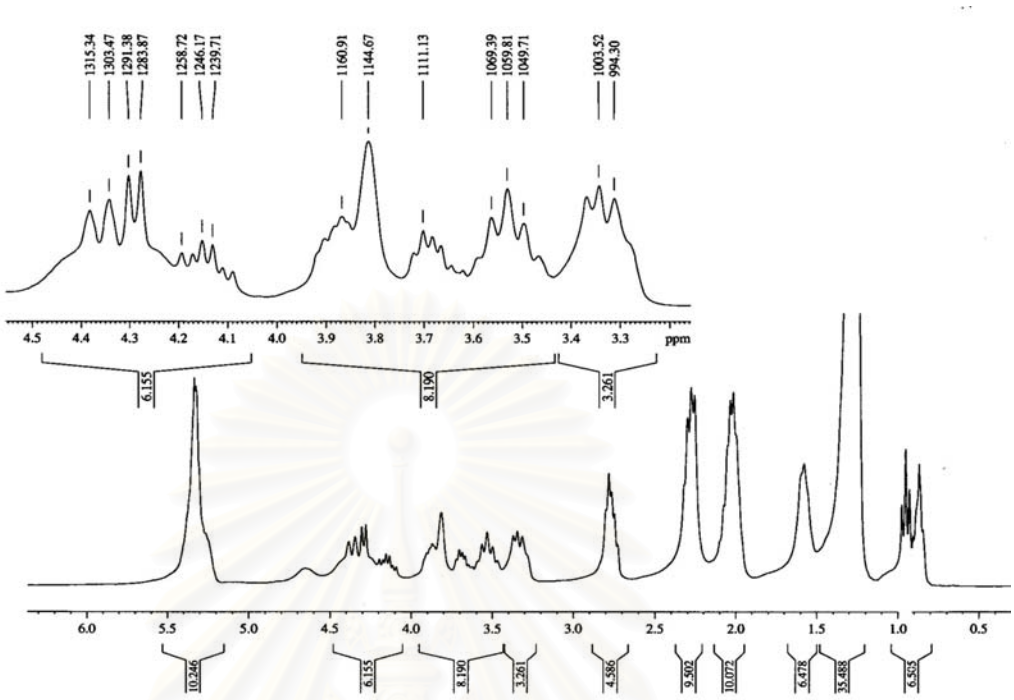

Figure 134. The 300 MHz ^{1}H-NMR spectrum of 1-*O*-linolenoyl-2-*O*-linoleoyl-3-*O*-β-D-glucopyranosyl-*rac*-glycerol (**6p**) in $CDCl_3$.

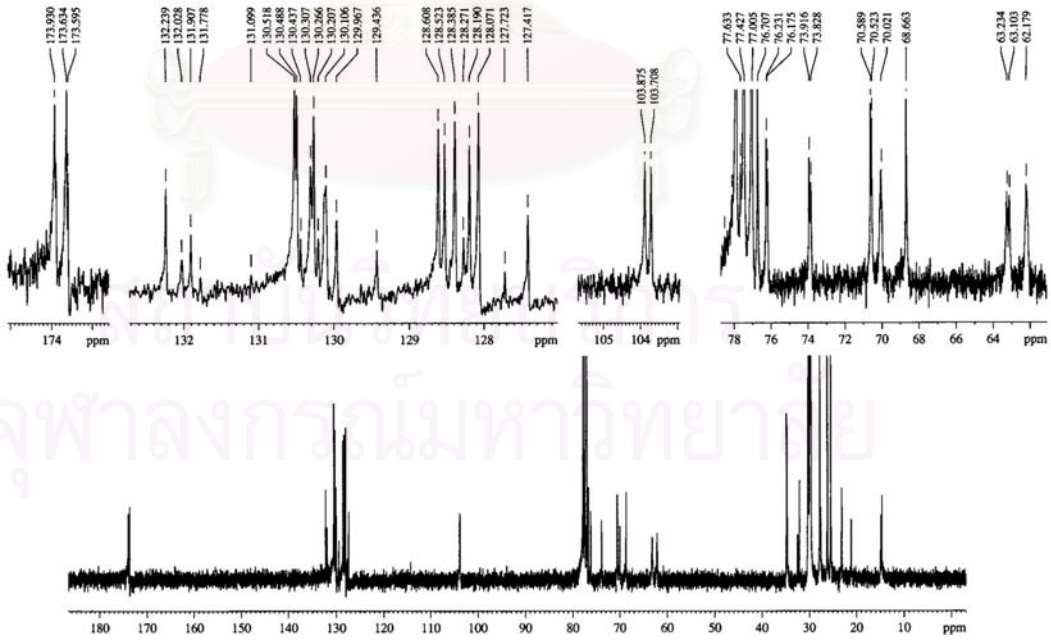

Figure 135. The 75 MHz ^{13}C-NMR spectrum of 1-*O*-linolenoyl-2-*O*-linoleoyl-3-*O*-β-D-glucopyranosyl-*rac*-glycerol (**6p**) in $CDCl_3$.

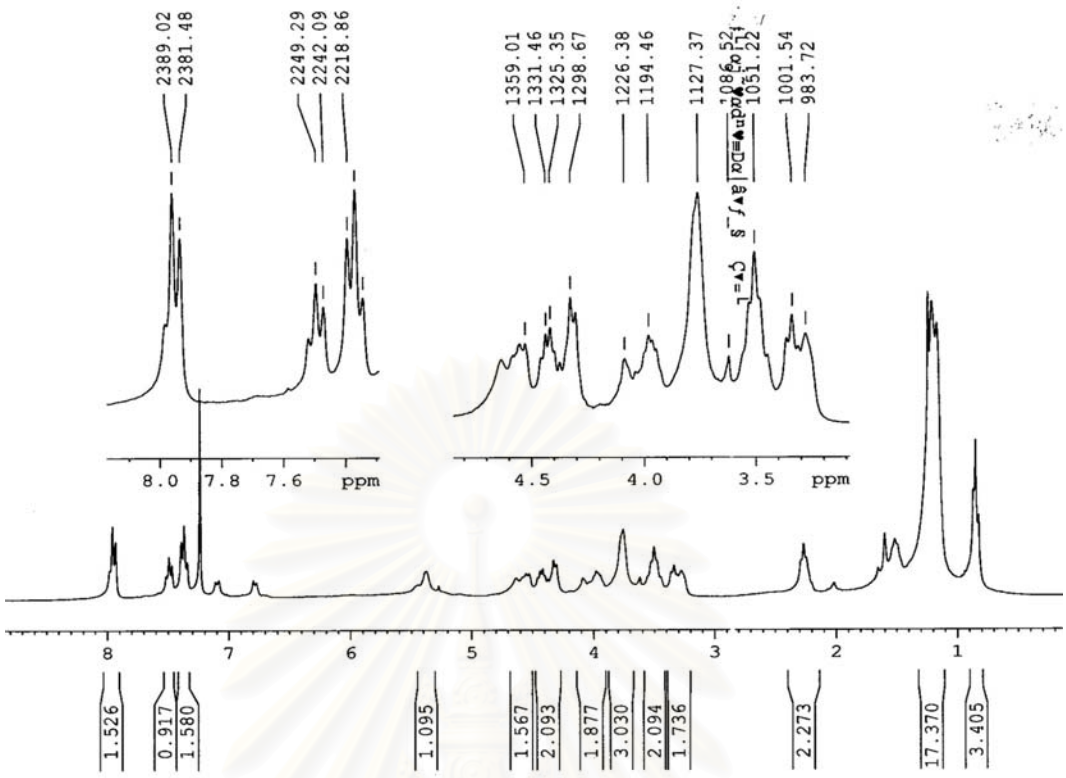

Figure 136. The 300 MHz ^{1}H-NMR spectrum of 1-*O*-benzoyl-2-*O*-lauroyl-3-*O*-β-D-glucopyranosyl-*rac*-glycerol (**6q**) in $CDCl_3$.

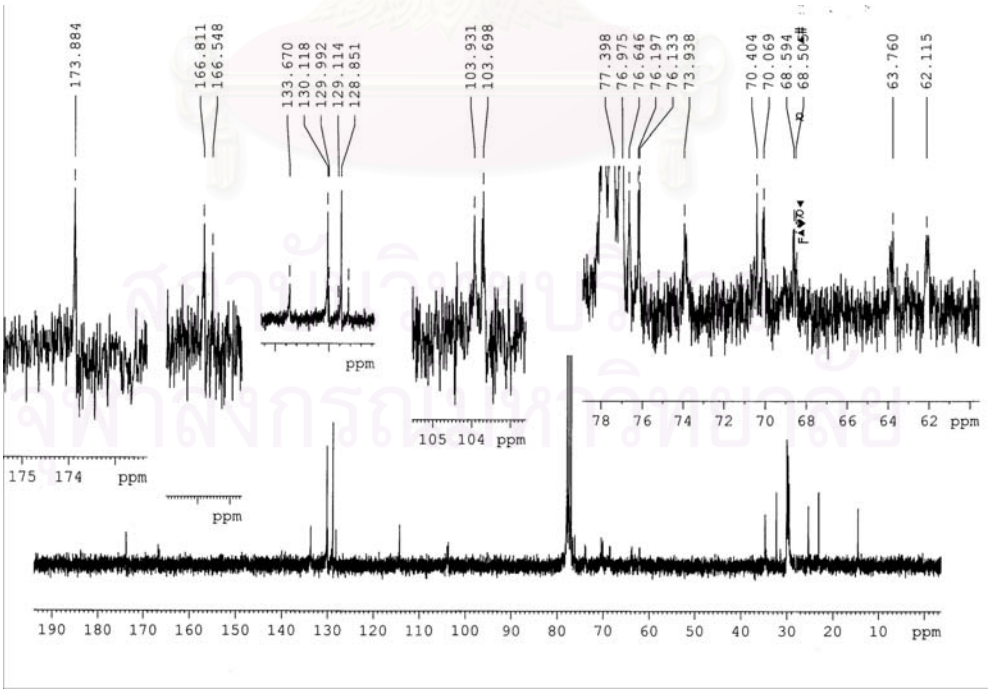

Figure 137. The 75 MHz ^{13}C-NMR spectrum of 1-*O*-benzoyl-2-*O*-lauroyl-3-*O*-β-D-glucopyranosyl-*rac*-glycerol (**6q**) in $CDCl_3$.

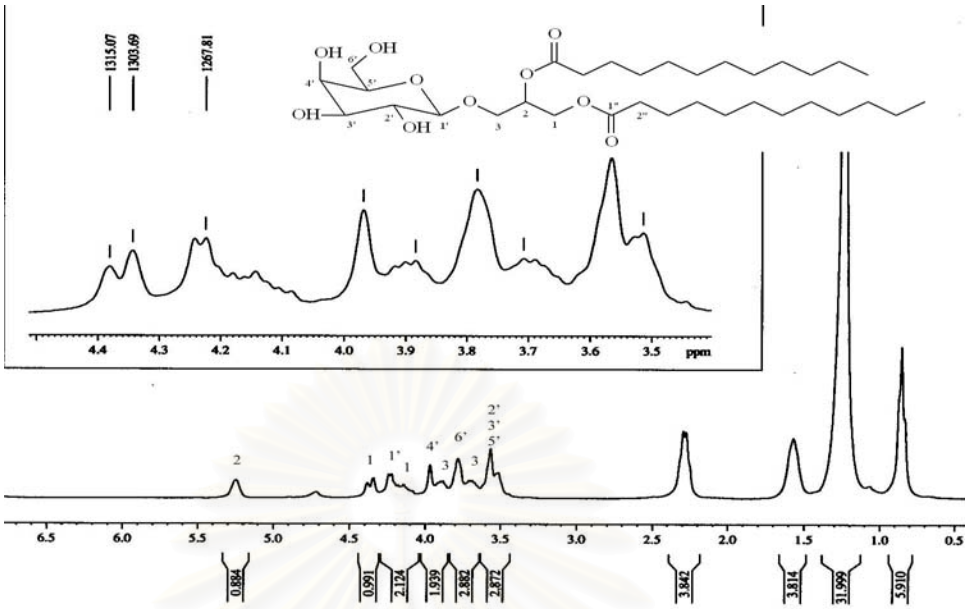

Figure 138. The 300 MHz ^{1}H-NMR spectrum of 1,2-di-*O*-lauroyl-3-*O*-β-D-galactopyranosyl-*rac*-glycerol (**13a**) in $CDCl_3$.

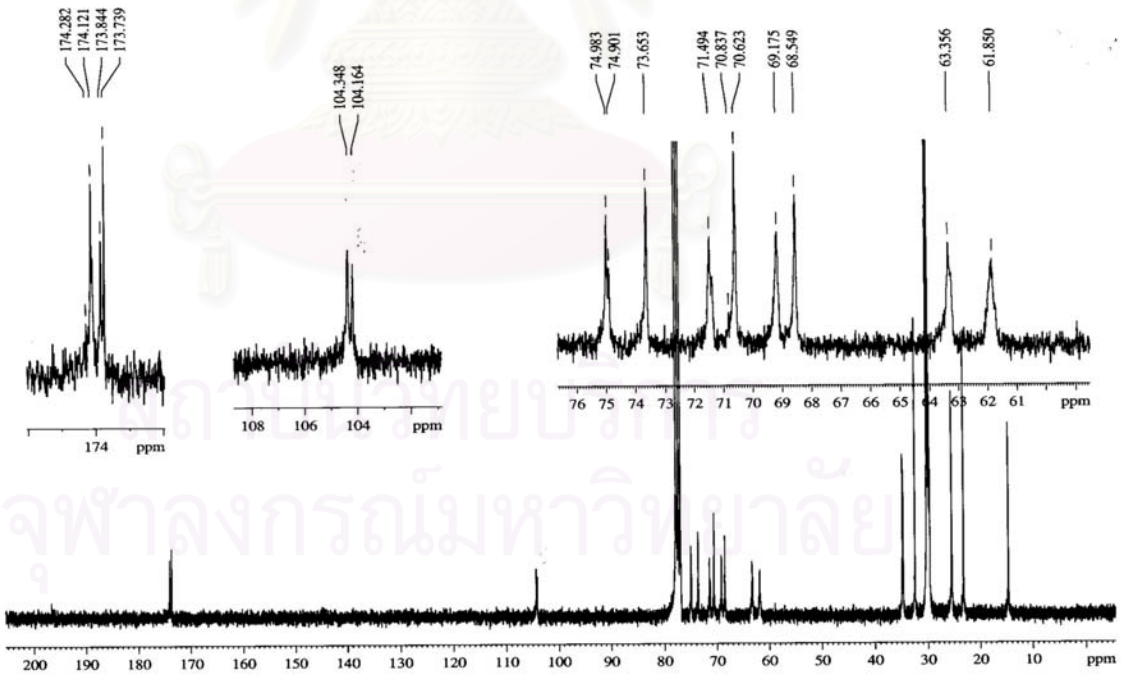

Figure 139. The 75 MHz ^{13}C-NMR spectrum of 1,2-di-*O*-lauroyl-3-*O*-β-D-galactopyranosyl-*rac*-glycerol (**13a**) in $CDCl_3$.

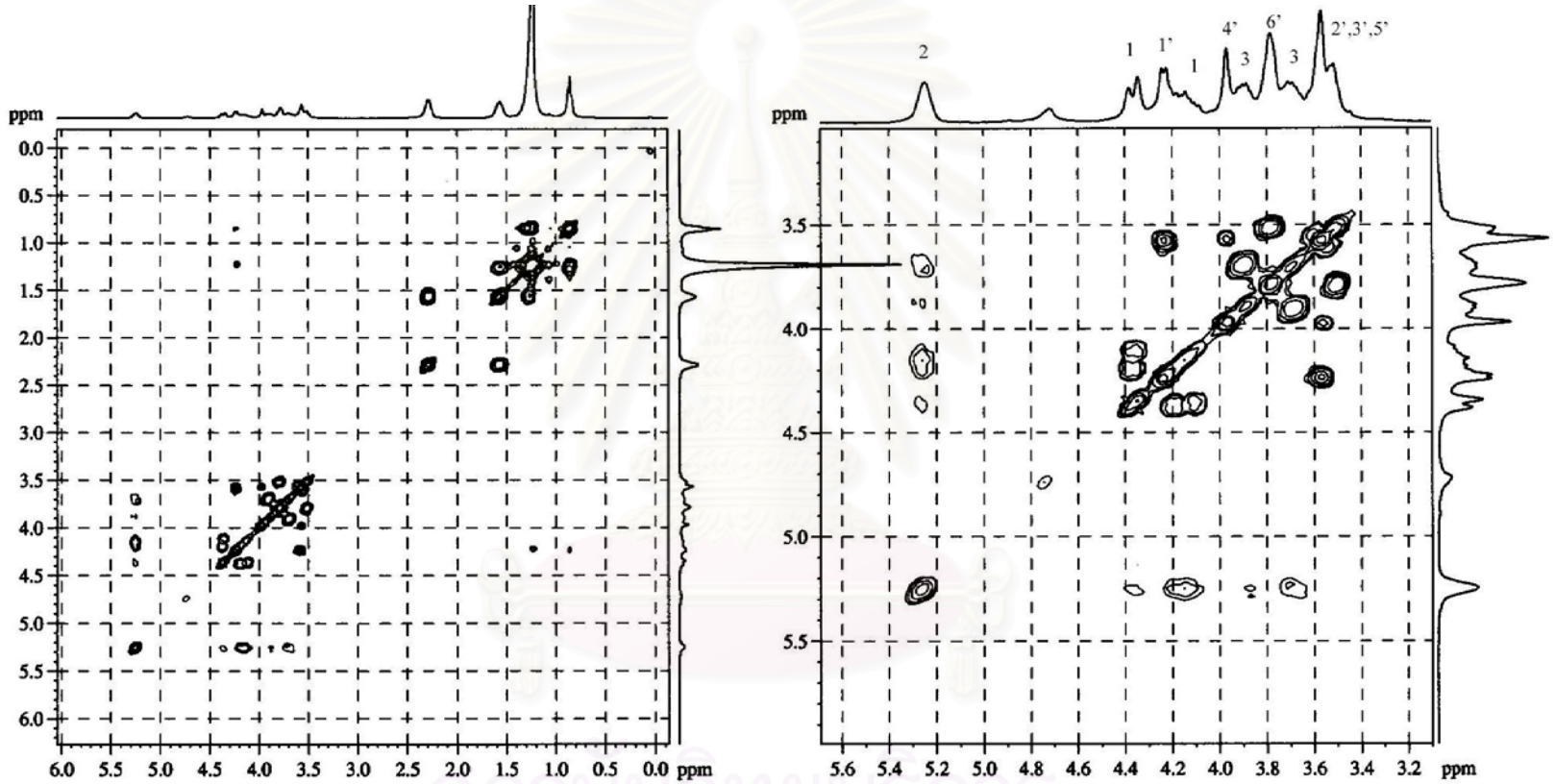

Figure 140. The ^{1}H-^{1}H COSY spectrum of 1,2-di-*O*-lauroyl-3-*O*-β-D-galactopyranosyl-*rac*-glycerol (**13a**) in $CDCl_3$.

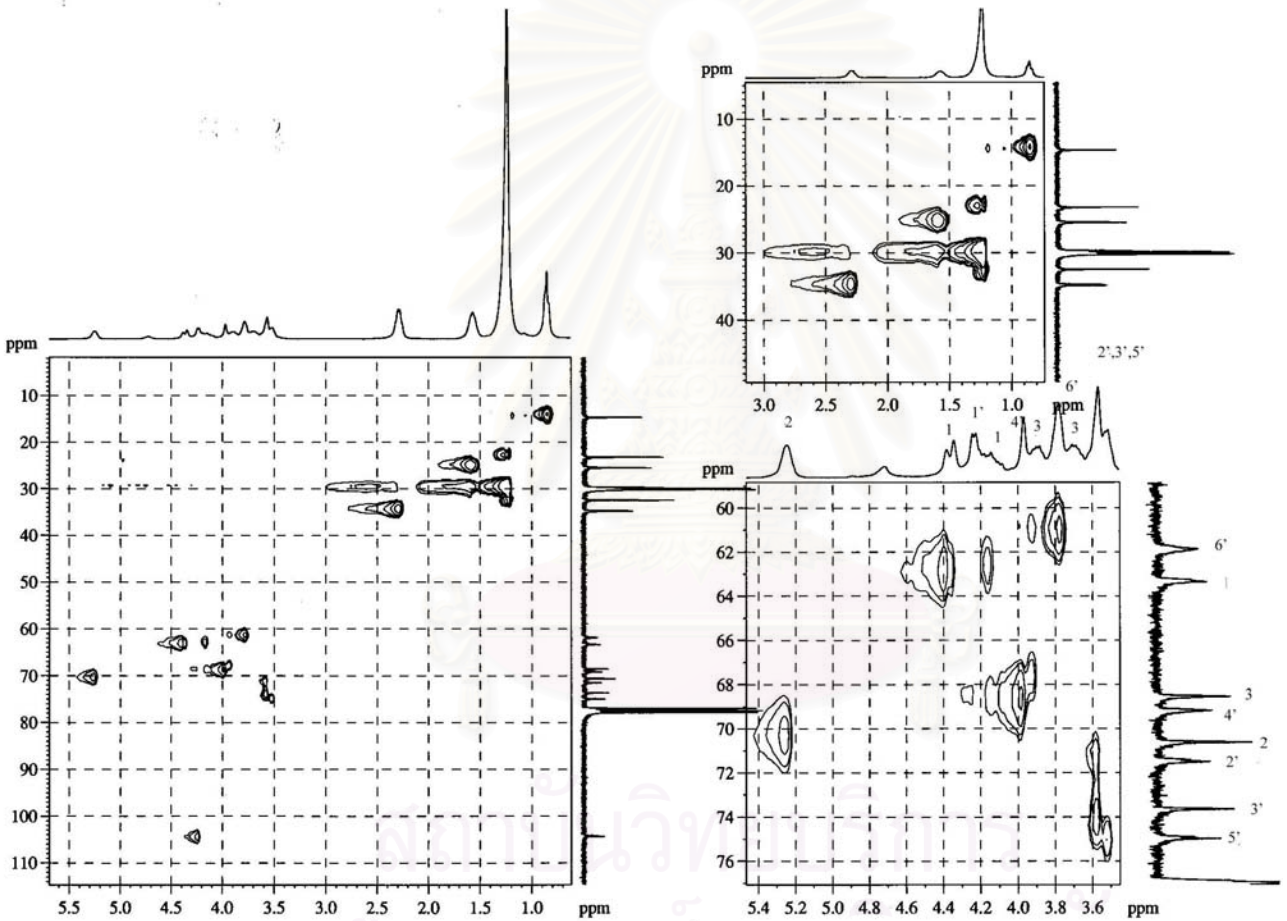

Figure 141. The HMQC spectrum of 1,2-di-*O*-lauroyl-3-*O*-β-D-galactopyranosyl-*rac*-glycerol (**13a**) in $CDCl_3$.

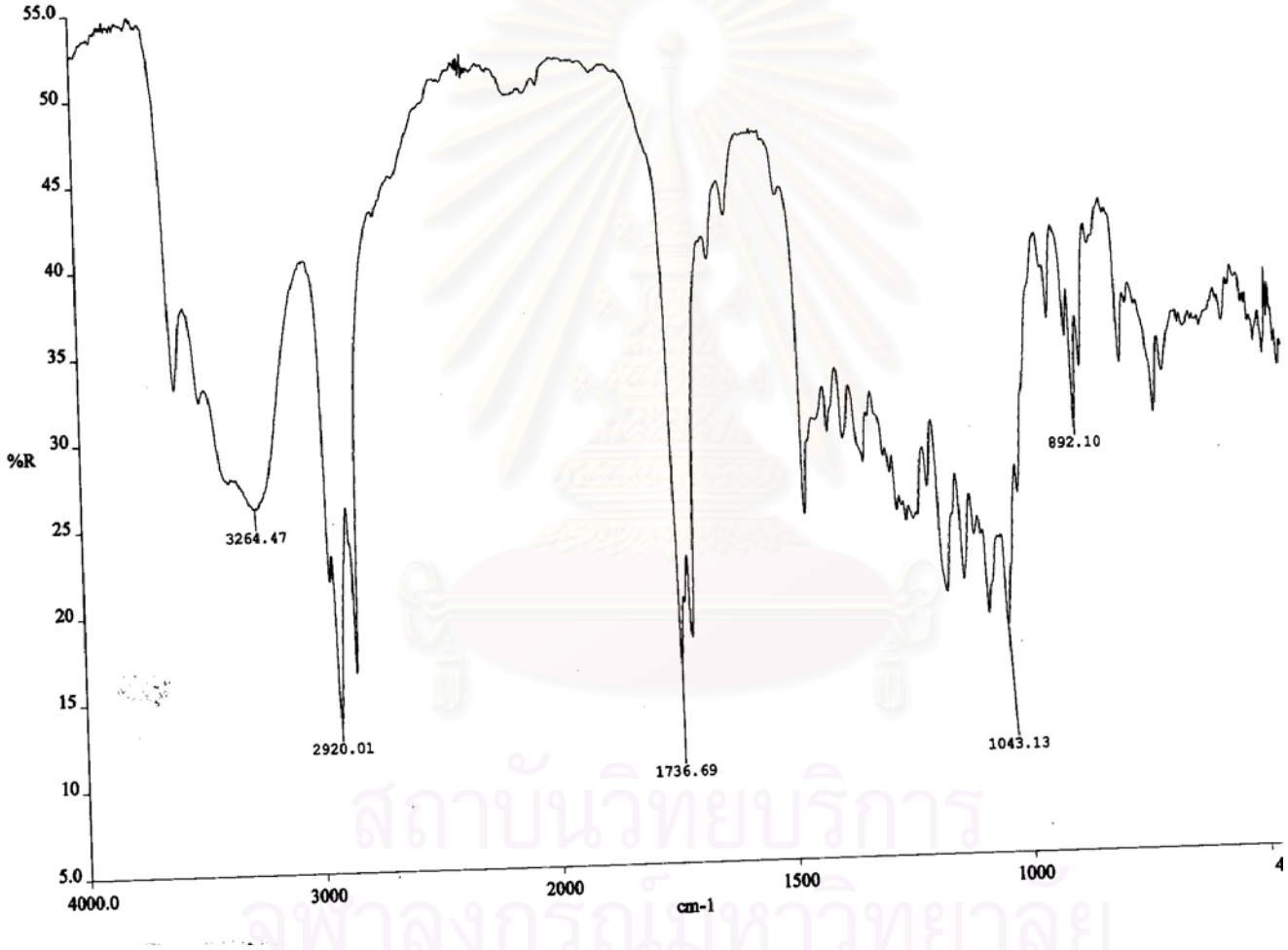

Figure 142. The infrared spectrum of 1,2-di-*O*-lauroyl-3-*O*-β-D-galactopyranosyl-*rac*-glycerol (**13a**).

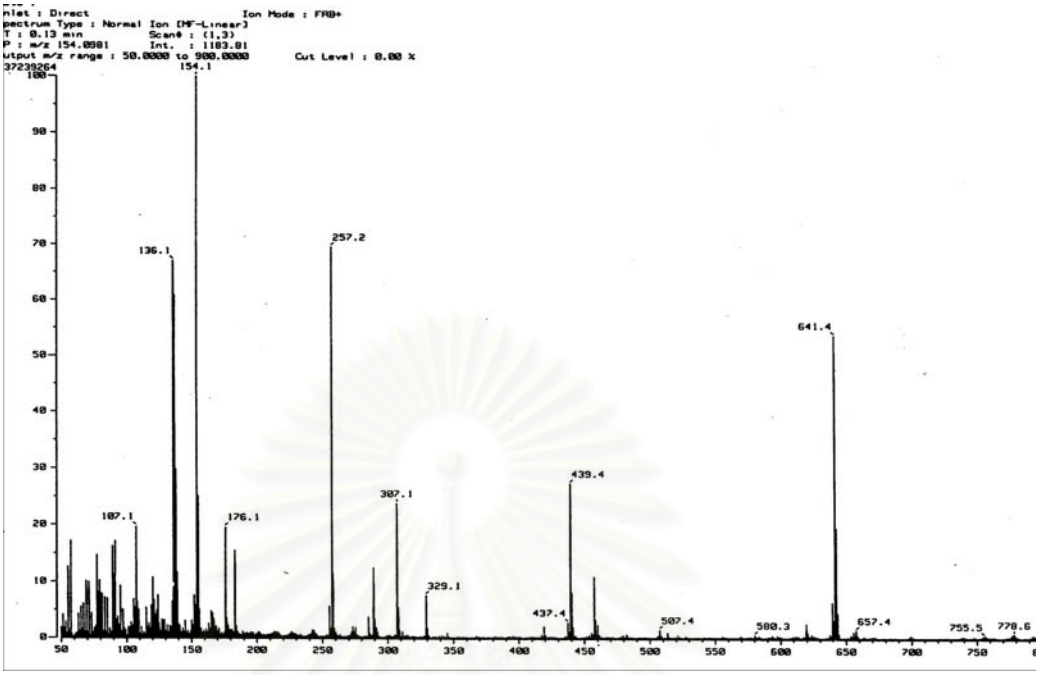

Figure 143. The positive ion FABMS of 1,2-di-*O*-lauroyl-3-*O*-β-D-galactopyranosyl-*rac*-glycerol (**13a**).

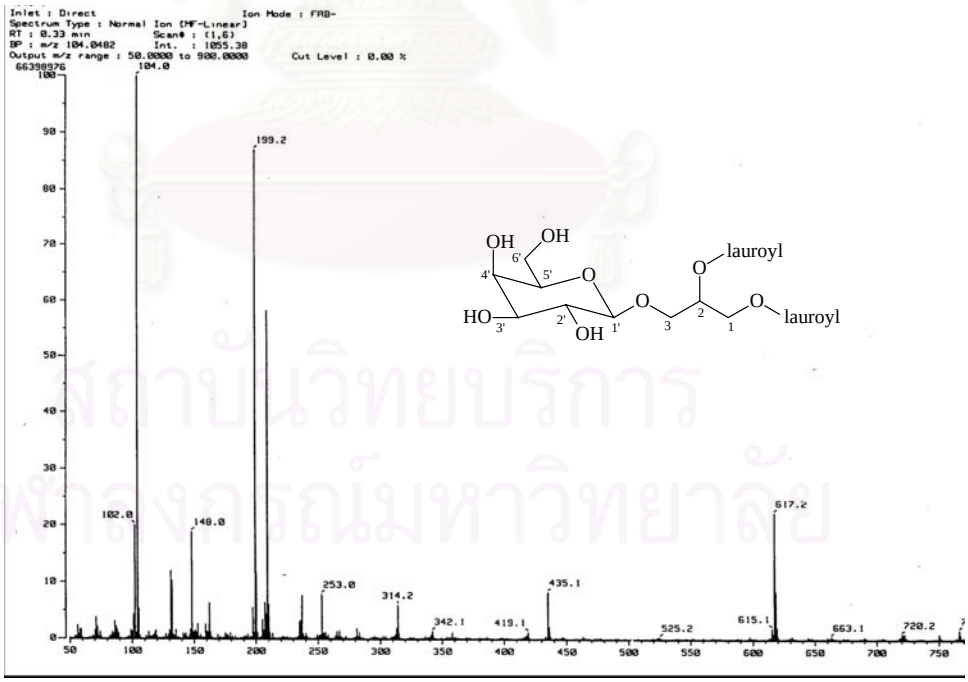

Figure 144. The negative ion FABMS of 1,2-di-*O*-lauroyl-3-*O*-β-D-galactopyranosyl-*rac*-glycerol (**13a**).

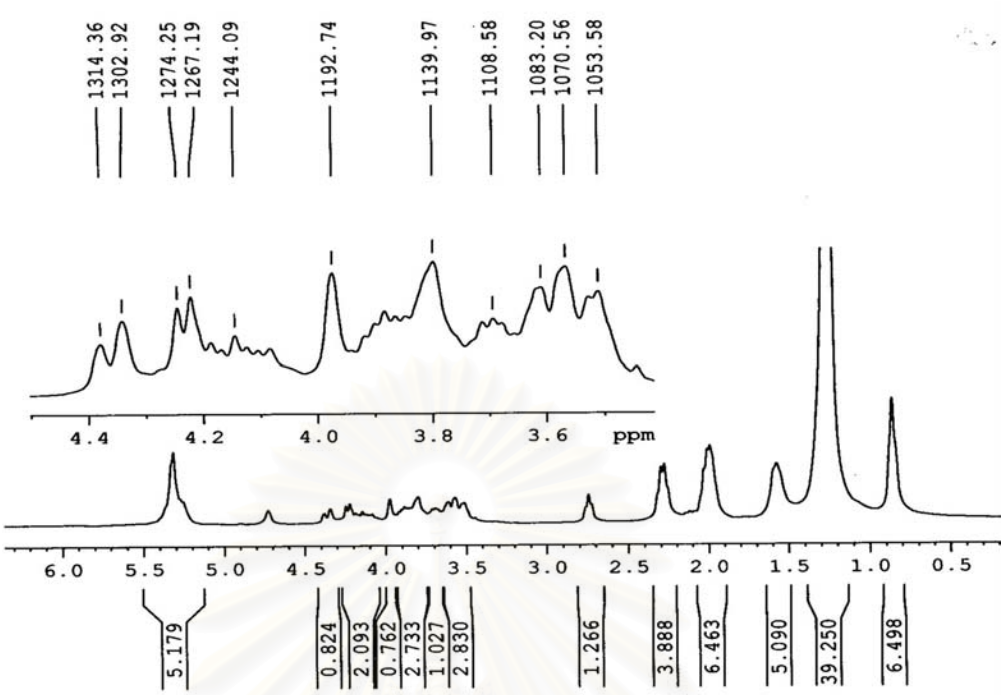

Figure 145. The 300 MHz ^{1}H-NMR spectrum of 1,2-di-*O*-linoleoyl-3-*O*-β-D-galactopyranosyl-*rac*-glycerol (**13b**) in $CDCl_3$.

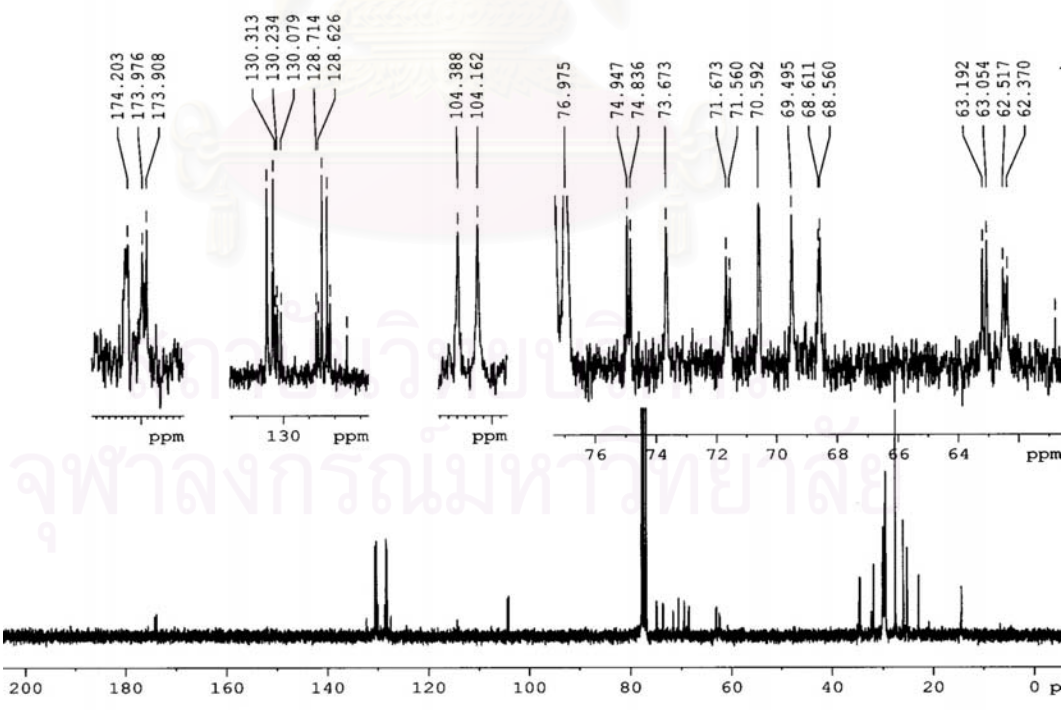

Figure 146. The 75 MHz ^{13}C-NMR spectrum of 1,2-di-*O*-linoleoyl-3-*O*-β-D-galactopyranosyl-*rac*-glycerol (**13b**) in $CDCl_3$.

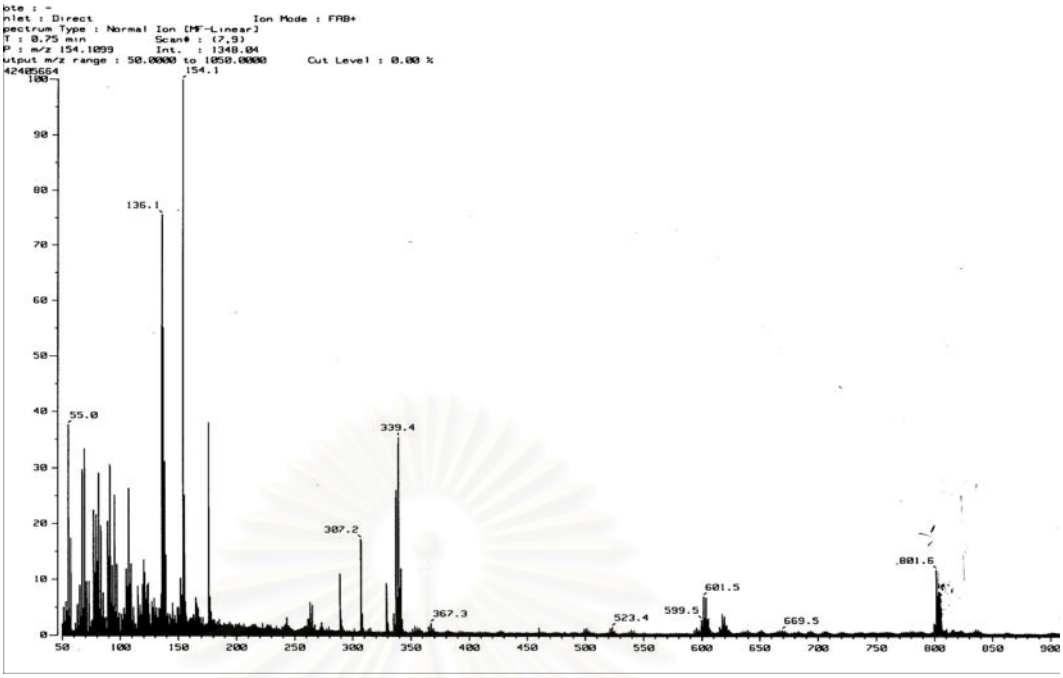

Figure 147. The positive ion FABMS of 1,2-di-*O*-linoleoyl-3-*O*-β-D-galactopyranosyl-*rac*-glycerol (**13b**).

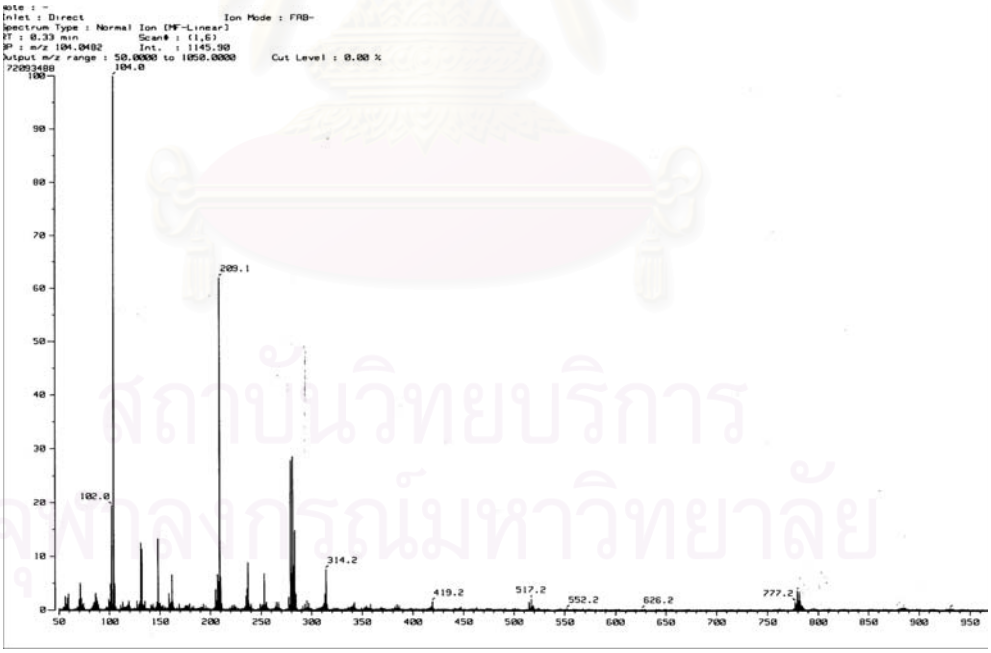

Figure 148. The negative ion FABMS of 1,2-di-*O*-linoleoyl-3-*O*-β-D-galactopyranosyl-*rac*-glycerol (**13b**).

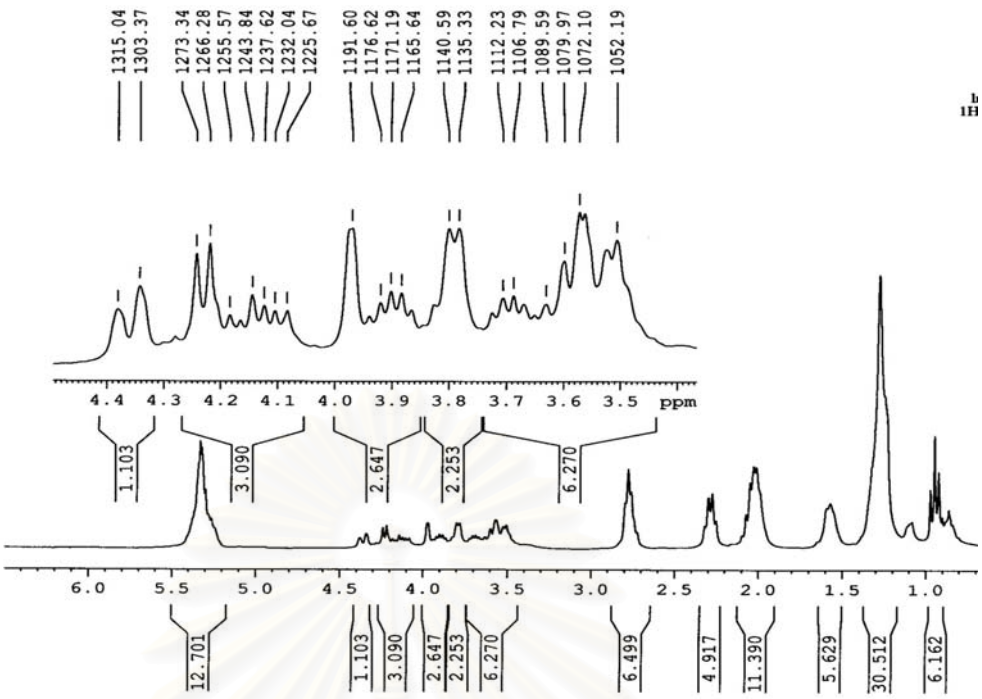

Figure 149. The 300 MHz ^{1}H-NMR spectrum of 1,2-di-*O*-linolenoyl-3-*O*-β-D-galactopyranosyl-*rac*-glycerol (**13c**) in $CDCl_3$.

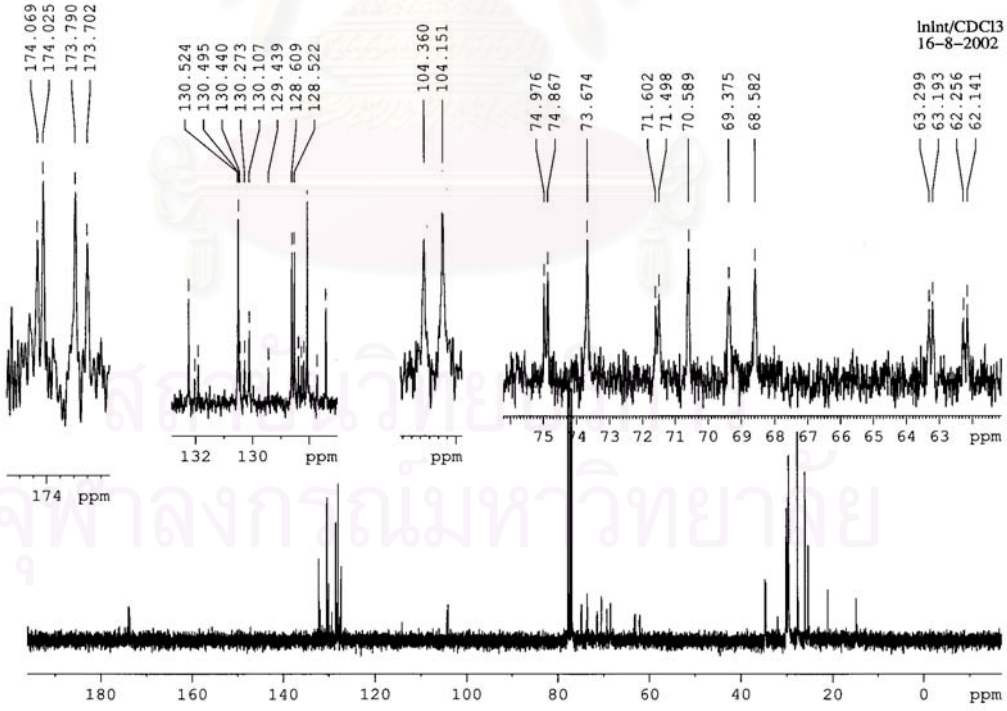

Figure 150. The 75 MHz ^{13}C-NMR spectrum of 1,2-di-*O*-linolenoyl-3-*O*-β-D-galactopyranosyl-*rac*-glycerol (**13c**) in $CDCl_3$.

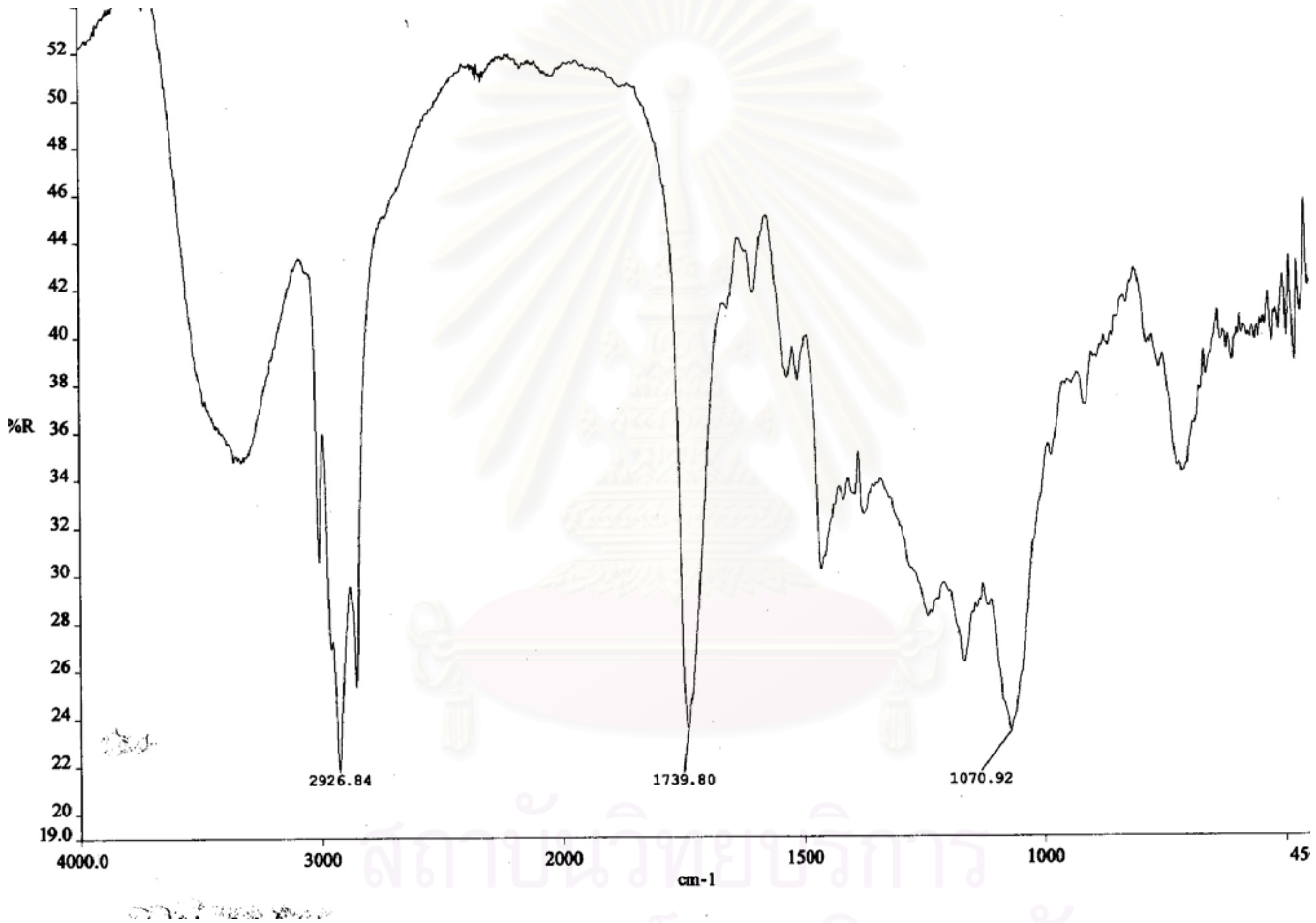

Figure 151. The infrared spectrum of 1,2-di-*O*-linolenoyl-3-*O*-β-D-galactopyranosyl-*rac*-glycerol (**13c**).

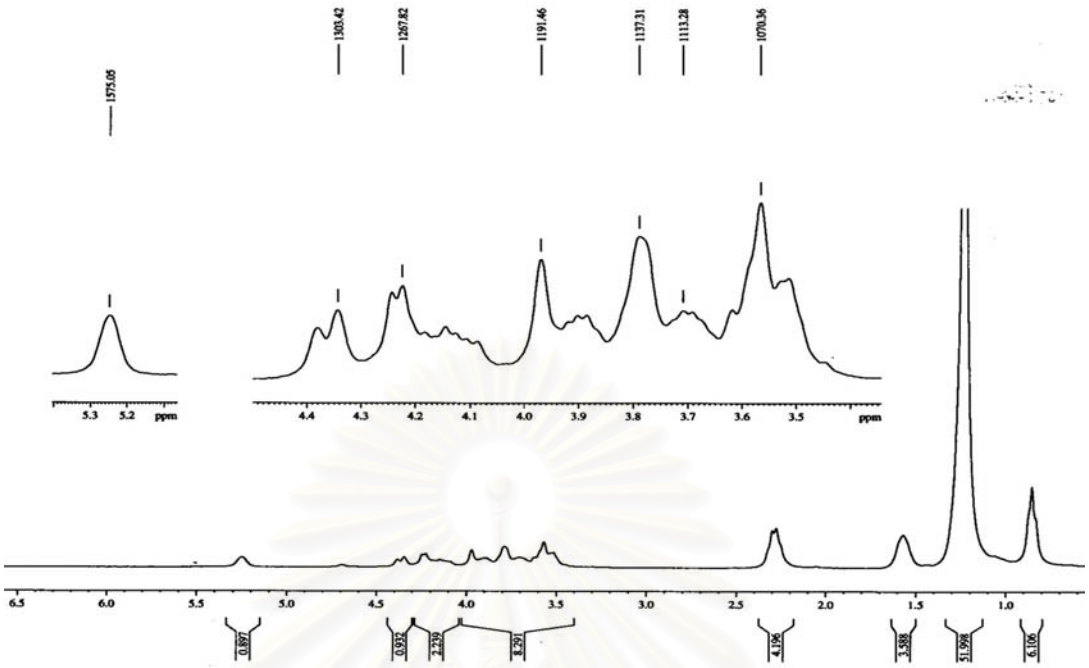

Figure 152. The 300 MHz ^{1}H-NMR spectrum of 1-*O*-behenoyl-2-*O*-lauroyl-3-*O*-β-D-galactopyranosyl-*rac*-glycerol (**13d**) in $CDCl_3$.

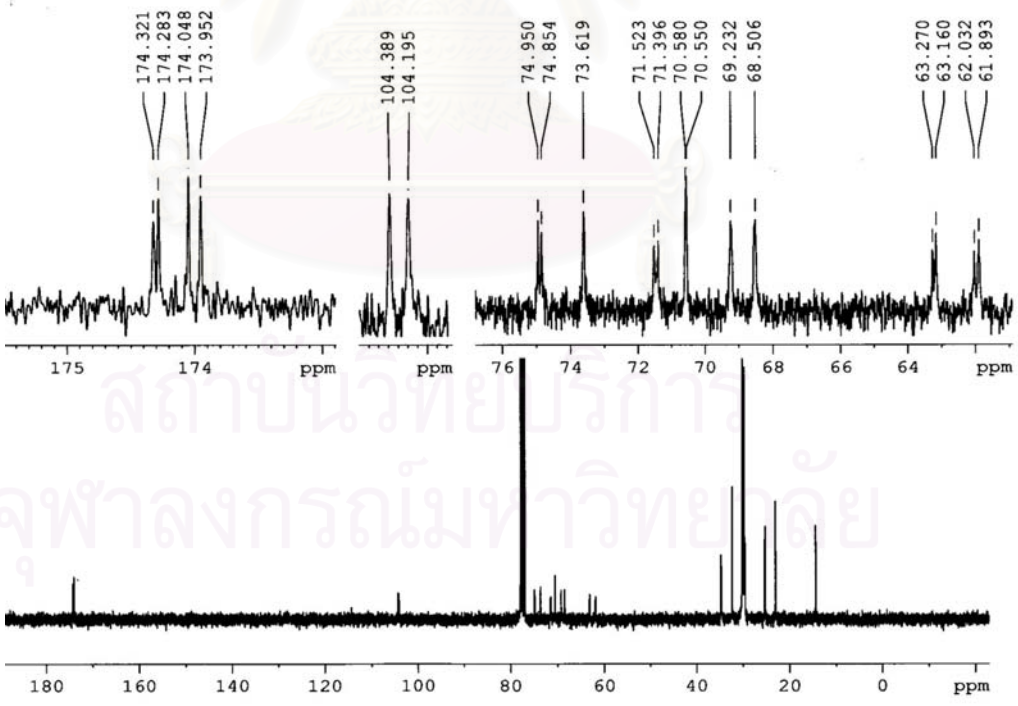

Figure 153. The 75 MHz ^{13}C-NMR spectrum of 1-*O*-behenoyl-2-*O*-lauroyl-3-*O*-β-D-galactopyranosyl-*rac*-glycerol (**13d**) in $CDCl_3$.

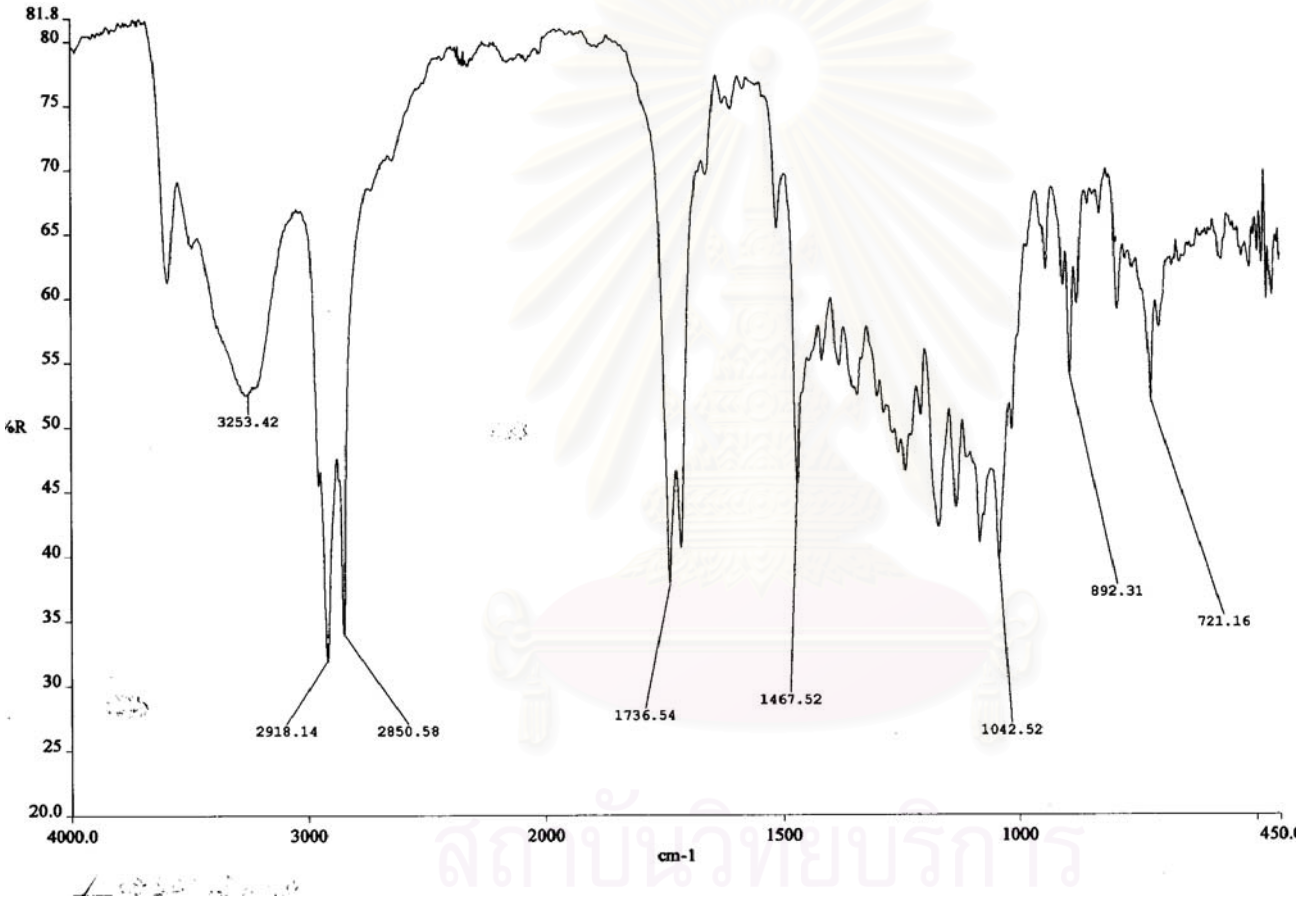

Figure 154. The infrared spectrum of 1-*O*-behenoyl-2-*O*-lauroyl-3-*O*-β-D-galactopyranosyl-*rac*-glycerol (**13d**).

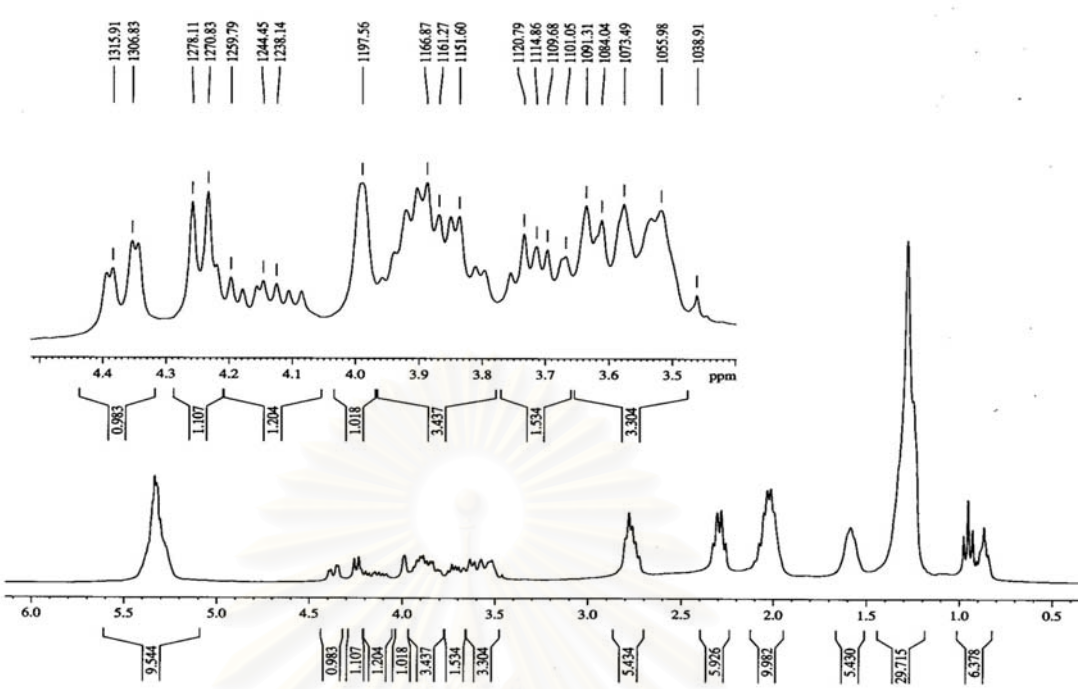

Figure 155. The 300 MHz ^{1}H-NMR spectrum of 1-*O*-linolenoyl-2-*O*-linoleoyl-3-*O*-β-D-galactopyranosyl-*rac*-glycerol (**13e**) in $CDCl_3$.

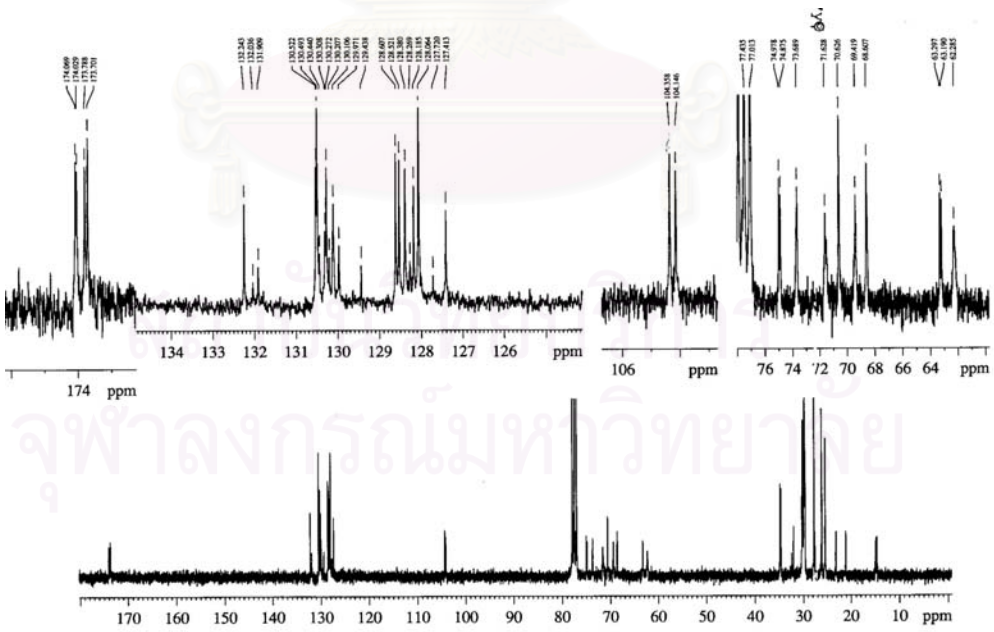

Figure 156. The 75MHz ^{13}C-NMR spectrum of 1-*O*-linolenoyl-2-*O*-linoleoyl-3-*O*-β-D-galactopyranosyl-*rac*-glycerol (**13e**) in $CDCl_3$.

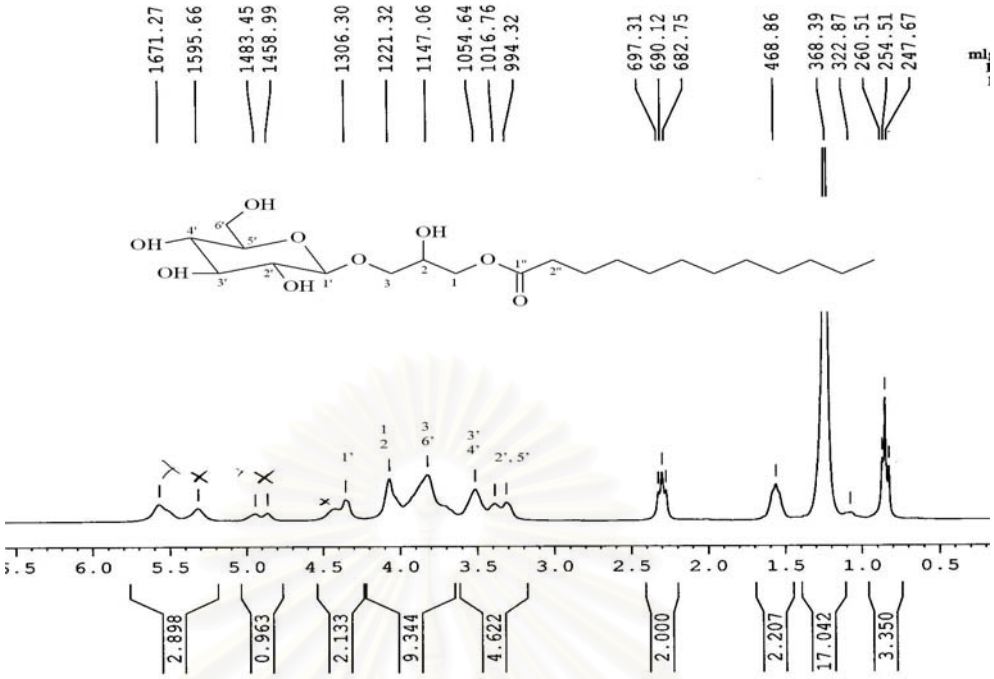

Figure 157. The 300 MHz ^{1}H-NMR spectrum of 1-*O*-lauroyl-3-*O*-β-D-glucopyranosyl-*rac*-glycerol (**8a**) in $CDCl_3$.

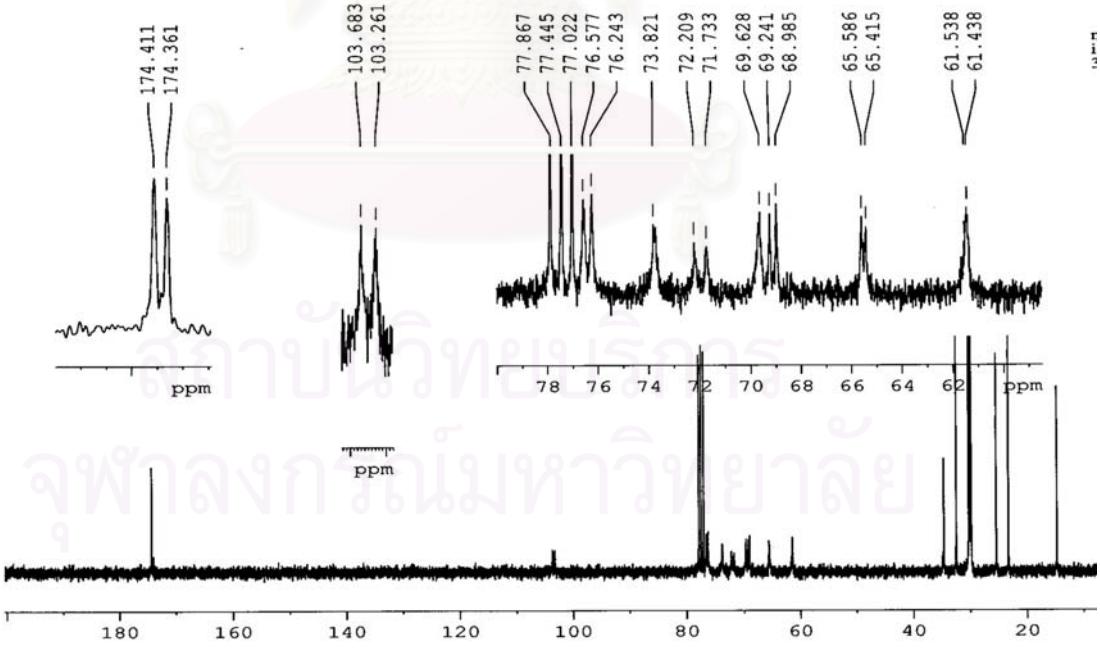

Figure 158. The 75 MHz ^{13}C-NMR spectrum of 1-*O*-lauroyl-3-*O*-β-D-glucopyranosyl-*rac*-glycerol (**8a**) in $CDCl_3$.

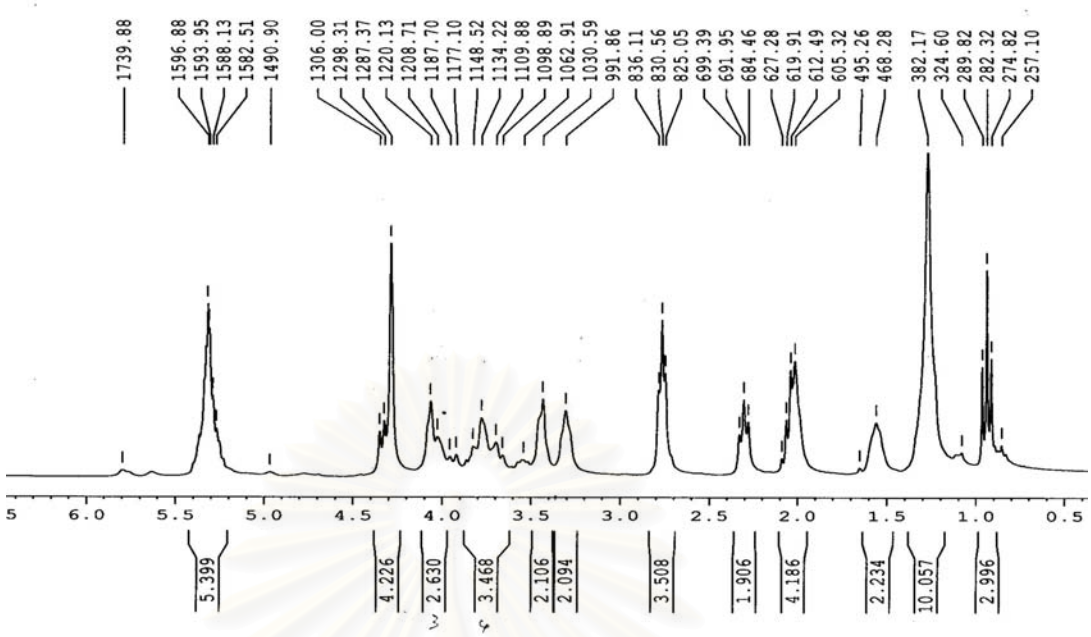

Figure 159. The 300 MHz ^{1}H-NMR spectrum of 1-*O*-linolenoyl-3-*O*-β-D-glucopyranosyl-*rac*-glycerol (**8b**) in $CDCl_3$.

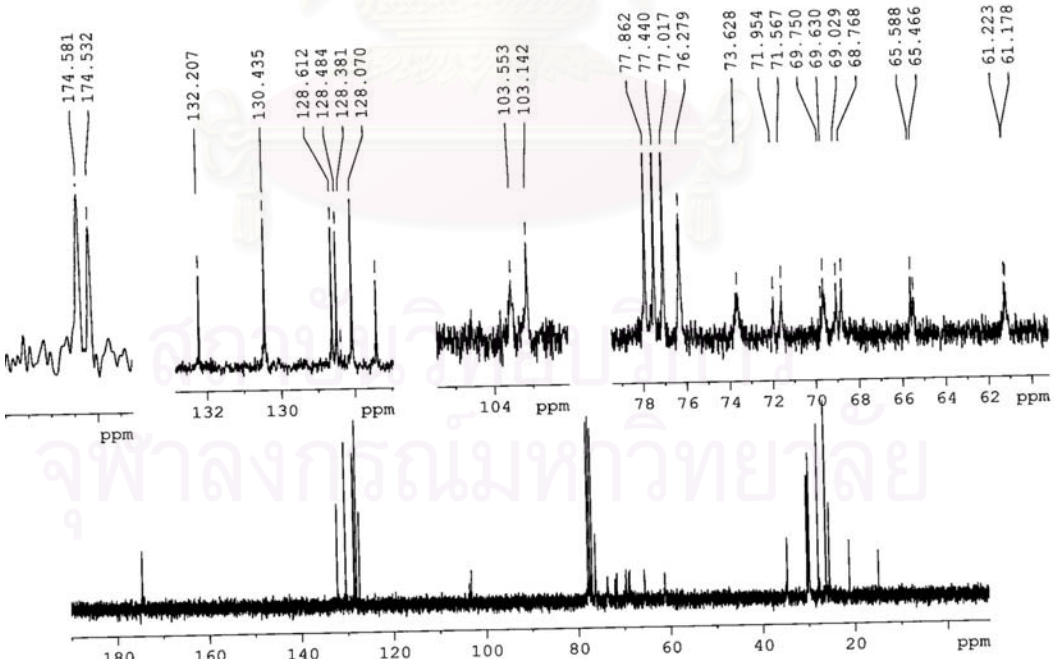

Figure 160. The 75 MHz ^{13}C -NMR spectrum of 1-*O*-linolenoyl-3-*O*-β-D-glucopyranosyl-*rac*-glycerol (**8b**) in $CDCl_3$.

Figure 161. The 300 MHz ^{1}H-NMR spectrum of 1-*O*-linolenoyl-3-*O*-β-D-galactopyranosyl-*rac*-glycerol (**15**) in $CDCl_3$.

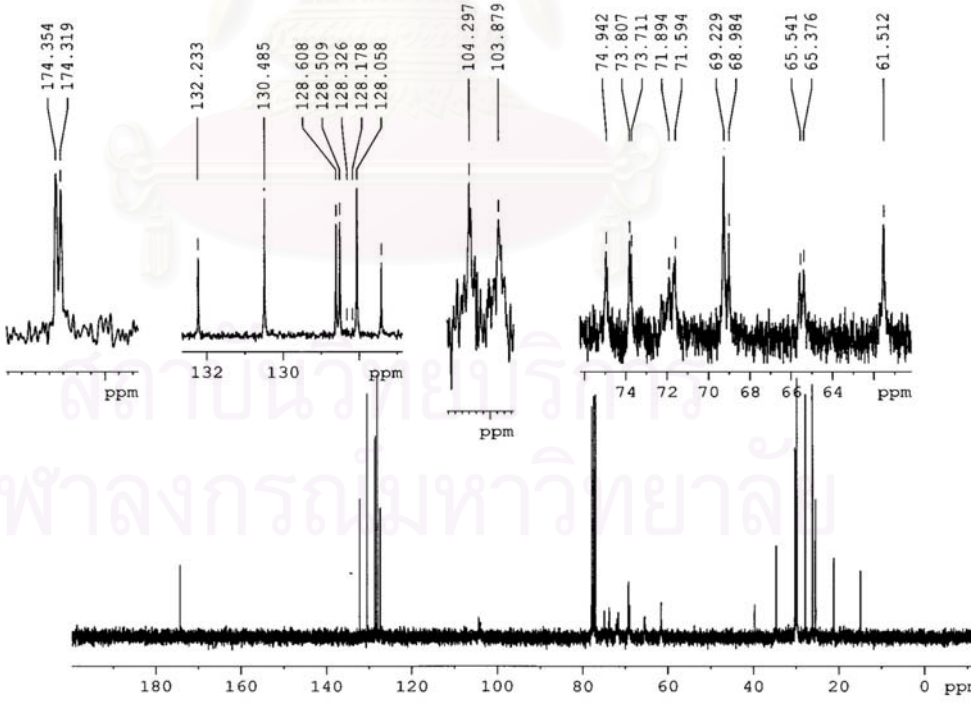

Figure 162. The 75 MHz ^{13}C-NMR spectrum of 1-*O*-linolenoyl-3-*O*-β-D-galactopyranosyl-*rac*-glycerol (**15**) in $CDCl_3$.

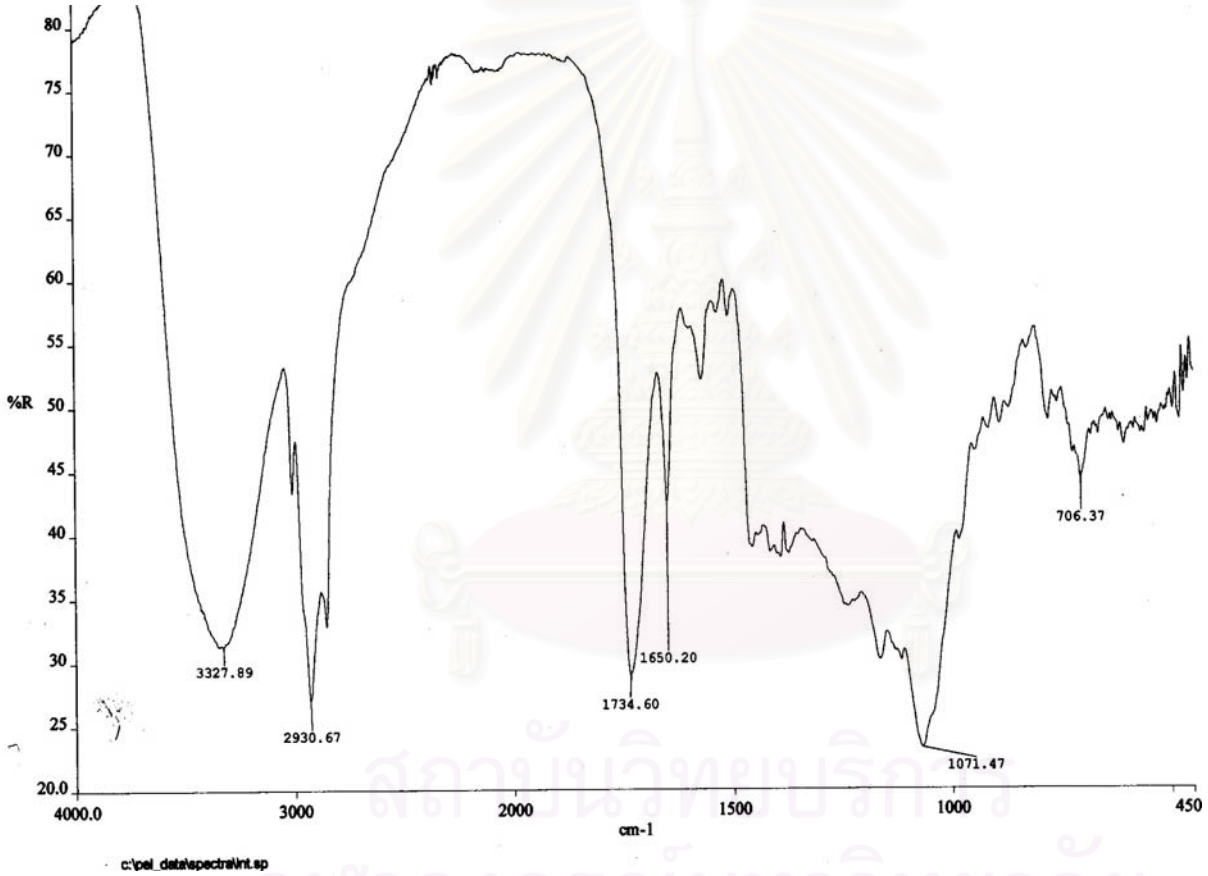

Figure 163. The infrared spectrum of 1-*O*-linolenoyl-3-*O*-β-D-galactopyranosyl-*rac*-glycerol (**15**).

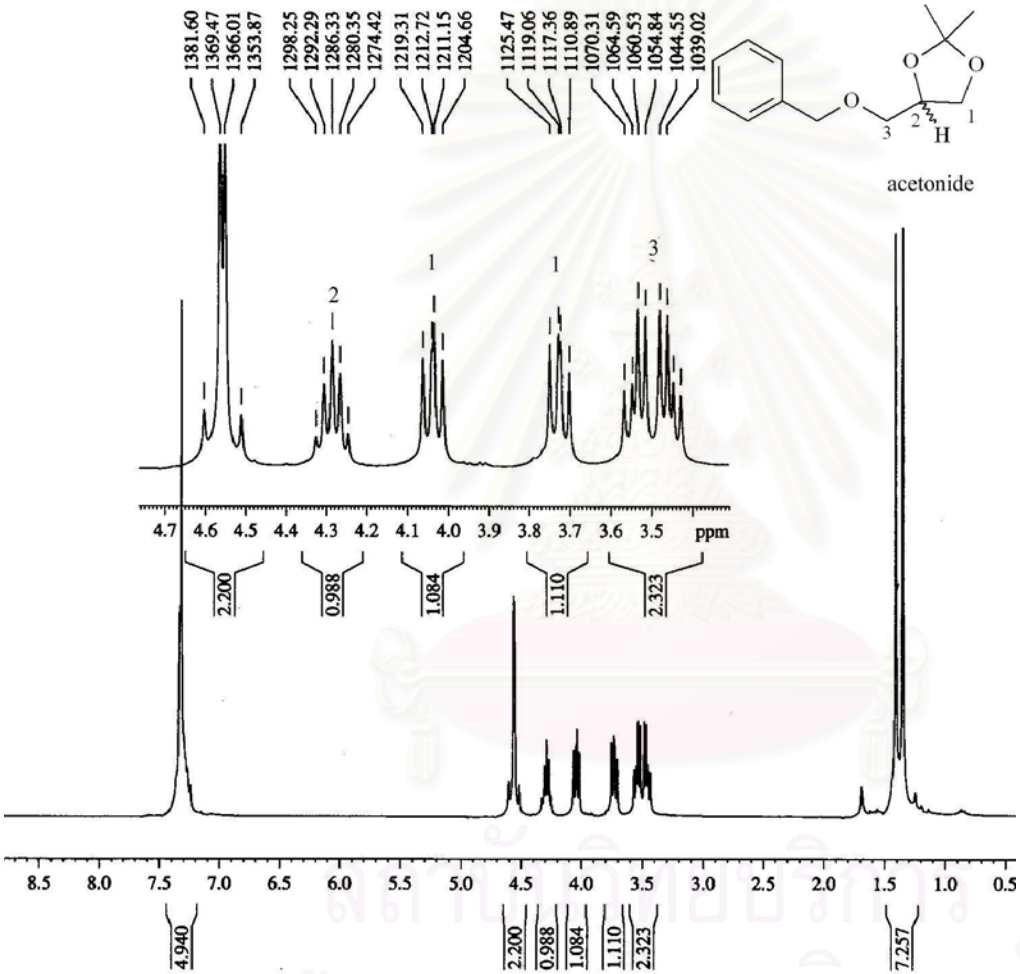

Figure 164. The 300 MHz ^{1}H-NMR spectrum of 1,2-*O*-isopropylidene-3-*O*-benzyl-*rac*-glycerol (**16**) in $CDCl_3$.

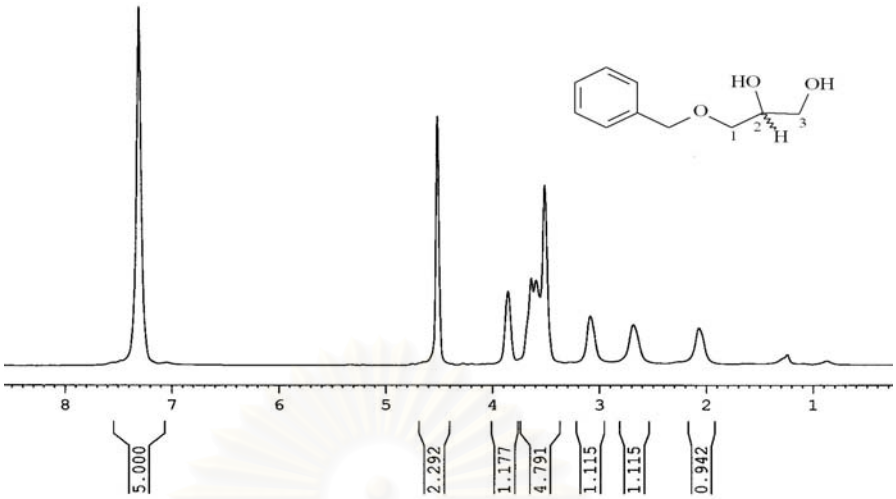

Figure 165. The 300 MHz ^{1}H-NMR spectrum of 1-*O*-benzyl-*rac*-glycerol (**17**) in $CDCl_3$.

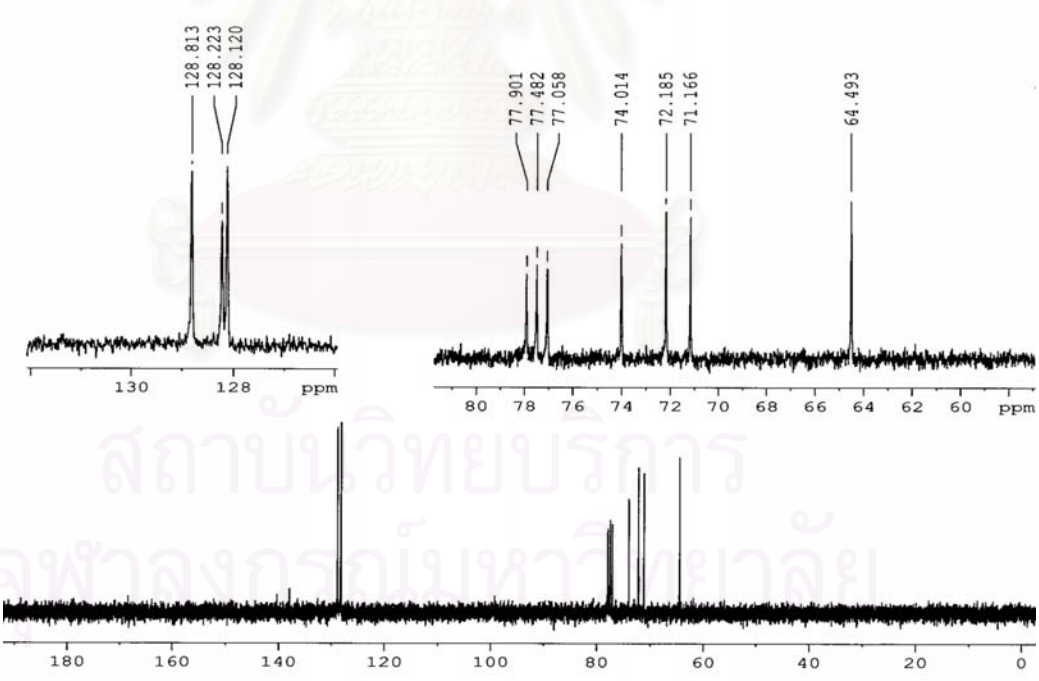

Figure 166. The 75 MHz ^{13}C-NMR spectrum of 1-*O*-benzyl-*rac*-glycerol (**17**) in $CDCl_3$.

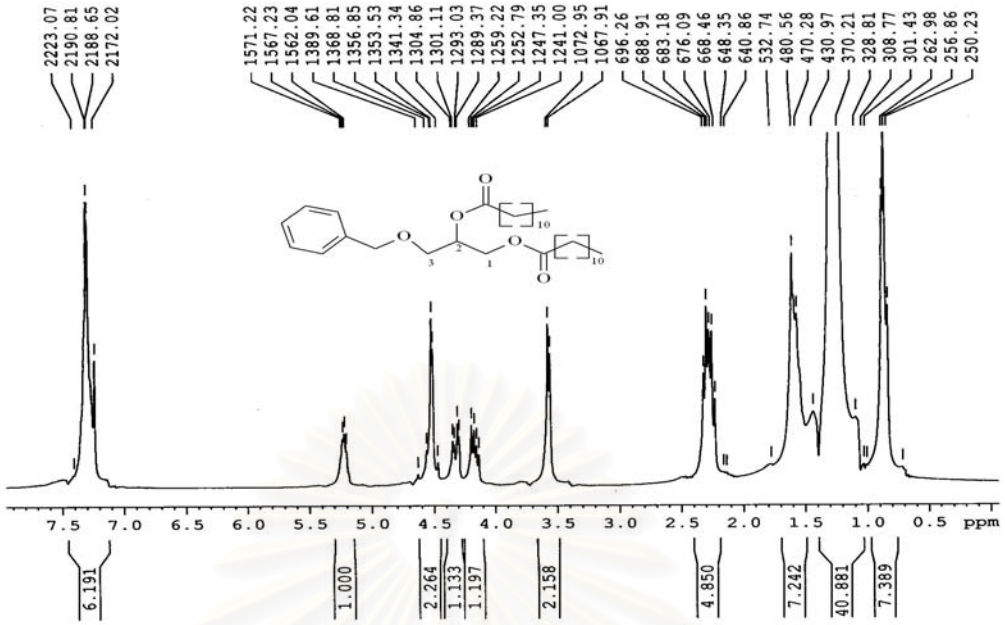

Figure 167. The 300 MHz ^{1}H-NMR spectrum of 1,2-*O*-dilauroyl-3-*O*-benzyl-*rac*-glycerol (**18**) in $CDCl_3$.

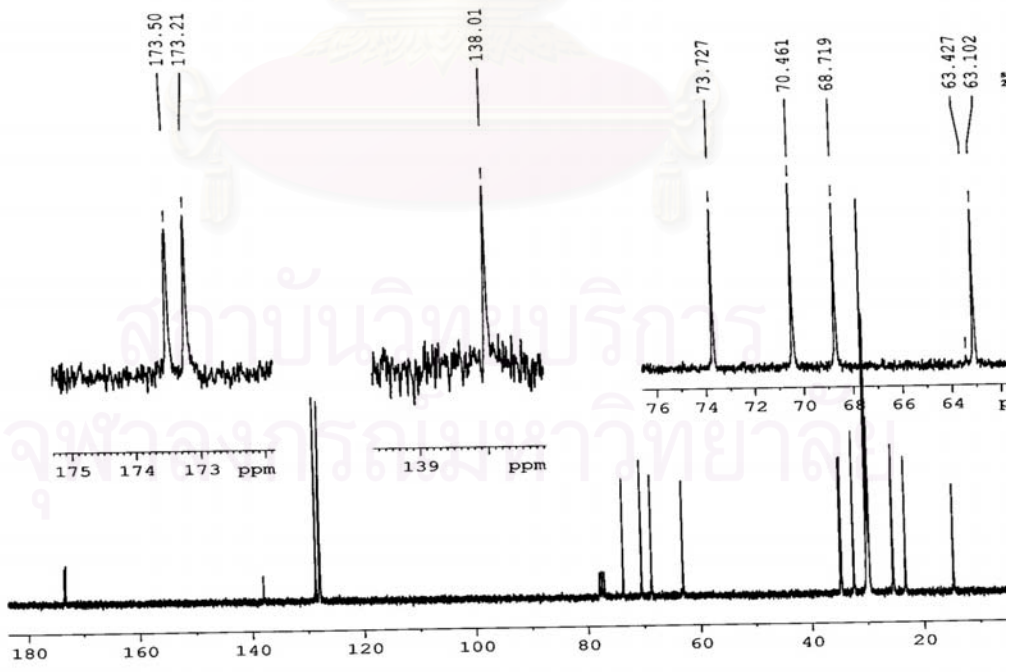

Figure 168. The 75 MHz ^{13}C-NMR spectrum of 1,2-*O*-dilauroyl-3-*O*-benzyl-*rac*-glycerol (**18**) in $CDCl_3$.

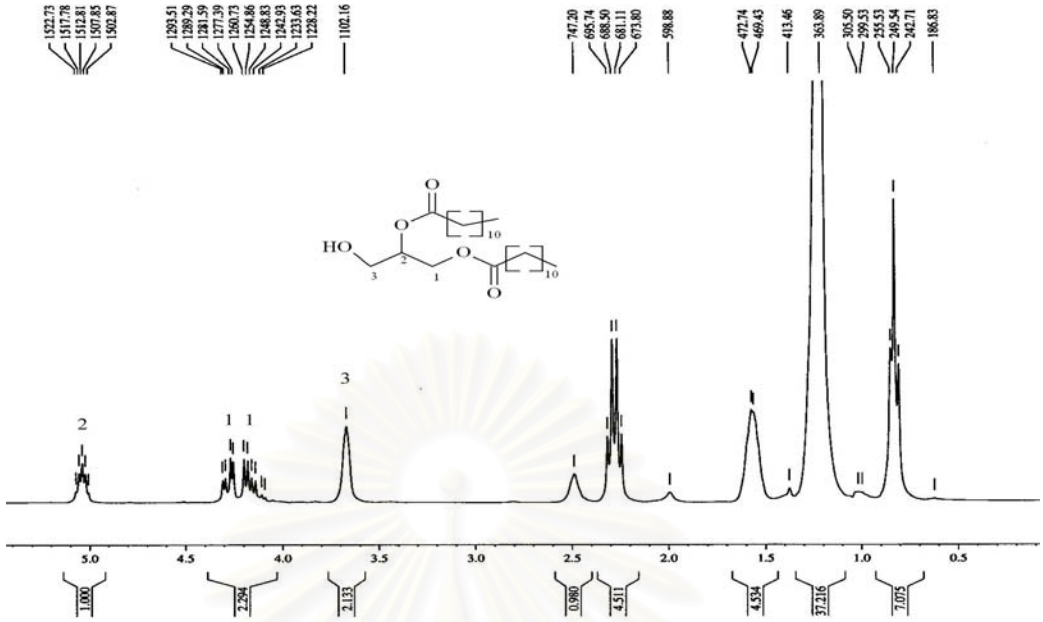

Figure 169. The 300 MHz ^{1}H-NMR spectrum of 1,2-*O*-dilauroyl-*rac*-glycerol (**19**) in $CDCl_3$.

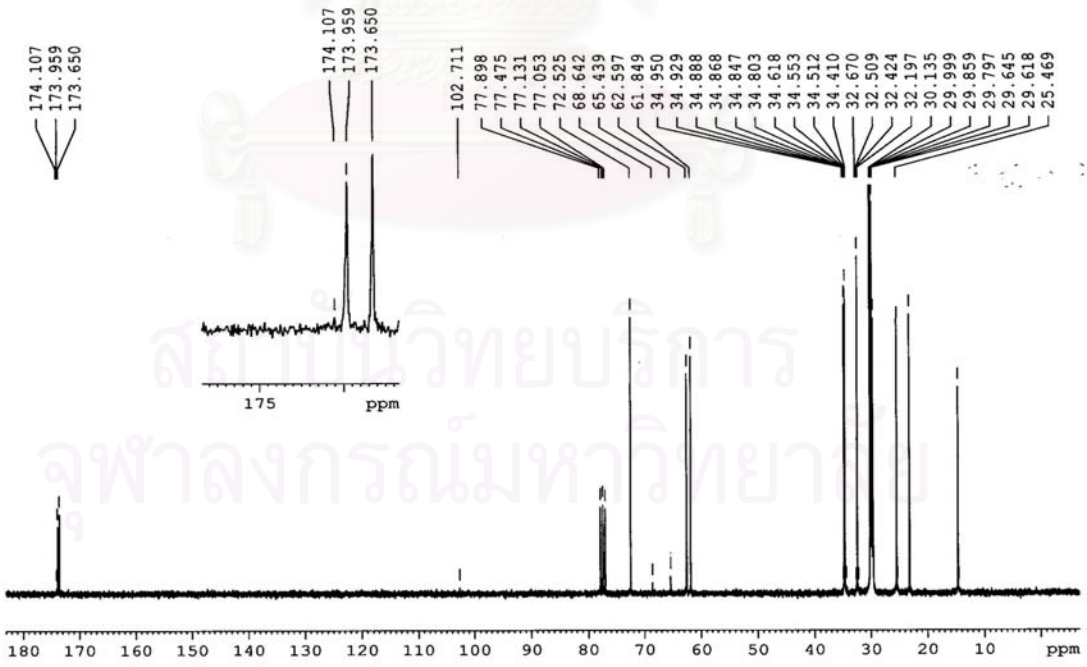

Figure 170. The 75 MHz ^{13}C-NMR spectrum of 1,2-*O*-dilauroyl-*rac*-glycerol (**19**) in $CDCl_3$.

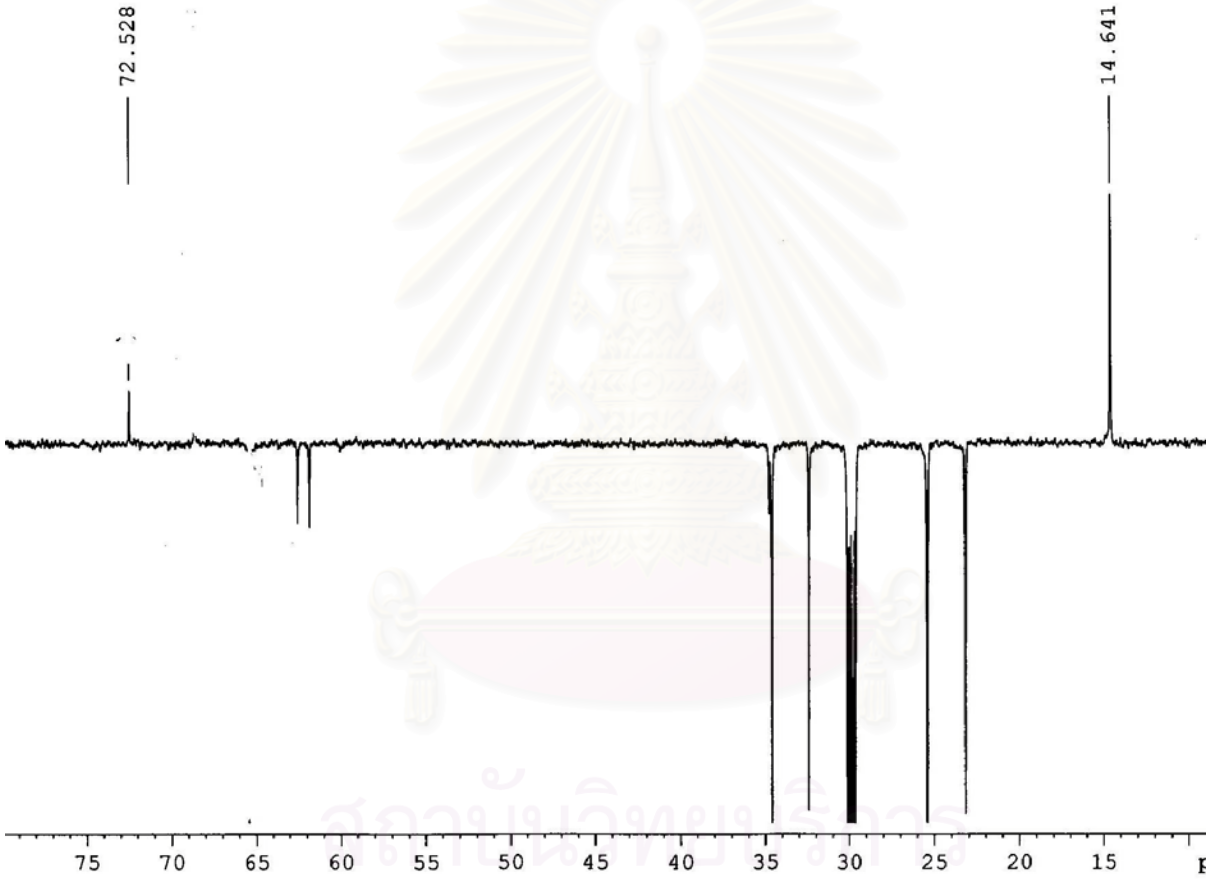

Figure 171. The DEPT 135 spectrum of 1,2-*O*-dilaurovl-*rac*-glycerol (**19**) in $CDCl_3$.

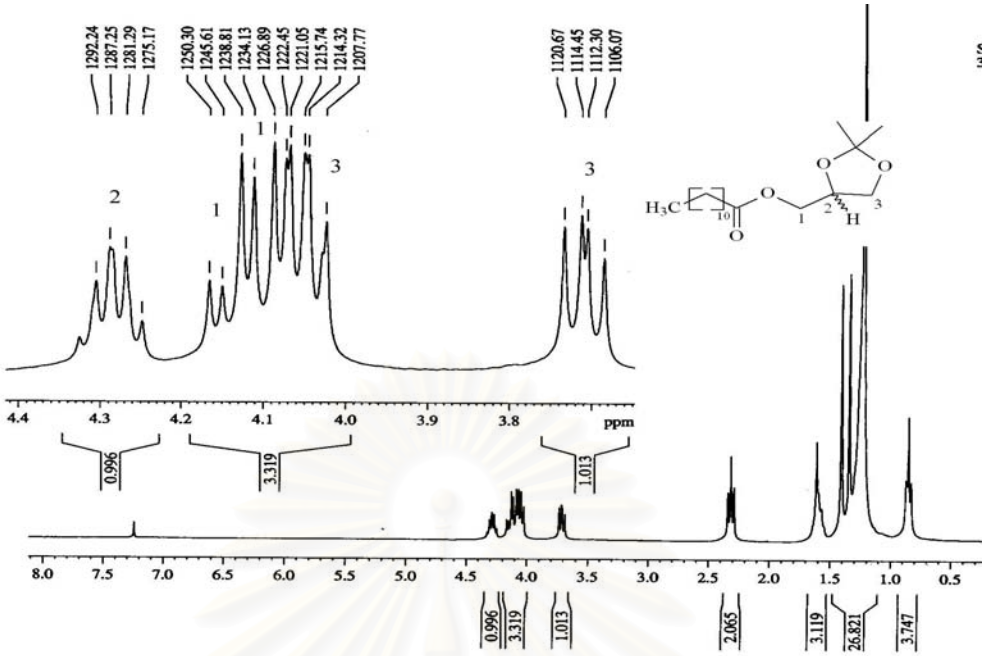

Figure 172. The 300 MHz ^{1}H-NMR spectrum of 1-*O*-lauroyl-2,3-isopropylidene-*rac*-glycerol (**20a**) in $CDCl_3$.

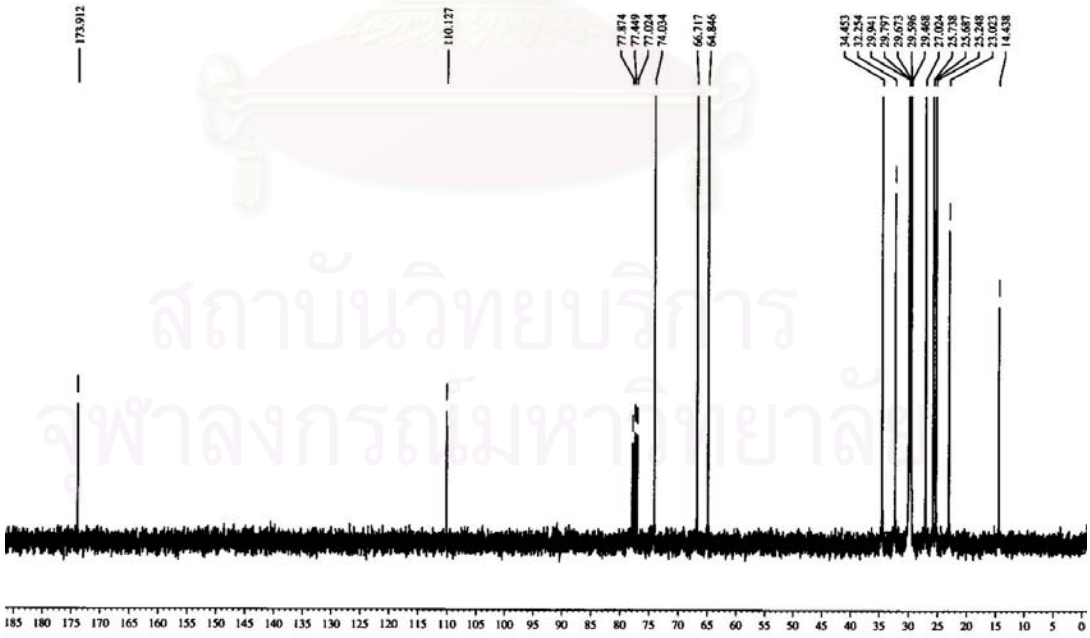

Figure 173. The 75 MHz ^{13}C-NMR spectrum of 1-*O*-lauroyl-2,3-isopropylidene-*rac*-glycerol (**20a**) in $CDCl_3$.

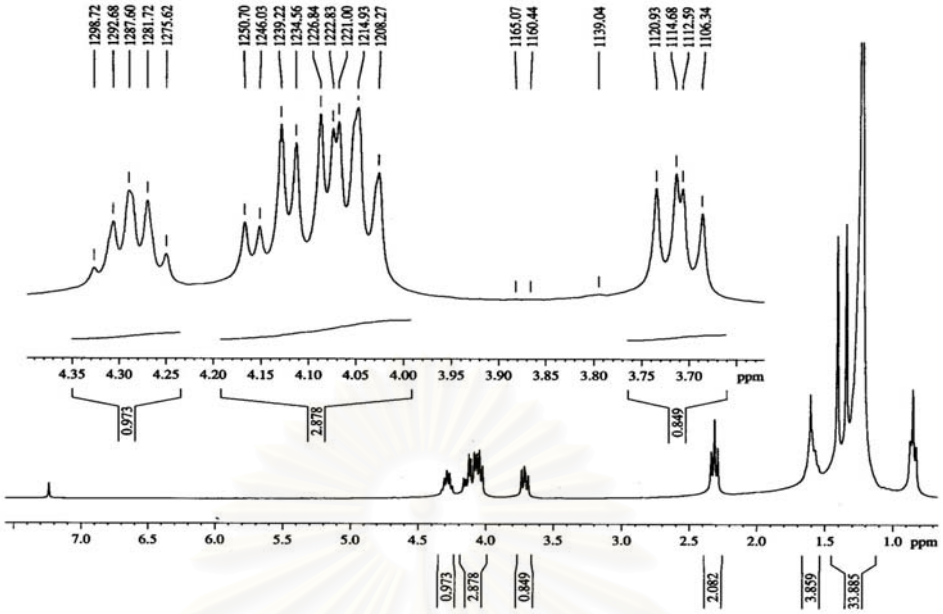

Figure 174. The 300 MHz ^{1}H-NMR spectrum of 1-*O*-stearoyl-2,3-isopropylidene-*rac*-glycerol (**20b**) in $CDCl_3$.

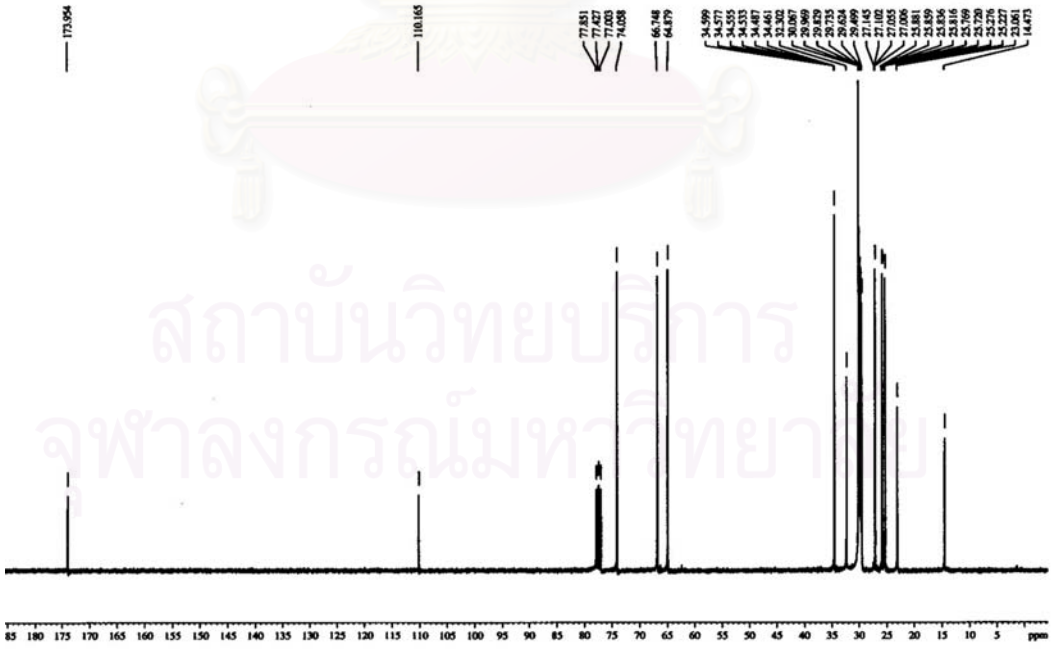

Figure 175. The 75MHz ^{13}C-NMR spectrum of 1-*O*-stearoyl-2,3-isopropylidene-*rac*-glycerol (**20b**) in $CDCl_3$.

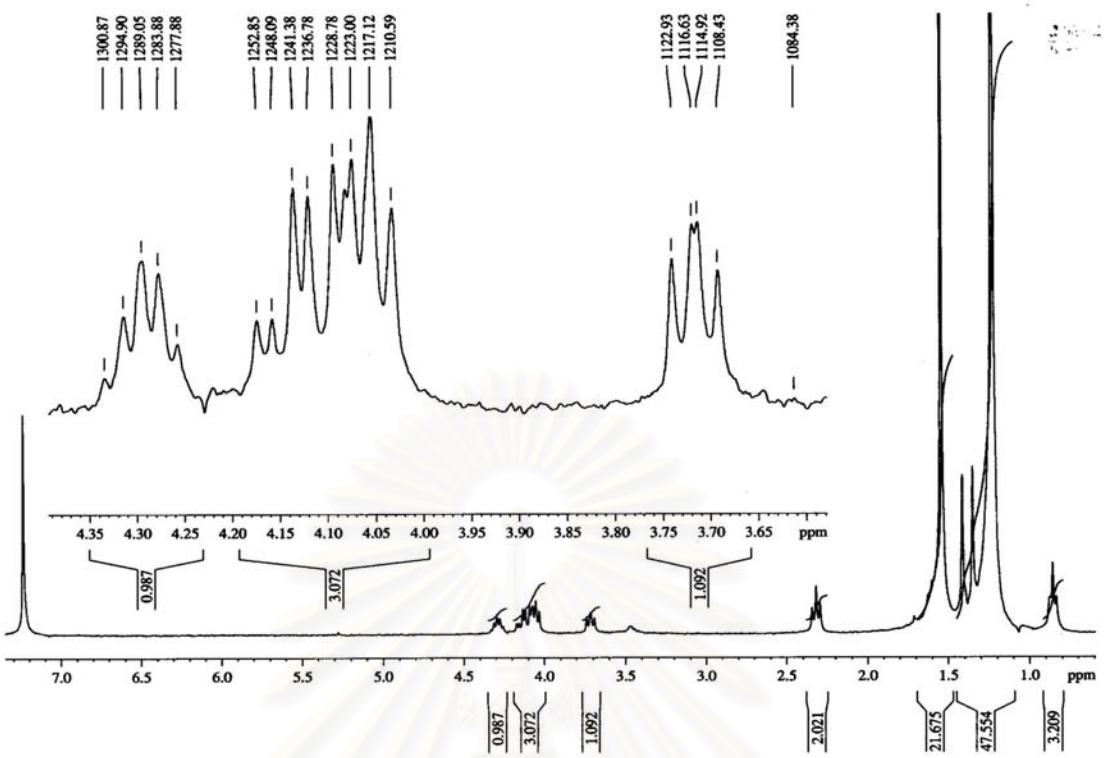

Figure 176. The 300 MHz ^{1}H-NMR spectrum of 1-*O*-behenoyl-2,3-isopropylidene-*rac*-glycerol (**20c**) in $CDCl_3$.

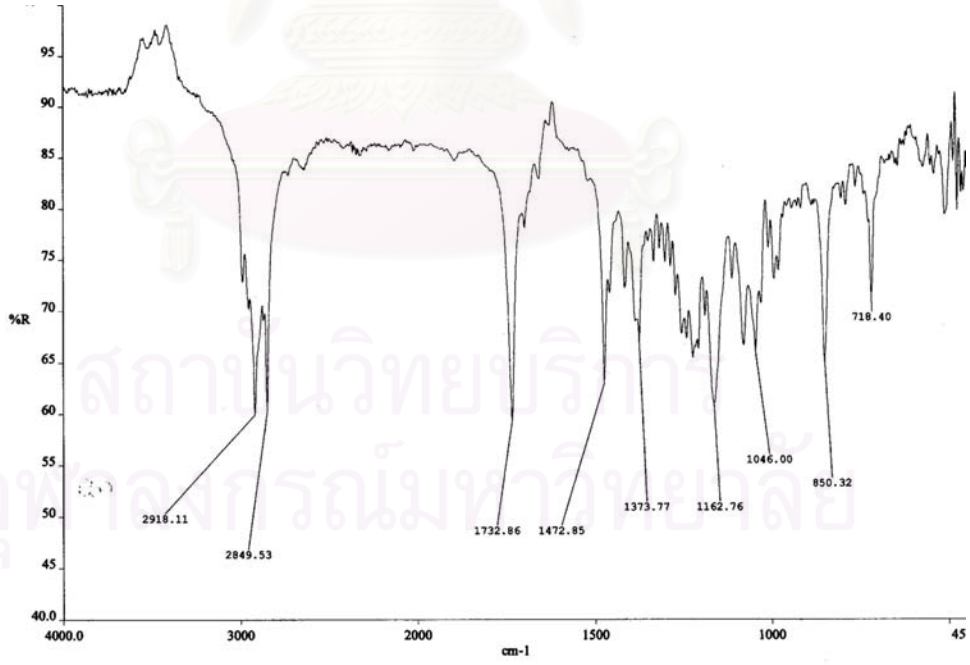

Figure 177. The infrared spectrum of 1-*O*-behenoyl-2,3-isopropylidene-*rac*-glycerol (**20c**).

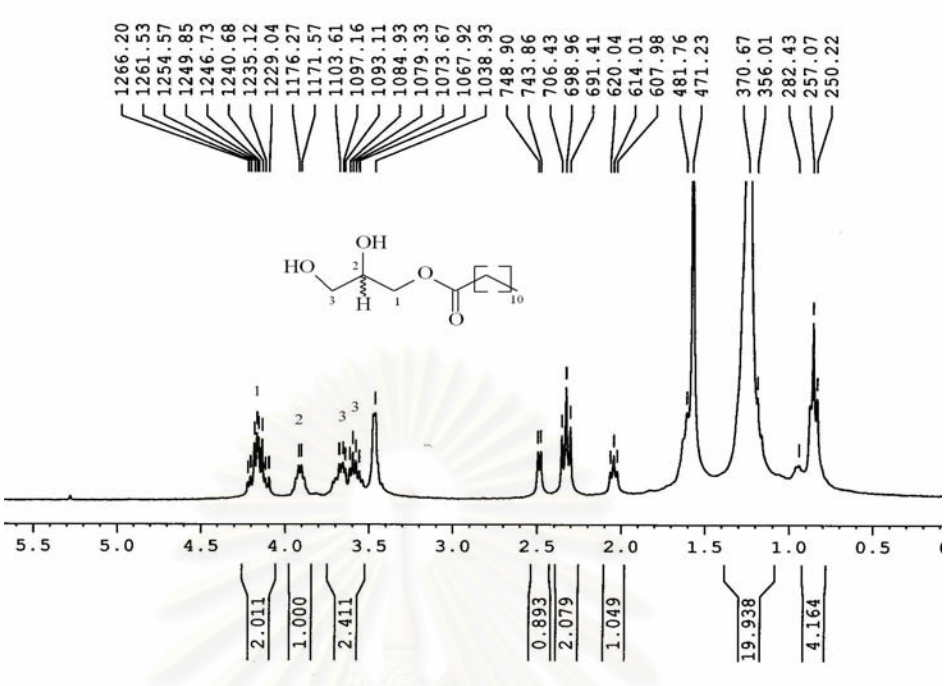

Figure 178. The 300 MHz ^{1}H-NMR spectrum of 1-*O*-lauroyl-*rac*-glycerol (**21a**) in $CDCl_3$.

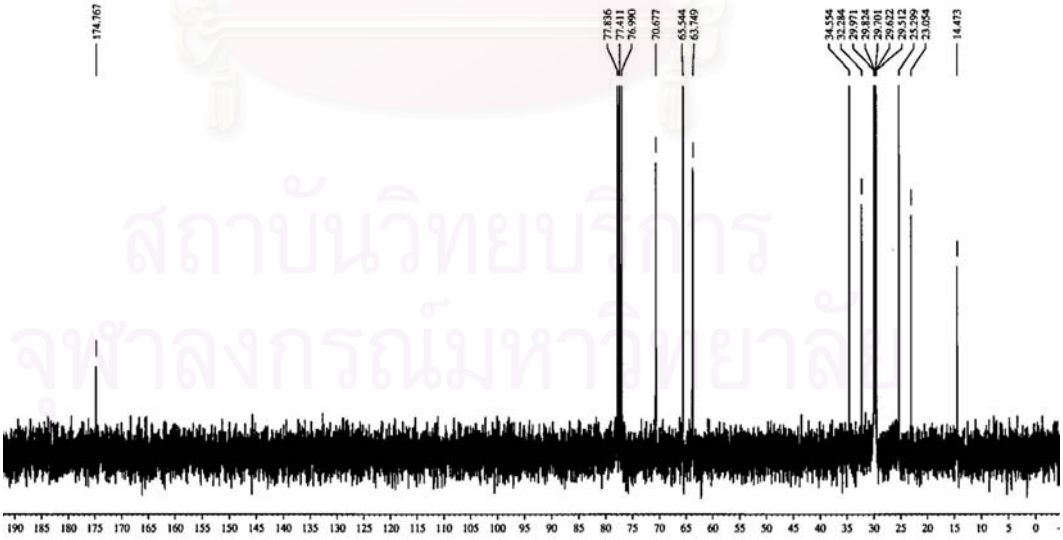

Figure 179. The 75 MHz ^{13}C-NMR spectrum of 1-*O*-lauroyl-*rac*-glycerol (**21a**) in $CDCl_3$.

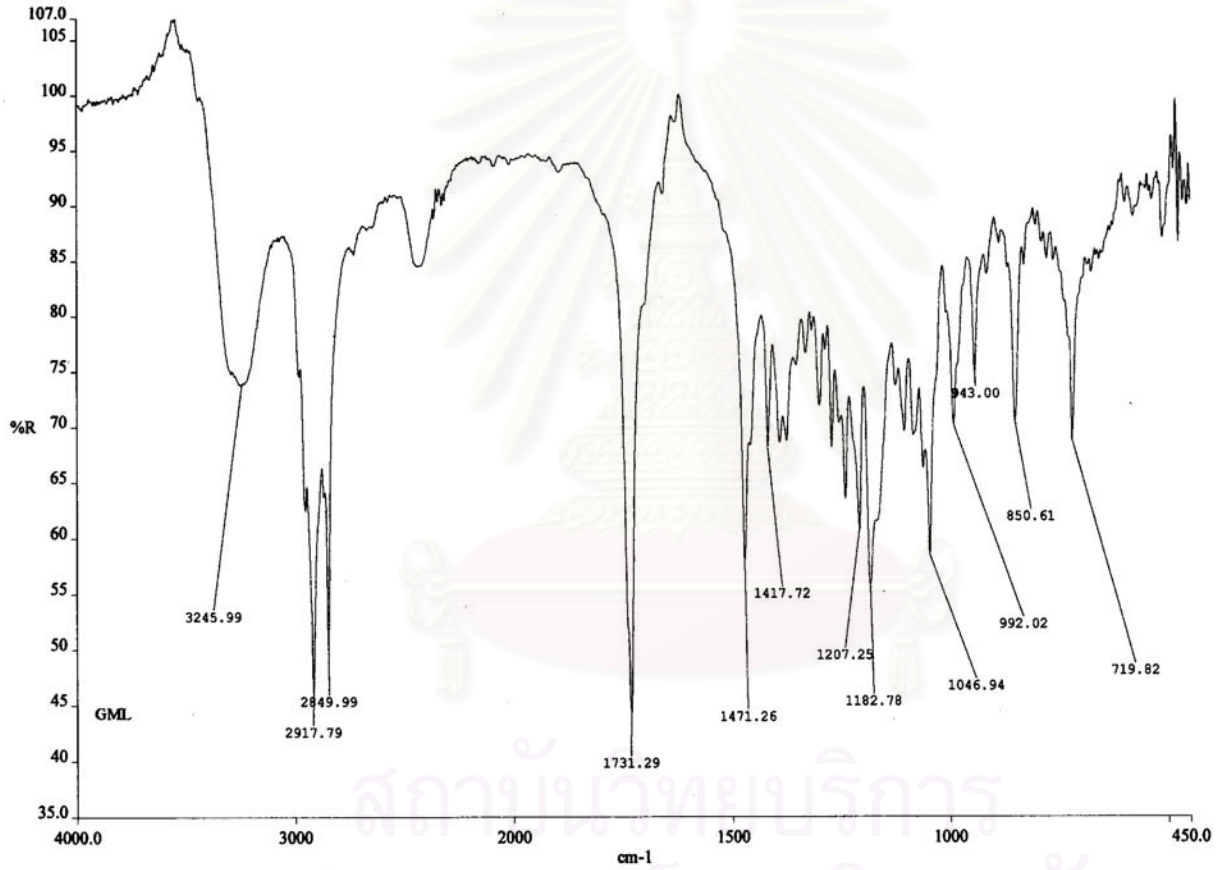

Figure 180. The infrared spectrum of 1-*O*-lauroyl-*rac*-glycerol (**21a**).

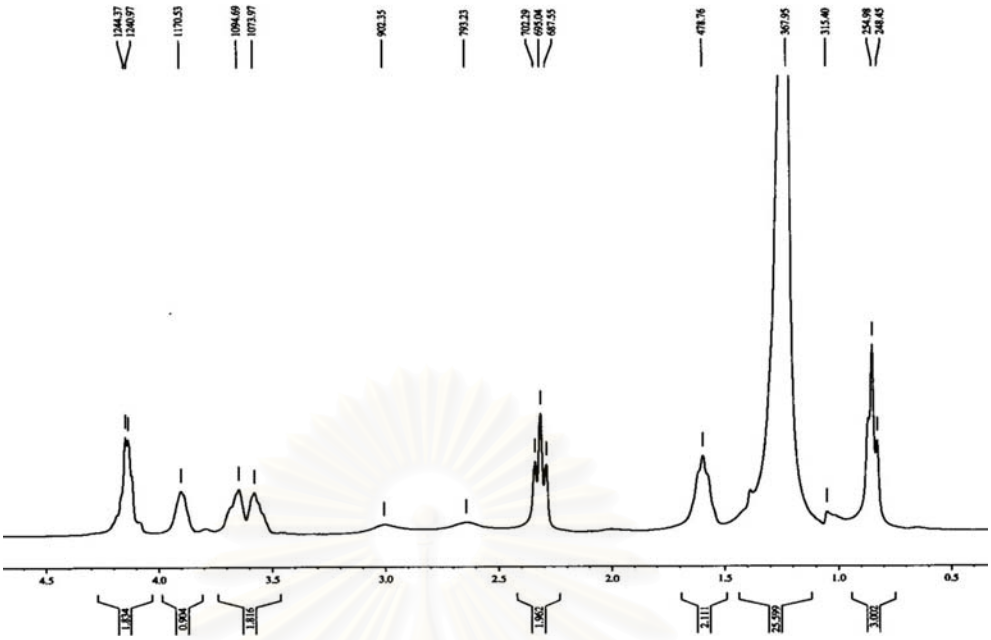

Figure 181. The 300 MHz ^{1}H-NMR spectrum of 1-*O*-stearoyl-*rac*-glycerol (**21b**) in $CDCl_3$.

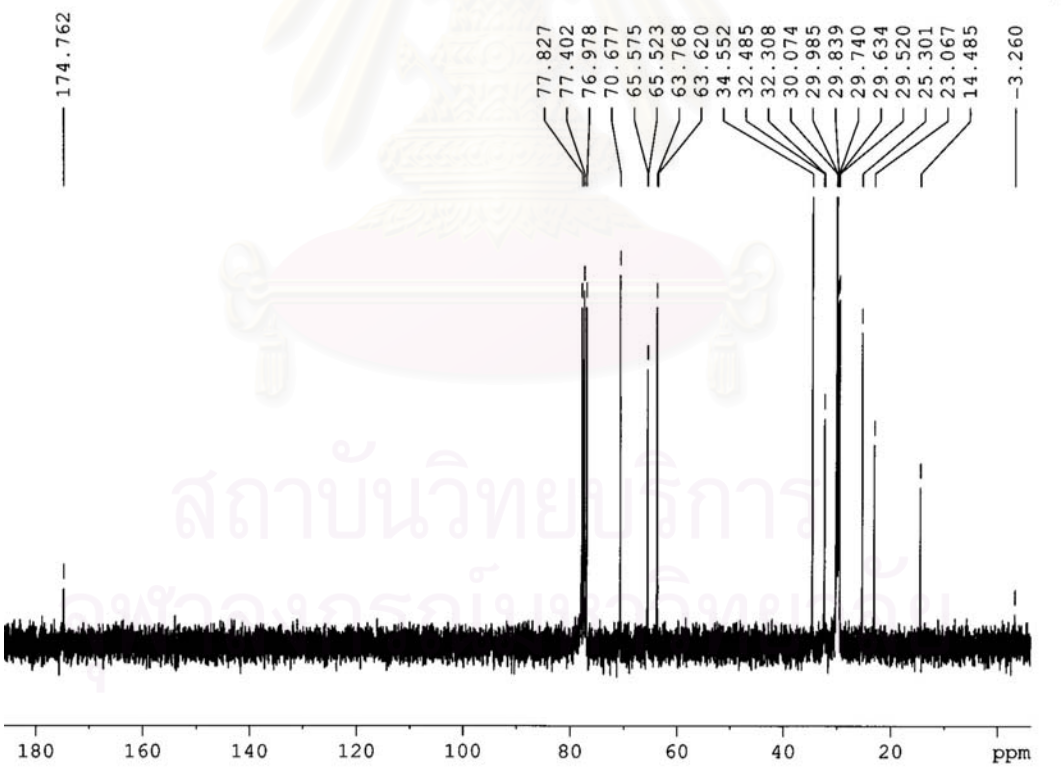

Figure 182. The 75 MHz ^{13}C-NMR spectrum of 1-*O*-stearoyl-*rac*-glycerol (**21b**) in $CDCl_3$.

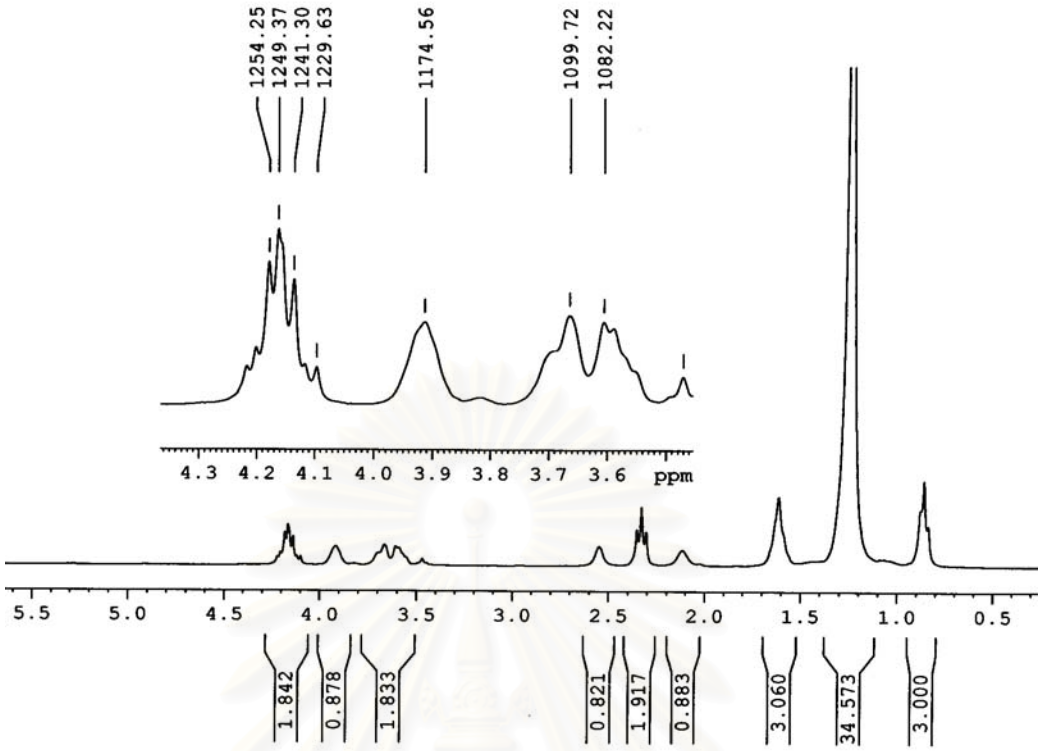

Figure 183. The 300 MHz ^{1}H-NMR spectrum of 1-*O*-behenoyl-*rac*-glycerol (**21c**) in $CDCl_3$.

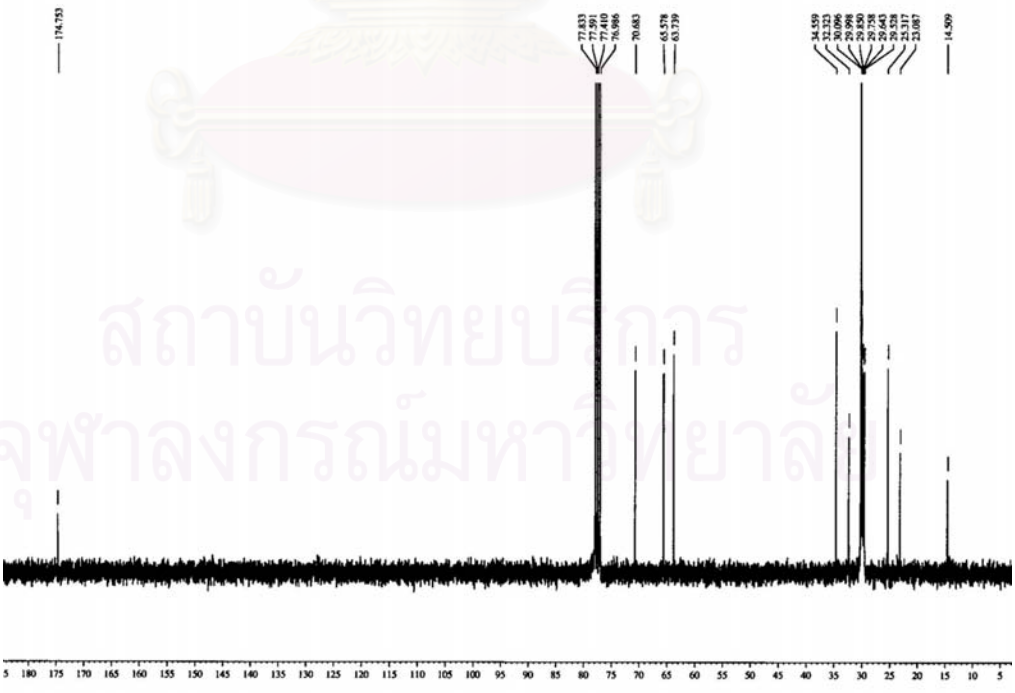

Figure 184. The 75 MHz ^{13}C-NMR spectrum of 1-*O*-behenoyl-*rac*-glycerol (**21c**) in $CDCl_3$.

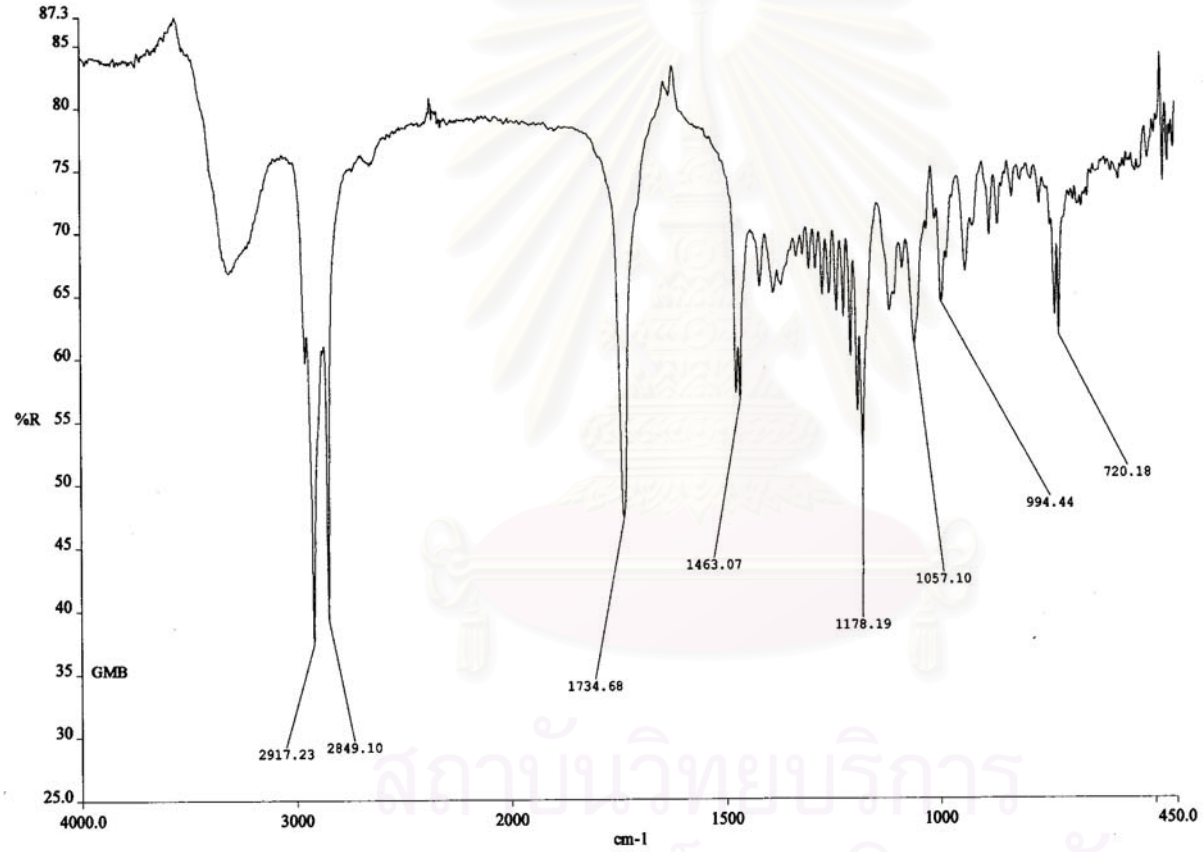

Figure 185. The infrared spectrum of 1-*O*-behenoyl-*rac*-glycerol (**21c**).

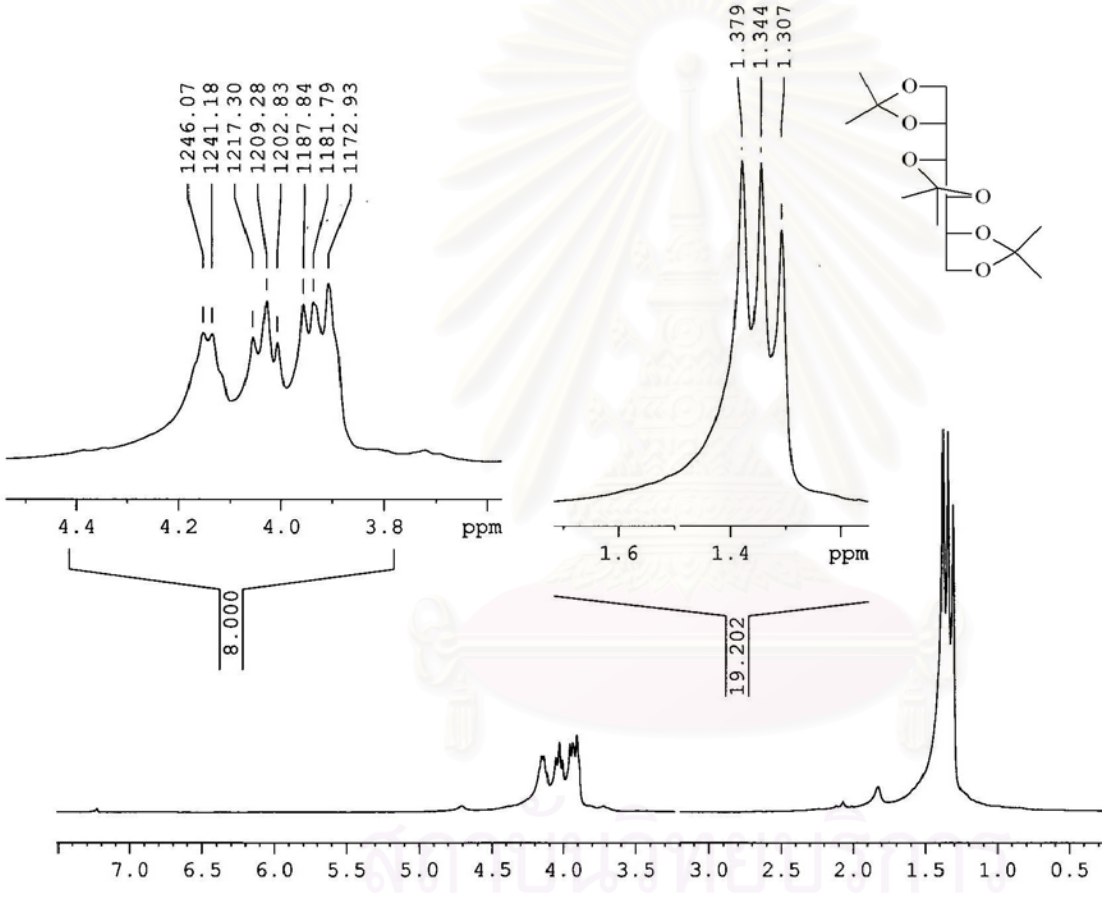

Figure 186. The 300 MHz ^{1}H-NMR spectrum of 1,2:3,4:5,6-tri-*O*-isopropylidene-D-mannitol (**23**) in $CDCl_3$.

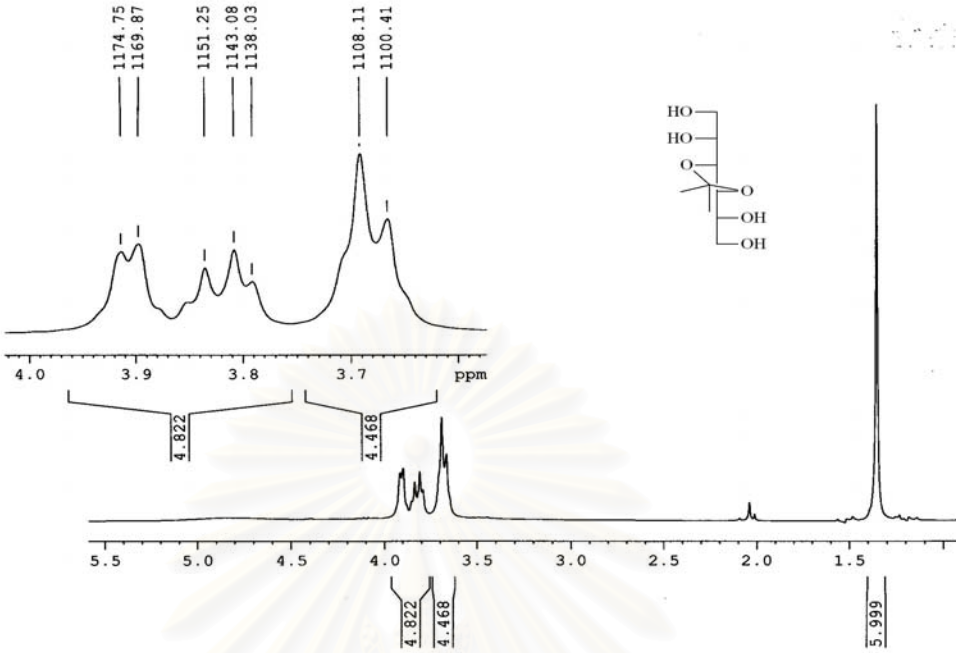

Figure 187. The 300 MHz ^{1}H-NMR spectrum of 3,4-*O*-isopropylidene-D-mannitol (**24**) in $CDCl_3$.

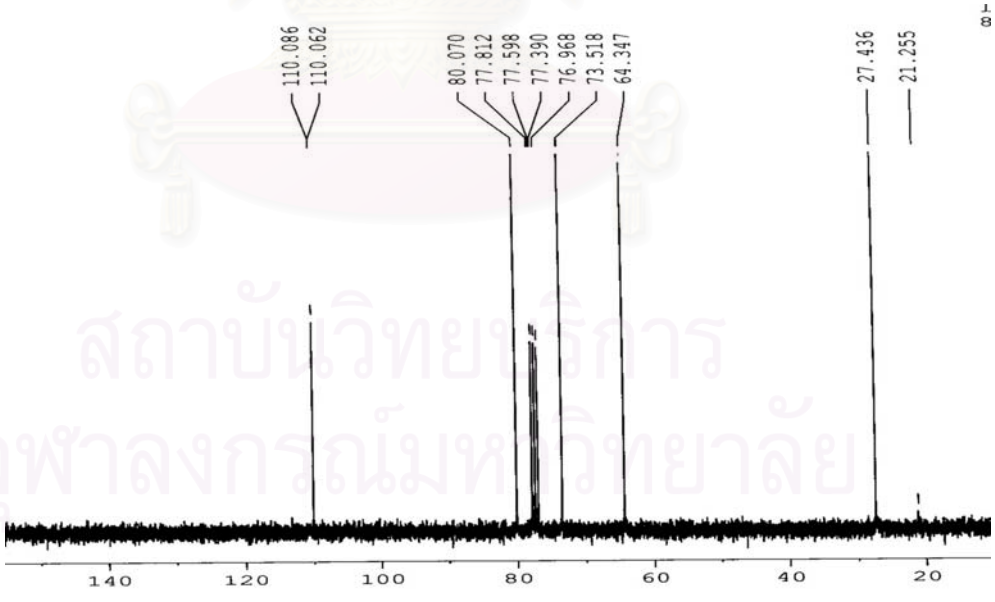

Figure 188. The 75 MHz ^{13}C-NMR spectrum of 3,4-*O*-isopropylidene-D-mannitol (**24**) in $CDCl_3$.

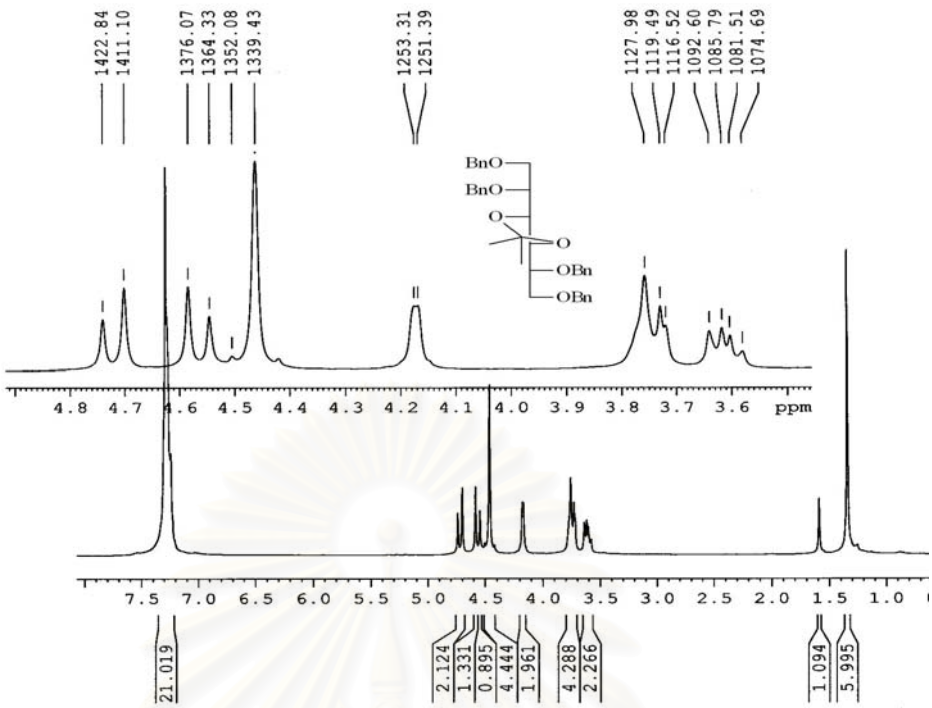

Figure 189. The 300 MHz ^{1}H-NMR spectrum of 1,2:5,6-tetra-*O*-benzyl-3,4-*O*-isopropylidene-D-mannitol (**25**) in $CDCl_3$.

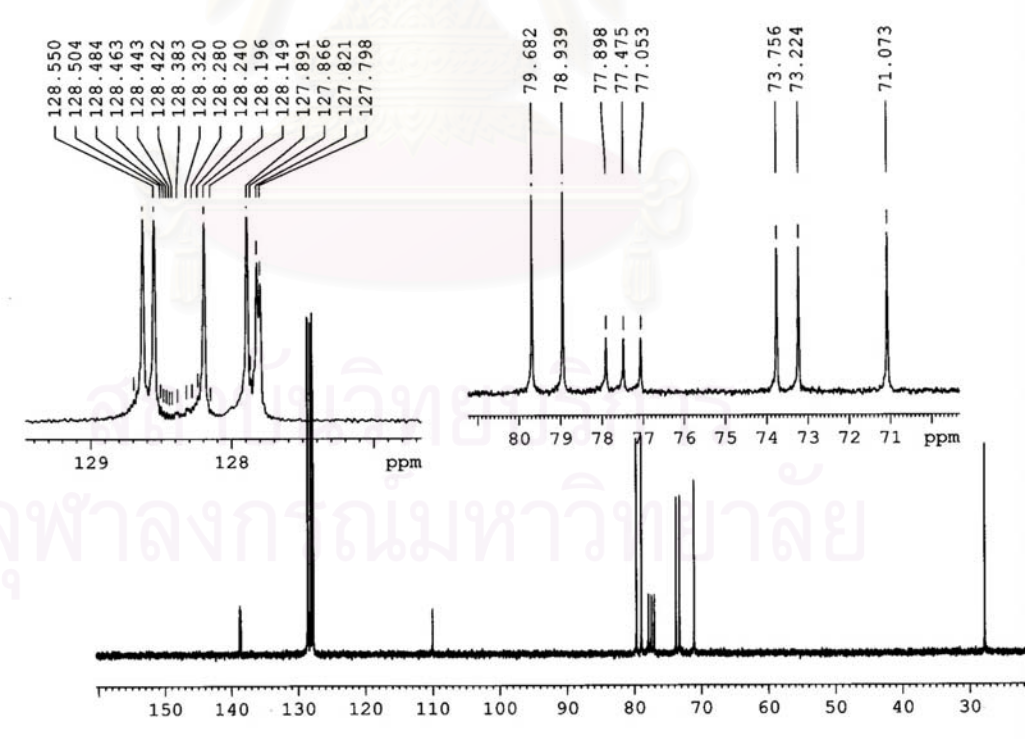

Figure 190. The 75 MHz ^{13}C-NMR spectrum of 1,2:5,6-tetra-*O*-benzyl-3,4-*O*-isopropylidene-D-mannitol (**25**) in $CDCl_3$.

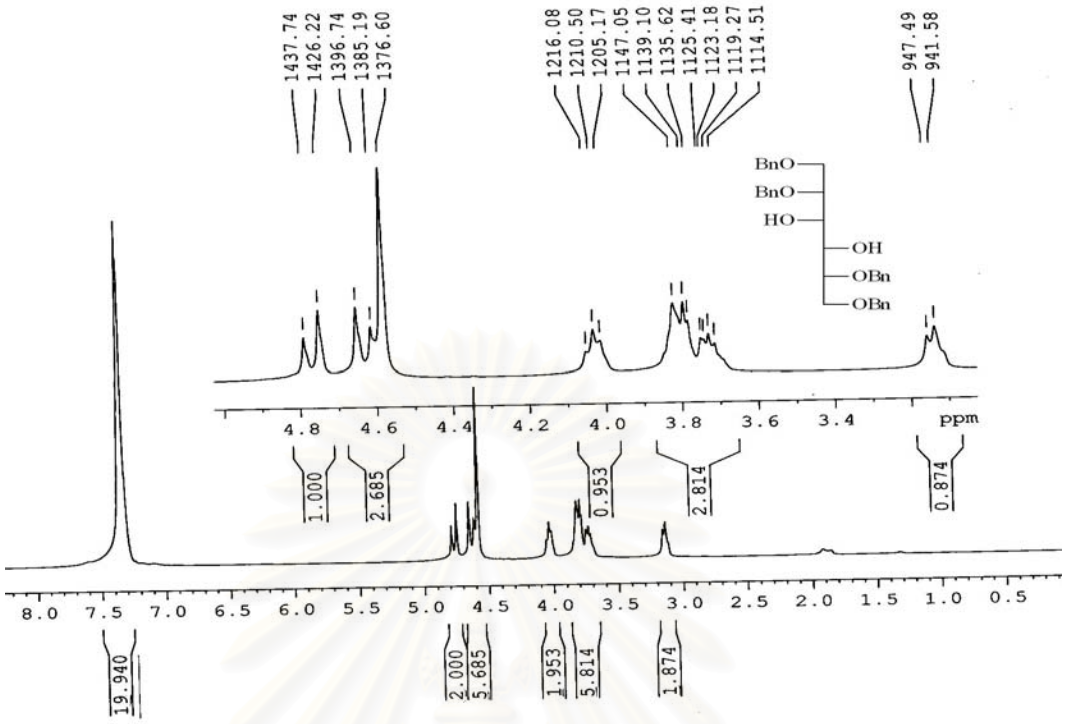

Figure 191. The 300 MHz ^{1}H-NMR spectrum of 1,2:5,6-tetra-*O*-benzyl-D-mannitol (**26**) in $CDCl_3$.

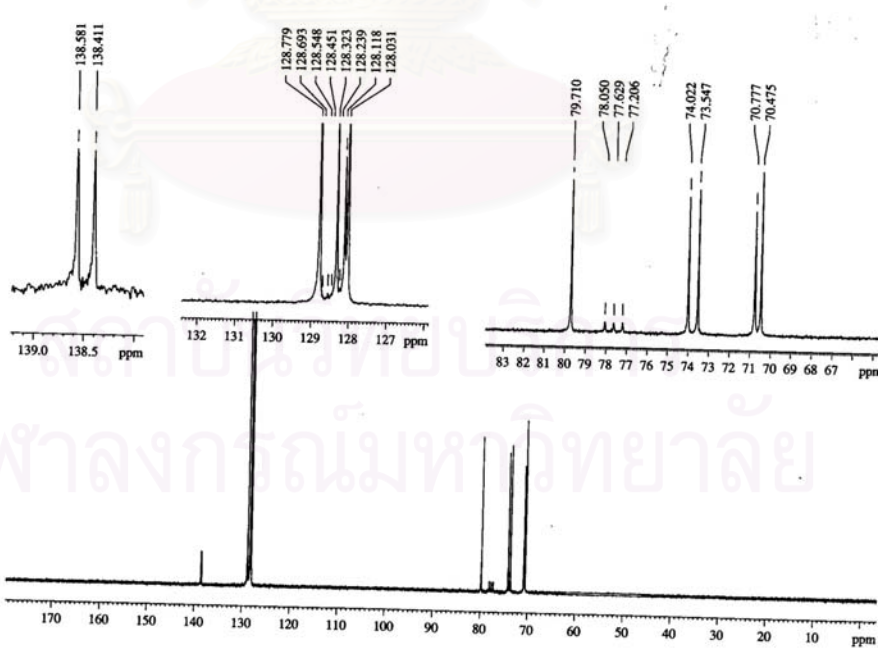

Figure 192. The 75 MHz ^{13}C-NMR spectrum of 1,2:5,6-tetra-*O*-benzyl-D-mannitol (**26**) in $CDCl_3$.

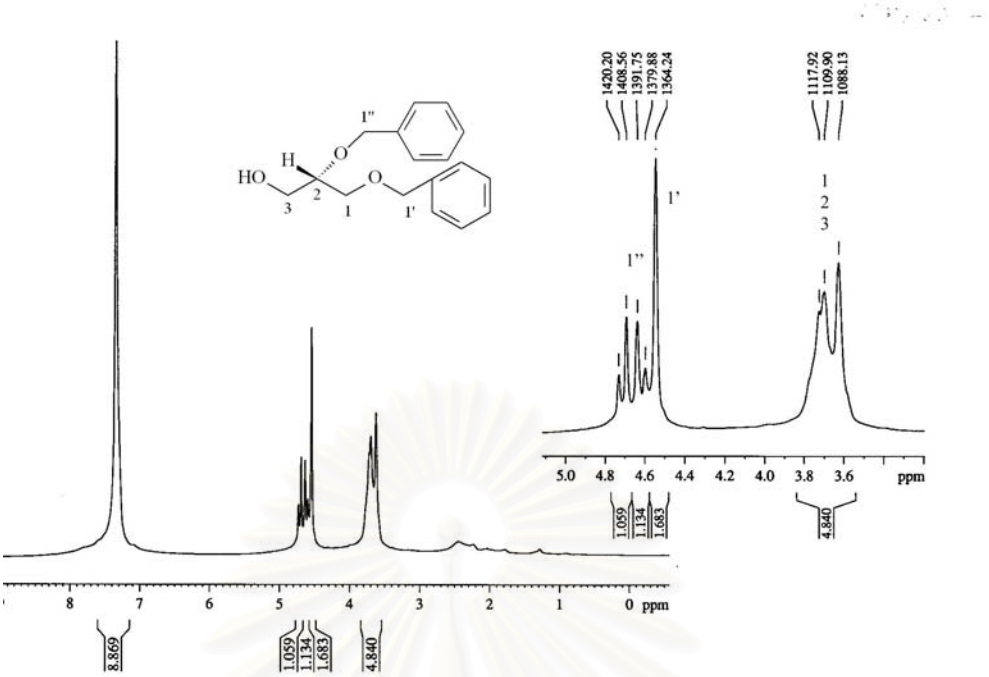

Figure 193. The 300 MHz ^{1}H-NMR spectrum of 1,2-di-*O*-benzyl-*sn*-glycerol (**28**) in $CDCl_3$.

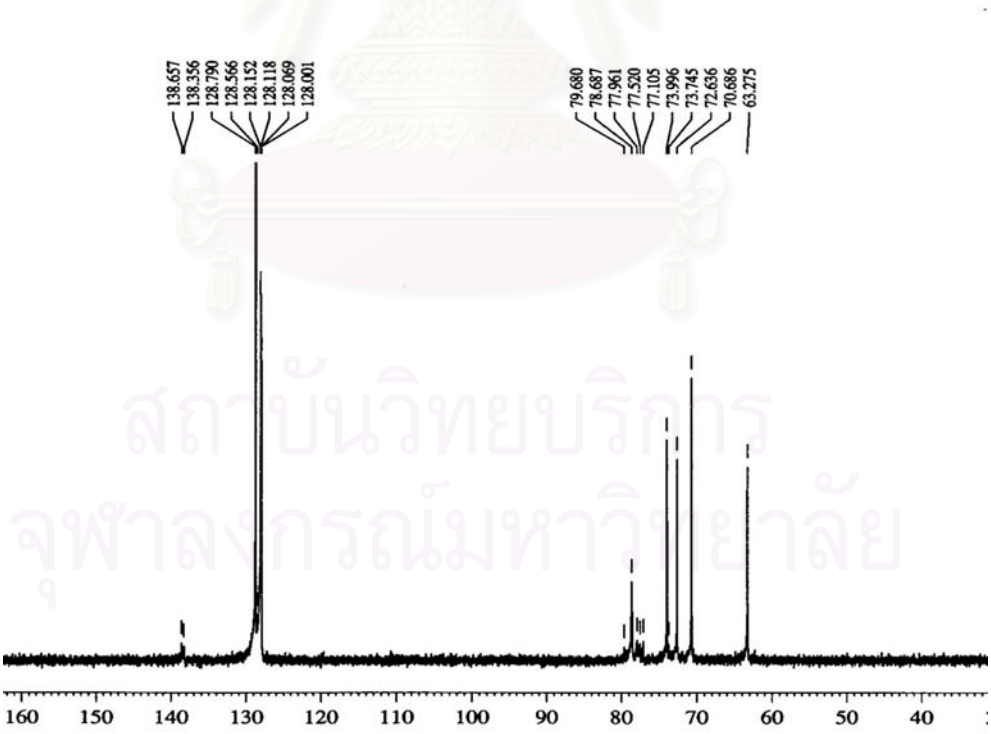

Figure 194. The 75 MHz ^{13}C-NMR spectrum of 1,2-di-*O*-benzyl-*sn*-glycerol (**28**) in $CDCl_3$.

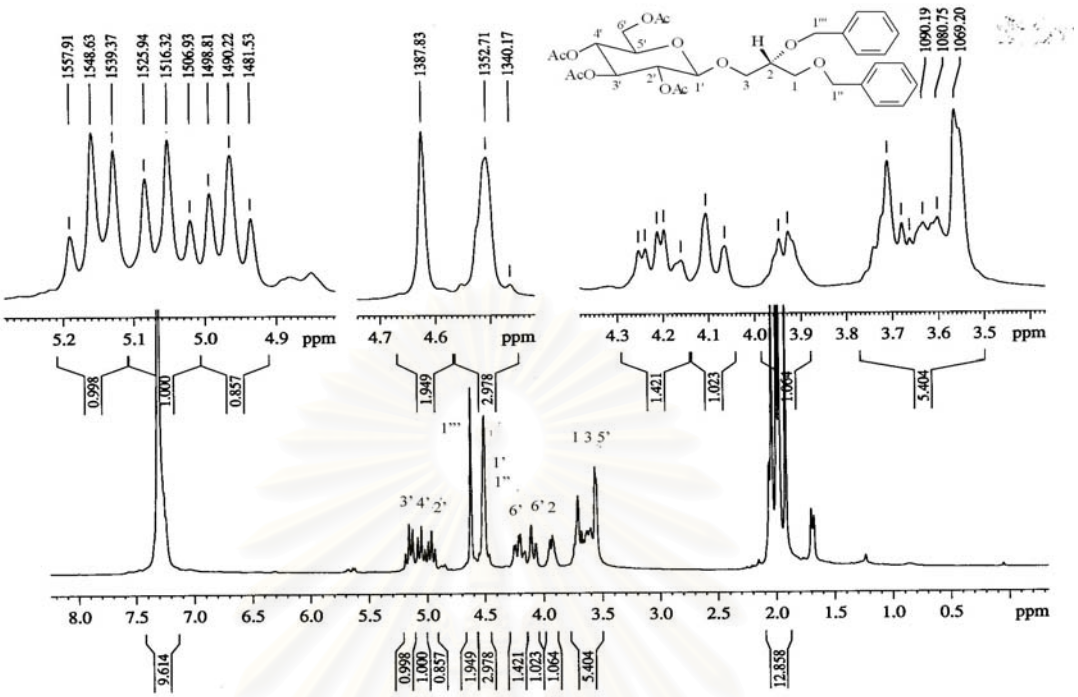

Figure 195. The 300 MHz ^{1}H-NMR spectrum of 1,2-di-*O*-benzyl-3-*O*-(β-D-2′,3′,4′,6′-tetra-*O*-acetyl-glucopyranosyl)-*sn*-glycerol (**29**) in $CDCl_3$.

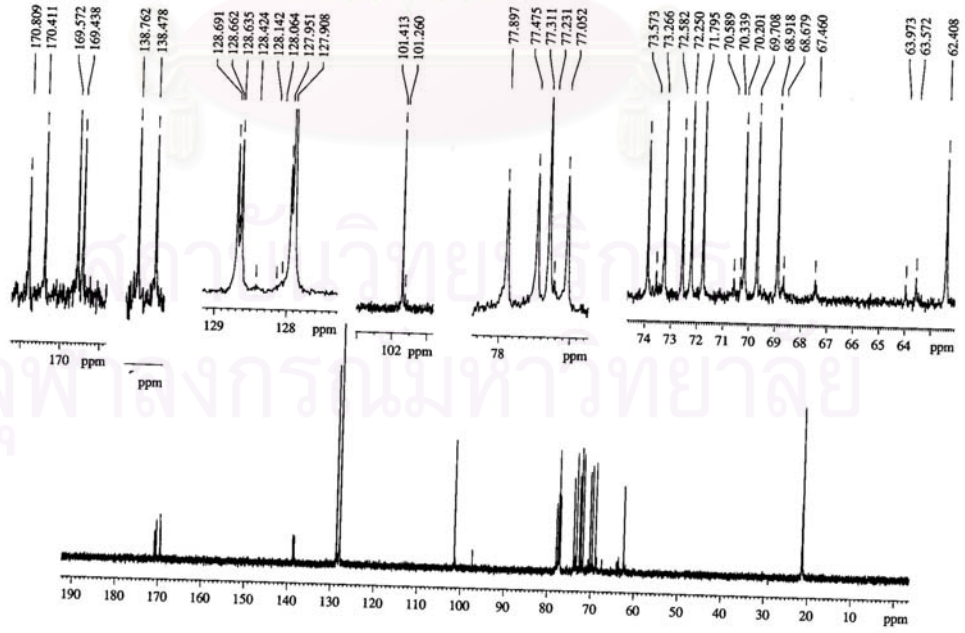

Figure 196. The 75 MHz ^{13}C-NMR spectrum of 1,2-di-*O*-benzyl-3-*O*-(β-D-2′,3′,4′,6′-tetra-*O*-acetyl-glucopyranosyl)-*sn*-glycerol (**29**) in $CDCl_3$.

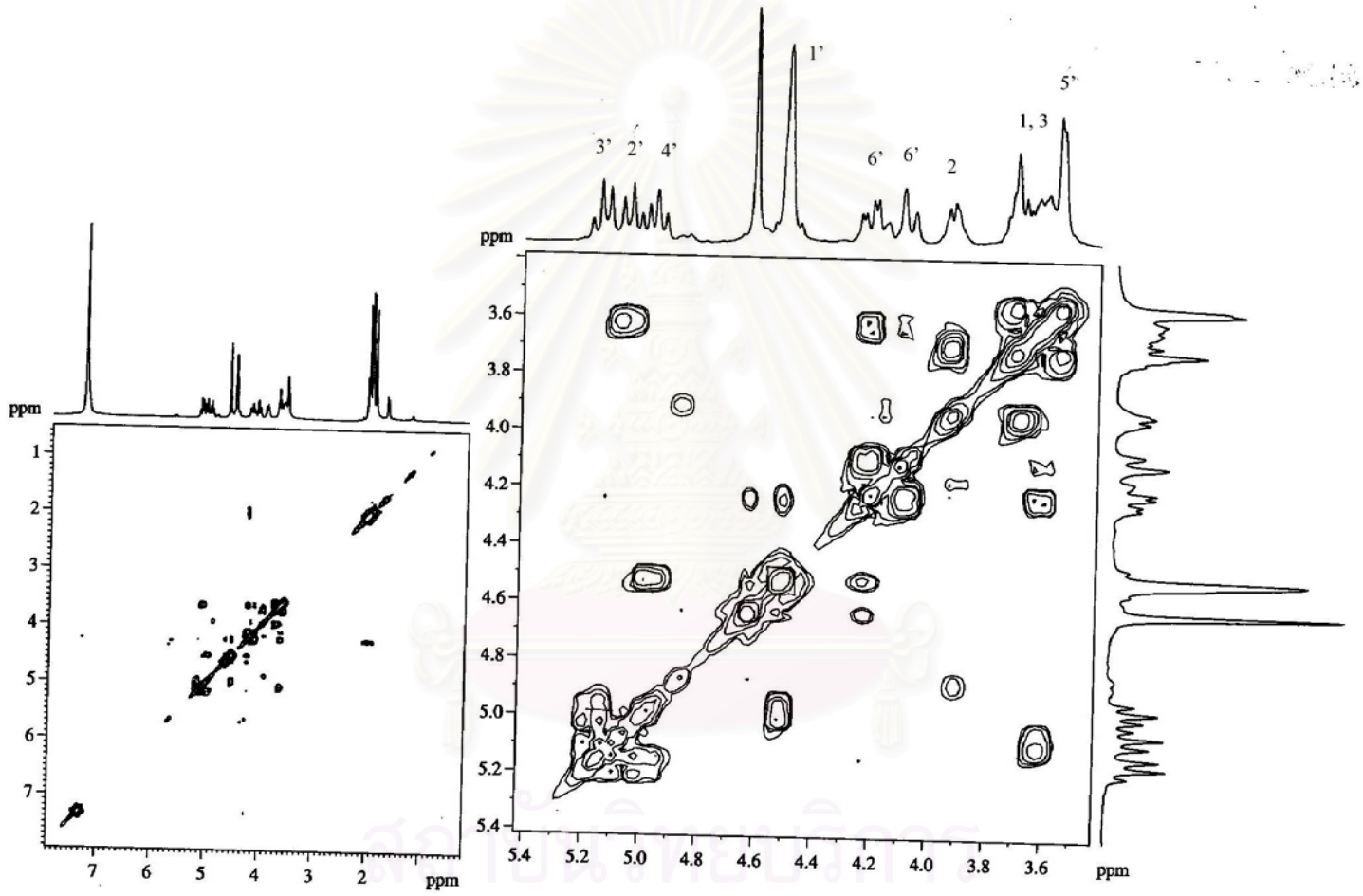

Figure 197. The ^{1}H-^{1}H COSY spectrum of 1,2-di-*O*-benzyl-3-*O*-(β-D-2′,3′,4′,6′-tetra-*O*-acetyl-glucopyranosyl)-*sn*-glycerol (**29**) in $CDCl_3$.

Figure 198. The 300 MHz ^{1}H-NMR spectrum of 1-*O*-(β-D-2′,3′,4′,6′-tetra-*O*-acetyl-glucopyranosyl)-*sn*-glycerol (**30**) in $CDCl_3$.

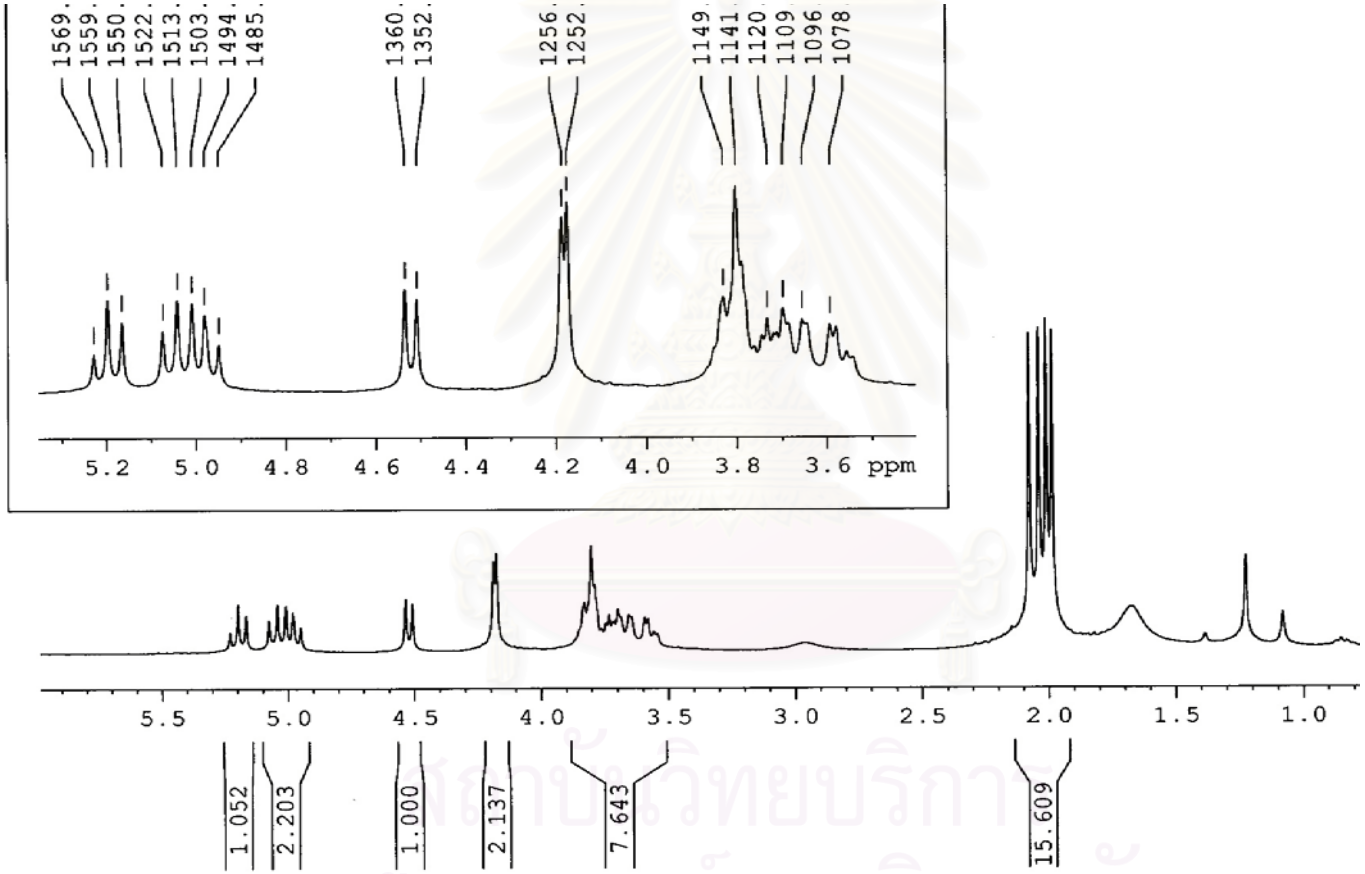

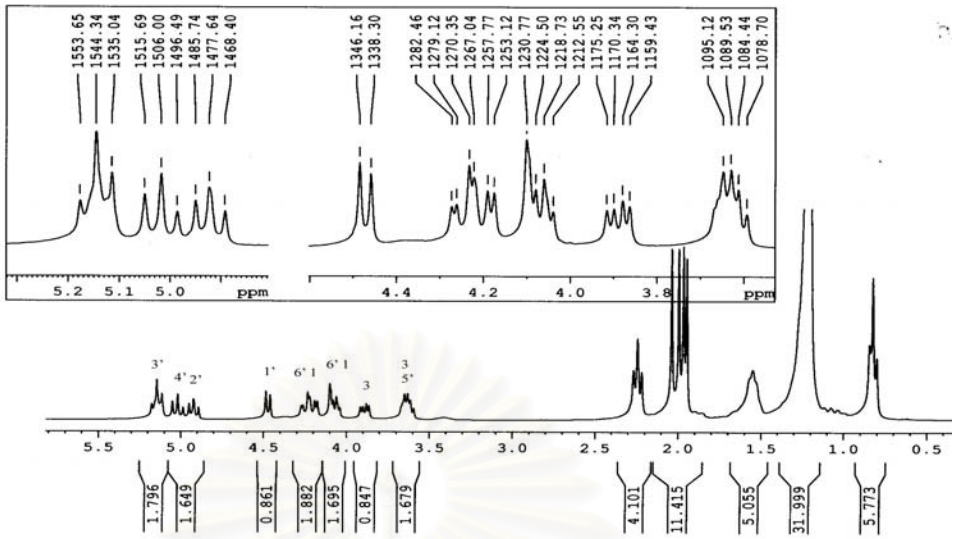

Figure 199. The 300 MHz ^{1}H-NMR spectrum of 1,2-di-*O*-lauroyl-3-*O*-(β-D-2′,3′,4′,6′-tetra-*O*-acetyl-glucopyranosyl)-*sn*-glycerol (**31a**) in $CDCl_3$.

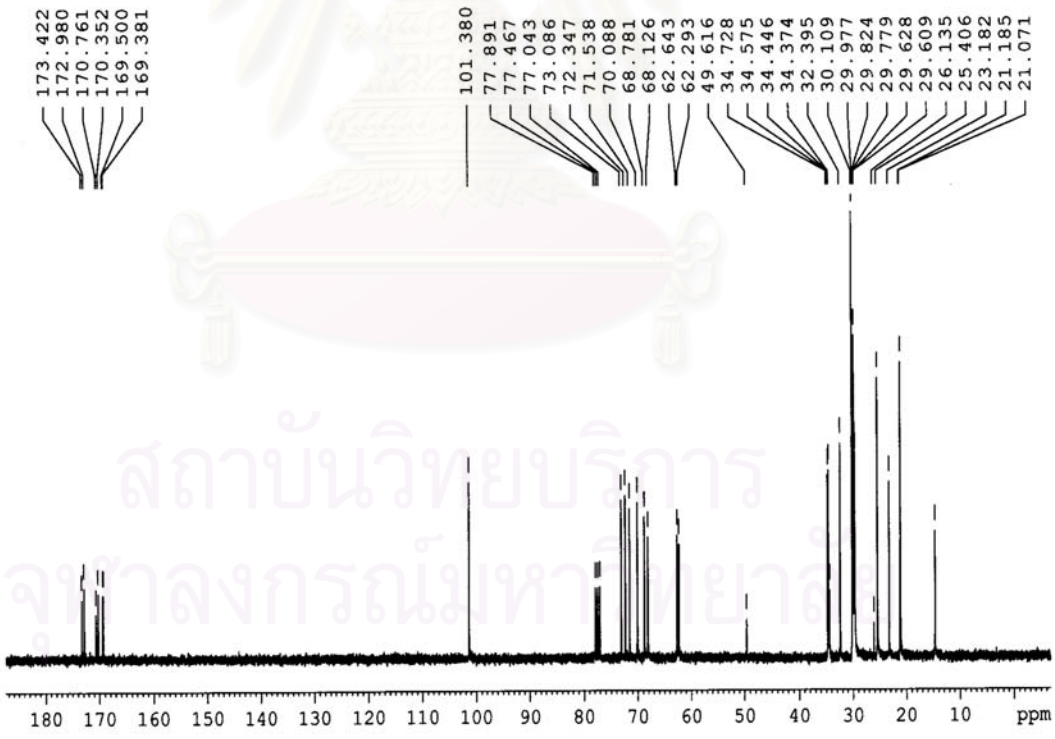

Figure 200. The 75 MHz ^{13}C-NMR spectrum of 1,2-di-*O*-lauroyl-3-*O*-(β-D-2′,3′,4′,6′-tetra-*O*-acetyl-glucopyranosyl)-*sn*-glycerol (**31a**) in $CDCl_3$.

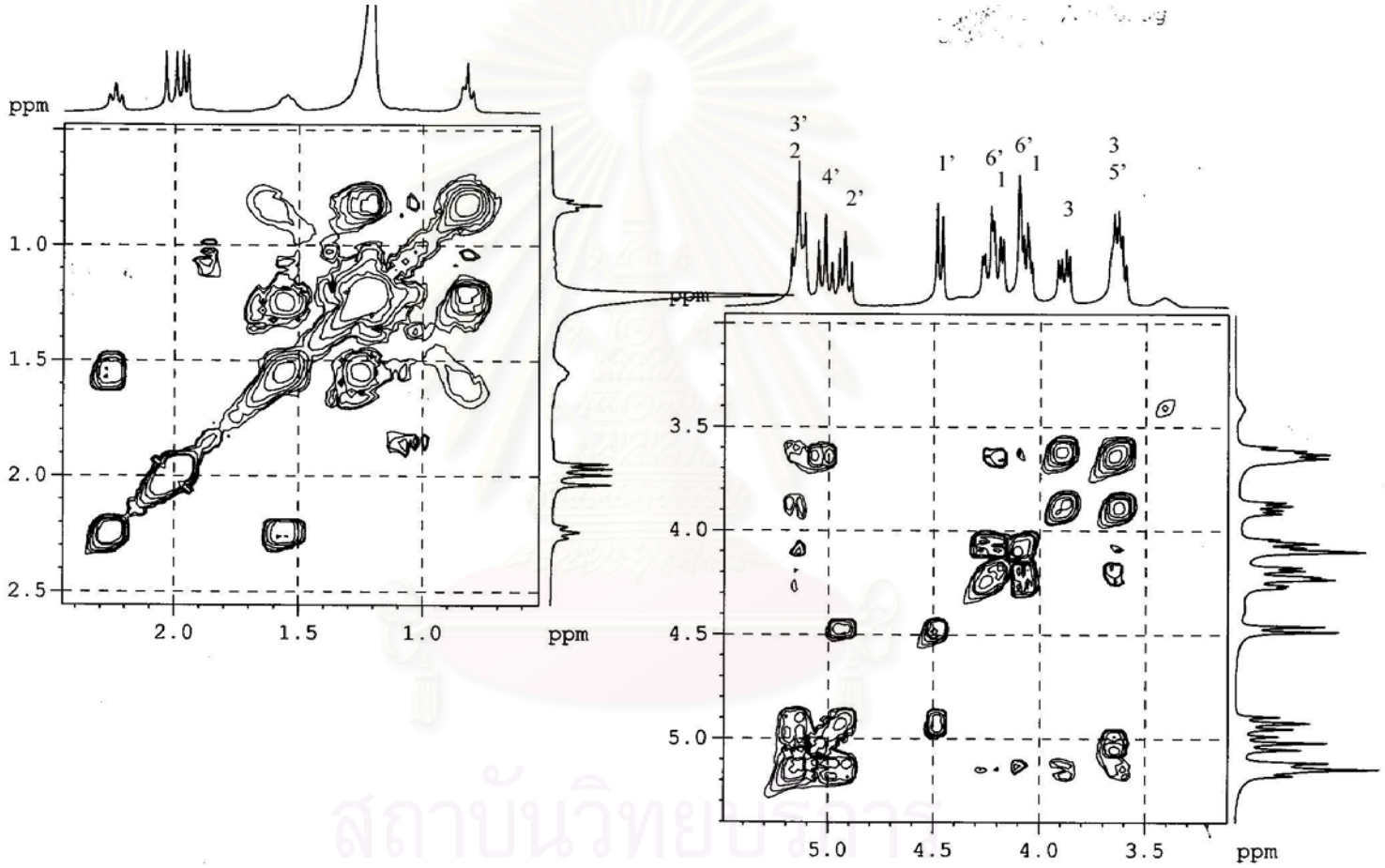

Figure 201. The ^{1}H-^{1}H COSY spectrum of 1,2-di-*O*-lauroyl-3-*O*-(β-D-2′,3′,4′,6′-tetra-*O*-acetyl-glucopyranosyl)-*sn*-glycerol (**31a**) in $CDCl_3$.

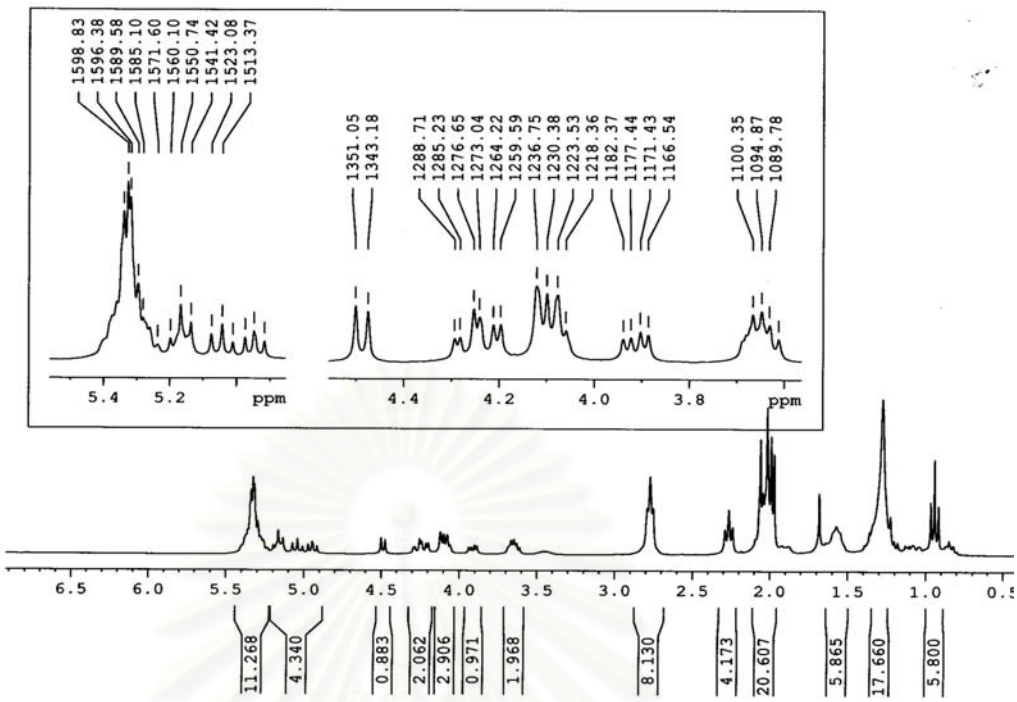

Figure 202. The 300 MHz ^{1}H-NMR spectrum of 1,2-di-*O*-linolenoyl-3-*O*-(β-D-2′,3′,4′,6′-tetra-*O*-acetyl-glucopyranosyl)-*sn*-glycerol (**31b**) in $CDCl_3$.

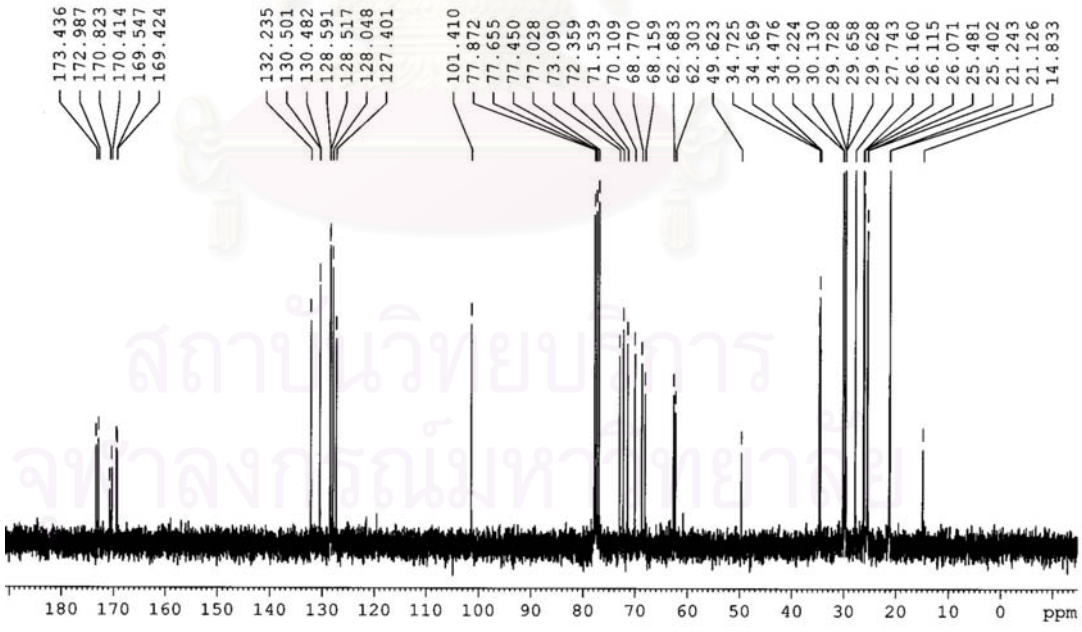

Figure 203. The 75 MHz ^{13}C-NMR spectrum of 1,2-di-*O*-linolenoyl-3-*O*-(β-D-2′,3′,4′,6′-tetra-*O*-acetyl-glucopyranosyl)-*sn*-glycerol (**31b**) in $CDCl_3$.

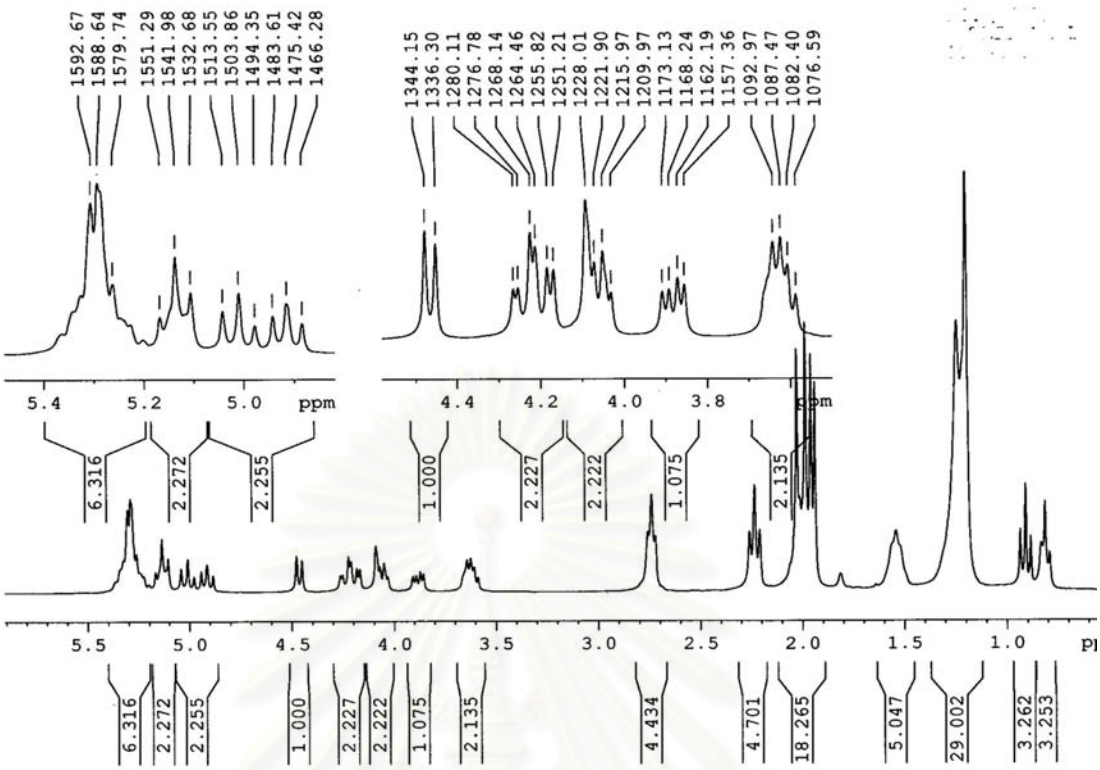

Figure 204. The 300 MHz ^{1}H-NMR spectrum of 1-*O*-linolenoyl-2-*O*-lauroyl-3-*O*-(β-D-2′,3′,4′,6′-tetra-*O*-acetyl-glucopyranosyl)-*sn*-glycerol (**31c**) in $CDCl_3$.

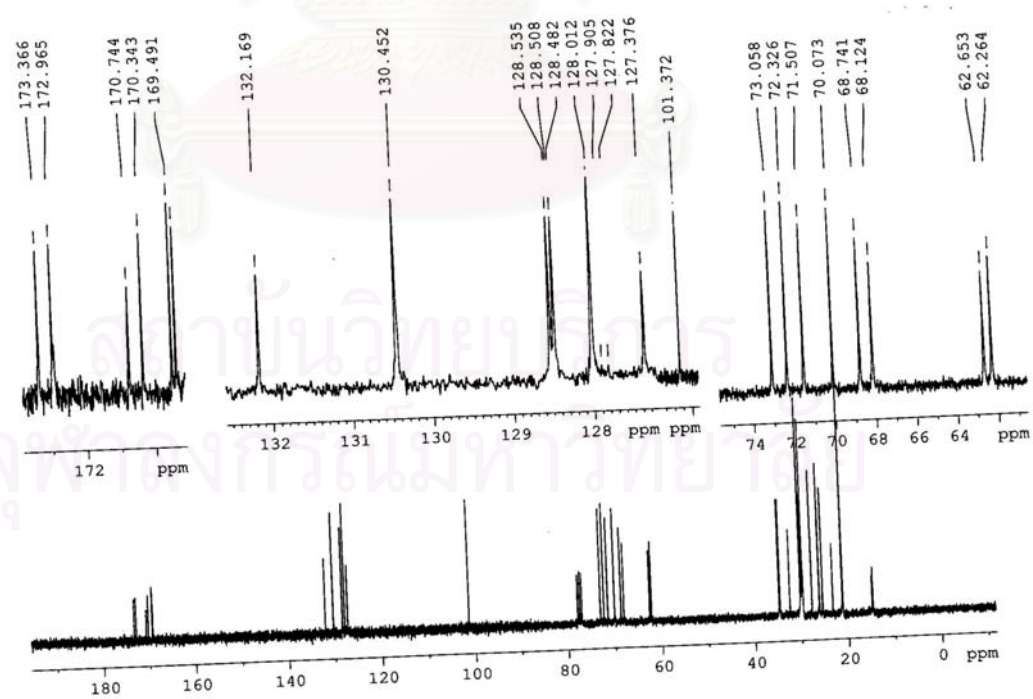

Figure 205. The 75 MHz ^{13}C-NMR spectrum of 1-*O*-linolenoyl-2-*O*-lauroyl-3-*O*-(β-D-2′,3′,4′,6′-tetra-*O*-acetyl-glucopyranosyl)-*sn*-glycerol (**31c**) in $CDCl_3$.

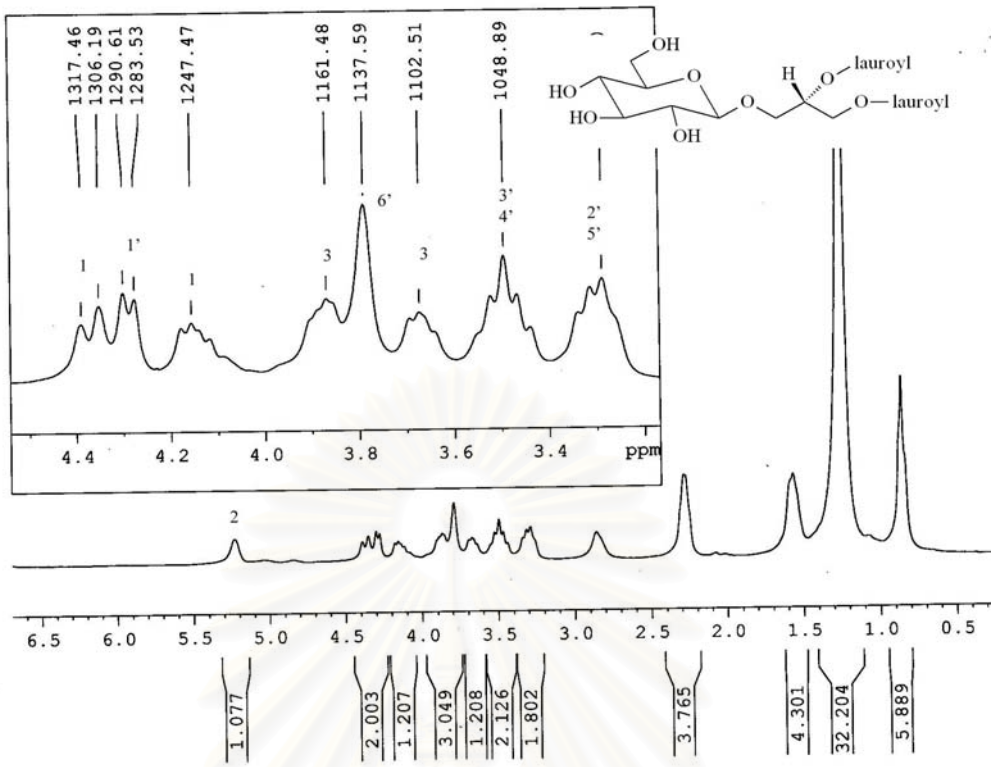

Figure 206. The 300 MHz ^{1}H-NMR spectrum of 1,2-di-*O*-lauroyl-3-*O*-β-D-gluucopyranosyl-*sn*-glycerol (**32a**) in $CDCl_3$.

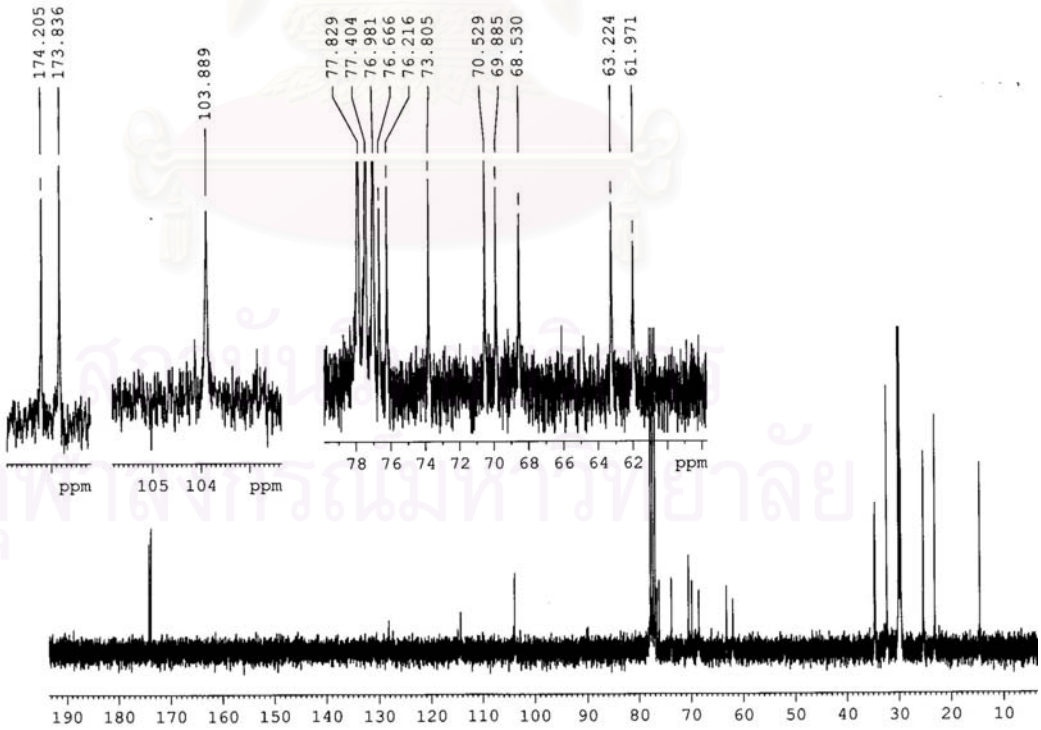

Figure 207. The 75 MHz ^{13}C-NMR spectrum of 1,2-di-*O*-lauroyl-3-*O*-β-D-gluucopyranosyl-*sn*-glycerol (**32a**) in $CDCl_3$.

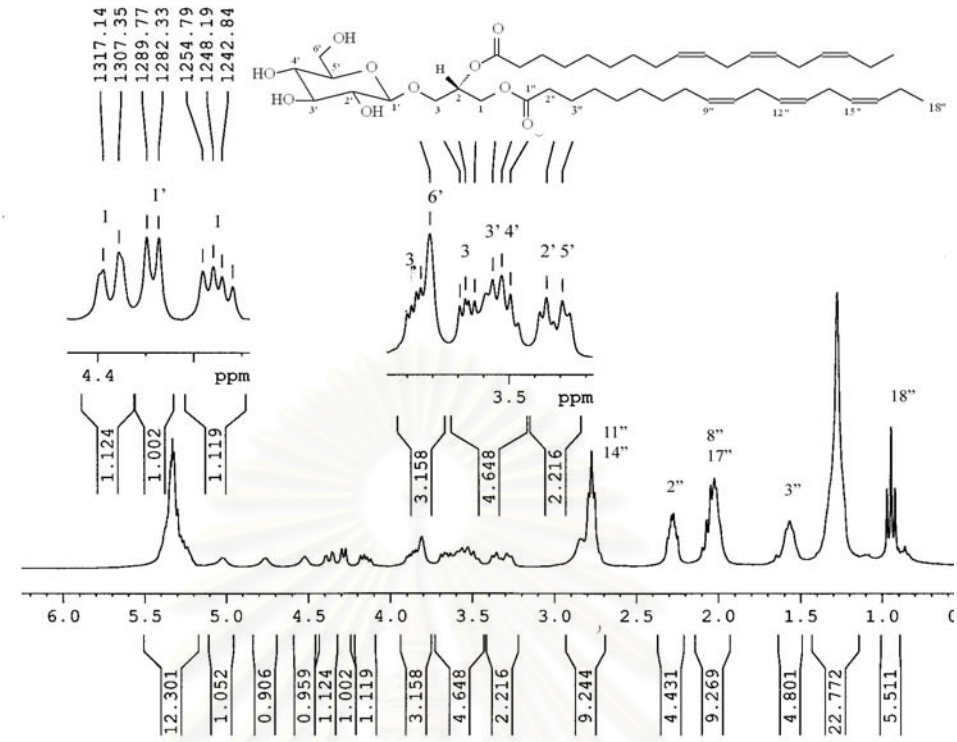

Figure 208. The 300 MHz ^{1}H-NMR spectrum of 1,2-di-*O*-linolenoyl-3-*O*-β-D-glucopyranosyl-*sn*-glycerol (**32b**) in $CDCl_3$.

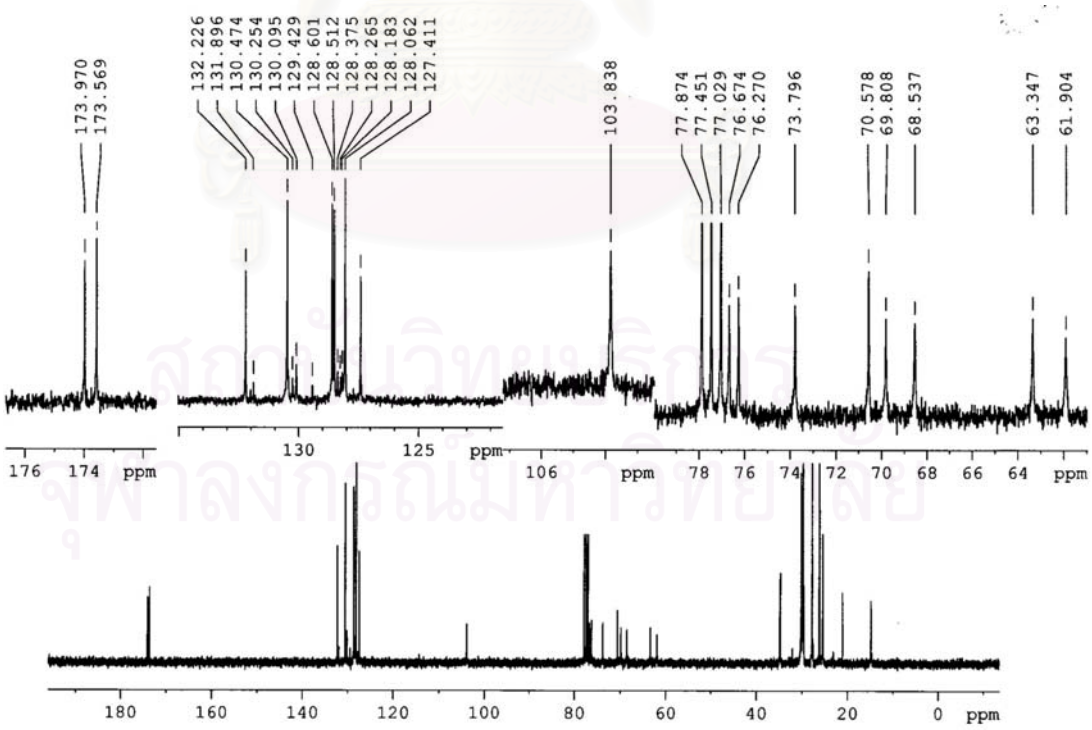

Figure 209. The 75 MHz ^{13}C-NMR spectrum of 1,2-di-*O*-linolenoyl-3-*O*-β-D-glucopyranosyl-*sn*-glycerol (**32b**) in $CDCl_3$.

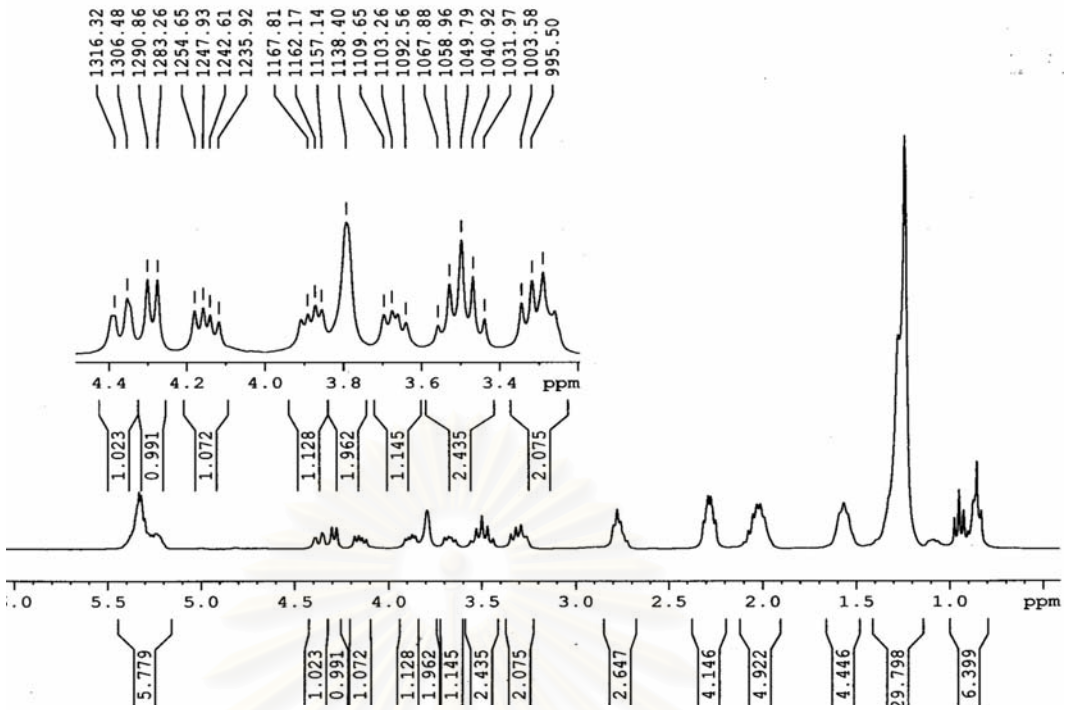

Figure 210. The 300 MHz ^{1}H-NMR spectrum of 1-*O*-linolenoyl-2-*O*-lauroyl-3-*O*-β-D-glucopyranosyl-*sn*-glycerol (**32c**) in $CDCl_3$.

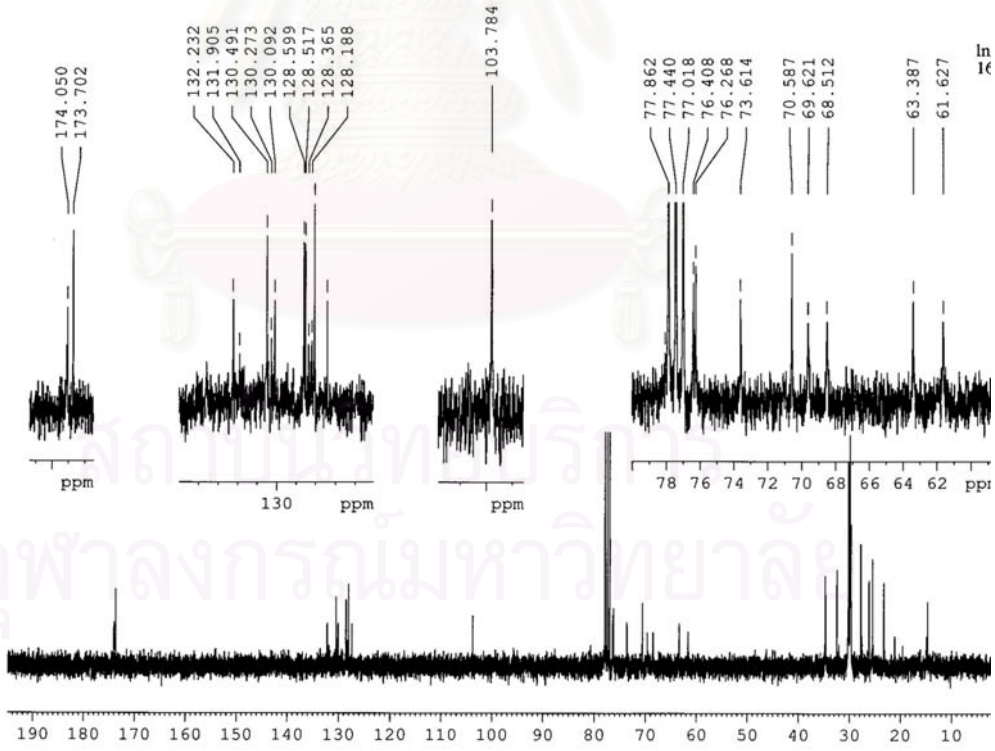

Figure 211. The 75 MHz ^{13}C-NMR spectrum of 1-*O*-linolenoyl-2-*O*-lauroyl-3-*O*-β-D-glucopyranosyl-*sn*-glycerol (**32c**) in $CDCl_3$.

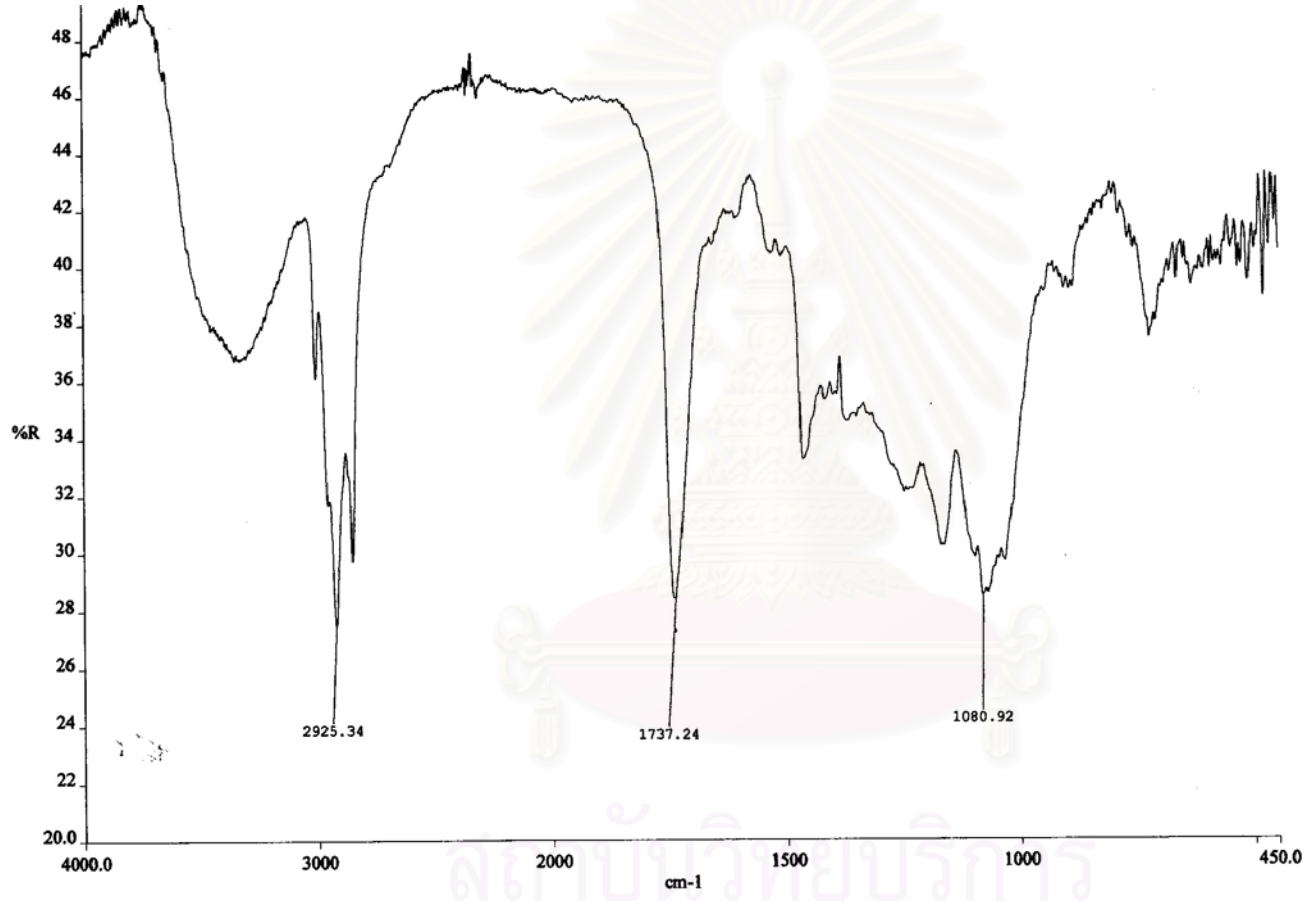

Figure 212. The infrared spectrum of 1-*O*-linolenoyl-2-*O*-lauroyl-3-*O*-β-D-glucopyranosyl-*sn*-glycerol (**32c**).

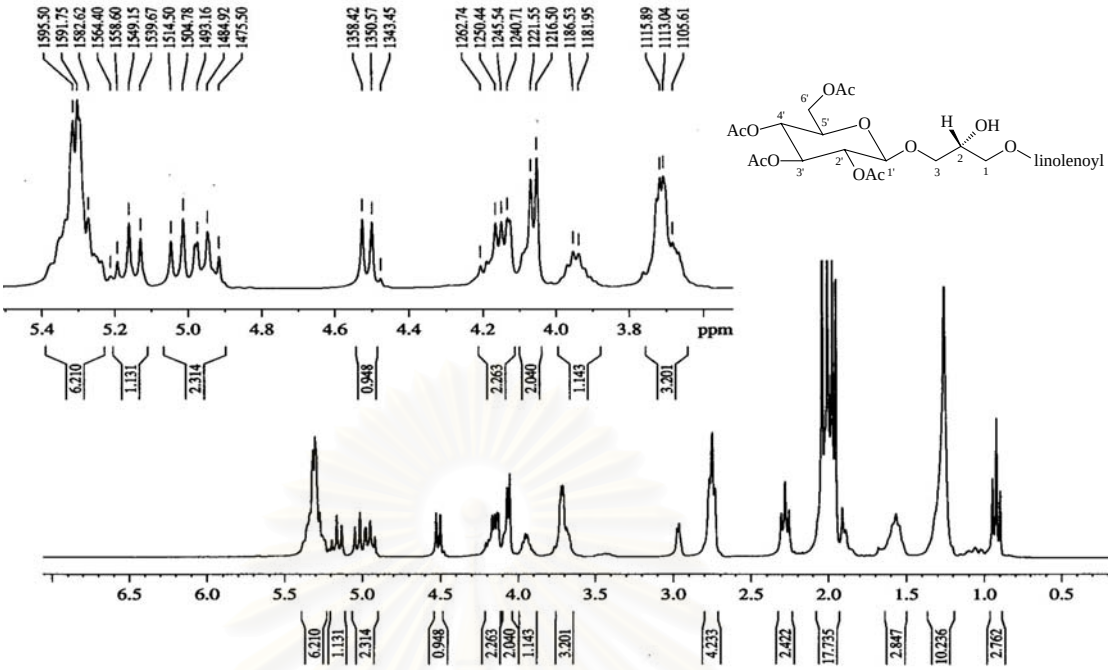

Figure 213. The 300 MHz ^{1}H-NMR spectrum of 1-*O*-linolenoyl-3-*O*-(β-D-2′,3′,4′,6′-tetra-*O*-acetyl-glucopyranosyl)-*sn*-glycerol (**33**) in $CDCl_3$.

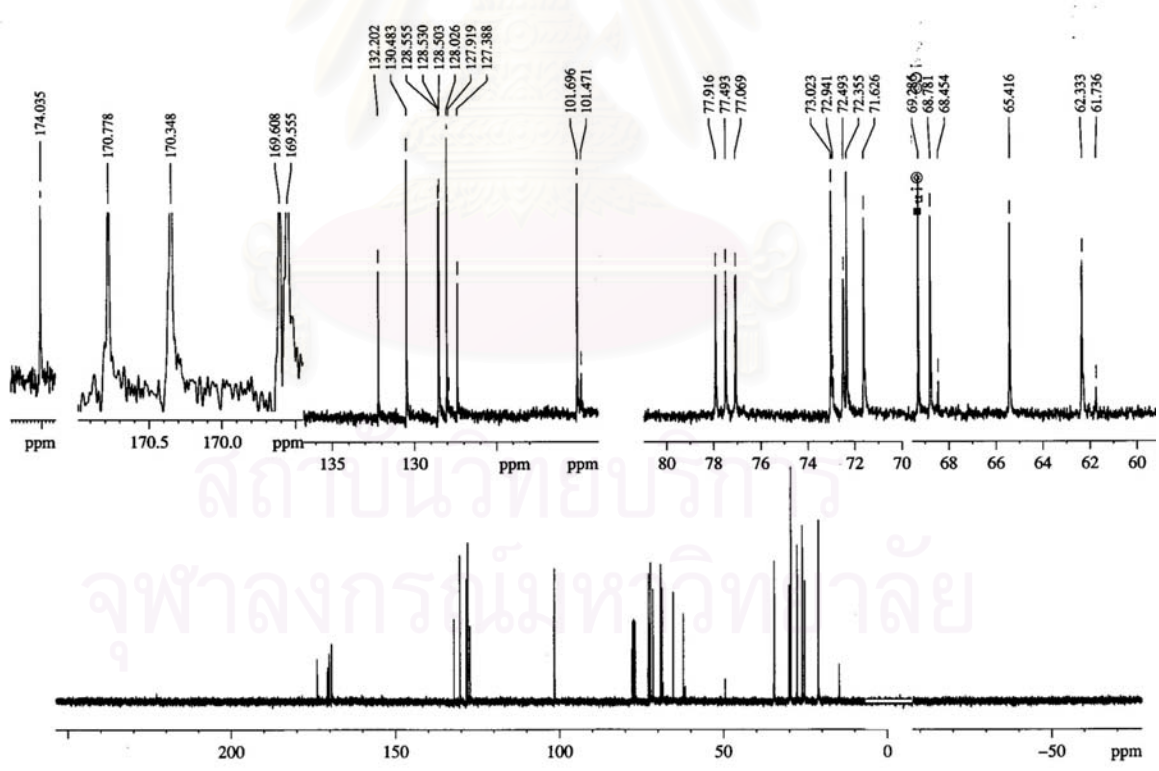

Figure 214. The 75 MHz ^{13}C-NMR spectrum of 1-*O*-linolenoyl-3-*O*-(β-D-2′,3′,4′,6′-tetra-*O*-acetyl-glucopyranosyl)-*sn*-glycerol (**33**) in $CDCl_3$.

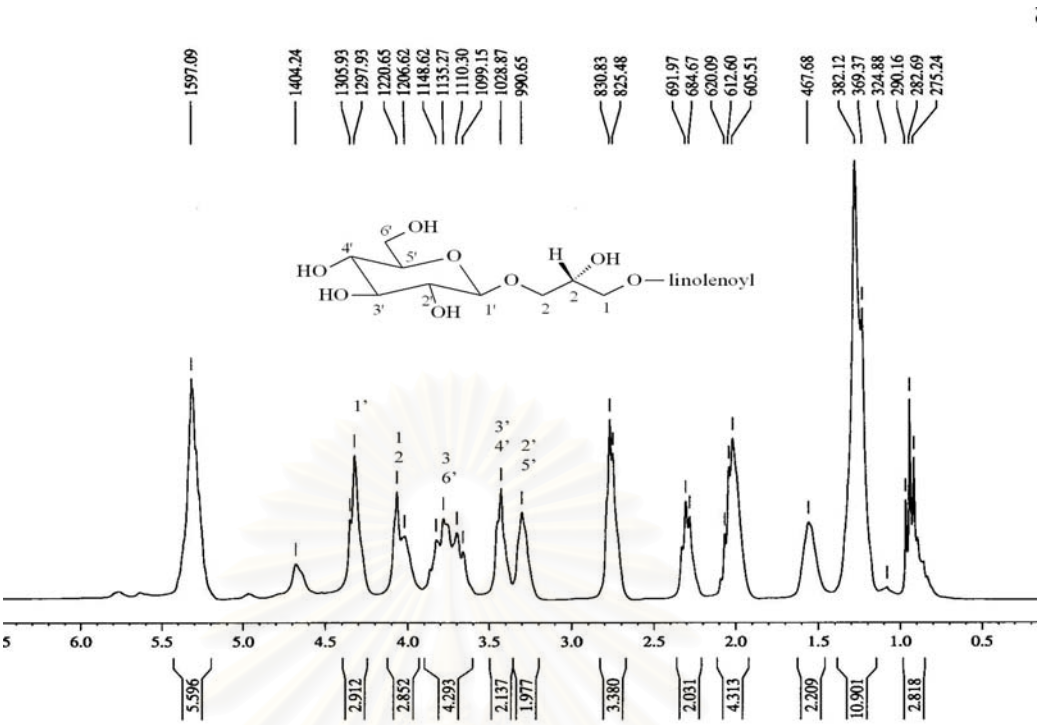

Figure 215. The 300 MHz ^{1}H-NMR spectrum of 1-*O*-linolenoyl-3-*O*-β-D-glucopyranosyl-*sn*-glycerol (**34**) in $CDCl_3$.

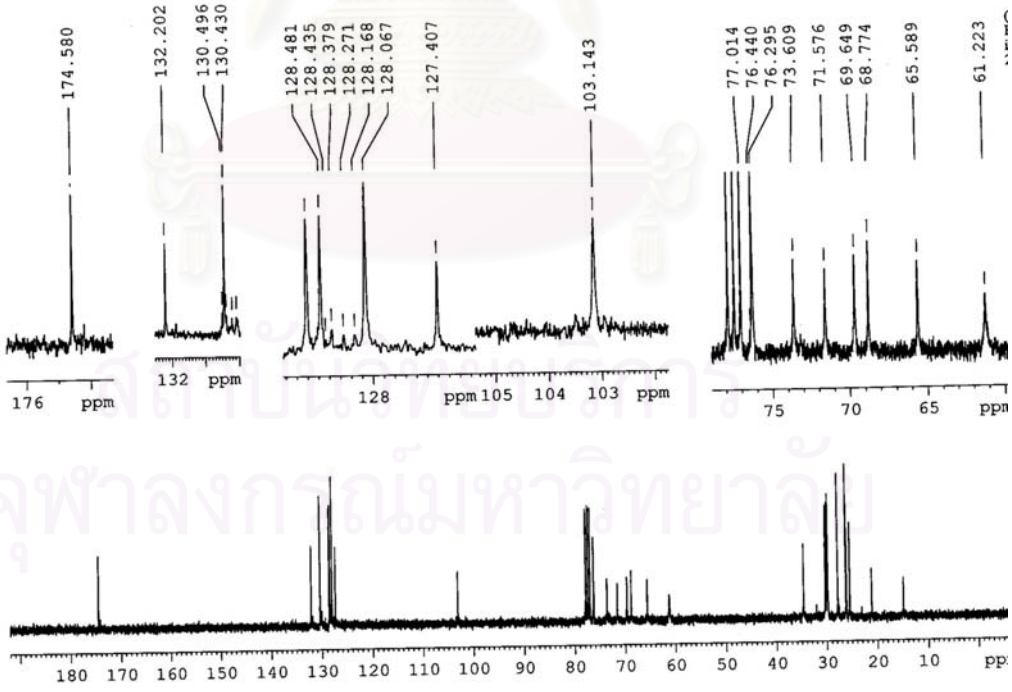

Figure 216. The 75 MHz ^{13}C-NMR spectrum of 1-*O*-linolenoyl-3-*O*-β-D-glucopyranosyl-*sn*-glycerol (**34**) in $CDCl_3$.

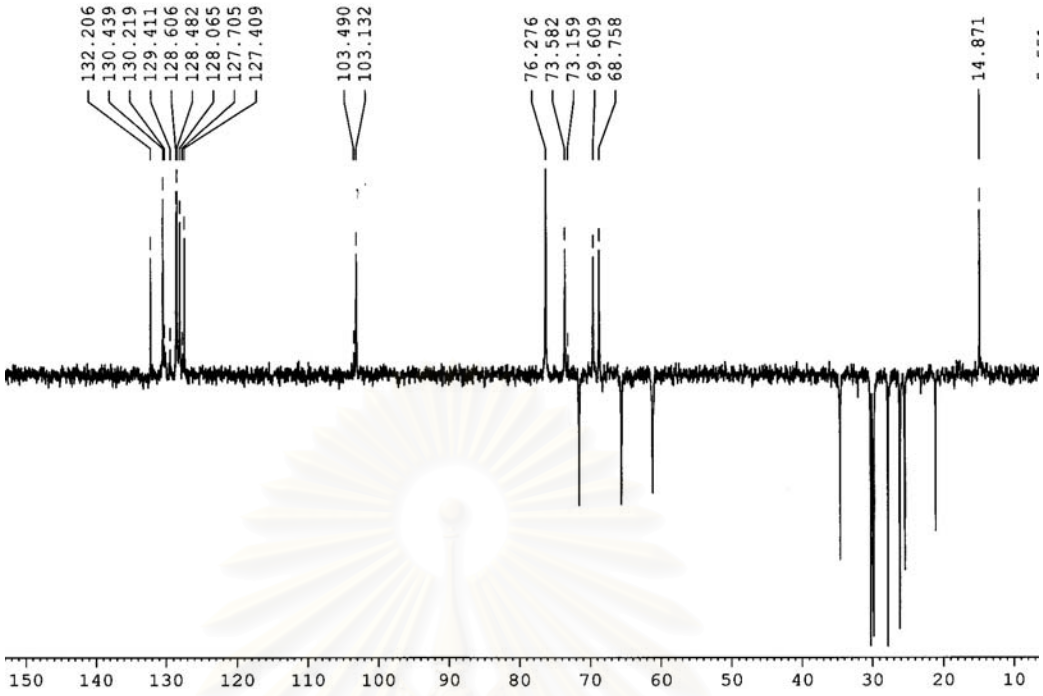

Figure 217. The DEPT 135 spectrum of 1-*O*-linolenoyl-3-*O*-β-D-glucopyranosyl-*sn*-glycerol (**34**) in $CDCl_3$.

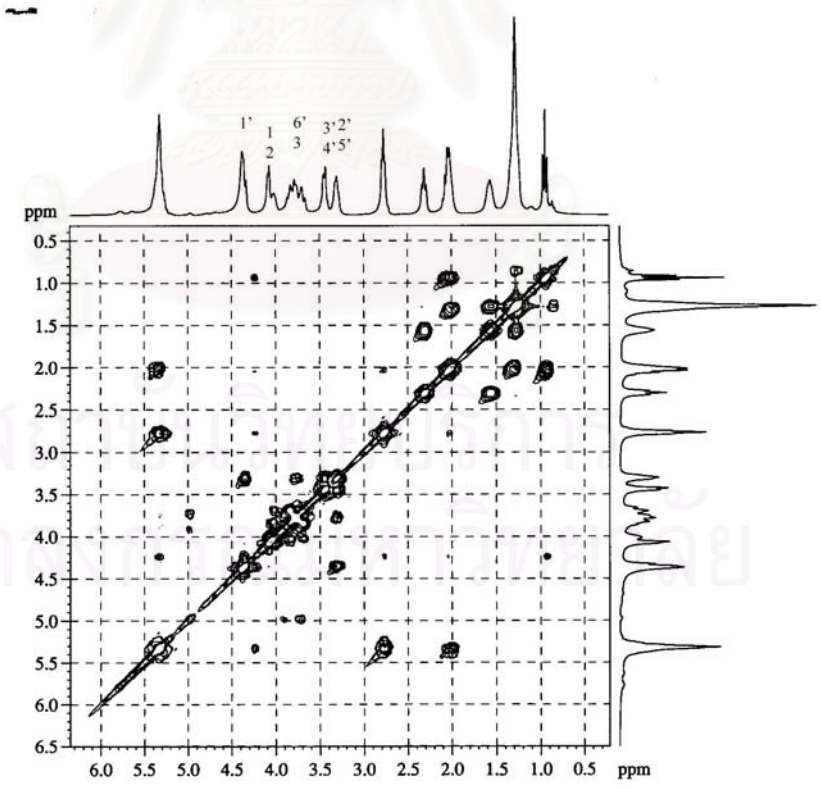

Figure 218. The ^{1}H-^{1}H COSYspectrum of 1-*O*-linolenoyl-3-*O*-β-D-glucopyranosyl-*sn*-glycerol (**34**) in $CDCl_3$.

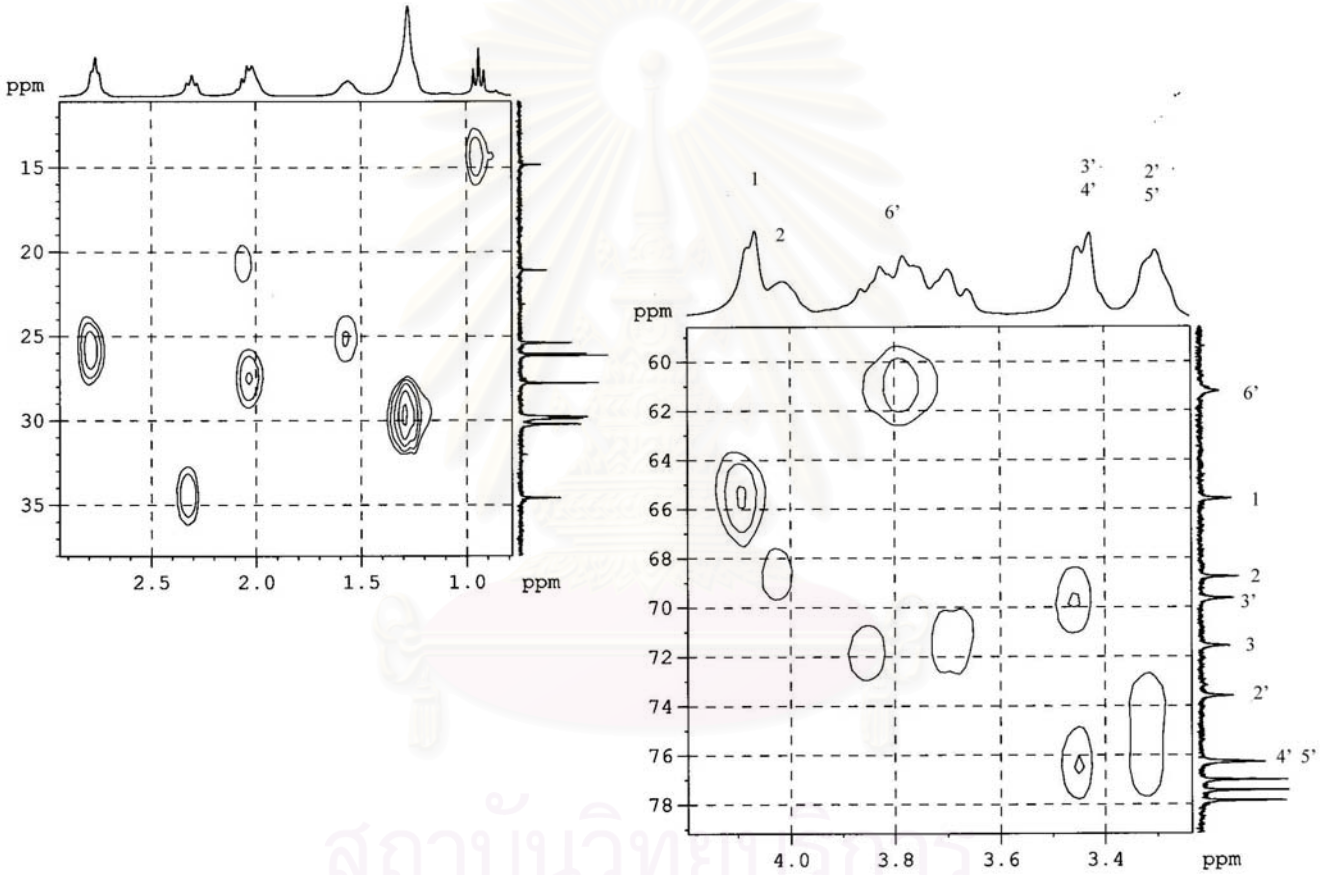

Figure 219. The HMQC spectrum of 1-*O*-linolenoyl-3-*O*-β-D-glucopyranosyl-*sn*-glycerol (**34**) in $CDCl_3$.

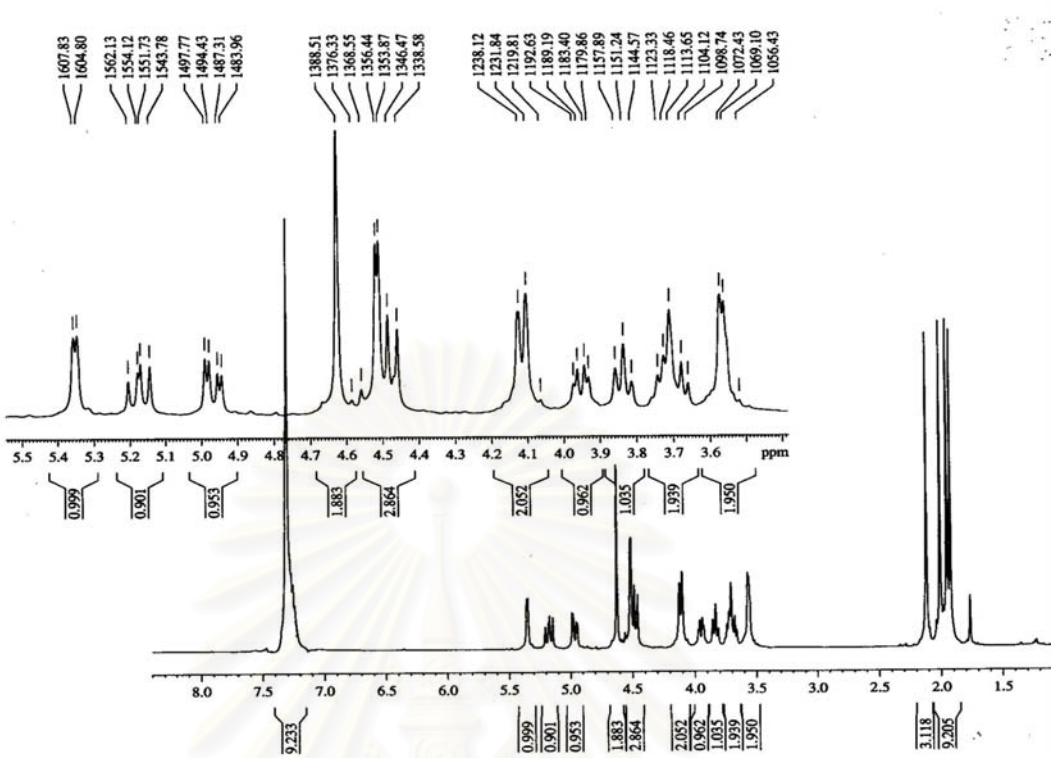

Figure 220. The 300 MHz ^{1}H-NMR spectrum of 1,2-di-*O*-benzyl-3-*O*-(β-D-2′,3′,4′,6′-tetra-*O*-acetyl-galactopyranosyl)-*sn*-glycerol (**35**) in $CDCl_3$.

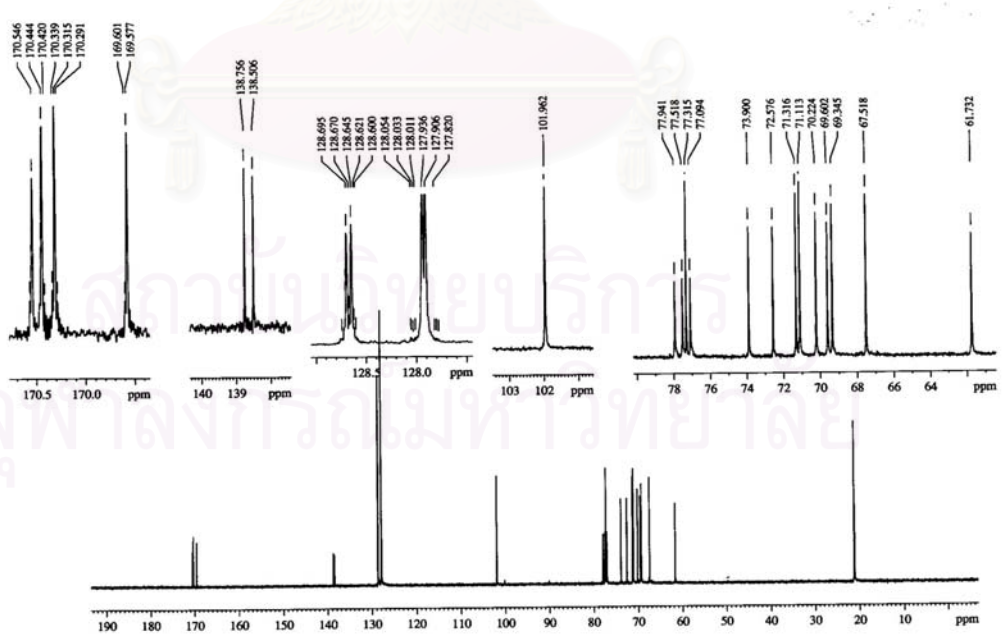

Figure 221. The 75 MHz ^{13}C-NMR spectrum of 1,2-di-*O*-benzyl-3-*O*-(β-D-2′,3′,4′,6′-tetra-*O*-acetyl-galactopyranosyl)-*sn*-glycerol (**35**) in $CDCl_3$.

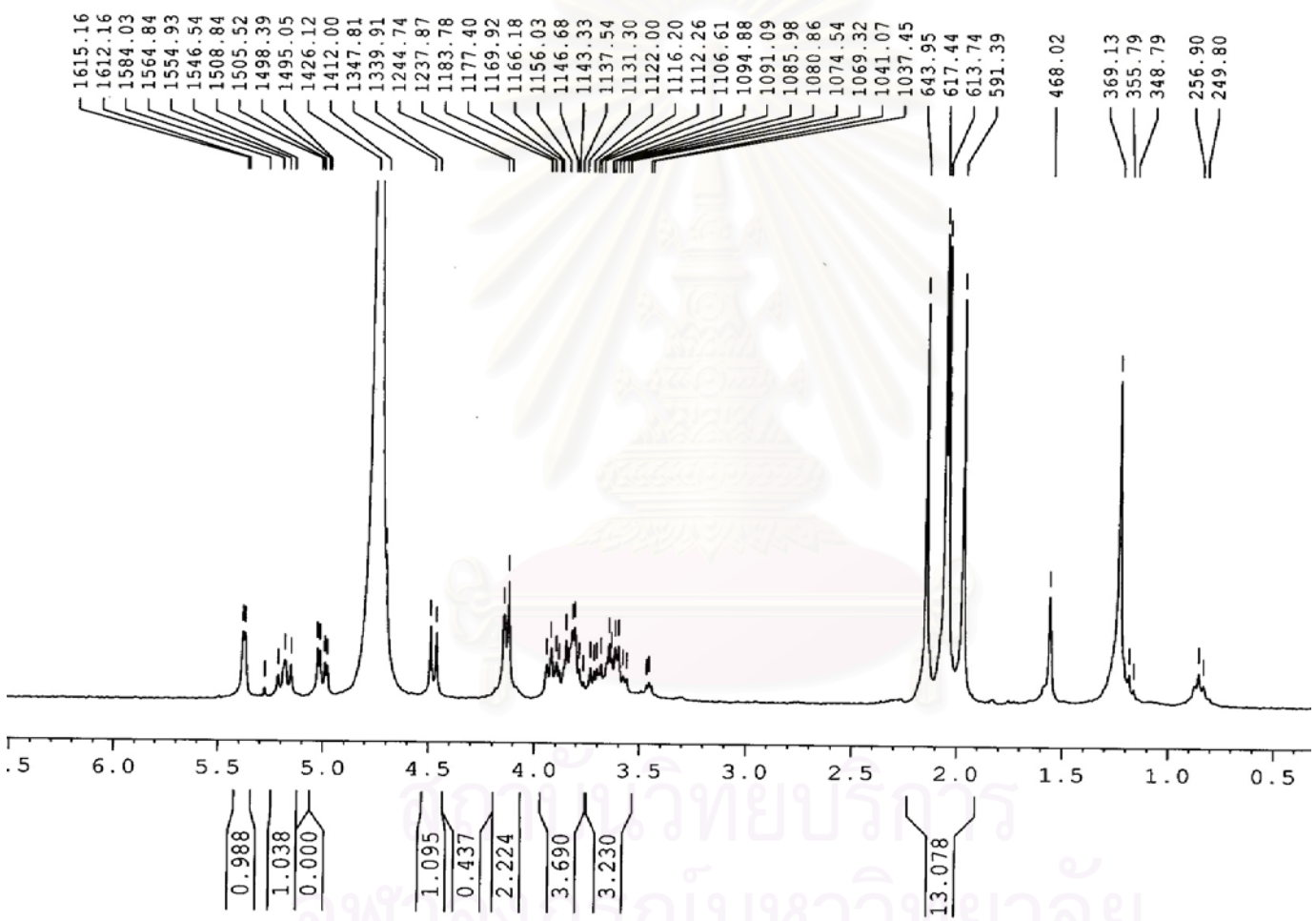

Figure 222. The 300 MHz ^{1}H-NMR spectrum of 1-*O*-(β-D-2′,3′,4′,6′-tetra-*O*-acetyl-galactopyranosyl)-*sn*-glycerol (**36**) in $CDCl_3$.

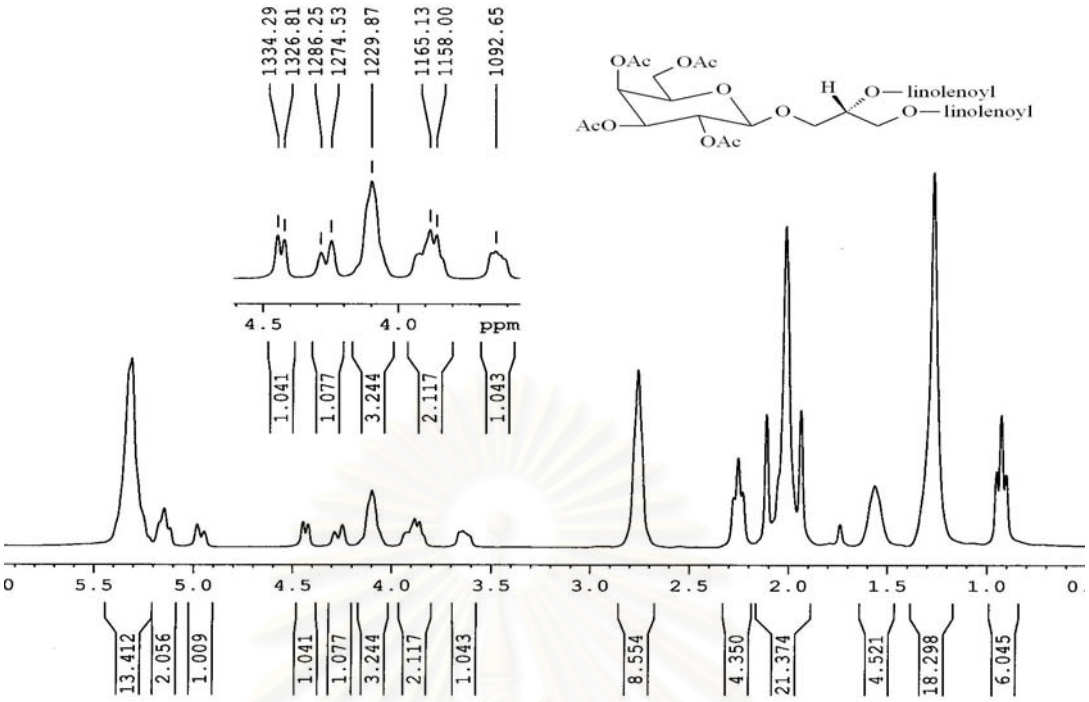

Figure 223. The 300 MHz ^{1}H-NMR spectrum of 1,2-di-*O*-linolenoyl-3-*O*-(β-D-2′,3′,4′,6′-tetra-*O*-acetyl-galactopyranosyl)-*sn*-glycerol (**37**) in $CDCl_3$.

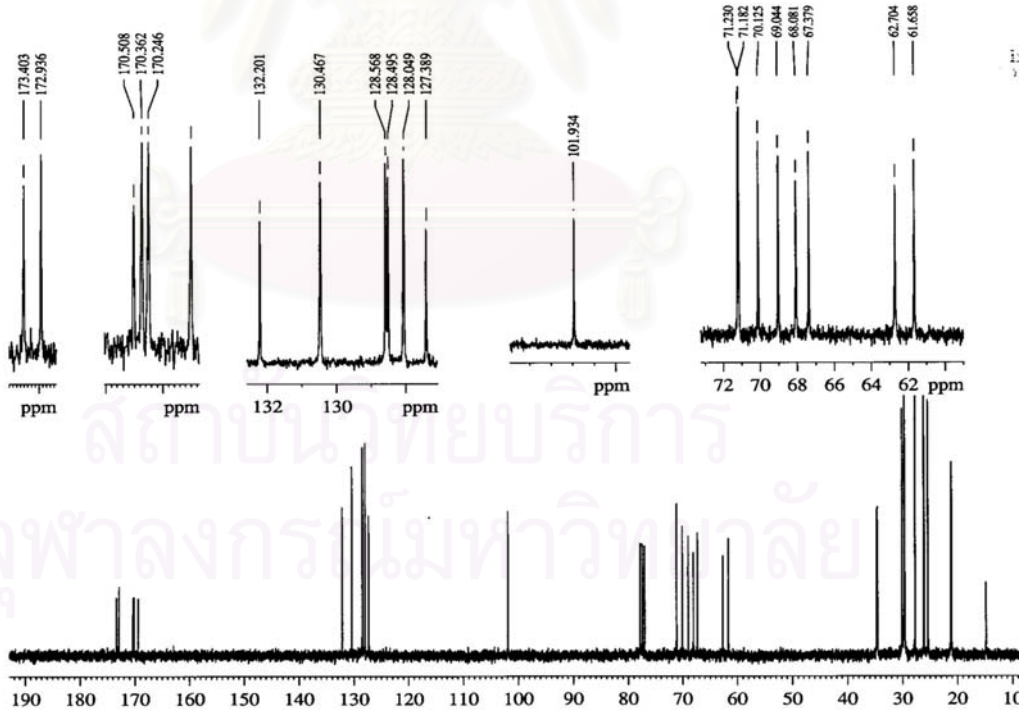

Figure 224. The 75 MHz ^{13}C-NMR spectrum of 1,2-di-*O*-linolenoyl-3-*O*-(β-D-2′,3′,4′,6′-tetra-*O*-acetyl-galactopyranosyl)-*sn*-glycerol (**37**) in $CDCl_3$.

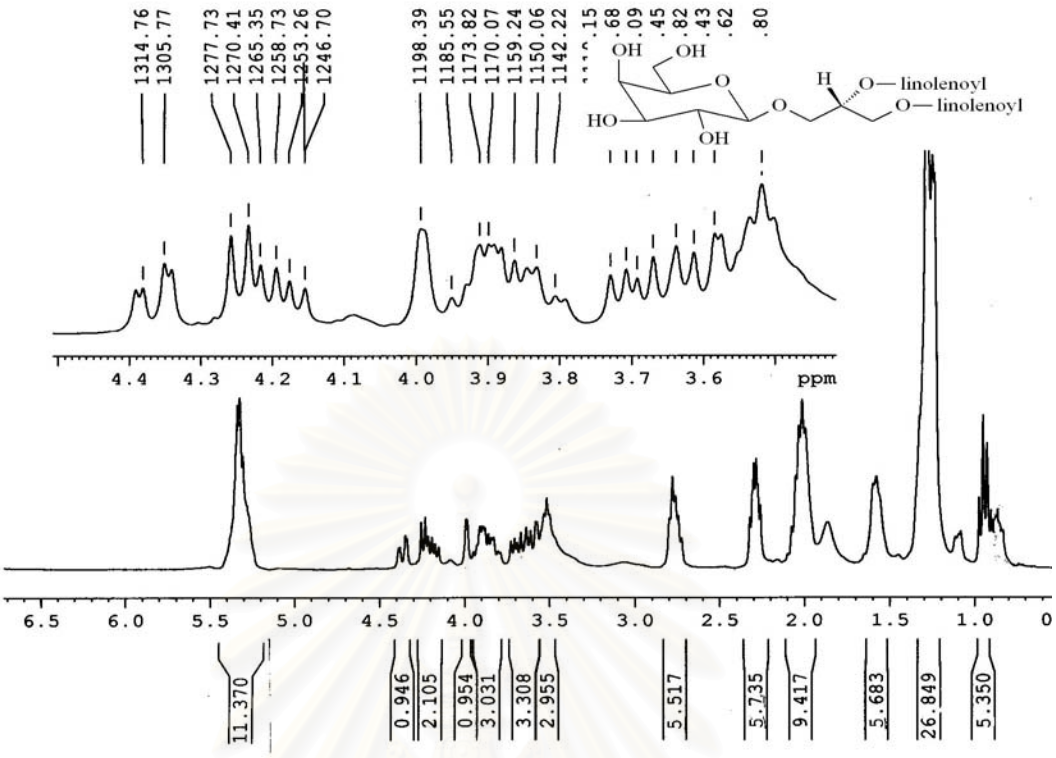

Figure 225. The 300 MHz ^{1}H-NMR spectrum of 1,2-di-*O*-linolenoyl-3-*O*-β-D-galactopyranosyl-*sn*-glycerol (**38**) in $CDCl_3$.

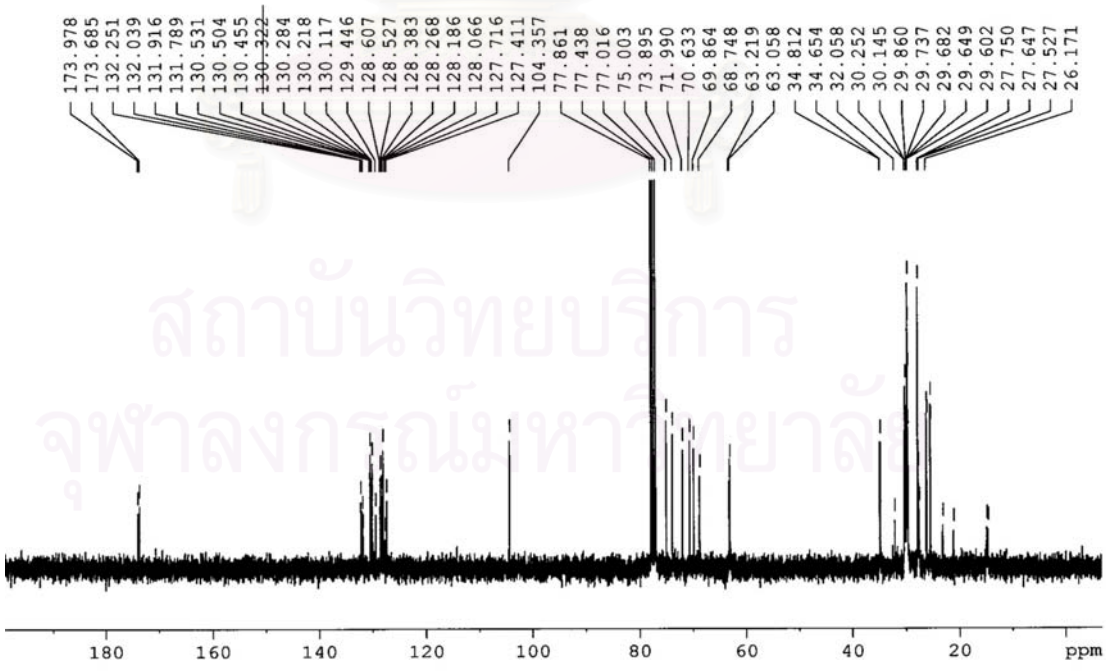

Figure 226. The 75 MHz ^{13}C-NMR spectrum of 1,2-di-*O*-linolenoyl-3-*O*-β-D-galactopyranosyl-*sn*-glycerol (**38**) in $CDCl_3$.

VITA

Mr. Wicharn Janwitayanuchit was born on October 1, 1964 in Bangkok, Thailand. He received his Bachelor of Science in Pharmacy with second class honor in 1989 and Master of Science in Pharmacy in 1992 from the Faculty of Pharmaceutical Sciences, Chulalongkorn University, Thailand. In 1992 to 1994, he worked as a lecturer at the Department of Pharmaceutical Chemistry, Faculty of Pharmacy, Prince of Songkla University. Since June, 1994 he has become a staff of the Department of Pharmacognosy and Pharmaceutical Chemistry, Faculty of Pharmaceutical Sciences, Huachiew Chalermprakiet University. He has held an appointment as Assistant Professor since 1999.